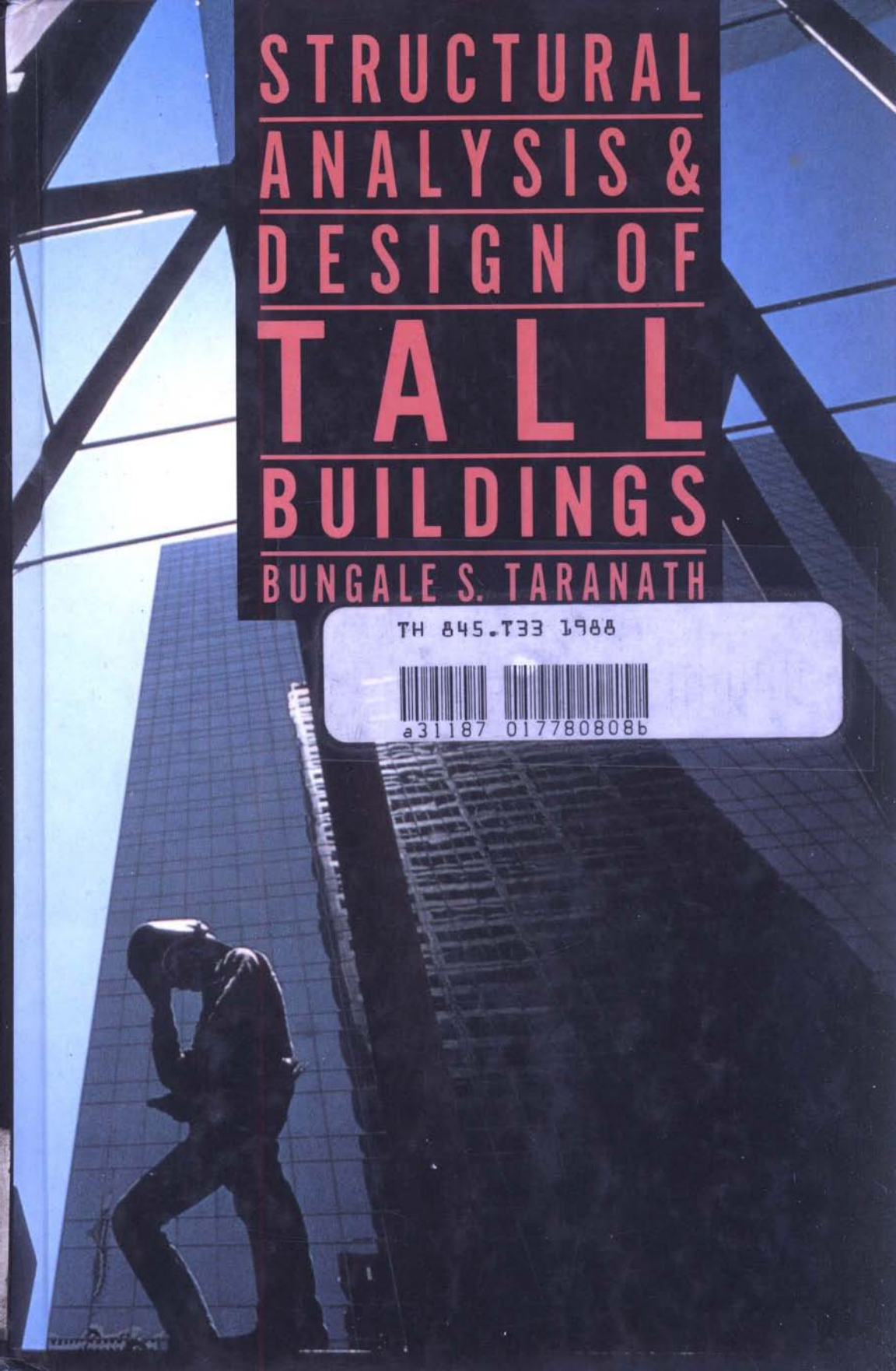

STRUCTURAL ANALYSIS & DESIGN OF TALL BUILDINGS

BUNGALE S. TARANATH

Structural Analysis and Design of Tall Buildings

Bungale S. Taranath

McGraw-Hill Book Company
New York St. Louis San Francisco Auckland
Bogotá Hamburg London Madrid Mexico
Milan Montreal New Delhi Panama
Paris São Paulo Singapore
Sydney Tokyo Toronto

Library of Congress Cataloging-in-Publication Data

Taranath, Bungale S.
Structural analysis and design of tall buildings.

Includes index.
1. Tall buildings—Design and construction.
I. Title.
TH845.T33 1988 624.1'7 87-29317
ISBN 0-07-062878-5

1234567890 DOC/DOC 89321098

ISBN 0-07-062878-5

The editors for this book were Nadine Post and Dennis Gleason, the designer was Naomi Auerbach, and the production supervisor was Dianne Walber. It was set in Century Schoolbook by The William Byrd Press, Inc.

Printed and bound by R. R. Donnelley & Sons Company.

DEDICATED TO

My Wife Saroja
Daughter Anupama
and
Son Abhiman

Contents

Preface

Tall buildings have a unique appeal, even an air of romance and mystery associated with their design. Developments in the last decade have produced many slender high-rise buildings, demanding that particular attention be paid to their complex behavior under lateral loads. Economic considerations routinely call for leaner and sparser designs that increasingly challenge the design professional to come up with safe and economical structural solutions. Existing technical literature is limited and until now there have been no books that deal exclusively with tall buildings. Most handbooks have limited sections, if any, on slender structures and their analysis.

Many admirable textbooks are available that address the design and analysis of building components, such as beams, columns, and trusses. Available books that consider the conceptual design of structures are broad in scope and are primarily intended to promote mutual understanding between architects and engineers. In today's engineering practice it is not unusual for the structural engineer to be called upon to conceptualize schematic options and to provide comparative alternatives before a final scheme is selected. Even experienced engineers find it hard to readily come up with various structural concepts because, other than their own library of experience, very little reference material is available. This book attempts to alleviate this problem by providing a systematic basis for conceptualizing different structural systems and by providing an orderly method of arriving at preliminary structural schemes.

High-rise architecture is continually changing, and prismatic shapes that were once very popular have given rise to terraced, set-back, and splayed elevations. Computers have given the structural engineer of today the tools to respond to this changing architecture with daring structural solutions. No longer does the structural engineer require that the building be regular in plan and the interior and exterior columns line up with each other. Although the engineer may influence the locations of certain obvious structural elements, the trend today is to let the architect define the building appearance and

then to come up with an economical structural system within the confines of the architect's requirement. This trend has resulted in some innovative and daring structural schemes. Fortunately for the layperson, the result has been usually an interesting, varied, and sometimes flamboyant architecture that adds to the variety and interest of the skyscapes in urban cities.

Therefore, there is a need today for the structural engineer to be knowledgeable not only about the run-of-the-mill type of design but also about some of the less usual structural solutions. To this end, emphasis is placed in this book on the methodology of incorporating well-established structural solutions to modern high-rise architecture. Application of the state-of-art solutions which have evolved as a natural extension of the proven systems are also discussed.

In attempting to set a stage for the rest of the book, Chapter 1 introduces the evolution of high-rise architecture and its impact on the relative size and locations of various structural elements. An attempt is made in this chapter to lay the general foundation for the understanding of future chapters dealing with specific structural systems and their merits.

Tall buildings are uniquely characterized by requiring that lateral loads be a major design consideration. Two types of loads normally associated with lateral loads are wind and earthquake loads. Today the state of the art in determining the design wind load on a tall building, and indeed to verify the serviceability of the building in terms of comfort to the occupants, is to perform a wind tunnel test under simulated conditions. Chapter 2 deals with the characteristics of wind and their treatment in various building codes. The complex field of wind tunnel engineering is presented in a simplified manner.

Chapter 3 outlines seismic design, highlighting dynamic behavior. Static, dynamic, and time history analyses are outlined, with emphasis on practical analysis rather than on intriguing mathematical manipulations which fail to develop physical understanding of earthquake phenomena.

The fourth, fifth, and sixth chapters present various structural systems that are currently in vogue using steel, concrete, and various combinations of these materials, called composite construction. Much of the material has been drawn from author's experience. Actually built or proposed structural systems of tall buildings are discussed in terms of their response to lateral loads.

The seventh, eighth, and ninth chapters consider the gravity design of vertical and horizontal systems using steel, concrete, and composite systems. In addition to the more common systems, the behavior and practical design of some of the novel systems such as composite stub and haunch girders are also discussed.

Chapter 10 is dedicated to the analysis of structural systems. Approximate methods which are more appropriate for certain types of structures than more time-consuming methods are discussed first, followed by modeling techniques for two- and three-dimensional analysis. Finite element applications for slab and shear wall systems are discussed, followed by a thorough coverage of warping behavior of open-section shear walls. Some of the original work done by the author that highlights the torsional behavior of open-section shear walls is presented for the first time. Practical solutions using commercially available computer programs are discussed.

Chapter 11 deals with problems unique to tall buildings and should be of interest to practicing engineers and be of assistance to the young engineers in developing an intuitive feeling for the structural behavior of tall buildings.

In short, this book attempts to achieve a number of objectives: it is intended to bridge the gap that exists between a novice and an experienced high-rise designer. It systematically introduces the complex issues of conceiving and manipulating design options. The scope of the book is broad, but the author believes that enough in-depth material is included to make this book useful to practicing engineers. It is hoped that this book will also serve as a teaching tool for advanced high-rise structure courses in universities and in advanced seminars.

My sincere thanks to Mr. John L. Tanner, Dr. Madhu B. Kanchi, Mr. James S. Notch, and Mr. Mysore V. Ravindra who read parts of the manuscript and offered many helpful suggestions. Thanks are also due to Mr. Mark P. Pavluvcik for his help in computer analysis and to Mr. Heinz Winkler for his help in preparing illustrations. Parts of Chapter 10 dealing with warping torsion are based on the author's doctoral thesis work conducted at the University of Southampton in England. Thanks are extended to Dr. B. Stafford Smith for supervision and valuable suggestions, and to the British Research Council for support during the research at the university. My gratitude is extended to Mrs. Pam Finch, Mrs. Valarie Griffin, and Mrs. Saroja Taranath for typing the manuscript. Finally, both love and gratitude to Anu and Abhi for allowing daddy to write relatively free of interruption. My wife Saroja's help and patience are acknowledged. Without her help this book could not have been written.

BUNGALE S. TARANATH
Houston, Texas

Chapter

1

General Considerations

1.1 Introduction

1.1.1 Historical background

Throughout the recorded history of building, perhaps nothing is more captivating than the human aspiration to create increasingly tall structures. Pride seems to have been the prime motivation for the building of such ancient structures as the Tower of Babel, Colossus of Rhodes, the pyramids of Egypt, the Mayan temples of Mexico, and the Kutub Minar of India. Ego and competition still play a part in determining the height of a building, but various other social and economic factors, such as increases in land values in urban areas and higher density of population, have led to a great increase in the number of tall buildings all over the world. What was once considered to be an American urban phenomenon can now be seen in many small towns and even in open country. The skylines of the world's cities are continually being pierced by distinct and identifiable tall buildings as impressive as mountain ranges, and reaching upward continues to be the challenge and goal.

The ancient tall structures, which can be considered as prototypes of present-day high-rise buildings, were protective or symbolic in nature and were infrequently used. Tall buildings such as the Egyptian pyramids and Mayan temples were primarily solid, serving more as monuments than as space enclosures. Throughout history, people had

to make use of the available building materials. The Pyramid of Cheops, for example, was built by piling huge masonry blocks one on top of another to a peak of 481 ft (146.7 m), equivalent to a modern 40-story office building. The two basic materials, masonry and timber, used in construction through the early centuries had their limitations. The spans which timber and stone could bridge, either as beams, lintels or arches, were limited. Wood was not strong enough for large structures, nor did it possess fire-resisting characteristics. Brick and stone masonry, in spite of their excellent strength and fire resistance, suffered from the drawback of weight. The mass of masonry required to carry the weight of a structure was too great to allow anything but a token usable space within it. The percentage of area occupied by the vertical structural elements, i.e., columns, walls, and braces, was inordinately large when compared to the gross floor area. This percentage was at a maximum value for the pyramids. The weight limitation of masonry materials established the aesthetics of classic, Gothic, and Renaissance architecture.

Masonry construction reached its zenith in 1891 with the construction of the 17-story, 210-ft (64-m) Monadnock Building in Chicago, an impressive structure that has gained historic landmark status. Gravity and the overturning moment caused by wind are resisted solely by the load-bearing masonry walls, which are 7 ft (2.13 m) thick at ground level. The area occupied by the walls of this building is 15 percent of the gross area at the ground floor.

In 1885, an American engineer named William LeBaron Jenny became the creator of the modern skyscraper when he realized that an office building could be constructed using totally different materials. He chose structural steel and incorporated it into a revolutionary system that was to make possible the soaring office towers that now symbolize the modern metropolis. Instead of relying on heavy masonry walls to support the weight of upper floors, Jenny had the ingenious idea of supporting the gravity loads of the 10-story Home Insurance Building in Chicago on a steel framework and hanging the masonry walls from this skeleton. The appropriateness of a steel skeleton for this purpose was acknowledged almost immediately. Its emergence was further influenced by factors such as economic expansion, the financial and institutional character of American business, and the intense use of urban land in central business districts. Still, very few buildings above 10 stories were built.

Two technological developments, the elevator and modern metal frame construction, removed the prevailing limitations on the height of the buildings, and the race for tallness was on. Competition to be the leading metropolis as judged by building heights developed between Chicago and New York. By the turn of the century, the downtown

business district around Wall Street in New York had achieved the status of the nation's foremost financial center. The great demand for office space saw the construction of several 20-story steel-skeleton buildings in this area.

In 1913, the Woolworth building was the first to reach 60 stories, soaring up 792 ft (242 m) in lower Manhattan. This Gothic cathedral style building is still in vigorous use after 70 years of service and the installation of air conditioning and automatic elevators. There was a temporary lull in high-rise construction during World War I, but activity picked up with renewed vigor after the war. Many excellent structures were built in New York, such as the 66-story, 950-ft (290-m) 60 Wall Tower Building; 71-story, 927-ft (283-m) Cities Service Building; and 77-story, 1046-ft (319-m) Chrysler Building.

The demand for tall buildings increased because large corporations recognized the advertising and publicity advantages of connecting their names with imposing high-rise office buildings even though their operations required a relatively small percentage of floor space. The surplus space was leased out to eager business tenants, making the investment in high-rise development not only a source of publicity and pride but also a sound financial investment as an income generator.

The collapse of the financial market during the depression put an end to speculative high rises, and only in the late 1940s in the wake of World War II did a new era of high-rise building set in. In addition to the stimulus of the new resources provided by technology was the spur of necessity. With the population doubling in almost every generation and production growing at an even faster pace, developers could scarcely keep up with the demand for space. In the frenzy of new building, the race for height ended for the time being, in 1930, with the construction of the Empire State Building in New York City. This building, measured without the 222-ft (67.7-m) television antenna added later, was 1250 ft (381 m) high, taller than the 984-ft (300-m) Eiffel Tower in Paris, which was the highest structure of the nineteenth century. In 1968 the John Hancock Center in Chicago rose to a height of 1127 ft (344 m) plus 344 ft (105 m) of television antennas. The World Trade Center in New York City rises higher than the Empire State Building, to an awe-inspiring height of 1350 ft (412 m). In 1974, however, the 110-story Sears Tower in Chicago took the crowning title as the world's tallest building at 1450 ft (442 m).

Despite some opposition, tall buildings continue to pop up across the country. Sixteen American cities boast at least one building among the world's tallest. Houston has numbers 8 and 9, the Texas Commerce Bank at 75 stories, or 1002 ft (305 m), and Allied Bank Plaza at 71 stories, or 970 ft (296 m). Controls already imposed by American cities on high-rise development suggest that the world's next tallest sky-

scraper may be seen not in the United States but in a booming foreign city probably in Asia.

There have been several proposals for buildings which will exceed 100 stories. Whether the next assault will be on the American skyline remains to be seen. Perhaps the fabled King Kong will make his next climb atop a high-rise building in Hong Kong. Builders have no doubt that such behemoths could be constructed, and they believe that a strong economy, a strong demand for office space, and strong popular or political support will once again sow the seeds of competitiveness for supertall structures.

In the early period of their building, most high rises tended to be prismatic in shape, but today even the most conservative architects are designing buildings with a touch of flamboyance. Owners and developers, who were once suspicious of daring designs, have come to expect them. In response, current architecture is producing buildings with from three to as many as ten sides, as well as round buildings. Some buildings proudly express on their surfaces, bold structures, others are clad in smooth architectural curtain walls. Some consist of a single tower; others of two, sometimes identical twins, looking at each other in perpetual challenge.

The current flamboyance in architecture has not deterred the structural engineer from coming up with economical support systems. In fact, it has stimulated the profession to give almost total freedom in the architecture of the high-rise structures. Today, with the use of computers, buildings are planned and designed which have little or no historic precedent. New structural systems are conceived and applied to extremely tall buildings in a practical demonstration of the engineer's confidence in the predictive ability of the analysis, the methods used, and the reliability of computer solutions. Computers have made once difficult calculations easy, allowing the engineer to experiment with new configurations in an overall effort to reduce the structural cost.

Compared to advances in other engineering disciplines, the increase in the height of buildings brought about by structural innovation and computer technology is only modest; compare the height of the Empire State Building, which was completed in 1931 using a semirigid connection in a record time of 18 months from preliminary architectural drawings to final completed structure, to the skyscrapers built today, such as the 110-story Sears Tower or the twin towers of the World Trade Center. What is more important in the present context is the significant decrease in structural materials the engineer has been able to effect because of innovative design techniques. Before examining the reasons for the steady decrease in the material quantities, it is instructive to follow the development of twentieth-century high-rise

architecture because structural quantities are closely related to the architecture of the building.

1.1.2 Review of twentieth-century architecture

The architecture of the United States in the twentieth century can be traced to several nineteenth-century roots. One was the advent of new forms of structural and other materials so strikingly displayed in the building technology of the American skyscraper. This has allowed greater scope of aesthetic expression and innovation in architectural practice. Another was the development of expressive new idioms of form and space. The development of metal trusses made it possible to roof column-free interior spaces easily and economically. Such roofs were used for railroad stations, market halls, exhibition palaces, and domes.

The nineteenth century was one of the most technically inventive centuries. It witnessed the application of new techniques and of new mechanical means in virtually every human activity. It became clear in time that the innovation in architecture would come from those who grasped the possibilities of the new materials and techniques. Revolutionary methods of building with wood were developed in the 1830s to meet the demands for speedy construction and to overcome the shortage of skilled labor. Cast iron was developed into a building material lighter and more adaptable than masonry, and combined with other inventions, notably the elevator, paved the way for tall buildings unprecedented not only for height but ease of construction.

In Chicago during the later part of the nineteenth century, a school of architects of whom Louis Sullivan and Frank Lloyd Wright were the most famous members, originated a new American style of domestic architecture. Their designs, primarily houses, were long, informal, and organic. Their ideas were ignored for more than a decade in America, but were taken up abroad and developed into the so-called International Style. The International Style was also influenced by the German Bauhaus school, founded by Walter Adolf Gropius, and by the abstract artists interested in using pure forms for buildings. This style was the architectural response to the machine age. Simplicity meant elegance derived from "pure" forms. Display of the structural muscle beyond the tightly stretched curtain wall was widely accepted as the "in thing." Structures designed in this era incorporated three distinct elements of the new style: (1) a new vocabulary of forms borrowed largely from abstract art, consisting of planes, lines, and rectangles without ornaments or mouldings; (2) the representation of interior space and exterior facade as a cohesive unit; and (3) the use of new structural materials such as steel and concrete.

The new style, with its angular forms, plane surfaces, and lack of conventional ornament, met with some resistance from the public, which tended to regard it as bare and inhuman. But by the middle of the twentieth century the style had become dominant across the country. Bold use of modern construction methods and structural materials became common. Noteworthy among the latter are glass tinted to reduce glare; glass brick designed to admit additional light while preventing glare and furnishing effective insulation against heat, cold, and noise; artificial stone; plastics; chromium, aluminum, and other metals; and above all steel and concrete.

The early stages of American architecture lacked truly monumental structures. The monumental idea was gradually added to American architectural forms, reaching its apex with the construction of Rockefeller Center in New York City. The center represented a new concept of building a city within a city, containing a towering 60-story structure surrounded by a number of smaller high-rise office buildings and recreational facilities. This complex of skyscrapers has exercised increased influence since 1931, the year work on the center was started. The building represents a departure in architectural thinking from a single-use, single-building concept to multiuse, multicomplex structures on a community scale. Because of that practical example, American architects have responded more and more creatively to such demands of contemporary American life-style as rapid intercommunication and integration of city and surrounding region. Another recent example of multibuilding planning is the World Trade Center in New York City, consisting of twin 110-story towers and four smaller buildings grouped around a plaza.

During the period of 1950 to the mid-1960s, the International Style of architecture was embraced by prominent American architects and resulted in sleek boxlike glass and steel high rises which integrated the concept of purity of design into the architecture of the structure. Notable examples are the Seagram Building (1950) and the Whitney Museum (1966), both in New York City, and the John Hancock Center (1968) in Chicago.

During the mid-1960s a reaction developed to the International Style that emphasized greater freedom of design. Figuratively speaking, the concept of glass box was beginning to shatter. It was no longer a misdeed to hide a structure behind a more aesthetic exterior. The building and construction industry saw the advent of new forms of structural and other materials which allowed greater scope for aesthetic expression and innovation. Within the last decade many major cities have had imaginative new shapes thrusting above their skylines using plan shapes that are other than prismatic. American corporations have built a new generation of flamboyant headquarters build-

ings that are altering the urban skyline and bringing new vigor to cities. Many are spectacle buildings—giant architectural logos that draw enormous public attention and increased revenues to the companies that build them. They are going up in cities and suburbs across the United States. These grand new buildings are emerging as good investments, serving not only as advertising symbols and marketing tools but also as sources of above-market rents for excess office space. The distinguishing architectural features for this new generation of buildings are sculptural shapes at their tops and elaborate detailing at their bases. The buildings generally divide into two types: modern, dramatically shaped masses, and postmodern structures with a romantic recollection of historical styles.

1.1.3 Functional requirements

Building configurations are tremendously varied, and their derivation seems to be random, at times even whimsical, although the configuration tries to simultaneously satisfy (1) the requirements of site, (2) the requirements of the building program, and (3) the requirements of appearance. The first requirement imposes constraints of site geometry and location, the second represents the requirements imposed by the planning and occupancy needs, and the third represents the designers' desires for physical images that express the aspirations of the building owner, the users and, of course, the designers themselves.

Buildings of the 1950s and 1960s responded to the functionalist ideas of the 1920s that the aesthetic and utilitarian aspects of the building are to be simultaneously satisfied. Such an idea is still being practiced, although currently functionalism is being hotly disputed. For a building to be successful, it should do the following:

1. Create a friendly and inviting image that has positive values to building owners, users, and observers.
2. Fit the site, providing proper approaches to the plaza with a layout congenial for people to live, work, and play.
3. Be energy-efficient, providing space with controllable climate for its users.
4. For office buildings, allow flexibility in office layout with easily divisible space.
5. Offer spaces oriented to provide the best views.
6. Most of all, the building must make economic sense, without which none of the modern high-rise development would be a reality.

1.2 Definition of a Tall Building

It is difficult to distinguish the characteristics of a building which categorize it as tall. After all, the outward appearance of tallness is a relative matter. In a typical single-story area, a five-story building will appear tall. In Europe, a 20-story building in a city may be called a high rise, but the citizens of a small town may point to their skyscraper of six floors. In large cities, such as Chicago or Manhattan, which are comprised of a vast number of tall buildings, a structure must pierce the sky around 70 to 100 stories if it is to appear tall in comparison with its immediate neighbors (Fig. 1.1). *Tall building* cannot be defined in specific terms related to height or number of floors. There is no consensus on what constitutes a tall building or at what magic height, number of stories, or proportion a building can be called tall. Perhaps the dividing line should be drawn where the design of the structure moves from the field of statics into the field of structural dynamics.

From the structural design point of view, it is simpler to consider a building as tall when its structural analyses and design are in some way affected by the lateral loads, particularly sway caused by such loads. Sway or drift is the magnitude of the lateral displacement at the top of the building relative to its base. As building heights increase, the forces of nature begin to dominate the structural system and take on increasing importance in the overall building system. Structural systems have to be developed around concepts associated entirely with resistance to turbulent wind. Over the past two decades, remarkable improvement has been achieved in the structural engineer's ability to develop appropriate building systems. Equally important, the structural engineer has developed a far more complete understanding of these forces of nature, particularly atmospheric wind.

1.3 Lateral Load Design Philosophy

In contrast to vertical load, lateral load effects on buildings are quite variable and increase rapidly with increases in height. For example, under wind load the overturning moment at the base of a building varies in proportion to the square of the height of the building, and lateral deflection varies as the fourth power of the height of the building, other things being equal.

There are three major factors to consider in the design of all structures: strength, rigidity, and stability. In the design of tall buildings, the structural system must also meet these requirements. The strength requirement is the dominant factor in the design of low-height structures. However, as height increases, the rigidity and stability requirements become more important, and they are often the

Figure 1.1. The tallness of a building is relative. (*a*) The Iah Tower in Mysore, India, is considered a tall building in a predominantly one- and two-story residential neighborhood. (*b*) A building must soar 70 to 100 stories in Manhattan to be considered tall. (*Top photo courtesy of B. M. Prasanna.*)

dominant factors in the design. There are basically two ways to satisfy these requirements in a structure. The first is to increase the size of the members beyond and above the strength requirements. However, this approach has its own limits, beyond which it becomes either impractical or uneconomical to increase the sizes. The second and more elegant approach is to change the form of the structure into something more rigid and stable to confine the deformation and increase stability. If design for lateral load, be it due to wind or earthquake, is of importance in tall buildings, what then are the criteria for the design of these loads? Let us consider designing for wind loads.

It is significant that there are no reports of completed tall buildings having collapsed because of wind load. Analytically, it can be shown that a tall building under the action of wind will reach a state of collapse by the so-called p-Δ effect, in which the eccentricity of the gravity load increases to such a magnitude that it brings about the collapse of the columns as a result of axial loads. Therefore, an important stability criterion is to assure that predicted wind loads will be below the load corresponding to the stability limit. The second consideration is to limit the lateral deflection to a level that will ensure that architectural finishes and partitions are not damaged. Although less severe than the collapse of the main structure, the floor-to-floor deflection normally referred to as the *interstory drift* nevertheless has to be limited because of the cost of replacing the windows and the hazard to pedestrians of falling glass.

Slender high-rise buildings should be designed to resist the dynamic effects of vortex shedding by adjusting the stiffness and other properties of the structure such that the frequency of vortex shedding does not equal the natural frequency of the structure. Lateral deflections of buildings should be considered from the standpoints of serviceability and comfort. The peak acceleration at the top floors of the building resulting from frequent windstorms should be limited to minimize possible perception of motion by the occupants.

In earthquake-resistant designs it is necessary to prevent outright collapse of buildings under severe earthquakes while limiting the nonstructural damage to a minimum during frequent earth tremors. The building should be designed to have a reserve of ductility to undergo large deformations during severe seismic activity.

1.4 Concept of Premium for Height

If there were no lateral loads such as wind or earthquake, any high-rise building could be designed primarily for gravity loads. Such a design would not impose any premium for height. Since there is no way to circumvent the gravity loads resulting from dead and live loads, the minimum possible material for a building of any number of stories

cannot be less than that required for gravity loads alone. Qualitatively, from the structural point of view, this corresponds to the most efficient or optimum system. Ideally, the structure needs to be designed for gravity loads only, whereas the stresses caused by lateral loads will automatically be limited to the 33 percent overstress allowed in most codes.

When the structure for a low- or mid-rise building is designed for gravity loads, it is very likely that the structure can carry most of the lateral loads. In general, this is not so for high-rise buildings because resistance to overturning moment and lateral deflection will almost always require additional material over and above that required for gravity load alone. Assuming equal bay sizes, the material quantities required for gravity floor framing in low- and high-rise structures are essentially identical; it makes no difference in the required quantities whether the floor being framed is at the second level of a low-rise building or at the 70th level of a high-rise building. The material required for floor framing is a function of the column-to-column span and not the building height. However, the material required for the vertical system, such as columns and walls, in a high-rise structure is substantially more than that for a low-rise building. The material increases in the ratio $(n + 1)/2$, where n is the number of floors, because the vertical components carrying the gravity load will need to be strengthened for the full height of the building, requiring more vertical steel than a one-story structure having the same floor area.

The quantity of materials required for resisting lateral loads is even more pronounced and would soon far outstrip all other structural costs if rigid frame action were employed in very tall buildings. The graph shown in Fig. 1.2 illustrates how the unit weight of a structural material such as steel increases as the number of floors increases. Wind begins to show its dominance at about 50 stories and becomes increasingly important with greater height. For example, in a steel building using rigid frame action, the total weight of, say, 24 psf (1149 Pa) of structural steel is split evenly at about 8 psf (383 PA) for each of the three subsystems, namely, (1) floor framing, (2) gravity columns, and (3) wind bracing system. Above 50 stories, wind bracing ingenuity often makes the difference between an economical solution and an expensive one. The objective is to arrive at a wind bracing system that keeps the additional material required for lateral loads to a reasonable quantity.

The material quantities needed with reinforced concrete buildings also increase as the number of stories increases. The increase in material for gravity load is more than for steel, whereas the additional material required for lateral load is not as high as for steel, since weight of additional gravity loads helps to resist the lateral deflection

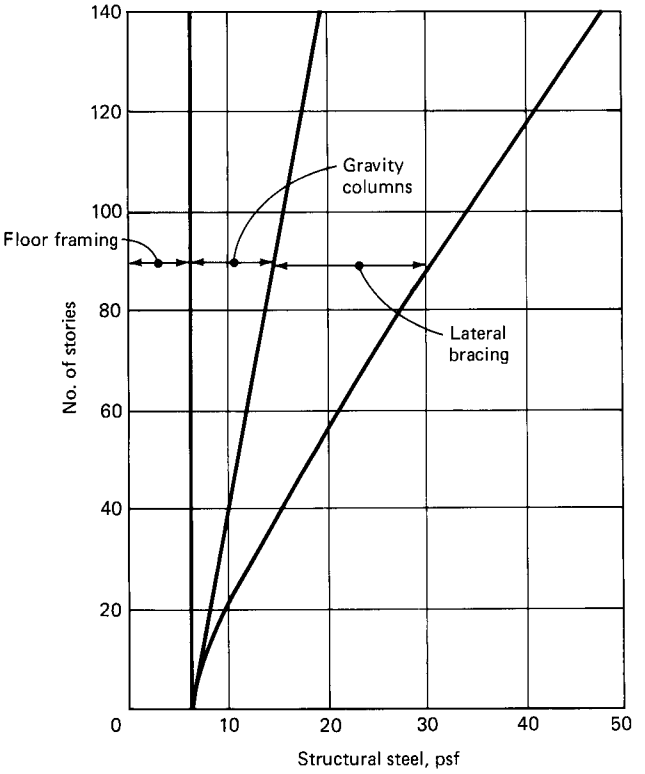

Figure 1.2. Structural steel quantities for gravity and wind systems.

and overturning moment. The additional gravity load, on the other hand, can aggravate the problem of designing for earthquake forces.

1.5 Relative Structural Cost

The structure usually accounts for 20 to 30 percent of the cost of a tall building. For buildings above 50 stories, the cost of a reasonable wind bracing system may work out, at most, to one-third of the structural cost. Therefore, compared to the total cost of the building, wind bracing costs, which are in the range of 7 to 10 percent, represent far from an overwhelming portion of the total construction dollar. The cost of the exterior wall alone can be half as much or may even be in excess of the cost of the total structure, depending upon its complexity and composition. The heating, ventilating, and air conditioning system often stands out in the cost picture.

In order to be economically competitive with low rises, tall buildings must offer savings other than in the structural system. Structural

optimization to carry the intended loads with minimum material may not allow a reduction in the overall cost of the building. The goal, therefore, is to optimize the overall cost, a process that normally takes place in the early stages of the project development. The structural cost is almost invariably studied together with the impact of the structure on other items such as increased or decreased floor-to-floor height, leasability of floors, etc.

It may appear from the foregoing that optimization of the structural cost alone may not be worth the effort. Nothing could be further from the truth. Indeed, the increased demand for bigger, taller buildings, coupled with freeform neomodern architecture, has created more need for innovative systems to cope with the economic demands. The technique of optimization is not a new feature for structural engineers. Engineering judgments have always included considerations of optimum structures, usually in the form of minimum weights for steel members and repetition of formwork in concrete structures. However, optimization of the integrated structure in terms of wind bracing, gravity columns, and floor framing in concert with each other and with the architecture of the building has not come about as a well-defined routine procedure. Each building, of course, is a response to a unique set of circumstances brought about by the real estate market, zoning laws, client priorities, and architects' tastes and fantasies. It is this singularity of tall buildings that has given impetus to the innovations in the art of structural engineering. High interest costs and scarcity of capital are additional factors demanding leaner designs.

1.6 Factors Responsible for Slimming Down the Weight of Structural Frame

Historically, the unit weight of structural framing members in terms of, say, average weight per square foot of floor area appears to be progressively decreasing over the years. For example, a survey of tall steel buildings built over the past 40 years will verify that today it is possible to build a 100-story building with perhaps no more than 30 psf (1437 Pa) of weight as compared to the 42 psf (2011 Pa) used for the Empire State Building in the 1930s. The reasons for this gradual decrease are manyfold, as can be seen by the following list.

1. Innovative design concepts. For medium high-rise buildings in the range of 30 to 40 stories, other factors being equal, the lateral load design methodology, although important, will not make a dramatic impact in the weight of structural framing materials. For taller buildings, the ingenuity of lateral design makes a big difference in the material quantities. Therefore, structural engineers are continually seeking better and more efficient methods of resisting the

lateral loads. Some of the common approaches are: (1) increase the effective width of subsystems to resist the overturning moment; (2) design systems such that the components interact in the most efficient manner; (3) use interior or exterior bracing for the full width of the building; (4) arrange floor framing in such a way that all or most of the gravity loading is directly carried by the primary lateral-load-carrying components; (5) manipulate the dispersion of materials in composite construction consisting of concrete and structural steel in a manner such that both materials are used to their best advantage; (6) minimize the bending induced by wind loads in the primary components; (7) employ truss action to eliminate bending in columns and spandrels; (8) slope exterior columns a slight amount to reduce drift; (9) use rounded plan shapes to reduce the magnitude of wind pressure; (10) arrange closely spaced columns at the exterior to support most or all of the gravity loads and all the lateral loads; (11) suspend floors from a central core such that the total gravity load acting on the core will induce enough holddown forces to counteract the overturning moment; (12) use an interior-braced core that interacts with exterior columns via belt and outrigger trusses; (13) use exterior steel plate curtain walls to resist lateral forces. All these methods essentially strive to obtain a structure that behaves like a cantilever of the ground with a minimum of secondary effects. A building system that utilizes columns located ideally at the perimeter of the building and tied together in such a manner that only axial loads are induced in the columns results in one of the most optimal solutions for lateral bracing.

2. Use of high-strength low-alloy steels. Today it is a common practice to use 50-ksi (345-MPa) steel in most composite floor-framing systems, gravity columns, and not too infrequently in lateral-load-resisting elements.
3. Increased use of welding as compared to bolting, which effects a savings in the range of 8 to 15 percent in the weight of steel.
4. Increased use of composite construction. Steel and concrete are being mixed and matched in various proportions to give the most cost-effective solutions.
5. Application of computers to both the design and the analytical processes. Interactions between two structural elements which were considered minor and neglected previously are being included in routine analysis.
6. Gradual increase in the allowable stresses in the materials based on research and successful past performance.

7. A reduction in the weight of other construction materials. Heavy partition walls have been almost completely replaced by drywall partitions. Exterior masonry has given way to more slick-looking glass curtain walls. Even when the building exterior calls for stone cladding, reduction in weight is being achieved with lighter backup materials. Changes in stone fabrication methods and finishings have made the use of relatively thin $\frac{7}{8}$- to $1\frac{3}{8}$-in (20- to 35-mm) stone sections feasible. Heavy masonry or concrete backup has gradually given way to much lighter systems, such as aluminum mullions that incorporate the stone attachment system with the curtain wall system. The increased use of prefabricated steel trusses is yet another innovation that has reduced the weight of exterior skin of the building.

In concrete construction, major factors responsible for reducing the reinforcement and concrete quantities are:

1. New framing techniques, such as skip joist construction in which every other joist is eliminated, have caught on in high-rise construction with a consequent reduction in the weight of structural frame.
2. Increased use of mechanical couplers in reinforcement for transferring both compression and tensile forces.
3. Use of welded cage for column ties, beam stirrups, etc., which reduces the amount of reinforcement steel.
4. Use of high-strength concrete; 6000 psi (41,370 kPa) is quite common, and strengths up to 10,000 psi (68,950 kPa) are being specified on vertical components of high rises.
5. Use of lightweight aggregate typically reduces 10 to 20 psf (479 to 958 Pa) in the dead load of the structure, resulting in savings of approximately 10 to 15 percent in the reinforcement requirement.
6. Most fire codes do not require as great a thickness of slabs when structural lightweight concrete is used. Typically a thickness of at least $\frac{1}{2}$ in (12.5 mm) of concrete can be taken off from floor slabs without reducing the fire rating.
7. Use of 75-ksi (517-MPa) steel reinforcement.
8. Use of state-of-the-art design methods.

All these factors have contributed to the reduction in the weight of structures. Some of the new glass curtain wall skyscrapers weigh 8 to 9 lb/ft^3 (1.25 to 1.41 kN/m^3) as compared to 15 lb/ft^3 (2.35 kN/m^3) for some buildings built in the 1940s. In addition to the above factors, use

of wind-tunnel tests gives an opportunity for rational design by making possible a reduction in the magnitude of wind pressures.

1.7 Development of High-Rise Architecture

The high-rise architecture of the United States in the twentieth century shows such a wide diversification as to defy distinct classification. Nevertheless, the development of high-rise architecture can be traced, perhaps somewhat imprecisely, in five phases. In the early 1940s before the advent of air conditioning and fluorescent light fixtures, the building form was controlled by the need for natural daylight and ventilation and thus required a form somewhat similar to the layout of contemporary apartments and hotels. The building width had to be limited to ensure that light and air reached all parts of the building. A building width of 55 to 60 ft (16.7 to 18.3 m) that gave office spaces on either side of a double-loaded corridor was common. To achieve more leasable space in a given rectangular or square block, plan forms with a central core and radiating wings were conceived. Still, the plan form did not allow for maximization of the site area. The limited width of the floor plan usually resulted in a relatively closely spaced column layout of 20 to 25 ft (6.1 to 7.6 m). The building usually had heavy masonry cladding that added enormously to the dead load and gave the building a holding down force to counteract the uplift effect of wind loads. Also, light-gauge metal deck and sprayed-on fireproofing had not come about. The required fireproofing was obtained by enclosing the structural steel beams and columns with an envelope of cast-in-place concrete, thereby increasing the stiffness enormously, which in turn limited the wind drift. Instead of realizing the benefits of the composite nature of steel and concrete, early designs penalized the design of steel members by requiring the weight of surrounding concrete to be treated as additional dead load.

The second phase of building configuration is the result of the interactions between the desire to create an increasing amount of rentable area in a given space and the advent of air conditioning and fluorescent lighting. This period is also characteristic of the modern movement in architecture stressing the aesthetic value of simplicity in facade treatment and simple cubic shapes, such as rectangles, squares, circles, and sometimes ovals. The curtain wall was stretched tightly over the skin and the building shot up toward the sky in one regular prismatic shape. In keeping with the International Style, it was not offensive—in fact, it was highly promoted to display the structural muscle. Glass boxes with exposed structural steel or concrete constituted the backbone of the International Style.

The third phase of high-rise architectural development is a result of

interaction between marketing experts and a mild boredom of the architectural community toward the repetitive nature of the boxes on the cityscapes. The simplest prismatic shape has only four corners, and therefore could offer at best four corner offices. Even those corner offices more than likely displayed corner columns positioned in the most logical location. From the point of view of leasing there was no great advantage in having many corner offices with views on two sides. Now, however, corner offices have become the most sought after lease space almost overnight, and the demand appears to be on the increase. In an overbuilt high-rise market, it is a well-proven fact that corner offices providing unobstructed views bring in more rental dollars or facilitate earlier leasing of space than a single-view office. Whether or not the views one sees from these offices have improved over the period is debatable; at least in the urban setting it is more than likely that one has nothing to look at but the curtain wall of another high-rise building. Thanks to the marketing experts, irrespective of the quality of view, it appears that corner offices are still perceived as the most desirable lease space by corporations and small renters alike. To capture this market, the trend in high-rise floor planning is to have as many corner offices as possible. This is achieved by undulating the exterior and providing nicks, notches, and other contortions at the perimeter of the building. Sometimes to create visual identity and interest, setbacks are provided at intermediate levels. Sometimes an otherwise simple plan shape is sliced and diced again, creating vertical lines to emphasize the verticality of the building and simultaneously providing for additional corner offices.

A fourth phase of office design known as postmodern architecture is currently sweeping through the profession, bringing in daringly articulated buildings. These buildings not only have stepbacks, angles, notches, and curves, but the resulting articulations are so severe as to preclude the use of any one type of structural system. This phase of office design, which began around 1970, is considered primarily an aesthetic reaction to the cubism period. This reaction has evolved gradually in three stages. First, the flat roof, which is all that is necessary from the functional point of view of the fifties and sixties, started receiving architectural attention to gain identity in the city skyline. Today, many buildings' tops are either a peaked roof, a pyramid, a dome, or any combination of these. Figure 1.3 shows an example of a medium high-rise building sporting a peaked roof and a mast. The second stage is characterized by the creation of elaborate entrances to the building in an effort to give it a street-level identity. The third stage is a continuation in the battle for identity. Articulations at the extremities are no longer sufficient to create a building's identity. The whole architectural facade needs to proclaim the identity

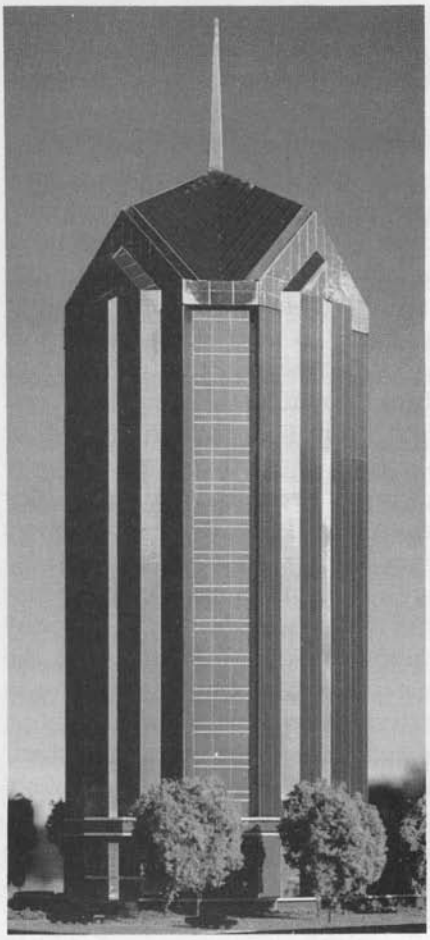

Figure 1.3. Example of transitional postmodern high-rise architecture, The University Tower, Durham, N.C. (Architects, Pickle and Thomas, Inc., structural engineers, Ellisor & Tanner, Inc., Dallas, Texas)

of the building. To this end, terracing of building plans, cutouts, slicing and dicing, and overhanging features are added to the building throughout its height.

The fifth phase can be looked upon as a modification of the current building shapes in the energy conservation context. We are witnessing buildings suitable for natural daytime lighting with courtyards, light wells, and skylights. Energy conservation efforts have brought about an understanding of spaces as a whole, especially in relation to how light influences the space. Instead of depending totally on mechanical heating and cooling and electric light, architects are considering the possible solar controls outside and in as an integral part of both engineering and architectural design. The architect is considering

lighting design not from an electrical engineering standpoint but from the various light sources outside the building.

It is of interest to trace the development of structural systems corresponding to the previously mentioned architectural trends. As mentioned earlier, ancient monuments such as the pyramids required very little attention in terms of lateral load resistance, nor did the early 10-story high rises of the 1870s. The high rises prior to the advent of air conditioning and fluorescent lights were of limited width and could accommodate interior columns at a relatively close spacing of 20 to 25 ft. Deep girders were moment-connected across the columns to create a rigid frame for providing lateral stiffness and stability. Often the rigid frame action was supplemented by using cross braces around utility cores. In addition to this bracing, the heavy masonry partitions and exterior cladding used in these buildings added a form of passive resistance to the stability of the building. Because rigid frame action and bracing across limited width of core are somewhat inefficient for tall buildings, the amount of material used in these buildings was relatively high; for example, the Empire State Building used 42 psf of structural steel (2011 Pa) in the gross area of the building as compared to the 33 psf (1580 Pa) in the Sears Tower.

The International Style of architecture, which started with the second phase of high rises, disrobed the building of its heavy partitions and cladding. Also, leasing requirements demanded column-free space between the central core and exterior columns. Even when the building exterior is clad in stone, relatively lightweight backup systems using stones which are only $\frac{7}{8}$ to $1\frac{3}{8}$ in (20 to 35 mm) thick are commonly employed. Thus the built-in heavy gravity loads which could be counted on in the design of the first phase of high rises are no longer available to perform the holding down function. The combination of long-span moment frames and bracing systems, when placed within the confines of the service core, are therefore no longer economical for modern tall buildings. A natural structural response to the economic requirement was to move the bracing from the interior to the exterior of the building, thereby obtaining maximum separation between the windward and leeward columns. To make the separation structurally meaningful, i.e., to make the windward and leeward columns work not as two separate rows of columns but as integral parts of a tube, it was necessary to introduce a shear-resisting element between the columns. This was achieved either by providing diagonal bracing between the exterior columns or by a system of closely spaced columns and deep spandrels along the building periphery. Thus a new system termed a *tube structure* was introduced into the structural vocabulary. The tube structure immediately freed up the economical height restrictions of moment frames and interior bracing systems. Note the simplicity of

the system, which was first introduced by the late Dr. Fazlur Khan of the architectural and engineering firm of Skidmore, Owings, and Merrill; it did not require invention of new materials nor did it require new framing or erection techniques. It employed the very basic elements of high-rise structures, namely beams and columns, and by strategically deploying their locations a very economical structural system had been found almost overnight. Also, the system did not require new methods of analysis other than encouraging the engineer to think in three dimensions. The emergence of the tube as the most logical form for high-rise structures is reflected by the innumerable examples of such buildings built in almost every growing metropolis in the world. The tube structure was suited admirably to the International Style. Buildings were prismatic with compact plan forms, and therefore did not penalize the efficiency of the framed tubes.

The radical departure from the pure prismatic shapes occurred over a period of time. First, the building top, which was invariably flat in keeping with the "less is more" norm, began to take on new forms, giving identity to the building in an otherwise anonymous cityscape. Perhaps the best example of this is the headquarters building of the Transamerica Corporation in San Francisco. Here the architect used the sloped-column approach to create a 48-story American version of the pyramid.

The third phase of high-rise architectural development with its many corner offices did not entirely preclude the use of a tube system because the basic prismatic shape of the building was still being preserved for almost the entire height of the building. The seemingly restrictive form of the tube, which was confined to square and rectangular shapes, very quickly found application in nonprismatic shapes. The tube was so benign to engineers that they could even rupture it without paying a significant penalty in structure, as long as the discontinuity was filled in with another structural element.

Then came the period where elaborate entrances and tops to the buildings were created to identify the building at the base and on the skyline. None of these changes, namely seductive tops to the buildings, the undulations of the exterior, or the appendages to the building entrance, precluded the deployment of the structural logic so brilliantly conceived by Fazlur Khan. The tube system, either with its rhythmic columns connected by a pattern of deep exterior spandrels or as an exterior braced tube with its bold diagonals on the building face, could still be used for buildings of this period. Whether the diagonals were expressed on the building face as in the John Hancock Tower in Chicago, or were hidden behind a smooth glass wall as in the Citicorp Building in Manhattan, was, or course, a matter of how strongly the

architect felt about preserving the International Style; the structural logic was still the same.

The current state of high-rise architecture is characterized by the use of articulated sculptured forms. Owners and developers are demanding, and the public has come to expect, these daring shapes. Buildings are designed not to express the pure form of the structural elements but to express the technological progress by creating facades that appear to be structural feats. The goal is the expression of the architectural envelope, not the structure. Today's bracing design required to limit the sway or wind drift of the building calls for ingenuity not in terms of visualizing a single pure structural system but in combining several systems to make the dramatic design concepts of the architect an economic reality. The work of the structural engineer comes in refinements to proven structural schemes with particular attention to details.

Logical structural solutions which could be used in the earlier versions are no longer sufficient to take into account the structural discontinuities. In fact, there no longer is one system applicable for the whole height of a building. In keeping up with the architectural slicing and dicing, the engineer has to follow suit. The engineer has to cut a brace here, introduce a partial tube there, and so on. In other words, the engineer goes around the building facade and height introducing whatever structural element possible behind the facade without undue regard to the one next to, above, or below it. The job is to find spaces for the structural system behind the building facade and to interconnect different elements to obtain overall continuity. For example, the building shape may permit the use of perimeter bracing for the bottom 10 floors, the next 10 floors could accommodate a framed-tube solution, and so on.

In spite of the cacophony of forms currently accepted as different architectural styles, large, many-sided prismatic shapes with hints of flamboyance are still dominating the architectural vocabulary because they have the backing of large corporations seeking prestigious symbols. As mentioned earlier, the tube is still the workhorse structural system of these buildings, as demonstrated by the number being constructed. With these practical displays of the tube characteristics, is it not conceivable that this is the most logical solution for all high rises? Should not the proven economy of this system put an end forever to the search by engineers for a suitable system on each project? The questions are perhaps deceptively simple. To be sure, the tube system is very economical, but even with its adaptability, it requires a certain amount of structural discipline that restricts the use of free-form architecture. The current flamboyance in architecture has necessitated

that several schemes be studied and comparatively priced before the adoption of a final scheme. The reasons for this are several.

First, every building is a unique response to a particular set of conflicting demands. For example, architecturally it may be desirable to have a sculptured profile without structural intrusions. This may have to be compromised by the structural desire to provide bracing at the perimeter. The size of vision panels may have to be curtailed by the structural requirement of deep spandrels. Interior beams and girders working efficiently for gravity loads may require expensive penetrations for passages or air conditioning ducts or may require an increase in the floor-to-floor height. Suboptimizing of the structure without due regard to the opposing demands of other disciplines may eventually result in an increase in the total cost of the building. Therefore, less efficient structural systems often need to be studied in the interest of bringing in the total project cost within the allotted budget.

1.8 Structural Concepts

In structural engineering practice, one of the foremost requirements is for the architect and the engineer to participate in the conceptional stages of the project in order to come up with an economical building. Although there is a general awareness in the architectural community about the concept of premium for height, there is insufficient understanding of the structural engineering discipline that is so integral a part of architecture, mainly because the necessary engineering information is not accessible in a concise form. It is necessary for the architect to get involved in the structural field because structural cost accounts for 20 to 30 percent of a building and, therefore, will have profound influences on the design, the aesthetics, and the manipulation of all resources to make the most beautiful project. Even in today's postmodern architectural environment with its hint of antitechnology there is a need for the architect to assume the traditional role as master builder—not in the sense that architects should learn how to design and analyze structural elements, but they should know how these elements will affect the general flow of natural forces in the building frame. Although it is impossible and indeed unnecessary to know all the aspects of structural analysis, the architect should be able to grasp the idea of "pounds per square foot" of the structure just as he or she would know the watts per square foot on the electrical system or the Btus per square foot as related to the energy efficiency of the building.

It is both interesting and necessary for architects and engineers to explore the idea of different structural systems and their related impact on the economy and the architecture of high-rise structures. To

this end, a critical appraisal of structural systems of a high-rise building as related to the architecture is presented in this section. In particular, the study will focus on certain aspects of exterior tube columns such as their size, location, number, and effect on the interior layout of the offices. This study is partly based on the work done by the author as a principal with the firm of Walter P. Moore and Associates. The building to be discussed was scheduled for construction in Houston during the year 1982–1983. The study was undertaken because a review of a typical floor plan of the project from marketing, leasing, and space planning viewpoints raised concerns about the size and location of columns. The leasing market was very soft, requiring all prudent concerns to be addressed before committing the finances to the project.

The main purpose of this section is to give an overview of the many possible structural solutions that are normally considered in the development of a high-rise project. Details of structural analyses are not given in this section, and only passing remarks are made about the behavior of each structural system since these will be described in greater detail throughout the remainder of this work.

1.8.1 Structural scheme options

A schematic elevation of the proposed 62-story building and plan of the typical floor are shown in Figs. 1.4 and 1.5. The building has 1.7 million square feet (157,935 m^2) of office space, with 62 floors extending above a landscaped plaza and a two-level basement below an entire city block. The building is fairly narrow, with a height-to-width ratio of approximately 6:1. The floor plan is noncompact, with a length-to-width ratio of approximately 2:1. Relatively stiffer elements are required parallel to the short face to resist wind on the long faces. This may be achieved by selecting a framed tube solution with columns at approximately 10-ft (3.0-m) centers along the short faces and 15 ft (4.58 m) along the long faces. A deep spandrel connecting the perimeter columns completes the framed tube system. The building may be conceived in steel, concrete, or a combination of the two, known as a composite system, utilizing the advantages of both concrete and structural steel: concrete for stiffness and steel for speed of construction. One of the methods of composite construction popular in certain parts of North America uses small, wide flange shapes as exterior erection columns with a planned initial growth of 10 to 12 floors, which are subsequently enclosed in reinforced concrete. The exterior spandrels consist of rolled wide flange beam shapes. The composite tube system was chosen as the most economical based on comparative studies done on similar projects that were under construction at the time the project was being designed.

The structural schemes presented in this section for this project may

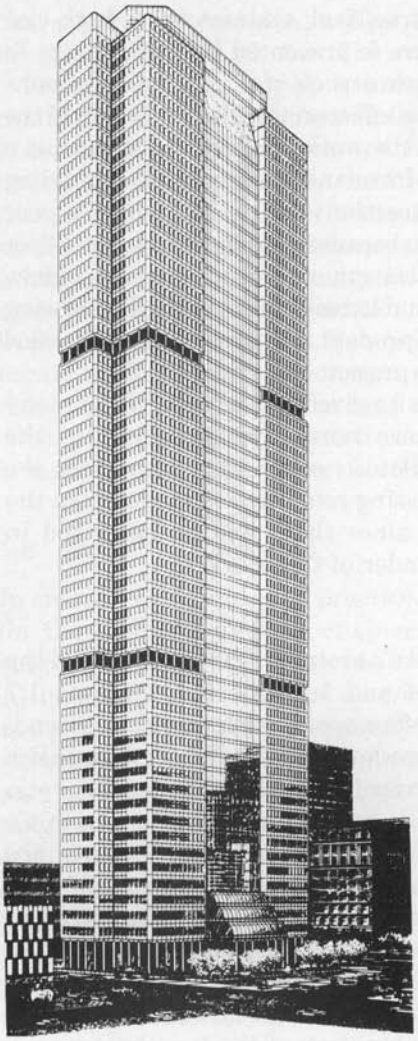

Figure 1.4. Model photograph of a 62-story high-rise project. (Architects, Hellmuth, Obata, Kassabaum, Dallas, Texas; structural engineers: Walter P. Moore and Associates, Houston, Texas)

be broadly classified into three categories. The first consists of cross-bracing schemes, the second, of framed tubes with deep spandrels and closely spaced columns, and the third consists of an assortment of schemes ranging from those utilizing shear wall frame interaction to a 14-column scheme interconnected with Virendeel trusses spanning the full width of the building. A brief description of each scheme is given in the following.

1. Cross-bracing systems
   a. Exterior braced tube. An all-steel scheme which consists of a series of eight-story-high exterior X braces is utilized to wrap

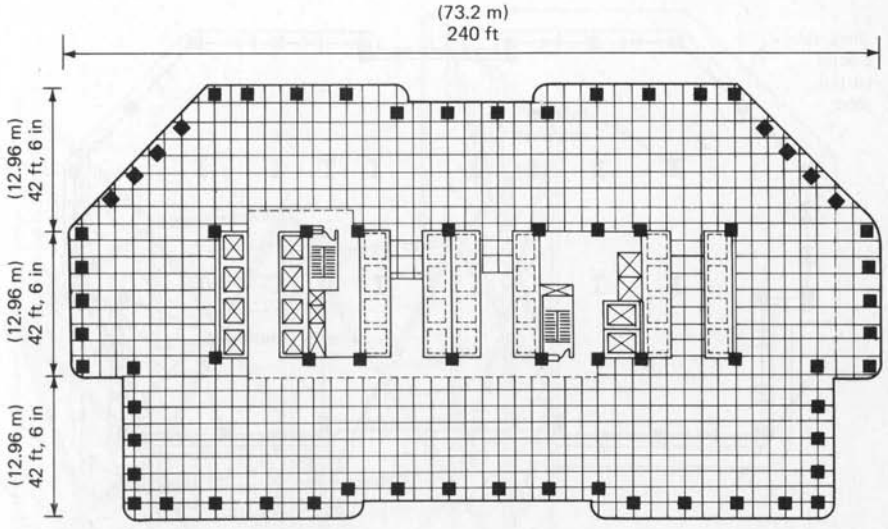

Figure 1.5. Typical floor plan.

around the two short faces and a significant portion of the flange faces as shown in Figs. 1.6 and 1.7. It was not necessary to encompass the whole building with the X braces; the center portion of the two broad faces could be kept free of vision-impairing columns and braces. These column-free areas would provide for dramatic views, thus enhancing the leasability of the building. Note that the exterior bracing follows the contour of the exterior face of the building. Its efficiency is unimpaired by its in-and-out modulations. As compared to the orthogonal bracing of a rectangular building, the skew bracing has some fabrication premium, but otherwise the structural efficiencies are identical.

An alternative to the X-bracing scheme which uses a four-story-high K brace is shown in Fig. 1.8. Note that moment-connected spandrels are utilized on one face (two for the whole building) to maintain the tube action across this face. As in the previous scheme, no columns or braces were anticipated behind all glass faces.

b. Interior braced tube. From the structural bracing point of view, the plan layout is as though the building is of a rectangular shape. Note that the bracings across the building width penetrate the interior space, creating somewhat of a restriction on the leasability of space, as shown in Figs. 1.9 and 1.10. This is equivalent to having a sloping interior column at each floor. As a trade-off, the two short faces

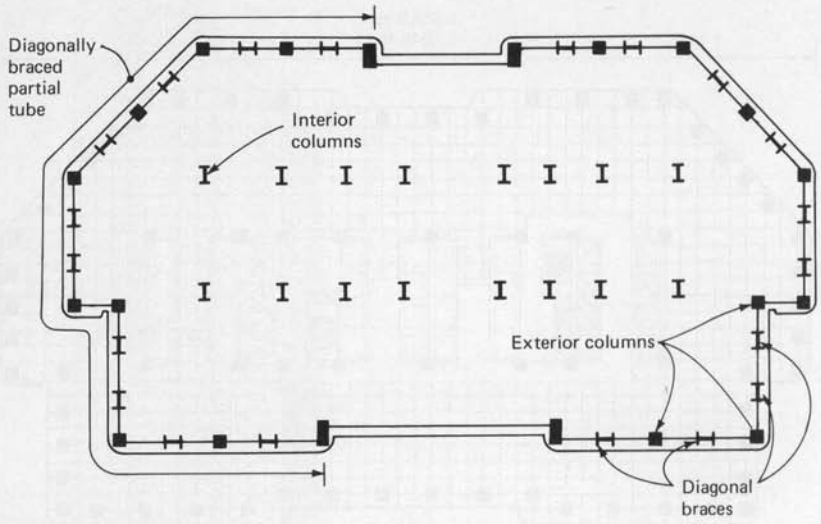

Figure 1.6. Exterior braced tube system: plan.

containing premium lease space (corner offices) are unobstructed by braces or closely spaced columns.

c. Braced and framed tube combination. The proposed scheme is evident from Figs. 1.11 and 1.12. A framed tube attached to a cross bracing at the extremities provides the required structural action.

2. Framed tube systems

a. Framed tube with 10- and 15-ft (3- and 4.58-m) column spacings. The exterior columns are spaced at approximately 10-ft (3-m) centers on the short faces and are opened up to 15-ft (4.58-m) centers on the long faces as shown in Fig. 1.13. This type of spacing is ideally suited for noncompact plan forms and has found applications in many tall buildings. This is the base scheme under which the working drawings were completed for this building. In scheme 4, 40 by 38 in (1016 by 965 mm) composite columns are used on the exterior.

Scheme 5 is identical to scheme 4 with the exception that smaller composite columns 40 by 27 in (1016 by 686 mm) are used in an effort to provide more flexibility in the office layout adjacent to the windows. An all-steel scheme which would give the smallest size of columns 36 by 20 in (914 by 508 mm) is used in scheme 6. Note the actual size of finished steel column with the required fireproofing and gypboard finishing tends to approach the size of composite columns.

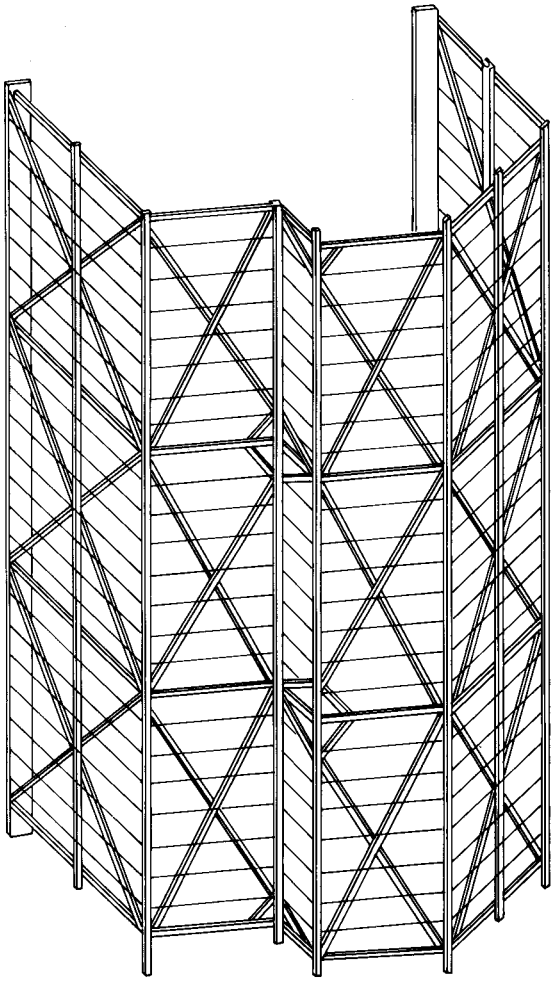

Figure 1.7. Isometric view of exterior braced tube.

b. Framed tube with 10-ft (3-m) column spacing. A 10-ft (3-m) spacing for exterior columns all around the perimeter of the building is used as shown in Fig. 1.14. Although many buildings have been built using 10-ft (3-m) and in some cases even smaller spacings, of late this type of spacing has fallen out of favor; some owners and architects consider the spacing to be too close. In scheme 8, 48 by 27 in (1220 by 686 mm) composite columns are used, while 36 by 20 in (914 by 508 mm) wide flange-shaped steel columns are used in scheme 7.

c. Twin tubes with 10-ft (3.0-m) column spacing. The efficiency of a framed tube is to a great extent dependent on the so-called

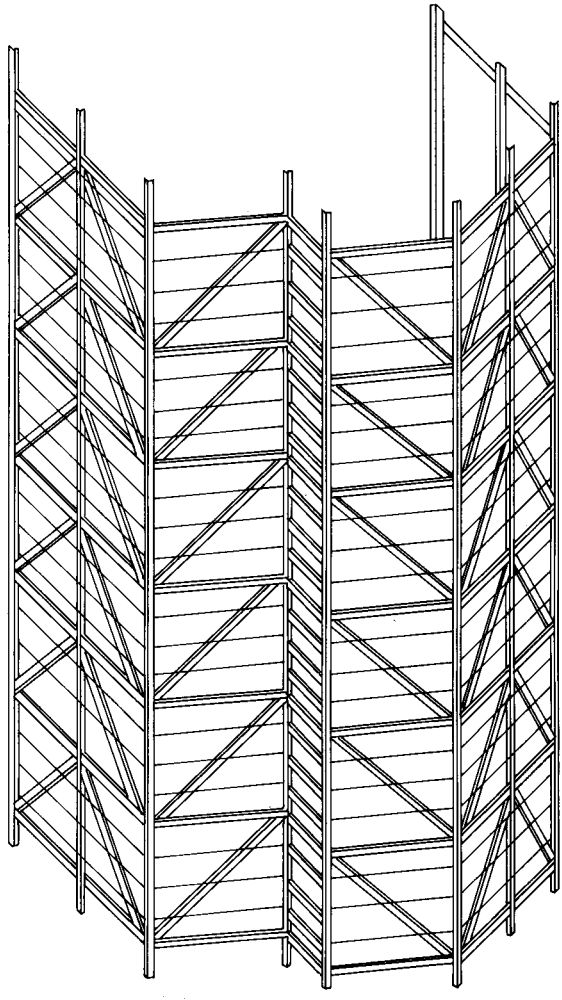

Figure 1.8. Isometric view of alternately braced tube.

shear lag phenomenon. When the plan shape of the building is oblong, it so happens that for wind loads on the long faces, the flange columns do not fully participate in resisting the lateral loads. Because of the large distance that exists between the web frames, the columns at the center of the broad faces are virtually unstressed. A technique that minimizes this problem employs a minimum number of interior columns in the lease space (two in this building), creating a rigid frame across the middle of the building floor plan. The oblong tube is, therefore, made structurally more efficient by making it work as though it is a bundled

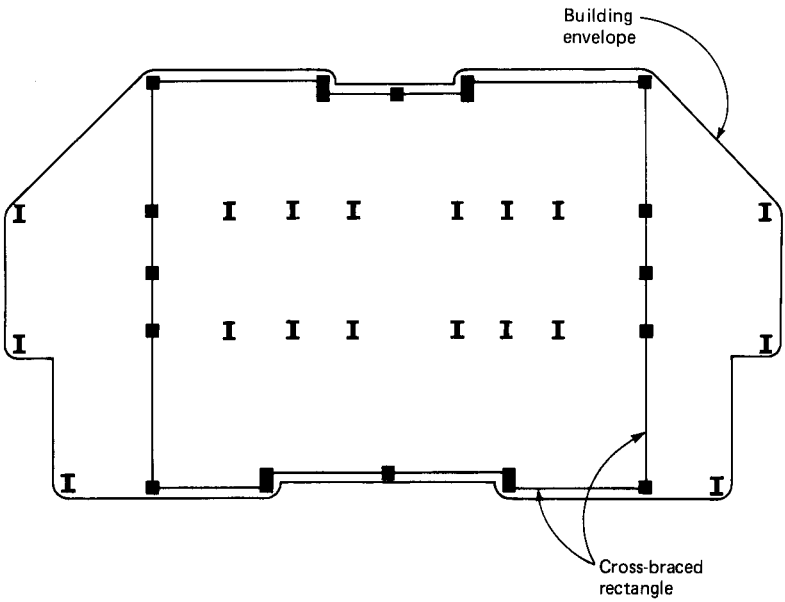

Figure 1.9. Interior cross bracing system: plan.

tube, as shown in Fig. 1.15. Of course, as noted earlier, to achieve this structural efficiency, interior layout has to be compromised because of the interior columns. Scheme 9 was engineered with an all-steel structure, while scheme 10 used composite columns. The typical exterior column sizes were respectively 33 by 20 in (838 by 508 mm) and 45 by 27 in (1143 by 686 mm).

d. Framed tube with 15-ft (4.58-m) column spacing. The exterior columns are spaced approximately 15 ft (4.50 m) on center all around the building perimeter as shown in Fig. 1.16. The size of typical exterior columns for steel and composite schemes (schemes 11 and 12) were, respectively, 40 by 22 in (1016 by 559 mm) and 48 by 36 in (1219 by 914 mm).

e. Twin tubes with 15-ft (4.58-m) column spacing. The structural concept is similar to schemes 9 and 10 with the exception that columns are spaced on approximately 15-ft (4.58-m) centers around the perimeter, as shown in Fig. 1.17. The size of typical exterior column for steel and composite schemes (schemes 13 and 14) were, respectively, 36 by 20 in (914 by 508 mm) and 40 by 36 in (1016 by 914 mm).

f. Framed tube with 20-ft (6.1-m) column spacing. The structural analysis for this column spacing, which is shown in Fig. 1.18, confirms the intuitive observation that the column spac-

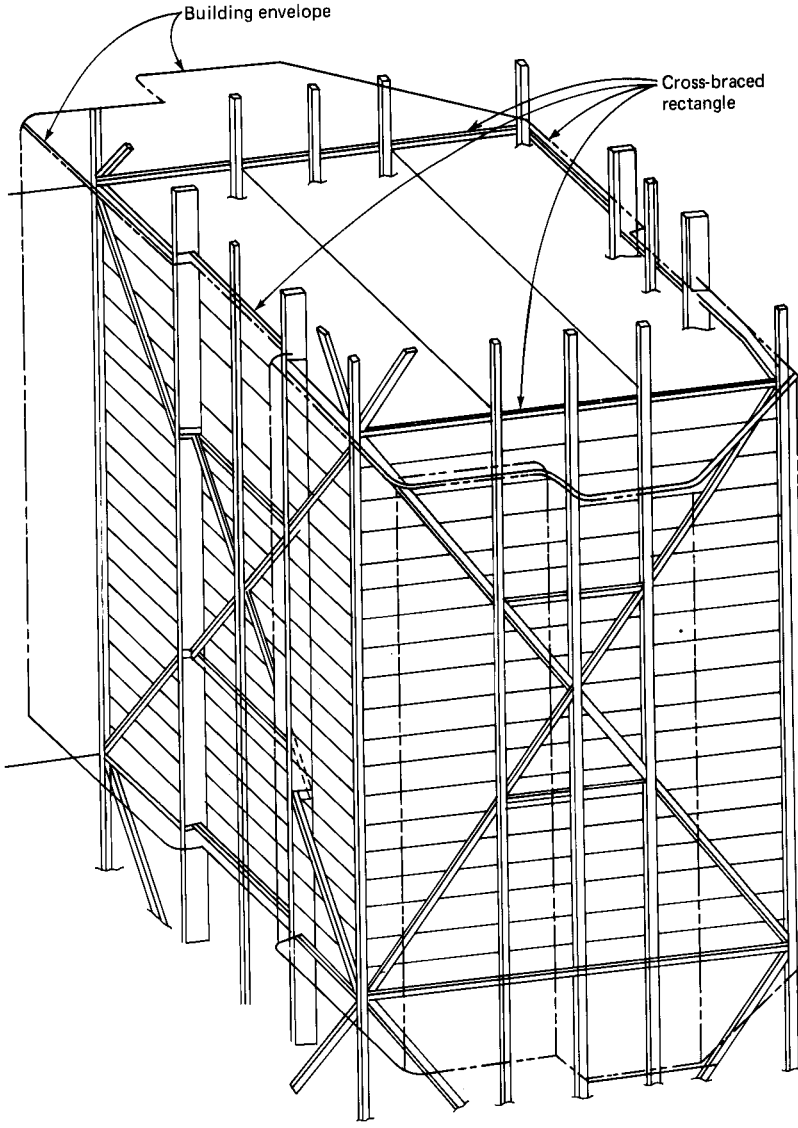

Figure 1.10. Isometric view of interior cross bracing system.

ing is too large to make this scheme economically feasible. Built-up steel spandrels of the order of 40 in (1016 mm) in depth are required at the perimeter to limit the sway at the top floors. The exterior column sizes for steel and composite schemes (schemes 13 and 14) were, respectively, 45 by 24 in (1143 by 610 mm) and 60 by 36 in (1524 by 914 mm).

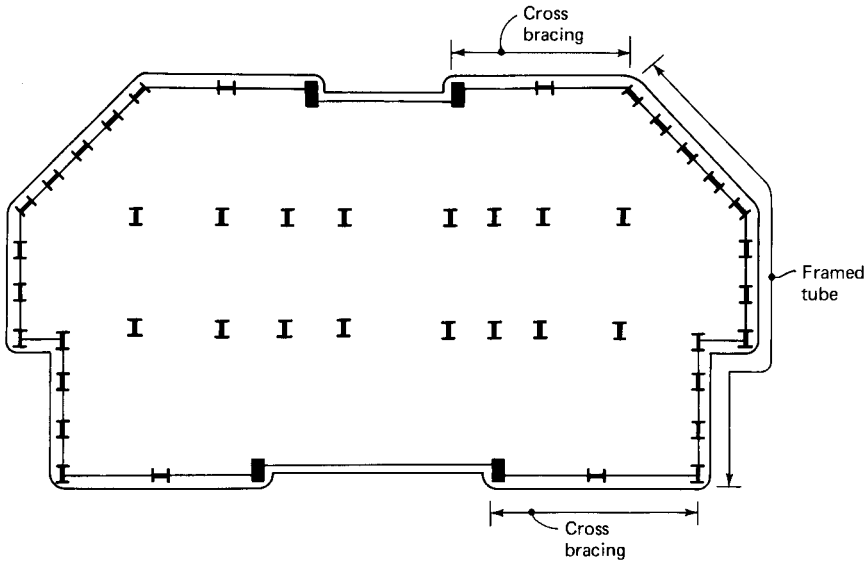

Figure 1.11. Braced and framed tube system: plan.

g. Twin tubes with 20-ft (6.1 m) column spacing. The column layout is as shown in Fig. 1.19. The shear lag phenomenon predominant in the single tube solution improves considerably because of bundling of the tubes and results in somewhat smaller perimeter column sizes. For the steel scheme (scheme 17), the required size is 42 by 24 in (1067 by 610 mm), while for the composite scheme (scheme 18) the column size works out to be 57 by 32 in (1448 by 813 mm).

3. Nontubular schemes
   a. Shear wall frame interaction. Closely spaced columns and deep spandrels on the short faces constitute efficient moment frames, as shown in Fig. 1.20. These acting together with shear walls which drop off at various heights provide for the lateral load resistance. Scheme 19, which uses steel columns for moment frames, requires 36 by 20 in (914 by 508 mm) columns on the short faces, while for scheme 20 the corresponding composite column size is 40 by 27 in (1016 by 686 mm). Both schemes require 20 by 17 in (508 by 432 mm) columns on the long faces.
   b. Moment frames and core braces. A steel scheme that employs core bracing and moment-connected frames at each column line along the width of the building was analytically tested as a possible solution, although it was intuitively clear that this would not work. However, the efficiency was im-

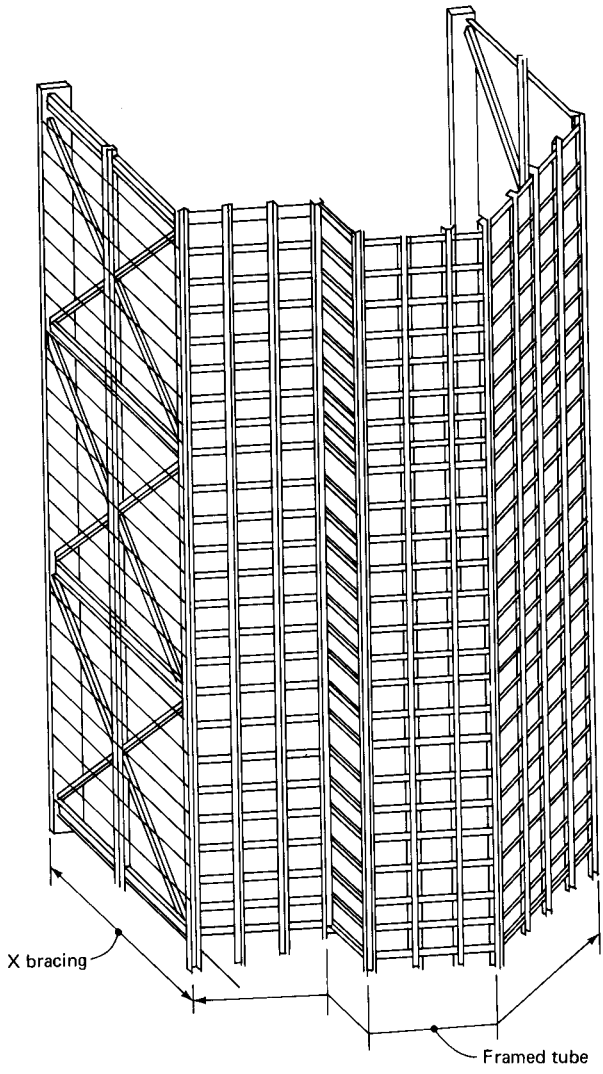

Figure 1.12. Isometric view of braced and framed tube system.

proved in this scheme by providing interior columns as shear links at every other floor as shown in Fig. 1.21. Although the interior columns are not continuous, they provide considerable resistance to the bending deformation of the girders by effectively reducing their span by half. The presence of interior columns at every other floor may be objectionable from leasing considerations but is included in the study for comparative purposes.

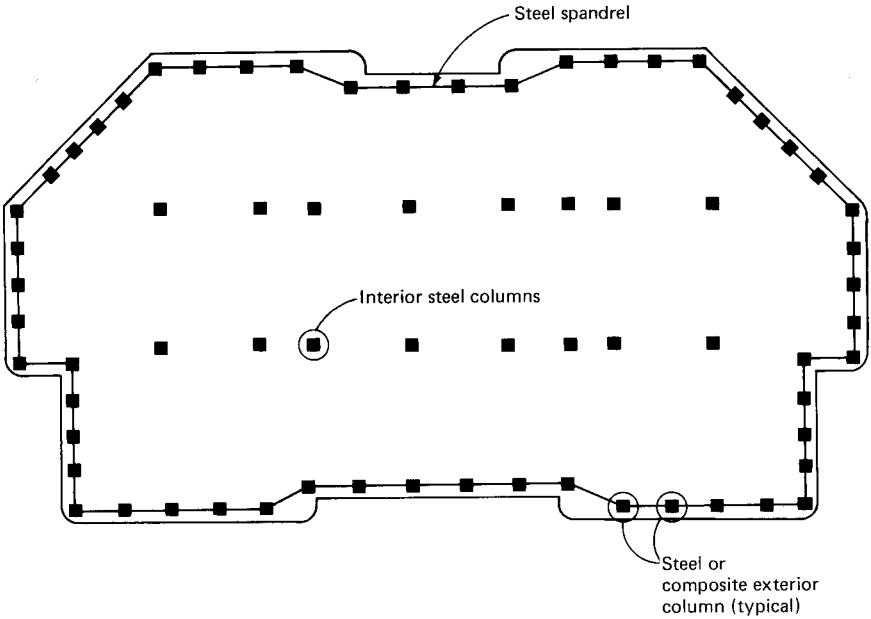

Figure 1.13. Framed tube with 10- and 15-ft (3- and 4.57-m) column spacing.

c. Outrigger and belt trusses. The idea of providing belt and outrigger trusses at various heights to engage the perimeter columns to participate in the lateral load resistance has been known for some time and been used on several notable buildings. The stiffening effect of outrigger and belt trusses is akin to a moment-resistant spring which tends to induce a reversal of curvature in the cantilever bending of the braced core. Using certain simplified assumptions, it can be shown that these trusses can be located at various floor levels without unduly decreasing their efficiency. Based on this premise and combined with the desired architectural elevation for the building, an analysis was made by placing the trusses at levels 20 and 40. The structural schematic plan is shown in Fig. 1.22. Although the structural efficiency is increased by the addition of these trusses, note that interior planning is disrupted at two levels. In buildings which cannot make use of these floors as mechanical floors usually there is a strong objection to running the outrigger trusses around the building. On this project, levels 20 and 40 were dedicated as premium lease spaces with an extra high floor-to-floor height; clearly the outrigger and belt trusses were architecturally unacceptable but were included in the structural study for comparative purposes.

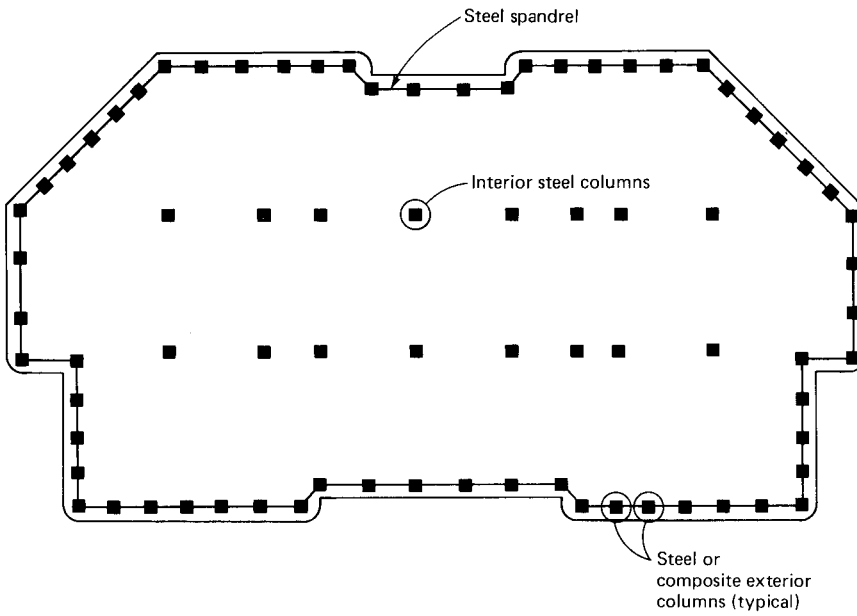

Figure 1.14. Framed tube with 10-ft (3-m) column spacing.

d. Jumbo column scheme. This scheme, which is shown in Fig. 1.23, was investigated at a conceptual level only and was based on the idea that an efficient structural solution is obtained by transferring all the gravity loads to wind-resisting columns. The columns, as in framed and braced tubes, work most efficiently when placed at maximum distance apart and connected by a shear-resisting element so that they work as compression and tension members of a truss whose depth is equal to the building width. For this building, vierendeel and/or interior diagonal trusses spanning the full width of the building were envisaged as the shear-resisting elements. A majority of the gravity loads are channeled to the 14 jumbo columns. Four relatively small columns are introduced at the building perimeter to simplify gravity framing and to eliminate long cantilevers.

1.8.2 Space efficiency of high-rise building columns

A high-rise building structure essentially consists of vertical elements such as columns, walls, and braces and horizontal planes that are the floor structure. The depth of the floor structure, although quite important from the overall economic considerations, does not pose

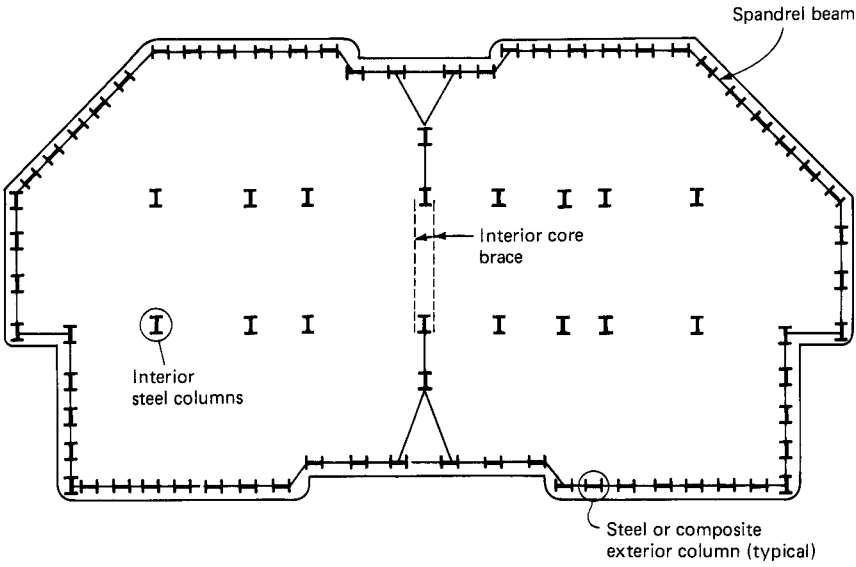

Figure 1.15. Twin tube system with 10-ft (3-m) column spacing.

undue limitations on the architectural space planning. After the initial discussion of the project during which ceiling and floor-to-floor heights, required cavity for air conditioning ducts, lights, and sprinkler system are discussed, the beam and girder depths hardly evoke the emotional discussion that pursues the determination of location

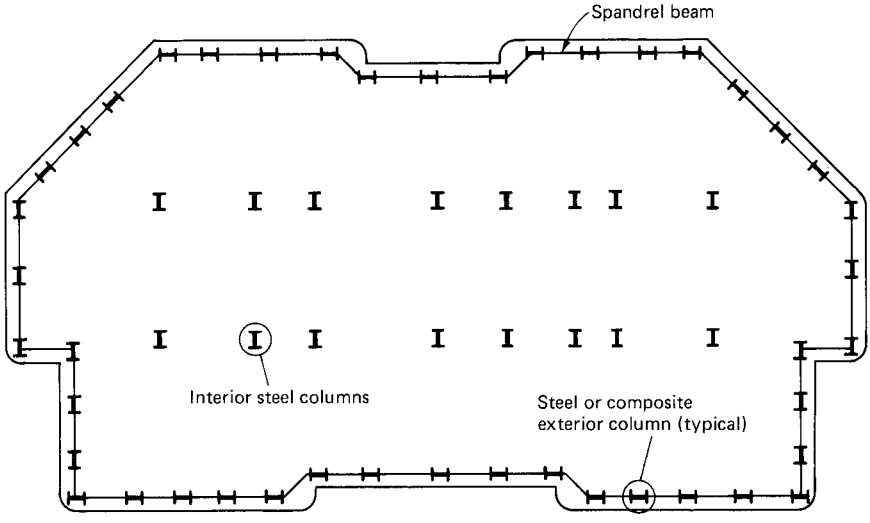

Figure 1.16. Framed tube with 15-ft (4.57-m) column spacing.

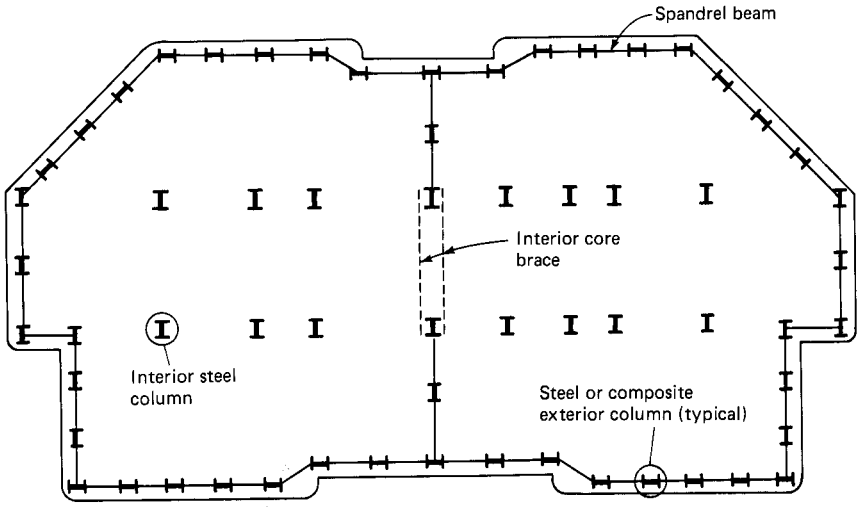

Figure 1.17. Twin tube system with 15-ft (4.57-m) column spacing.

and size of vertical elements. The size of floor beams becomes almost inconsequential because it literally hides in the ceiling cavity and escapes the scrutiny of any number of consultants, architects, interior space planners, marketing experts, lease space consultants, and, of course, the developer who is looking for maximization of rentable space. While it is possible that seemingly alike columns of two buildings may have somewhat different sizes, it appears that from an

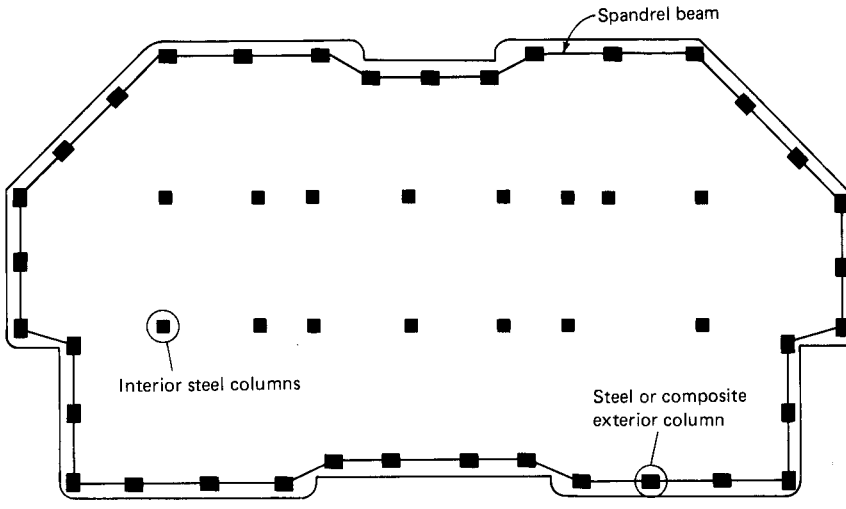

Figure 1.18. Framed tube with 20-ft (6.1-m) column spacing.

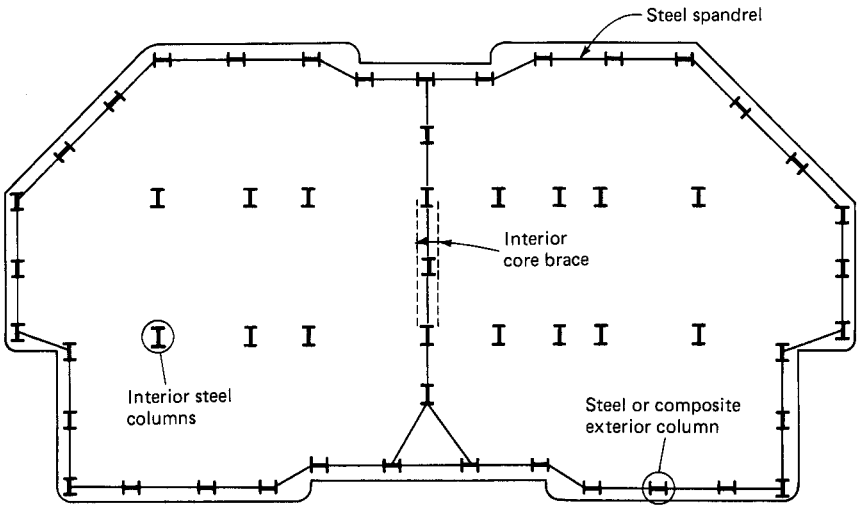

Figure 1.19. Twin tube system with 20-ft (6.1-m) column spacing.

overall perspective, in comparison to floor area, the area taken up by vertical structural elements does not differ significantly from one scheme to another and for that matter from one high rise to another. Irrespective of the location of building, material used for the building, and the system employed for the building, the finished size of vertical elements appears to vary within a very narrow band, say to within 1 percent of the gross ground floor area. It is of interest to explore this rather interesting phenomenon historically as it relates to modern high rises.

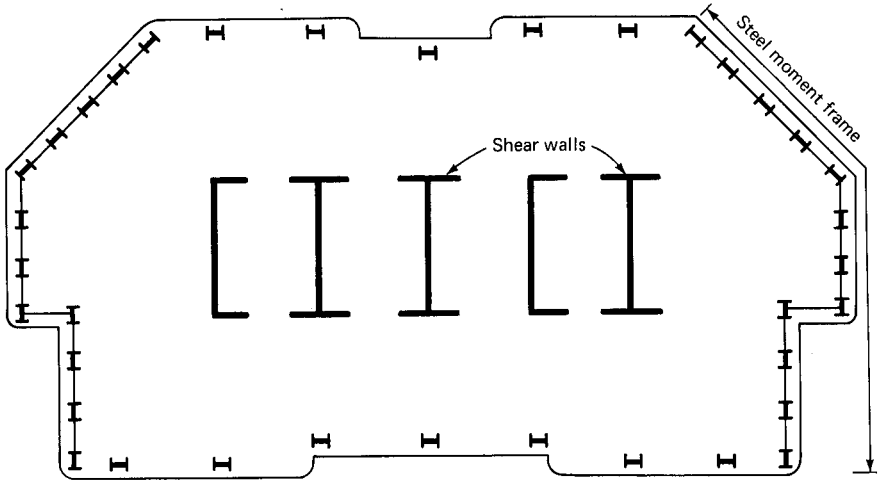

Figure 1.20. Shear wall frame interacting system.

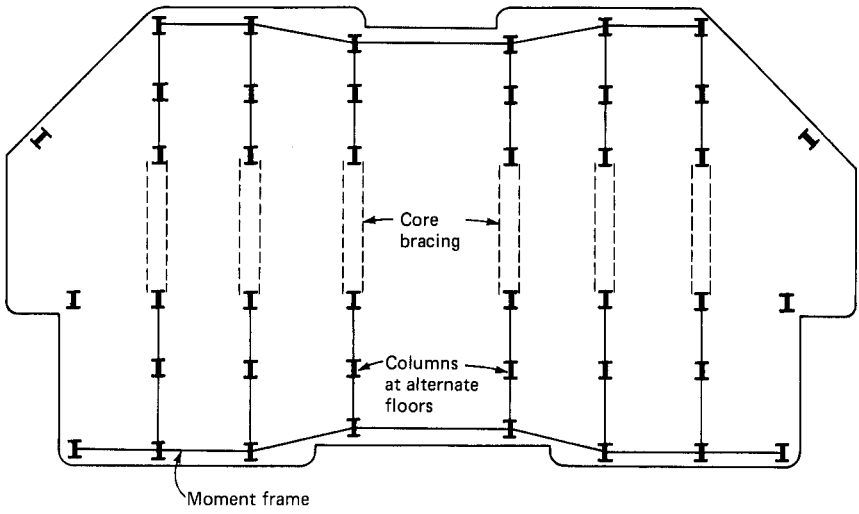

Figure 1.21. Moment frame and braced core system.

The size and density of structural elements in a modern tall building are strikingly less than in the buildings of former centuries. Real estate market considerations and aesthetic principles have motivated us to continuously push this trend to further limits. It is interesting to study in a contemporary high-rise building the structural plan density

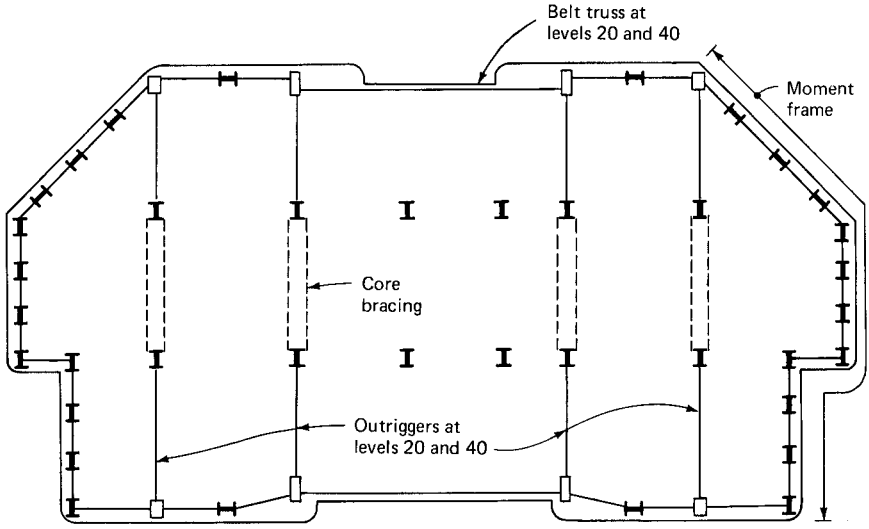

Figure 1.22. Outrigger and belt truss system: schematic plan.

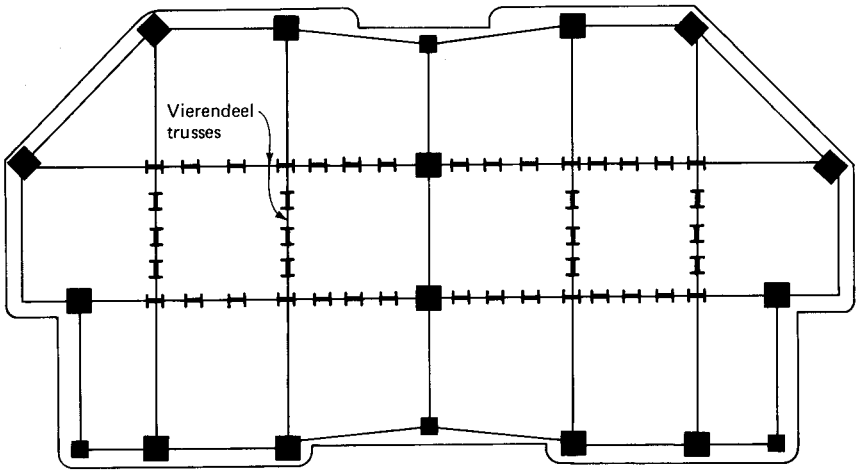

Figure 1.23. Jumbo column scheme.

index, which is defined as the total area of all vertical structural elements divided by the gross floor area of the footprint of the building at the ground level. Historically, this ratio is decreasing. Monumental structures such as the pyramids of Egypt and more recently the Washington Monument did not require usable spaces within and, therefore, the structural plan density index is close to 100 for these structures. This ratio is reduced to 50 for the Taj Mahal in India and 25 for St. Peter's in Rome. The 17-story, 210-ft (64-m) Monadnock Building constructed in Chicago in 1891 sports 7-ft (2.13-m) thick masonry walls at the ground floor, taking up as much as 15 percent of the floor area at ground level. Contemporary high rises, because of their lightweight construction, improved high-strength materials, and innovative structural techniques require a rather modest 2 to 3 percent of the gross area of the ground floor; the higher percentage is most often found in buildings using shear walls as a basic structural element. The Sears Tower in Chicago is supported by 112 major steel built-up columns varying in size from 39 by 39 in to 39 by 24 in (990 by 990 mm to 990 by 610 mm) at the ground floor, taking up no more than 2 percent of the ground floor area.

With the above buildings as a guide, it is interesting to compare the plan density indexes for the various structural schemes for the project referenced earlier. The comparison is shown in Table 1.1. It is assumed in this study that structural steel columns are finished to rectangular shapes with an allowance of $2\frac{1}{2}$ (64 mm) for fireproofing and drywall construction at each face.

TABLE 1.1 Structural Cost and Column Density Comparison

Scheme no.	Column spacing, ft	Exterior column type	Relative structural cost	Plan density index
		Framed Single Tubes		
4	10 & 15	Composite	1.00	2.5
5	10 & 15	Composite	1.06	1.95
6	10 & 15	Structural steel	1.10	1.87
7	10	Composite	0.97	2.13
8	10	Structural steel	1.09	2.57
11	15	Structural steel	1.18	1.83
12	15	Composite	1.04	2.39
15	20	Structural steel	1.30	1.76
16	20	Composite	1.09	2.38
		Twin Tubes		
9	10	Structural steel	1.01	2.07
10	10	Composite	0.96	2.50
13	15	Structural steel	1.12	1.68
14	15	Composite	1.01	2.14
17	20	Structural steel	1.26	1.73
18	20	Composite	1.07	2.15
		Nontubular Schemes		
19	Shear walls and steel frame		1.15	2.66
20	Shear walls and composite frame		1.10	2.66
21	Shear links		1.32	1.28
22	Outrigger and belt trusses		1.20	1.36
23	14 jumbo columns		1.24	2.15

1.8.3 Structural cost and column space efficiency comparison

All in all, including slight variations of certain schemes, a total of 23 alternative schemes were evaluated for the project as shown in Fig. 1.24. Structural costs were obtained on the basis of unit prices for in-place structural steel and concrete. It was assumed in the cost study that additional construction time required for composite construction (which was estimated to be 4 to 6 weeks) had negligible effect on cost comparisons. During the early design stages cross-bracing schemes were comparatively priced on an earlier architectural version of the tower but were ruled out by the owners in preference to a tubular scheme. Therefore, these schemes were not priced in the final comparison. Table 1.1 shows a summary of the structural cost comparison for various schemes. For comparative purposes the relative cost of the base scheme is considered as 1.0. The comparison is based on unit prices obtained in the early part of 1983 in the Houston construction

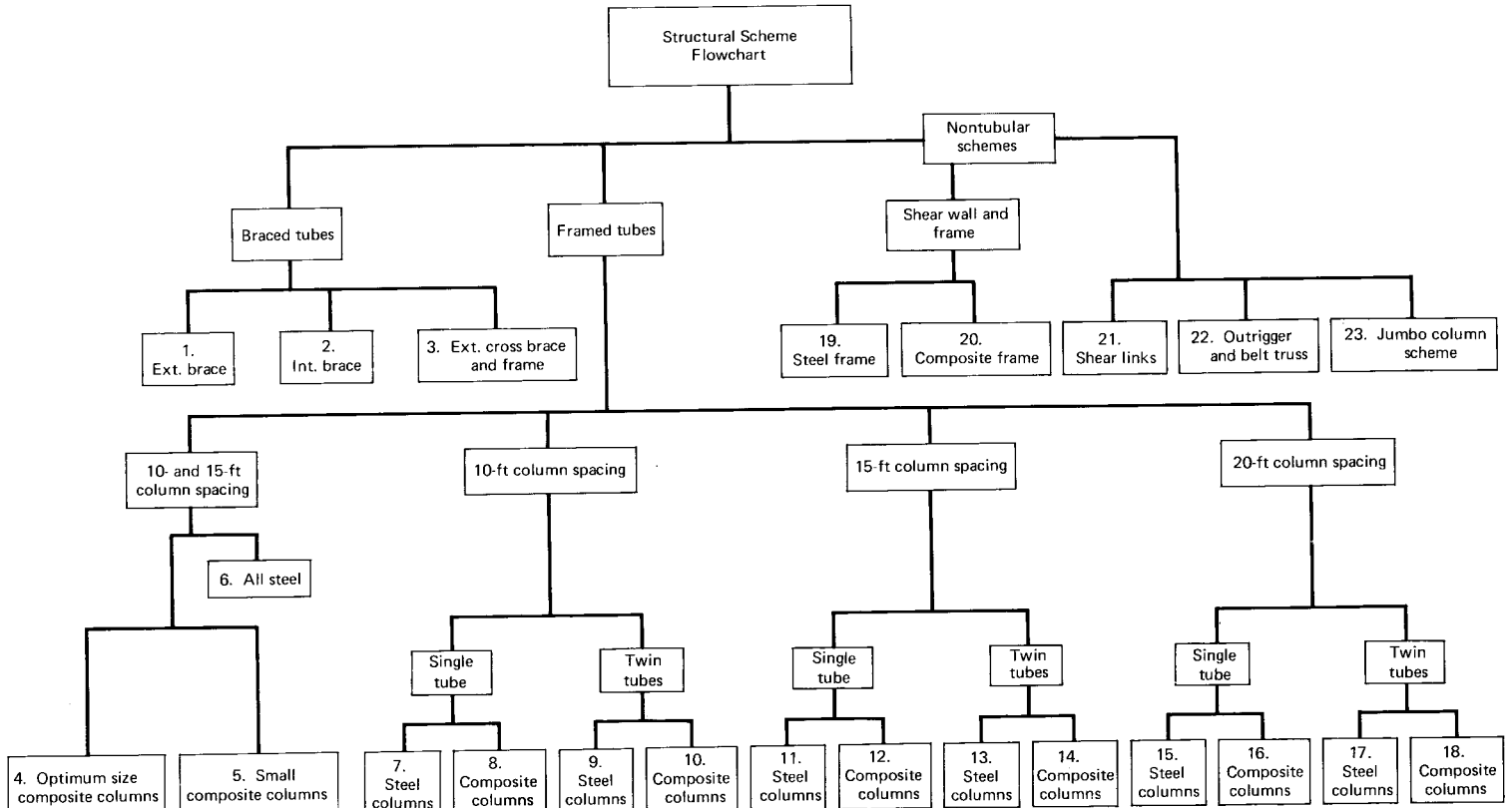

Figure 1.24. Structural scheme flowchart.

market. It is seen from the table that the framed tube option dominates the picture, with a relative cost index varying from a low of 0.97 to a high of 1.30 depending upon the exterior column spacing and the material makeup of the column. The study clearly demonstrates that the Houston version of composite construction, which utilizes exterior columns and steel spandrel beams, is more economical than an all-steel scheme, irrespective of the column spacing. The twin-tube scheme with the 10-ft (3-m) spacing worked out to be the most economical.

The scheme which employed a combination of 10- and 15-ft (3- and 4.58-m) column spacing was well in line with the most economical scheme. At the other end of the comparative scale, schemes that depart from the compact tube concept add a distinct premium to the structural cost. It is likely that further refinements of these schemes would have reduced the premium, but not to a level where they would compete with the base scheme. The study demonstrates that the base scheme chosen for the project is just as economical as the most economical scheme. Minor revisions such as reduction in size and relocation of certain columns are feasible to improve the leasability without paying undue penalty in the structure.

The plan density indexes, which are a reflection of the size of vertical elements, are seen in this study to vary over a very slight range from a low of 1.28 to a maximum of 2.66. Maximum economy is achieved by maintaining this index around 2.5. Whether or not it is justified to incur an additional cost of about 30 percent of the structural cost to reduce this index to around 1.8 is a matter to be decided for each project on its own merit. However, from the study it appears that the premium for holding down the size of vertical elements is way out of proportion to the planning flexibility obtained by smaller columns.

1.9 Summary

Ancient tall buildings such as the Egyptian pyramids and Mayan temples were primarily solid structures serving as monuments rather than as space enclosures. Contemporary tall buildings by contrast are conceived to serve as space enclosures, although the shear magnitude and audacity in scale of some tall buildings may give them the dubious title of monuments. Refinement from solid structures to space enclosures in itself does not change the basic issues of providing overall structural stability. The issues are the same, but the method of achieving the required structural action has changed considerably.

In the early monumental buildings it was unnecessary to consider the spatial interaction between subsystems because there was no subsystem to speak of. Massiveness of the structure provided for the

stability of the buildings without requiring great ingenuity on the part of the structural engineer. The size and density of structural elements in a modern tall building are strikingly less than in the buildings of former centuries. Structural technology has allowed and real estate market and aesthetic principles have motivated us continuously to push this trend to further limits.

The high-rise building technology can be thought of as a progressive reduction of material used within the space occupied by the building. Physically it can be pictured as hollowing of the interior of the building. For a tall building to be successful, it has to satisfy concurrently the requirements of site, building program, and above all make economic sense. From structural design considerations, a building can be considered tall when the effects of lateral loads are some way reflected in its design. Lateral deflections of tall buildings due to wind and earthquake loads should be limited to prevent damage to both structural and nonstructural elements. The accelerations at the top floors during frequent windstorms should be kept within acceptable limits to minimize discomfort to the building occupants.

The trend today in high-rise architecture is to have a free-form shape that fulfills the dual function of creating an exciting exterior and at the same time provides interior spaces that are highly desirable to lessees. The structural engineer, who at one time dominated the process of determining building form, no longer considers the domination a necessity. Instead, with the immense analytical backup provided by the computers, the structural engineer has set architecture free of the structural restraints. Needless to say, free-form architecture has demanded closer scrutiny of the proven systems, challenging the engineer to either modify the proven system or to come up with new structural solutions altogether. Although it is possible to arrive at a number of structural solutions which are readily applicable to high-rise buildings, the final scheme may well depend on how best it meets other nonstructural requirements. Optimization of structural systems is thus a task to be studied together with other building disciplines.

Chapter

2

Wind Effects

2.1 Design Considerations

Windy weather poses a variety of problems in new skyscrapers, causing concern for building owners and engineers alike. The forces exerted by winds on buildings increase dramatically with the increase in building heights. Static wind effects increase as the square of a structure's height, and the high-rise buildings of the 1970s and 1980s, which are at times 1000 feet (305 m) tall, must be 25 times stronger than the typical 200-foot (61-m) building of the 1940s. Moreover, the velocity of wind increases with height, and the wind pressures increase as the square of the velocity of wind. Thus, the wind effects on a tall building are compounded as its height increases.

In designing for wind, a building cannot be considered independent of its surroundings. The influence of nearby buildings and of the land configuration can be substantial. The swaying of the top of a high building caused by wind may not be seen by a passerby, but it may feel substantial to those who occupy the top floors. The horizontal swings may not be dangerous but may cause motion sickness in the occupants. There is scant evidence that winds, except in the case of a tornado or hurricane, have caused major structural damage to any of the new high rises. However, the modern skyscraper, which uses lightweight curtain walls, dry partitions, and high-strength materials, is more prone to wind motion problems than the early skyscrapers, which had

enormous weight of the masonry partitions, heavy stone facades, and massive structural members.

To be sure, all buildings sway during windstorms, but the motion in earlier tall buildings with locked-in gravity forces from their enormous weight is usually imperceptible and certainly has not been a cause for concern. Structural innovations and lightweight construction technology have disrobed the modern high-rise buildings of their stiffness. Wind action has become a major problem for the designer of today's high-rise buildings. In buildings prone to wind motion problems, objects in a room may vibrate, catching the occupant's eye. Doors and chandeliers swing, pictures lean, and books fall sideways off shelves. If the building has a twisting action, the occupants may get an illusory sense that the world outside is moving, creating symptoms of vertigo and disorientation. In more violent storms, windows can blow out, creating safety problems to pedestrians below. Sometimes, strange and often frightening noises are heard by the occupants as the wind shakes elevators, strains floors and walls, and whistles around the sides.

Keeping the movements in the upper levels of the building to acceptable human tolerances is the goal of the structural engineer. Exactly what this tolerance is has been very difficult to assess. Engineers today try to design structures that have inherent stiffness achieved through engineering techniques rather than depending upon dead weight to stabilize the structure. In spite of all the mathematical and engineering sophistication possible with a computer, wind has still managed to dodge complete quantitative analysis, mainly because of two major problems. First, unlike dead loads which are permanent and unchanging and live loads which are tacitly assumed to change slowly, wind loads change rapidly and even abruptly, creating effects much larger than if the same loads were applied gradually. The other major problem is that of providing comfort for the occupants, called "creature comfort." The true complexity of wind action and acceptable human tolerance for wind motions of tall buildings have just begun to be investigated. There is still a need for understanding the nature of wind and its interaction with a tall building, with particular reference to allowable deflections and comfort of occupants. In designing tall buildings to withstand wind forces, the following are important factors that must be considered:

1. Strength and stability requirements of the structural system
2. Fatigue in structural members and connections caused by fluctuating wind loads
3. Excessive lateral deflection that causes cracking of partitions and

external cladding, misalignment of mechanical systems and doors, and possible permanent deformations

4. Frequency and amplitude of sway that can cause discomfort to the occupants
5. Possible buffeting that may increase the magnitudes of wind velocities on neighboring buildings
6. Effects on pedestrians
7. Annoying acoustical disturbances
8. Resonance of building oscillations with the vibrations of elevator hoist ropes

Before discussing the details of the wind-related problems, it is useful to review the nature of wind as related to the behavior of tall buildings.

2.2 Nature of Wind

2.2.1 Introduction

Wind is the term used for air in motion and is usually applied to the natural horizontal motion of the atmosphere. Motion in a vertical or near vertical direction is called a *current.* Winds are produced by differences in atmospheric pressure, which are primarily attributable to differences in temperature. These temperature differences are caused largely by unequal distribution of heat from the sun, together with the difference in the thermal properties of land and ocean surfaces. When temperatures of adjacent regions become unequal, the warmer and thus lighter air tends to rise and flow over the colder, heavier air. Winds initiated in this way are usually greatly modified by the rotation of the earth.

Movement of air near the surface of the earth is three-dimensional in nature, with a horizontal motion which is much greater than the vertical motion. Motion of air is created by solar radiation, which generates pressure differences in air masses. Vertical air motion is of great importance in meteorology but is of less importance near the ground surface. The surface boundary layer involving horizontal motion of wind extends upward to a certain height above which the horizontal airflow is no longer influenced by the ground effect. The wind speed at this height is called the *gradient wind speed* and generally occurs at an altitude greater than 1500 ft (458 m). In this boundary layer is precisely where most of the human activity is conducted, and therefore how the wind effects are felt within this zone is of great concern in engineering.

Although one cannot see the wind, it is a common observation that its flow is quite complex and turbulent in nature. Imagine taking a walk outside on a reasonably windy day. You no doubt experience the constant flow of wind, but intermittently you will experience sudden gusts of rushing air. This sudden variation in wind speed is called gustiness or turbulence. The up-and-down fluctuations of speed about the mean velocity that occur over long periods of time due to solar energy cycles are of little importance in engineering, but the shorter-period peaks resulting from surface-generated turbulence are of great importance for the human activity in the earth's boundary layer.

In describing global circulation and specific recurrence of certain types of wind, modern meteorology relies on wind terminology used by early long-distance sailors. For example, terms like trade winds and westerlies were used by sailors who recognized the occurrence of steady winds blowing for long periods of time in the same direction. A broad indication of the flow of wind in the lower levels resulting from the general circulation of the atmosphere can be obtained by considering the interface between the cold winds from the polar regions and the westerlies. This is considered next.

Near the equator, the lower atmosphere is warmed. This air rises, depositing much precipitation and creating a uniform low-pressure area. Into this low-pressure area air is drawn from the relatively cold high-pressure regions from northern and southern hemispheres, giving rise to trade winds between the latitudes of 30° from the equator. The air going aloft flows counter to the trade winds to descend into these latitudes, creating a region of high pressure. Flowing northward and southward from these latitudes in the northern and southern hemispheres, respectively, are the prevailing westerlies, which meet the cold dense air flowing away from the poles in a low-pressure region characterized by stormy variable winds. It is this interface between cold, dense air and warm, moist air which is of main interest to the television meteorologists of northern Europe and North America.

Air above hot earth expands and rises. Air from cooler areas such as the oceans then floats in to take its place. The process is called *circulation*. Two kinds of circulation produce wind: (1) general circulation extending around the earth, and (2) smaller secondary circulations producing local wind conditions. Figure 2.1 shows a greatly simplified theoretical model of the circulation of prevailing winds which result from the general movement of air around the earth. There are no prevailing winds within the equatorial belt, which lies roughly between latitudes 10° S and 10° N. Therefore, near the equator and up to about 700 miles (1127 km) on either side of it there lies a low-pressure belt in which the air is hot and calm. The air in this region rises above the earth instead of moving across it, creating a

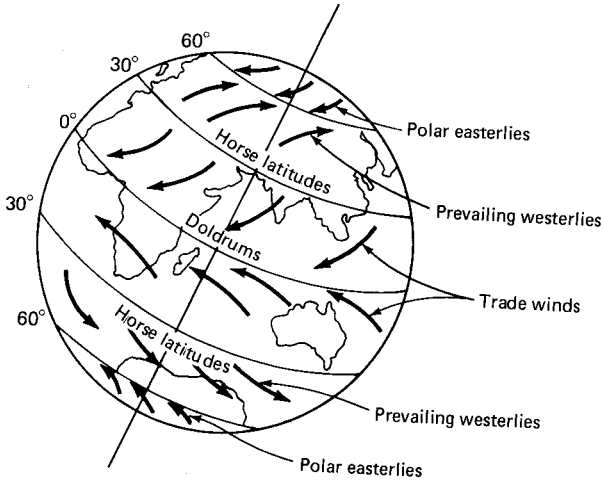

Figure 2.1 Circulation of world's winds.

region of relative calm called the *doldrums*. In both hemispheres, some of the air that has risen at the equator returns to the earth's surface at about 30° latitude, producing no wind. These high-pressure areas are called *horse latitudes*, possibly because many horses died on the sailing ships that were stalled because of lack of wind. The winds that blow between the horse latitudes and the doldrums are called *trade winds* because sailors once relied on them in sailing trading ships. The direction of trade winds is greatly modified by the rotation of the earth, and they blow somewhat from east to west. Two other kinds of winds that result from the general circulation of the atmosphere are called the *prevailing winds* and the *polar easterlies*. The prevailing winds blow in two belts bounded by the horse latitudes and 60° north and south of the equator. The polar easterlies blow in the two belts between the poles and about 60° north and south of the equator. Thus the moving surface air produces six belts of winds around the earth as shown in Fig. 2.1.

2.2.2 Types of wind

Of the several types of wind that encompass the earth's surface, winds which are of interest in the design of tall buildings can be classified into three major types: the prevailing winds, seasonal winds, and local winds.

1. *The prevailing winds.* Surface air moving from the horse latitudes toward the low-pressure equatorial belt constitutes the prevailing winds or trade winds. In the northern hemisphere, the northerly

wind blowing toward the equator is deflected by the rotation of the earth to become northeasterly and is known as the northeast trade wind. The corresponding wind in the southern hemisphere is called the southeast trade wind.

On the polar sides of the horse latitudes, the atmospheric pressure diminishes and the winds set in motion toward the poles are deflected by the earth's rotation toward the east. Because the winds are known by the direction from which they blow, these winds are known as the prevailing westerlies. The winds from the poles, particularly in the southern hemisphere, are deflected to become the polar easterlies. In comparison to the westerlies, the trade winds and the polar easterlies are shallow, and above a few thousand feet they are generally replaced by westerlies.

2. *The seasonal winds.* The air over the land is warmer in summer and colder in winter than the air adjacent to oceans during the same seasons. During the summer, the continents thus become seats of low pressure, with winds blowing in from the colder oceans. In the winter, the continents are seats of high pressure with winds directed toward the warmer oceans. These seasonal winds are typified by the monsoons of the China Sea and Indian Ocean.

3. *The local winds.* Corresponding with the seasonal variation in temperature and pressure over land and water, daily changes occur which have a similar but local effect, penetrating to a distance of about 30 miles (48 km) on and off the shores. Similar daily changes in temperature occur over irregular terrain and cause mountain and valley breezes. Other winds associated with local phenomena include whirlwinds and winds associated with thunderstorms.

All three types of wind mentioned here are of equal importance in the design of high-rise buildings. However, for purposes of evaluating the wind load on high-rise structures, the characteristics of the prevailing and seasonal winds are analytically studied together, while those of local winds are studied separately. This grouping is for analytical convenience and to distinguish between the widely differing scale of fluctuations of the winds; prevailing and seasonal wind speeds fluctuate over a period of several months, whereas the local winds vary almost every minute. The variations in the speed of prevailing and seasonal winds are referred to as *fluctuations* in mean velocity. The variations in the local winds, which are of a smaller character, are referred to as *gusts*.

Flow of wind, unlike that of other fluids, is not steady and fluctuates in a random fashion. Because of the randomness of its variation, the properties of wind are studied statistically. The roughness of the earth's surface produces frictional drag in the flow of air, causing a

gradual decrease in its velocity near the earth's surface. Also, turbulence is caused by surface roughness. Before these characteristics are studied in greater detail, it is of interest to have an overview of other types of extreme wind conditions and their effect on structures. This is considered more in the next section.

2.3. Extreme Wind Conditions

2.3.1 Introduction

Human beings and their works are subjected to hazards arising from forces and disturbances occurring in the natural environment. One of these natural hazards is the dynamic action of wind in the shape of hurricanes and tornadoes. These winds cause direct economic damages exceeding several million dollars in any given year. The large risk to both investment and human life which occurs from wind makes necessary an understanding of the physical phenomenon involved in the wind hazard and the development of improved planning and design methods. Wind engineering is, therefore, important, both in terms of potential economic damage and life loss and in human comfort.

Extreme winds, such as thunderstorms, hurricanes, tornadoes, and typhoons, impose loads on structures that are many times more than those normally assumed in their design. Some standards, such as ANSI A.58.1-1982, published by the American National Standards Institute, provide for hurricane wind speeds for a specified probability of occurrence but do not consider directly the effect of other types of extreme wind conditions. A brief description of the characteristics of extreme winds and their effect on structures follows.

2.3.2. Thunderstorms

Thunderstorms are one of the most familiar features of temperate summer weather, characterized by long hot spells punctuated by release of torrential rain. The essential conditions for the development of thunderstorms are warm, moist air in the lower atmosphere and cold, dense air at higher altitudes. Under these conditions warm air at ground level rises, and once it has started rising it continues to rise faster and faster, building storm clouds in the upper atmosphere. Thunder and lightning accompany downpours, creating gusty winds that sometimes blow violently at great speeds. Wind speeds of 20 to 70 mph (9 to 31 m/s) are typically reached in a thunderstorm and are often accompanied with swirling wind action exerting high suction forces on roofing and cladding elements.

2.3.3 Hurricanes

Hurricanes are severe atmospheric disturbances that originate in the tropical regions of the Atlantic Ocean or Caribbean Sea. They travel north, northwest, or northeast from their point of origin and usually cause heavy rains. They originate in the doldrums and consist of high-velocity winds blowing circularly around a low-pressure center known as the eye of the storm. The low-pressure center develops when the warm saturated air prevalent in the doldrums interacts with the cooler air. From the edge of the storm toward its center the atmospheric pressure drops sharply and the wind velocity rises. In a fully developed hurricane, winds reach speeds up to 70 to 80 mph (31 to 36 m/s), and in severe hurricanes can attain velocities as high as 200 mph (90 m/s). Within the eye of the storm, the winds cease abruptly, the storm clouds lift, and the seas become exceptionally violent. The most destructive hurricane in U.S. history hit the Atlantic seaboard in June, 1972. Hurricane Agnes caused at least 122 deaths and damage amounting to over $3 billion.

The maximum basic wind velocity for any area of the United States specified by code is 120 mph (54 m/s), which is less than the highest wind speeds in hurricanes. Except in rare instances, such as defense installations, a structure is not normally designed for full hurricane wind speeds.

The hurricane is one of the most spectacular forms of terrestrial disturbances and produces the heaviest rains known on earth. Hurricanes have two basic requirements, warmth and moisture, and consequently they develop only in the tropics. Almost invariably they move in a westerly direction at first and then swing away from the equator, either striking land with devastating results or moving out over the oceans until they encounter cool surface water and die out naturally. The region of greatest storm frequency is the northwestern Pacific, where the storms are called *typhoons*—a name of Chinese origin meaning "wind which strikes." The storms which occur in the Bay of Bengal and the seas of north Australia are called *cyclones*. Although there are some general characteristics common to all hurricanes, no two are exactly alike. However, a typical hurricane can be considered to have a 375-mile (600-km) diameter, with its circulating winds spiraling in toward the center at speeds up to 112 mph (50 m/s). The size of the eye can vary in diameter from as little as 3.7 to 25 miles (6 to 40 km). However, the typhoon which roared past the island of Guam in 1979 had a very large diameter of 1400 miles (2252 km) with the highest wind speed reaching 190 mph (85 m/s). Storms of such violence have been known to drive a plank of wood right through the trunk of a tree and blow straws end-on through a metal deck. Fortunately, storms of such magnitude are not common.

2.3.4 Tornadoes

Tornadoes develop within severe thunderstorms and sometimes hurricanes and consist of a rotating column of air usually accompanied by a funnel-shaped downward extension of a dense cloud having a vortex of several hundred feet, typically 200 to 800 ft (61 to 244 m) in diameter whirling destructively at speeds up to 300 mph (134 m/s). A tornado contains the most destructive of all wind forces, usually destroying everything along its path, which is approximately 10-miles (16-km) long and directed predominantly toward the northeast. Tornadoes form when a cold storm front runs over warm, moist surface air. The warm air rises through the overlaying cold storm clouds and is intercepted by the high-altitude winds which are even colder and are rapidly moving above the clouds. Warm air collides with the cooler air and begins to whirl. The pressure at the center of the spinning column of air is reduced because of the centrifugal force. This reduction in pressure causes more warm air to be sucked into it, creating a violent outlet for the warm air trapped under the storm. As the velocity increases, more warm air is drawn up to the low-pressure area created in the center of the vortex. As the vortex gains strength, the funnel begins to extend toward the ground, eventually touching it. Funnels usually form close to the leading edge of the storm. Larger tornadoes may have several vortices within a single funnel. If the bottom of the funnel can be seen, it usually means that the tornado has touched down and begun to pick up visible debris from the ground.

A typical tornado travels 20 to 30 mph (9 to 14 m/s), touches ground for 5 to 6 miles (8 to 10 km), and has a funnel 300 to 500 ft (92 to 152 m) wide. Distance from the ground to the cloud averages about 2000 ft (610 m). Tornadoes contain the most powerful of all winds, causing damage well in excess of $100 million a year in the United States. Although it is impractical to design buildings to sustain a direct hit from a tornado, it behooves the engineer to pay extra attention to anchorage of roof decks and curtain walls for buildings in areas of high tornado frequency.

Rolling plains and flat country make a natural home for tornadoes. Statistically, flat plains get more tornadoes than other parts of the country. In North America communities in Kansas, Nebraska, and Texas have many tornadoes and are classified as "tornado belt" areas. No accurate measurement of the inner speed of a tornado has been made because tornadoes destroy standard measuring instruments. However, photographs of tornadoes suggest that wind speeds are of the order of 167 to 224 mph (75 to 100 m/s). Although there definitely are tornado seasons, tornadoes can occur at any time.

Like a hurricane, the tornado consists of a mass of unstable air

rotating furiously and rising rapidly around the center of an area with low atmospheric pressure. The similarity ends here, because whereas the hurricane is generally of the order of 300 to 400 miles (483 to 644 km) in diameter, a large tornado is unlikely to be more than 1500 feet (458 m) across. However, in terms of destructive violence no other atmospheric disturbance compares with the tornado.

Wind alone is not the only damaging element at work in a tornado. The pressure at the center of a tornado is extremely low, so that as the storm passes over a building, the pressure inside the structure is far greater than that outside, causing the building to literally explode. Currently, ordinary buildings are not designed to withstand a direct hit from a tornado. However, for those buildings which are deemed essential, such as defense installations and nuclear facilities, sufficient information is available to implement tornado-resistant design. This information is in the form of tornado risk probabilities, tornado wind speeds, and accompanying forces.

2.4 Characteristics of Wind

2.4.1 Introduction

Wind is a phenomenon of great complexity because of the many flow situations arising from the interaction of wind with structures. However, in wind engineering simplifications are made to arrive at meaningful predictions of wind behavior by characterizing the flow states into the following distinguishing features:

1. Variation of wind velocity with height
2. Turbulent nature of wind
3. Probabilistic approach
4. Vortex shedding phenomenon
5. Dynamic nature of wind structure interaction

A brief description of each of these features follows.

2.4.2 Variation of wind velocity with height

At the interface between a moving fluid and a solid surface, viscosity manifests itself in the creation of shear forces aligned opposite to the direction of fluid motion. A similar effect occurs between the surface of the earth and the atmosphere. Viscosity reduces the air velocity adjacent to the earth's surface to almost zero. A retarding effect occurs in the layers near the ground, and these inner layers in turn successively slow down the outer layers. The slowing down is less at each

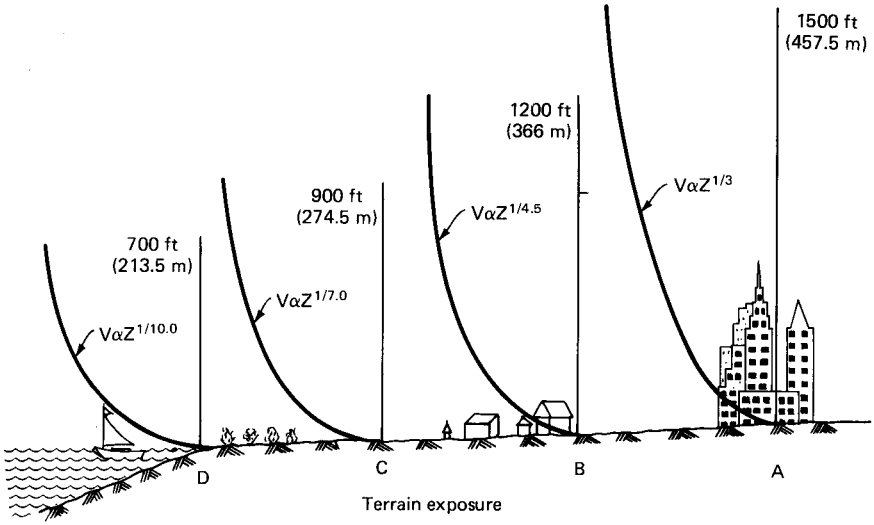

Figure 2.2 Variation of wind velocity with height.

layer and eventually becomes negligibly small. It is evident that the velocity increase which takes place along a vertical line must be continuous from zero on the surface to a maximum at some distance away. The height at which the velocity ceases to increase is called the *gradient height*, and the corresponding velocity, the *gradient velocity*. The shape and size of the curve depends less on the viscosity of the air than on the type and predominance of the turbulent and random eddying motions in the wind, which in turn are affected by the type of terrain over which the wind is blowing (see Fig. 2.2). This important characteristic of variation of wind velocity with height is a fairly well understood phenomenon and is reflected in higher design pressures given at higher elevations in most building codes.

The variation of velocity with height can be considered as a gradual retardation of the wind nearer the ground as a result of surface friction. At heights of approximately 1200 ft (366 m) from the ground, the wind speed is virtually unaffected by surface friction and its movement is solely dependent on the prevailing seasonal and local wind effects. The height through which the wind speed is affected by the topography at ground level is called the *atmospheric boundary layer*. The wind speed profile within this layer is in the domain of turbulent flow. The variation of wind speed in this layer can be mathematically predicted from a logarithmic equation. However, in engineering practice wind profile in the atmospheric boundary layer is well represented by the so-called power law expression of the form:

$$V_Z = V_g \, (Z/Z_g)^{\alpha} \tag{2.1}$$

where V_Z = the mean wind speed at height Z above the ground surface
V_g = gradient wind speed assumed constant above the boundary layer
Z = height above the ground
Z_g = depth of boundary layer
α = power law coefficient

Therefore, by knowing the mean wind speed at gradient height and the value of exponent α, the wind speeds are easily calculated by using Eq. (2.1). The exponent α and the depth of boundary layer Z_g vary with terrain roughness. The value of α ranges from a low of 0.14 for open country to about 0.5 for built-up urban areas, signifying that wind speed reaches its maximum value over a longer height in an urban terrain than in open country. The pressure and suction on a tall building generated by wind are a function of the wind speed, and therefore they increase with the building height.

2.4.3 Turbulent nature of wind

The motion of wind in general is turbulent. A concise mathematical definition of turbulence is difficult to give, except to state that it occurs in wind flow because air has a very low viscosity of about one-sixteenth that of water. Any movement of air at speeds greater than 2 to 3 mph (0.9 to 1.3 m/s) is turbulent, causing particles of air to move in all directions. This is in contrast to the laminar flow of particles of heavy fluids, which move predominantly parallel to the direction of flow.

The variation of wind velocity with height describes only one aspect of wind in the boundary layer. Superimposed on the mean wind speed is the turbulence or gustiness of wind, which produces deviations in the wind speed above and below the mean, depending upon whether there is a gust or lull in the wind action. Turbulence is created as a result of shearing velocity gradient in viscous fluid. The layers of wind slide relative to one another because wind near a solid boundary has a near-zero velocity, whereas the adjacent layers have a definite velocity giving rise to gradient distribution.

Flow of air near the earth's surface changes in speed and direction because of the obstacles which introduce random vertical and horizontal components at right angles to the main direction of flow. Turbulence thus generated generally influences the wind flow not only in the immediate vicinity, but it may persist downward from projections as much as a hundred times their height. These gusts have a random distribution over a wide range of frequencies and amplitudes, both in

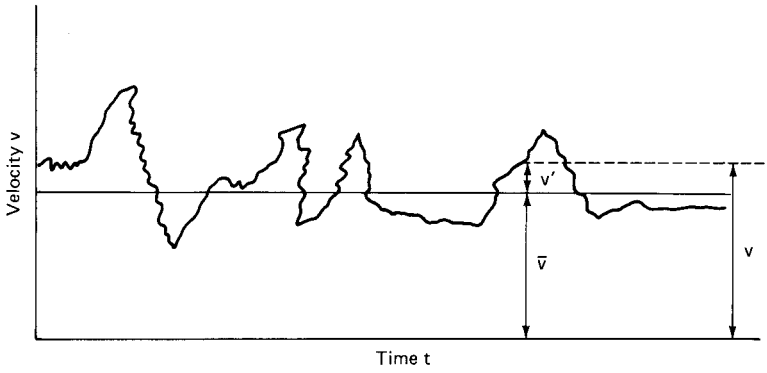

Figure 2.3 Variation of wind velocity with time.

time and space. Shown in Fig. 2.3 is a schematic representation of wind speed as measured by a typical anemometer, which clearly shows the unsteady nature of wind.

The scale and intensity of turbulence can be likened to the size and rotating speed of the eddies or vortices that make up the turbulence. It is generally found that the size of the flow affects the size of the turbulence within it. Thus, the flow of a large mass of air has a larger overall turbulence than a corresponding flow of a small mass of air. Because of the randomness of its variation, the properties of wind are studied statistically. A statistical property is the mean or the average. Because the wind speed changes constantly, different averages are obtained by using different averaging times. For example, while a one-hour average of wind speed may be 30 mph (13.4 m/s), the same wind averaged for one minute may be as high as 80 mph (35.8 m/s). This shows that it is necessary to specify averaging time whenever a mean velocity of wind is mentioned. However, one of the strange phenomena that occur when measuring wind speed is that averages taken over periods between 10 and 60 min adequately avoid the violent peaks and valleys due to gustiness. The averages taken over 10-, 20-, and 60-min intervals are nearly the same. This characteristic of the wind records allows the comparison of mean data taken over the different time periods used by different countries.

For structural engineering purposes, the characteristics of the natural wind in the atmosphere near the earth's surface can be considered as being made up of a mean velocity whose value increases with height in some way and on which are superimposed turbulent fluctuations as velocity components along the wind direction. This can be visualized in another way by considering the mean velocity as increasing with height as before, but subject to vortices or eddies (small currents of air spinning in space) oriented randomly to the mean direction. By

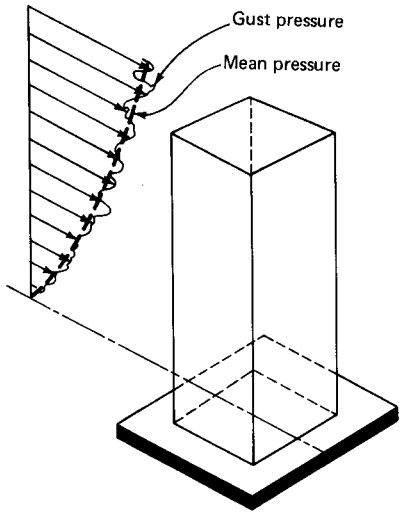

Figure 2.4 Schematic representation of mean wind and gust velocity.

assigning different size and rates of spin for these vortices, one can equate these to the wavelength and frequency of variable components. Fluctuation in the turbulence of wind is a random phenomenon.

Spectral analysis techniques provide a convenient tool for dealing with the random turbulence of wind. A complete treatment of the method is beyond the scope of the present work except to state that the method has some similarities with structural problems, wherein a required solution, for example, the deflection of a simply supported beam, can be obtained by superposition of a sufficiently large number of deflection patterns with different amplitudes and shapes.

The velocity at any instant v_t can be represented as the summation of the average velocity and the instantaneous value of velocity fluctuation about the mean value as shown in Fig. 2.3. Thus

$$v_t = \bar{v} + v' \tag{2.2}$$

where v_t = velocity at instant t
$\bar{v}$ = average or mean velocity
v' = instantaneous velocity fluctuation about the mean velocity $\bar{v}$

Figure 2.4 schematically represents the fluctuation of mean and gust velocity along the height of a building.

The longest averaging time used in structural engineering practice is one hour. As the averaging time decreases, the maximum speed of wind increases. The average or mean wind speed used in many building codes of the United States is the *fastest-mile wind*, which can

be thought of as the maximum velocity measured over one mile of wind passing through an anemometer. Normally, the wind speed in structural design is in the range of 60 to 120 mph (97 to 154 m/s), giving an averaging period of 30 to 60 s.

Rapid bursts in the velocity of wind are called gusts. Tall buildings are sensitive to gusts that last about one second. Therefore, the fastest mile wind (which has the averaging period of 30 to 60 s) is inadequate for design of tall buildings. One must use the gust speed rather than the mean wind speed in the determination of wind loads. The gust speed can be obtained by multiplying the mean wind speed by a gust factor G_v. Thus

$$V_g = G_v V \tag{2.3}$$

where G_v = the gust factor
V_g = the gust speed
V = the mean wind speed

Not all buildings are equally sensitive to gusts. In general, the more flexible a structure is, the more sensitive it is to gusts. The only accurate way to determine the gust factor (also called gust response factor) is to conduct a wind tunnel test. However, attempts are made in some contemporary wind load standards to give analytical procedures which yield different gust factors for buildings with different dynamic characteristics.

2.4.4 Probabilistic approach to wind load determination

In many engineering sciences the intensity of particular events is considered as a function of duration recurrence interval (return period). For example, in hydrology the intensity of rainfall expected in a region is considered to be a function of return period; the rainfall that is expected to be repeated once in 10 years is likely to be less than expected once in every 50 years. Similarly, in wind engineering the speed of wind is considered to vary with duration and return period. For example, the fastest-mile wind 33 ft (10 m) above the ground in Dallas, Texas, corresponding to a 50-year return period is 67 mph (30 m/s) as compared to the value of 71 mph (31.7 m/s) for a 100-year recurrence interval.

A 50-year return period wind of 67 mph (30 m/s) means that on the average, Dallas will experience a wind faster than 67 mph within a period of 50 years. A return period of 50 years corresponds to a probability of occurrence of 1/50 = 0.02 = 2 percent. Thus the chance that a wind exceeding 67 mph (30 m/s) will occur in Dallas within a given year is 2 percent. Suppose a building is designed for a 100-year

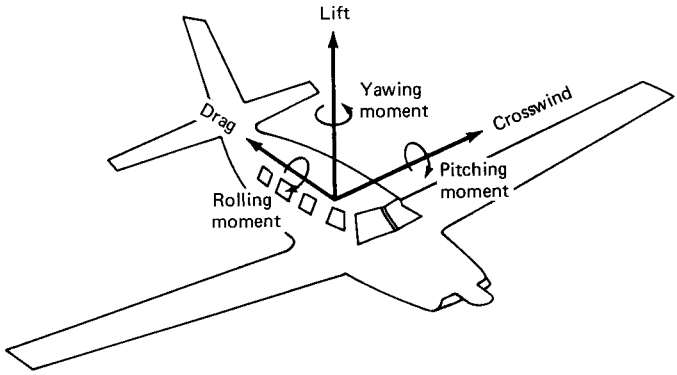

Figure 2.5 Six components of wind.

lifetime using a wind speed of 67 mph. What is the probability that wind will exceed the design speed within the lifetime of the structure? The probability that this wind speed will not be exceeded in any year is 49/50. The probability that this speed will not be exceeded in 100 years in a row is $(49/50)^{100}$. Therefore, the probability that this wind speed will be exceeded at least once in 100 years is

$$1 - \left(\frac{49}{50}\right)^{100} = 0.87 = 87 \text{ percent}$$

This signifies that although a wind with low annual probability of occurrence such as a 50-year wind is used to design structures, there exists still a high probability of the wind being exceeded within the lifetime of the structure. However, in structural engineering practice it is believed that the actual probability of overstressing a structure is much less because of the factors of safety and the general conservative values used in design.

2.4.5 Vortex shedding phenomenon

In general, wind blowing past a body can be considered to be diverted in three mutually perpendicular directions, giving rise to forces and moments about the three directions. In aeronautical engineering special terminology is used to describe these forces and moments as shown in Fig. 2.5. Although all six components are significant in aeronautical work, in civil and structural engineering, the force and moment corresponding to the vertical axis (lift and yawing moment) are of little significance. The flow of wind can be considered to be two-dimensional, as shown in Fig. 2.6.

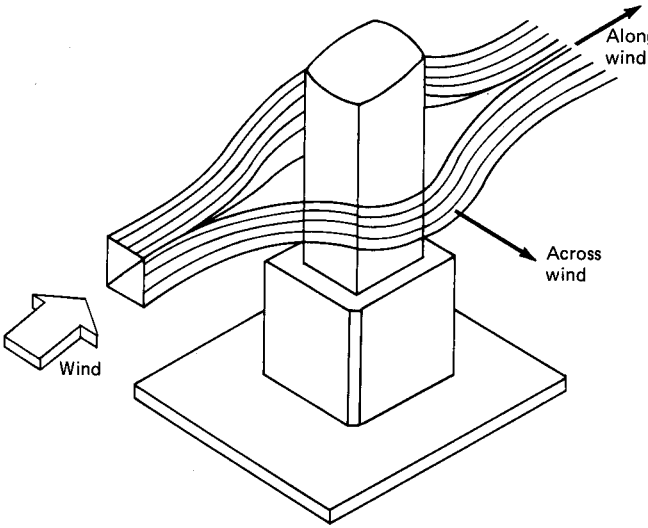

Figure 2.6 Simplified two-dimensional flow of wind.

Along wind or simply *wind* is the term used to refer to drag forces and *transverse wind* is used to refer to crosswind. The crosswind response, that is, motion in a plane perpendicular to the wind, dominates over the along wind response for most tall buildings. The complex nature of wake-excited response is a result of interaction of turbulence, building motion, and the dynamics of wake formation.

It is perhaps baffling to the uninitiated engineer to learn that a tall building is subject to wind excitations not only in a direction parallel to the wind but also in a direction perpendicular to it. Yet in many instances, the major criterion for design of very tall buildings is the crosswind response. Since the dynamic forces arising from wind loads are normally at right angles to the wind direction, not only are the coefficients for calculating wind loads given in most codes inappropriate, but the bracing necessary to ensure dynamic stability may well be misplaced in another plane.

There appear to be three distinctly different reasons why a building responds in a direction at right angles to the applied wind forces; these are: (1) the biaxial displacement induced in the structure because of either asymmetry in geometry or in applied wind loading, (2) the turbulence of wind, and (3) the negative-pressure wake or trail on the building sides. For tall buildings it appears that the crosswind response is caused mainly by the wake.

Consider a cylindrically shaped building subjected to a smooth wind flow. The originally parallel stream lines are displaced on either side of the cylinder, and this results in spiral vortices being shed periodically

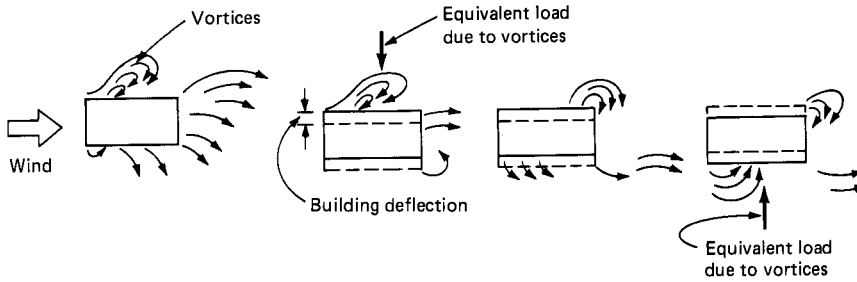

Figure 2.7 Vortex shedding phenomenon.

from the sides of the cylinder into the downstream flow of wind which is called the wake. At low wind speeds of say 50 to 60 mph (22.3 to 26.8 m/s), the vortices are shed symmetrically in pairs one from each side. These vortices can be thought of as imaginary projections attached to the cylinder that increase the drag force on the cylinder. When the vortices are shed, i.e., break away from the surface of the cylinder, an impulse is applied to the cylinder in the transverse direction. This phenomenon of alternate shedding of vortices for a rectangular tall building is shown schematically in Fig. 2.7.

At low wind speeds, since the shedding occurs at the same instant on either side of the cylinder, there is no tendency for the cylinder to vibrate in the transverse direction. The structure is therefore subject to along-wind oscillations parallel to the wind direction. At higher speeds, the vortices are shed alternately first from one and then from the other side of the cylinder. When this occurs, there is an impulse in the along-wind direction as before, but in addition, there is an impulse in the transverse direction. The transverse impulses are, however, applied alternately to the left and then to the right. Thus the frequency of transverse impulse is precisely half that of the along-wind impulse. This kind of shedding which gives rise to structural vibrations in the flow direction as well as in the transverse direction is called *vortex shedding* or the *Karman vortex street*, a phenomenon well known in the field of fluid mechanics.

There is a simple formula to calculate the frequency of the transverse pulsating forces caused by vortex shedding.

$$f = \frac{V \times S}{D} \tag{2.4}$$

where f = the frequency of vortex shedding in hertz
V = the mean wind speed at the top of the building
S = a dimensionless parameter called the Strouhal number for the shape
D = the diameter of the building

In the Eq. (2.4), the parameters V and D are expressed in consistent units such as ft/s and ft, respectively.

The Strouhal number is not a constant but varies somewhat irregularly with the wind velocity. At low air velocities, S is also low and increases with the velocity up to a limit of 0.21 for a smooth cylinder. This limit is reached for a velocity of about 50 mph (22.4 m/s) and remains almost constant at 0.20 for wind velocities between 50 and 115 mph (22.4 and 51 m/s).

Consider for illustration purposes, a circular prismatic-shaped high-rise building having a diameter equal to 110 ft (33.5 m) and a height-to-width ratio of 6 with a natural frequency of vibration equal to 0.16 Hz. Assuming a wind velocity of 60 mph (27 m/s), the vortex shedding frequency is given by

$$f = \frac{V \times 0.2}{110} = 0.16 \text{ Hz}$$

where V is in ft/s.

If the wind velocity increases from 0 to 60 mph (27.0 m/s), the frequency of vortex excitation will rise from 0 to a maximum of 0.16 Hz. Since this frequency happens to be very close to the natural frequency of the building, and assuming a very low damping, the structure would pulsate as if its stiffness were zero at a wind speed somewhere around 60 mph (27 m/s). Note the similarity of this phenomenon with the ringing of church bells or the shaking of a tall lamppost whereby a small impulse is added to the kinetic energy possessed by the moving mass at each end of the cycle. This results in a slight increase in deflection at the end of each swing. Only damping by air resistance, friction damping provided in a bolted steel joint or a crack in concrete, or the damping provided by the internal dissipation of energy can lose energy. If these damping characteristics are small, the vortex shedding at the natural frequency of the structure can cause displacements far beyond those predicted on the basis of static analysis. The displacements are limited only by the plastic yielding in steel members and cracking in concrete members.

When the wind speed is such that the shedding frequency becomes approximately the same as the natural frequency of the cylinder, a resonance condition is created. After the structure has begun to resonate, further increases in wind speed by a few percent will not change the shedding frequency, because the shedding is now controlled by the natural frequency of the structure. The vortex shedding frequency is, so to speak, locked in with the natural frequency. When wind speed increases above that causing the lock-in phenomenon, the frequency of shedding is again controlled by the speed of the wind. The

structure vibrates with the resonant frequency only in the lock-in range, and for wind speeds either below or above this range, the vortex shedding will not be critical.

Vortex shedding is also generated for other than cylindrical shapes. The value of S for different shapes is determined by placing the various shapes in wind tunnels and measuring the frequency of shedding for a range of wind velocities. One does not have to know the value of S very precisely because the lock-in phenomenon occurs within a range of about 10 percent of the exact frequency of the structure.

The crosswind response mechanism is very complex, and an exact analytical method that takes into account the variables of turbulence, building shape, structure stiffness, damping, and density has not been introduced into structural engineering practice. In cases where the crosswind response may become the controlling factor in the design, the only recourse left for the engineer is to resort to an aeroelastic wind tunnel investigation. Even then it has to be recognized that even very expensive model tests cannot simultaneously scale the Reynolds number, Strouhal number, the fluctuating lift and drag coefficients, the structural stiffness, the aerodynamic damping, and so on.

2.4.6 Dynamic nature of wind

When wind hits a blunt body in its path, it transfers some of its energy to the body. The measure of the amount of energy transferred is called the *gust response factor*. As mentioned earlier, wind turbulence (also called gustiness) is affected by terrain roughness and height above ground. The gust response factor is, therefore, dependent on the roughness of the terrain and the height above ground. A tall, slender, and flexible structure could have a significant dynamic response to wind because of buffeting. This dynamic amplification of response would depend on how the gust frequency correlates with the natural frequency of structure and also on the size of the gust in relation to the building size.

Unlike the mean flow of wind, which can be considered as static, wind loads associated with gustiness or turbulence change rapidly and even abruptly, creating effects much larger than if the same loads were applied gradually. Wind loads, therefore, need to be studied as if they were dynamic in nature. The intensity of a wind load depends on how fast it varies and also on the response of the structure. Therefore, whether the pressures on a building created by a wind gust, which first increases and then decreases, are considered as dynamic or static loads depends to a large extent on the structure to which it is applied.

Let us consider the movement of a tall building acted upon by a wind gust. Under the wind pressure, the building bends slightly and its top moves. It first moves in the direction of wind, say with a magnitude of

2 ft (0.61 m), and then starts oscillating back and forth. Its top goes through its neutral position, then moves approximately 2 ft (0.61 m) in the opposite direction, and continues oscillating back and forth until it eventually stops. The time it takes a building to swing through a complete oscillation is known as a *period*. The period of oscillation for a tall steel building in the height range of 700 to 1400 ft (214 to 427 m) normally is in the range of 5 to 10 s, whereas for a 10-story concrete or masonry building it may be in the range of 0.5 to 1 s. The action of a wind gust depends not only on how long it takes to reach its maximum value and decrease again, but on the period of the building on which it acts. If the wind gust reaches its maximum value and vanishes in a time much shorter than the period of the building, its effects are dynamic. The gusts can be considered as static loads if the wind load increases and vanishes in a time much longer than the period for the building. For example, a wind gust growing to its strongest pressure and decreasing to zero in 2 s is a dynamic load for a tall building with a period of, say, 5 to 10 s, but the same 2-s gust is a static load for a low-rise building with a period of less than 2 s.

2.5 Code Wind Loads

2.5.1 Introduction

Building codes and standards are documents which serve as compendiums for technical information and as sources for extracting minimum requirements of accepted design and construction practices. Codes and standards are, in fact, dynamic instruments that are revised periodically to reflect the state of the art. Although building codes vary from state to state, they are laws nevertheless. With the exception of some large cities in the United States which have adopted their own independent codes, about 85 percent of state and local governments have adopted or patterned their regulations on the provisions given mainly in three model codes. These are the *Basic Building Code* issued by the Building Officials and Code Administrators (BOCA) International, *Standard Building Code* (SBC) issued by Southern Building Code Congress International, and the *Uniform Building Code* (UBC) issued by the International Conference of Building Officials.

Because considerable differences exist among the provisions given in the model codes, the salient features of each code as related to wind loads are discussed separately in the following sections instead of collectively. Also discussed are the provisions of the National Building Code of Canada and the American National Standard ANSI A58.1-1982.

2.5.2 The Basic Building Code (BOCA 1984)

The BOCA code gives a table of effective velocity pressures at different heights for various 50-year wind speeds. The pressures are for locations such as suburban and wooded terrain, called exposure B. For buildings located in flat and open terrain, the code requires a higher load to be used in the design without giving any specific value. Similarly, the code allows the designer to scale down the pressures for buildings located in urban and hilly terrain. The code stipulates that the effective velocities should be multiplied by distribution coefficients equal to the pressure and suction values of 0.8 and 0.5 on the windward and leeward walls for buildings with height-to-width ratios and height-to-length ratios not exceeding 2.5. For higher ratios, values of 0.8 and 0.6 are stipulated. A suction distribution coefficient of 0.7 is specified for leeward walls of all buildings.

2.5.3 Standard Building Code (SBC 1985)

The basic wind speed used in obtaining the design pressure is a 100-year wind. Lower pressures are officially acceptable if their validity is shown to be based on rational data.

The design pressure is given by the formula

$$P = 0.0025\, V^2 \left(\frac{H}{30}\right)^{2/7} \qquad \text{for } H \geq 30 \text{ ft} \tag{2.5}$$

where P = basic wind load pressure in psf
V = 100-year recurrence of fastest-mile wind velocity
H = height above grade at which pressure is being computed

The pressures thus obtained are to be multiplied by appropriate shape factors (1.3 for rectangular prismatic structures and 0.70 for cylindrical shapes). No exposure factors are distinguished in the code.

2.5.4 Uniform Building Code (UBC 1985)

For nonslender buildings up to 400 ft in height, the UBC adopts the minimum 50-year wind as the basic wind speed. Two types of exposures, B and C, are considered. C is the more severe exposure and is applicable to buildings in open and flat terrain. Exposure B is for a terrain which has buildings, forests, or surface irregularities of 20 ft (6.0 m) minimum in height. Design wind pressure P, which is applicable to both the structural system and components of the structure, is given by the formula

$$P = C_e C_q q_s I \tag{2.6}$$

where P = design wind pressure
C_e = a factor that combines the effects of height, exposure, and gust factor
C_q = pressure coefficient which takes into consideration whether the structural system such as the building bracing or portion of a curtain wall is being designed
q_s = wind pressure at a standard height of 33 ft (10 m) corresponding to the 50-year wind speed with a value of 26 psf (1245 Pa) for a 100-mph (44.7-m/s) wind speed and varying as the square of the wind speed
I = importance factor, which increases the pressure by 15 percent for essential buildings such as medical facilities and communication centers

For buildings taller than 400 ft (122 m) and slender structures sensitive to dynamic effects, UBC refers to a national standard, presumably the American National Standard Institute ANSI A58.1 for the calculation of wind loads.

Two methods, the normal force method and projected area method, are given in the UBC for obtaining the pressure coefficient C_q. The normal force method is mandatory for gabled structures but is also applicable to flat-roofed buildings. Values of 0.8 and 0.5 are given for the pressure and suction coefficients for the windward and leeward walls, giving a total pressure coefficient of 1.3 for a building. The projected area method gives a similar value of 1.3 for a structure less than 40 ft high, and a value of 1.4 for structures over 40 ft but less than 200 ft in height.

2.5.5 National Building Code of Canada (NBC 1980)

The NBC is perhaps the most exhaustive treatise to address the wind loading on tall buildings with consideration given to building dimensions, shape, stiffness, damping ratios, site topography, climatology, boundary layer meteorology, bluff body aerodynamics, and probability theory. The code gives three different approaches for determining wind loads on buildings: (1) simple procedure, (2) experimental procedure, and (3) detailed procedure.

Simple procedure. The simple procedure is applicable for determining the structural and wind loads for the majority of low- and medium-rise buildings and also for cladding design of low-, medium-, and high-rise buildings. This approach is similar to other code approaches in which

the dynamic action of wind is dealt with by equivalent static loads defined independently of the dynamic properties of wind. The external pressure or suction on the building surface is given by the equation

$$P = qC_eC_gC_p \tag{2.7}$$

where P = the design static pressure on suction acting normal to the surface
q = the reference wind pressure or suction
C_e = the exposure factor that reflects the changes in wind speed with height and as a result of variations in the surrounding terrain
C_g = the gust factor, with a value of 2.0 for the structure as a whole and 2.50 for cladding
C_p = the external pressure coefficient averaged over the area of the surface considered.

The pressure q is determined from the reference wind speed v by the following equation:

$$q = cv^2 \tag{2.8}$$

where c is a conversion factor depending upon the air temperature and atmospheric pressure. If the wind speed is in miles per hour, the design pressure q in pounds per square foot can be obtained by using a value of 0.0027 for the conversion factor c. The reference wind pressure is calculated for three different levels of probability being exceeded per year (1/10, 1/30, and 1/100), that is, return periods for 10, 30, and 100 years, respectively. A 10-year recurrence velocity is used for the design of cladding and for the serviceability check of structural members for deflection and vibration. A 30-year wind is used for the strength design of structural members of all buildings except those which are classified as postdisaster buildings. A 100-year wind is used for the design of such buildings as hospitals.

The exposure factor C_e is based on the $\frac{1}{5}$ power law, which is appropriate for wind gust pressures in open terrain. An averaging period of 3 to 5 s is used in determining the gust factor. The gust represents a "parcel" of wind which is assumed to be effective over the whole of the building. For tall buildings, the reference height for pressures on the windward face correspond to the actual height above ground, and for suctions on the leeward face the reference height is half the height of the structure.

For nearly 25 years wind speed records have been kept at a large number of wind-measuring stations in Canada and the United States. These stations have recorded the number of miles of wind that pass an anemometer head at each hour. This is also referred to as the hourly

average speed. These stations usually are at airports and thus located in open terrain, and the measured wind speeds are at a representative height of 33 ft (10 m). Using this data base from over 100 stations, a statistical analysis has been performed to calculate the wind speed that would have one chance in 10, 30, and 100 of being exceeded in any one year. Obviously, the 100 or so wind-measuring stations are not sufficient to cover the whole country. Therefore, values of 30-year wind for an additional 500 stations have been estimated, and by further mathematical calculations 10- and 100-year wind speeds have been computed for over 600 locations.

The pressure and suction generated on the building face depend not only on the wind speed but also on factors like air density and temperature and atmospheric pressure. The air pressure is dependent on elevation above sea level and varies with the changes in weather systems. Monthly average values of these differing parameters in the windy part of the year have been used to compute the velocity pressures given in the NBC. Note that the pressures given in the NBC have not been modified for gust factors, and therefore gust factor has to be accounted for separately in the design.

Pressure coefficient C_p is a nondimensional ratio of wind-induced pressure on a building to the velocity pressure of the wind speed at the reference height. It depends on the shape of the building, wind direction, and the profile of the wind velocity, and can be determined most reliably from wind tunnel tests on building models. However, based on some limited measurements obtained on full-scale buildings supplemented with wind tunnel tests, the NBC gives certain values of C_p for both suction and pressure for tall rectangular buildings for which the height-to-width ratios are greater than 2.0. These are given as follows:

Windward wall: $C_p = 0.8$ for the entire height (2.9)

End walls (walls parallel to the direction of wind): $C_p = -0.7$ (suction) (2.10)

Leeward wall: $C_p = -0.5$ (suction) (2.10*a*)

The code specifies that in calculating the exposure factor for both the structural and cladding design that $\frac{1}{2}H$ should be used for the leeward walls, H for roof and side walls, and the actual height Z to the level under consideration for the windward wall.

The interior pressure coefficient for a tall building without openings is given a value of $C_{pi} = -1.0$ and may occur anywhere over the wall area. Since the same internal pressure is assumed to occur at both the leeward and the windward walls, the values of structural loads are not affected by the internal pressure but are needed for the cladding

design. For buildings with openings, the following values of internal pressure coefficients are given for the cladding design, depending upon the location of the opening:

1. Openings in windward wall, $C_{pi} = +0.7$
2. Openings in leeward wall, $C_{pi} = -0.5$
3. Openings in walls parallel to wind direction, $C_{pi} = -0.7$
4. Openings distributed uniformly in all four walls, $C_{pi} = -0.3$

Wind blowing on the building faces creates air pressures inside the building due to minute leakage of air through cladding systems. This effect is defined by prescribing internal pressure coefficients C_{pi} at various locations inside the building and are important in the design of both cladding elements and the overall structure. It is rather difficult, if not impossible, to determine the magnitude and distribution of these coefficients because of the uncertainties associated with the influence of openings either intended in the design or caused by window breakage. Also it is very difficult to estimate the effect of ventilation leakage of the building envelope.

Experimental procedure. The second approach given in the NBC for wind load analysis is to use the results of special wind tunnel or other experimental procedures whenever the building is likely to be susceptible to wind-induced vibrations. This is appropriate for tall, slender structures for which wind loading plays a major role in the structural design. A wind tunnel test is also recommended for determining exterior pressure coefficients for cladding design of buildings whose geometry deviates markedly from more common shapes for which information is already available.

Detailed procedure. The third approach given in the NBC consists of a series of calculations intended for a more accurate determination of the gust factor C_g, the exposure factor C_e, and the pressure coefficient C_p. The end product of the calculations yields a static design pressure which is expected to produce the same peak effect as the actual turbulent wind, with due considerations for the building properties such as height, width, natural frequency of vibration, and damping. This approach is primarily for determining the overall wind loading and response of tall slender structures and is not intended for determining exterior pressure coefficients for cladding design.

The code gives procedures for calculating the dynamic effects of vortex shedding for slender cylindrical towers and for tapered structures. Since the available data are limited for slender structures with cross sections other than circular, wind tunnel tests are recommended

for estimating the likely response. To limit the cracking of masonry and interior finishes a maximum lateral deflection limitation of 1/500 is specified unless detailed analysis is made and precautions are taken to permit larger movements.

The code recognizes that maximum accelerations of a building leading to possible human perception of motion or even discomfort may occur in a direction perpendicular to the wind. A tentative acceleration limit of 1 to 3 percent of gravity for a 10-year return wind is recommended to limit the possibility of perception of motion.

2.5.6 ANSI Standard A58.1-1982

The full title of this standard is *American National Standard Minimum Design Loads for Buildings and Other Structures.* It was first published in 1972 and subsequently expanded and revised in 1982. One of its nine sections prescribes the procedures for calculating design wind loads. It takes into consideration the differences between those wind loads which act on the building as a whole and those which dictate the design of individual structural components and cladding of buildings. Two procedures, one analytical and one experimental, using wind tunnel tests and similar tests employing fluids other than air are given in the ANSI Standard. The analytical procedure applies to the majority of buildings, and due consideration is given to the load magnification effect caused by gusts which may be in resonance with the along-wind vibrations of the structure. This procedure does not consider the phenomenon of vortex shedding, nor does it consider buildings having unusual shapes or response characteristics. Since it is not possible to particularize the influence of site locations which can create channeling effects or upwind obstructions analytically, a wind tunnel procedure is recommended for such situations.

Basic wind speeds for any location in the continental United States and Alaska are shown on a map having isotachs representing the fastest-mile velocities at 33 ft (10 m) above the ground. For Hawaii and Puerto Rico, the basic wind speeds are given in a table as 80 and 95 mph (35.7 and 42.4 m/s), respectively. The map is for a 50-year recurrence interval for flat, open country and grasslands with an open terrain and scattered obstructions generally less than 30 ft (9 m) in height. The minimum basic wind speed provided in the standard is 70 mph (31.3 m/s). Upgrading of minimum wind speed for special topographies such as mountain terrain, gorges, and ocean fronts is recommended.

The wind speed map for the United States and adjoining land masses is based on the data collected over a long period of time at 129 U.S. weather stations located throughout the country. The maximum ve-

TABLE 2.1 Classification of Buildings and Other Structures for Wind, Snow, and Earthquake Loads

Nature of occupancy	Category
All buildings and structures except those listed below	I
Buildings and structures where the primary occupancy is one in which more than 300 people congregate in one area	II
Buildings and structures designated as essential facilities, including, but not limited to:	III
(1) Hospital and other medical facilities having surgery or emergency treatment areas	
(1) Fire or rescue and police stations	
(3) Primary communication facilities and disaster operation centers	
(4) Power stations and other utilities required in an emergency	
(5) Structures having critical national defense capabilities	
Buildings and structures that represent a low hazard to human life in the event of failure, such as agricultural buildings, certain temporary facilities, and minor storage facilities	IV

This material is reproduced with permission from American National Standard *Minimum Design Loads for Buildings and Other Structures*, ANSI A58.1–1982, copyright 1982 by the American National Standards Institute. Copies of this standard may be purchased from the American National Standards Institute at 1430 Broadway, New York, NY 10018.

locity to be expected at any location in the continental United States can be found simply by reference to the wind velocity map.

Because of the relatively rare occurrence of hurricanes, records of sufficient length are not available to map the wind speed contours in the hurricane-prone regions. To alleviate this lack of available data, mathematical simulation of hurricanes has been used to analytically generate wind speed records in 58 coastal points. These have been incorporated in the wind speed map.

Calculation of design wind pressure on wind bracing systems. The procedure for calculating wind loads may be summarized as follows:

1. Determine I, the importance factor, for wind from the nature of occupancy of the building and its proximity to hurricane-prone oceanlines. Tables 2.1 and 2.2 give the type of occupancy and the importance factor I, respectively. Buildings are classified into four categories depending upon the primary purpose of occupancy. Assembly buildings and essential facilities are treated as either category II or III, requiring design for larger wind loads. Buildings with low hazard to human life in the event of failure are considered as category IV, and all other buildings are classi-

TABLE 2.2 Importance Factor, *I* (Wind Loads)

	I	
Category*	100 miles from hurricane oceanline, and in other areas	At hurricane oceanline
I	1.00	1.05
II	1.07	1.11
III	1.07	1.11
IV	0.95	1.00

* See Table 2.1.

Notes:

1. The building and structure classification categories are listed in Table 2.1.
2. For regions between the hurricane oceanline and 100 miles inland the importance factor *I* shall be determined by linear interpolation.
3. Hurricane oceanlines are the Atlantic and Gulf of Mexico coastal areas.

fied as category I. *I* essentially recognizes that buildings near hurricane-prone oceanlines are buffeted by stronger winds. For example, an essential building of category II located adjacent to the Atlantic Ocean or Gulf of Mexico has a value of 1.11 for *I* as compared to 1.07 for the same building located inland 100 miles (1690 km) from the ocean.

2. Select the basic wind speed *V* for the location of the building from the 50-year mean recurrence interval map which is shown in Fig. 2.8.
3. Determine the ratio of height to least horizontal dimension of the building. If it is less than 5, the building can be considered nonflexible, permitting simpler expressions for determining gust factors. If the ratio is larger than 5, the building is considered flexible and the fundamental frequency of the building must be determined. Use of a series of empirical parameters and graphs is required to arrive at gust response factors. We will defer the presentation of these parameters and graphs until later in this section where examples of gust factors will be given both for flexible and nonflexible buildings.
4. Determine the external pressure coefficient C_p for average loads on main wind-force-resisting systems from a knowledge of plan dimensions and building elevation.
5. Determine the exposure category that adequately reflects the characteristics of the ground surface irregularities at the building site, taking into account both natural topography and man-made features. ANSI has four categories of exposures to take into

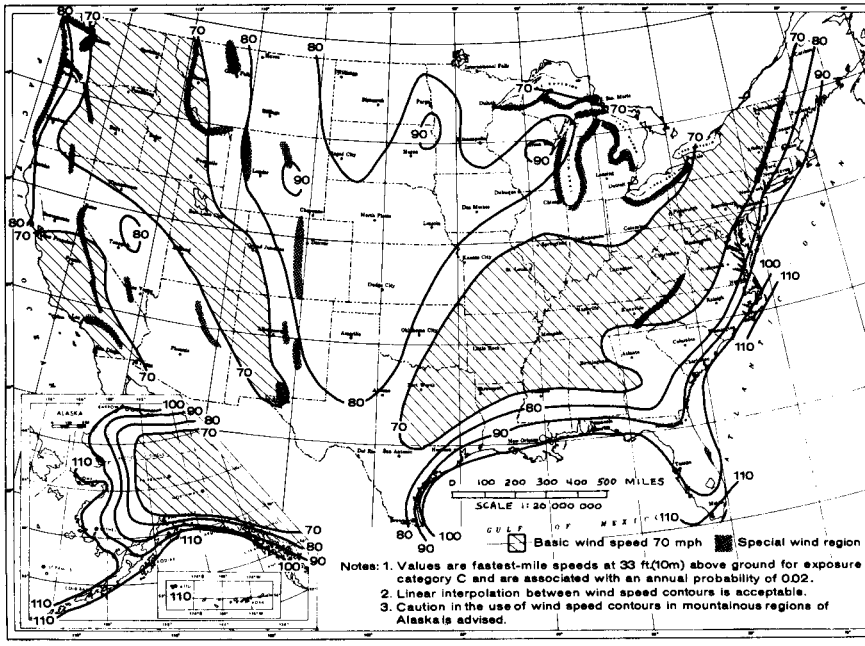

Figure 2.8 Wind velocity map. (*Reproduced from ANSI A58.1-1982 by permission*)

account the terrain effect on design wind loads for buildings. A brief description of these categories follows:

Exposure A: Heavily built-up urban locations protected by surrounding buildings with at least 50 percent of the buildings being more than 70 ft (21.4 m) in height.

Exposure B: Urban and suburban areas, towns, city outskirts, wooded areas, or other terrain with obstructions having the size of single-family dwellings or larger.

Exposure C: Flat, open country and grasslands with scattered obstructions [generally less than 30 ft (9.14 m)].

Exposure D: Flat, unobstructed coastal areas directly exposed to wind flowing over large bodies of water.

The gradient height varies from a high of 1500 ft (457 m) for densely built up urban locations (exposure A) to a low of 700 ft (213.4 m) for coastal areas (exposure D). The corresponding values for exposures B and C are, respectively, 1200 and 900 ft (366 and 274 m).

6. Determine the velocity pressure exposure coefficient K_z, which depends on the type of exposure and height above ground. This is

determined by using the power law expressions given in ANSI; thus

$$K_z = 2.58\left(\frac{Z}{Z_g}\right)^{2/\alpha} \qquad \text{for } Z \geq 15 \text{ ft} \tag{2.11}$$

$$K_z = 2.58\left(\frac{15}{Z_g}\right)^{2/\alpha} \qquad \text{for } Z < 15 \text{ ft} \tag{2.12}$$

Z_g is the gradient height above which the frictional effect of terrain becomes negligible. As noted earlier, this height varies with the characteristics of the ground surface irregularities of the building site, which arise as a result of natural topographic variations as well as manmade features.

The power coefficient α is the exponent for velocity increase in height and has values of 3.0, 4.5, 7.0, and 10.0, respectively, for exposures A, B, C, and D. To eliminate the necessity of making these computations, ANSI A58.1-1982 gives a table for computed values of K_z for various exposures up to a height of 500 ft (152.6 m). An extended version of the ANSI table for velocity pressure coefficient K_z for buildings up to 1500 ft (457 m) is given in Table 2.3.

7. Determine the velocity pressure q_z in pounds per square foot

$$q_z = 0.0025K_z(IV)^2 \tag{2.13}$$

8. Determine the design wind pressure P by the relation

$$P = q\bar{G}C_p \tag{2.14}$$

where $q = q_z$ for windward wall at height Z above ground
$q = q_h$ for leeward wall at mean roof height
$\bar{G}$ = the gust response factor
C_p = external pressure coefficient

Experiments conducted in wind tunnels have shown that for nonwindward faces, the wind pressure for the design of main wind-force-resisting systems does not vary appreciably with respect to height. Therefore, in determining external pressure coefficients for these faces, the design pressures are assumed to be uniformly distributed with respect to height and evaluated at mean roof height.

Determination of gust response factor. The wind velocity map presented in ANSI is based on the fastest-mile speed measured at a standard height of 33 ft (10 m) above the ground. The fastest-mile velocity

TABLE 2.3 Velocity Pressure Exposure Coefficient (K_zANSI A58.1–1982)

Height above ground Level Z, ft	K_z			
	Exposure A	Exposure B	Exposure C	Exposure D
0	0.00	0.00	0.00	0.00
15	0.12	0.37	0.80	1.20
20	0.15	0.42	0.87	1.27
25	0.17	0.46	0.93	1.32
30	0.19	0.50	0.98	1.37
40	0.23	0.57	1.06	1.46
50	0.27	0.63	1.13	1.52
60	0.30	0.68	1.19	1.58
70	0.33	0.73	1.24	1.63
80	0.37	0.77	1.29	1.67
90	0.40	0.82	1.34	1.71
100	0.42	0.86	1.38	1.75
120	0.48	0.93	1.45	1.81
140	0.53	0.99	1.52	1.87
160	0.58	1.05	1.58	1.92
180	0.63	1.11	1.63	1.97
200	0.67	1.16	1.68	2.01
250	0.78	1.28	1.79	2.10
300	0.88	1.39	1.88	2.18
350	0.98	1.49	1.97	2.25
400	1.07	1.58	2.05	2.31
450	1.16	1.67	2.12	2.36
500	1.24	1.75	2.18	2.41
550	1.32	1.82	2.24	2.46
600	1.40	1.90	2.30	2.50
650	1.48	1.96	2.35	2.54
700	1.55	2.03	2.40	2.58
750	1.63	2.09	2.45	2.62
800	1.70	2.15	2.49	2.65
850	1.77	2.21	2.54	2.68
900	1.84	2.27	2.58	2.71
950	1.90	2.33	2.62	2.74
1000	1.97	2.38	2.66	2.77
1050	2.03	2.43	2.70	2.80
1100	2.10	2.48	2.73	2.82
1150	2.16	2.53	2.77	2.85
1200	2.22	2.58	2.80	2.87
1250	2.28	2.63	2.83	2.90
1300	2.35	2.67	2.87	2.92
1350	2.40	2.72	2.90	2.94
1400	2.46	2.76	2.93	2.96
1450	2.52	2.81	2.96	2.98
1500	2.58	2.85	2.99	3.00

TABLE 2.4 Exposure Category Constants

Exposure category	α	z_g	D_o
A	3.0	1500	0.025
B	4.5	1200	0.010
C	7.0	900	0.005
D	10.0	700	0.003

shown on the wind speed map is the wind speed in miles per hour based on the shortest recorded time interval in which one mile of wind passed the recording instrument. Wind speed usually varies from approximately 10 mph (4.47 m/s) to a maximum of approximately 60 mph (26.82 m/s), which means the recorded time for one mile length of wind to pass over the recording instrument is anywhere from 1 to 6 min. Gusts of much shorter duration often occur, and these have significantly greater speed. Therefore, the fastest-mile velocity shown on the map is not the greatest wind velocity to be anticipated at that location; a gust factor must be applied to the measured velocity to provide for the effect of turbulence in computing the design wind load. We will now consider determination of gust response factor with respect to two examples.

Example 1 Consider a tall building 550 ft (167.6 m) in height located in Dallas, Texas, with an importance factor $I = 1.0$ and a type B exposure. Assume a rectangular plan dimension of 120 by 180 ft (36.57 by 54.86 m) for the full height of the building. The ratio of height to width, 550/120 = 4.58, is less than 5.0. Therefore, the building can be considered nonflexible for purposes of determining gust response factor. The expression for gust factor G_h is given by the expression

$$G_h = 0.65 + 3.65T_z \tag{2.15}$$

where T_z is the exposure factor at mean roof height given by the relation

$$T_z = \frac{2.35(D_0)^{1/2}}{(Z/30)^{1/\alpha}} \tag{2.16}$$

D_0 is a surface coefficient factor and is given as a function of type of exposure in ANSI Table A6, which is reproduced here as Table 2.4. Substituting the exposure category constants $D_0 = 0.010$ and $\alpha = 4.5$, we get

$$T_z = \frac{2.35\ (0.010)^{0.5}}{(550/30)^{1/4.5}} = 0.123$$

TABLE 2.5 Gust Response Factors G_h and G_z

Height above ground level Z, ft	G_h and G_z			
	Exposure A	Exposure B	Exposure C	Exposure D
0–15	2.36	1.65	1.32	1.15
20	2.20	1.59	1.29	1.14
25	2.09	1.54	1.27	1.13
30	2.01	1.51	1.26	1.12
40	1.88	1.46	1.23	1.11
50	1.79	1.42	1.21	1.10
60	1.73	1.39	1.20	1.09
70	1.67	1.36	1.19	1.08
80	1.63	1.34	1.18	1.08
90	1.59	1.32	1.17	1.07
100	1.56	1.31	1.16	1.07
120	1.50	1.28	1.15	1.06
140	1.46	1.26	1.14	1.05
160	1.43	1.24	1.13	1.05
180	1.40	1.23	1.12	1.04
200	1.37	1.21	1.11	1.04
250	1.32	1.19	1.10	1.03
300	1.28	1.16	1.09	1.02
350	1.25	1.15	1.08	1.02
400	1.22	1.13	1.07	1.01
450	1.20	1.12	1.06	1.01
500	1.18	1.11	1.06	1.00

Notes.

1. For main wind-force-resisting systems, use building or structure height $h = z$.
2. Linear interpolation is acceptable for intermediate values of z.
3. For height above ground of more than 500 ft Eq. (2.5) may be used.
4. Value of gust response factor shall be not less than 1.0.

Substituting T_z in Eq. (2.15), we get

$$G_h = 0.65 + 3.65 \times 0.123 = 1.099$$

For buildings up to 500 ft (152.4 m) in height, gust response factors can be obtained directly from ANSI Table 8, which is reproduced here as Table 2.5. For wind on the broad face of the building, the ratio of plan dimensions is less than 1.0. The combined pressure coefficient for determining wind loads on the main wind-force-resisting system is, therefore, equal to 0.8 + 0.5 = 1.3. The velocity pressure $q_z = 0.0025K_z(IV)^2 = 0.0025K_z\ (1 \times 70)^2 = 12.25K_z$. The design pressure P_1 is given by $P_1 = q_z\, G_h\, C_p = 12.25 \times 1.3 \times 1.099K_z = 17.51K_z$. The variation of P_1 along the building height is then obtained by using values of K_z given in Table 2.3.

Example 2: Assume that the building given in Example 1 is increased to 685 ft (208.8 m) in height and has a natural period of 7 s (i.e., natural frequency f = 0.143 Hz) and a damping coefficient of 0.02. The height-to-width ratio is 685/120

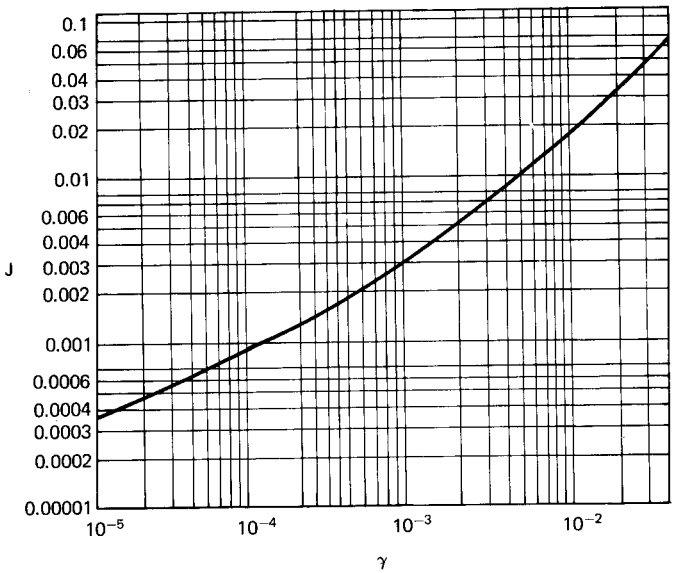

Figure 2.9 Pressure profile factor J as a function of γ. (*Reproduced with permission from ANSI A58.1-1982.*)

= 5.7, and is thus greater than 5. Therefore, the gust response factor is determined by using the expressions and graphs given in ANSI for flexible buildings. The gust factor is given by the relation

$$\overline{G} = 0.65 + \left[\frac{P}{\beta} + \frac{(3.32\ T_1)^2 S}{1 + 0.0002c}\right]^{1/2} \tag{2.17}$$

where P = a power factor = $\overline{f}JY$

$$\overline{f} = 10.5fh/sv \tag{2.18}$$

J = pressure profile factor given as a function of parameter given in Fig. 2.9*

γ = a parameter that depends on the exposure category given in Table 2.6

Y = a resonance factor given as a function of width-to-height ratio c/h of the building in Fig. 2.10

β = the damping coefficient = 0.02 for the example problem

T_1 = the exposure factor evaluated at two-thirds the mean roof height of the structure

*Equations, tables, and graphs presented in this section are reproduced with permission from American National Standard A58.1-1982, *Minimum Design Loads for Buildings and Other Structures*, copyright 1982 by the American National Standards Institute. Copies of this standard can be purchased from the American National Standards Institute at 1430 Broadway, New York, N.Y. 10018.

TABLE 2.6 Parameters S and γ

Exposure category	S	γ
A	1.46	8.20/h
B	1.33	3.28/h
C	1.00	0.23/h
D	0.85	0.02/h

This material is reproduced with permission from American National Standard *Minimum Design Loads for Buildings and Other Structures*, ANSI A58.1–1982, copyright 1982 by the American National Standards Institute. Copies of this standard may be purchased from the American National Standards Institute at 1430 Broadway, New York, NY 10018.

s = the surface friction factor given in Table 2.6
S = the structure size factor given in Fig. 2.11
c = the average horizontal dimension of the building perpendicular to wind direction

We will now proceed to calculate the gust response factor G for the example problem. Surface friction factor s and parameter γ for type B exposures are obtained as 1.33 and $3.28/h = 0.0048$, respectively, from Table 2.6. From Eq. (2.18),

$$\bar{f} = \frac{10.5 \times 0.143 \times 685}{1.33 \times 70} = 11.048$$

From Fig. 2.9, J is obtained as 0.01 for $\gamma = 3.28/685 = 0.0048$, and from Fig. 2.10, resonance factor Y is obtained as 0.045 for $\bar{f} = 11.048$ and $c/h = 0.17$.

$$P = \bar{f}JY = 11.048 \times 0.01 \times 0.045 = 0.005$$

T_1 is calculated at two-thirds the mean roof height by the relation

$$T_1 = \frac{2.35(D_0)^{0.5}}{(2/3 \times 685/30)^{1/4.5}} = \frac{2.35\ (0.010)^{0.5}}{(2/3 \times 685/30)^{1/4.5}} = 0.1283$$

Substituting values for the various parameters in Eq. (2.17), we get

$$\bar{G} = 0.65 + \left\{\frac{0.005}{0.02} + \frac{[3.32\ (0.1283)]^2 \times 0.75}{1 + 0.002 \times 120}\right\}^{1/2} = 1.25$$

The design pressures at various heights of the building can be obtained as before.

External wind coefficients. Wind, when buffeted by buildings of different shapes, produces quite a different loading effect on each face of the building. For example, wind acting on a building of rectangular plan shape produces positive (inward-acting) load only on the windward face of the building; the other three sides are subjected to

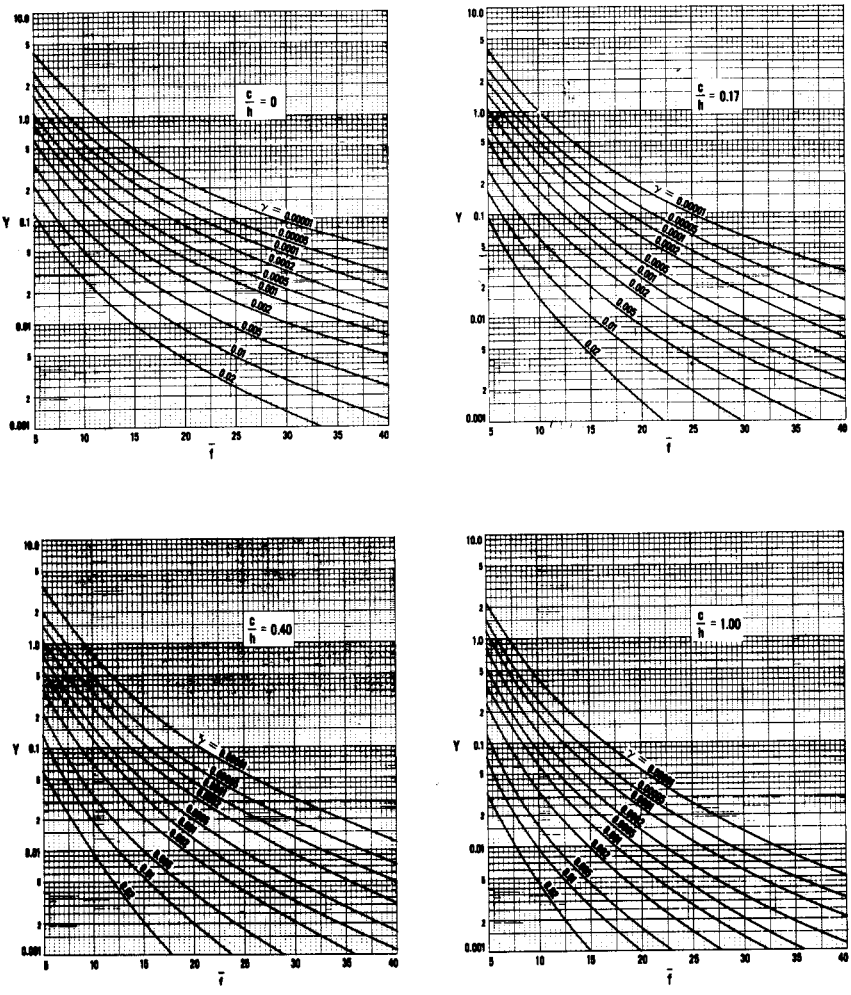

Figure 2.10 Resonance factor Y as a function of γ and the ratio c/h. (*Note*: The four sets of curves correspond to four different values of the ratio c/h.) (*Reproduced with permission from ANSI A58.1-1982.*)

negative (outward-acting) or suction loads. The pressure distribution becomes even more complicated when wind direction is angular to the building face. The distribution of positive and negative pressures is also influenced by the plan aspect ratio of the building. The pressure coefficients on the roof vary with the direction of wind and also with the pitch of the roof. The ANSI standard has assembled a table of pressure coefficient values for walls and roofs of buildings based on wind tunnel tests, actual data collected from full-scale measurements,

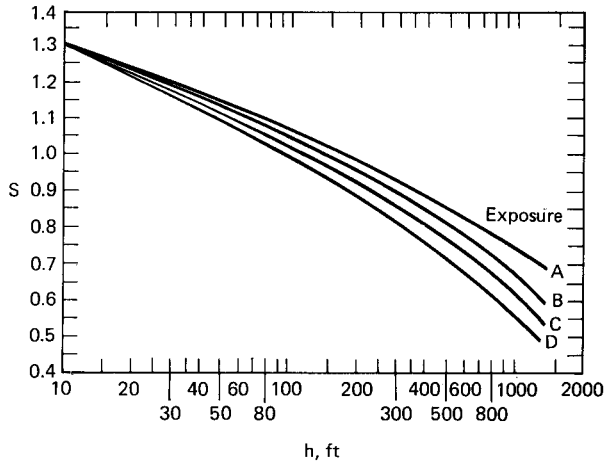

Figure 2.11 Structure size factor S. (*Reproduced with permission from ANSI A58.1-1982.*)

and data published in other standards, such as the Australian standard. The pressure coefficient values for the windward wall are referenced to the velocity pressure q_z. The design wind pressure, therefore, varies with the height above the ground. The coefficients for suction on the leeward wall are referenced to a single velocity pressure that is evaluated at the mean roof height. If the building has a flat roof, it is referenced to the velocity pressure at the top of the building.

Two sets of external pressure coefficients are given, one for determining the overall design forces on the wind-bracing system of the building and the other to determine the design forces on the components and cladding of the building. For the design of cladding, a distinction is made between buildings with a mean roof height of 60 ft (18.3 m) or smaller, and taller buildings. Separate values of pressure coefficients are given for each type.

The values of external pressure coefficients to be used in the design of bracing systems of the buildings are reproduced in a pictorial form in Fig. 2.12. Linear interpolation is permitted for intermediate values of the plan aspect ratio L/B.

The external pressure coefficients to be used in the design of components and cladding of tall buildings are reproduced from ANSI in Fig. 2.13. As in the case of pressure coefficients for the design of the bracing system, the positive pressure-coefficient values for the windward wall are referenced to velocity pressure q_z; thus the positive pressure on the cladding varies with the height above ground. The negative pressure coefficient values for the cladding design on the leeward face and the sides of the building are referenced to the velocity

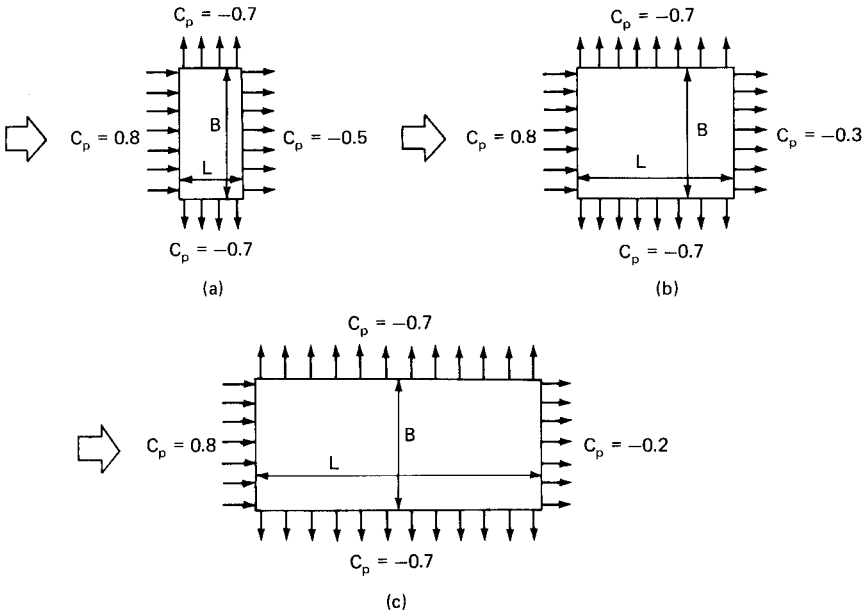

Figure 2.12 Variation of external pressure coefficients with plan dimensions (*a*) $0 \leq L/B \leq 1$; (*b*) $L/B = 2$; (*c*) $L/B \geq 4$.

pressure q_h evaluated at the mean roof height of the building. Since the wind can blow from any direction, each component and cladding member should be designed for maximum positive and negative pressure. In determining the design forces on the cladding, due consideration should be given to its location and its tributary area. Similar to the live load reduction allowed for gravity design of members based on the tributary area of loading, some reduction in design pressure is allowed for in the lateral design of cladding components.

Internal pressure coefficients. Another important consideration in the design of cladding of tall buildings is the pressure existing within the building. This pressure is the accumulative effect of wind seepage through the building enclosure, mechanical ventilation and air conditioning, and stack effect. The stack effect, which is also called the chimney effect, is a result of temperature difference between the interior and exterior of the building and is particularly significant in tall buildings in the colder climates. The internal pressure also depends on either the intentional openings in curtain walls, such as operable windows, or accidental openings likely to be caused because of glass breakage during windstorms. Because loss of window glass during high winds cannot be predicted with any certainty, the net

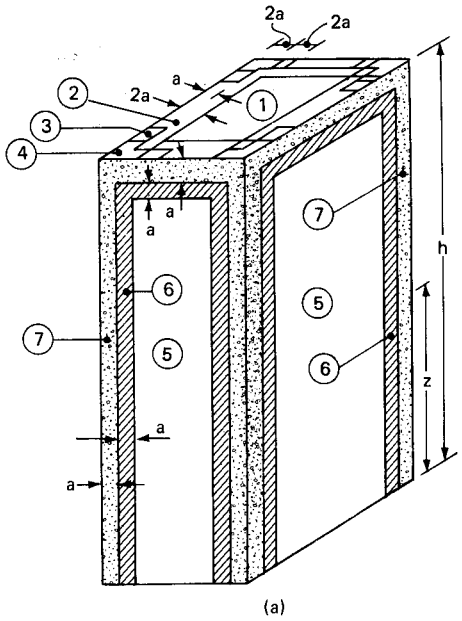

Figure 2.13 External pressure coefficients for cladding design. (*a*) Schematic elevation identifying various zones. (*Adapted from ANSI A58.1 1982.*)

internal pressure is variable in character and seldom can be predicted with great accuracy. On the basis of information gathered through wind tunnel tests conducted primarily on low-rise buildings, ANSI gives a value of ± 0.25 for GC_{pi}, the internal pressure coefficient for buildings with uniformly distributed openings in the walls. For other cases, the value of GC_{pi} could vary from a positive value of 0.75 to a suction value of -0.25. Note the suffix G in the expression for internal pressure coefficient, which signifies that the values are combined values of gust response and internal pressure coefficient.

2.6 Cladding Pressures

2.6.1 Introduction

In recent years the design of cladding for lateral loads has become a major concern to architects and engineers. Although the failure of exterior cladding resulting in broken glass or falling cladding may be of less consequence than major collapse of the structure, the expense of its replacement and hazards posed to pedestrians require that careful attention be given to its design. Cladding breakage in a windstorm is a complicated phenomenon as witnessed in hurricane Alicia, which

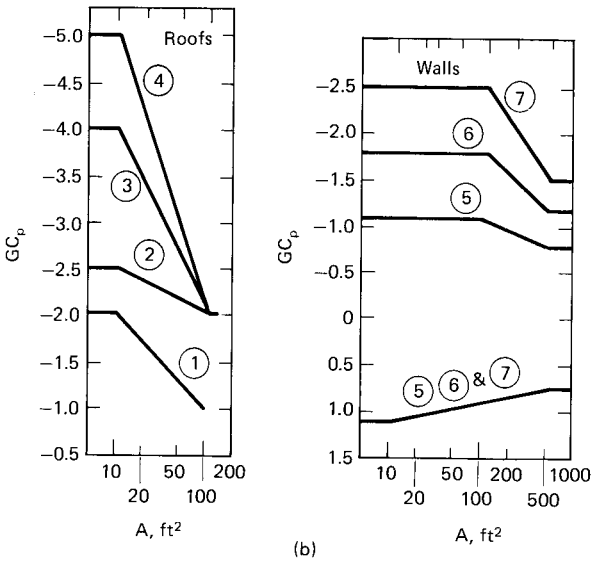

Figure 2.13 (*Continued*) (*b*) Relation between pressure coefficient and tributary area. Notes: (1) Vertical scale denotes GC_p to be used with appropriate q_z or q_h; (2) horizontal scale denotes tributary area A, in square feet; (3) use q_h with negative values of GC_p and q_z with positive values of GC_p; (4) each component shall be designed for maximum positive and negative pressures; (5) if a parapet is provided around the roof perimeter, zones 3 and 4 may be treated as zone 2; (6) for roofs with slope of more than 10°, use GC_p from ANSI A58.1 Fig. 3*b* and attendant q_h based on exposure C; (7) plus and minus signs signify pressures acting toward and away from the surfaces, respectively; (8) notation: g: 5% of minimum width or $0.5h$, whichever is smaller; h: mean roof height, in feet; z: height above ground, in feet. (*Reproduced from ANSI A58.1 1982 with permission.*)

blew into Galveston and downtown Houston on August 18, 1983 causing breakage of glass in several tall buildings. Wind forces play a major role in glass breakage, which is also influenced by other factors, such as solar radiation, mullion and sealant details, tempering of the glass, double or single glazing of glass, and fatigue. It is known with certainty that glass failure starts at nicks and scratches which may be caused during manufacturing and handling operations.

At the time of this writing, there is no analytical approach available for the rational design of curtain walls. Although most codes have tried to identify regions of high wind loads around the building surface, the modern trend in architecture of using nonprismatic and curvilinear plan shapes for high-rise buildings, combined with the unique topography of the surrounding site, has necessitated experimental determination of wind loads for each building.

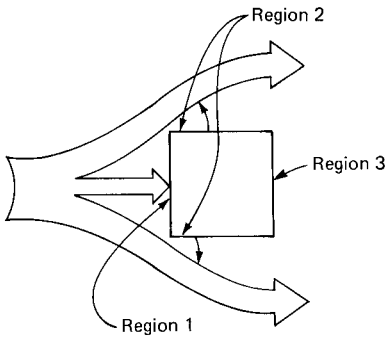

Figure 2.14 Distribution of pressures and suctions.

It has become routine to obtain the design information concerning the distribution of wind pressures over the surface of the building by conducting wind tunnel studies on small scale models. In the past two decades, the modern curtain wall has developed into an ornamental item and has emerged as a significant element of the building. Sizes of window panes have increased considerably, requiring that the glass lights be designed as structural elements for various combinations of forces due to wind, shadow effects, and temperature movement. Glass in curtain walls not only has to resist large forces, particularly in tall buildings, but must also be designed to accommodate the various distortions of the total building structure. Breaking of large panes of glass in tall buildings can cause serious damage to neighboring properties and can injure pedestrians.

2.6.2 Distribution of pressures and suctions

It has been known for some time that when air flows around the edges of a structure, the pressures produced at the corners are much in excess of the normal pressure on the center of elevation, as evidenced by damage caused to corner windows, eave and ridge tiles, etc., in a windstorm. Wind tunnel studies conducted on scale models of buildings have shown that three distinct pressure areas are developed when wind blows on a tall building. These are shown schematically in Fig. 2.14 and are listed below.

1. Positive-pressure zone on the upstream face (Region 1)
2. Negative pressure zones at the upstream corners (Regions 2)
3. Negative pressure zone on the downstream face of the building (Region 3).

Highest negative pressures are created in the upstream corners designated as Regions 2 in Fig. 2.14. These have been measured in

wind tunnel investigations and also have occurred in practice. Wind pressures on the building surface are not constant, but fluctuate almost continuously. The positive pressure on the upstream or the windward face fluctuates more than the negative pressure on the downstream or the leeward face. The negative-pressure region remains relatively steady as compared to the positive-pressure zone. The fluctuation of pressure is random with time and also varies from point to point on the building surface. Therefore, the design of the cladding is strongly influenced by local pressures. As mentioned earlier, the design pressure on cladding can be thought of as a combination of the mean velocity and the fluctuating velocity of wind. As in the design of buildings, whether or not the pressure component arising from fluctuating velocity of wind is treated as a dynamic load or as a pseudo-static load is a function of the period of the cladding. The period of cladding on a building is usually on the order of 0.2 to 0.02 s, which is very much shorter than the period it takes for wind to fluctuate from a gust velocity to a mean velocity. Therefore, it appears that it is sufficiently accurate to consider both the static and the gust components as equivalent static loads in the design of cladding.

Strength of glass, and indeed any other cladding material, is not known in the same manner as for steel or concrete. For example, it is not possible to buy glass based on yield strength criteria as for concrete or steel. Therefore, the selection, testing, and acceptance criteria for glass must necessarily be based on statistical probabilities rather than on absolute strength. The glass industry has addressed this problem, and commonly uses eight failures per thousand lights of glass as an acceptable probability of failure in the selection of glass.

2.6.3 Local cladding loads and overall design loads

In the practice of structural engineering in the United States and western European countries, the structural engineer's concern and responsibility are to determine the overall load for the designing of the building structure. It is generally the architect's responsibility to design the building skin to withstand the local wind loads. The overall wind load, which is the composite effect of positive and negative pressures that govern the design of the building structure, is needed by the structural engineer in order to determine the required strength and stiffness of the building frame. The local wind loads which act on the various areas of the building enclosures are needed by the architect for dictating the strength and stiffness of wall and roof elements and for specifying the adequacy of their fastenings. The two types of loads differ significantly, and it is important that these differences be

understood. The inherent differences between the two types of loading are:

1. Local winds are more influenced by the configuration of the building surface on which they act than the overall loading.
2. The local load is the maximum load that may occur at any location at any time on any wall surface, whereas the overall load is the summation of all loads (with due regard to their sign) occurring simultaneously on all the building surfaces.
3. The intensity and character of local loading for any given wind direction and velocity differ substantially on various parts of the building surface, whereas the overall load is considered to have a specific intensity and direction.
4. The local loading is sensitive to the momentary nature of wind, but in determining the critical overall loading, only gusts of about 2 s or more are significant.
5. Generally, maximum local loads are of greater intensity than the overall load and are usually negative in character.
6. Internal pressures caused by leakage of air through cladding systems have a significant effect on local loads but usually are of no consequence in determining the overall load.

The relative importance of providing for these two types of wind loading is quite obvious. Although the results of underestimating the overall wind load on a building are likely to be tragic, very few, if any, buildings have been toppled by winds. There are no classic examples of building failures comparable to the Tacoma bridge disaster. On the other hand, local failures of roofs, windows, and wall cladding are not uncommon, and in aggregate such failures have cost millions of dollars.

The analytical determination of the actual wind pressure or suction existing at a given point on the surface of a building under a given wind direction and velocity is a very complex problem. Contributing to the complexity are the vagaries of wind action as influenced both by adjacent surroundings and the configuration of the wall surface itself. Much more research is needed on the microeffects of such architectural features as projecting mullions and column covers and deep window reveals. In the meantime, increasing use of model testing in boundary layer wind tunnels is providing vital information on wind loads on building surfaces.

Probably the most important fact established by these tests is that the negative or outward-acting wind loads on wall surfaces are greater

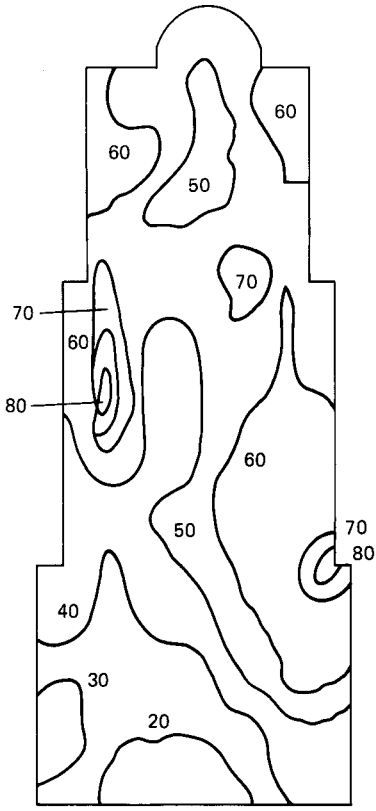

Figure 2.15 Distribution of positive pressures, in psf.

and more critical than had formerly been assumed. It may be as much as twice the amount of the positive loading. In most instances of local wall failure, glass or panels have been blown off of the building, not into it, and the majority of such failures have occurred in areas near the building corners. Obviously this underlies the importance of giving careful attention to the design of both anchorage and glazing details to resist outward-acting forces, especially near the corners of high-rise buildings.

Another feature that has come to light from model testing is that wind loads, both positive and negative, on tall buildings do not vary in proportion to height above ground. Typically, the positive-pressure contours instead of being horizontal are usually found to follow a more concentric pattern such as illustrated diagrammatically in Fig. 2.15, with the highest pressure being near the upper center of the facade and pressures at the very top being somewhat less than those a few stories below the roof.

2.7 Wind Tunnel Engineering

2.7.1 Introduction

It is fairly easy to visualize wind loading as an equivalent horizontal load causing shear and overturning effects on a building. But the complex action of wind, with its turbulent fluctuations about a mean value, drag, vortex shedding, and separation effects, not only results in shear and overturning effects but also induces dynamically fluctuating loads on the overall structure and its smaller components such as curtain walls. Methods of analysis which can be used to predict the complicated flow of wind and its effect on the response of the building and its components have not been developed for routine office use. In the design of very tall buildings it is recognized that use of the wind tunnel approach is a more refined method for arriving at design wind loads. Although some uncertainties still exist in the wind tunnel tests because of the complicated characteristics of natural wind, in today's engineering practice, wind tunnel results are the state of the art in tall building design.

Although wind tunnel model testing has gained wide acceptance, it is important to note that the action of wind in many situations is adequately covered in existing codes. It is therefore necessary to identify situations where wind tunnel tests are required in order to achieve reliable structural performance. Also, wind tunnel model studies generally indicate lower wind loads than prescribed in the codes and lead to more cost-effective designs. Although it is hard to quantify which buildings need to be selected as candidates for wind tunnel tests, it is prudent to include those buildings which have an unusual sensitivity to the action of wind and generally fall outside existing experience. Buildings with unusual aerofoil shapes and which are torsionally flexible may need to be wind-tunnel-tested even when height is not a major design consideration. Prismatic shapes, as a rule of thumb, can be considered as candidates for wind tunnel test when the height exceeds the range of 40 to 50 stories.

Use of wind tunnels for testing buildings has been an offshoot from aeronautical engineering. From time immemorial, builders have known something about the wind factor, at least from experience, and used this more or less crudely in their designs. Gustave Eiffel, the noted engineer and constructor of the 984-ft (300-m) tower for the Paris Exposition of 1889, was the first one to use an assumed wind loading on a major building-like structure. However, it was not until early this century with the coming of the airplane that the methods necessary for the understanding of aerodynamics began to appear. At first, methods were crude and results were largely empirical. Later, with the greater complexity of engineering systems brought about by

the Second World War, wind engineering analysis developed rapidly. A renewal of concern among engineers with the effects of wind on buildings and structures was brought about by the collapse of the Tacoma Narrows Bridge in 1940. This suspension bridge was designed to resist a steady wind of at least 100 mph (44 m/s). However, a few months after completion, the main span began to oscillate in both horizontal and torsional modes under a wind speed of 42 mph (18.8 m/s). Within a few hours, the vibrating structure literally tore itself apart. This episode led to an extensive study of the effect of wind on structures. All the studies were conducted in aeronautical wind tunnels with relatively short sections.

In aeronautics, it is necessary to duplicate the flow of wind at high altitudes. Wind above gradient height is uniform with very little turbulence. The impact of turbulent flow (which is typical of the wind that blows on structures) on the wind tunnel measurements was not understood until 1958, and since then the techniques for modeling wind effects have improved considerably. Today, there are over 20 wind tunnel facilities in North America alone, attesting to the rapid growth in the field of wind engineering and more specifically wind tunnel testing of buildings and structures.

2.7.2 Description of wind tunnels

Aeronautical wind tunnels are designed to minimize the effects of turbulence and the boundary layer because the majority of airplane flights, except for brief periods of landing and takeoff, occur at a height well above the so-called boundary layer. Building activity, on the other hand, occurs precisely within this atmosphere boundary layer, which is characterized by the gradual retardation of wind speed and high turbulence near the surface of the earth. Therefore, aeronautical wind tunnels are not directly suitable for measuring wind effects on buildings. Existing aeronautical wind tunnels have been modified and entirely new facilities have been built in an effort to reproduce the natural flow of wind within the boundary layer.

Wind tunnel facilities in North America vary in size and shape, with testing facilities ranging from 5 to 20 ft (1.52 to 6.1 m). The essential features of a boundary layer wind tunnel are that it should:

1. Be large enough to contain models with enough clearance to facilitate easy installation and removal.
2. Be large enough to generate a natural wind profile over a wide range of speeds. The turbulence generated should match that found in the atmosphere.

3. Provide for a rotating model.
4. Be capable of employing a wide range of testing techniques with very low wind speeds of 1 to 2 mph (0.4 to 0.9 m/s) for smoke visualization and higher speeds of 60 to 70 mph (25 to 31 m/s) for wind pressure measurements and to meet the dynamic similarity parameters.

Various approaches are used in the aeronautical tunnels to generate turbulence and a thickened boundary layer, such as screens, spires, and grids. Special boundary layer wind tunnels have been in use with a long test section in which a thickened turbulent boundary layer is generated by installing appropriate roughness elements in the upstream flow. Another approach is to use a counterjet technique. In every case there is always some question whether the natural wind turbulence characteristic is appropriately modeled and proper gust simulation is included. The degree of scaling required to appropriately account for these may yield a very extreme scale for the building on the order of 1:500 or even more for urban environment studies.

A relatively stable turbulent boundary wind layer with duplicated mean velocity profile can be achieved in a 65- to 100-ft (20- to 30-m) long tunnel. The floor of the tunnel is covered with appropriately located roughness elements consisting of blocks of Styrofoam or other suitable material. At the test section located at the end of a long fetch, a test model is installed in a surrounding consisting of duplicate models of the actual buildings that are around the building being tested.

Although the techniques used in the wind tunnel facilities to simulate turbulent flow vary considerably, it is generally agreed that the techniques reproduce the near flow of wind with reasonable accuracy.

2.7.3 Objectives of wind tunnel tests

The objective of wind tunnel tests, as noted before, is to study as precisely as possible the effect of natural wind on the buildings. Topics that are important with regard to high-rise buildings are:

1. Boundary layer vertical profiles and turbulence intensities
2. Intensity and duration of extreme winds
3. Influence of nearby structures and the effects of the proposed building on the behavior of an existing building
4. Wind loading on tall buildings as related to:
   a. Drag, vortex shedding, and separation
   b. Dynamic response
   c. Loads on cladding and glass

5. Near zone effects—stability of vehicles and pedestrians
6. Motion tolerance—occupancy discomfort
7. Legal factors
   a. Buffeting of downstream structures
   b. Missile damage caused by other structures
8. Moisture penetration of buildings
9. Study of solutions for problematic snow accumulation and pollution control problems

Although not common, sometimes model testing is undertaken to study the effect of wind on various building configurations in order to determine the most suitable building shape. The structural engineer engaged in the design of tall buildings relies on the wind engineer to obtain the following quantitative data for use in the building design.

1. The intensity and scale of pressure fluctuations on exterior panels and glass surfaces
2. The overturning moments and shears that should be used in the building design
3. The oscillation response of the structure, in terms of becoming a major creature comfort problem
4. The change in the wind environment at the ground in terms of it becoming uncomfortable or even dangerous to pedestrians

A brief description of these items, which are of immediate interest to the engineer and architect, is given in the next section.

2.7.4 Rigid model studies

Within the past 20 years, the field of wind engineering has experienced tremendous growth and has become a primary tool for assessing the wind load characteristics on tall buildings. Daring architectural forms executed with lightweight building materials have created a compelling need to obtain a better description of the wind effects than described in the codes. Analytical approaches that take into account the specific design parameters created by the uniqueness of the building shape, near field turbulence characteristics of wind, etc., are not readily available for use in practice. Cladding pressure study is of great concern to the professional architectural engineer because of the large number of inadequately performing or failed curtain wall systems. Although some of the more advanced building codes have attempted to establish design loads with due considerations to shape factors, turbulence, and dynamic characteristics of buildings, it has

become industry practice to resort to wind tunnel tests because it is generally felt by owners and developers that the confidence in cladding wind loads obtained in wind tunnels far outweighs the cost. Many curtain wall suppliers in North America hesitate to undertake jobs if the cladding pressure studies are not available. Although the cladding results may show a larger dispersion with lower than code pressures in some areas and larger ones in others, the risk factor associated with the larger rather than the economic implications of the lower loads is the prime motivation behind the curtain wall pressure study.

Although the basic purpose of rigid model study is to obtain the local pressure fluctuations, the results can nevertheless be extrapolated to obtain the design pressure on the overall structural system for buildings that are not sensitive to aeroelastic interaction. A brief description of experimental and analytical techniques used for obtaining the cladding and overall design loads is given in the following section.

Modeling criteria. The underlying principle in model studies is that forces acting on the model should be proportional to the forces on the prototype. The four forces usually considered in fluid mechanics (of which wind engineering can be considered a branch) are inertia, gravity, viscosity, and surface tension. Usually it is not possible to have all forces in the model in the same proportions as they are in the prototype, and in most model studies it is sufficient to have only two forces the same without introducing serious errors. The inertial force, which is generally a predominant force, and one other force are made proportional. In fluid mechanics three nondimensional parameters are used to represent the ratios of forces of gravity, viscosity, and surface tension to the force of inertia and are called, respectively, Froude number, Reynolds number, and Weber number. Depending upon the nature of the problem being investigated, equality among different numbers is sought. For example, equating the Froude numbers of the model and prototype ensures that the gravitational and inertial forces are in the same proportions. Likewise, similarity of Reynolds numbers assures that viscous and inertial forces are in the same proportion. Equating the Weber numbers results in proportionality between surface tension and inertial forces.

In wind tunnel tests of structures it is important to simulate the mean wind profile, the turbulence intensity, and the length scale of turbulence within the atmospheric boundary layer. The gradual retardation of the wind speed as it approaches the ground results in the wind profile. The wind turbulence intensity is a measure of the velocity fluctuations, which increase with the terrain roughness and are more predominant near the ground. The effect of turbulence extends to a height of 500 ft (152 m) or so in the boundary layer.

To simulate the wind profile correctly in a wind tunnel, it is necessary to have geometric and kinematic similarity of the wind velocity gradients, intensities of turbulence, and turbulence spectrums between the prototype and the model. Dynamic similarity is not required since the fluid employed for testing is the same as the prototype.

The effect of rotation of the earth on the wind profile depends upon the geographical location of the building. Rotation effects are greatest at the poles and smallest at the equator. This effect is neglected in wind tunnel tests. The wind velocity gradient governs the mean wind load; the intensity of turbulence influences the magnitude of the pressure fluctuation; and the turbulence spectrum affects the aeroelastic interaction between the wind and the building. Wind profile, as mentioned earlier, is simulated in a number of ways. Placing of screens, stacked plates, or honeycombs of varying thicknesses in the wind tunnel are some of the methods used to generate a velocity profile. Although they are quite effective in simulating the velocity profile, they cannot be used to control the turbulence characteristics. However, the boundary layer which grows along a sufficiently long stretch of wind tunnel gives a good simulation of turbulence. Therefore, when the length of the wind tunnel is limited, some artificial method of creating the turbulence is required. Barriers, mixing devices, and grids are some of the devices used to assist in the generation of turbulence.

Most commonly, pressure study models are made from methyl methacrylate sheets. This material is commonly known as Plexiglas, Lucite, and Perspex and has several advantages over wooden or aluminum alloy models in that it can be easily and accurately machined and drilled and is transparent, facilitating observation of the instrumentation inside the model. It can also easily be formed into curved shapes by heating the material to about 200°C. Model panels can either be cemented together or joined by using flush-mounted screws.

A scale model of the prototype in a 1:300 and 1:500 range is constructed by the wind tunnel laboratory using drawings that are usually provided by the architect. In a rigid model, important building features which have significance in regard to the wind flow, such as building profile, protruding mullions, and overhangs, are simulated to the correct length scale. Because the model is rigid, measurements are obtained only for the mean and fluctuating pressures acting on the building. In a rigid model study no attempt is made to simulate the dynamic response characteristics of the building. Characteristics, such as the mass and stiffness distribution which determine the natural frequency and mode of vibration, together with the damping characteristics, are precisely the features that require simulation in an elastic model study as discussed later in this chapter.

(a)

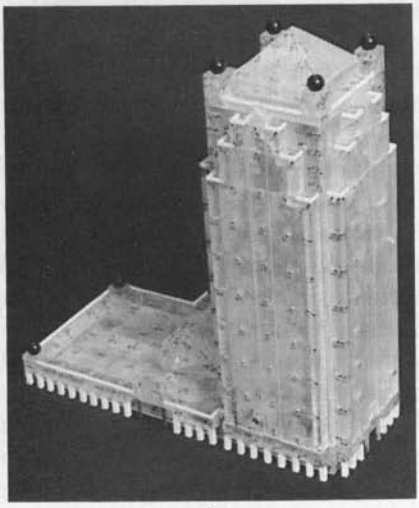

(b)

Figure 2.16 (*a*) Rigid model of high-rise building in wind tunnel. (*b*) Closer view of pressure models. (*Photographs courtesy of Dr. Peter Irwin of Rowan, Williams, Davis & Irwin, Inc.*)

Measurement techniques. The model is instrumented with a large number of pressure taps, sometimes as many as 500 to 700, and is tested in a boundary layer wind tunnel in the presence of a detailed modeling of the nearby surroundings within a radius of 1500 ft (457/m), as shown in Fig. 2.16. Flexible, transparent vinyl or polyethylene tubing of about $\frac{1}{16}$-in (1.5-mm) internal diameter is used as pressure tappings and is located around the exterior surface of the model. Generally a liberal number of tappings are deployed around the

model surface to obtain a good distribution of pressure. Pressure tap locations are generally more concentrated in regions of high pressure gradients such as around corners.

The pressure tappings are connected by short plastic tubing to miniature electronic pressure transducers. The length of plastic tubing is kept as short as possible to minimize damping of fluctuating pressure by the column of air trapped in the tube. Pressure transducers are used instead of monometers because of the ability of transducers to measure fluctuating loads.

It is not usually feasible to attach a separate transducer to each of the pressure tappings for reasons of economy and available space. Therefore, the pressure transducer is mounted to a pressure-scanning device such as a Scanivalue, which has the capability to automatically switch the pressure transducer to as many as 40 or 50 pressure taps one at a time. The electrical output signals from the transducers are processed through a computerized automatic data acquisition system. The pressure transducer is calibrated such that the electrical output signal is converted to an equivalent pressure or velocity. Static pressure upstream of the tunnel is used as reference, since only the pressure differentials are measured by the transducer. The pressure data acquisition is done by an on-line computer system capable of sampling data in a short period of time.

The wind tunnel test is run for a duration of about 60 s, which corresponds to approximately 1 hour in real time. Sufficient numbers of readings are obtained from each port to obtain a stationary value such that fluctuations become independent of time. From the values thus obtained, the mean pressure and the root-mean-square value of the pressure fluctuations are evaluated. The rate of sampling of the pressure signal by the computer corresponds to a very small time interval, such as half a second at full scale. The computer record is divided into subintervals, and the maximum and minimum values of pressures are calculated for each subinterval. These individual maximum and minimum values are used in an extreme-value analysis to determine the most probable maximum and minimum values applicable for the whole sample period.

The boundary layer wind tunnel, by virtue of having a long working section with roughened floor and turbulence generators at the upwind end, is expected to correctly simulate the mean wind speed profile and turbulence of natural wind. The model is mounted on a turntable, thus allowing any wind direction to be simulated by rotating the model to the appropriate angle. As in other wind studies, it is necessary to simulate the features surrounding the building under study. Generally polystyrene foam is used to simulate the near field characteristics because of the ease of construction. The building model and the near

field characteristics are mounted on a turntable in the test section and rotated to change the direction of the wind.

Cladding pressures. Measurements are taken for all wind directions spaced at about 10 to 20° apart. The data are then converted into pressure coefficients that are derived from the measured dynamic pressure of the wind above the boundary layer. From the data acquired, full-scale peak exterior pressures and suctions for selected return periods at each tap location are derived by combining the wind tunnel data with a statistical model of windstorms expected at the building site. The results are given for various return periods such as 25, 50, and 100 years. A detailed account of the probability procedure used by wind engineers to analyze the meteorological data and to combine this information with the wind tunnel results to produce the peak suction and pressure values at each port is beyond the scope of this book. Suffice it to say that the method involves fitting the measured data to a probability distribution and computer simulation and analysis of hurricane events.

In order to get a feel for the amount of data that is handled by the computer, let us take a closer look at a practical example. Consider the model shown in Fig. 2.16*a* which is a 1:400 scale model for a 50-story building. Assume the model is instrumented with 703 pressure taps and measurements are taken for 36 wind directions at 10° intervals. If the rate of sampling is half a second at full scale, 120 readings for each port for each wind direction are required for a full-scale test duration of 1 hour. For 703 pressure taps with 36 wind directions, the total number of readings for each configuration is equal to $703 \times 120 \times 36 = 3{,}036{,}960$. This enormous amount of data is condensed into recommended cladding design loads and presented by the wind engineer in the form of block diagrams as shown in Fig. 2.17. Sometimes the information is presented in the form of pressure contours or isobars, as shown in Fig. 2.18.

In evaluating the peak wind loads on the exterior of the prototype, effects of internal pressures arising from air leakage, mechanical equipment, and stack effect should be included. In performing the internal pressure calculations, it may be necessary to take into account the possibility of window breakage caused by roof gravel scoured from roofs of adjacent buildings and other flying debris during a windstorm. As a rough guide, the resulting internal pressure can be considered to be in the range of ± 5 psf (25 kg/m^2) at the base of the building to as much as ± 20 psf (100 kg/m^2) at the roof for a 50-story building. In tall buildings in general, the positive pressures are lower in magnitude than the negative pressures. Wind tunnel study is typically repeated to consider the effects of proposed buildings, and the results of the configuration that gives the highest loads are adapted in the design.

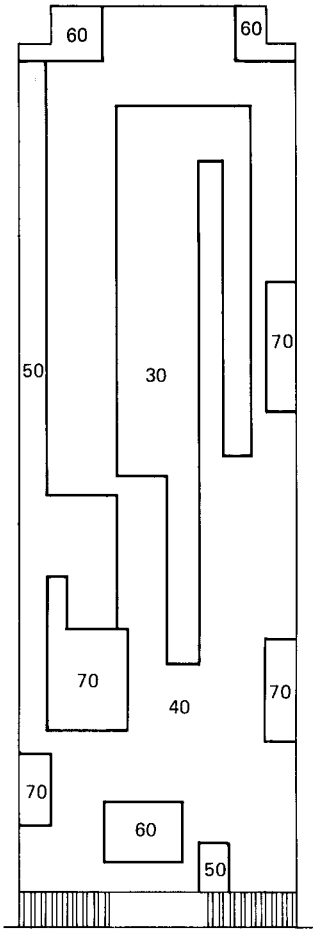

Figure 2.17 Block pressure diagram, in psf.

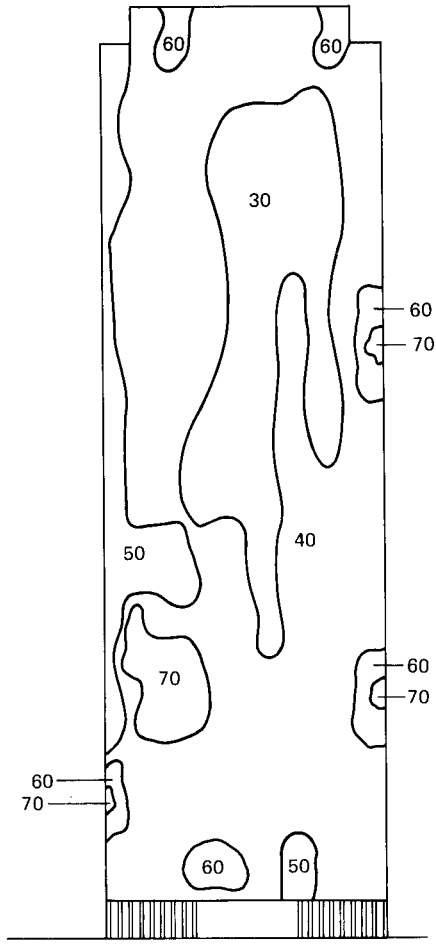

Figure 2.18 Pressure contours, in psf.

In the design of glass, 1-minute loading is commonly used. In wind tunnel study the duration of measured peak pressures is different than the 1-minute interval; usually it corresponds to 5 to 10 s or less in terms of real time. Therefore, it is necessary to use some reduction in peak loads obtained from the wind tunnel tests. Empirical reduction factors of 0.80, 0.94, and 0.97 have been given in glass manufacturers' recommendations for three different types of glass, namely annealed float glass, heat-strengthened glass, and tempered glass, respectively.

Overall building loads. The results obtained in a rigid model test are used to predict the local wind environment for the design of glass and

cladding. However, for buildings that are not dynamically sensitive to wind, the results can be extrapolated to obtain the design pressure on the overall structural system. This procedure involves introducing a gust factor for converting the mean wind load to gust loads. An appropriate gust factor estimation should take into account the averaging period of the mean wind load; the terrain roughness in relation to the building height; the peak gust factor, which depends on the natural frequency of the building; the effect of turbulence; and the critical damping ratio of the building. Rigid model wind study does not take into account all of these factors, yet is considered to provide adequate design data for buildings with a height-to-weight ratio of less than 5.

The procedure for converting results of pressure model tests to obtain overall structural loads can be outlined as follows. The first step is to delineate the exterior surfaces of the building into small zonal areas tributary to each pressure tap. This is similar in procedure to assigning tributary areas for computing gravity loads in column design. The next step is to compute the wind force components F_x and F_y by multiplying the tributary area corresponding to each pressure tap by the mean pressure. A gust factor appropriate to the overall loading is introduced at this stage to convert the hourly mean wind results to include effects of gusts. The components F_x and F_y can be appropriately summed over the building to obtain the distribution of wind loads and by statics the moments at each floor are obtained. Torsional moments are obtained by appropriate summation forces F_x and F_y about the vertical axis.

Although the primary purpose of pressure model study is to obtain the peak loads to be used in the design of glass and cladding, as a by-product it is becoming more and more common to use the results to design the overall structural frame. As compared to the aeroelastic and high-frequency force balance studies, the method used in rigid model study to obtain mean pressure may appear to be tedious, but it should be noted that it is the only test that provides information on the magnitude of local pressure fluctuations, which are essential to an economical and satisfactory design of cladding and glass panels.

2.7.5 Aeroelastic study

Although a good estimate of the mean wind load on the building as a whole can be obtained from rigid model study by integration of local pressures over the surface, the uncorrelated nature of local peak pressures precludes such an integration being carried out for the overall peak dynamic loads. A gust load factor selected for an appropriate wind gust duration, of course, can be used to increase the mean hourly load to that of a gust whose duration is sufficient for its entire effect to be fully felt by the structure. Selection of a proper gust factor that takes into account all the variables present in a wind-structure

interaction is not always obvious. Although many of the interaction effects can be described qualitatively, in practice precise analytical quantification of these effects is not possible. Aeroelastic model study attempts to take the guesswork out of the gust factor computation by measuring directly the dynamic loads in the wind tunnel. The fluctuating aerodynamic loads can be measured on a variety of models ranging from very simple rigid models to models exhibiting the multimode vibration characteristics of tall buildings. The more common types of models that are of immediate interest in the aeroelastic study of tall buildings can be broadly classified into the following two categories: (1) stick models, and (2) multi-degree-of-freedom models.

In this section a brief description of each of these models is presented. Before this is undertaken, a few comments that in general apply to aeroelastic studies are necessary.

General comments. In tall, slender, and flexible buildings, dynamic loads are induced by the buffeting action of atmospheric turbulence. The wind-induced excitations can be significantly amplified by the dynamic response of the building, which contributes up to 50 percent or even more to the total response of the building. Wind-induced horizontal accelerations are also significantly amplified, requiring consideration of occupant comfort and perception of motion. As in the case of rigid model studies, analytical procedures for determining the dynamic effects of wind loads are not available as a design procedure, thus necessitating wind tunnel tests to simulate unique characteristics of the building and its specific setting.

In addition to the similarity of the exterior geometry, the aeroelastic studies require similarity of the inertia, stiffness, and damping characteristics of the building. Although a building in reality responds dynamically to wind loads in a multimode configuration, enough evidence exists to show that the dynamic response occurs primarily in the lower modes of vibration. As a result, it is possible to study the dynamic behavior of the building by using simple dynamic models.

Aeroelastic study basically examines the wind-induced sway response of a tall building, in addition to providing information on the overall wind-induced mean and dynamic loads. These tests are important for slender, flexible, and dynamically sensitive structures where aeroelastic or body-motion-induced effects are of significance. When a tall building sways and twists under wind action, the movement makes the building produce inertial loads, causing fluctuating stresses. At any given instant, the amplitude of twisting and swaying motion is not just a function of the magnitude of wind load at that instant but also depends on the integrated effect of the wind over the several previous minutes. Therefore, it is important to consider the

building's dynamic response when predicting the loads on the structure. In addition to providing an accurate assessment of loads for structural design, an aeroelastic model test provides one of the most reliable approaches to predicting the building response to wind which can be used by the designer to ensure that the predicted motion will not cause discomfort to the building occupants in the upper floors.

Typically, aeroelastic measurements are carried out at several wind speeds covering a range selected to provide information on both relatively common events, such as 10-year wind loads, which may influence the serviceability and occupant comfort, and relatively rare events, such as 100-year winds, which govern the strength design. The modeling of dynamic properties requires the simulation of inertial, stiffness, and damping characteristics. It is necessary, however, to simulate these properties for only those modes of vibration which are susceptible to wind excitation.

It is often difficult to determine quantitatively when an aeroelastic study is required on a building project. The following factors can be used as a guide in making a decision.

1. The building height-to-width ratio is greater than about 5; i.e., the building is slender.
2. Approximate calculations show that there is a likelihood of vortex shedding phenomenon.
3. The structure is light in density on the order of 8 to 10 lb/ft^3 (1.25 to 1.57 kN/m^3).
4. The structure has very little inherent damping, such as a welded steel construction.
5. The structural stiffness is concentrated in the interior of the building, making it torsionally flexible.
6. The calculated period of oscillation is long, on the order of 5 to 10 s.
7. Existence of unusual near field conditions that could create torsional loads and cause strong buffeting action.
8. The building is sited such that predominant winds blow from a direction most sensitive to the building oscillations.
9. The building occupancy is such that the occupants' comfort plays a more predominant role. People in high-rise apartments, condominiums, and hotels are likely to experience more discomfort from building oscillations than those in office buildings.

The development during the past two decades of aeroelastic direct modeling techniques for predicting the behavior of tall buildings has been influenced by the following factors:

1. Tall buildings, although slender from structural considerations, aerodynamically speaking behave more like three-dimensional structures. Therefore, analytical formulations applicable for very slender tall structures such as chimneys cannot be successfully applied to tall buildings.
2. Gust factor methods are inadequate to describe the crosswind response of tall buildings, necessitating aeroelastic studies for slender buildings with a height-to-width ratio greater than 6 or so.
3. In most instances the surroundings have a beneficial shielding effect, but in certain situations the wake buffeting can significantly increase the dynamic response of the building.
4. Current modern architecture often results in buildings which have an erratic distribution of mass because of leaveouts, stepbacks, etc. Response of such buildings tends to be highly complex, defying analytical solutions. The complicated structural features are relatively easy to reproduce physically, thus favoring model testing.
5. Aeroelastic study provides perhaps the most sought after answer to the expected response of the building in terms of human comfort. Acceleration at the upper levels of the prototype can be predicted based on measurements on the model.

Model requirements

1. Characteristics of wind simulated in the wind tunnel should represent the mean and turbulent nature of wind. This requirement is not unique to aeroelastic studies and applies equally to all wind studies of buildings.
2. The depth of boundary layer and the scale of turbulence intensity that can be simulated in a wind tunnel must be consistent with the scale of the model.
3. Although mismatching of Reynolds number is of little concern in turbulent flows, for building shapes that are unusually smooth, special precautions such as scoring the surface of the model may be necessary to increase the turbulence of wind.
4. The model mass and stiffness values should correspond to the prototype values.
5. The damping device attached to the model should represent the damping characteristics of the prototype. Usual values assumed in practice for critical percentage of damping are 1.0, 1.5, and 2.0, for steel, composite, and concrete constructions, respectively.

The entire phenomenon of wind loading on the prototype cannot be modeled in the wind tunnel at a consistent geometric scale. However, it is agreed by researchers in this field that representative results can be obtained as long as the depth of boundary layer and turbulence characteristics are maintained in the wind tunnel.

Rigid aeroelastic models. The main objective of aeroelastic study is to obtain a more accurate prediction of design wind loads and to determine the degree of occupant sensitivity to building motion. For the results to be accurate, it is necessary that the model respond in the same way as the prototype building. Fortunately, this can be achieved without having to miniaturize all the curtain wall or structural member characteristics. It is possible to capture the essential behavior of the prototype by simpler models.

A rigid model is used based on the premise that the fundamental mode of displacement for a tall building, which is made up of a combination of shear and bending action, can be approximated by a straight line. In terms of aerodynamic modeling, it is not necessary to achieve the correct density distribution along the building height as long as the mass moment of inertia about the pivot point is the same as that of the correct density distribution. It should be noted that the pivot point is chosen to obtain a mode shape which provides the best agreement with the calculated fundamental mode shapes of the prototype. For example, modal calculations for a tall building with a relatively stiff podium may show that the pivot point is located at the intersection of podium and the tower. Therefore the pivot point for the model should be at a location corresponding to this intersection point rather than at the base of the building. The springs located near the gimbals are chosen to achieve the correct frequencies of vibration in the two fundamental sway modes. An electromagnet or an oil dashpot provides the model with a damping corresponding to that of the full-scale tower. Figure 2.19 shows a rigid aeroelastic model mounted on gimbals.

An alternate method of obtaining a rigid aeroelastic model is to mount the model on a flexible steel bar attached to a vibration-free table. The width and thickness of the bar are chosen to properly simulate the tower stiffnesses in two horizontal directions. Damping is simulated by employing dashpots. Figure 2.20 shows a schematic elevation of a rigid aeroelastic model mounted to a flexible steel bar. Shown in Fig. 2.21 is a photograph of an aeroelastic model of a 62-story building. In either type of model torsional modes are not simulated because the model effectively rotates as a rigid body about the vertical axis.

In a tall building with a torsionally stiff structural system, such as

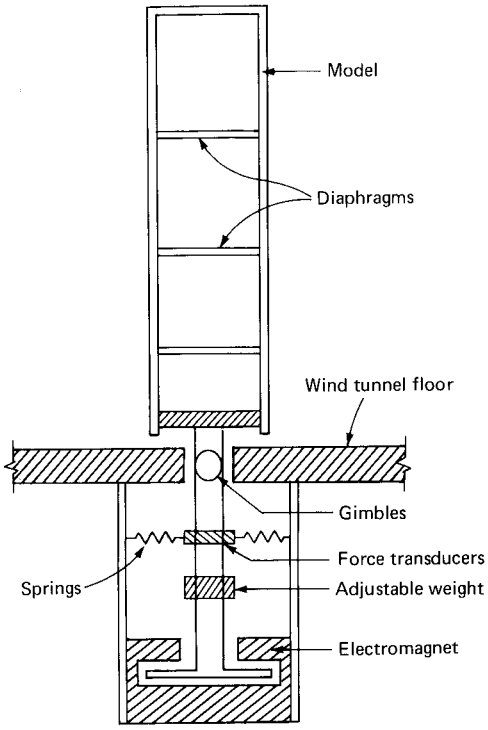

Figure 2.19 Rigid aeroelastic model with gimbal.

a perimeter tube system, the torsional deformation from lateral loads may be of minor consequence when compared to the bending deformations. It is not necessary in such cases to simulate the torsional motions of the prototype in the wind tunnel model. In regard to the sway or the bending deformations, a fairly accurate representation can be obtained by approximating the mode shape by a straight line. A correct distribution of the mass on the model is obtained by building the model with a light material such as balsa wood and then adding weights at appropriate locations. The damping of sway motion can be achieved in a number of ways, such as using hydraulic dampers, springs in two mutually perpendicular directions, electromagnetic devices, or dashpots. As in other types of model testing, certain nondimensional parameters must be made the same on the model as in full-scale building in order for the model to experience the same nondimensional moment, shear force, and acceleration as the prototype. A complete discussion of deducing these nondimensional parameters using classical methods such as Buckingham's PI theorem is beyond the scope of this work.

The quantities that are of interest to the structural engineer are the wind pressure, shear force, moment, and acceleration that occur on the

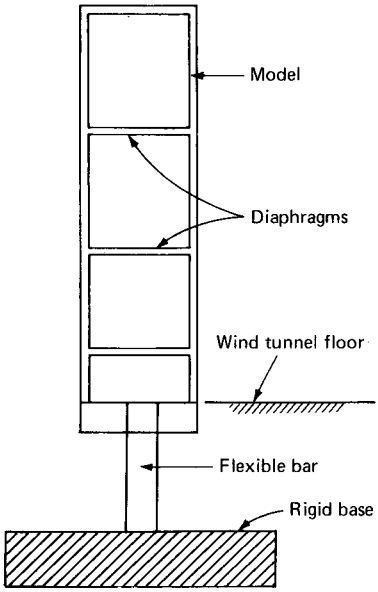

Figure 2.20 Rigid aeroelastic model mounted to flexible steel bar.

full-scale building. These are related to the model quantities by the nondimensional rations of length and the frequency scales as follows:

$$P_p = P_m\left(\frac{N_p^2 b_p^2}{N_m^2 b_m^2}\right) \tag{2.18}$$

$$F_p = F_m\left(\frac{N_p^2 b_p^4}{N_m^2 b_m^4}\right) \tag{2.19}$$

$$M_p = M_m\left(\frac{N_p^2 b_p^5}{N_m^2 b_m^5}\right) \tag{2.20}$$

$$a_p = a_m\left(\frac{N_p^2 b_p}{N_m^2 b_m}\right) \tag{2.21}$$

where P, F, M, and a denote the pressure, shear force, moment, and acceleration, respectively. The subscripts p and m are used to denote the prototype and model quantities.

The model frequency N_m can be any value deemed convenient for testing. Assuming it to be 10 Hz and using a value of 0.166 Hz for N_p, the frequency of the full-scale building which is representative of a

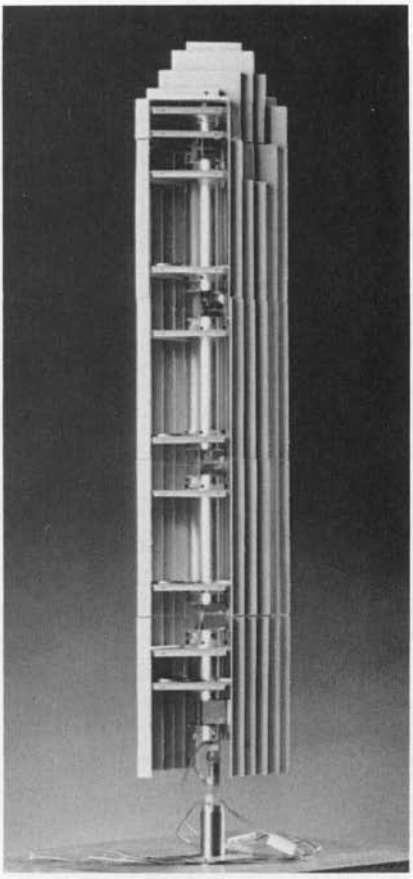

Figure 2.21 A rigid aeroelastic model. (*Photograph courtesy of Dr. Peter Irwin, Rowan, Williams, Davis & Irwin, Inc.*)

60-story steel building, we obtain the ratio $N_p/N_m = 0.0166$. Usually the wind tunnel model is constructed to a length scale of 1:400, giving the ratio $b_p/b_m = 400$. Using these values in Eqs. (2.22) through (2.25), we get

$$P_p = 44.1P_m \tag{2.22}$$

$$F_p = 7.05 \times 10^6 F_m \tag{2.23}$$

$$M_p = 2821.7 \times 10^6 M_p \tag{2.24}$$

$$a_p = 0.11a_m \tag{2.25}$$

The relation between the model time t and full-scale time is given by the relation $t_m = t_p(N_p/N_m)$. The model events in the example are therefore compressed to about one-sixtieth of the full time duration. Thus, 1 hour of full-scale event is typically compressed to 60 s on the model.

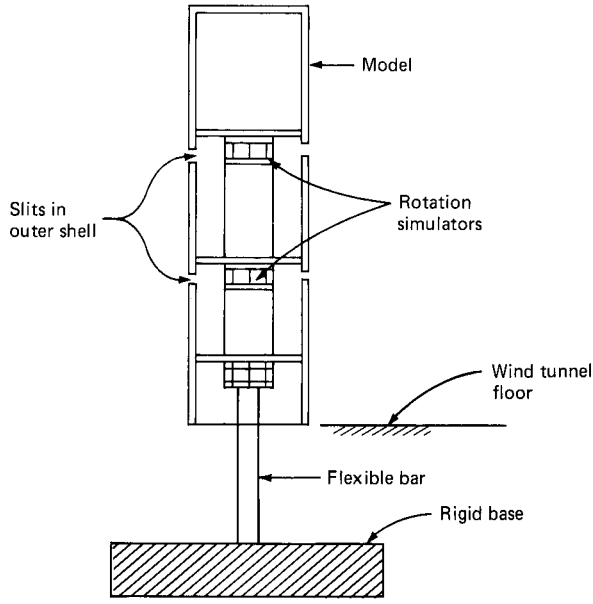

Figure 2.22 Rigid aeroelastic model with provisions for simulating torsion.

Rigid models simulating torsional modes. Torsion is a consequence of unsymmetrical distribution of building stiffness about the shear center, or it may occur because of eccentric disposition of the lateral loads with respect to the center of stiffness of the building. Centrally supported concrete-core buildings often use open section shear walls which may have their shear centers located at considerable distance from the geometrical center of the building. Unless additional lateral resisting elements such as moment frames, braces, or shear walls are used on the building perimeter, the torsional characteristics of the building may play an important role in the overall behavior of the structure. It is necessary in such instances to simulate in the aeroelastic model not only the bending characteristics of the building but also the torsional behavior. This is achieved with sufficient accuracy by introducing torsional springs at appropriate locations along the building height. The torsional mode shapes of the full-scale building are simulated in a stepwise manner by this aeroelastic model. In order to allow one section of the model to rotate relative to the next, the model shell is cut around the periphery. Figure 2.22 shows a schematic representation of a model with two cuts. The two sections of the model with the lumped masses behave as a two-degree-of-freedom system and therefore can capture essential dynamic behavior of the two lowest torsional modes.

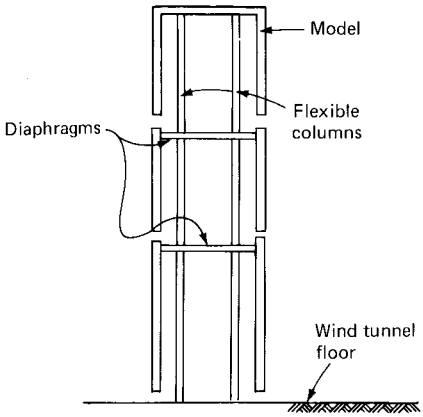

Figure 2.23 Flexible aeroelastic model.

Flexible model. If the building geometry is uniform for the whole height, it is reasonable to assume that the sway modes of vibration vary linearly along the height. By using only the lowest modes, it is possible to obtain acceptable results for the dynamic behavior of the building. However, for buildings of complex shapes with stepbacks and similar major variations in stiffness, this assumption may not yield acceptable results because: (1) the fundamental mode shapes may vary in a manner other than a linear shape, and (2) the higher modes could contribute significantly to the dynamic behavior. In such cases it is essential to capture the multimode behavior of the building in the aeroelastic model. This is achieved by selecting a discrete model comprised of several lumped masses interconnected with elastic columns. A schematic representation of the aeroelastic model of a tall building is shown in Fig. 2.23. The building is divided into three convenient zones, with the mass of each zone located at the center of the zones. In this model the masses are concentrated in the diaphragm representing the floor system and are interconnected by flexible columns. A lightweight shell that represents the building shape encloses the assembly of the floor system, masses, and columns. The shell is made discontinuous in three zones to allow for relative movements between the masses. The similarity between the elastic properties of the prototype and the model can be achieved in varying degrees. For example, the behavior of the so-called shear building in which the girder rotations and column axial deformations are neglected can be duplicated in the model by using a rigid diaphragm and flexible columns. The effect of girder rotations and axial deformation of the columns can, however, be simulated in the aeroelastic model at considerable fabrication effort.

Instrumentation. As mentioned previously, the aeroelastic study is undertaken to obtain forces and moments to be used in the design of the overall structural system and to evaluate the effect of the building motion on the occupants' comfort. Local pressures that are required for the design of the curtain wall and glass are not obtained, nor are the effects of wind on the pedestrian. To obtain the bending and torsional moments and shear forces, strain gauges are attached to the metal bars and calibrated by subjecting the model to known forces. Instrumentation connected to the on-line computer system gives a continuous history of these quantities for a given wind direction and speed. Figure 2.24 shows a schematic representation of measured overturning moments for a period of 3 min at full scale. These figures are for wind buffeting the broad face of the building that is shown schematically in Fig. 2.24. To correlate these measured moments with the physical behavior of the model, it is useful to decompose the continuously varying moments into mean values about which the maximum and minimum values oscillate.

It is easy to visualize that the quasi-static component of the wind on the broad face is giving rise to the mean moment M_x as shown in Fig. 2.24*b*. The oscillations of variable amplitudes that occur about the mean value are a consequence of the dynamic characteristics of the tower motion. They occur primarily at one frequency that corresponds to the fundamental frequency of the building and are caused by the inertial loads somewhat similar to the lateral loads generated during earthquakes. Depending upon the slenderness of the building, it is entirely possible for the dynamic component to be as large as the steady component. Hence in very tall buildings with a height-to-width ratio of greater than 5 or so, it is important to account for peak excursions of the moment rather than just the mean value.

So far, we have discussed only one component of the moment, namely M_x. Wind tunnel measurements typically show that for tall buildings, in addition to this well-understood phenomenon, there is another excitation the building is subjected to, the vortex shedding phenomenon. The building oscillates not only in the direction of wind but also at right angles to it as shown in Fig. 2.24*c*. Often the building motion is greatest in the across-wind direction, with the corresponding overturning moment due to the across-wind motion exceeding that due to alongside wind. As mentioned previously, this phenomenon is rather intriguing and is real for slender buildings. The overturning moment due to alongside wind increases more or less proportionately with the wind speed as expected. The across-wind moment, on the other hand, shows a distinct peak due to vortex shedding excitation. The wind speed at which vortex shedding occurs is a function of Strouls number.

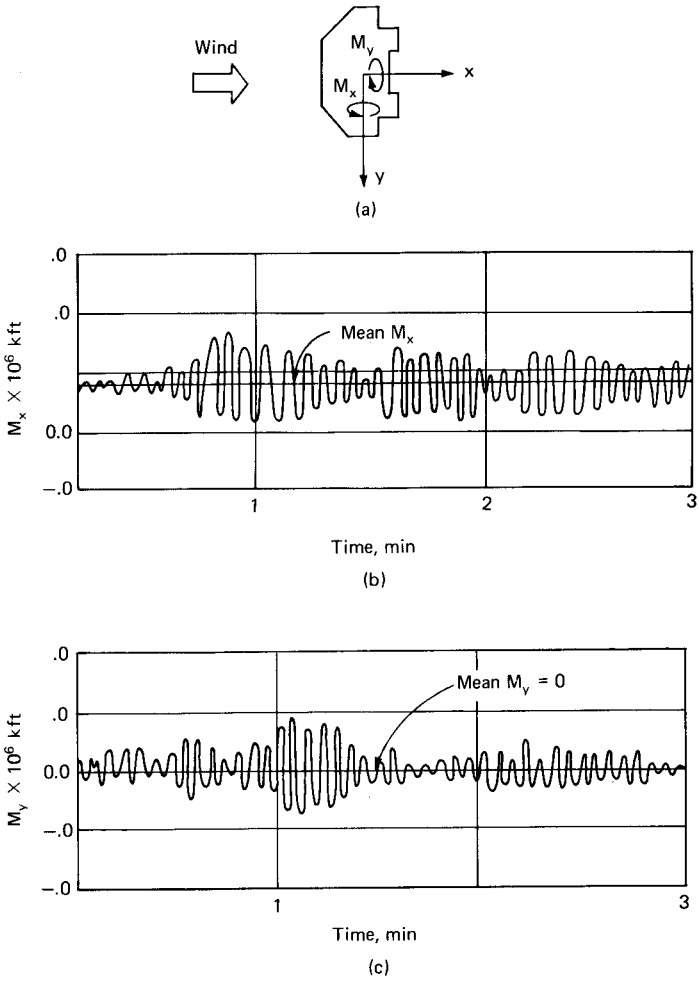

Figure 2.24 Variation of wind moments. (*a*) Building plan; (*b*) moment parallel to wind direction; (*c*) moment perpendicular to wind direction.

If this speed corresponds to the design speed, it is very likely that the building will be subjected to dangerously high moments. One method of substantially reducing the likelihood of vortex shedding is to increase the damping of the building. An alternate approach is to increase the building's natural frequency such that the peak excitation occurs well above the design speed range. Analytical methods are not available for calculating wind speeds that correspond to the peak excitation of buildings of arbitrary shapes subjected to real wind climate, so it is almost mandatory to undertake aeroelastic wind

tunnel test in cases where the vortex shedding phenomenon is suspected.

Derivation of equivalent lateral loads. As mentioned earlier, the response of a tall building to wind loads in general is two-dimensional. For a given wind direction, one would have to consider forces in both the x and y directions. The force occurring at any instant can be considered as the summation of the effects arising from the mean and dynamic components. Aeroelastic testing measures the peak moment at the base of the structure. For structural analysis, however, a floor-by-floor distribution of lateral forces is required. The task then is to convert the measured peak overturning moment into a system of equivalent static forces acting at each floor level. This is achieved as follows. In order to make the description simple it is useful to consider a specific example.

Assume that a model of a 60-story building is tested aeroelastically in the wind tunnel giving peak values of 1,500,000 kft (2,033,700 kNm) and 600,000 kft (813,480 kNm) for base overturning moments M_x and M_y for a particular wind direction. Since these are peak values, they include the effect of dynamic components. Assume that cladding pressure study results are available. As described in previous sections, it is possible to obtain the floor-by-floor loads from the results of the pressure study model by simply integrating the pressure measured at each port over an area corresponding to the tributary area for the port. Summation of these forces times the distance to the base yields the static components of the moments M_x and M_y. Let us assume that these values for the example problem are 1,000,000 and 500,000 kft (1,356,000 and 678,000 kNm). Out of the 1,500,000 kft (2,033,700 kNm) of peak moment M_x we have accounted for 1,000,000 kft (1,356,000 kNm) as the static component. The difference of 500,000 kft (678,000 kNm) that corresponds to the dynamic component remains to be distributed as an equivalent lateral load at each level. This is approximated from the mode shape of vibration and the mass distribution.

The summation of the mean force obtained from the pressure model study and the dynamic force obtained by assuming mode shape distribution yields the equivalent static force to be used in the structural analysis.

Biaxial nature of wind. As mentioned many times, wind tunnel tests are conducted for several wind directions to account for wind's random nature. For a given wind direction, it is highly unlikely that the peak overturning moment about the x axis will coincide exactly in time with the peak overturning moment about the y axis. Therefore it is

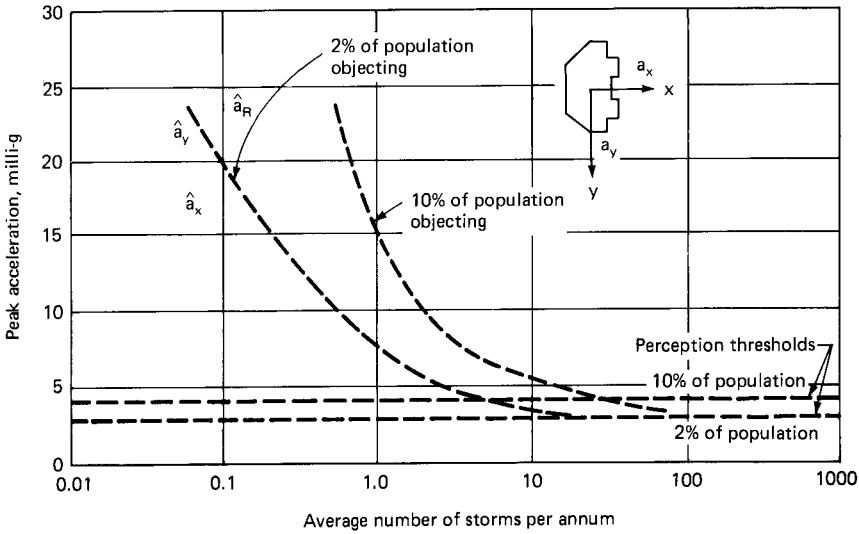

Figure 2.25 Davenport's criterion for perception of motion.

justifiable to reduce the peak moments when considering the biaxial behavior of the building.

Recommendations for combining the force values for key wind directions are normally given in the wind tunnel reports, and may vary from one facility to another.

Prediction of building acceleration and human comfort. One of the basic reasons for undertaking aeroelastic study is to ensure that the building motion will not cause discomfort to the building occupants in the upper floors. It is generally known that quantitative prediction of human discomfort is difficult if not impossible to define in absolute terms because the perception of sway and associated discomfort are subjective by their very nature. However, in practice certain thresholds of comfort have been established relating to the acceleration at the top floors to the frequency of windstorms. One such criterion first given by Davenport is shown in Fig. 2.25. Accelerations at the top of the model are measured directly by installing three accelerometers, two of which measure the acceleration components in the x and y directions; the third is used to deduce the torsional component. The peak acceleration is evaluated from the expression:

$$\bar{a} = G_p \sqrt{a_z^2 + a_y^2 + a_z^2} \tag{2.26}$$

where $\bar{a}$ = peak acceleration
G_p = a peak factor for acceleration usually in the range of 3.0 to 3.5
a_x and a_y = accelerations due to the sway components in the x and y directions
a_z = acceleration due to torsional component

The peak acceleration is measured for a series of wind directions and speeds. It is then combined with the meteorological data to predict the frequency of occurrence for various levels of accelerations. A commonly accepted criterion is that for human comfort the maximum acceleration in the upper floors should not exceed 2.0 percent of gravitational acceleration for a 10-year return period storm.

2.7.6 High-frequency force balance model

In a tall flexible building the effect of wind load can be looked upon as created from three distinctly different contributions. First, there is the mean wind load, the effect of which is very easy to visualize. Since the mean wind load by definition is a constant load, it simply bends and twists a building, which returns to its normal undeflected position upon load removal. Then there is the fluctuating load resulting from the unsteady nature of the wind which brings about the oscillation of the building about the steady deflected shape. The third contribution comes from the inertia forces of the building; it is somewhat similar to the lateral forces induced in a building by earthquakes and depends at any particular instant on the deflection history of the building several minutes preceding that instant. For design purposes it is convenient to consider the inertial effects as an equivalent wind load.

A rigid model offers a convenient method of obtaining local wind pressures on the building faces, which in general consist of positive and negative pressures distributed uniquely for each building. It is possible to sum these local forces horizontally at each pressure tap level to obtain the net lateral forces in two perpendicular directions and torsional moment at each level. By interpolating the values obtained at each pressure tap level, which in general may not correspond to the floor level of the prototype, it is possible to derive the forces and torsional moments at each floor level. The cumulative shear and overturning and torsional moments at each floor are easily obtained from simple statics, as are the base shear and overturning moments. These values, which are calculated from the mean measurements of the wind tunnel tests, would have an excellent correlation with the overall lateral load to be used in the design of the bracing system of the building, except for the fact that they ignore the influence of the gust factor. Therefore, when rigid model pressure

studies are used to predict the structural loads for frame design, it is necessary to assume a conservative gust factor value to multiply the mean values. An alternate and better approach is to take the guesswork out of gust factor calculation by experimentally determining the gust factor.

A wind-tunnel-tested aeroelastic model provides comprehensive information on the dynamic loads and motions of the full-scale building because the essential structural features such as flexibility, mass, and damping of the prototype are simulated in the model. However, an aeroelastic model is quite complex to design and build and takes the best part of 10 to 12 weeks to complete the wind tunnel tests. During the last decade, the beneficial effects of reduced wind loads on the economy of the structural system were becoming known to engineers and owners alike, but the time element involved in the aeroelastic model testing often precluded the use of wind tunnel test data in the actual design. The flurry of high-rise activity and the tight schedules for design did not allow for an orderly method for incorporating the wind tunnel test results.

In response to this demand, wind tunnel engineers came up with a substitute. The high-frequency force balance approach provides an alternate, more economical, and time efficient method of furnishing the desired information.

Two basic types of force balance models are in vogue. In the first type the outer shell of the model representing the architectural shape is connected to a flexible metal cantilever bar. Accelerometers and strain gauges are fitted into the model, and the aerodynamic forces are derived from the acceleration and strain measurements. In the second type, a simple foam model of the building is mounted on a five-component, high-sensitivity force balance which is used to measure bending moments and shear forces in two orthogonal directions and torsion about the vertical axis. In both methods, resulting fluctuating loads on the model as a whole are determined, and by making certain simplifying assumptions, the information of interest to the structural engineer, namely the floor-by-floor lateral loads and the expected behavior of the building in terms of acceleration at the top floor, is deduced. A brief description of the concept behind each of the two force balance models is given below.

Flexible support model. In this method, a lightweight rigid model is mounted on a high-frequency-response force balance and tested in a wind tunnel to obtain the overturning moments. The full-scale building loads and motions are computed from the measured power spectrum. This method is applicable in cases where building motion does not itself affect the aerodynamic forces and where torsional effects are

not of prime concern. In practice, this method is applicable to many tall buildings.

It is not cost effective and may be impossible to measure the dynamic forces on the entire height of the building. Instead, in the force balance study, dynamic bending and torsional moments are measured at the base of the building and are used to calculate the dynamic response of the building. In simple terms, this means that accelerations are calculated at different heights, and from a knowledge of the weight of the building at different levels, the corresponding inertial loads are computed. The measured dynamic forces are combined with the inertial loads to obtain a peak dynamic load, which represents the gust factor contribution to the mean loading. A model analysis is used that is similar to approaches used in aeroelastic model studies to correlate the test data to the prototype. Since the dynamic loads are obtained directly from the model without reference to the prototype structural stiffness and mass distribution, it is possible to calculate the dynamic response for several alternative structural systems and cladding variations.

The objectives of the technique are: (1) to provide data on wind-induced forces and moments for design of the building's structural frame and (2) to determine the wind-induced accelerations. The high-frequency force balance model is constructed to a small scale of the order 1:500 and is tested in a wind tunnel that simulates the wind environment of the prototype in a manner similar to the pressure model tests. The balance shown in Figs. 2.26 and 2.27 consists of a rectangular steel bar about 6 in (152 mm) long. The cross-sectional dimensions of the bar are chosen to give a very high bending stiffness that results in natural frequencies of the order of 50 Hz. A set of bars, usually four, which are relatively thin compared to their width, is installed on top of the stiff bar by a flat plate to simulate the torsional stiffness of the building. These bars, because of their proportions, contribute very little to the bending stiffness of the balance, but because of their disposition about the center of rotation, they simulate the torsional mode. The bending and torsional frequencies of the balance are controlled independently of each other. The model itself is constructed out of a very lightweight material such as balsa wood and is mounted on top of the torsion spring through a relatively rigid plate. Strain gauges are attached to the bars that simulate the bending and torsional stiffness of the model. The gauges are calibrated by applying a range of known loads to the model. Tests are conducted in the wind tunnel for various wind directions, and the instantaneous base overturning and torsional moments are read from the strain gauges. Two sets of strain gauges are attached to the flexural bar to facilitate

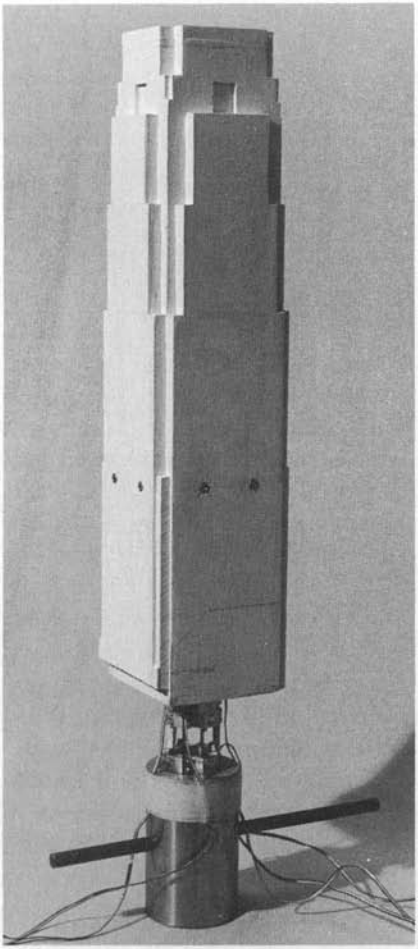

Figure 2.26 The model shown is a high-frequency force balance model which is itself lightweight and rigid. It is attached to a fast-response force balance that measures the instantaneous base moments, base torsional moment, and base shear forces. The building's response and wind-induced dynamic loads are computed from the base measurements using spectral methods. (*Photograph courtesy of Dr. Peter Irwin, Rowan, Williams, Davis & Irwin, Inc.*)

calculation of base shear by taking the difference of overturning measurements.

The instantaneous data records obtained from the strain gauge readings are analyzed to obtain the root-mean-square values for base overturning moments, torsional moments, and base shear for each of the wind directions for which the model is tested. Power spectral density functions are computed for the overturning and torsional moments and correction factors are applied to remove the effect of model resonance. Reduction factors to the measured values are determined to account for the directional nature of wind, wind statistics for the site, and probability distribution of wind speeds. Neglecting the reduction factor amounts to making the conservative assumption that the design wind comes with equal probability from any direction.

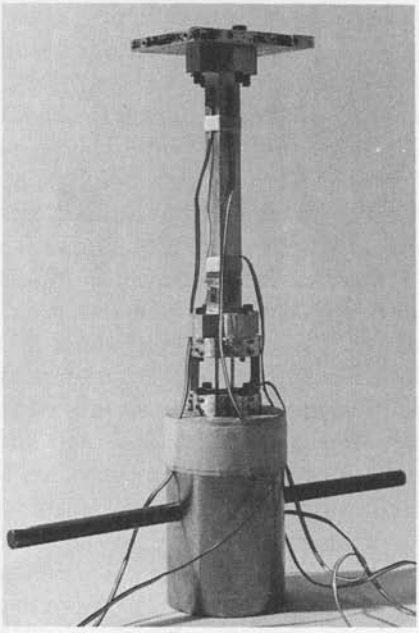

Figure 2.27 Detailed view of a high-frequency force balance. It uses strain gauges attached to flexural members to make the necessary measurements. (*Photo courtesy of Dr. Peter Irwin, Rowan, Williams, Davis & Irwin, Inc.*)

Meteorologically, it is known that strong winds generally have preferred directions of flow, which vary from region to region. Wind tunnel tests routinely take account of this phenomenon.

From the measured bending and twisting movements and known frequency and mass distribution of the prototype, it is possible to calculate the information of interest to the engineers, namely the wind forces at each floor and the expected peak accelerations.

Five-component force balance model. In this method, the prototype building is represented as a rigid model made out of lightweight material such as polystyrene foam. The stress components of interest at the base are the base moments, shear forces, torsional moment, and axial load. The model is attached to a measuring device consisting of a set of five highly sensitive load cells attached to a three-legged miniature frame and an interconnecting rigid beam. The arrangement is shown in Fig. 2.28 in which the load cells are schematically represented as extension springs. Horizontal forces acting in the x direction produce extension of the vertical spring at 1, which can be related to the base overturning moment M_x by knowing the extension of the spring and the pivotal distance P_x. Similarly, the base overturning moment M_y can be calculated from a knowledge of extension of the spring at 2 and the pivotal distance P_y. The horizontal spring at 3 measures the shear force in the x direction, while those at 4 and 5

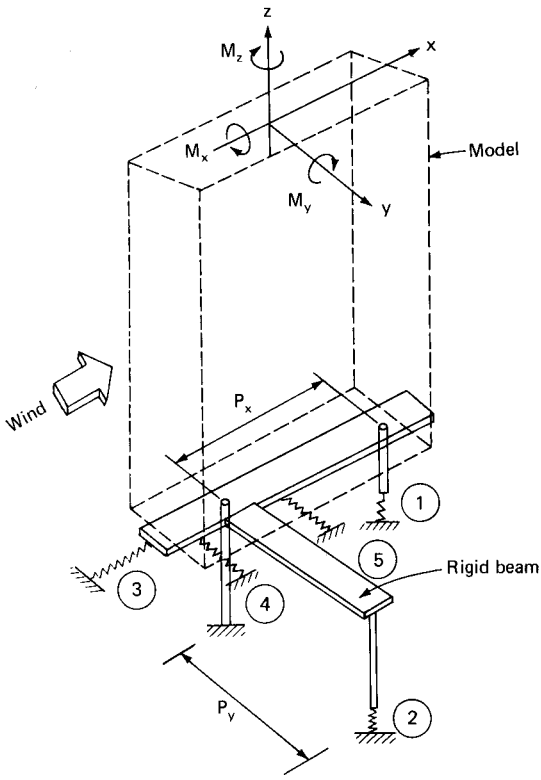

Figure 2.28 Schematic representation of five-component force balance model.

measure the shear force in the y direction. The difference in the measurements of springs at 4 and 5 serves to compute the torsional moment at the base about the z axis. However, the results obtained for torsion are an approximation to the true response of the building because the model does not account for the relative twist present in the prototype.

From the measurements of the fluctuating aerodynamic loads at the base of the rigid model of the building, the dynamic response is calculated by modal methods. The force balance measurements are in the form of mean and root-mean-square fluctuating aerodynamic components of the base shear and overturning moments about two orthogonal axes and a torsion for the full range of wind directions. Dynamic response calculations are based on the principle that the aerodynamic forces are proportional to the overturning moments and the torque measured in the wind tunnel. This assumption holds reasonably well for transitional modes, but not so for torsional modes because of the rigid body rotation of the model. However, this assump-

tion normally gives conservative results for torsional forces and is considered sufficiently accurate for design purposes.

In the foregoing an attempt is made to describe the principle features of the five-component force balance study. A detailed description of the instrumentation technique and discussion of advantages and shortcomings of the method are considered beyond the scope of the present work. The interested reader is referred to Ref. 38 for further details.

2.7.7 Pedestrian wind studies

A sheet of air moving over the earth's surface is reluctant to rise when it meets an obstacle such as a tall building. If the topography is suitable, it will prefer to flow around the building rather than over it. There are good physical reasons for this tendency, the predominant one being that the wind will find the path of least resistance, i.e., a path that requires minimum expenditure of energy. As a rule, it requires less energy for the wind to flow around the obstacle at the same level than for it to rise, which requires more potential energy. Also, if the wind has to go up or down, additional energy has to be expended in having to compress the column of air above or below it. Generally wind will try to seek a gap at the same level. However, during high winds when the air stream is blocked by the broad side of a tall, flat building, its tendency is to drift in a vertical direction rather than to go around the building at the same level; the circuitous path around the building would require expenditure of more energy. Thus the wind is driven in two directions. Some of the wind will be deflected upward, but most of it will spiral to the ground creating a so-called standing vortex or a minitornado at the sidewalk level.

Thus tall buildings and their smooth walls are not the only victims of wind buffeting. Pedestrians who walk past tall, smooth-skinned skyscrapers may be subjected to what someone has called the "Mary Poppins syndrome," referring to the tendency of the wind to lift the pedestrian literally off his or her feet. Another effect of this phenomenon has frequently been observed and is known as the "Marilyn Monroe effect," referring to the billowing action of ladies' skirts in the turbulence of wind around and in the vicinity of the building. Whatever the popular name may be, the point is that during windy days even a simple task such as crossing the plaza or taking an afternoon stroll becomes an extremely unpleasant experience to pedestrians, especially during winter months around buildings in the cold climates. Pedestrian footsteps become irregular, and for female pedestrians hair and skirts are considerably disturbed. Walking may become irregular, and the only way to keep walking in the direction of wind would be to bend the upper body windward. In extreme cases walking can

become dangerous for elderly persons, who may be blown sideways or leeward. Walking into the wind direction is possible only by facing backward.

In the case of skyscrapers, the strong downward wind can be generated along the windward faces of the buildings, causing strong ground-level winds in certain places near the building, which can create havoc for pedestrians and shops. The effect at the ground level is often amplified when there are other tall buildings nearby lined up to form what is usually termed a street canyon.

A dramatic example of wind modification by buildings is arcades under tall buildings. Because of the high stagnation pressure on the upwind side of the building and the large suction on the downward side, a strong draft is generated through the arcade. Tall buildings supported by stilts have the same problem as arcades. Other examples are shown in Fig. 2.29.

For a successful design of a building at the pedestrian level, studies are therefore necessary to assist the building planners in overcoming the uncomfortable or dangerous wind conditions which often occur at the base of the buildings. Planners, designers, and developers are becoming increasingly aware of the potential for pedestrian-level problems and generally acknowledge that design assistance is required to predict the microclimate that will be adversely affected by a proposed design.

Although one can get some idea of wind flow patterns from the above examples, analytically it is impossible to estimate pedestrian-level wind conditions in outdoor areas of buildings and building complexes. There are innumerable variations to location, orientation, shapes, and topography, making it impossible to even attempt formulating an analytical solution to the problem. Based on actual field experience and results of wind tunnel studies, it is, however, possible to qualitatively recognize situations that adversely affect the pedestrian comfort within a building complex.

Model studies can provide reliable estimates of pedestrian-level wind conditions based on considerations of both safety and comfort. These studies require geometrically scaled models, including aerodynamically significant details in areas of interest. Simulation of characteristics of natural wind, including the simulation of the salient properties of the approach wind and the influence of nearby building structures and significant topographic features, is required for an accurate estimate of pedestrian wind conditions. Model studies are used to evaluate a building design and offer remedial suggestions where unacceptable pedestrian-level wind speeds are created. A model is constructed and pedestrian-level wind speed measurements are made at various locations for all the prevailing wind directions. The

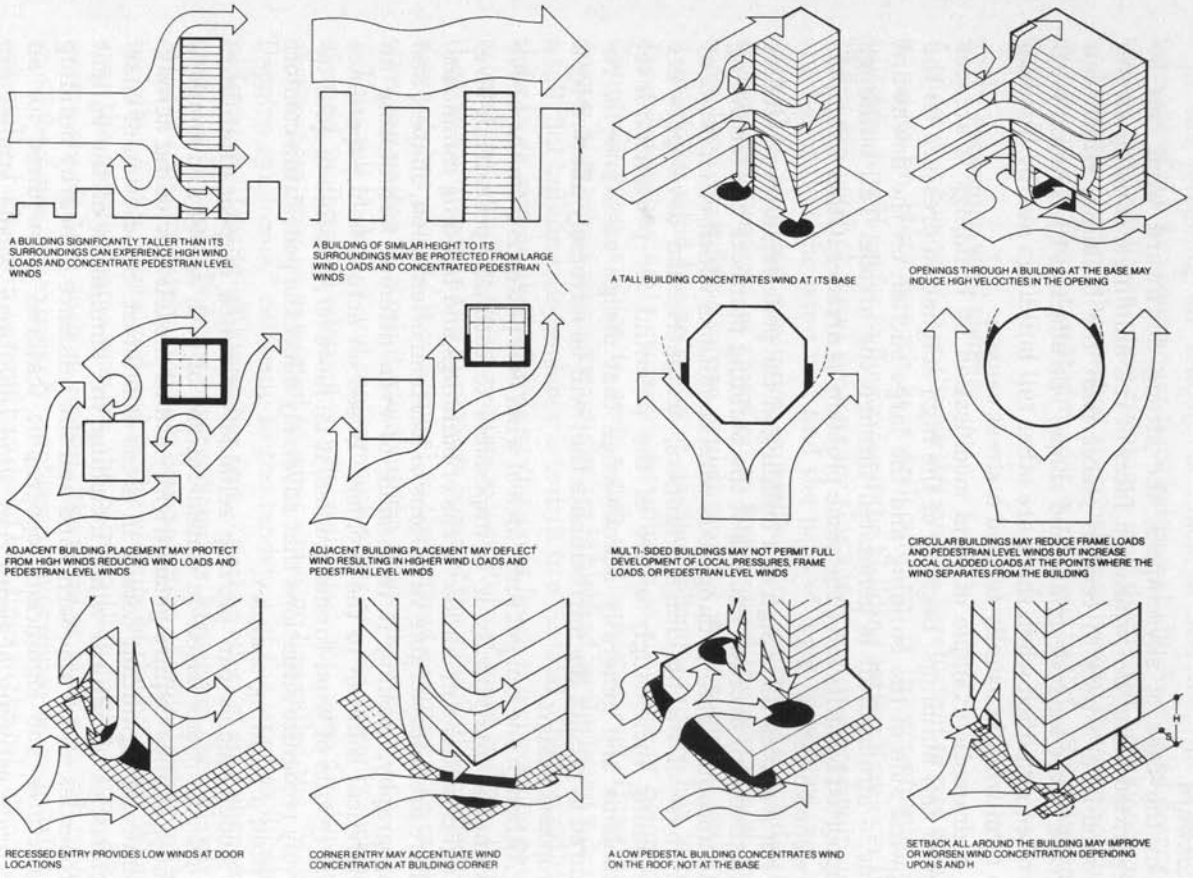

Figure 2.29 Near wind climate. (*Reproduced by permission from Progressive Architecture.*)

effects of adding a proposed building to an existing cluster of buildings are obtained by comparing measured wind speeds with and without the proposed building to a set of standard acceptance criteria. The acceptance criteria state how often a wind speed occurrence is permitted to occur for various levels of activity. This is done for both the summer and winter seasons with acceptance criteria being more severe during the winter months. For example, an occurrence once a week of a mean speed of 15 mph (6.7 m/s) is considered acceptable for walking during the summertime, whereas only 10 mph (4.47 m/s) is considered acceptable during winter months.

2.8 Field Measurements of Wind Loads

Gustave Eiffel, the noted engineer for the Eiffel Tower, was, perhaps, the earliest researcher to conduct studies and make measurements of the displacements of the top of his tower under the action of wind. His observations between 1893 and 1895 showed that under the effect of wind, the displacements at the top of the tower resembled an elliptical shape whose measured values, which ranged from 2.3 to 2.75 in (60 to 70 mm), were considerably less than those predicted by him. At about the same period, a series of tests were conducted on the 16-story Monadnock Building in Chicago to measure the movement of structure. The building's vibration characteristics were checked by measuring the oscillations of plumb bobs suspended in the stair shaft from the sixteenth floor. These observations were also cross-checked by transits and showed that the building was very stiff with a measured deflection of about $\frac{1}{2}$ in (12.7 mm). The next set of activities was spurred during the boom years of high-rise construction in the 1940s. New York's Empire State Building was the first to be instrumented for wind load measurements. Rathbun (1940) in his ASCE paper which describes the observations on the Empire State Building, compared the building oscillations to the tines of a tuning fork. His observation showed that the building's sway motion occurs primarily in the fundamental frequency of the building. In the next two decades no similar studies involving the measurement of the wind response of tall buildings were conducted. Since 1960, however, the flurry of high-rise building activity rekindled the interest in full-scale studies in a number of countries, the most important work coming from Canada, England, Australia, Hong Kong, and Holland. In Canada, Dalghish (Ref. 38) studied three buildings in the range of 34 to 58 stories. His work encompasses multiple aspects of wind engineering that include studies of cladding pressures, meteorological data for predicting overall structural loads, and measurements of mean and fluctuating pressures.

In England, Lee (Ref. 38) has carried out full-scale studies of the

structural behavior of a 157-ft (48-m) tall concrete building by subjecting the building to forced vibrations. In comparison to the number of tall buildings completed in the United States, the number of buildings instrumented to validate wind tunnel tests has been very small. Some buildings have been instrumented, but because of the nature of the tests, it will be some time before enough data are gathered for results to be published.

There are difficulties in measuring the reference conditions under which the full-scale tests take place. Stack effects can create pressure differences as large as a moderate wind. Engineers and researchers alike have been interested in comparing the results of model testing with those of the prototype in order to determine what improvements are needed in testing, and in some cases to get a better picture of the actual physical phenomenon. Full-scale tests are required to obtain confidence in model scale tests and to improve our knowledge about the effects that we do not fully understand as yet such as Reynolds number and turbulence effects. Certain scaling inequalities presented in the wind tunnel tests appear to promote the lingering doubt about the validity of wind tunnel tests.

The measured mean and fluctuating loads as compared to those predicted by the wind tunnel studies appear to show a moderate amount of agreement, but more often these studies expose the shortcomings of field studies. It is agreed among researchers in this field that there simply are not enough field data on full-scale buildings to validate wind tunnel techniques. Therefore, it is unreasonable to expect the wind tunnel results to be any more precise than any of the other parameters encountered in structural engineering practice, such as the calculation of natural frequencies and damping of tall buildings. The level of structural damping is at best an educated guess. Thus, there are many uncertainties in the wind design of tall buildings, signifying once again that structural engineering is as much an art as it is a science.

Amidst this rather pessimistic observation, structural engineer Halvorson and wind engineer Isyumov have brought in recent evidence (1986) which appears to confirm the accuracy of the current state-of-art procedure for high-rise building design. Their work consisted of a field-monitoring program to measure the dynamic response characteristics of Allied Bank Plaza Tower, a 71-story steel building in downtown Houston. The field-monitoring instrumentation consisted of two accelerometers located at the 71st floor of the tower. Wind measurements were made under two significant wind events, one an extratropical windstorm on April 1, 1983, with gust speeds of up to 56 mph (25 m/s), and Hurricane Alicia on August 18, 1983, with fastest-mile wind speeds approaching the code-specified 50-year recurrence

wind speed of 90 mph (40 m/s). Their observations showed that the sway response of the tower varies in a sinusoidal manner corresponding to the fundamental modes of vibration of the building. Full-scale measurements of accelerations showed excellent agreement with those predicted from the wind tunnel data. Based on the comparison between field measurements and wind tunnel results, the following conclusions are made by Halvorson and Isyumov.

1. The magnitude of structural loads experienced during Hurricane Alicia (which was determined as a 50-year recurrence event) are in very good agreement with the loads predicted by the wind tunnel tests. The Houston code wind loads, on the other hand, overestimated the wind loads by approximately 100 percent.
2. The mean wind loads are only about 20 to 30 percent of the total structural loads. Dynamic effects brought about by wind gusts are 3 to 5 times as significant as the mean loads.
3. The lateral drift, which is a combination of mean and dynamic peak displacements, was evaluated from wind tunnel measurements and field records, respectively. Calculated drift indices in two directions were $2\frac{1}{2}$ and 2 ft (0.76 and 0.61 m) and compared very well with the measured values of 2.58 and 1.25 ft (0.78 and 0.38 m).
4. Davenport's criterion of limiting the acceleration for a 10-year windstorm to approximately 20 milli g appears to serve well the serviceability requirements of a tall building in regard to motion perception by building occupants.
5. Estimates from the field records indicate that the building exhibits a damping characteristic equivalent to 1.4 to 1.6 percent of the critical damping, which is somewhat higher than the rule-of-thumb value of 1 percent used for steel buildings. The additional contribution appears to come from soil structure interaction provided by the foundation system, which consists of a $9\frac{1}{2}$-ft (2.89-m) thick mat founded on overconsolidated clay at a depth of 55 ft (16.77 m) below grade.

In addition to details of instrumentation and measurement techniques, the paper contains excellent discussion on other aspects of high-rise structural engineering such as joint stiffness factors, p-Δ effects, dynamic analysis, soil structure interaction, and biaxial nature of wind loads. The reader is referred to the paper for further details.

Chapter

3

Seismic Design

3.1 Introduction

3.1.1 Nature of earthquakes

Catastrophic earthquakes appear in the headlines with discomforting frequency, causing thousands of lives to be lost and property damage running into hundreds of millions of dollars. This truly global phenomenon has just begun to be understood, and considerable emphasis is being placed on the analytical studies of earthquake response of buildings, supported by experimental studies both in the laboratory and in the field in an effort to prevent much of this destruction and loss of life.

Accounts of destructive earthquakes appear all through recorded history. Early humans, in their inability to comprehend such a strange and destructive phenomenon, attributed the whole mechanism of earthquake to the angry work of gods. Although in ancient times it was tempting to think of earthquakes as somehow otherworldly, they are in fact, among the most common of the earth's phenomena.

We will limit our discussion to the class of earthquakes in which this energy release is both near the earth's surface and large enough to damage structures. It is known that such shallow-focus earthquakes are related to the forces which bring about the deformation of the earth as a whole. These distortions are gradually taking place in the earth's crust. Their cause is not completely understood, but their occurrence is

certain. According to a well-established theory known as the *elastic rebound theory*, the distortions and the associated strains and stresses in the outer layers of earth build up with the passage of time until ultimately the stress at some location becomes high enough to fracture the rock or cause it to slip along some previously existing fault plane. Slippage at one location causes an increase in the stress in the adjacent rock, so that the slippage propagates rapidly along the fault plane. The result is the sudden rebound of the elastic strain. The strain energy that has accumulated in the rock is suddenly released and propagates in all directions from the source in a series of shock waves. If the amount of energy released is small, or if the fault slippage occurs in an uninhabited region, the shock waves travel unnoticed except by sensitive seismographs. If this energy release is great, the effect at nearby locations is chaotic. The earth may experience violent motion in all directions, lasting for a few seconds in a moderate earthquake or for a few minutes in a very large earthquake.

Although most of the earthquakes of record have occurred in what can be classified as well-defined earthquake belts, an examination of earthquake records for the world reveals the truly global nature of this phenomenon. Thus, even in the seismically inactive parts of the world, some measure of earthquake resistance should be built into the design of all structures in which failure will be a major catastrophe.

The earth's crust is composed of a dozen or so large plates and several smaller ones ranging in thickness from 20 to 150 miles (32 to 241 km). The plates are in constant motion, riding on the molten mantle below and normally traveling at the rate of a millimeter a week, equivalent to the growth rate of a fingernail. The plates' travels result in continental drift and the formation of mountains, volcanoes, and earthquakes. If plates carrying two continental masses grind past each other, as the Pacific and the North American plates do under California's San Andreas Fault, friction locks them together. When slippages occur, the earth around the fault creates a so-called strike-slip earthquake. Still another kind of tectonic phenomenon results when an oceanic and a continental plate meet each other. For example, the oceanic plate which forms part of the Pacific floor off Mexico is pushing northeastward against the North American plate, which is creeping westward. The oceanic plate dips under the continental crust, but the relative movement between the two plates is resisted by friction. When frictional forces are overcome, the stuck section of the plate lurches forward, generating the shock waves of a thrust quake similar to the one responsible for the Mexican disaster of 1985.

Scientists estimate that over one million earthquakes occur every year. Some are very small and cause no damage, while others are violent and cause severe damage. One of the largest and most violent

earthquakes to hit North America occurred near Anchorage, Alaska, in 1964. In the twentieth century there have been only three earthquakes of Richter 8 or larger magnitude to affect a metropolitan area. The first one was the 1906 earthquake which destroyed much of San Francisco, California, estimated at 8.3 on the Richter scale. In 1923, Tokyo and Yokohama in Japan were badly damaged, and the third was the September 1985 quake which hit Mexico City. The most powerful earthquake ever recorded was off the coast of Chile in May, 1960. It reached 9.5.

The devastating earthquake which hit Mexico City measured 8.1 on the Richter scale. In just 4 minutes an estimated 300 buildings collapsed in downtown Mexico City. Fifty more were later judged dangerously close to falling, and hundreds of others were regarded as unsafe. Just 36 hours after the first tremor, the second earthquake, known as the aftershock, battered Mexico City. This tremor, which lasted for about a minute and was not as powerful as the first, toppled some already weakened buildings. The estimated death toll numbered over 8000 persons and property damage is estimated at $8 billion. The strength of this earthquake set the skyscrapers swinging as far north as Houston, 1100 miles (1770 km) from the epicenter. Tidal waves rolled ashore on the coast of El Salvador more than 800 miles (1287 km) to the southeast. The widespread damage is a chilling reminder that the world's well-defined quake-prone areas can be struck at any time without warning and with deadly effect. The same region in which the September 1985 earthquakes occurred had experienced six earthquakes with a magnitude of at least 7.0 since 1911. Thus, the latest shocks came as no surprise to seismologists.

Mexico City has a shaky geological base that makes it especially susceptible to earthquakes. It is built on the soft, moist sediment of an ancient lake bed, which when jolted shakes like a bowl of jelly. In addition, the city is undergoing subsidence at the rate of up to 10 in (25.4 mm) annually, creating uneven settlement in some building foundations. The unusual severity of the quake and the resonance of the soil structure are probably major factors behind the extent of the damage. It is estimated that because of the soft subsoils some buildings were subjected to acceleration equal to 1.0 g. Most seriously affected by the earthquakes were structures in the 5- to 15-story range which had natural frequencies close to that of the soil, causing them to resonate with greater vigor than other buildings.

During the 1985 Mexican earthquake, coastal towns only 50 miles (80 km) from the epicenter suffered less damage than Mexico City, which was 200 miles (320 km) from the epicenter, because the shoreline is made of solid rock and thus shakes less violently than the alluvial lake bed on which Mexico City is built. Thus even though the

seismic waves were diminished in intensity in their travel from the epicenter, they were amplified by the city's foundation.

When rocks in the earth's crust break, waves travel through the earth in all directions, causing shaking and trembling of the ground. The motion of the ground causes buildings to sway and, if they are not engineered properly, makes them fall. The most common cause of earthquakes is faulting. During faulting, parts of the earth's crust are pushed together or pulled apart, making the rocks break and slide past each other, releasing energy during the process.

The San Andreas Fault in California is a very long fault that passes under the Gulf of California through the Great Valley and San Francisco. It continues under the Pacific Ocean off the coast of Northern California. The land west of the San Andreas Fault is slowly moving north, while the land east of the fault is moving south. In 1906, movement along the San Andreas Fault caused the famous San Francisco earthquake.

Some faults are deep and others are close to earth. The point beneath the surface where the rocks break and move is called the *focus* of an earthquake. Directly above the focus, on the earth's surface, is the *epicenter*. The most violent shaking is found at the epicenter of an earthquake.

Three types of waves are caused during an earthquake: (1) The primary, or P waves, which travel the fastest, pulling and pushing rock particles; (2) secondary waves, or S waves, which are slower than P waves and cause the rock mass to move in a direction at right angles to their movement; (3) the surface, or the L waves, which are the slowest and travel from the focus directly upward to the epicenter and move along the earth's surface, similar to the way waves travel in an ocean. L waves cause most of the damage during an earthquake because they bend and twist the earth's surface.

Earthquakes often occur in the same three parts of the world. One major earthquake zone extends nearly all the way around the edge of the Pacific Ocean, going through New Zealand, the Philippines, Japan, Alaska, and along the western coasts of North and South America. The San Andreas Fault, where as many as 30 major earthquakes have occurred, is part of this zone. A second major zone of earthquakes is found near the Mediterranean Sea, extending across Asia, encompassing Italy, Greece, Turkey, and part of India. The third zone is located from Iceland through the middle of the Atlantic Ocean.

3.1.2 Seismograph

For purposes of seismic engineering, strong earthquakes are recorded on a strong-motion accelerograph. The accelograph is normally at rest and is triggered only when the ground acceleration exceeds a preset

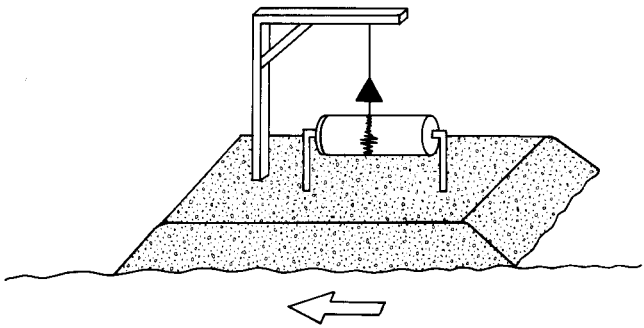

Figure 3.1 Conceptual model of displacement seismograph.

value. Earthquake records can be made for three components of ground acceleration, two horizontal and one vertical. There are about 4000 strong-motion accelerographs installed around the world.

A basic seismograph consists of a writing device at the end of a heavy pendulum that is attached to a frame in such a way that it will remain nearly still even when the earth moves. A constantly moving drum, attached to the ground through a heavy foundation mass, is placed under the writing device. When the earth is still, the writing device records a straight line, and a zig-zag or wavy line during an earthquake. The higher the wavy lines on the seismograph, the stronger the earthquake.

When an earthquake wave travels through the ground underneath such a pendulum, the motion of the ground is traced by the pen. This is because the pendulum stays stationary because of inertia forces and the trace is actually the movement of the drum. In most seismographs used today, the ground motion is made to produce a small electric signal, and this signal records the motion.

In the seismograph shown in Fig. 3.1, the lengths of wavy lines are proportional to the ground motion. This type of seismograph is called a *displacement seismograph*. It is possible, however, to record the ground acceleration by appropriately changing the period and damping of the pendulum. Such a device is called an *acceleration seismograph*. The current method of recording earthquakes is by the use of accelerograms which produce an analog trace of acceleration versus time in the form of either a photographic trace on film or paper or a scratch on waxed paper.

3.1.3 Scale and intensity of earthquakes

Earthquake intensities and magnitudes are described according to two scales, the modified Mercalli and the Richter scales. The Richter scale is based on the maximum trace amplitude of a seismogram written by

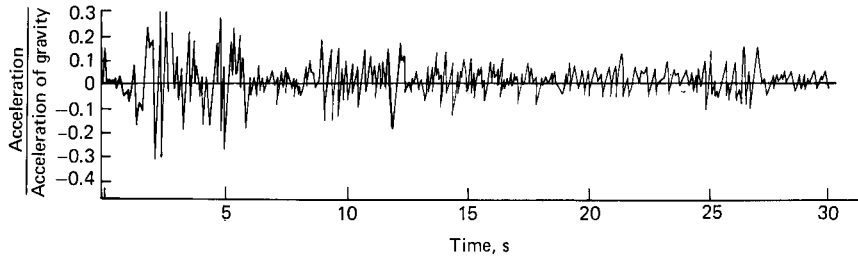

Figure 3.2 El Centro, California, earthquake ground acceleration record.

a horizontal pendulum seismograph with a 0.8 natural period, and defines more accurately than the Mercalli scale the energy released by an earthquake. It uses a base 10 logarithm of the ratio of an observed trace amplitude to the standard maximum trace. The distance of the seismograph from the quake is also taken into account. The quakes that occurred between 1900 and 1950 for which seismograph traces are available lie between 0 and 8.6 on the Richter scale. Because the open-ended Richter scale is logarithmic, each increment on the scale represents a tenfold increase in magnitude. For example, a quake registering 6.2 is ten times more powerful than one measuring 5.2. A quake of 7.0 is capable of inflicting major damage, while those recorded at more than 8.0 are classified as great earthquakes.

The modified Mercalli scale intensity refers to the degree of shaking on a scale of 1 to 12 and is expressed in Roman numerals (I, II, . . ., XII). The successive degrees are not derived from physical measurement of any kind, but merely represent ratings given to earthquake effects upon the people and the amount of damage to buildings. The Mercalli scale levels are represented by a rather long description of earthquake effects. The scale ranks earthquake intensity from I (barely felt) to XII (total destruction). Destructive earthquakes of modified Mercalli intensity IX or X generally register more than 6.5 on the Richter scale.

3.1.4 Seismic design

For structural engineering purposes, an accelerogram record of the time history of ground shaking gives the best measure of earthquake intensity. Figure 3.2 shows schematically the recorded ground acceleration at El Centro, California. This is representative of large earthquake ground motions in the United States. During a short initial portion, the intensity of ground acceleration increases to strong shaking, followed by a strong acceleration phase of shaking, which is followed by a gradual decreasing of motion. There are also records available of vertical accelerations and displacements. From the measured acceleration, it is possible to obtain the ground velocity and

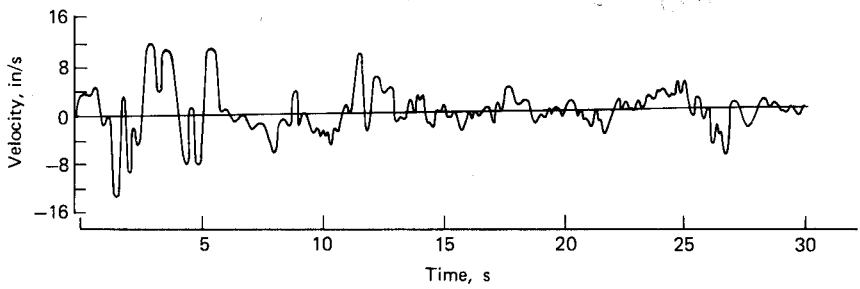

Figure 3.3 El Centro, California, earthquake ground velocity record.

displacements as a function of time. Figures 3.3 and 3.4 show the ground velocity and displacement plotted as functions of time. The maximum recorded ground acceleration is about 0.33 g, where g is the acceleration due to gravity of 32 ft/s^2 (9.75 m/s^2). The maximum ground velocity is 13.7 in/s (0.348 m/s), and the maximum ground displacement from the initial position is about 8.3 in (211 mm).

It is not possible to predict accurately when and where earthquakes will occur, how strong they will be, and what characteristics the ground motions will have; therefore, the engineer must estimate the ground shaking. The simplest method is to use a seismic risk map, such as those used in conjunction with building codes. Different zones indicate different intensities of ground motion to be considered in the design. The construction of a risk map is based mainly on the seismic history from a probabilistic point of view. As a refinement, in addition to the seismic history, the geological information is taken into account to construct a detailed seismic risk map. The most detailed method of establishing a design earthquake is to conduct a seismic site evaluation, which takes into account seismic history, active faults in the vicinity of the building site, and the stress-strain properties of materials through which the seismic waves travel.

Earthquake forces result from the random vibratory motion of the

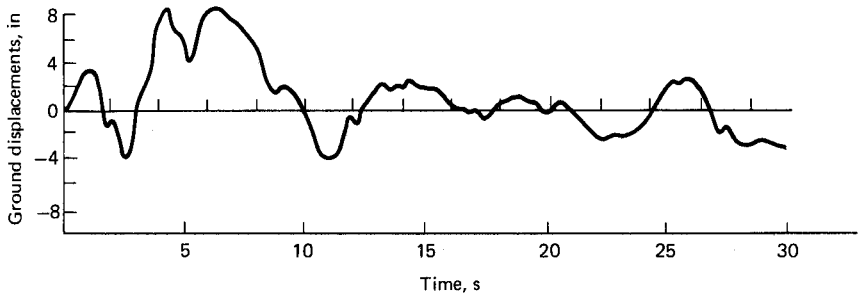

Figure 3.4 El Centro, California, earthquake, ground displacement record.

ground on which the structure is supported. The vibratory motion of the ground sets up inertia forces both vertically and horizontally, but it is customary to neglect the vertical components, since most structures have adequate reserve strength for these loads because of the safety factor requirements that are specified in most codes for gravity loads. The horizontal forces, equal to mass times acceleration, represent the inertia forces occurring at the critical instant of maximum deflection and zero velocity during the largest cycle of vibration as the structure responds to the earthquake motion. In virtually all earthquake design practice, the structure is analyzed as an elastic system, although it is acknowledged that the elastic limit of the structural members will be exceeded during the violent shaking of a major earthquake.

At present, there are three accepted methods by which the magnitude and the distribution of the earthquake-induced lateral forces are estimated on structures. These are (1) equivalent static (building code) method, (2) the response spectrum method, and (3) time history method. Each method has certain areas of applicability and each has disadvantages. A brief review of each of the methods is discussed later in this chapter. Before this is undertaken, it is instructive to consider the behavior of tall buildings under seismic action.

3.2 Tall Building Behavior During Earthquakes

3.2.1 Introduction

The behavior of a tall building during an earthquake is a vibration problem. The seismic motions of the ground do not damage a building by impact as does a wrecker's ball, or by externally applied pressure such as wind, but rather by internally generated inertial forces caused by vibration of the building mass. An increase in the mass has two undesirable effects on the earthquake design. First, it results in an increase in the force, and second, it can cause buckling of vertical elements such as columns and walls when the mass pushing down exerts its force on a member bent or moved out of plumb by the lateral forces. This phenomenon is known as the p-Δ effect. The greater the vertical force, the greater the movement due to p-Δ. Although buildings generally have larger vertical-load-carrying capacity because of gravity load requirements of the codes, the p-Δ problem is not mitigated. It is almost always the vertical load that causes buildings to collapse; in earthquakes, buildings do not fall over —they fall down. The seismic motions of the ground cause the structure to vibrate, and the amplitude and distribution of dynamic deformations and their duration are of concern to the engineer. The chief objective of earth-

quake design is that the building should not be a hazard to life and limb in the event of a strong shaking. During moderate ground shaking that has a significant probability of occurrence during the life of the structure, the vibrations may be in the elastic range with no damaging amplitude, but during strong ground shaking, members may undergo plastic strain and there may be some cracking.

3.2.2 Response of tall buildings

In general, tall buildings respond to seismic motion somewhat differently than low-rise buildings. The magnitude of the horizontal inertia forces induced by earthquakes depends on the building mass, ground acceleration, and the nature of the structure. For a hypothetical rigid building founded on infinitely stiff foundation, the inertia force F for a given ground acceleration a is given by Newton's Law $F = Ma$, where M is the building mass. Since all structures deform, the deformation absorbs some energy; the force F tends to be less than the product of mass and ground acceleration. A tall structure tends to be more flexible than a low-rise building, and in general would experience accelerations much less than a low-rise building. On the other hand, a very flexible tall structure subjected to motion for a prolonged time may experience much larger forces if its natural period is near that of the ground waves. Thus, the magnitude of lateral force in a tall building is influenced to a great extent by the type of response of the structure itself. This is shown schematically in Fig. 3.5.

Consider, for example, the behavior of a 60-story building during an earthquake. Although the motion of the ground is erratic, it can be considered to have horizontal components in two mutually perpendicular directions. These components typically have varying periods and can be considered as short-period components when the period is less than 0.5 s or so, and long-period components for periods in excess of 0.5 s. The period of fundamental frequency T_1 of a tall building is a function of its stiffness, mass, and damping characteristics, and can range anywhere from 0.05 to 0.15 times the number of stories, depending upon the materials used in the construction and the structural system employed. As a preliminary approximation for steel-framed buildings, the period T_1 is approximately equal to 0.1 N, where N is the number of stories. A typical 60-story building would have a fundamental period of 6 s, with the periods of the next two higher modes, T_2 and T_3, approximately equal to $T_2 = T_1/3$ and $T_3 = T_1/5$. The second and third modes of vibration for the 60-story building are thus approximately equal to 2 and 1.2 s. During the first few seconds of earthquake, the acceleration of the ground reaches a peak value and is associated with relatively short-period components of the range 0 to 0.5 s, which have little influence on the fundamental

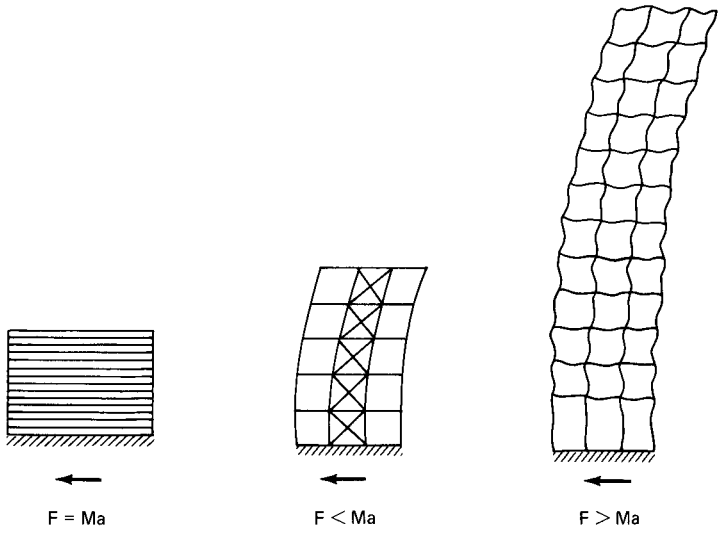

Figure 3.5 Schematic representation of seismic forces in low, mid-, and high-rise buildings.

response of the building. On the other hand, the long-period components that occur at the tail end of the earthquakes, and have periods closer to the fundamental period of the building have a profound influence on its behavior.

The intensity of ground motion reduces with the distance from the epicenter of the earthquake. However, weakening of the ground motion occurs at a faster rate for higher-frequency components than for lower-frequency components. The cause for this attenuation phenomenon is not understood, but its existence is certain. This is a significant factor in the design of tall buildings, because it means that a tall building, although situated farther from a causative fault than a low-rise building, may experience greater ground motion. Therefore, the area covered by ground shaking potentially damaging to, say, a 50-story building is much greater than the area covered by ground shaking potentially damaging to one-story buildings.

3.2.3 Influence of soil

The seismic motion that reaches a structure on the surface of the earth is influenced by the local soil conditions. The subsurface soil layers underlying the building foundation may amplify the response of the building to earthquake motions originating in the bedrock. Although it is somewhat difficult to visualize, it is possible that a number of underlying soils can have a period similar to the period of vibration of

the structure. Greater structural distress is likely to occur when the period of the underlying soil is close to the fundamental period of the structure. Tall buildings tend to experience greater structural damage when they are located on soils having a long period of motion because of the resonance effect that develops between the structure and the underlying soils. If a building resonates in response to ground motion, its acceleration is amplified. This amplification can be great. However, buildings are prevented from resonating with the purity of a tuning fork because they are damped; the extent of damping depends upon the construction materials, types of connections and the presence of nonstructural elements. Damping is measured as a percentage of critical damping.

3.2.4 Damping

Critical damping refers to the minimum amount of damping necessary to prevent oscillation altogether. To get a mental picture of critical damping, imagine a tightly tensioned string immersed in a tank containing water. When the string is plucked, it oscillates about its mean position several times before coming to rest. If we replace water with a liquid of higher viscosity in the container, the string will probably oscillate, but certainly not as many times as it did in water. By progressively increasing the viscosity of the liquid, it is easy to visualize that a state can be reached where the string, once plucked, will return to its neutral position without ever crossing it. The minimum viscosity of the liquid that prevents the vibration of the string altogether can be thought of as the equivalent to critical damping.

The damping of structures under earthquake disturbances is influenced by a number of external and internal sources. Chief among them are:

1. External viscous damping is caused by air surrounding the building. Since the viscosity of air is small, this effect is negligible in comparison to other types of damping.
2. Internal viscous damping is associated with the material viscosity. This is proportional to the velocity, so that the damping ratio increases in proportion to the natural frequency of the structure. In dynamic analysis, internal viscous damping is included by introducing a dashpot in the mathematical model. It is frequently used to represent the effect of other types of damping as well.
3. Friction damping, also called Coulomb damping, occurs because of friction at connections and support points of the structure. It is a constant, irrespective of the velocity or amount of displacement. In

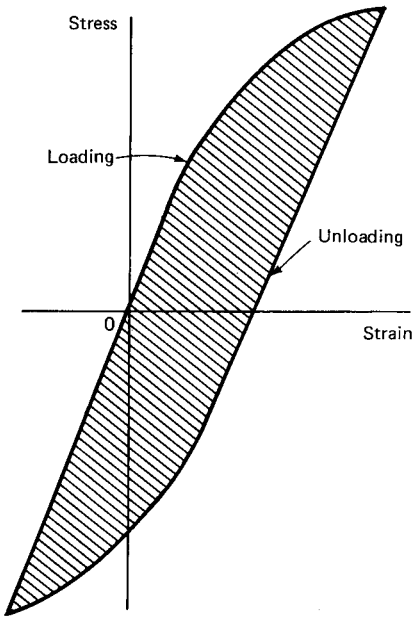

Figure 3.6 Hysteresis damping.

dynamic analysis its effect is included as internal viscous damping when the level of displacements is small or as hysteresis damping when it is large. Steel buildings with bolted connections typically have more friction damping characteristics as compared to a fully welded construction. A prestressed concrete building has fewer damping characteristics as compared to a mild-steel-reinforced construction because in prestressed concrete the level of cracking is relatively less and hence it experiences less body friction.

4. Hysteresis damping manifests itself when the structure is subjected to load reversals in the inelastic range. Figure 3.6 shows the hysteresis loop for one cycle of loading. The area inside of the loop corresponds to the energy dissipated in the cycle. This dissipation of energy is defined as hysteretic damping. It increases with the level of displacement and is independent of the velocity of the structure. The effect of hysteretic damping can be included in an elastic analysis by assuming equivalent viscous damping.
5. Radiation damping refers to the energy dissipation that takes place through the ground on which the structure is built and is a function of the characteristics of the ground such as density, Poisson ratio, and shear modulus and modulus of elasticity. It also depends on the relative stiffness of the structure and the ground and the depth to which the structure is embedded in the ground.

6. Hysteresis damping around the foundation is caused by the inelastic deformation of the ground adjacent to the foundation.

It is common practice in dynamic analysis of buildings to lump all the various sources of damping into one type and to represent it as viscous damping. To arrive at a precise value of viscous damping that can effectively take into account all the aforementioned characteristics is hard if not impossible. Representative values of damping ratios used in practice vary anywhere from 0.02 to 0.05 depending upon the material used for the building and the method of connection of its members. Damping ratios obtained from vibration tests of existing buildings vary from a low of 0.005 to a high of 0.075, making a precise recommendation difficult.

In earthquake design, the idea of critical damping is used to modify the ground response spectrum by assuming percentages of damping that represent reasonable values for buildings, generally of the order of 2 to 15 percent of critical. Figures at the low end are used in wind engineering, whereas upper-end figures are used in earthquake engineering.

A level of acceleration generally at 0.1 g where g is the acceleration due to gravity is sufficient to produce some damage to weak construction. Between 0.1 and 0.2 g, most people feel sickness symptoms. An acceleration of 1.0 g, or 100 percent of gravity, is analytically equivalent, in the static sense, to a building that cantilevers horizontally from a vertical surface.

3.2.5 Building deflections

Earthquake-induced motions, even when they are more violent than those induced by wind, evoke a totally different type of human response. First, because earthquakes occur much less frequently than windstorms, and second, because the duration of motion caused by earthquake is generally short and transient in nature. People who experience earthquakes are grateful that they have survived the trauma and are less inclined to be critical of building motion. Earthquakes are, therefore, a safety rather than a human discomfort phenomenon.

Static lateral deflections similar to those caused by wind loads have an important effect on the structural integrity of the components of the buildings. These should be limited so as not to cause any distress in structural frames, members, or connections, as well as such architectural components as partitions, claddings, and windows.

Therefore, in addition to evaluating the dynamic characteristics of the primary structural system, it is necessary to provide for large deformations that occur between various components of a building.

Prevention of outright collapse of the building under severe but rare earthquakes while limiting the nonstructural damage to a minimum during frequent but moderate earth tremors forms the basic underlying philosophy of seismic design. This is considered in the following section.

3.3 Philosophy of Earthquake Design

3.3.1 Introduction

In earthquake-resistant design, it is not sufficient to make a member "strong." It must also have a reserve of ductility. In most structural engineering problems, we can evaluate with a fair degree of accuracy the dead loads and the live loads which the structure must be able to support. The strength and properties of materials used in the construction of a structure are well defined by many tests. With the available theories of mechanics and digital computers we can determine to a high degree of precision the moments, shears, and thrusts that the members will be subjected to. From the material and geometric properties, the amount of resistance the members can provide to these forces can be assessed. With this complete and adequate information, a very realistic factor of safety against collapse can be established.

Consider, for example, the lateral design of a tall building subjected to wind loads. Unless the building is very slender, with a height-to-width ratio of greater than 6 or so, the building, if designed for code-designated wind forces, is more than likely to perform adequately throughout its life span. Even when the slenderness ratio is greater than 6 and the building shape is unusual, the engineer can fairly accurately determine the design lateral loads by either using correction factors to the basic wind loads to take into account the dynamic nature of wind or by resorting to wind tunnel tests to determine the worst possible wind load that can be expected over the life of the building. In other words, engineers can get a fairly reasonable estimate of lateral loads either by analytical procedures or by wind tunnel experiments. The measured wind loads on actual buildings, although the available data are limited, seem to indicate that the actual wind loads on buildings are somewhat smaller than those usually assumed in the design, adding an additional degree of confidence.

The situation with regard to earthquake forces is entirely different. The seismic forces specified in the code are quite small relative to the actual forces expected at least once in the life cycle of the building. It is important to understand the principles behind the code specifications and the justification for designing for lateral earthquake forces of 3 to 20 percent of gravity as compared to dynamic analysis requirements of over 50 percent of gravity. Accelerations derived from actual

earthquakes are surprisingly high when compared to the code forces used in design. A design based on manipulation of numbers to come up to code requirements without appreciation of the code intent will certainly not assure adequate earthquake resistance in case of a major earthquake. A better approach is to design on some reasonable basis, recognizing the uncertain nature of demands and to provide for all the reserve capacity that can be accomplished at little or no extra cost in initial construction or at only a slight sacrifice in architectural features. This in essence is the underlying philosophy of earthquake design.

3.3.2 Uncertainties in earthquake design

The seismic loads on the structure during an earthquake result from internal inertia forces, which are created by ground accelerations. The magnitude of these loads is a function of the following factors:

1. Mass of the building
2. The dynamic properties of the building, such as its mode shapes, periods of vibration, and its damping characteristics
3. The intensity of ground motion and soil structure interaction

From the structural viewpoint, the intensity of vibrations of the earth's surface at the building site is of interest. Such intensity of vibration is a function of (1) amount of energy released, (2) distance from center of earthquake to the structure, and (3) character and thickness of foundation material. The magnitude of the earthquake, which is a function of the energy released, can be predicted on a regional basis from probability theories. Mathematical theories are available to predict the effect of distance for various soil conditions underlying a site using assumed bedrock vibrations. However, there are too many unknowns to be able to predict quantitatively with any degree of certainty the foundation vibration for some unknown future earthquake. Qualitatively, the following are apparent:

1. Ground shaking is strongest in the vicinity of the causative fault, and the intensity diminishes with distance from the fault.
2. The period of ground motion increases with an increase in the distance from the causative fault.
3. Deep deposits of soft soils tend to produce ground surface motions having predominantly long-period characteristics.
4. Shallow deposits of stiff soils result in ground motions having predominantly short-period characteristics.

5. The soil amplification varies with frequency and intensity of the bedrock motions.

In spite of the great strides made in earthquake engineering during the last two decades, numerous uncertainties still exist. The traditional static approach of determining the force level for a given earthquake motion and designing the structure to withstand these forces with a considerable degree of safety has very serious limitations because of the following problems:

1. There simply are not enough empirical data available at the present time to make a reliable prediction as to the intensity and nature of future earthquakes at a given time.
2. Foundation and soil interaction and geological conditions have a profound effect on the structural performance, but at present there exists no clear-cut method which can correctly incorporate these effects.
3. Analysis by elastic assumptions does not take into account the change in properties of the building materials during the progress of an earthquake.

Because of these uncertainties, it is necessary when applying the static load criteria to evaluate the capabilities of the structure to perform satisfactorily beyond the elastic-code-stipulated stresses. Ductility, which involves deformations into the inelastic range is a necessity if structures designed for the static forces are to be capable of resisting earthquakes of the intensity of those which have been actually recorded.

Recent codes now require that the function of buildings be taken into account in the earthquake design. This is a direct consequence of the lessons learned from the San Fernando earthquake, in which several medical facilities were rendered useless and vacated, becoming liabilities rather than maintaining emergency service. Higher loads are specified for other vital public buildings whose functioning is considered indispensable in rescue and recovery efforts.

In earthquake-resistant design, it is not necessary to consider the simultaneous action of wind earthquake loads, since the probability of this occurrence is quite low. There is no record of an extreme wind and earthquake load hitting a building at the same time. It is expected, as in the case of wind loads, that under the action of ordinary earthquake loads, the building structure will remain within the elastic range. Under code-specified earthquake forces, which represent the action of a moderately heavy earthquake, it is reasonable to expect the structure to maintain elastic behavior. In the case of catastrophic earth-

quakes, however, a different philosophy exists that permits the building to venture into the plastic range. Certain portions of the building are permitted to suffer minor damage, provided the stability of the structure as a whole is not impaired. The occasional excursion of the building into the plastic range is accepted on the premise that the peak forces produced by earthquakes are of short duration and therefore can be more readily absorbed by the movement of the building than a sustained static load.

3.3.3 Architectural and structural considerations

It is often expensive, and perhaps economically prohibitive, to achieve a sound structure if the building is conceived in seismically disadvantageous configuration. It is necessary that both the architect and engineer be familiar with the performance characteristics of different types of materials as well as different configurations and framing systems. The overall architectural concept has a direct bearing on the alleviation of the structural hazard. The architectural concept must be a logical blending of all design components into a total system, with complete continuity of structure rather than an assembly of unconnected parts. The structure should have an inherent resistance to lateral forces. Complex asymmetrical shapes which invite torsion, reverse pendulums produced by placing heavy or overhanging loads on the upper stories, structural discontinuity, and abrupt changes in the structure stiffness, all make the problem of reducing seismic risks more difficult.

A building's shape, symmetry, and general layout as developed in the conceptual stage are more important or make for greater differences in the performance of a structure than the accurate determination of the code-prescribed forces. The seismic design thus begins with and is dominated by the architectural concept of the building. Selection of a basically sound and economical system is more important than the computations of stresses and deflections. During an earthquake the structure is compelled to conform to ground motions. Thus, the criterion for design is one of ability to absorb imposed deformations rather than a requirement of strength to resist applied forces. The inherent properties of the materials and the structural system should be used to their fullest and should not be sacrificed for minor economies or architectural effect. Damage control, as it applies to mechanical and electrical features, as well as structural elements, must be included in the criteria for seismic design. Architect and engineer must work closely together to achieve the most desirable building that will be seismic-resistant as well as functionally and aesthetically pleasing. Damage control features should provide for details which allow struc-

tural movement without damage to nonstructural elements. For example, extra clearance at edges of glass should be provided to minimize its breakage from frame distortions. Damage to nonstructural elements may constitute a major financial loss even though the damage to structural elements is minor. Special care is required in detailing to minimize this type of damage.

The first step is to develop an architectural concept which will avoid as many problems as possible. Architects and engineers must realize the significance of (1) symmetry in basic plan layout; (2) reentrant corners in L-, T-, or U-shaped buildings; (3) participation of nonstructural elements in earthquake resistance; and (4) omission of major structural elements to create an open ground floor that may cause abrupt changes in the rigidities at that level. All these and other factors which affect the response of the building are discussed in the following section.

Lightweight construction. Other things being equal, the greater the structural mass, the greater the seismic forces. In contrast to wind design, seismic design calls for lighter construction with a high strength-to-weight ratio to minimize the inertial forces. However, it should be noted that lightweight construction which minimizes seismic forces may not necessarily result in lower cost.

Structural symmetry. Experience with past earthquakes has shown that buildings which are unsymmetrical in plan have greater susceptibility to earthquake damage than symmetrical structures. The asymmetric design induces torsional oscillations in the structure. At times it may become necessary to use irregular plan shapes such as L, T, or U shapes because the available site may impose restrictions on planning. In such cases asymmetry in plan can be eliminated by use of seismic joints at junctions of individual wings. When this is done, each part of the building must be considered as a separate structure with its own independent bracing system. In an otherwise regular structure, asymmetry can be caused by eccentric disposition of structural elements. Such a condition can exist, for example, in a building with a large front opening and an essentially stiff rear wall. Attempts should be made to avoid this type of condition by better conceptual planning, or this type of design can be improved by introducing additional structural elements so as to make the center of rigidity of vertical elements more nearly coincide with the center of lateral forces.

Ductility. Ductile materials are highly desirable for earthquake-resistant design because earthquake design should satisfy two basic objectives: (1) to prevent loss of life and serious injury and to prevent

buildings from collapse and dangerous damage under a maximum intensity earthquake; (2) to ensure buildings against irreparable damages under moderate to heavy earthquakes. The strength built into the structure alone cannot create an earthquake-resistant design. Earthquake resistance requires energy absorption, which means the structure should have predictable ductility as well as strength. The ductility of the structure can be visualized as its capacity to undergo large deformations without appreciably losing its load-carrying capacity. If such a ductility is present, the building is prevented from collapse even if it is seriously damaged. Therefore, in addition to seismic strength design, the ductility of the building should be given due consideration.

The required ductility can be achieved by proper choice of framing and connection details. A minimum ductility ratio of the order of 4 to 6, which can be achieved in most structural materials, is a reasonable criterion for earthquake design. Brittle material such as concrete should be properly reinforced to resist seismic forces. Due regard should be given to the common mode of failure of concrete columns by buckling of the main steel and by spalling of the concrete cover brought about by the combined effect of compression and flexure. Particular attention must be given in the design and detailing of ductile moment-resisting concrete frames. A limit must be placed on the amount of tensile reinforcement to avoid compression failures in flexural compression. Additional strength and ductility on the compression side can be obtained by using compressive reinforcement. Failure of concrete in shear or diagonal tension also reduces the ductility of reinforced concrete. Therefore, appropriate shear reinforcement in the form of stirrups or inclined bars should be provided in beams. In columns greater ductility can be achieved by providing spiral reinforcement or closely spaced ties. The concrete within the ties is restrained, adding to the compressive strength as well as ductility of the column. Appropriate bond and anchorage must be provided for all reinforcement to avoid premature failure of the member by loss of anchorage. Tensile forces in concrete columns must be avoided.

The above problems for steel are similar in principle, but the detailing is different. Connections should be designed to avoid tearing or fracture. To avoid instability problems, particularly in the inelastic range, adequate stiffness and restraint must be provided. The column in the lower stories should have a reserve of compressive strength for additional flexural and overturning compression that may arise from earthquake forces.

Damping. The damping characteristics of a structure have a major effect on its response to ground motions because a small amount of

damping significantly reduces the maximum deflections due to resonant response. In this connection, reinforced concrete has a higher degree of damping than structural steel. However, damping in itself is not a complete index of the antiseismic value of material or system.

Adequate foundations. Differential movement of buildings caused by seismic action is an important cause of structural damage, especially to heavy rigid structures that cannot accommodate these movements. Adequate design must minimize the possibility of relative displacement between the various parts of the foundation and between foundation and superstructure. Earthquake vibrations can cause consolidation or liquefaction of soils, resulting in uneven settlement. Either the stabilization of the soil prior to construction, or the use of piles, caissons, or deep piers bearing on deep stratum is a solution to this problem. The lateral load capacity of the piles, which depends on the properties of the soil, the size and length and material of the pile, the pile grouping and spacing, and the frequency and duration of loading should be verified. When horizontal load is greater than the value suitable for piles, batter piles can be used.

Short-column effects. A column will carry a larger portion of the load than assumed if restraints are introduced in the construction that were not assumed in the analysis. In past earthquakes, column failures have frequently been inadvertently caused by the shortening effect of stairways, partial height filler walls, or intermediate bracing members. Unless considered in the analysis, such stiffening members should be isolated from the columns by proper detailing.

Separation of structures. In past earthquakes, the mutual hammering received by buildings in close proximity of one another has caused significant damage. The simplest method of preventing damage is to provide sufficient clearance so that free motion of the two structures can occur. The motion to be provided for results partly from the deflections of the structures themselves and partly by the rocking or settling of foundations. For tall flexible buildings, the width of seismic joint between the structures should be equal to 3 to 4 times the calculated elastic deflection under code-prescribed loads, plus the tipping distance due to foundation rotation as determined by rational methods.

Plan dimensions. The ratio of plan dimensions should not be inordinately large to prevent different types of forces acting on different plan sections. If this cannot be achieved, then seismic joints should be provided in such a building. It is desirable to retain the plan shape

uniform throughout the building height, thus avoiding setbacks. Sudden changes in the vertical distribution of strength and stiffness should be kept to a minimum. If this cannot be achieved, it is necessary to perform dynamic response analysis to ensure that the expected behavior of the building is simulated in the analytical model.

Deflections. As mentioned earlier, during earthquakes buildings do not fall over; they fall down, implying that the vertical elements are crushed because of the large p-Δ effects. Therefore, a building exhibiting large lateral displacement under horizontal loads is more prone to damage than a building with moderate lateral displacement. Buildings with a large height-to-width ratio that are prone to large deformations need special attention.

In high-rise buildings, although outright structural collapse is rare, damage to exterior cladding materials could be severe because of the flexibility produced by the large height-to-width ratios of such buildings. Injuries from falling cladding and debris may be more severe than life loss in buildings. Extreme care should be taken while developing the connection details of the exterior cladding materials to the building components.

In conclusion, it can be said that increased earthquake safety, which would radically cut loss of life and property, can be attained with today's technology at relatively low cost in comparison to the total budgeted for construction. The additional cost of seismic- over wind-resistant design may vary from 5 to 15 percent of the building cost, a low enough premium which would prevent loss of human lives in case of severe earthquake.

We will now consider each of the three accepted methods of seismic design, namely, (1) the equivalent static, or the building code, method: (2) the response spectrum method; and (3) the time history method. The advantages, disadvantages, and the range of applicability for each method are discussed in the following sections.

3.4 Static Approach

3.4.1 Introduction

Current American codes for seismic design are based on three broad objectives: (1) to minimize loss of human life and personal injury, (2) to assure continuity of vital services, and (3) to minimize damage to property. Codes generally recognize that it is not economically feasible to give complete protection to buildings in the event of a worst-case earthquake; it is tacitly accepted that structural damage should be prevented and nonstructural damage minimized in the occasional moderate earthquake and that serious damage or collapse should be

prevented in the much rarer severe earthquake. Static analysis is used with equivalent static loadings to represent the dynamic action of the earthquake on the structure. The continued use of the static approach in the design of buildings is based on the premise that buildings so designed have performed well in past earthquakes. This good performance may have been due to other factors that were present in the older buildings but were ignored in the analysis, such as contribution to strength and stiffness by nonstructural elements and ductility of the structure. These factors may not always be present, especially in tall buildings, and therefore special care should be exercised in their design. The vertical seismic forces are not generally considered for the design of structures except for the effect of uplift forces and for very important structures such as nuclear reactor buildings. In typical building design only the horizontal components of earthquake forces are considered and are assumed to act nonconcurrently along the two main structural axes.

Control of lateral deflection or drift of a story relative to adjacent stories is considered with a view to limiting the damage to nonstructural components such as glass and curtain wall panels. It is perhaps unreasonable to limit the interstory drift purely for the reason of preventing discomfort to the occupants because people realize that they are lucky to have survived an earthquake and very rarely complain about the oscillations of the building.

Earthquake-resistant design involves engineering judgment and experience as well as an application of scientific principles. The design involves economic considerations and probabilities. Although it is entirely possible to design a structure to resist the greatest earthquake experienced thus far, and even greater, such economic investment is considered unwarranted in view of the small probabilities of occurrence of major earthquakes at any specific location. The results have been good when buildings designed according to seismic codes have been subjected to earthquakes. To achieve this objective it is necessary to prevent buildings from collapse and dangerous major damage. By providing this protection against severe earthquakes, as a by-product resistance against property damage in the more frequent, less severe earthquake is also achieved.

Earthquake resistance calls for energy absorption (or ductility) rather than strength resistance only. If a building is able to deflect horizontally by several times the amount envisioned under the basic seismic design load and still maintain its vertical-load-carrying capacity, it will be able to absorb earthquakes considerably heavier than the design earthquake. If such ductility is present, collapse of the building can be prevented even if the building is seriously damaged. Thus, in

addition to seismic load design, the ductility of the building should be given due consideration.

Great progress in earthquake engineering has thrown considerable light onto the effect of earthquakes on buildings, and this is reflected in the seismic design codes. However, numerous uncertainties still exist. Among these are the probable intensity and character of the maximum earthquake, the damping characteristics of the actual building, the effect of the soil structure interaction, and the effect of inelastic behaviors of the building. However, for convenience in design, an earthquake is translated into an equivalent static load acting horizontally on the building and is intended to represent the inertial force, which is mass times acceleration occurring at the critical instant of maximum deflection and zero velocity during the largest cycle of vibration as the structure responds to the earthquake motion. These design loadings, however, incorporate modifying factors to cover local variations in seismicity, type of construction, soil conditions, usage of building, etc.

The concept of an assumed constant lateral acceleration permits the determination of lateral force as simply the product of weight of the element considered and the ratio of the selected lateral acceleration to the acceleration due to gravity. This is called the *seismic coefficient* and is the basis of most codes. The provisions for earthquake design as given in the Uniform Building Code (UBC 1985), the American National Standards Institute standard (ANSI A53-82), and the Applied Technology Council Recommendations (ATC 3-06) are outlined in the following sections.

3.4.2 Uniform Building Code (UBC 1985) method

UBC uses equivalent horizontal static forces to design the building for maximum earthquake motion. Using Newton's second law of motion, the total lateral seismic force, also called the base shear, is determined by the relation

$$V = Ma$$

where V = total horizontal seismic force over the height of the building (also called the base shear)
M = mass of the building
a = the maximum acceleration of the building

Since

$$M = W/g$$

where W = building weight
g = acceleration due to gravity

$$V = Wa/g = WC$$

where C is called the seismic coefficient, which represents the ratio of maximum earthquake acceleration to the acceleration due to gravity.

The base shear is distributed over the height of the structure by considering the response of the structure during an earthquake. The seismic coefficient is modified by factors which take into account (1) dynamic properties of the structure (i.e., natural period of vibration, modal shapes, and damping); (2) type of construction, with particular reference to ductility or energy-absorptive capacity of the structure; (3) importance of the structure as related to its use; (4) seismicity of the region; (5) subsoil conditions; and (6) allowable stresses and load factors. Only horizontal components of the seismic forces are considered, and they are assumed to act nonconcurrently along the two main structural axes. Vertical seismic forces should, however, be considered in cases where uplift forces, column stability, and p-Δ effects govern the design. The weight of the building consists of the total dead load plus probable live load, and in areas subject to heavy snow, the probable snow load.

The minimum total lateral force assumed to act nonconcurrently in the direction of each axis of the structure is given by the formula

$$V = ZIKCSW \tag{3.1}$$

where Z = the numerical coefficient dependent upon the seismic probability zone factor
I = the occupancy importance factor
K = the horizontal force factor
C = the ratio a/g
S = the coefficient for the site structure resonance
W = the weight of the building

The seismic probability zone factor Z is based on the seismic risk map of the United States, which is reproduced by permission from UBC in Fig. 3.7. The values for the numerical coefficient Z for zones 0, 1, 2, 3, and 4 correspond to the following:

Zone 0 — No damage, $Z = 0$
1 — Minor damage, $Z = \frac{3}{16}$
2 — Moderate damage, $Z = \frac{3}{8}$
3 — Major damage, $Z = \frac{3}{4}$
4 — Those areas within zone 3 that are in proximity to certain major known faults, $Z = 1.0$

Although it is not possible to predict the maximum earthquake at any location, history and experience together with geological observations have shown that the maximum probable earthquakes do vary with

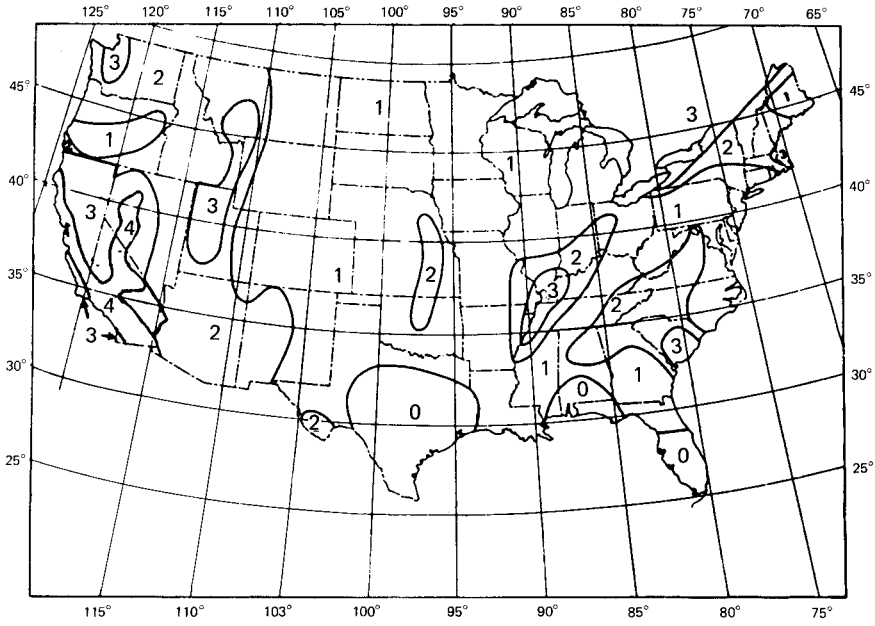

Figure 3.7 UBS seismic risk map. (*Reproduced from 1985 Uniform Building Code.*)

various areas, thus requiring that different seismic design loads be specified for different areas. Thus, the continental United States has been divided into four zones of approximately equal seismic probability. Zone 4 is the very heavy earthquake zone and zone 0 has practically no earthquake expectation. Although provisions of the code are largely empirical, they do represent an acceptable method of computing seismic loads. Corresponding to these loads, the normal design stresses can be increased by one-third, similar to the wind load design, and under the action of these seismic loads the building structure may still not reach its yield point. If the seismic force greatly exceeds the design loads, plastic behavior or ductility of the structure will be called into action, thus providing reserve energy absorption in preventing collapse or catastrophic damage.

The horizontal force factor K depends on the type of structural system employed and is a constant, favoring or penalizing different types of construction. It reflects reserve capacity of the structure to resist collapse under high overloads and is based on previous experience. It varies from 0.67 to 1.33 for buildings, but could be as large as 2.5 for structures such as overhead water tanks. The high-energy-absorbing ductile-moment-resisting frame has a low factor, whereas a rigid shear wall structure has a high factor because it experiences a higher degree of damage.

I is an occupancy importance factor which was introduced into the

code after the San Fernando earthquake, in which many essential facilities such as hospitals and trauma centers were rendered unusable. To prevent this mishap, the code specifies higher values for I of 1.5 for essential facilities and 1.25 for assembly buildings. All other types of occupancies are designed for a value of I equal to unity.

The coefficient C is related to the stiffness of the structure and is determined in accordance with the formula

$$C = \frac{1}{15\sqrt{T}} \tag{3.2}$$

where T is the period of the building, which is established by using the structural properties and deformational characteristics of the elements. T is the fundamental period of vibration of the structure in seconds in the direction under consideration. The value of T can be estimated or computed by sophisticated methods. Since during the preliminary design stage T is not known, an estimate is made on the basis of measurements made on many existing structures and is approximated by the relation

$$T = \frac{0.05\, h_n}{\sqrt{D}} \tag{3.3}$$

where h_n = building height, in feet, above base
D = the dimension of the structure, in feet, in the direction parallel to the applied forces

The equation $C = 1/15\sqrt{T}$ is in effect a plot of the response spectrum. Therefore, the use of equivalent static forces is a spectrum analysis for the first mode only, with an assumed straight-line mode that uses equation $C = 1/15\sqrt{T}$ as an assumed spectrum. The participating contribution of higher modes is given some consideration by arbitrary coefficients which give higher values for local effects and adjusts the load distribution and overturning moments.

S is another coefficient included in the base shear expression to account for the influence of local soil conditions on the seismic motion of the structure. It is a site-structure resonance factor that amplifies the response of the building to earthquake motions originating in bedrock. The amplification is maximum, attaining a value of 1.5 when the site and building periods are identical, and tapering off to a minimum value of 1 or slightly higher when the site and structure periods are substantially different. Two different expressions are used to define S depending upon the value of the ratio of building period to site period, T/T_s, as follows:

$$S = 1.0 + \left(\frac{T}{T_s}\right) - 0.5\left(\frac{T}{T_s}\right)^2 \qquad \text{for values of } \frac{T}{T_s} = 1 \qquad (3.4)$$

and

$$S = 1.2 + 0.6\left(\frac{T}{T_s}\right) - 0.3\left(\frac{T}{T_s}\right)^2 \qquad \text{for values of } \frac{T}{T_s} > 1 \qquad (3.5)$$

UBC stipulates a maximum value for T_s irrespective of the value obtained through geotechnical investigation. The building period must be substantiated by calculations or comparison to other similar buildings. In the absence of a properly established value for T_s, a maximum value of 1.5 can be used for any structure. The product of C and S need not exceed 0.14.

In the 1985 edition of the UBC, an alternate method, called Method B, is given for evaluating S, the numerical coefficient for site-structure resonance. Depending upon the profile type of the soil, the values of 1.0, 1.2, and 1.5 are given for S. The value of $S = 1.0$ is for rock or for other types of soils exhibiting rocklike characteristics with regard to shear wave velocity; $S = 1.25$ for stable deposits of sands, gravels, and stiff clays; $S = 1.5$ for soft to medium-stiff clays and sands. A conservative value of 1.5 is required to be used for S if the exact nature of the soil cannot be determined in sufficient detail to classify the soil according to the descriptions given in the UBC.

An inspection of the equivalent static forces established by the UBC shows that this procedure is highly arbitrary. The coefficients Z and K are not based on quantitative measured data but represent expressions of qualitative judgment. The coefficient C makes an attempt to include the dynamic approach, but is in effect a response spectrum, only vaguely resembling that of a few strong-motion earthquakes, and gives values far below the measured records of moderately strong earthquakes. In this day and age of computer analysis, the code method may appear crude, but it behooves one to note that buildings honestly designed for the code forces have generally performed well in moderately strong earthquakes, and for that reason alone the code is likely to be in use for a long time. It should be noted that the level of protection intended by the code is to prevent damage only in moderate earthquakes and to prevent collapse in a great earthquake. Some damage is expected in a strong or great earthquake.

The other essential items covered in the UBC include: (1) lateral distribution of horizontal shear, (2) evaluation of overturning moments and horizontal torsional moments, (3) drift limitation and

separation of buildings, (4) setbacks, (5) structural design requirements, and (6) lateral forces on parts of buildings. These are outlined in the following sections.

Lateral distribution of base shear. The formula $V = ZIKCSW$ does not indicate the manner in which the shear force is to be distributed throughout the height of the structure. The shear force at any level depends on the dynamic characteristics of the structural deformation, the mass at that level, and the amplitude of oscillation. The earthquake forces deflect the structure into certain shapes known as natural modes of vibration, and related to the shape of each mode is a certain distribution of lateral forces. Examples of the first eight modes are shown in Fig. 3.8 for a uniform shear type of building. Instantaneous lateral forces are found by superposition of the forces resulting from each mode. Because of the nature of mode shapes, sometimes the forces add up and sometimes the forces cancel one another. The resulting maximum shear envelope is as shown in Fig. 3.9. The UBC specifies a triangular lateral load distribution for symmetrical building structures with equal floor weights along the height.

Recognizing the whiplash effect of slender buildings, the code places a part of the base shear as an extra concentrated force F_t at the top of the building. The concentrated force at the top can be determined by the formula $F_t = 0.07TV$. F_t need not exceed $0.25V$ and can be zero for buildings with periods of 0.7 s or less. The remaining portion of the base shear is then distributed over the height of the structure, including the top level, according to the formula:

$$F_x = \frac{(V - F_t)\, w_x h_x}{\sum_{i=1}^{n} w_i h_i} \tag{3.6}$$

Evaluation of overturning and torsional moments. Since a building, especially a tall building, oscillates with the participation of not only the fundamental but also the higher modes of vibration, an accurate evaluation of the overturning moment at a given level of the building can be made only by dynamic methods of analysis. The distribution of earthquake forces prescribed in the UBC primarily represents the forces that are developed by the dominant fundamental mode. Therefore, it is entirely possible that the overturning moments computed by the distributed earthquake forces prescribed in the code are conservative for the calculation of axial loads on vertical elements. However, reduction factors for overturning moments at any given level are not given in the current UBC in light of damage to buildings during the

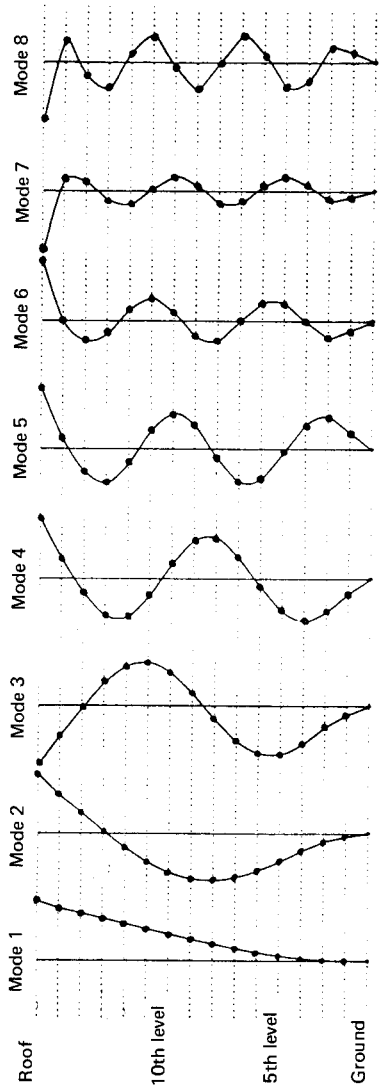

Figure 3.8 First eight modes of vibration.

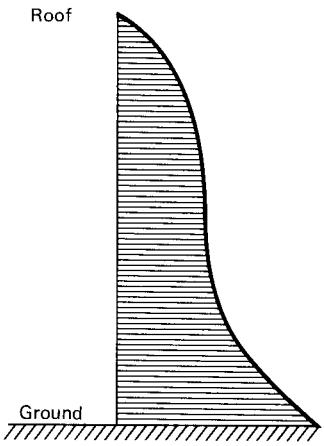

Figure 3.9 Envelope of maximum shears.

1967 Caracas, Venezuela, earthquake. Observation of buildings in the aftermath of the earthquake revealed failure of a number of building columns which could be attributed to the effect of overturning moments.

The overturning moment at any level should be distributed to various resisting elements in the same proportion as the distribution of shear in the resisting system. Where other vertical members are provided which are capable of partially resisting the overturning moment, a redistribution can be made to these members if framing members of sufficient strength and stiffness to transmit the required load are provided. If the vertical resisting element is discontinuous, the overturning moment carried at the lowest story of that element shall be carried down as loads to the foundation. The rigidity of horizontal bracing diaphragm is to be taken into account in the distribution of shear among various lateral force resisting elements.

The torsional effects of the earthquake forces are considered in the seismic design of structures when the center of mass and center of rigidity do not coincide. Even otherwise, possible additional torsional response is to be expected because of errors in the estimation of relative rigidities of structural elements and the errors in the estimation of distribution of dead and live loads at the floor levels and the torsional input motions of the ground. The product of the shear force in the story and the distance between the center of mass and the shear center of the building gives a horizontal torsion that must be accounted for in the design. Even for perfectly symmetrical buildings, which are of course rare in today's high-rise architectural environment, the code stipulates design for an accidental torsion assumed to be equivalent to the story shear acting with an eccentricity of not less than 5 percent of the width of the building at that level. Additional shear forces

statically equivalent to the torsion should be applied to the vertical resisting elements. The beneficial effect of negative torsional shears on the vertical elements should be neglected.

Drift limitation and separation of buildings. Control of lateral deflection or drift of a relative story to its adjacent story deals with the problem of (1) restriction of damage to the nonstructural components such as glass panels, curtain wall panels, plaster walls, and other partitions, and (2) protection from motion sickness or discomfort. Note that realistic interstory drifts during earthquakes are best estimated by computations using a method of dynamic analysis. However, in the UBC no definite value is given for the total building drift, but 0.005 of the story height is recommended as the allowable story drift. Higher values of story drift are permissible if proper provisions are made in the connection of nonstructural elements to prevent distress. For buildings having structural systems such as moment-resistant frames, the code stipulates that the displacements calculated on the basis of applied horizontal forces should be increased by a factor $1.0/K$, with a lower limit set at 1.0 for the ratio $1.0/K$. Although at first this requirement might appear to indicate that more stringent limits are imposed on more ductile structures, it is in reality an attempt to unify the stiffness requirement of all types of structures independent of the K factor.

A separation is required between buildings or between portions of structure such that they are structurally separated by a distance sufficient to avoid contact under deflection from seismic action or wind forces.

Setbacks. UBC specifies that if the plan dimension of a building at any level corresponds to at least 75 percent of the plan dimension of the lower part, then the building can be considered as a uniform building without setbacks provided other irregularities do not exist. For structures having irregular shapes or framing systems, UBC recommends that the distribution of lateral forces be determined using a dynamic analysis of the structure.

Structural design requirements. UBC allows a one-third (33 percent) increase in all allowable stresses of structural materials and soil bearing values when combined vertical and earthquake forces are considered in a working stress design. The loading combinations prescribed for working stress design are as follows:

1. Dead load plus floor live load plus roof live load (or snow load)
2. Dead load plus floor live load plus wind load (or seismic load)

3. Dead load plus floor live load plus wind load plus half snow load
4. Dead load plus floor live load plus snow load plus half wind load
5. Dead load plus floor live load plus snow load plus seismic load

For buildings using the strength design approach, the code stipulates the following load combinations:

$$U = 1.4D + 1.7L \tag{3.7a}$$

$$U = 0.75(1.4D + 1.7L \pm 1.87E) \tag{3.7b}$$

$$U = 0.75(1.4D + 1.7L \pm 1.7W) \tag{3.7c}$$

$$U = 0.9\text{D} \pm 1.43E \tag{3.7d}$$

$$U = 0.9D \pm 1.3W \tag{3.7e}$$

$$U = 1.4D + 1.7L + 1.7H \tag{3.7f}$$

$$U = 0.9D + 1.7H \tag{3.7g}$$

$$U = 0.75\,(1.4D + 1.4T + 1.7L) \tag{3.7h}$$

$$U = 1.4(D + T) \tag{3.7i}$$

For reinforced concrete buildings subjected to earthquake motions, load combinations containing the earthquake term [Eqs. (3.7*b* and *e*)] are modified as follows:

$$U = 1.4(D + L \pm E) \tag{3.7j}$$

$$U = 0.9D \pm 1.4E \tag{3.7k}$$

The notations used in Eqs. (3.7*a* to *k*) are as follows:

U = required strength to resist factored loads or related internal moments and forces
D = dead loads or related internal moments and forces
L = live loads or related internal moments and forces
W = wind loads or related internal moments and forces
E = load effects of earthquake or related moments and forces
T = internal moments and forces due to differential settlement, creep, shrinkage, or temperature effects
H = moments or forces due to earth pressure

Lateral forces on parts of buildings. The UBC specifies that parts of buildings and their anchorages are to be designed on the basis of the

formula

$$F_p = Z_i I C_p W_p$$

where F_p = the lateral force on the part being considered
Z = the zonal probability factor
W_p = the weight of the part being considered
C_p = the horizontal force factor as given in Table No. 23-J of UBC
I = the importance coefficient, which has the same value as used for the building

In an earthquake, the ground motion is highly erratic and includes vibrations of a wide range of frequencies. As a result, each component of the building may vibrate at its own frequency and produce local accelerations in miscellaneous parts of the building considerably greater than those of the building as a whole. Also, the damping that is usually present for the building as a whole may be completely lacking for many of the building parts. To account for these local conditions, the code specifies higher accelerations for various parts of buildings when considered as isolated elements. These appear as a factor C_p in a separate table in the UBC. The numerical value of C_p again has been assigned by arbitrary judgment based primarily on observation of earthquake damage. For example, C_p for cantilevered parapets is 1; for exterior precast panels, 2.0; for walls and partitions, 0.20. It is not intended that the coefficient specified for the design of these parts of structures be used simultaneously in the design of the whole structure. However, code coefficients apply in both directions. If a wall, for example, is to be designed for a factor C_p of 0.20, this force must be considered to be applied in either direction normal to the face of the wall. The same is true for floor diaphragms, roof diaphragms, parapet walls, and all other parts.

The elements of a building in some degree affect its overall dynamic properties; they may also affect the damping capacity and the energy dissipation characteristics of the building. The reactions for the building elements under their seismic design coefficient must also be provided for at the connections. They must be connected in such a way that there will be strength and inherent ductility whatever the direction of the motion. A great deal of improvement in seismic resistance can be obtained by a thorough planning and detailing of the parts, regardless of the specific design coefficients used.

3.4.3 American National Standard Institute (ANSI A58.1-1982) method

The minimum earthquake design loads given in the ANSI standard are primarily based on the 1979 UBC with some modifications. The

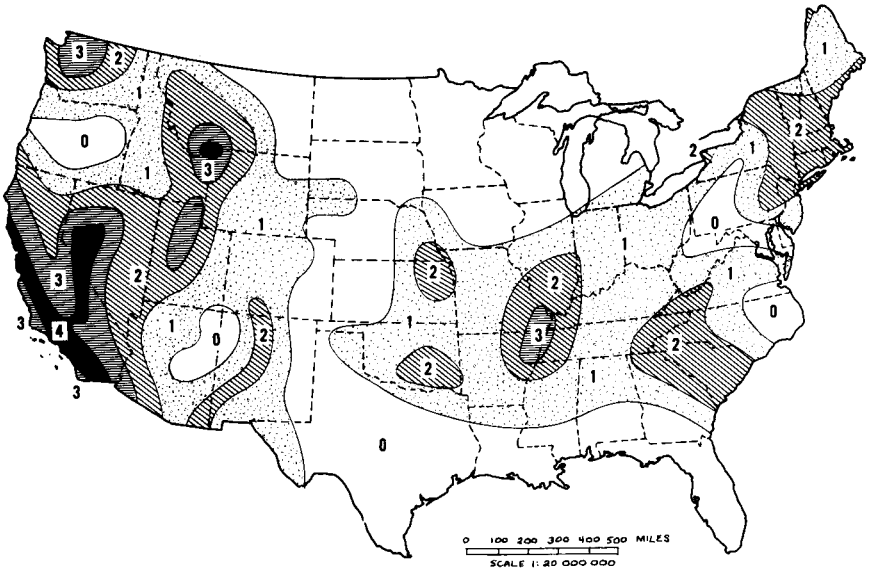

Figure 3.10 Map for seismic zones for 48 contiguous states. (*This material is reproduced with permission from ANSI A58.1-1982, copyright 1982 by the American National Standards Institute. Copies of this standard may be purchased from the American National Standards Institute, 1430 Broadway, New York, NY 10018*).

basic equation that defines the minimum lateral seismic forces acting nonconcurrently in the direction of each of main axis of the building is given by the formula:

$$V = ZIKCSW \tag{3.8}$$

For determining the seismic zone coefficient Z, ANSI has adapted the velocity-related zoning map (Fig. 3.10) from the Applied Technology Council publication ATC 3.06. ATC uses two types of zoning maps based on the concept of effective peak acceleration and the effective peak velocity, which are referred to as EPA and EPV maps, respectively. Several nontechnical reasons influenced the choice of the EPV map over the EPA map. First, because EPA contours are closely spaced for California and Nevada, it would have required subdividing these states into five zones. Second, in the interest of simplicity, it was preferable to use the more conservative EPV map. Third, use of the EPV map resulted in fewer changes to the zoning as given in the UBC. The ANSI zoning map subdivides the continental United States into five seismic zones: 0, 1, 2, 3, and 4, with corresponding Z values of $\frac{1}{8}$, $\frac{3}{16}$, $\frac{3}{8}$, $\frac{3}{4}$, and 1.0, respectively, as shown in Fig. 3.10.

The occupancy importance coefficient I has three values: 1.0, 1.25, and 1.50. The lower value of 1.0 applies to all buildings such as office and residential buildings which are not primarily used for assembly

purposes. Buildings primarily used for the congregation of more than 300 people are given a higher value of 1.25. Essential facilities such as hospitals, fire and police stations, communication centers, and defense installations are given an I value of 1.5.

The coefficient K gives the energy dissipation capacity that compensates for the difference between measured accelerations in an earthquake and the pseudo-acceleration used in the calculation of earthquake forces. The energy dissipation capacity is primarily due to the ductility and damping characteristics of the structural system.

The values of K given in the ANSI standard are identical to the 1979 UBC values with three exceptions. (1) The K value has been reduced from 1.33 to 1.0 for one-, two-, or three-story box structures with diaphragms, shear panels, joists, studs, and sheathing materials. These have been found to have good resistance to strong ground motion as compared to box structures having walls and diagonal bracing elements. (2) To emphasize the idea that ordinary unbraced moment-resisting concrete frames are not desirable in high seismic zones 2, 3, and 4, no value of K has been given for such structures. However, moment-resisting frames are permitted in these zones using a value $K = 1$ provided that special details that impart ductility to the frame are employed. The details may not be as stringent as those required for systems using $K = 0.67$. Buildings in seismic zones 0 and 1 for which I is less than 1.5 can be detailed without undue concern for ductility as long as anchorages between walls, floors, and roof are designed to resist the seismic horizontal forces and continuous load paths are provided between the resisting element and the element that transmits the seismic forces; minimum force for connection design is specified as equal to $0.15ZI$ or 0.05, whichever is greater, times the weight of the element being connected to the resisting element.

An alternate approach to the design of structures in zones 2, 3, and 4 is to omit the ductility requirements altogether and to use a value of $K = 2.50$. (3) For unreinforced masonry, no horizontal force factor K is given for seismic resistance in zones 2, 3, and 4 because of the inability of unreinforced masonry to undergo significant inelastic deformation. A higher value of $K = 4.5$ is considered acceptable in the design. All buildings in zone 0 and buildings with I less than 1.5 in zone 1 can be designed with unreinforced masonry provided anchorages meet requirements outlined in 2 above for concrete moment frames.

The seismic coefficient C is determined by the formula

$$C = \frac{1}{15\sqrt{T}}$$

where T is the fundamental elastic period of vibration of the building in the direction under consideration, measured in seconds.

A number of simple equations that involve only a general description of the building type and overall dimensions are given for estimating the building period. An increase of 20 percent above the simple period formulas is allowed when using a more exact formula that uses the stiffness properties and deformation characteristics of the structure. The simple formulas for estimate of period for different building types are as follows:

1. For shear walls or exterior concrete frames utilizing deep beams or wide piers, or both,

$$T = \frac{0.05\ h_n}{\sqrt{D}} \tag{3.9}$$

where h_n = building height in feet
D = dimension of the structure in a direction parallel to the direction under consideration, in feet

2. For isolated shear walls not interconnected by frames or for braced frames

$$T = \frac{0.05\ h_n}{\sqrt{D_s}} \tag{3.10}$$

where D_s = maximum dimension of shear wall or braced frame parallel to the applied forces, in feet

3. Moment-resisting steel space frames

$$T = 0.035 h_n^{3/4} \tag{3.11}$$

4. Moment-resisting concrete space frames

$$T = 0.025 h_n^{3/4} \tag{3.12}$$

Many of the formulas for building fundamental periods given in ANSI are based on data and recommendations presented in ATC 3.06.

A more exact formula for the period T that incorporates the stiffness and deformational characteristics of the building is given by the relation

$$T = 2\pi \sqrt{\frac{\sum_{i=1}^{n} w_i \delta_i^2}{g \sum_{i=1}^{n} f_i \delta_i}} \tag{3.13}$$

where δ_i = deflection of level i relative to the base due to applied lateral forces, Σf_i

f_i = any lateral force at level i, obtained on the basis of a rational distribution of the elastic deflection at level i
g = acceleration due to gravity

S is the soil factor in Eq. (3.8) that attempts to combine the effect of underlying soil on the dynamic characteristics of the building. Soil profile is categorized into three types, S_1, S_2, and S_3, and relies on word descriptions for soil profiles. A different S factor is assigned to each type of soil profile: 1.0 for S_1, 1.20 for S_2, and 1.50 for S_3. An upper limit of 0.14 is placed for the product CS, except for soil profile S_3 in seismic zones 3 and 4, in which the product CS need not exceed 0.11.

The total base shear V is distributed over the height of the structure according to the relation

$$V = F_t + \sum_{i=1}^{n} F_i \tag{3.14}$$

where F_t = the additional lateral force at top to account for whiplash effect and effects of higher modes and is equal to $0.07TV$
F_i = the lateral force at level i

The maximum value for F_t is stipulated as $0.25V$ and may be neglected for relatively stiff buildings with fundamental period of 0.7 or less. The distribution of remaining base shear over the height is given by the relation

$$F_x = \frac{(V - F_t)\, w_x h_x}{\sum_{i=1}^{n} w_i h_i} \tag{3.15}$$

Other salient features of the ANSI code are as follows.

Since the static analysis is based on a fairly uniform structure, ANSI requires that irregularly shaped buildings, and buildings having large differences in structural stiffness of adjacent stories, be analyzed by a dynamic analysis. In distributing the horizontal shear to various lateral-force-resisting systems due consideration is to be given for the relative rigidities of the various vertical elements as well as the in-plane rigidity of the floor system. As in UBC, ANSI requires a minimum torsion equal to the lateral force times 5 percent of the dimension of the building in the direction of forces to be considered in the design. Diaphragms such as floor and roof systems must be designed for a minimum lateral force of $0.14ZIw_{px}$, where w_{px} is the weight of floor or roof diaphragms and collectors and elements tributary to it at level x, plus 25 percent of the storage live load for warehouse occupancies.

A reduction in the calculated overturning moment is allowed for tall buildings because the envelope of story shears overestimates the overturning moments in such structures. Whether or not this reduction is justified in light of observation of earthquake behavior of buildings during the 1967 earthquake in Caracas, Venezuela, has been a subject of much debate. No reduction is allowed for the top 10 stories of a tall building because of the whiplash effect. A reduction of 20 percent of overturning moment is permitted for the twentieth story from top and those below it. A linear interpolation between 0 and 20 percent is allowed for stories between the tenth and the twentieth stories below the top. Drift and building separation requirements are identical to UBC requirements.

Elastic or inelastic dynamic analysis is permitted for establishing magnitudes of lateral forces and their distribution provided that (1) base shear shall not be less than 90 percent of the value obtained by the equivalent static analysis, (2) a value of $K = 0.67$ to 2.5 is used for structural systems that meet the detailing requirements for a level of ductility consistent with the value of K, (3) the drift limitation of 0.005 times the story height shall be satisfied using the equivalent static forces. (4) The dynamic analysis is performed by using either a smooth response spectrum or by inputting ground motion time histories that reflect the characteristics of the structure and site.

With regard to seismic detailing of steel structures, reference is made to the detailing requirements of part II of AISC specifications which give specific criteria for (1) minimum width or depth to thickness ratios, (2) bracing requirements to inhibit lateral torsional buckling, and (3) connections that are capable of developing plastic hinges. For concrete structures, reference is made to the ACI 318, Appendix A, which gives ductility requirements for $K = 0.67$.

All buildings are required to achieve a minimum degree of seismic resistance because even buildings in zone 0 are not totally immune from small intensities of ground shaking.

Non-load-bearing exterior panels are required to be designed for a seismic load given by the relation

$$F_p = ZIC_pW_p \tag{3.16}$$

where F_p = lateral force on the panel in the direction under consideration
C_p = Horizontal force factor for the panel with a typical value of 0.30
W_p = weight of the panel

Allowance should be made at the connection of panels to the structure to accommodate a minimum of $\frac{1}{2}$ in (12.7 mm) of relative

story deflection or $3.0/K$ times the calculated elastic deflection, whichever is greater. Connection should be detailed to have sufficient ductility to alleviate premature fracture of concrete. The connection is required to resist $1\frac{1}{3}$ times the inertia force of the panel as given in Eq. (3.16). Individual fasteners such as anchor bolts and inserts must be designed for four times the load given in Eq. (3.16). Positive attachment of fasteners embedded in concrete is required to transfer the load to the reinforcement effectively. A value of $I = 1.0$ is used in Eq. (3.16) for the design of connection and fasteners.

3.4.4 Applied Technology Council (ATC 3-06) provisions

The Applied Technology Council, a research and development subsidiary of the Structural Engineers Association of California (SEAOC), sponsored the development of a seismic code in 1974 by taking a fresh look at all aspects of earthquake-resistant design that would be applicable throughout the United States. The outcome of this project is a massive 505-page document, *Tentative Provisions for the Development of Seismic Regulations for Buildings*, known as ATC 3-06, published in 1978. The report is not a code but is of interest to engineers concerned with the design of seismic-resistant buildings. It is currently being reviewed by code-governing bodies for possible adaptation of certain sections.

ATC 3-06 assigns buildings into different categories in accordance with concern for life safety. The configuration of the building together with the category to which the building is assigned dictates primarily what method of analysis should be used for designing its seismic resistance system. These seismic performance categories are classified into four types as follows:

Category A: Limited to low-seismic-risk areas requiring only wind-resistant design. Some minimum resistance to earthquake is provided by ties and wall anchorages.

Category B: Some earthquake-resistant requirements, but these are less stringent as compared to requirements in areas of high seismicity.

Category C: The level of seismic resistance requirements compares roughly to the current design practice on the west coast for buildings other than schools and hospitals.

Category D: Critical structures in relatively high seismic zones require this construction. As much redundancy as possible should be provided for the lateral bracing systems of buildings in both categories C and D.

The ATC 3-06 provisions contain several noteworthy departures from the other building codes. First, ATC 3-06 attempts to establish a

uniform seismic risk throughout the country by considering both the intensity of ground motion and frequency of seismic events. Seismicity in a region is related to the ground motion indexes that take into account not only seismic motion at the source but also the attenuation with distance from the source. The zone coefficient is tied to two indexes related to effective peak acceleration (EPA), and effective peak velocity (EVA), plus a seismic index. This dual approach is an attempt to capture a realistic response of both short-period structures which are governed by the maximum acceleration characteristics of ground motion, and longer-period structures which are influenced by the peak velocity of ground motion. ATC 3-06 provides two seismic risk maps for establishing the design acceleration by using two coefficients: (1) A_a, a coefficient representing effective peak acceleration, and (2) A_v, a coefficient representing effective peak velocity-related acceleration. The former is associated with local seismicity, whereas the latter reflects possible effects of distant earthquakes on longer-period structures. Both these maps, referred to as EPA and EPV maps, divide the country into seven distinct zones relating each zone to A_a and A_v, which are expressed in decimal fractions of g, the acceleration due to gravity.

The equivalent lateral force V to be applied on the building is given by the relation

$$V = C_s W \tag{3.17}$$

where W = the total gravity load of the building, including partitions and permanent equipment and operating contents, with proper allowance for snow loads for buildings and 25 percent of live load for storage and warehouse

C_s = a seismic design coefficient related to (1) both effective peak acceleration coefficient A_a and effective peak velocity coefficient A_v, (2) soil coefficient S, (3) fundamental period of building T, (4) structural system response modification factor R

The seismic coefficient is given by the relationship

$$C_s = \frac{1.2A_vS}{RT^{2/3}} \tag{3.18}$$

The value of C_s need not be greater than 2.50. For type S_3 soil where A_a is equal to or greater than 0.30, the value of C_s need not exceed $2A_a/R$. The term S in Eq. (3.18) represents the characteristics of the site. It has the numerical value of 1.0 for type S_1 soil, 1.2 for type S_2

soil, and 1.5 for type S_3 soil. The soil characteristics are summarized as follows:

S_1 = stable deposits of sand, gravel, or stiff clays with a maximum overburden depth of 200 ft (61. 6 m).

S_2 = stable deposits of sand, gravel, or still clays in excess of 200 ft (61. 6 m) of overburden.

S_3 = deposits of soft to medium-stiff clays with or without intervening layers of sand or other cohesionless soils. A minimum depth of 30 ft (10 m) is stipulated for cohesive deposits.

The response modification factor R is somewhat similar to the ductility coefficient used in the UBC. However, a major difference exists between UBC and ATC 3-06 approaches regarding the manner in which the structure's inherent ductility is taken into account when specifying lateral design forces. In the UBC, the magnitude of the basic design force is computed for a structure of average ductility, then adjusted upward or downward by the use of the K factor. Structures with lower energy dissipation capacity are adjusted upward, and those with greater energy dissipation capacity are adjusted downward.

In the ATC 3-06 approach, the magnitude of reduction between the forces due to elastic response and forces to be used in design is obtained explicitly by the use of response modification factor R. Structures with significant redundancy and ductility qualify for greater force reductions, while those with relatively little redundancy and ductility qualify for relatively small force reductions. For example, the recommended R for a partially reinforced shear wall is 1.25, while that for a specially reinforced concrete moment frame is 7.

The value of R varies from a low of 0.25 to a high of 8, as compared to the values of K in UBC which vary from 0.65 to 2.5. The seemingly large difference is due to the fact that ATC 3-06 stipulates that the approximate period values, which are based on the geometric parameters, be used for the preliminary design only. It is the intent that the final design be based on a more rational value of T calculated using the methods of structural dynamics. These refined values of periods are typically larger than those based on geometrical considerations alone and hence are likely to produce similar values of base shear as in other codes.

Special provisions are made to reduce the base shear by taking into account the soil structure interaction. An upper limit of 30 percent is placed for the maximum reduction of base shear. The distribution of base shear as lateral forces at different heights is accomplished by a relationship that provides linear distribution for short-period buildings and a parabolic distribution for long-period buildings. This is in

view of the fact that higher modes are more significant for long-period structures.

Horizontal torsion is taken into account at each story by considering an accidental eccentricity of 5 percent of the plan dimension in the appropriate direction. The effects of accidental torsion are to be combined with those for calculated torsion. The overturning moments computed from the lateral forces are modified by a reduction factor with a value of 1.0 for the top 10 stories, 0.8 for the twentieth story and floors below it, and linearly interpolated value for stories between 10 and 20.

ATC 3-06 stipulates that story drift be calculated as the elastic deflection of the structure with fixed base and subjected to lateral seismic forces. The calculated values are amplified by coefficient C_d that depends on the type of seismic-resisting system employed. The maximum allowable story drift varies from 0.01 to 0.02 times the story height, depending upon the seismic hazard exposure and building group.

The secondary effect on shears and moments of frame members due to the p-Δ effect that is induced by the action of vertical loads and displacements of the building due to seismic forces are to be considered when the relation $P\Delta/VhC_d$ is greater than 0.10 for any story.

ATC 3-06 provisions are based on strength design rather than working stress concept and give capacity reduction factors to reflect the limit-state design. Biaxial effects are considered by combining the effects of 100 percent of the load in one direction with 30 percent of the effects in the perpendicular direction.

The equivalent lateral force procedure is not recommended for buildings that are irregular in shape, either in terms of abrupt changes in the structural stiffness or inertia properties. Such buildings must be analyzed with special consideration for their dynamic characteristics.

ATC 3-06 stipulates two methods of dynamic analysis. The first method is called *analysis by mathematical model* and the second is *modal analysis*. The first method is intended for irregular buildings in seismic performance Categories C and D, which are located in areas of high seismicity whose failure will result in significant hazard to the public. Modal analysis for such buildings may not yield realistic results because of its inability to properly account for irregular distribution of story strengths, thus requiring concentration of ductility demand in a few stories of the building.

A more rigorous procedure, in which the actual strength properties of the various components of a building can be explicitly considered, is preferable in such cases. A nonlinear time history analysis is one such procedure. It consists of step-by-step integration of coupled equations of motions, taking into account the inelastic behavior of the structural

system. The procedure for inelastic time analysis is similar to the elastic procedure, except at each step of integration the stiffness matrix of the structure is modified to account for yielding.

In modal analysis, the response of a multi-degree-freedom structure is captured by the superposition of responses of individual natural modes of vibration, each mode responding with its own frequency and mode shape. In a planar analysis the building is modeled as a system of masses lumped at the floor levels, with each mass having one degree of freedom, that of lateral displacement in the direction under consideration. However, for buildings with vertical irregularities or with nearly equal lower natural frequencies, the effects of torsion should be accounted for by a modal analysis with at least three degrees of freedom per floor, two translational and one torsional. The design values of base shear, lateral force, and deflection at each level are determined by combining their modal values. The modal analysis can be used for buildings in Categories C and D having irregularities of mass and stiffness over the height.

3.5 Dynamic Approach: Spectrum Method

3.5.1 Introduction

Determining the behavior of a structure during an earthquake is basically a vibration problem. The seismic motions of the ground cause the structure to vibrate and the amplitude of vibration of this dynamic deformation and its duration are of concern to the engineer. Using dynamic analysis, calculations can be made of the earthquake-induced vibrations of the structures, and these will indicate the general nature and amplitude of the deformation that can be expected during the earthquake. The actual earthquake design criteria must be based on a number of considerations, such as the probability of occurrence of strong ground shaking, the characteristics of the ground motion, the nature of the structural deformation, the behavior of the building materials when subjected to oscillatory strains, the nature of the building damage that may be sustained, and the cost of repairing the damage as compared to the cost of providing additional earthquake resistance. Earthquake design criteria must specify the desired strength of structures so that there is approximately a uniform factor of safety for different structures and for different parts of the same structure.

With the advent of computers and greater understanding of the earthquake phenomenon, the structural engineering profession has gradually moved toward more exact approaches in the seismic design of multistory buildings. Relatively simple methods based on equivalent static loads are no longer satisfactory. The current design practice

often requires more precise determination of local seismicity and critical ground motion characteristics and application of advanced dynamic analysis techniques using sophisticated computer programs. These techniques generally lead to improved accuracy in predicting structural response.

For most buildings, an inelastic response can be expected to occur during a major earthquake. Although nonlinear inelastic programs are available, these are not representative of state-of-the-art analysis and are rarely employed in practice because (1) their proper use requires special background, (2) results produced are difficult to interpret and apply to traditional design criteria, and (3) the necessary computations are prohibitively expensive. Therefore, analyses used in practice are essentially based on linear elastic analysis. There are three choices available for applying the dynamic earthquake loads, namely, the time history, the frequency domain, or the response spectrum methods. Both the time history and frequency domain methods require prescription of a specific ground motion record which requires prediction of the future critical seismic ground motion that can occur at a given site. The difficulties associated with prescribing appropriate earthquake motions are numerous because of the highly indeterminant nature of estimating future seismic ground motions that may occur at a site during the useful life of a structure. Therefore, it is prudent to base seismic design on a range of possible earthquake ground motions rather than a single assumed earthquake motion. This is obtained by using a so-called response spectrum, which represents an envelope of upperbound responses based on several different ground motion records. The method, based on response spectrum, is generally cost effective and therefore is the most widely used approach for representing dynamic earthquake loading. This method, which is generally considered as the state of art among structural engineers, is considered next.

3.5.2 Spectrum analysis

The word "spectrum" is used to reflect the fact that a broad range of related quantities is summarized on one graph. For a given earthquake record and a given percentage of critical damping, the graph shows related quantities such as acceleration, velocity, or deflection for a complete range or spectrum of building periods.

The plot of a response spectrum can be explained with reference to Fig. 3.11 by visualizing it as the response of a series of progressively longer cantilever pendulums with increasing natural periods subjected to a common lateral agitation at the base. Assume that the common base is moved through a ground motion corresponding to the motion that would occur in a given earthquake. A plot of maximum response

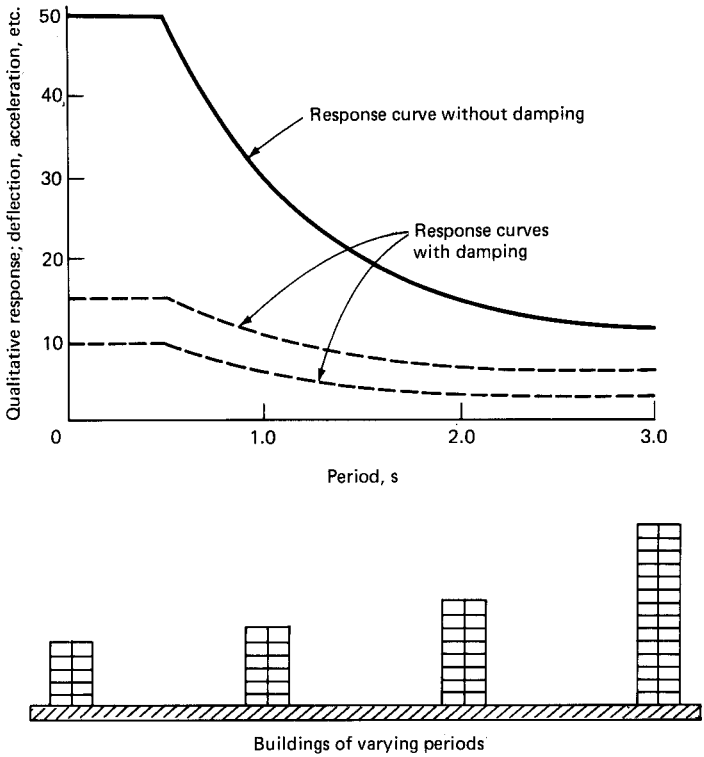

Figure 3.11 Response spectrum.

such as acceleration versus the period of the pendulums will provide the acceleration response spectrum as shown in Fig. 3.11. The absolute value of the peak acceleration response occurring during the excitation for each pendulum is represented by a point on the acceleration spectrum curve. In Fig. 3.12 the generation of the response spectrum for the 1940 El Centro earthquake is illustrated. Using the ground acceleration as input, a family of response spectrum curves can be generated for various levels of damping, where higher values of damping result in lower spectral response.

In order to establish the concept of spectrum method, let us consider a single-degree-of-freedom structure such as an elevated water tank supported on columns or a revolving restaurant supported at the top of a tall concrete core. These structures can be adequately modeled as single-degree-of-freedom structures by considering the columns and the core as flexible cantilevers and the tank or the restaurant as the only mass at the tip of the cantilever; the mass of the columns or core is ignored. Let us assume that we are required to design the structures for an earthquake which will have the same characteristics as the 1940

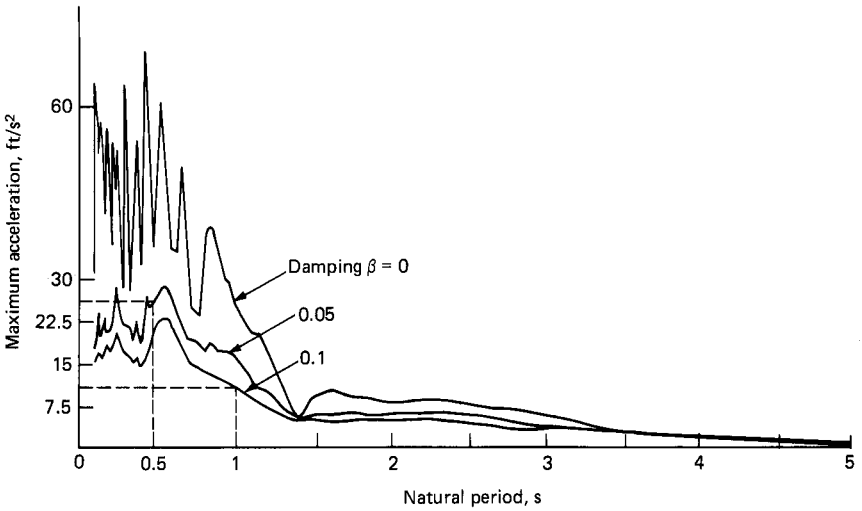

Figure 3.12 Acceleration spectrum: El Centro earthquake.

El Centro earthquake. The recorded ground acceleration for the first crucial 30 s of the earthquake is shown in Fig. 3.2. The maximum acceleration recorded is 0.33 g, which occurred at about 2 s after the start of the record.

The dynamic problem then is to analytically subject the base of the structure to the same acceleration as the El Centro recorded acceleration and to calculate the maximum acceleration experienced by the mass during the first 30 s of the earthquake. In structural dynamics it is possible to obtain the maximum response such as displacement, velocity, and accelerations of a single-degree-of-freedom system by assuming that the ground motion corresponds to a series of impulsive loads. The maximum response can be obtained by integrating the effect of individual impulses over the duration of the earthquake. This procedure is called *Duhamel integration* and is widely used for obtaining maximum response of earthquakes. In the seismic analysis of buildings it is generally not necessary for the engineer to carry out the complicated integration procedures because the maximum response values for many recorded earthquakes are already established. For example, the acceleration response derived for the north-south component of the El Centro earthquake is shown in Fig. 3.12.

To design the two structures mentioned earlier, assume the tank and restaurant structures weigh 720 kips (3202 kN) and 2400 kips (10,675 kN), with corresponding period of vibration of 0.5 and 1 s, respectively. Since the response of the structure is strongly influenced by the damping factor, it is necessary to estimate the critical damping for the two structures. Let us assume the critical dampings for the two structures are 0.05 and 0.1, respectively. From Fig. 3.12, the acceler-

ation for the water tank is 26.25 ft/s^2, giving a horizontal force in kips equal to the mass of the tank, w/g, times the acceleration

$$F = \frac{720}{32.2} \times 26.25 = 587 \text{ kips } (2611 \text{ kN})$$

The acceleration for the restaurant from Fig. 3.12 is 11.25 ft/s^2, and the horizontal force in kips would be equal to the lumped mass at the top of the core times the acceleration, or $2400 \times 11.25/32.2 = 838.51$ kips (3730 kN). The two structures can then be designed by applying horizontal forces at the top and determining the associated forces and moments. The lateral load, which is obtained by multiplying the response spectrum acceleration by the lumped mass of the system, is referred to as the *base shear*, and its evaluation forms one of the major tasks in earthquake analysis.

In the previous example a single-degree-of-freedom example was chosen to illustrate the underlying principle of spectrum analysis. Multistory buildings, however, cannot be modeled as single-degree-of-freedom systems and their analysis is necessarily more complicated than the previous examples.

A multistory building will have as many modes of vibration as it has degrees of freedom. The use of lumped mass models to represent the actual distributed mass of a structure is a convenient tool for reducing the infinite degrees of freedom of the structure to a manageable few. In multistory buildings it is generally sufficient to assume the masses as concentrated at the floor levels and to formulate the problem in terms of these masses.

Assuming that masses are concentrated at each level, for a planar analysis the number of modes of vibration corresponds to the number of levels in the multistory structure. Each mode of vibration has its own characteristic frequency or period of vibration. The actual motion of a tall building at any instant is a unique linear combination of its natural or principal modes of vibration. During vibration, the masses of the structure vibrate in phase with displacements as measured from its initial position, always having the same relationship to each other. All masses vibrating in one of the natural modes pass the equilibrium position at the same time and reach their extreme positions at the same instant.

Using certain simplifying assumptions, it can be shown that each component mode of vibration behaves as an independent single-degree-of-freedom system with a characteristic frequency. The assumptions required for and the proof of the proposition will not be attempted in this section because it is explained in subsequent sections. For now, suffice it to note that this method called the *modal*

superposition method, consists of obtaining the total response of the building by appropriately combining the first few selected modes of vibration.

Since a multistory building has several degrees of freedom, in general it vibrates with as many different mode shapes and periods as it has degrees of freedom. Each mode of vibration contributes to the base shear, and for elastic action of the structure, this base shear can be determined by multiplying an effective mass by an acceleration read from the response spectrum for the period of that mode and for the assumed damping. Therefore, the procedure for determining the base shear for each mode of a multi-degree-of-freedom structure is the same as that for determining the base shear for a single-degree-of-freedom structure except that an effective mass is used instead of the total mass. The effective mass is a function of the actual mass at each floor and the deflection at each floor and is greatest for the fundamental mode and becomes progressively less for higher modes. The mode shape must therefore be known in order to compute the effective mass.

Since the actual deflected shape of the building consists of linear combinations of the modal shapes, higher modes of vibration also contribute, though to a lesser degree, to the structural response. These can be taken into account by using the concept of a participation factor. Further mathematical explanation of this concept is deferred for a later section, but suffice it to note that inertia force, also called the base shear, for each mode is determined as the summation of products of effective mass and spectral acceleration. The force at each level for each mode is obtained by distributing the base shear in proportion to the product of the floor weight and displacement. The total design values are then computed by taking the square root of sum of the squares of the forces thus obtained at each floor level. These forces are applied as static loads, and the structural analysis is carried out in the familiar manner. Other methods of modal combinations, such as complete quadratic combination techniques, are available but will not be discussed.

3.5.3 Development of design spectrum

In the usual practice of structural engineering of tall buildings it is very rare that the structural engineer is called upon to develop a design response spectrum. However, it is of practical value to understand the various assumptions and limitations that go into the development of response spectra. To this end a brief description of the three basic approaches used in the development of design spectra is given in the following sections. The three approaches are:

1. The use of actual earthquake records
2. The use of smoothed design spectra
3. Use of unique design spectra reflecting the actual site conditions

Response spectrum from actual earthquake records. The generation of a response spectrum curve can be idealized by subjecting a series of damped single-degree-of-freedom mass spring systems with continuously varying natural periods to a given ground excitation as explained in the previous section. Response spectrum graphs are generated by numerical integration of actual earthquake records to determine maximum values for each period of vibration.

Spectral curves developed from actual earthquake records are quite jagged, being characterized by sharp peaks and troughs. Because the magnitude of these troughs and peaks can vary significantly for different earthquake records and because of the uncertainties of future earthquakes, it is wise to consider several possible earthquake spectra in the evaluation of the structural response for design purposes. Thus, if response to actual recorded earthquakes is to serve as a design basis, analysis should be performed using several selected spectra that are believed to be representative of critical ground motions that may occur at the site.

Smooth design spectra. As an alternative to the use of several earthquake spectra for design, researchers have developed smooth design spectra that represent approximate upper-bound response envelopes based on critical levels of ground motion. The sharp peaks in earthquake records indicate the resonant behavior of the system when the natural period of the system coincides with the period of the forcing function, especially for systems with little or no damping. However, as can be seen from the spectra, even a moderate amount of damping has a tendency to smooth out the peaks and reduce the spectral response. Because most buildings in practice possess at least some degree of damping, the peaks in response spectra are of little significance. Therefore, it is justifiable to smooth out the spectra without losing their practical value. Figure 3.13 shows the smoothed-out acceleration spectra for the El Centro, California, earthquake as first defined by Housner. The other two response spectra for velocity and displacement, shown in Figs. 3.14 and 3.15, are obtained from the acceleration spectrum, since they are related to one another. The three spectra can be drawn in one figure, as shown in Fig. 3.16. In this figure the horizontal axis denotes the natural period and the ordinate denotes the spectrum velocity, with both these axes following a logarithmic scale. The acceleration and displacement are read from diagonal axes in-

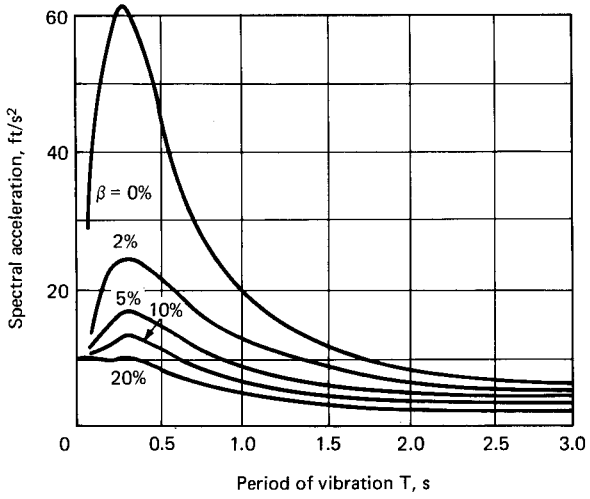

Figure 3.13 Smoothed-out acceleration spectra for El Centro earthquake.

clined at 45° to the horizontal axis. Such a plot, which encompasses all the spectral parameters, is called a *tripartite diagram*. From this plot the following observations can be made.

1. For extremely short periods, i.e., for very high frequency, hence very stiff, structures, the spectral acceleration values approach magnitudes equal to maximum acceleration. The structure would move like a rigid body attached to the ground.
2. For moderately short periods of the order of 0.1 to 0.3 s, the spectral accelerations are about twice as great as the maximum ground acceleration.

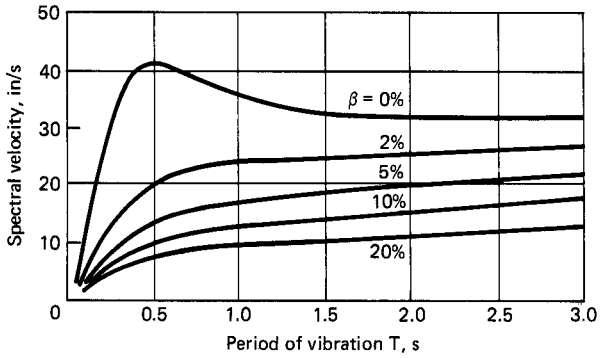

Figure 3.14 Smoothed-out velocity spectra for El Centro earthquake.

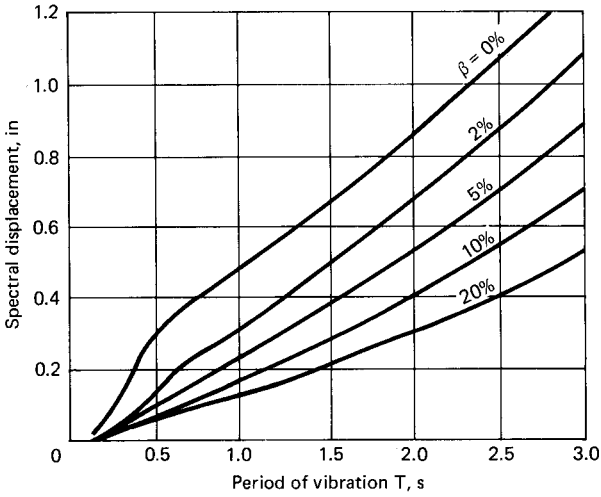

Figure 3.15 Smoothed-out displacement spectra for El Centro earthquake.

3. For very long periods, i.e, for very low frequencies, hence for slender buildings, the maximum spectral displacements approach the maximum ground displacements.
4. For intermediate frequencies, the maximum spectral velocity has a magnitude several times the input velocity.

In the low-period range, the variation of the spectrum curve tends to show correlation with the line of maximum ground acceleration. In the medium-period range, the variation of the spectrum curve tends to show correlation with the line of maximum ground velocity. In the higher-period range, the variation of the spectrum curve tends to show correlation with the displacement.

Because of the above characteristics, it is possible to represent an idealized upper-bound response spectrum curve by three straight lines that envelop the spectral displacement, velocity, and acceleration. To illustrate the development of smooth design response spectra, the values of maximum ground acceleration ($\bar{a}$ = 0.348 g), maximum velocity ($\bar{v}$ = 1.10 ft/s), and maximum displacement ($\bar{d}$ = 0.36 ft) that occurred during the El Centro earthquake are also shown in Fig. 3.16.

By drawing lines parallel to the ground motion maxima, an approximate smooth spectrum curve can be constructed as shown in Fig. 3.16 by applying factors of proportionality to the peak values of the ground acceleration, velocity, and displacement. In this way, the smooth response spectrum curve can be constructed using various factors of proportionality applied to the ground motion maxima over different

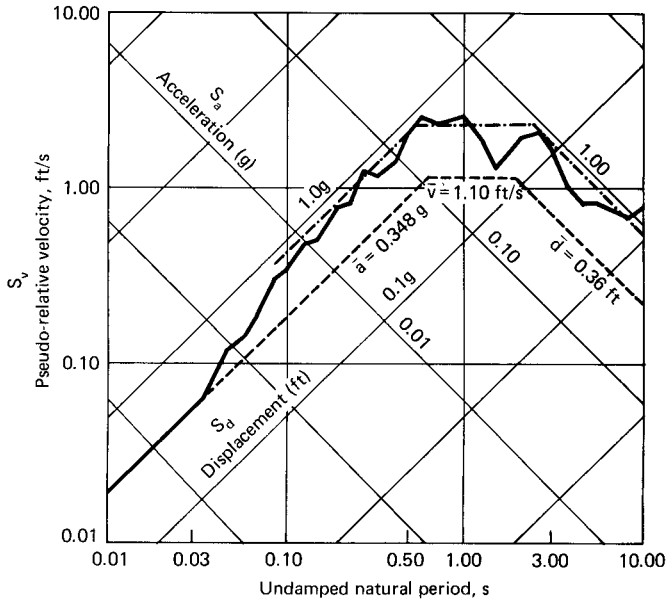

Figure 3.16 Tripartite response spectra of El Centro earthquake (5 percent damping, north-south component).

ranges. Note that, the proportionality factors required to produce reasonable approximations to actual spectra vary significantly for different earthquake records. However, reasonably smooth design spectra based on enveloping the spectral response of several earthquake records of similar intensities and site conditions can be constructed from a limited number of baseline parameters that reflect the influences of expected ground motion maxima as well as other ground motion characteristics. Different recommended procedures are based on the construction of response spectra for different sets of peak ground motion parameters.

Local soil characteristics can have an important influence on the relative spectral amplifications in these zones by influencing the surface ground motion that results from a given base rock excitation. For these reasons, many recommended design spectra make allowance for the influence of soil type on the shape of the spectrum curve. The general tendency of overlaying soil is to pull the response spectrum curve further out along the period scale, causing greater amplification in the longer-period range. Greater effective peak ground velocity and displacement are expected for sites with softer soil conditions. Local soil conditions are accounted for by classifying the site into one of the limited number of soil type categories and by applying different spectrum modifications for each category. It should be recognized that

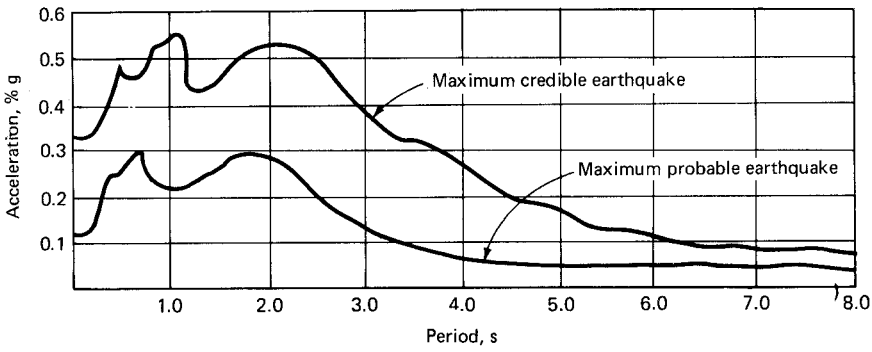

Figure 3.17 Unique design spectra.

significant differences exist among the various recommended spectrum profiles, although all are based on the same peak ground acceleration and damping. These differences are especially significant in the longer-period range where larger relative variations in spectral amplitude are noted.

Unique design spectra. For especially important structures or where local soil conditions are not amenable to simple classification, the use of recommended smooth spectrum curves is inadequate for final design purposes. In such cases, site-specific studies are performed to determine more precisely the expected intensity and character of seismic motion. The development of site-specific ground motions is generally the responsibility of geotechnical consultants working with the structural engineer's design criteria. A schematic representation of unique design spectra is shown in Fig. 3.17.

Concluding remarks. Irrespective of the method of development, the design spectrum is not a specification of a particular earthquake ground motion. It depicts only the relative behavior of single-degree-of-freedom structures of different periods and damping. In order to design the structures, it is necessary to specify the damping and allowable stresses. The actual earthquake forces calculated for use in the design of a structure will strongly depend on the damping that the structure is assumed to have. Using a large design spectrum and a larger value of damping may give a smaller design force than using a small spectrum with a small value of damping. The actual damping the structure may have when vibrating strongly is not well known, so it must be estimated.

In summary, the response spectrum method is a technique that is available for theoretical analysis of structures subjected to ground motion records. These solutions are becoming mandatory for multi-

story buildings which fall outside of the assumptions made in the empirical code seismic loads.

A brief recap of the procedure for spectrum analysis is as follows:

1. Select the design spectrum.
2. Determine the mode shapes and periods of vibration to be included in the analysis.
3. Read the level of response from the spectrum for the period of each of the modes considered.
4. Calculate participation of each mode corresponding to the single-degree-of-freedom response read from the curve.
5. Add the effect of modes to obtain combined maximum response.
6. Convert the combined maximum response into shears and moments for use in design of the structure.
7. Analyze the building for the resulting moments and shears in the same manner as for static loads.

3.6 Time History Analysis

3.6.1 Introduction

The mode superposition or the spectrum method outlined in the previous section is a useful technique for the elastic analysis of structure. It is not directly transferable to inelastic analysis because the principle of superposition is no longer applicable. Also, the analysis is subjected to uncertainties inherent in the modal superimposition method. The actual process of combining the different modal contributions is, after all, a probabilistic averaging technique and in certain cases may lead to results not entirely representative of the actual behavior of the structure. Time history analysis overcomes these two uncertainties, but it requires large computational effort. It is not normally employed as an analysis tool in practical design of high-rise buildings. However, a brief description of the method is given in this section for the sake of completeness in the presentation of earthquake design. The method consists of a step-by-step direct integration in which the time domain is discretized into a number of small increments δt, and for each time interval the equations of motion are solved with the displacements and velocities of the previous step serving as initial functions. The method is applicable to both elastic and inelastic analyses. In elastic analysis the stiffness characteristics of the structure are assumed to be constant for the whole duration of the earthquake. In the inelastic analysis, however, the stiffness is assumed to be constant through the incremental time δt only. Modifications to

structural stiffness caused by cracking, formation of plastic hinges, etc., are incorporated between the incremental solutions. A brief outline of the method, which is thus applicable to both elastic and inelastic analysis, is given below.

3.6.2 Analysis procedure. In this method of dynamic analysis, instead of going through a process of determining a response spectrum for a given ground motion and then applying the results to a given structure, it is possible by using computers to apply the earthquake motion directly to the base of a given structure. Instantaneous stresses throughout the structure are calculated at small intervals of time for the full duration of the earthquake or the significant portion of it. The maximum stress in any member that occurs during the earthquake can then be found by scanning the output record and the design reviewed. Even with the availability of high-speed computers, this method is restricted to the research field and to the design of special structures such as nuclear facilities and military installations. Because of high computer demands and consequent cost, the method is not being used as a routine design tool.

The procedure usually includes the following steps:

1. The earthquake record is selected which represents the expected earthquake.
2. The record is digitized as a series of small time intervals of about $\frac{1}{40}$ to $\frac{1}{25}$ of a second with given levels of acceleration occurring for each interval.
3. A mathematical model of the structure is set up. It usually consists of a series of lumped masses linked by elastic links with damping factors. Each lumped mass represents one floor, and each link represents the elastic stiffness of the framing members. The damping factors are introduced as expressions varying with the relative velocity of adjacent lumped masses.
4. The digitized record is applied to the model as accelerations at the base of the structure.
5. The computer integrates the motion equations of each mass as it is subjected to increments of elastic and damping forces through the connecting links and gives a complete record of the acceleration, velocity, and displacement of each lumped mass.

The accelerations and relative displacements of the lumped masses are translated into member stresses. The maximum values can then be found by scanning the output record.

This procedure automatically includes various modes of vibration

and combines their effect as they occur, thus eliminating the uncertainties of combining the modes which are inherent to the spectrum analysis.

The time history analysis technique represents the most sophisticated of the analysis methods in general use; however, it also has the following sources of uncertainty:

1. The input data or design earthquake is still an assumption.
2. As long as the analysis uses unchanging values for elastic constants and damping values, it will not reflect the accumulative effects of changing properties and progressive damage related to the duration of the earthquake.
3. Uncertainty related to the erratic nature of earthquakes. By pure coincidence, the maximum response of the calculated time history could fall at either a peak or a valley of the theoretical spectrum, presenting the possibility of a single time history response representing an unusual coincidence. This drawback can be overcome by supplementing the time history analysis with a spectrum analysis or by running time history studies from a number of different earthquakes.
4. Small inaccuracies in estimating properties of the structure will have considerable effect on the level of maximum response.
5. Errors latent in the magnitude of the time step chosen are hard to assess unless the solution is repeated with smaller time steps.

3.7 Practical Method of Dynamic Analysis

3.7.1 Introduction

Selection of a method for lateral analysis of earthquake motions is a personal choice and may vary from one design office to another and even within a single office. However, in all these methods, assumptions and analysis techniques are invariably based on elastic behavior. Although nonlinear analysis techniques are available, generally speaking their use within the design office is a long way from finding common application. Therefore, the discussion is limited to the elastic analysis techniques currently available.

Present-day codes in North America require that dynamic analysis be carried out for tall buildings unless they are very regular in shape and exhibit a reasonably uniform stiffness throughout the height. The seismic criteria and dynamic analysis procedures are based on the premise that the structure should meet two different levels of performance depending upon the magnitude of the earthquake event. The first level of performance requires essentially an elastic response

without significant structural damage under a moderate earthquake, which is likely to occur during the economic lifespan of the building. The spectrum curve which defines this criterion is the so-called maximum probable earthquake spectrum and is used to determine design forces and drift at design force level. It prescribes the lateral forces which the structure must resist without significant damage to structural elements and with the structure remaining essentially elastic. An earthquake capable of generating such a force level would have a moderate probability of occurrence during the anticipated life of the structure.

The second level of performance requires that the structure not collapse under the most severe earthquake that is geologically foreseeable. Substantial structural and nonstructural damage are considered to be acceptable under such a major seismic event. This second criterion is the so-called maximum credible earthquake spectrum. This is used to determine maximum building deflections, required ductility, and p-Δ effects. This spectrum is utilized to evaluate the capacity of the structure to resist collapse within the prescribed limits of permissible nonelastic action and ductility limits. The response levels specified by this spectrum could be generated by an earthquake having a low probability of occurrence during the anticipated life of the structure. Data from seismicity studies are used to determine appropriate magnitude for the two postulated earthquakes and are normally provided by the project geotechnical engineer.

Numerous computer analysis techniques for use in the seismic design of tall buildings are available to the design engineer. Nevertheless, certain assumptions about earthquake characteristics and building behavior are still necessary to convert complex structural systems that defy regularity and symmetry into a manageable computer model. Because of the many simplifying assumptions that go into the modeling technique, it behooves the engineer to address the inherent inaccuracies encountered in computer analysis techniques and to adjust and correct the results in order to avoid unnecessarily wasteful conservative designs in certain areas and a lack of strength in others.

Many sophisticated computer programs supported by numerous universities and major networks are available. Some are tailored to the analysis of buildings. For example, some programs make use of the commonly accepted assumption that the floors behave as a rigid diaphragm to reduce the number of degrees of freedom.

The most important phase in working with computer analysis techniques is to create a mathematical or analytical model that faithfully represents all the structural characteristics. It is indeed possible that more than one computer model may be necessary to study

the essential building responses to overcome the inherent modeling problems. The underlying principle behind the modeling technique is to obtain a realistic distribution of earthquake forces, floor shears, and overturning moments for the design of the structural system. The aim is to obtain elastic lateral forces, which as mentioned many times over are substantially smaller than those expected in real seismic situations. The concepts of ductility and damping are required to account for the differences. It is necessary to properly conceive and detail the lateral-force-resisting systems to develop the overall ductility. The analytical model used for deriving the lateral forces should recognize the principles of structural dynamics with due consideration for stiffness, mass, and damping of the actual structure. The model is then excited in order to derive the lateral forces as a percent of acceleration due to gravity and distributed over the height of the building in a manner consistent with its modes of vibration.

3.7.2 Analysis and design

In general, both the static and dynamic analyses of tall buildings are conducted with the use of mathematical models. A brief description of each is given in the following sections.

Static analysis. Static analyses of high-rise structures are in general performed by constructing a mathematical model of the building by using standard building-analysis-oriented computer programs. The model usually includes each column and beam and diagonals that act as part of the lateral-force-resisting system. The model is analyzed for the following cases: DL, LL, W_x, W_y, E_x, E_y, and accidental torsion, where

DL is the dead load.

LL is the live load.

W_x and W_y are the wind forces in two mutually perpendicular directions.

E_x and E_y are the earthquake forces in two mutually perpendicular directions.

The dead loads are calculated from the weight of the materials and the floor area usage. To begin with, the provisions of the applicable building code such as UBC are followed in calculating the lateral wind and seismic forces. The periods used to define the lateral force for the static analysis are calculated using the formulas given in the codes. Even though a modal analysis may indicate substantially longer periods, usually no attempt is made to use the longer periods to lower

the static design force levels because the use of these larger static forces will minimize the adjustment of member sizes as dictated by the dynamic analysis.

Dynamic analysis. A response spectrum method of dynamic analysis is usually chosen. A mathematical model for the building is constructed similar to the static model. Story translational and rotation masses are put into the computer program. These, together with the structural stiffness matrix, are used to determine the building's vibrational modes and periods. The program then determines the response of each mode to earthquakes by calculating a participation factor for each mode and selecting the spectral acceleration from the input spectrum that corresponds to the modal periods. The modal responses, including the acceleration and displacement at each story, are used to determine individual frame displacements. The displacements are used to calculate the modal member forces. The process is repeated for each mode specified in the analysis. The results of a selected number of modes are combined in the computer by taking either the square root of sum of the squares (SRSS) of each modal response or by other recognized methods appropriate for the building.

Members are designed for forces and deflections representing the combination of all significant modal responses of the building, using the maximum probable earthquake spectrum and appropriate damping factors. Where shear forces are transferred or offset between horizontal existing elements, a detailed analysis may be required to determine the most critical combination of shear from the various modes instead of using the SRSS method. This is so because the SRSS method may be a poor estimater of total peak responses when applied to systems with coupled modes having closely spaced periods. In particular, response quantities such as story shears or overturning moments parallel to the earthquake in two directions will be underestimated because SRSS ignores all cross-modal contributions. The amount of underestimation is dependent upon the severity of the modal coupling. This can be assessed by comparison of individual modal responses for the modes having closely spaced periods. The idea is to make sure that the masses at all levels are fully participating in the dynamic model.

The model is used to analyze the building response to the moderate and major earthquakes in each of its principal directions. The results of the static analyses are generally used to establish member sizes in compliance with the code requirements. Ductility demand ratios are calculated from the results of the dynamic analysis and to determine whether adjustment of member sizes is necessary for conformance with the seismic criteria developed for the particular project.

As mentioned previously, elastic dynamic analysis is the most preferred method by practicing engineers. However, because strictly elastic behavior is not expected of the structure under either a moderate or major earthquake, the design procedure allows for a controlled degree of inelastic behavior in the structural elements. This is accomplished by specifying allowable curvature and ductility factors. If ductility is defined as the ratio of maximum elastic moment M to plastic moment capacity M_P, the allowable ductility μ can be expressed by the equation $\mu = M_P/M$.

For steel structures, the ductility ratios usually used for the beams are 2.0 and 4.0 for moderate and major earthquakes, respectively. For columns, the respective values are 1.25 and 2.0. The structural elements are designed so that the ductility specifications are not exceeded. The results from the dynamic and static analysis are combined and divided by the appropriate ductility factor and checked against the plastic moment capacity. Beams that do not satisfy these requirements are resized. The columns in general are designed according to a weak beam–strong column concept, ensuring that plastic hinging will take place in the beams and not in the columns. In summary, the structural system is designed (1) to remain essentially elastic under loads and deformations caused by maximum probable earthquake, and (2) to have sufficient ductility to undergo displacements indicated by the maximum credible earthquake without exceeding permissible ductility or collapse. For rigid-frame structures, ductility demand calculations are done to assure that the seismic resisting elements and the joints have sufficient ductility to undergo maximum credible earthquake displacements. Braced-frame and shearwall structures are required to remain elastic under both the maximum probable and maximum credible earthquakes.

All seismic resisting elements in framed structures are checked for safety against collapse. This is assured when the lateral force required to form a full-story mechanism and as produced by p-Δ effects due to the maximum credible earthquake exceeds the lateral force caused by the yield-level earthquake.

3.8 Dynamic Analysis: Theory

3.8.1 Introduction

A good portion of the loads that occur in multistory buildings can be considered as static loads requiring static analysis only. Although almost all loads except dead loads are transient, it is customary in most designs to treat these loads as static. For example, lateral loads imposed by transient wind pulses are usually treated as static loads. Even in earthquake design, which is clearly a dynamic problem, one of

the acceptable methods of design is to use the so-called equivalent force system that is supposed to represent the static equivalent of dynamic forces. Under such assumptions, the analysis of a multistory building reduces to obtaining a single solution of the problem under static loads. The magnitude, nature, and origin of loads can be clearly visualized, and with the availability of computer programs the analysis can be performed without undue complexities. For example, once the wind load, building geometry, and member properties are known, the analysis for forces and deflections becomes a trivial computing task.

Although the equivalent static load approach is a recognized method of earthquake analysis, the state-of-the-art method for high-rise buildings uses a dynamic solution. Indeed, most building codes make the dynamic analysis mandatory for buildings whose configurations violate the assumptions made in the derivation of code equivalent forces. In today's architectural environment, it is more than likely that a tall building will not meet the spirit of the code assumptions either because the building has vertical steps, has a nonuniform configuration, or any other idiosyncrasies. It is, therefore, necessary for structural engineers to have a thorough understanding and mastery of the concepts and methods of solutions used in dynamic analysis.

Consider a multistory, multibay plane frame structure subjected to lateral wind loads. Although wind load is dynamic in nature, normal design practice, except in the case of very slender buildings, is to treat the wind load as an equivalent static load. The variation of wind load with respect to time is not considered, and the load is assumed to be applied gradually to the structure. Under these assumed ideal conditions, the analysis of the structure to determine the forces and displacements becomes somewhat trivial. For a given system of loads and known properties of the members and boundary conditions, there is but one unique solution which defines the equilibrium and compatibility conditions.

Assume that the structure, instead of being subjected to wind loads, is subjected to a seismic load. During an earthquake the structure is subjected to rapid ground displacements and experiences a number of different internal forces that include inertia forces, damping forces, and elastic forces. Although there is no external force per se applied to the structure, the mass of the structure generates an equivalent forcing function when subjected to acceleration.

It is easy to visualize this force by considering a somewhat simplified response of the structure during an earthquake. Before the start of the earthquake, the structure is in static equilibrium and would remain so if the movement of the ground from an earthquake takes place very slowly; the structure would simply ride to the new displaced position. When the ground moves suddenly, inertia of masses distributed in the

structure attempts to prevent the displacement of the structure, thus creating seismic loads somewhat analogous to externally applied lateral forces. The magnitudes of these forces are, of course, a function of masses and the length of time during which the displacement takes place.

These forces are considered to be dynamic, meaning that they vary with respect to time. Because the loading is time-varying, the response of the structure, including deflections, forces, and bending moments, which are a consequence of the loading, are also time-dependent. Instead of a single solution that can be obtained for the static case of wind load, a separate solution is required at each instant of time during the entire duration of earthquake. Since the deflections during the earthquake vary with time, accelerations and corresponding inertia forces are generated which have to be evaluated before internal forces and moments in the structure can be determined. The inertia forces developed in the system are a function of deflections, which are themselves related to the inertia forces. In structural dynamics it is therefore necessary to formulate the problem in terms of differential equations by relating the inertia forces to the second derivative of structural displacements. The resulting equations are called equations of motion which express the dynamic equilibrium of all forces, including the inertia forces acting on the structure.

Although courses in structural engineering cover this topic, engineers practicing in areas of the world not normally considered as earthquake zones seldom are exposed to the method. This section is, therefore, written in a review form, starting with the basic principles of structural dynamics, with particular reference to earthquake analysis. Although present-day computer programs have taken out the drudgery of calculations, the need to have an understanding of dynamic analysis is necessary in order to properly formulate the dynamic problems and to interpret the computer results.

In the following sections a brief mathematical treatment is presented for single-degree-of-freedom systems with and without damping forces, followed by multi-degree-of-freedom systems. The modal superposition method and orthogonality conditions which form the backbone of dynamic analysis of tall buildings are explained with reference to a system with two degrees of freedom to show how coupled equations of motions for a multi-degree-of-freedom system are transformed into a set of independent single-degree-of-freedom systems. The section concludes with a summary highlighting the practical aspects of dynamic analysis.

3.8.2 Systems with single degree of freedom

Consider a portal frame structure as shown in Fig. 3.18 consisting of an infinitely stiff beam supported by flexible columns. Assuming that

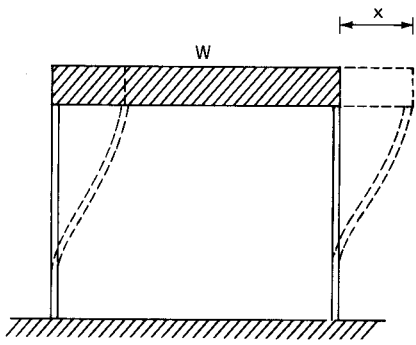

Figure 3.18 Single-bay single-story portal frame.

the beam is completely rigid and that columns do not have any mass as compared to the beam, the structure can be visualized as a spring-supported mass for horizontal motion of the beam.

The analytical model which has only one translation capability is thus referred to as a one-degree-of-freedom model. Mathematically it does not make any difference if the model is turned 90° as shown in Fig. 3.19, but it is easier to visualize the displacements of such a model. Under the action of gravity force W, it is easy to see that the spring will be extended by a certain amount. If the spring is very stiff, the extension is small, and vice versa.

The extension x experienced by the spring can be related to the stiffness of the spring k by the relation

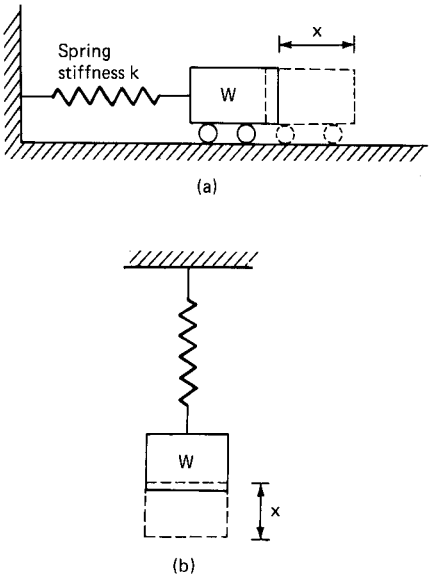

Figure 3.19 Single-degree-of-freedom system analytical models. (*a*) Model in horizontal position; (*b*) model in vertical position.

$$x = \frac{W}{k} \tag{3.19}$$

k is called the spring constant or spring stiffness and denotes the load required to produce unit extension of the spring. If W is measured in kips and the extension in inches, the spring stiffness will have dimensions of kips per inch. The weight W comes to rest after the spring has extended by the amount x. Equation (3.19) expresses the familiar static equilibrium condition between the internal force in the spring and the externally applied force W.

If a vertical force is applied or removed suddenly, vibrations of the system are produced. Such vibrations, maintained by the elastic force in the spring alone, are called free or natural vibrations. The weight moves up and down, and therefore is subjected to an acceleration given by the second derivative $\ddot{x}$ with respect to time. At any instant t, then, there are three forces acting on the body: the dynamic force equal to the product of the body mass and its acceleration, the gravity force W acting downward, and the force in the spring equal to $W + kx$ for the position of weight shown in Fig. 3.19. These are in a state of dynamic equilibrium given by the relation

$$\frac{W}{g}\ddot{x} = W - (W + kx) = -kx \tag{3.20}$$

The above is the most simple equation of motion in dynamics of structures. It is called Newton's law of motion and is governed by the equilibrium balance of inertia force that is a product of the mass W/g, acceleration $\ddot{x}$, and the resisting forces that are a function of the stiffness of the spring. We will now consider the equations of motion for a damped single-degree-of-freedom system.

The principle of virtual work can be used as an alternate to Newton's law of motion. This principle is useful for relatively complex structural systems which contain many interconnected parts. Although the method of virtual work was developed for static problems, it can readily be applied to dynamic systems by simple recourse to D'Alembert's principle, which establishes dynamic equilibrium by the inclusion of inertial forces in the system.

The principle of virtual work can be stated as follows: For a system that is in equilibrium, the work done by all the forces during an assumed virtual displacement is equal to zero. Consider a damped oscillation subjected to a time-dependent force $F_{(t)}$ as shown in Fig. 3.20*a*. The free-body diagram of the oscillator subjected to various forces is shown in Fig. 3.20*b*. Since the inertial force has been included

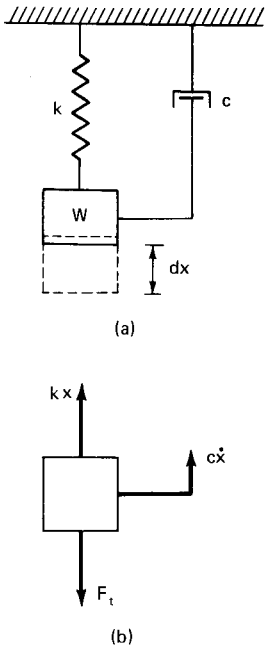

Figure 3.20 Damped oscillator. (*a*) Analytical model; (*b*) forces in equilibrium.

in the system, we can consider the dynamic equilibrium of the system from the principle of virtual work.

Let δx be the virtual displacement. The total work done by the system is zero and is given by

$$m\ddot{x}\,\delta\dot{x} + c\dot{x}\,\delta x + kx\,\delta x - F_{(t)}\,\delta x = 0 \tag{3.21}$$

$$(m\ddot{x} + c\dot{x} + kx - F_{(t)})\,\delta x = 0 \tag{3.22}$$

since δx is arbitrarily selected,

$$m\ddot{x} + c\dot{x} + kx - F_{(t)} = 0 \tag{3.23}$$

This is the differential equation of motion of the damped oscillator.

The differential equation of motion for an undamped system can also be obtained from the principle of conservation of energy, which states that if no external forces are acting on the system and there is no dissipation of energy due to damping, then the total energy of the system must remain constant during motion and consequently its derivative with respect to time must be equal to zero.

Consider again the oscillator shown in Fig. 3.20*a* without the damper. The two energies associated with this system are the kinetic energy of the mass and the potential energy of the spring.

The kinetic energy of the spring

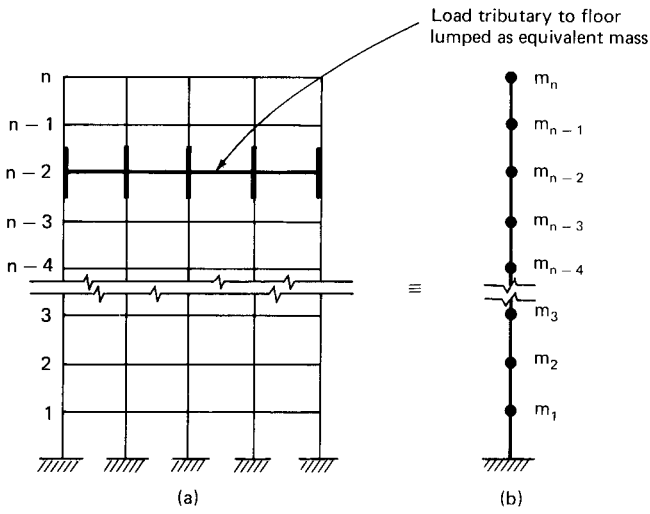

Figure 3.21 Multi-degree-of-freedom system. (*a*) Multistory frame; (*b*) analytical model with lumped masses.

$$T = \tfrac{1}{2} m\dot{x}^2 \tag{3.24}$$

where $\dot{x}$ is the instantaneous velocity of the mass.

The force in the spring is kx; work done by the spring is $kx\ \delta x$. The potential energy is the work done by this force and is given by

$$V = \int_0^x kx\ \delta x = \frac{1}{2} kx^2 \tag{3.25}$$

The total energy is constant. Thus

$$\frac{1}{2} m\dot{x}^2 + \frac{1}{2} kx^3 = \text{constant } c_0 \tag{3.26}$$

Differentiating, we get

$$m\dot{x}\ddot{x} + kx\dot{x} = 0 \tag{3.27}$$

Since $\dot{x}$ cannot be zero for all values of t, we get

$$m\ddot{x} + kx = 0 \tag{3.28}$$

which has the same form as Eq. (3.20). This has a solution of the form:

$$x = A \sin(\omega t + \alpha) \tag{3.29}$$

$$\dot{x} = \omega A \cos(\omega t + \alpha) \tag{3.30}$$

where A is the maximum displacement and ωA is the maximum velocity.

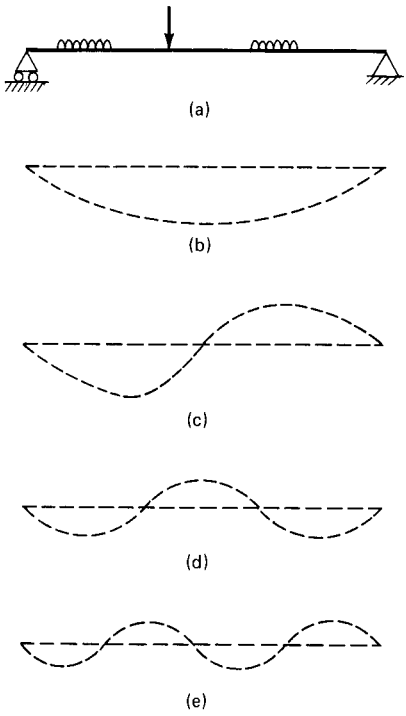

Figure 3.22 Generalized displacement of simply supported beam. (*a*) Loading, (*b*) full sine curve; (*c*) half sine curve; (*d*) one-third sine curve; (*e*) one-fourth sine curve.

Maximum kinetic energy is

$$T_{\max} = \frac{1}{2} m(\omega A)^2 \tag{3.31}$$

Maximum potential energy is

$$V_{\max} = \frac{1}{2} kA^2 \tag{3.32}$$

Since $T = V$,

$$\frac{1}{2} m\,(\omega A)^2 = \frac{1}{2} kA^2$$

or

$$\omega = \sqrt{\frac{k}{m}} \tag{3.33}$$

which is the natural frequency of the simple oscillator. This method, in which the natural frequency is obtained by equating maximum kinetic energy and maximum potential energy, is known as *Rayleigh's method.*

3.8.3 Multi-degree-of-freedom systems. Multiple-degree-of-freedom systems are systems, the configuration of which can be determined by a finite number of displacement coordinates. The true response of a multidegree system such as a multistory building can be determined only by evaluating the inertia effect at each mass particle because structures are continuous systems and therefore possess an infinite number of degrees of freedom. Although analytical methods are available to describe the behavior of continuous systems, such methods are limited to structures which have uniform material properties and regular geometry. The methods of analysis are complex, requiring considerable mathematical formulation of partial differential equations. The analysis is greatly simplified if the entire displacement of the structure can be specified by a limited number of displacement components. Further simplification that is customary in the dynamic analysis of buildings is to assume that the entire mass of the structure is concentrated in a number of discrete points located at each floor level of a multistory building. The one-story idealizations presented in earlier sections are particular cases of systems with multiple degrees of freedom. Closed-form solutions to obtain dynamic characteristics of one- and two-degree systems subjected to harmonic excitations can be formulated without undue complexity if damping forces are not considered. However, as the number of degrees of freedom increases, these formulations become increasingly unwieldy because of the large number of terms to be included in the equations of motion, thus requiring matrix formulation suitable for computer techniques.

Consider a multistory building with n degrees of freedom as shown schematically in Fig. 3.21. The dynamic equilibrium equations for undamped free vibration can be written in the general form

$$\begin{bmatrix} m_{11} & m_{12} & m_{13} & \cdots & m_{1n} \\ m_{21} & m_{22} & m_{23} & \cdots & m_{2n} \\ m_{31} & m_{32} & m_{33} & \cdots & m_{3n} \\ \cdots & \cdots & \cdots & \cdots & \cdots \\ m_{n1} & m_{n2} & m_{n3} & \cdots & m_{mn} \end{bmatrix} \begin{bmatrix} \ddot{x}_1 \\ \ddot{x}_2 \\ \ddot{x}_3 \\ \vdots \\ \ddot{x}_n \end{bmatrix} + \begin{bmatrix} k_{11} & k_{12} & k_{13} & \cdots & k_{1n} \\ k_{21} & k_{22} & k_{23} & \cdots & k_{2n} \\ k_{31} & k_{32} & k_{33} & \cdots & k_{3n} \\ \cdots & \cdots & \cdots & \cdots & \cdots \\ k_{n1} & k_{n2} & k_{n3} & \cdots & k_{nm} \end{bmatrix} \begin{bmatrix} x_1 \\ x_2 \\ x_3 \\ \vdots \\ x_n \end{bmatrix} = 0$$

The above system of equations can be written in matrix form:

$$[M]\{\ddot{x}\} + [K]\{x\} = 0 \tag{3.34}$$

where [M] = the mass or inertia matrix
$\{\ddot{x}\}$ = the column vector of accelerations
$[K]$ = the structure stiffness matrix
$\{x\}$ = the column vector of displacements of the structure

If we had considered the general case of forced vibrations that included the effect of damping, the equations of motion would be of the form

$$[M]\{\ddot{x}\} + [C]\{\dot{x}\} + [K]\{x\} = \{P\}$$

where [C] = the damping matrix
$\{\dot{x}\}$ = the column vector of velocity
$\{P\}$ = the column vector of external forces

Methods for solving these systems of equations are available, but they tend to be cumbersome. However, in solving seismic engineering problems simplified methods are used in which the vibration problem is first solved by neglecting the presence of damping. Its effects are later included in the design by modifying the design spectrum to account for the damping. Absence of precise data on damping does not usually justify a more rigorous treatment. Neglect of damping results in dropping the second term in the foregoing expression. Limiting the treatment of the problem to free vibrations results in dropping the right-hand side of the expression. The resulting equations of motion will become identical to Eq. (3.34). We will now consider in some detail the determination of natural frequencies and characteristic shapes of undamped systems subjected to free vibrations. This emphasis is deliberate because the procedure is a fundamental step in the dynamic analysis of the system and offers considerable insight into the vibration characteristics of structures.

During free vibration the motions of the system are simple harmonic, which means that the system oscillates about the stationary position in a sinusoidal manner; all masses follow the same harmonic function, having similar angular frequency ω. Thus

$$\begin{aligned} x_1 &= a_1 \sin \omega_1 t \\ x_2 &= a_2 \sin \omega_2 t \\ &\vdots \\ x_n &= a_n \sin \omega_n t \end{aligned}$$

or in matrix notation

$$\{x\} = \{a_n\} \sin \omega_n t$$

Where $\{a_n\}$ represents the column vector of modal amplitudes for the nth mode, and ω_n the corresponding frequency. Substituting for $\{x\}$ and its second derivative $\{\ddot{x}\}$ in Eq. (3.34) results in a set of algebraic expressions:

$$-\omega_n{}^2 [M] \{a_n\} + [K] \{a_n\} = 0 \tag{3.35}$$

Using a procedure known as Cramer's rule, the above expressions can be solved for determining the frequencies of vibrations and relative values of amplitudes of motion $a_{11}, a_{12}, \ldots, a_n$. The rule states that nontrivial values of amplitudes exist only if the determinant of the coefficients of a is equal to zero because the equations are homogeneous, meaning that the right-hand side of Eq. (3.35) is zero. Setting the determinant of Eq. (3.35) equal to zero, we get

$$\begin{bmatrix} k_{11} - \omega_1{}^2 m_{11} & k_{12} - \omega_1{}^2 m_{12} & k_{13} - \omega_1{}^2 m_{13} & \cdots & k_{1n} - \omega_n m_{1n} \\ k_{21} - \omega_2{}^2 m_{21} & k_{22} - \omega_2{}^2 m_{22} & k_{23} - \omega_2{}^2 m_{23} & \cdots & k_{2n} - \omega_n m_{2n} \\ k_{31} - \omega_3{}^2 m_{31} & k_{32} - \omega_3{}^2 m_{32} & k_{33} - \omega_3{}^2 m_{33} & \cdots & k_{3n} - \omega_n m_{3n} \\ \cdots - \cdots & \cdots - \cdots & \cdots - \cdots & \cdots \cdots - & \cdots \\ k_{n1} - \omega_n{}^2 m_{n1} & k_{n2} - \omega_n{}^2 m_{n2} & k_{n3} - \omega_n{}^2 m_{n3} & \cdots & k_{nn} - \omega_n m_{nn} \end{bmatrix} = 0 \tag{3.36}$$

With the understanding that the values for all the stiffness coefficients k_{11}, k_{12}, etc., and the masses m_1, m_2, etc., are known, the determinant of the equation can be expanded, leading to a polynomial expression in ω^2. Solution of the polynomial gives one real root for each mode of vibration, hence for a system with n degrees of freedom, n natural frequencies are obtained. The smallest of the values obtained is called the fundamental frequency and the corresponding mode the fundamental or first mode.

In mathematical terms the vibration problem is similar to those encountered in stability analyses. The determination of frequency of vibrations can be considered similar to the determination of critical loads, while the modes of vibration can be likened to evaluation of buckling modes. Such types of problems are known as *eigenvalue* or *characteristic value* problems. The quantities ω^2 which are analogous to critical loads are called eigenvalues or characteristic values, and in a broad sense can be looked upon as unique properties of the structure similar to geometric properties such as area or moment of inertia.

Unique values for characteristic shapes, on the other hand, cannot be determined because substitution of ω^2 for a particular mode into the dynamic equilibrium equation [Eq. (3.35)] results in exactly n unknowns for the characteristic amplitudes $x_1 \ldots . x_n$ for that mode. However, it is possible to obtain relative values for all amplitudes in terms of any particular amplitude. We are, therefore, able to obtain the pattern or the shape of the vibrating mode but not its absolute magnitude. The set of modal amplitudes that describe the vibrating pattern is called *eigenvector* or *characteristic vector*.

3.8.4 Modal superposition method

Modal superposition is a method in which the equations of motions are transformed from a set of n simultaneous differential equations to a set of n independent equations by the use of so-called normal coordinates. These equations are solved for the response of each mode, and the total response of the system is obtained by superposing individual solutions. Two concepts which are necessary for the understanding of the modal superposition method are (1) normal coordinates and (2) property of orthogonality. These will be explained first, followed by application of the method to a two-story structure. The treatments are necessarily incomplete in the mathematical sense but are sufficiently thorough to provide a sound conceptual understanding.

Normal coordinates. In static analysis it is common and convenient to represent the displacements of a structure by a system of geometric coordinates such as the cartesian system of coordinates that indicate the linear and angular positions of the elements with respect to a static position. For example, in a planar system, coordinates x and y and rotation θ are used to describe the position of the displaced structure. If the structure is restrained to move only in the horizontal direction and if rotations are of no consequence, only one coordinate is sufficient to describe the displacement. The displacements in general can also be obtained indirectly by any independent system of coordinates which are sufficient in number to specify the deflected position of all elements of the system. These coordinates are called generalized coordinates and their number is equal to the number of degrees of freedom of the system. In dynamic analysis, however, it is much more advantageous to use free-vibration mode shapes to represent the displacements because of their orthogonality properties, which will be explained shortly, and because a close approximation of the displacement can be made by considering only the first few modes.

Dynamic analysis of multi-degree-of-freedom systems becomes extremely difficult if a system of direct coordinates is employed to describe their motion. A static analysis, on the other hand, can be handled without undue complications by using any set of consistent coordinates, and the resulting forces and displacements can be converted from one set of coordinates to another without much difficulty. To avoid the computational problems, in structural dynamics the normal modes of vibration are employed as generalized coordinates to describe the motion. Using this system, the undamped motion equations become uncoupled, greatly simplifying their solution. While the mathematical description of normal modes and their properties is somewhat intriguing, there is nothing complicated about their con-

cept. Let us indulge in some trivial analogies to bring home their concept. For example, we can consider a set of normal modes as being similar to the primary colors, red, blue, and yellow. None of the primary colors can be constructed as a combination of the others, but any secondary color such as green or pink can be created by combining the primary colors, each with a distinct proportion. The proportions can be looked upon as scale factors, while the primary colors themselves can be considered similar to normal modes. To further reinforce the concept of generalized coordinates, it is helpful to recall its application in the solution of beam bending problems in which the deflection curve of the beam is represented in the form of trigonometric series. Considering the case of a simply supported beam subjected to vertical loads as shown in Fig. 3.22*a*, the deflection at any point can be represented by the following series:

$$y = a_1 \frac{\sin \pi x}{l} + a_2 \frac{\sin 2\pi x}{l} + a_3 \frac{\sin 3\pi x}{l} \tag{3.37}$$

Geometrically, this means that the deflection curve can be obtained by superposing simple sinusodial curves such as shown in Fig. 3.22*b* to *e*.

The first term in Eq. (3.37) represents the first curve, the second term, the second curve, etc. The coefficients a_1, a_2, a_3, etc., represent the maximum ordinates of the sine curves and the numbers 1, 2, and 3 the number of waves or mode shapes. By properly determining the coefficients a_1, a_2, a_3, etc., the trigonometric series can be made to represent any deflection curve with a degree of accuracy which depends on the number of terms considered in the series. A brief mathematical treatment of orthogonality condition follows.

Orthogonality. An important property of force displacement relationship that is rarely used in static problems but is very important in structural dynamics is the so-called orthogonal property. This property is best explained with reference to an example shown in Fig. 3.23.

Consider a two-story lumped-mass system subjected to free vibrations. The two modes of vibration can thus be considered as elastic displacements of the system due to two different loading conditions. A theorem known in structural mechanics as Betti's reciprocal theorem will be used to derive the orthogonality conditions. This law states that the work done by one set of loads on the deflection due to a second set of loads is equal to the work done by the second set of loads acting on the deflections due to the first. Using this theorem with reference to Fig. 3.23, we get

$$\omega_1^2 m_1 x_{1b} + \omega_1^2 m_2 x_{2b} = \omega_2^2 m_1 x_{1a} + \omega_1^2 m_2 x_{2a} \tag{3.38}$$

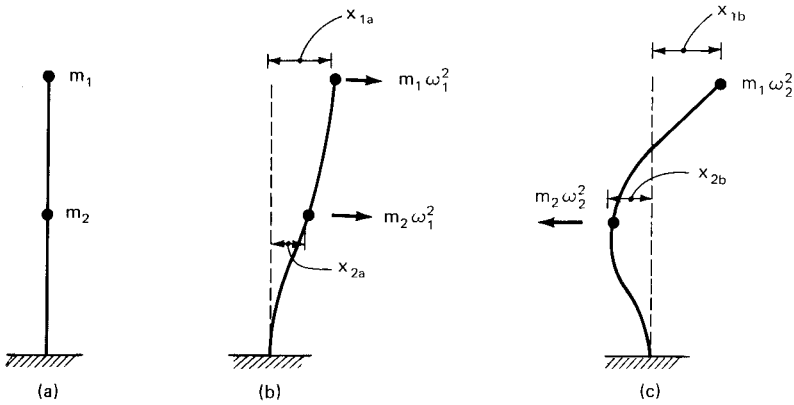

Figure 3.23 Two-story lumped-mass system illustrating Betti's reciprocal theorem. (*a*) Lumped model; (*b*) forces acting during first mode of vibration; (*c*) forces acting during second mode of vibration.

This can be written in matrix form

$$\omega_1^2 \begin{bmatrix} m_1 & 0 \\ 0 & m_2 \end{bmatrix} \begin{bmatrix} x_{1b} \\ x_{2b} \end{bmatrix} = \omega_2^2 \begin{bmatrix} m_1 & 0 \\ 0 & m_2 \end{bmatrix} \begin{bmatrix} x_{1a} \\ x_{2a} \end{bmatrix}$$

or

$$(\omega_1^2 - \omega_2^2) \{x_b\}^T [M] \{x_a\} = 0 \tag{3.39}$$

If the two frequencies are not the same, i.e., $\omega_1 \neq \omega_2$, we get

$$\{x_b\}^T [M] \{x_a\} = 0 \tag{3.40}$$

This condition is called the orthogonality condition, and the vibrating shapes $\{x_a\}$ and $\{x_b\}$ are said to be orthogonal with respect to the mass matrix $[M]$. By using a similar procedure it can be shown that

$$\{x_a\}^T [k] \{x_b\} = 0 \tag{3.41}$$

The vibrating shapes are therefore orthogonal with respect to stiffness matrix as they are with respect to the mass matrix. In the general case of the structures with damping, it is necessary to make a further assumption in the modal analysis that the orthogonality condition also applies for the damping matrix. This is for mathematical convenience only and has no theoretical basis. Therefore, in addition to the two orthogonality conditions mentioned previously, a third orthogonality

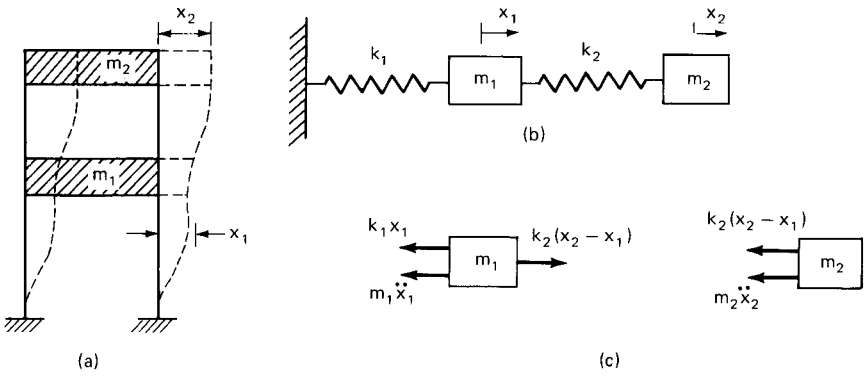

Figure 3.24 Two-story shear building—free vibrations. (*a*) Building with lumped masses; (*b*) mathematical model; (*c*) free-body diagram with lumped masses.

condition of the form

$$\{x_a{}^T\}\, c\, \{x_b\} = 0 \tag{3.42}$$

is assumed in the modal analysis.

To bring out the essentials of the normal mode method, it is convenient to consider the dynamic analysis of a two-degree-of-freedom system. We will first analyze the system by a direct method and then show how the analysis can be simplified by the modal superposition method.

Consider a two-story dynamic model of a shear building shown in Fig. 3.24 subject to free vibrations. The masses m_1 and m_2 at levels 1 and 2 can be considered connected to each other and to the ground by two springs having stiffnesses k_1 and k_2. The stiffness coefficients are mathematically equivalent to the forces required at levels 1 and 2 to produce unit horizontal displacements relative to each level.

It is assumed that the floors and therefore the masses m_1 and m_2 are restrained to move in the direction x and that there is no damping in the system. Using Newton's second law of motion, the equations of dynamic equilibrium for masses m_1 and m_2 are given by

$$m_1\ddot{x}_1 = -k_1x + k_2(x_2 - x_1) \tag{3.43}$$

$$m_2\ddot{x}_2 = -k_2(x_2 - x_1) \tag{3.44}$$

Rearranging terms in these equations gives

$$m_1\ddot{x}_1 + (k_1 + k_2)\, x_1 - k_2x_2 = 0 \tag{3.45}$$

$$m_2\ddot{x}_2 - k_2x_1 + k_2x_2 = 0 \tag{3.46}$$

The solutions for the displacements x_1 and x_2 can be assumed to be of the form

$$x_1 = A \sin(\omega t + \alpha) \tag{3.47}$$

$$x_2 = B \sin(\omega t + \alpha) \tag{3.48}$$

where ω represents the angular frequency and α represents the phase angle of the harmonic motion of the two masses. A and B represent the maximum amplitudes of the vibratory motion. Substitution of Eqs. (3.47) and (3.48) into Eqs. (3.45) and (3.46) gives the following equations.

$$(k_1 + k_2 - \omega^2 m_1)A - k_2B = 0 \tag{3.49}$$

$$k_2A + (k_2 - \omega^2 m_2)B = 0 \tag{3.50}$$

To obtain solution for the nontrivial case of A and $B \neq 0$, the determinant of the coefficients of A and B must be equal to zero, thus

$$\begin{bmatrix} (k_1 + k_2 - \omega^2 m_1) & -k_2 \\ -k_2 & (k_2 - \omega^2 m_2) \end{bmatrix} = 0 \tag{3.51}$$

Expansion of the determinant gives the relation:

$$(k_1 + k_2 - \omega^2 m_1)(k_2 - \omega^2 m_2) - k_2^2 = 0 \tag{3.52}$$

or

$$m_1 m_2 \omega^4 - m_1 k_2 + m_2 (k_1 + k_2)\omega^2 + k_1 k_2 = 0 \tag{3.53}$$

Solution of this quadratic equation yields two values for ω^2 of the form

$$\omega_1^2 = \frac{-b + \sqrt{b^2 - 4ac}}{2a} \tag{3.54}$$

$$\omega_2^2 = \frac{-b - \sqrt{b^2 - 4ac}}{2a} \tag{3.55}$$

where $a = m_1 m_2$
$b = -[m_1 k_2 + m_2 (k_1 + k_2)]$
$c = k_1 k_2$

As mentioned previously, the two frequencies ω_1 and ω_2 which can be considered as intrinsic properties of the system are uniquely determined.

The magnitudes of the amplitudes A and B cannot be determined uniquely but can be obtained in terms of ratios $r_1 = A_1/B_1$ and $r_2 = A_2/B_2$ corresponding to ${\omega_1}^2$ and ${\omega_2}^2$, respectively. Thus

$$r_1 = \frac{A_1}{B_1} = \frac{k_2}{k_1 + k_2 - {\omega_1}^2 m_1} \tag{3.56}$$

$$r_2 = \frac{A_2}{B_2} = \frac{k_2}{k_1 + k_2 - {\omega_2}^2 m_1} \tag{3.57}$$

The ratios r_1 and r_2 are called the amplitude ratios and represent the shapes of the two natural modes of vibration of the system.

Substituting the angular frequency ω_1 and the corresponding ratio r_1 in Eqs. (3.47) and (3.48), we get

$$x_1' = r_1 B_1 \sin(\omega_1 t + \alpha_1) \tag{3.58}$$

$$x_2' = B_1 \sin(\omega_1 t + \alpha_1) \tag{3.59}$$

These expressions describe the first mode of vibration, also called the fundamental mode. Substituting the larger angular frequency ω_2 and the corresponding ratio r_2 in Eqs. (3.47) and (3.48), we get

$$x_1'' = r_2 B_2 \sin(\omega_2 t + \alpha_2) \tag{3.60}$$

$$x_2'' = B_2 \sin(\omega_2 t + \alpha_2) \tag{3.61}$$

The displacements x_1'' and x_2'' describe the second mode of vibration. The general displacement of the system is obtained by summing the modal displacements, thus

$$x_1 = x_1' + x_1''$$

$$x_2 = x_2' + x_2''$$

Thus for systems having two degrees of freedom, we are able to determine the frequencies and mode shapes without undue mathematical difficulties. Although the equations of motions for multidegree systems have similar mathematical form, solutions for modal amplitudes in terms of geometrical coordinates become unwieldy. Use of orthogonal properties of mode shapes makes this laborious process unnecessary. We will demonstrate how the analysis can be simplified by using the modal superposition method. Consider again the equations of motion for the idealized two-story building discussed in the

previous section. As before, damping is neglected, but instead of free vibrations we will consider the analysis of the system subject to time-varying force functions F_1 and F_2 at levels 1 and 2. The dynamic equilibrium for masses m_1 and m_2 is given by

$$m_1\ddot{x}_1 + (k_1 + k_2)\, x_1 - k_2x_2 = F_1 \tag{3.62}$$

$$m_2\ddot{x}_2 - k_2x_1 + k_2x_2 = F_2 \tag{3.63}$$

These two equations are interdependent because they contain both the unknowns x_1 and x_2. These can be solved simultaneously to get the response of the system, which was indeed the method used in the previous section to obtain the values for frequencies and mode shapes. Modal superposition method offers an alternate procedure for solving such problems which, instead of requiring simultaneous solution of the equations, seeks to transform the system of interdependent or coupled equations into a system of independent or uncoupled equations. Since the resulting equations contain only one unknown function of time, solutions are greatly simplified. Let us assume that solution for the above dynamic equations is of the form:

$$x_1 = a_{11}z_1 + a_{12}z_2 \tag{3.64}$$

$$x_2 = a_{21}z_1 + a_{22}z_2 \tag{3.65}$$

What we have done in the above equations is to express displacement x_1 and x_2 at levels 1 and 2 as a linear combination of properly scaled values of two independent modes. For example, a_{11} and a_{12}, which are the mode shapes at level 1, are combined linearly to give the displacement x_1. z_1 and z_2 can be looked upon as scaling functions. Substituting for x_1 and x_2 and their derivitives $\ddot{x}_1$ and $\ddot{x}_2$ in the equilibrium Eqs. (3.62) and (3.63) we get

$$m_1a_{11}\ddot{z}_1 + (k_1 + k_2)a_{11}z_1 - k_2a_{21}z_1 + m_1a_{12}\ddot{z}_2 + (k_1 + k_2)a_{12}z_2 - k_2a_{22}z_2 = F_1 \tag{3.66}$$

$$m_2a_{21}\ddot{z}_1 - k_2a_{11}z_1 + k_2a_{21}z_1 + m_2a_{22}\ddot{z}_2 - k_2a_{12}z_2 + k_2a_{22}z_2 = F_2 \tag{3.67}$$

We seek to uncouple Eqs. (3.66) and (3.67) by using the orthogonality conditions. Multiplying Eq. (3.66) by a_{11} and Eq. 3.67 by a_{21} we get

$$m_1a_{11}^2\ddot{z}_1 + (k_1 + k_2)\, a_{11}^2\, z_1 - k_2a_{11}\, a_{21}z_1 + m_1a_{11}a_{12}\ddot{z}_2 + (k_1 + k_2)\, a_{11}a_{12}z_2 - k_2a_{11}a_{22}z_2 = a_{11}F_1 \tag{3.68}$$

$$m_2 a_{21}^2 \ddot{z}_1 - k_2 a_{11} a_{21} z_1 + k_2 a_{21}^2 z_1 + m_2 a_{21} a_{22} \ddot{z}_2 - k_2 a_{12} a_{21} z_2 + k_2 a_{21} a_{22} z_2 = a_{21} F_2 \quad (3.69)$$

Adding the above two equations, we get

$$(m_1 a_{11}^2 + m_2 a_{21}^2)\ddot{z}_1 + \omega_1^2 (m_1 a_{11}^2 + m_2 a_{21}^2) z_1 = a_{11} F_1 + a_{21} F_2 \quad (3.70)$$

Similarly, multiplying Eqs. (3.66) and (3.67) by a_{12} and a_{22} and adding we obtain

$$(m_1 a_{12}^2 + m_2 a_{22}^2)\ddot{z}_2 + \omega_2^2 (m_1 a_{12}^2 + m_2 a_{22}^2) z_2 = a_{12} F_1 + a_{22} F_2 \quad (3.71)$$

Equations (3.70) and (3.71) are independent of each other and are the uncoupled form of the original system of coupled differential equations. These can be further written in a simplified form by making use of the following abbreviations:

$$\left.\begin{aligned} M_1 &= m_1 a_{11}^2 + m_2 a_{21}^2 \\ M_2 &= m_1 a_{12}^2 + m_2 a_{22}^2 \end{aligned}\right\} \quad (3.72)$$

$$\left.\begin{aligned} K_1 &= \omega_1^2 M_1 \\ K_2 &= \omega_2^2 M_2 \end{aligned}\right\} \quad (3.73)$$

$$\left.\begin{aligned} P_1 &= a_{11} F_1 + a_{21} F_2 \\ P_2 &= a_{12} F_1 + a_{22} F_2 \end{aligned}\right\} \quad (3.74)$$

M_1 and M_2 are called the generalized masses, K_1 and K_2 the generalized stiffnesses, and P_1 and P_2 the generalized forces.

Using these notations, each of the Eqs. (3.70) and (3.71) takes the form similar to the equations of motion of a single-degree-of-freedom system, thus

$$M_1 \ddot{z}_1 + k_1 z_1 = P_1 \quad (3.75)$$

$$M_2 \ddot{z}_2 + k_2 z_2 = P_2 \quad (3.76)$$

The solution of these uncoupled differential equations can be found by any of the standard procedures given in textbooks on vibration analysis. In particular, Duhamel's integral provides a general method of solving these equations irrespective of the complexity of the loading function. However, in seismic analysis of tall buildings usually a response spectrum is available for the forcing function. Therefore, the maximum values of the response corresponding to each modal equa-

tion is obtained from the response spectrum. Direct superposition of modal maximum would, however, give only an upper limit for the total system which, in many engineering problems, would be too conservative. To alleviate this problem approximations based on probability considerations are generally employed. One method employs the so-called root mean square procedure, also called the square root of sum of the squares (SRSS) method. As the name implies, a probable maximum value is obtained by combining the square root of the sum of the squares of the modal quantities. Although this method is simple and widely used, it is not always a conservative predictor of earthquake response because more severe combinations of modal quantities can occur, for example, when two modes have nearly the same natural period. In such cases a more conservative combination of modal quantities is more appropriate.

An attempt has been made in this section to bring out the essentials of structural dynamics as related to seismic design of buildings. A certain amount of mathematical presentation has been unavoidable. Lest the reader lose the physical meaning of the various steps, it is worthwhile to summarize the essential features of dynamic analysis.

Dynamic analysis of high-rise buildings is accomplished by idealizing them as systems with multiple degrees of freedom. The dead load of the building together with a percentage of live load (estimated to be present during an earthquake) is modeled as a system of masses lumped at floor levels. In a planar analysis, each mass has one degree of freedom corresponding to lateral displacement in the direction under consideration, while in a three-dimensional analysis it has three degrees of freedom corresponding to two translational and one torsional displacement. Free vibrations of the buildings are evaluated, without including the effect of damping. Damping is taken into account by modifying the design response spectrum. The dynamic model representing the building has a number of mode shapes equal to the number of degrees of freedom of the model. Mode shapes have the property of orthogonality, which means that no given mode shape can be constructed as a combination of others. Yet any deformation of the dynamic model can be described as a combination of its mode shapes, each magnified by a scale factor which is determined mathematically. With each mode shape is associated a natural frequency of vibration. Mode shapes and frequencies are determined by solving the eigenvalue problem. The total response of the building to a given response spectrum is obtained by summing the number of modal responses. The number of modes required to adequately determine the forces for design is a function of the dynamic characteristics of the building. Generally for very tall and flexible buildings, six to ten modes in each direction are considered sufficient. Since generally each mass responds

to earthquakes in more than one pattern, it is necessary to evaluate effective modal mass values. These values indicate the percentage of the total mass that is mobilized in each mode. The acceleration experienced by each mass undergoing various modal deformations is determined from the response spectrum, which has been adjusted for damping. Product of acceleration for a particular frequency multiplied by the effective modal mass gives the static equivalent of forces at each discrete level. Since these forces do not reach their maximum values simultaneously during an earthquake event, statistical methods are used to achieve the combinations. The resulting forces are used as design static forces.

Chapter

4

Lateral Systems: Steel Buildings

4.1 Introduction

4.1.1 Steel in high-rise buildings

The monumental architectural and structural triumphs of ancient days—the pyramids of Egypt, the temples of Greece, the viaducts of Rome—were executed in stone or some form of masonry construction. Today's architects and engineers have building materials that are far superior. Structural steel is one such material which has been in use for a long time. Its use as a versatile and economical building material is on the increase. Within the past two decades, the steel producers have provided architects and structural designers with a broad spectrum of steels. A wider range of structural shapes, many of them in high-strength grades, is being produced.

Weathering steels that protect themselves with their own built-in resistance to corrosion are being increasingly used in many exposed applications. Improved fire protection techniques and new methods of fabrication and erection are some of the reasons for utilizing steel in a variety of structures from low-rise parking areas to 100-story skyscrapers. Radically new steel structural systems have evolved for resisting wind and earthquake forces and motions. In many cases bold

designs have been deliberately exposed to display the steel aesthetically.

Although the application of steel to structures can be traced back to 1856 when Bessemer's steel-making process was first introduced, its application to tall structures received its stimulus from the 984-ft (300-m) Eiffel Tower, which was constructed in 1889. After the turn of the nineteenth century, several tall buildings, from the 286-ft (87-m) Flatiron Building in 1902 to the 1046-ft (319-m) Chrysler Building in 1929, were constructed in the downtown areas of Chicago and Manhattan. This height record was broken by the 1250-ft (381-m) Empire State Building in 1931, the twin towers of the World Trade Center buildings at 1350 ft (412 m) in 1972, followed almost immediately by the 1450-ft (442-m) Sears Tower in Chicago in 1974. Rumors of even taller buildings being on the drawing boards of architects have since appeared in the press regularly, as though to remind structural engineers that the race for tallness is still on. The prediction of whether a taller steel building will be built within this decade is perhaps best left to the crystal ball gazers and soothsayers. The practical demonstration of the suitability of steel in the construction of tall buildings has been firmly established. The role of steel members, which in the early structures were relegated to carrying gravity loads only, has been completely upgraded to include wind systems with the advent of new structural systems ranging from the modest portal frame to the tubelike structures. Today, improved fabrication and erection techniques combined with the advanced analytical techniques made possible by computers have permitted the use of steel in just about any rational structural system for tall buildings.

4.1.2 Advantages of steel construction

Whether or not steel is the proper choice for framing a multistory building is a decision that invariably requires comparative studies. However, the following are some of the reasons normally associated with the competitive advantages of steel over concrete.

1. Construction speed, particularly during periods of high interest rates. Steel frames go up more rapidly, thus reducing construction financing costs and allowing the building to generate revenue sooner. As an example, on a $20-million loan at 13.5 percent interest, a savings of about $250,000 on interest and carrying charges would be realized for each month that the project completion time is reduced.
2. Availability of steel in a variety of grades and shapes that is suitable for economical framing of both short and long spans.

3. Steel offers economical design approaches for retrofit and rehab projects. Steel can be easily modified, expanded, or converted to suit future needs of owners and tenants. For this reason a steel frame is often referred to as a changeable frame.
4. In difficult foundation conditions, steel construction may result in reduced foundation costs because of its light weight. Steel frame is normally 25 to 35 percent lighter than a concrete frame and can permit the use of less expensive foundation systems. For example, in downtown Houston, which is underlain by soft compressible clay, a tall building normally has a mat foundation system. This type of foundation requires that the weight of soil removed as a consequence of building the substructure should not be less than a certain percentage of the load that will eventually be applied to the soil by the completed structure. This means that as the eventual structure becomes heavier, increasingly greater amounts of soil must be removed in order to limit the net pressure on the soil. With concrete construction, for a typical office building with about 1.5 million square feet of space in a 50-story building, no fewer than three below-grade levels are usually required. By changing the concrete framing system to steel, typically the requirement can be met with only two basements. By virtue of this substitution, not only is the substructure cost lowered, but the retention system installation and dewatering costs are also reduced.
5. Increasing acceptance by code-governing bodies of the rational methods for designing with fire-safe exterior structural steel. The methods define procedures for calculating heat transfer and for determining the temperature of the steel at critical points.
6. In severe cold weather conditions, structural steel framing is preferred because of less likelihood of "lost days" due to snow and icy conditions. However, it should be noted that winter protection in terms of wind drapes and artificial heat are required to raise the temperature of steel to at least 45°F in order that the fireproofing can be applied. This temperature has to be maintained for at least 24 hours following the application of sprayed-on fireproofing.

4.1.3 Structural systems in steel

One of the basic questions the structural engineer is called upon to answer very early in the design stage is which structural system is the most economical for the building. In providing preliminary estimates it is common practice to disregard the well-known fact that the structural cost of steel buildings is composed not only of the total tonnage of steel used, but also the fabrication and erection costs. Although the steel fabrication and erection prices are substantially

affected by the number and type of connections, broadly speaking it can be assumed that these costs remain the same for different structural schemes. This is an oversimplification of the actual condition, but it serves as a starting point for structural scheme selection.

The goal, then, is to find a structural system that will use a minimum amount of steel without requiring expensive compromises by other disciplines. As a general rule, other things being equal, the taller the building the more necessary it is to identify the proper system for resisting lateral loads. The project is first established by the architect in conceptual terms, identifying the overall shape of the building, approximate number of floors, and the size and location of service cores. The structural engineer is called upon at this stage to explore the structural options and to recommend a system that is not only economical in the structural sense but is also in concert with other major disciplines. Needless to say, each building is a product of a series of compromises between conflicting demands, making structural scheme selection one of the most challenging and interesting tasks for the engineer.

In order to determine the most economical framing system, it is necessary to evaluate both the horizontal floor framing system and the vertical elements of the structural frame. Attention is focused on lateral framing systems in this chapter. Floor framing options are studied in later parts of this book.

High-rise structures are generally offices or residential structures (apartments, hotels), and in some instances a combination of the two. They sometimes include parking garages. Studies done on structural systems pertain to specific structures, and the results obtained are not sufficiently general to favor a particular structural system even in seemingly similar conditions.

Today there are innumerable structural steel systems that can be used for the lateral bracing of tall buildings. It would be an exercise in futility to try to classify all these systems into distinct categories. However, for purposes of presentation, the different structural systems that are currently being used in the design of tall steel buildings are broadly divided into the following categories:

1. Semirigid frames
2. Rigid frames
3. Braced frames
4. Rigid frame and braced frame interaction
5. Belt and outrigger truss systems
6. Framed tube structures with regularly shaped tubes

7. Framed tube structures with irregular shapes
8. Exterior braced tubes with regular shapes
9. Exterior braced tubes with irregular shapes
10. Cellular tube structures
11. Megastructures (ultimate high-efficiency structures)

Descriptions of each system and its range of applicability are given in the following sections.

4.2 Semirigid Frames

4.2.1 Introduction

The use of portal frames, which consist of an assemblage of beams and columns, is one of the very popular types of bracing systems used in the design of tall buildings because of the minimum obstruction to architectural layout created by this system. In buildings of moderate heights and in tall structures which are not excessively slender, it may be preferable to resist lateral forces through bending of beams and columns. To achieve maximum frame action, the joints at the intersections of beams and columns are required to be rigid, meaning that any deformation at the connections should be negligible.

In tall buildings above 30 stories or so high, usually it is economical for the frame to develop its full frame resistance potential when moment-resistant frames are used as wind bracings. In such frames rigid connections are specified to assure the stiffest building frame. However, for buildings which are less than 25 to 30 stories, rigid framing may not yield the optimum solution. This is because heavier connection elements along with fully developed welds or large connectors are needed to obtain the desired fixity. In addition the gravity moment induced in external or unsymmetrically loaded interior columns may offset the advantages of reduced beam bending requirements and their attendant economic reduction in beam weight. At the other end of the spectrum is the simple framing, with very little, if any, resistance to bending requiring some other provision for carrying lateral loads in a tall building. Either shear walls, braced frames, or some other lateral bracing system is required in the planning of the building.

Semirigid connections can be defined as those connections whose behavior is intermediate between fully rigid and simple connections. Such connections offer substantial restraint to the end moment and can effect sufficient reduction in the midspan moment of a gravity-loaded beam. However, they are not rigid enough to prevent all the rotation of the end of the beam. Although the actual behavior of the

connection is complex, in practice simplified approaches are used in the design of such connections.

Although several specifications such as the AISC, the British, and the Australian codes offer a semirigid connection option to the designer, it has rarely been used because of the difficulty of obtaining a reliable analytical model to predict the rather complex response of connections. However, reasonable success has been obtained by another type of partially rigid connection which the AISC designates as Type 2 wind connection, with similar provisions found in the British and Australian codes.

In the following sections a brief description of the behavior of each type of connection is given with particular emphasis on the design of Type 2 wind connection.

4.2.2 Review of connection behavior

In structural steel design, different types of design assumptions are allowed, depending upon the rigidity of the connection used in the construction. For example, the American Institute of Steel Construction (AISC) specifications permit portal frames to be categorized into three different types of design:

1. Simple frames which use simple shear connections, called AISC Type 2 connections
2. Fully rigid frames which use rigid beam-to-column connections, called AISC Type I connections
3. Semirigid frames which use partially rigid beam-to-column connections, called the AISC Type 3 connections

The classification is based on the degree of restraint provided by the connection at the beam-to-column joint.

Connections in simple frames are designed to transfer vertical shear only, it being assumed that there is no bending moment present at the connection. Connections in fully rigid frames are called upon to develop full resistance to both shear and bending moment and are assumed to have sufficient rigidity to hold virtually unchanged the original angles between connecting members. Semirigid frames are those whose connection behavior is intermediate between simple and fully rigid connection.

Completely simple and completely rigid behavior are, of course, ideal conditions which can only be approached. Practically, it is necessary to accept something less than ideal, since real structural frames perform in the broad range between fully rigid and simple support action. For example, consider the typical beam-to-column connection consisting of a double-angle web connection as shown in

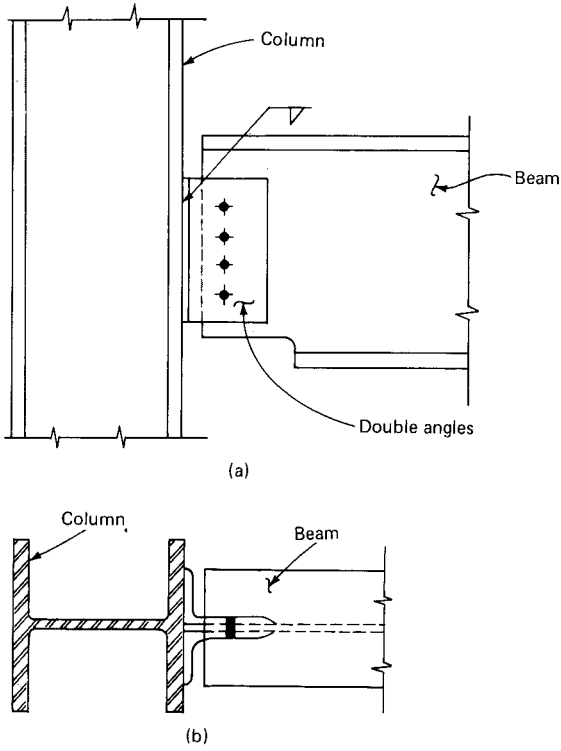

Figure 4.1 Beam-to-column field-bolted shear connection. (*a*) Elevation; (*b*) plan.

Fig. 4.1. The conventional framing angles that fasten to the beam web are usually considered to be completely flexible and are assumed to carry shear only. Actually, they offer limited restraint to moment and thus oppose to some extent the rotation at the end of the beam. The relationship between the applied moment and the rotation of a connection is determined generally by experiment. When rotation takes place, the upper part of the connection is in tension while the lower part is compressed against the column. The rotation is accommodated by deformation of the angles. Therefore, to minimize the rotational restraint, the angles should be as thin as possible.

Unstiffened seated beam connections as shown in Fig. 4.2 are also used for supporting the ends of unrestrained beams in Type 2 construction. The behavior of the seat angle is shown schematically in Fig. 4.3. The bottom angle acts as a cantilever, except that it is restrained by the bottom flange of the beam that is connected to it. The moment-rotation characteristics of a seat angle connection primarily depend on the depth of beam, stiffness of the top angle, stiffness of the bolts

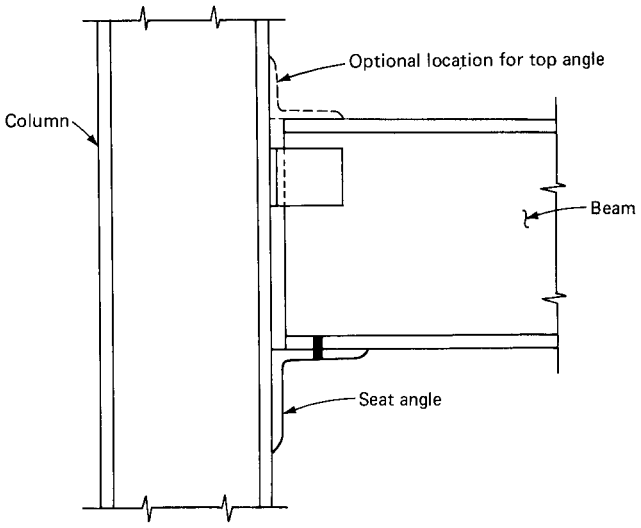

Figure 4.2 Unstiffened seated beam connection.

connecting the top angle to the column, and the stiffness of the column flanges to which the top angle is connected. Seat angle connections are typically stiffer than web angle connections but still are considered to be simple flexible connections. By combining the geometry of web angle and top and bottom angle connections it is possible to develop a connection that has greater moment resistance than either of the previously described connections.

The top and bottom angles are assumed to carry the moment, and the web angles the shear. Although the load distribution may appear to be arbitrary, such a division of function produces adequately

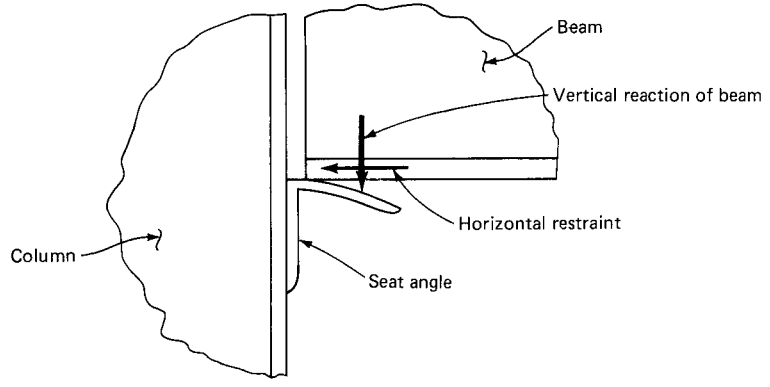

Figure 4.3 Cantilever bending of seat angle.

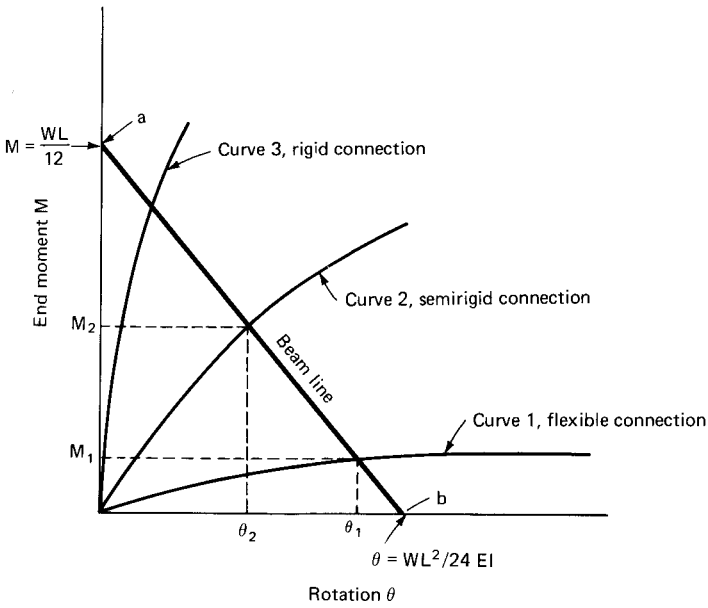

Figure 4.4 Beam line concept: Moment-rotation (M-θ) curves.

proportioned connections. Structural tees used in place of top and bottom angles of the flexible seat angle connection result in the most rigid connection of the semirigid types. The increase in rotational restraint occurs because the top tee is loaded in tension, which acts on the tee without any eccentricity, whereas the top angles are loaded eccentrically, resulting in large deformations.

4.2.3 Beam line concept

One of the methods of understanding the behavior of beam-to-column connection under load is to study a plot of its moment-rotation characteristics, as shown in Fig. 4.4. The vertical axis shows the end moment of the beam acting at the beam-column connection. The resulting rotation at the beam end is plotted along the horizontal axis in radians. This diagram is somewhat similar to a stress-strain diagram. Superimposed upon this plot is the so-called beam line, which expresses the resulting end moment M and rotation θ for a uniformly loaded beam for any end restraint, ranging from full fixity to simply supported condition.

The relation between end moment M and rotation θ can be expressed by the following equation.

$$M = -\frac{2EI\theta}{L} - \frac{WL}{12} \tag{4.1}$$

This is a straight-line relationship and can be plotted by considering the rotation of a simply supported beam and the fixed end moment of a completely restrained beam. Point a on the beam line is the end moment when the connection is completely restrained. Thus, in Eq. (4.1), rotation $\theta = 0$, giving

$$M = -\frac{WL}{12} \tag{4.2}$$

Point b is the rotation at the end of the beam when the beam has zero restraint at the ends. In other words, the beam behaves as a simply supported beam. Substituting $M = 0$ in Eq. (4.1), we get

$$\theta = -\frac{WL^2}{24EI} \tag{4.3}$$

The point at which the beam line intersects the connection line gives the resulting end moment and rotation under the given load. The dependence of the beam behavior on the rigidity of the connection can be studied by using this diagram. It is assumed that the behavior of the two end connections is the same and that the beam is subjected to loads placed symmetrically on the beam. The behavior of the three types of connections mentioned previously, namely the flexible connection, the semirigid connection, and rigid connection, can be studied by using the beam line diagram. Curve 1 represents a flexible connection which is typical of a double-angle web connection. Under a uniform load W, the beam ends rotate through an angle θ_1, which is very nearly equal to the rotation θ of a completely unrestrained beam. Corresponding to this rotation, a moment M is generated at the ends which signifies that even with the so-called flexible connections, some end moment is set up. Normally the bending moment developed is about 5 to 20 percent of the fully fixed moment.

Curve 2 represents a semirigid connection, such as that shown in Fig. 4.5, which consists of an end connecting plate so detailed that under working load it elastically yields to provide the necessary rotation of the connection. Although the beam is detailed to undergo a rotation equal to θ_2, significant moment M_2 corresponding to the rotation θ_2 develops at the beam ends. The restraint offered by this type of connection can vary anywhere from a low of 20 percent to a high of 90 percent of the full fixity. That is, the end moments could be 20 to 90 percent of the moment generated in a fully fixed beam.

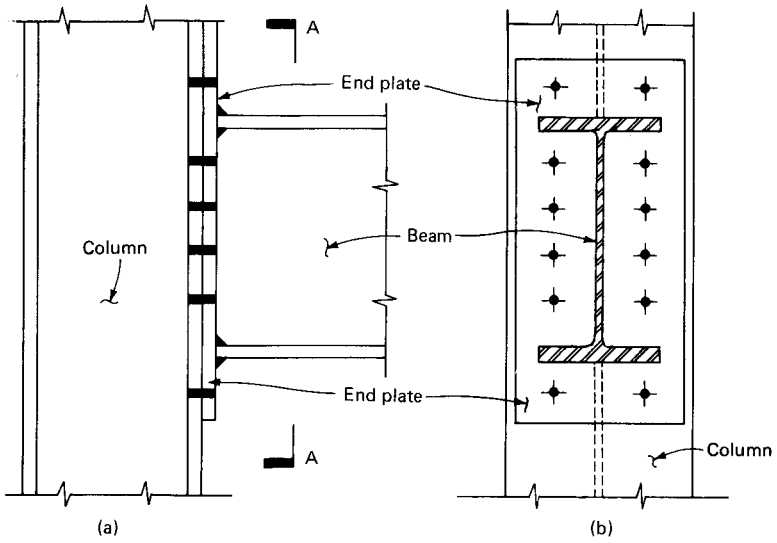

Figure 4.5 Column-to-beam bolted end plate connection. (*a*) Elevation; (*b*) section *A*-*A* side view.

Curve 3 represents the moment-rotation characteristics of a rigid connection so detailed as to allow virtually no rotation at the ends. Figure 4.6 shows typical welded beam-to-column connections normally used to achieve fully rigid connections. The beam develops end moments which are about 90 to 95 percent of the fully fixed condition, especially when column flange stiffeners are used as in Fig. 4.6.

Wind moments applied to flexible and semirigid connections present some very intriguing problems because some means of transferring these moments must be provided in these connections, which are supposed to be flexible. Additional restraint provided for carrying the wind load will result in an increase in the end moment due to gravity loads. A rigorous mathematical solution of flexible and semirigid connections is not possible, but based on the performance of buildings using these types of connections, AISC provides for two approximate solutions. In the first method the connection is designed for the moment caused by the combination of gravity and wind loads using a one-third increase in the allowable stresses. In the second method, the connection is designed for the moment induced by wind loads only, using a one-third increase in the stress allowances. The connection must, however, be designed to yield plastically for any combination of gravity and wind moments. Any additional moment that could occur at the ends beyond the wind moments is relieved because of the yielding of the connection. This type of connection necessitates some elastic but

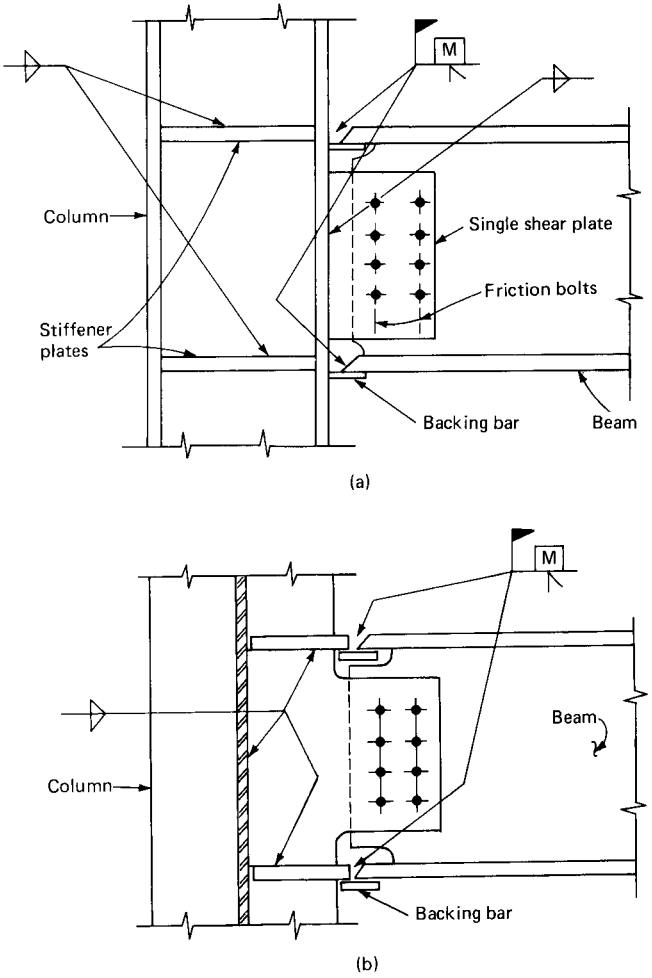

Figure 4.6 Beam-to-column welded moment connections. (*a*) Beam-to-column flange connection; (*b*) beam-to-column web connection.

self-limiting deformation of the connection plate without overstressing the fasteners. The term *self-limiting deformation* is included in the statement to prevent the use of semirigid connections for cantilever beams whose deflections are not limited by the rotation of the connection but may continue to progress, resulting in the failure of such connections.

Although the AISC specification permits the designer to take advantage of reduction in the midspan moment of a beam with semirigid connections, in practice this procedure has not found wide acceptance primarily because of lack of reliable analytical techniques. The Type 2

wind connection, which basically ignores the beam restraint for gravity loads, has found relatively greater acceptance. The behavior of the Type 2 wind connection is considered next.

4.2.4 Type 2 wind connection

Although the design of Type 2 wind connections is empirical in its approach, many significant tall buildings have been built with this technique, the most notable example being the Empire State Building, for many years the world's tallest. It must be pointed out, however, that significant stability and stiffness are incorporated into the structure by the exterior stone cladding and interior braces. Other major buildings that have used Type 2 construction are the United Nations Secretariat Building and the Chrysler Building, both in New York, and the Alcoa Building in Pittsburgh.

Type 2 wind connection is a compromise between the two extremes of the added expense of Type 1 connection and the lack of bracing of the simple Type 2 connection. Exploring this type of bracing for medium high-rise buildings may be well worth the effort because it can result in less expensive moment connections between beams and columns. As mentioned earlier, it is impossible to delineate precise practical boundaries between connection types. Many connections found in structures designed as simple connections are actually semirigid. Design of Type 2 wind connections for tall buildings is based on the practice of ignoring beam end moments generated by a connection's resistance to gravity load while counting on the same connection to resist wind moments calculated on the assumption of fully rigid behavior. This is a time-tested procedure and it is safe provided the actual end moment, which can be higher than the design moment, does not overstress the fasteners. Connections designed under this procedure are generally semirigid with components which, by deforming inelastically, prevent fastener distress. Since it is difficult to calculate the true combined moment at the connections, reliance must be placed on joint configurations of demonstrable ductility. Thus the Type 2 wind connection can be defined as a type of connection that develops lateral resistance through special wind connections which provide some restraint to the ends of a simple beam designed for gravity loads only. Basic to the Type 2 wind design is the requirement that the connection should have adequate inelastic deformation capacity to avoid connector overstress under full loading.

Since no advantage is taken of the end restraint to reduce the beam weight, frame stability is relatively unchanged. However, without the benefit of bracing or shear walls, drift requirements normally control the height to which this system can be used to advantage. Although a variety of technical factors, such as types of construction, bolted or

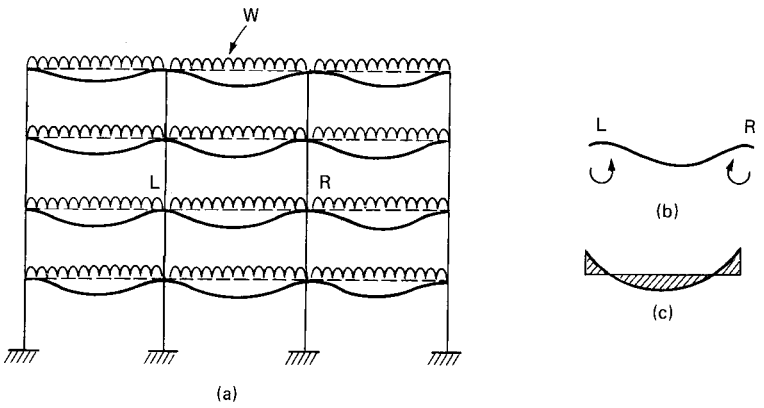

Figure 4.7 (*a*) Portal frame subjected to gravity loads; (*b*) end moments; (*c*) moment diagram.

welded joints with various connection configurations, are available, the selection of the optimum Type 2 wind connection based on a precise scientific evaluation is not routine office practice. In fact, Type 2 wind connection design is empirical. The structural performance of the connection itself in tall buildings is greatly influenced by whether gravity or horizontal loads are dominant, suggesting that connection details themselves should vary over the height of the building since the relative influence of gravity and lateral force varies throughout the height of the building.

To understand the Type 2 wind connection, it is instructive to trace its behavior through a complete sequence of loadings, starting from the gravity loads to reversible wind loadings. Figure 4.4 shows a moment-rotation curve for a beam with a known moment-rotation characteristic. The shape of the curve depends on the design of the connection and may range from the almost full fixity of Type 1 rigid frame construction to the Type 2 simple framing construction. In Fig. 4.4, point 1 at the intersection of the connection curve and the beam line *ab* represents the gravity moment M_1 and the corresponding rotation θ_1 at the ends due to a uniformly distributed load w. The end moment at the left-hand side of the girder is counterclockwise, while the end moment on the right-hand side is clockwise as shown in the free-body diagram of the beam in Fig. 4.7. The beam can be considered as a typical beam of a moment frame as shown in Fig. 4.7. The intersection points L_1 and R_1 in Fig. 4.9 represent the application of vertical load only to the beam; there is no wind moment acting on the connection or the beam. Assume that the frame is subject to wind loads acting from left to right, as represented in Fig. 4.8*a*. The beam is subjected to end moments

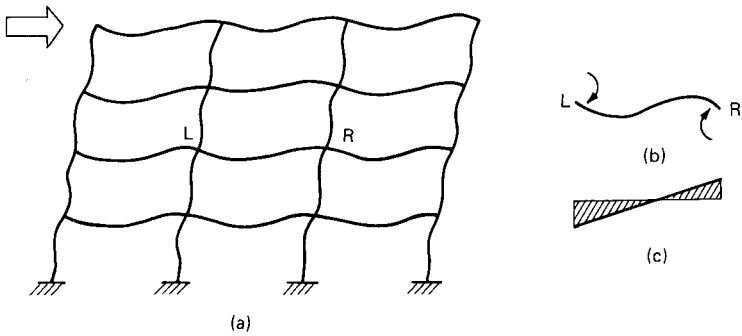

Figure 4.8 (*a*) Portal frame subjected to lateral loads from left; (*b*) end moments; (*c*) moment diagram.

which act in a clockwise direction as shown in the free-body diagram of the beam in Fig. 4.8*b*. The windward or the left-end moment acts in a direction opposite to the gravity moment, while the right-end or the leeward moment acts in the same sense as the gravity moment. The gravity moment at the left end is relieved by the wind action, while the right-end gravity moment becomes additive to the wind moment. Because of the additional moment, the right-end connection moves from the original point R_1 to R_2 along the connection curve. The left-end moment moves downward from L_1 to point L_2 because of the reduction in gravity moment. The windward moment does not retrace its path along the M-θ curve but travels on a line parallel to the slope of the curve. Recall that this characteristic is similar to the stress-strain diagram of a material such as steel subjected to load reversals. The decrease in moment occurs along a straight line because the moment is entirely elastic in this region. The rotations at the ends of the beam are, however, the same. The beam rotates by the same amount until the entire wind moment is developed between points R and L as illustrated in Fig. 4.9.

Since wind is a transient load, we have to consider the condition when it stops acting on the structure. The only loads on the beam are gravity loads similar to the condition that we started with, except the moment at the ends will not revert back to M_1 because during the loading cycle the connection has undergone inelastic rotations. The left-end connection goes from L_2 to L_3 and the right-end connection goes from R_2 to R_3. Both the connections move on an elastic line parallel to the initial slope. Static equilibrium requires that the moment at each end be the same. The resulting moment is, however, less than M_1.

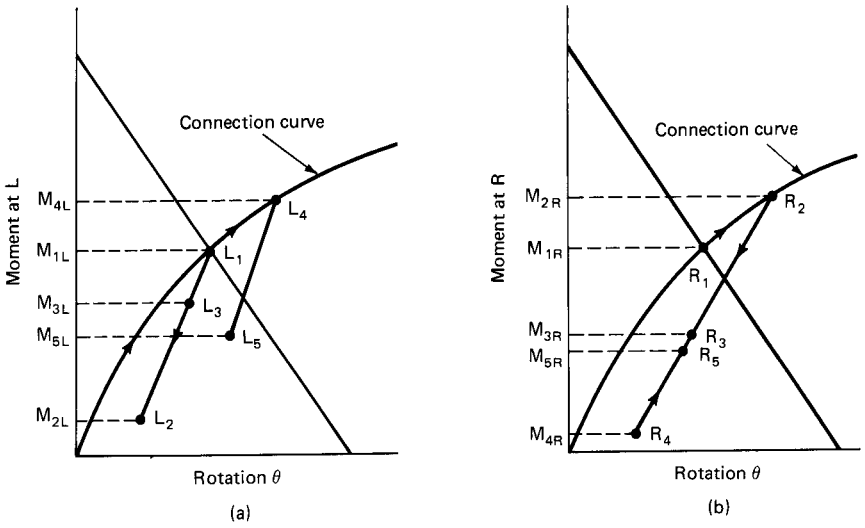

Figure 4.9 Behavior of semirigid wind connection. (*a*) Moment-rotation characteristics at left support; (*b*) moment rotation characteristics at right support; (*c*) summary of connection behavior.

Consider the wind now acting in the right-to-left direction as shown in Fig. 4.10*a*. The left-end connection receives additional moment and travels from L_3 to L_4. Part of this rotation is inelastic and part is elastic as shown in Fig. 4.9*a*. The right-end connection is partially relieved of the moment and moves down to point R_4 as shown in Fig. 4.9*b*. Both the connections rotate through the same angle until the entire moment is developed. Figure 4.9*a* and *b* shows the behavior when the wind stops and the only loads are gravity loads. The connections move from R_4 to R_5 and L_4 to L_5. Both ends have the same moment in order to satisfy static equilibrium. The moments corresponding to R_5 and L_5

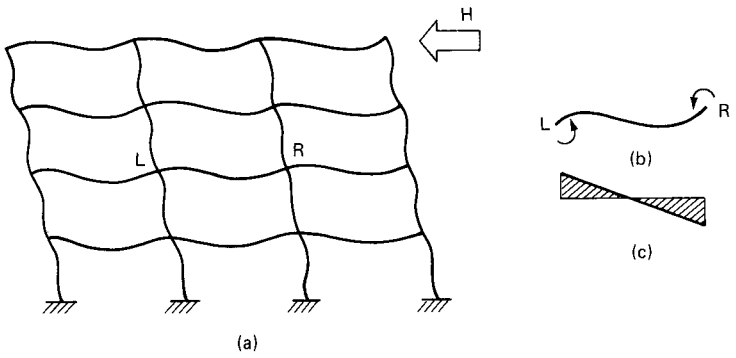

Figure 4.10 (*a*) Portal frame subjected to lateral loads from right; (*b*) end moments; (*c*) moment diagram.

are considerably less than the gravity moment at points R_1 and L_1 under gravity loads only. This phenomenon of reduction in moment due to cyclic loading is referred to as "shakedown." The gravity moment, therefore, has shaken down considerably. From this point on, the connection behaves entirely as an elastic connection. Regardless of the direction of wind, the maximum moment on the connection can never exceed points L_5 and R_5. The connection is said to have undergone a complete shakedown. After shakedown the maximum moment occurring at the connection is considerably smaller than the original gravity movement. A brief summary of the connections at the left and right ends is given in Table 4.1.

One of the drawbacks for the not-so-wide use of semirigid frames is the lack of sufficient information available to the designers about the moment-rotation relationship. The moment-rotation characteristics of a connection depend upon many physical parameters such as type of connection, the size of angles, end plates, top and bottom angles, and gauge for bolt location. In short, an exact relationship can only be obtained by conducting experiments. However, Lothers in his text *Advanced Design in Structural Steel*, has presented formulas for parameter Z to define the relationship between moment and rotation for the connections.

The factor Z for a connection is analogous to the stiffness factor $4EI/L$ which corresponds to the rotation at the end of a beam upon the application of a unit moment. The slope of the moment-rotation relation is one way of defining the parameter Z. Although the moment-rotation characteristics for most types of connections are nonlinear for the full spectrum of elastic and inelastic deformations, their behavior in the design range can be considered elastic. The reciprocal of the initial tangent to the moment-rotation curve can be considered as sufficiently accurate for determining the value of Z.

The theoretical expressions derived by Lothers for Z have been found to agree favorably with tests conducted by Rathburis. These values have been approximated for four types of connections by Defalco and Marino and are given in tabular form for connections with angle thickness and fastener sizes of practical proportions. These connections and their values of Z, which are reproduced by permission from the April 1960 AISC *Engineering Journal*, are shown as types A, B, C, and D in Figs. 4.11 through 4.14. Type A connection consists of a double-angle connection as shown in Fig. 4.11, while Type B, shown in Fig. 4.12, consists of a top and bottom clip angle connection. Type C connection in Fig. 4.13 is similar to type B with the exception that the shear capacity of the beam is augmented by bolting two angles to the beam web. Type D connection is a seat angle connection with a top plate connection as shown in Fig. 4.14. More important than the

TABLE 4.1 Summary of Connection Behavior

Load case		Moment at L	Moment at R	Connection behavior
1. Gravity	W	M_{1L}	M_{1R}	Equal gravity moments at each end
2. Gravity plus wind from left	$W + H$	M_{2L}	M_{2R}	L unloads elastically while R loads along connection curve
3. Remove wind from left	W	M_{3L}	M_{3R}	Elastic recovery of $M_{H/2}$ at both connections
4. Gravity plus wind from right	$W - H$	M_{4L}	M_{4R}	L loads elastically up to and then along the connection curve R unloads elastically
5. Remove wind from right	W	M_{5L}	M_{5R}	Elastic recovery of $M_{H/2}$ at both connections
6. Gravity plus wind from left	$W + H$	$M_{6L} = M_{5L} - \frac{M_H}{2}$	$M_{6R} = M_{5R} + \frac{M_H}{2}$	L unloads elastically by $M_{H/2}$ while R loads elastically by $M_{H/2}$
7. Remove wind from left	W	M_{5L}	M_{5R}	Elastic response at both ends. The connections have "shaken down" with the gravity moments considerably smaller than the initial gravity moments
8. Gravity plus wind from right	$W - H$	$M_{5L} + \frac{M_H}{2}$	$M_{5R} - \frac{M_H}{2}$	
9. Gravity plus wind from left	$W + H$	$M_{5L} - \frac{M_H}{2}$	$M_{5R} + \frac{M_H}{2}$	

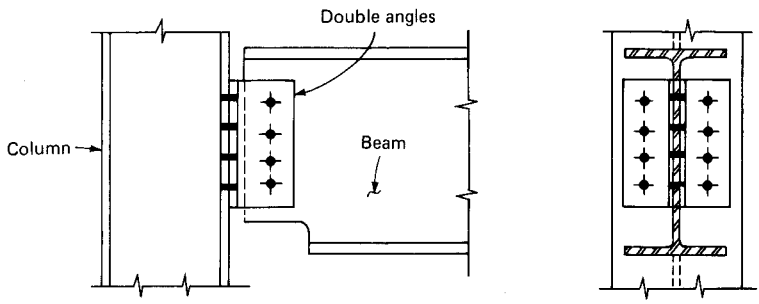

No. of rows of bolts	Z X 10^5, rad/kip-in
3	3.1
4	1.3
5	0.35
6	0.20
7	0.11
8	0.075
9	0.052
10	0.035

(c)

Figure 4.11 Double-angle connection (type A). (*a*) Elevation; (*b*) side view; (*c*) values of stiffness factor *Z*.

ultimate moment capacity is the initial stiffness of the curve, which is represented by the slope of the M-θ curve at the origin. The connection rotational stiffness, designated as Z, represents a zero value for a perfectly pin-ended connection and infinity for a fully fixed beam.

Analyses of frames that incorporate Type 2 wind and semirigid (Type 3) connections must include considerations of:

1. Connection ductility
2. Evaluation of the drift characteristics of frames with less than fully rigid connections
3. Effect of partial restraints on column and frame stability

Design outline for Type 2 wind connections

1. Calculate the allowable end reaction due to gravity loads.
2. Determine the magnitude of wind moment to be resisted at the beam end. This is obtained by the elastic analysis, assuming rigid frame action.

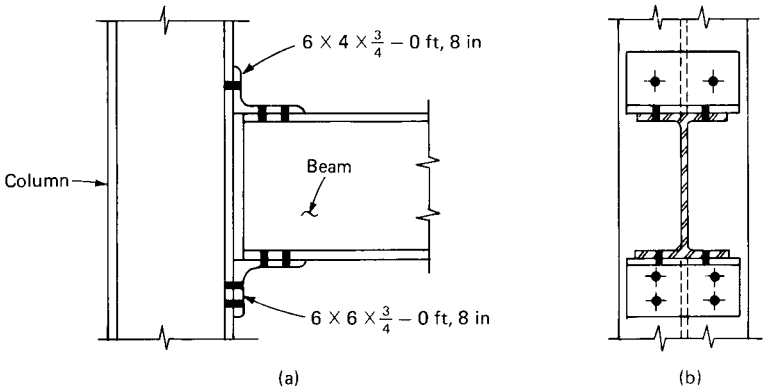

Depth of beam, in	Z X 10^5, rad/kip-in
8	0 046
10	0.036
12	0.028
14	0.023
16	0.018
18	0.014
21	0.012
24	0.010
27	0.0078
30	0.0066
33	0.0055
36	0.0046

(c)

Figure 4.12 Top and bottom clip angle connection (type B). (*a*) Elevation; (*b*) side view; (*c*) values of stiffness factor Z.

3. Assume that the type of semirigid connection to be used on the project is known beforehand. The connection could be any type of standard connection, such as double-angle, single-angle, the single shear plate tab, the top-and-seat angle, or the header plate connection. Make an initial guess on the various dimensions and thickness of connecting material.
4. Use this information to determine the moment-rotation characteristics of the connection to determine the Z value. Since currently available data do not include all conceivable types of connections, it is advisable to restrict connection designs to those for which M-θ curves have been well established. The AISC code, however, allows

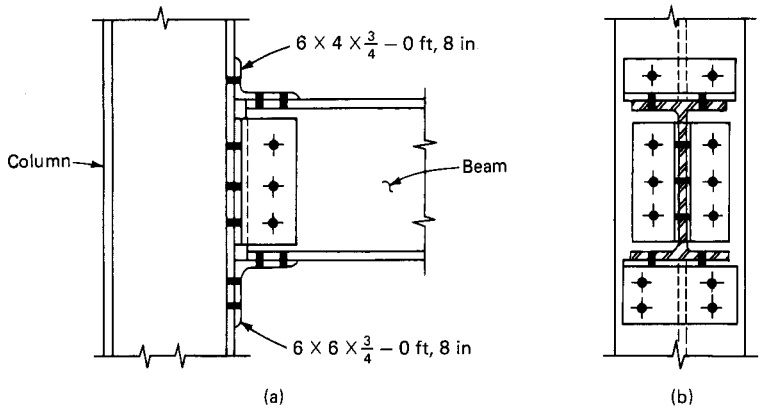

Depth of beam, in	Z X 10^5, rad/kip-in
8	0.046
10	0.036
12	0.028
14	0.024
16	0.020
18	0.015
21	0.013
24	0.011
27	0.0087
30	0.0076
33	0.0065
36	0.0054

(c)

Figure 4.13 Type C top and bottom clip angle connection. (*a*) Side view; (*b*) elevation; (*c*) values of stiffness factor *Z*.

use of any connection as long as its behavior can be demonstrated by either tests or by a rational analysis.

5. Proceeding on the assumption that the *Z* value for the chosen connection is available, plot the moment-rotation curve on the beam line. The straight-line relation for the beam rotation and end moment is conveniently obtained by calculating the beam line points *a* and *b* that correspond to the end moment of a fixed beam and the rotation of a simply supported beam subjected to the vertical loads.
6. Check the connection for wind moment by calculating the bolt tension, bolt shear, tension in the connecting angles, etc.
7. Check connection for ductility. This in essence requires that all

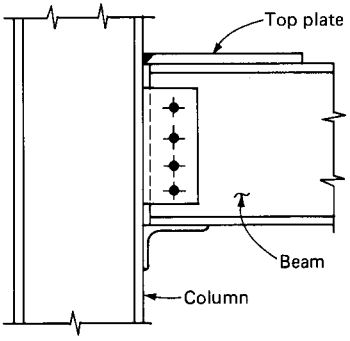

(a)

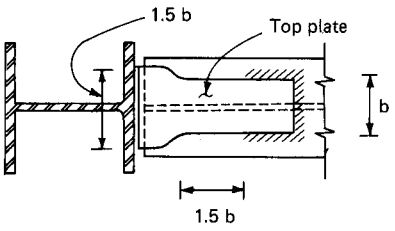

(b)

Depth of beam, in	Z X 10^5 rad/kip-in
8	0.21
10	0.13
12	0.093
14	0.068
16	0.052
18	0.041
21	0.030
24	0.023
27	0.018
30	0.015
33	0.012
36	0.010

(c)

Figure 4.14 Type D seat angle with top plate connection. (*a*) Side view; (*b*) elevation; (*c*) values of stiffness factor *Z*.

connection materials such as bolts, welds, and plates not be stressed beyond the material strengths (with a proper safety factor) under the simultaneous action of gravity and wind moments.

8. Since at the start we assumed in the wind analysis that connections are fully rigid, steps 1 through 7 yield a conservative design. If required, the connection design can be modified by incorporating the effect of nonrigid connections in the wind analysis. This can be done by using a reduced bending rigidity for the beam to account for less than 100 percent rigidity of the connection.

Iteration of steps 2 through 8 gives results that will converge to the optimum solution. Since semirigid connections provide less frame stiffness than fully rigid connections, it is necessary to use a modified girder stiffness which incorporates the Z factor as follows:

$$K_r = \frac{3\,(I/L)}{4\,(L'/L) - (L/L')} \tag{4.4}$$

where K_r = modified stiffness of beam
$L' = L + 3EIZ$
L = beam span
I = moment of inertia of the beam

Although the use of reduced stiffness of the beam in the determination of wind moments is optional, it is important that reduction in stiffness be accounted for in determining the lateral drift and p-Δ effects.

4.2.5 Concluding remarks

In spite of reported success of many buildings built by using Type 2 wind connections, there exists little unanimity of opinion about its applicability for buildings taller than five stories or so. Engineers who design buildings using Type 2 wind connections are automatically put in a defensive position of explaining the paradox of how the joints act as rigid for wind loading and as pins under gravity loading. A straightforward application of the method for frames can result in structures in which the columns are overstressed and exhibit sway deflections much in excess of calculated values. Other cautious approaches that take into consideration the relative softness of connections have been proposed by several investigators but have not found general application in the design office and therefore will not be discussed.

4.3 Rigid Frames

4.3.1 Introduction

Rigid connections are those with sufficient stiffness to hold the angles between members virtually unchanged under load. A frame that consists of such connections is defined as a rigid frame or an unbraced frame. It gets its strength and stiffness from the nondeformability of joints at the intersection of columns and girders. Rigid frames generally consist of a rectangular grid of horizontal beams and vertical columns connected in the same plane by means of rigid joints. The frame may be in the plane of an interior wall of the building or in the plane of the exterior face of the building. Because of the continuity of members at the joints, the rigid frame responds to lateral loads primarily through flexure of beams and columns as shown schemati-

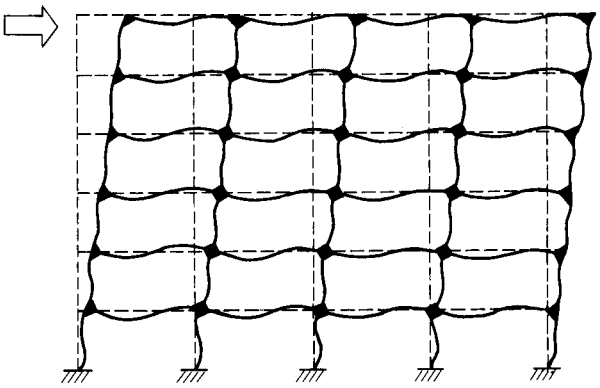

(a)

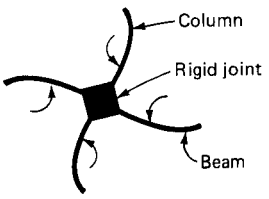

(b)

Figure 4.15 (*a*) Response of rigid frame to lateral loads; (*b*) flexural deformation of beams and columns due to nondeformability of connection.

cally in Fig. 4.15. This continuous character of the rigid frame is dependent upon the rotational resistance of the member connections not to permit any slippage.

4.3.2 Deflection characteristics

The lateral deflection components of a rigid frame can be thought of as being caused by two components similar to the deflection components of a cantilever beam. One component can be likened to the bending deflection and the other to the shear deflection of the beam. Normally for prismatic members when the span-to-depth ratio is greater than 10 or so, the bending deflection is by far the more predominant component. Shear deflections contribute a small portion to the overall deflection and are therefore generally neglected in calculating deflections of beams and columns of normal proportions. The deflection characteristics of a rigid frame, on the other hand, are just the opposite; the component analogous to the beam shear deflection dom-

inates the deflection picture and may amount to as much as 80 percent of the total deflection, while the remaining 20 percent comes from the bending component. The bending and the shear components of deflection are usually referred to as the cantilever bending and frame racking, each with a distinct deflection mode.

Cantilever bending component. This phenomenon is also known as *chord drift.* The wind load acting on the vertical face of the building causes an overall bending moment on any horizontal cross section of the building. This moment, which reaches its maximum value at the base of the building, causes the building to rotate about the leeward column and is called the *overturning moment.* In resisting the overturning moment, the frame behaves as a vertical cantilever responding to bending through the axial deformation of columns. This overturning moment causes compression in the leeward columns and tension or uplift in the windward columns. The columns lengthen on the windward face of the building and shorten on the leeward face. This column length change causes the building to rotate and results in the chord drift component of the lateral deflection. This mode of deformation accounts for about 90 to 95 percent of the total deflection in a normally proportioned cantilever beam. In the case of rigid frames, however, this phenomenon accounts for about 20 percent of the total drift of structure, the remainder coming from frame racking.

Shear racking component. This phenomenon is analogous to the shear deflection in a beam and is brought about in a rigid frame by the bending of beam and column elements. The lateral load on the rigid frame causes horizontal and vertical shear forces acting on columns and beams, respectively, which in turn produce bending moments in the members. Bending of individual columns and beams results in the entire frame distortion. This mode of deformation accounts for about 80 percent of the total sway of the structure. In a normally proportioned rigid-frame building with column spacing at about 35 to 40 ft (10.6 to 12.2 m) and a story height of 12 to 13 ft (3.65 to 4.0 m), beam flexure contributes about 50 to 65 percent of the total sway. The column rotation, on the other hand, contributes about 10 to 20 percent of the total deflection. This is because in most unbraced frames the ratio of column stiffness to girder stiffness is very high, resulting in larger joint rotations by unstiff girders. So generally when it is desired to reduce the deflection of unbraced frame, the place to start adding stiffness is in the girders. However, in nontypical frames, such as those that occur in framed tube structures where column spacing approaches the floor-to-floor height, it is necessary to study the relative girder and column stiffness before making adjustments in the member properties.

For a normally proportioned rigid frame, as a first approximation, the total lateral deflection can be thought of as a combination of three factors:

1. Deflection due to axial deformation of columns (15 to 20 percent)
2. Frame racking due to beam rotations (50 to 60 percent)
3. Frame racking due to column rotations (15 to 20 percent)

In addition to the above, there is a fourth component that contributes to the deflection of the frame and is due to deformation of the joint, because of high shears. In a rigid frame, since the sizes of joints are relatively small compared to column and beam lengths, it is common practice to ignore the effect of joint deformation. However, its contribution to building drift in very tall buildings consisting of closely spaced columns and deep spandrels could be substantial, warranting a closer study. This effect is called *panel zone deformation* and is discussed at length in Chap. 11.

4.3.3 Methods of analysis

Because of the large-scale availability of computers, the analysis of rigid-frame buildings, even in preliminary design stages, is accomplished most effectively by using stiffness analysis programs. Hand calculations are rarely undertaken except for very preliminary purposes because of the approximate nature of analysis and the longer time it takes to do hand computations.

Among the better known approximate methods of analysis, the cantilever and portal methods are perhaps the most popular and considered by some engineers to be sufficiently accurate for use in the final analysis of buildings of intermediate height range. The portal method is considered reasonably valid for buildings less than 25 stories, and the cantilever method is assumed to be valid for buildings in the 25- to 30-story range. A brief description of each method is given in Chap. 10.

4.3.4 Calculation of drift

Calculation of drift due to wind loads is a major element in the analysis of tall building frames. Although it is convenient to consider the lateral displacements to be composed of two distinct components, whether or not the cantilever or the racking component dominates the deflection is dependent on factors such as height-to-width ratio of the building and the relative rigidity of the column to girder connection. Unless the building is very tall or very slender, it is usually the racking component that dominates the deflection picture. A simple

method for determining the deflection of a tall building from chord drift is to assume that the entire structure acts as a vertical beam to which elementary beam theory applies; the axial stress in each column is proportional to its distance from the centroidal axis of the frame. This approach assumes that the frame is infinitely stiff with respect to longitudinal shear and hence requires that the girders be infinitely rigid. Since the girders are not infinitely rigid, this approach tends to underestimate the deflection due to cantilever bending. Methods of calculation which take into account the shear racking component are given in Chap. 10.

4.4 Braced Frames

4.4.1 Introduction

Pure rigid frame systems are not efficient for buildings higher than about 30 stories because the shear racking component of deflection produced by the bending of columns and girders causes the building drift to be too large. As mentioned earlier, its inherent weakness most often lies in the flexibility of girders. A braced frame attempts to improve upon the efficiency of pure rigid frame action by virtually eliminating the column and girder bending factors. This is achieved by adding truss members such as diagonals between the floor system. The shear is now primarily absorbed by the diagonals and not by the girders. The diagonals carry the lateral forces directly in predominantly axial action, providing for nearly pure cantilever behavior. All members are subjected to axial loads only, thereby creating an efficient structural system.

4.4.2 Types of braces

Any rational configuration of bracing can be used for bracing systems. Bracing types available for incorporation into the structural system range from a concentric simple K or X brace between two columns to knee bracing and eccentric bracing with complicated geometry requiring computer solutions. Figure 4.16 is a photograph showing inverted K bracing with double-angle connections.

In an eccentric bracing system the connection of the diagonal brace is deliberately offset from the connection between the beam and the vertical column. This system, although originally conceived for satisfying ductility requirements in seismic zones, can conveniently be employed in nonseismic applications. By keeping the beam-to-brace connections close to the columns, the stiffness of the system can be made very close to that of concentric bracing. By shifting the work point away from the column centerline to the column face, connection

Figure 4.16 Inverted K bracing with double-angle connections.

details can be made simpler. The economy of the system has proved itself in the application of temporary bracing systems required in composite high-rise construction. Design application of eccentric bracing systems is discussed in greater detail in later sections. Only concentric bracing systems are discussed in this section.

The selection of bracing type is a function of the required stiffness, but most often it is influenced by the size of wall opening required for circulation. Because of architectural requirements, sometimes only certain bays around elevator and stair shafts are braced. On occasion it may be possible to brace portions of the building without compromising the architecture, and in very rare cases it may even be possible to truss across the full width of the building, resulting in sloping interior columns. A very efficient three-dimensional system commonly known as a *braced tube system* results when the bracing encompasses the perimeter of the building. This system is discussed in greater detail in Sec. 4.8.

Common types of interior bracing employed in high-rise construction are shown in Fig. 4.17*a* through *n*. Figure 4.17*e* through *n* shows bracings across single bays in one-story increments. Figure 4.17*a* shows diagonal bracing in two-story increments. Shown in Fig. 4.17*b* and *c* is a K-braced frame, while Fig. 4.17*d* shows bracing for a three-bay frame. Any reasonable pattern of braces with singly or multiply braced bays can be designed, provided that shear is resisted at every story and that proper deflection calculations are made.

Finding an efficient and economical bracing system for a tall building presents the structural engineer with an excellent opportunity to use innovative design concepts. However, availability of proper depth for bracing trusses is often an overriding consideration. As a

preliminary guide, a height-to-width ratio of 8 to 10 is considered proper for a reasonably efficient bracing system. Finding space for such an optimum-width bracing without disrupting architectural planning may not always be possible, forcing the structural engineer to use less than optimum bracing systems.

4.5 Staggered Truss System

4.5.1 Introduction

Most high-rise residential-type structures such as apartments and hotels are generally in the neighborhood of 60 by 150 ft (18.3 × 45.75 m) to 200 ft (61 m) long. Their floor plans normally lend themselves to central double-loaded corridors of about 6 to 8 ft (1.83 to 2.43 m) in width. A study was done at the Massachusetts Institute of Technology in the mid-1960s under the sponsorship of U.S. Steel Corporation for the purpose of developing an economical framing system for such tall, narrow structures. The staggered truss system evolved as an outgrowth of the research done by the departments of architecture and civil engineering at MIT. The result is a system for high-rise structures which provides an efficient and economical use of structural steel combined with the efficiency and flexibility of unit layouts. The narrow tower width allows story-high trusses to span economically in the transverse direction between the columns at the exterior of the building. The required flexibility in unit layouts is achieved by arranging the trusses in a staggered plan at alternate floors, as shown schematically in Fig. 4.18. The floor system acts as a diaphragm transferring lateral loads in the short direction to the trusses. Lateral loads are thereby resisted by truss diagonals and are transferred into direct loads in the columns. The columns therefore receive no bending moments.

The truss diagonals are eliminated at the corridor location to allow for the opening. Since the diagonal is eliminated, the shear is carried by the bending action of the top and bottom chord members. Similarly, other openings can be provided for in the truss to allow for additional openings at a slight structural premium when required by architectural layout. The system was first used for a housing project for the elderly in St. Paul, Minnesota, completed in 1967. Since then, a number of long, narrow, high-rise buildings for apartment houses, hotels, and in some cases for office buildings have been built using this concept.

Because the staggered truss resists major gravity and lateral loads in direct stresses, the system is quite stiff. In general, no material needs to be added for drift control, and high-strength steels are conveniently used throughout the entire frame. The system has been

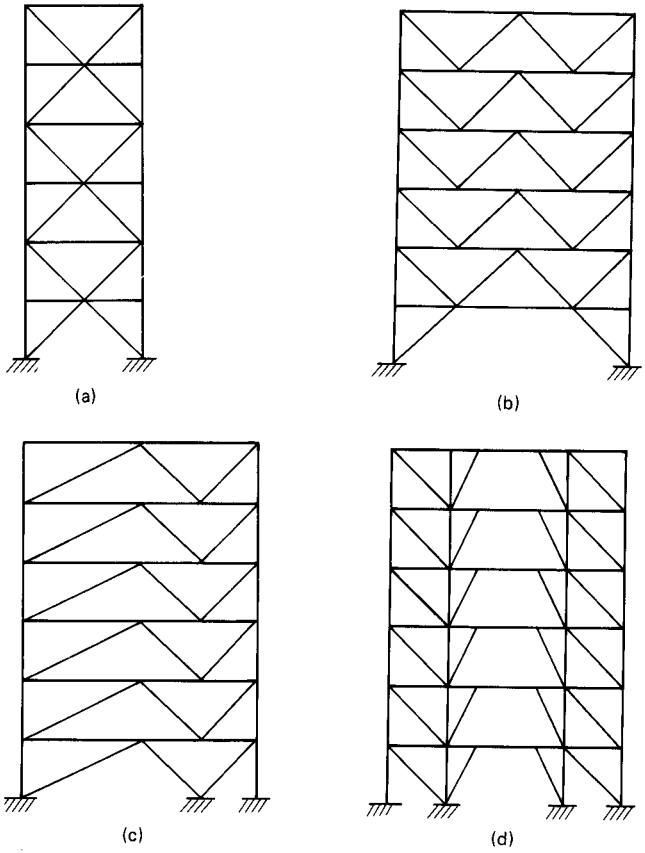

Figure 4.17 Common types of braced frames.

used for 35- to 40-story buildings. Spans must be long enough to make the trusses efficient, with 45 ft (13.72 m) being considered as the minimum practical limit. In a typical hotel or residential building, a staggered truss system will normally reduce the steel requirement by as much as 30 to 40 percent as compared to a conventional moment-connected framing. Since the trusses are supported only by the perimeter columns, the need for interior columns and associated foundations is eliminated, contributing to the economy of the system.

An added advantage of the system is that it allows for public spaces free of interior columns on the lower levels. The most economical use of staggered trusses is achieved by placing the trusses between units, since in a normal hotel or housing these units are spaced uniformly across the length of the building. It is possible to extend these units through trusses by providing for additional openings. However, varying the spacings could create a variety of unit sizes that can be

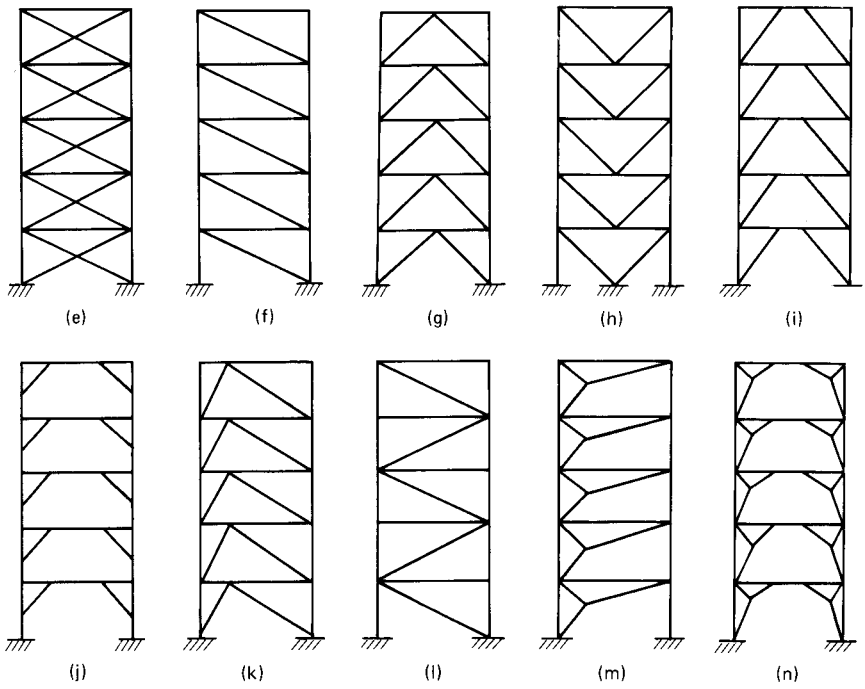

Figure 4.17 (*Continued*)

accommodated within the trusses. Thus, one-, two-, or three-bedroom apartments can be arranged on a single floor merely by varying the column spacings. The system is not limited to simple rectangular plans. It can be effectively used in curvilinear plans or can be used in a combination of offset rectangles. Figure 4.19 shows the staggered truss layout for a semicircular building.

4.5.2 Physical behavior

To understand the behavior of a staggered truss system it is helpful to consider the three-dimensional interaction between vertical bracing systems of a building through an interconnecting floor system. The behavior of a staggered truss system is not unlike that found in a structural system wherein the vertical bracing is transferred to another location. For purposes of illustration, consider a high-rise plan form shown in Fig. 4-20*a*. Assume that for architectural reasons it is required to eliminate the bracing at column lines A and B below level 2. If there is no other bracing below level 2, the columns at the extremities of the bracing must resist both the overturning moment and shear forces below level 2.

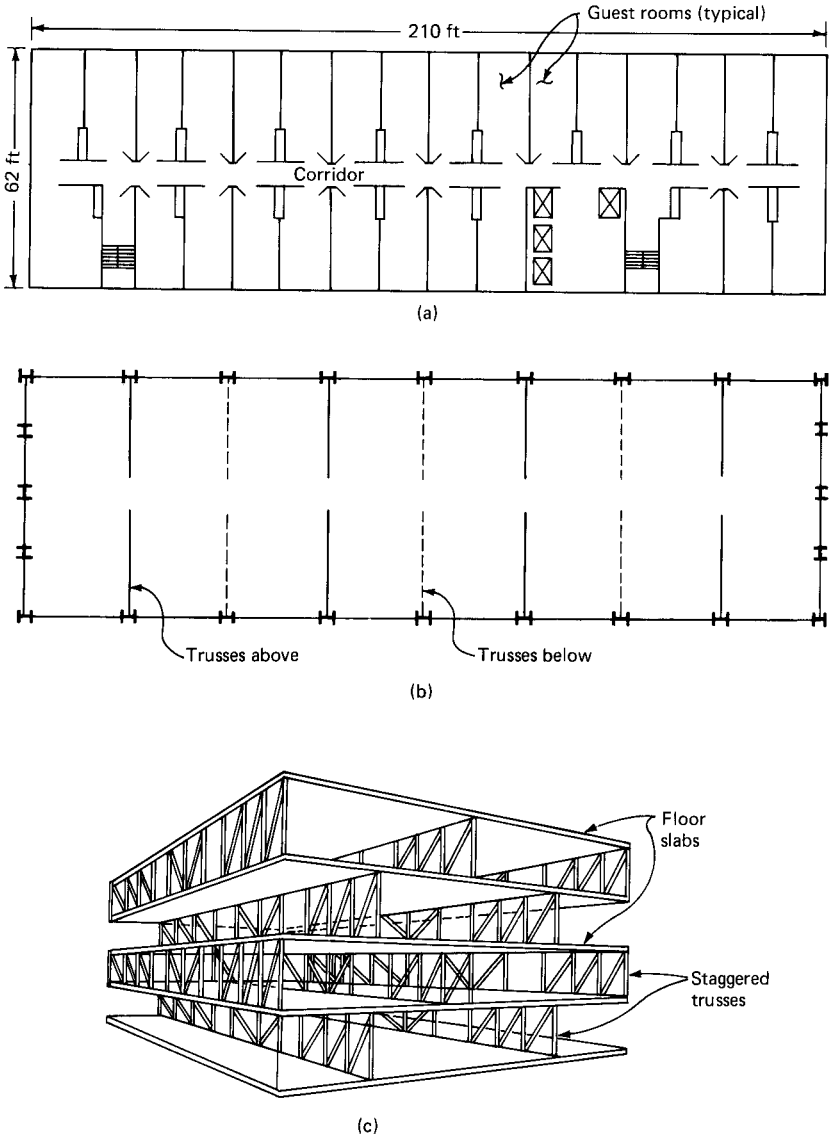

Figure 4.18 Staggered truss system. (*a*) Hotel plan showing layout of guest rooms; (*b*) arrangement of staggered trusses; (*c*) perspective view of truss arrangement.

The overturning moment manifests itself as compressive and tensile forces in the columns, while the shear forces introduce bending moments in the columns resulting in a rather inefficient structural system. Assume that architecturally it is permissible to introduce a bracing at the center of the building below level 2 as shown in Fig.

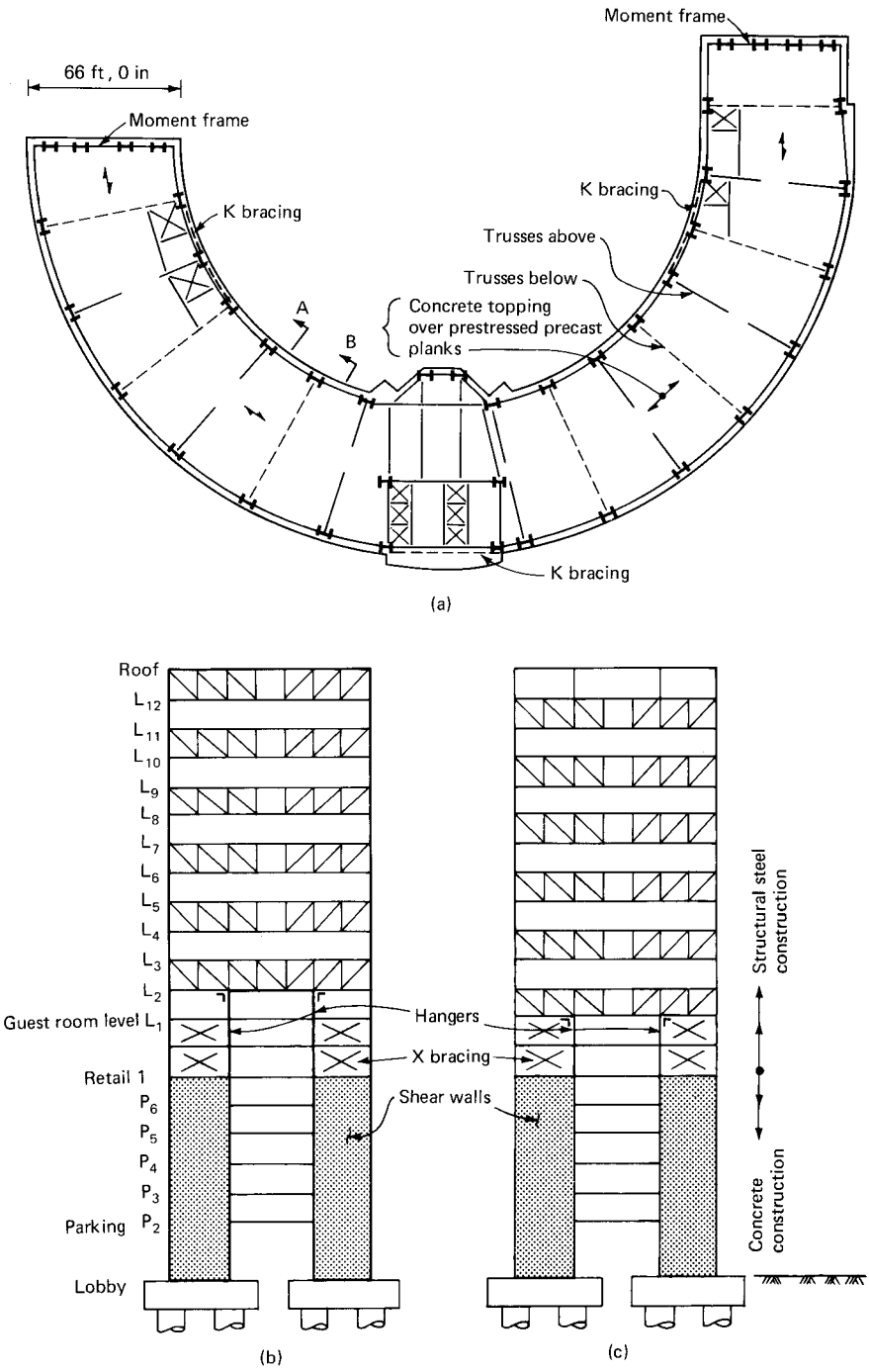

Figure 4.19 Staggered truss system for a semicircular building. (*a*) Building plan; (*b*) section A; (*c*) section B.

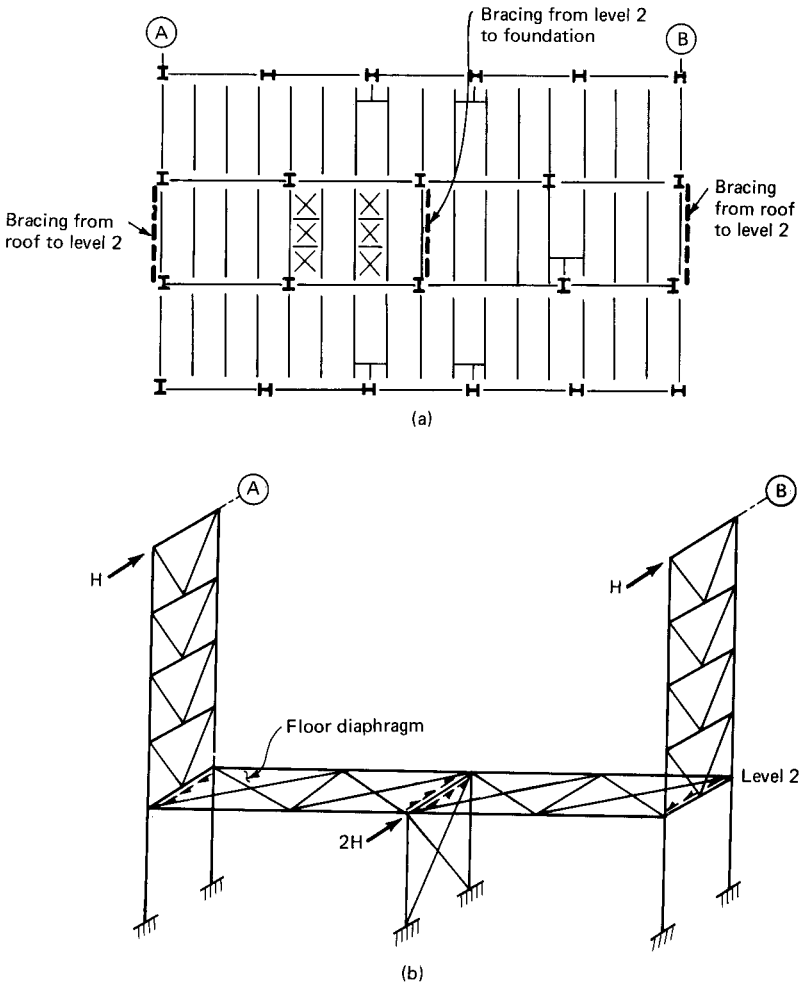

Figure 4.20 Conceptual model for staggered truss system. (*a*) Building plan; (*b*) lateral load transfer through diaphragm action.

4-20*a* and *b*. For purposes of lateral analysis, generally it is sufficiently accurate to assume that the slab diaphragm is rigid in its own plane. As a consequence of this assumption, most of the shear at the exterior braces at level 2 is transferred to the interior bracings through the diaphragm action of the floor slab. The columns under the exterior braces are therefore subjected to axial stresses only, while the shear at this level is resisted by the interior bracing. This in essence is the structural action in a staggered truss system in which the lateral force is transmitted across the floor to the truss on the adjacent column line and continues down on the truss line across the next floor down the

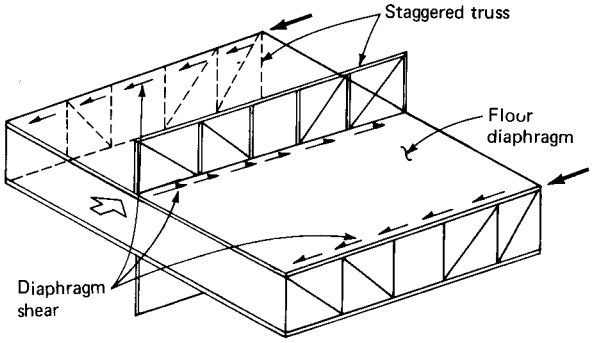

Figure 4.21 Load path in staggered truss system.

next truss, etc., as shown schematically in Figs. 4-21 and 4-22. Thus, between the floors, lateral forces are resisted by the truss diagonals, and at each floor these forces are transferred to the truss below by the floor system acting as a diaphragm. The columns between the floors receive no bending moments, resulting in a very efficient and stiff structure. Since the trusses are placed at alternate levels on adjacent column lines, two-bay-wide column-free interior floor space is created in the longitudinal direction.

4.5.3 Design considerations

Floor system. As in other structural systems, the floor system in a staggered truss scheme needs to fulfill two primary requirements: (1) collect and transmit the gravity loads to the vertical elements, and (2)

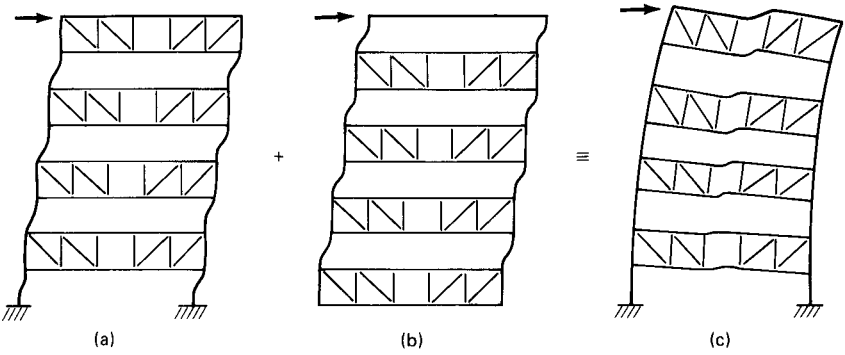

Figure 4.22 Conceptual planar model for staggered truss system. (*a*) and (*b*) Lateral deformation of adjacent bays; (*c*) overall behavior. Note the absence of local bending of columns.

resist the lateral loads as a shear diaphragm and provide a continuous path for transferring the lateral loads from the bottom chord of one truss to the top chord of the adjacent truss down through the structure. In addition to these structural requirements, the floor system must permit flexibility for apartment size and location, must provide fireproofing and an acceptable ceiling, and should be usable as temporary bracing during steel erection. Thus, one could use precast concrete planks, long-span composite steel decks, open-web joist system, or any other system consistent with the structural and architectural requirements. Precast planks and flat-bottomed steel decks are often used as exposed ceilings with minimum of finish. For spans up to 30 ft (9.15 m), 8-in (203-mm) planks are required, while for spans less than 24 ft (7.3 m), 6-in (152-mm) planks are adequate. In a composite steel deck system, a 7 ½-in (190-mm) deck is required for spans up to 30 ft (9.15 m), and for spans up to 24 ft (7.3 m), 6-in (152-mm) deep steel deck is adequate. When precast planks are used, shear transfer is achieved by the use of welded plates cast in the planks or by welding shear connectors on the truss chord.

In the case of a metal deck system, generally adequate shear transfer is obtained by the connection of the steel deck to the trusses. Planks used for erection purposes should have connection weld plates, even when shear connectors are provided. The choice of the floor system depends on the geographical location as well as local conditions. In earthquake zones the lighter floor produces smaller seismic forces. In cold climates the cost of grouting between precast planks in winter is increased by the necessity for heating. The floor system may consist of either a series of simple or continuous spans over the chords of the trusses. Because of the large spacing between the trusses, the continuous spans are usually limited to a maximum of two bays. Generally one end of each span is supported on the lower chord, while the other end is made continuous by simply running the floor slab across the top chord of the truss.

Since the trusses are staggered at alternate floors, the equivalent lateral load on each truss is equal to the wind load acting on two bays. Hence floor panels on each side of the truss must transmit half of that load to the adjacent truss in the story immediately below. The floor system acts as a deep beam resisting both the in-plane shears and bending moments. Adequate provision should be made to transfer longitudinal shear between each span so that the whole floor system acts as a single unit.

Although any floor system that is capable of carrying the gravity loads and the diaphragm shear can be used in staggered truss systems, economic considerations generally favor the use of either precast

concrete planks or long span composite metal deck, both with a topping of concrete reinforced with welded-wire fabric.

The design of the floor components for gravity loads is identical to that of a conventional high-rise building. Although continuity may be developed at the support connections to the truss chords, simple span behavior is assumed for convenience. Because the staggered truss system depends upon the diaphragm action of the entire floor to transfer lateral loads from one truss to another, the floor is assumed to have chords to resist the in-plane shears and moments. The bending can be resisted by the floor slab or by flange action at the exterior walls. The floor system of two adjacent bays is considered to be a continuous beam for the in-plane forces. Since there are no published criteria for general use, for any specific project it is advisable to study the diaphragm behavior in somewhat greater detail to develop and decide upon design procedures and criteria.

Columns. In the staggered truss system the lateral wind loads are taken out of the system by the floor, which acts as a diaphragm, and the truss diagonals, which act as vertical braces. Therefore, lateral loads are transferred into direct loads in the columns. No shear exists in the columns to create bending in the transverse direction of the building. Thus the columns can be designed as braced members to resist minor axis buckling, and the strong direction of the column can be used to resist lateral loads in the longitudinal direction. Another aspect of column design for staggered truss systems that should be considered is the effect of truss deflections in causing excessive weak-axis bending moment. The axial compression of the top chord and elongation of the bottom chord introduce bending in columns. This problem can be solved by introducing a camber in the truss by deliberately making the truss bottom chord smaller than the top chord. As an alternate, the connection between the bottom chord and column can be designed to slip under dead load conditions. Torquing the bolts after dead loads have been applied to the truss will limit the bending moments in the columns.

As a second alternate, the connection of the bottom chord can be designed to remain loose, increasing the effective length of the column in the weak axis to two stories between the top chords of the trusses at two levels. If none of the above procedures is applicable, then these moments should be provided for in the design of the columns.

Trusses. The design of the staggered truss system is quite conventional. Loading conditions and design methods are similar in principle to other framing systems. The floor system spans only from the bottom chord of one truss to the top chord of the next, and the resulting large

floor area supported by each truss allows maximum live load reduction.

In the transverse direction the lateral loads are transferred from the bottom chord of a truss to the top chord of an adjacent truss through floor diaphragm action down through the truss diagonals to the bottom chord. The sequence of events starts over, thus causing the entire transverse lateral load to be transferred through the floor system by diaphragm action and through the truss by direct stresses. The only additional bending occurs in the truss chords at the corridor openings or in other places where diagonals are eliminated.

The span-to-depth ratio of trusses is usually in the range of 6:1, giving adequate depth for the efficient design of top and bottom chords. Usually the panel width of trusses is not a governing criterion. Larger panel lengths with fewer web members decrease the fabrication costs and may work out to be more economical.

For maximum efficiency, just as in any other structural system, it is preferable to maintain a uniform spacing of trusses. This allows for maximization of typical truss units and reduces fabrication costs. However, when required by architectural arrangement, it is possible to vary the column and thus the truss spacing. Vierendeel openings other than those required for corridors should be avoided in the interest of economy. Truss design is based on continuous chord and pinned members, preferably using a computer analysis. Generally W or S shapes are selected for the chord members since angles are not efficient in resisting the secondary bending. Also, when planks are used wide flanges offer good bearing areas. Since the staggered truss system resists loads primarily by direct stresses, deflections are generally not a problem and therefore high-strength steels can be economically employed. The truss as a member supports a very large area and it is likely that if reduced live loads are used, the maximum live load reduction will be permissible. If any chord member is considered to support an area equal to the truss panel length times the bay spacing, it would be prudent to base the chord moment design on a reduced live load based on the smaller tributary area.

The simplest method of stacking trusses is a configuration called the checkerboard pattern, in which the trusses are placed at alternate columns and floors. It is possible, however, to obtain greater variety of spaces by using different layouts on alternate levels.

Longitudinally, the wind forces in a staggered truss structure can be resisted by any conventional bracing system such as braced frames and core shear walls. However, many projects lend themselves to the design of rigid frames on the two broad faces because (1) the main columns are oriented with webs parallel to the spandrels and (2) a large number of columns is generally available to participate in the

moment frame. In some cases deep precast fascia beams used for architectural reasons can be directly bolted to the columns to serve as stiff structural spandrels.

In the transverse direction, at the roof and at the bottom floors it is normally not possible to carry the rhythm of the staggered truss for the full height of the building. Posts and hangers are usually required to support these levels. At the bottom level the lateral loads may need to be transferred to the foundation by diagonal bracing. These are shown schematically in Fig. 4.19*b* and *c* with respect to the curvilinear layout of a staggered truss system shown in Fig. 4.19*a*.

4.6 Eccentric Bracing Systems

4.6.1 Introduction

Concentric braced frames are excellent from strength and stiffness considerations and are therefore used widely either by themselves or in conjunction with moment frames when the lateral loads are caused by the wind action. However, they are of questionable value when used alone in seismic regions because of their poor inelastic behavior. Moment-resistant frames possess considerable energy dissipation characteristics but are relatively flexible when sized from strength considerations alone. Eccentric bracing is a unique structural system that attempts to combine the strength and stiffness of a braced frame with the inelastic behavior and energy dissipation characteristics of a moment frame. The system is called eccentric bracing because deliberate eccentricities are employed between the beam-to-column and beam-to-brace connections in an effort to force shear yielding of the eccentric beam element. The eccentric beam element can thus be likened to a fuse that limits large forces from entering and causing buckling of braces. The system of eccentric bracing was first conceived by Professor Edgar P. Popov and his associates in the Department of Civil Engineering at the University of California at Berkeley. The unique system attempts to combine the advantages of braced and moment frames in a single structural system. As a characteristic feature of the system, the connection of the diagonal brace to the horizontal beam is deliberately offset from the connection between the beam and the vertical column. This offset or eccentricity, promotes formation of an energy-absorbing hinge in the portion of the beam between the two connections. This element functions as a fuse by undergoing flexural and shear yielding prior to formation of any additional plastic hinges in the bending members and well before buckling of any compression members. Thus the system maintains stability even under large inelastic deformations. The required stiffness during wind or minor earthquakes is maintained because no

plastic hinges are formed under these loads and all behavior is elastic. Although the deformation is larger than in a concentrically braced frame because of the bending and shear deformation of the "fuse," its contribution to deflection is not significant because of the relatively small length of the fuse. Thus the elastic stiffness of the eccentrically braced frame can be considered the same as the concentrically braced frame for all practical purposes.

4.6.2 Ductility

The ductile behavior is highly desirable when the structure is called upon to absorb energy. Steel's great capacity for deformation without fracture combined with its high strength makes it an ideal material for seismic structures. After the maximum load is reached, the material continues to withstand the load, undergoing large deformations without fracture. This capacity, by virtue of which the material can sustain the load without undergoing fracture, is attributed to steel's ductile nature. A brittle material, on the other hand, is not capable of undergoing large deformation at the onset of yielding and exhibits fracture on or about the point at which it reaches the maximum load. The large deformations associated with ductile behavior are highly desirable in earthquake-resistant design where the structure must be able to absorb energy. Steel is therefore suited admirably for eccentric bracing systems.

4.6.3 Behavior of frame

Eccentrically braced frames can be configured in various geometrical forms as long as the brace is connected to at least one link beam which can experience large deformations. The underlying principle of this system is to prevent the buckling of the brace from large overloads, such as those occurring during major earthquakes. This is achieved by sacrificing the link, making it deform plastically in shear. It is possible to calculate the theoretical load that would induce plasticity of the link, thus ensuring the magnitude of the axial load that goes into the bracing. A properly designed eccentrically braced frame is stiff to resist wind and moderate earthquake loads and is very ductile at the extreme overloads that are likely to occur during strong earthquake motions. The link enables the frame to absorb and dissipate large amounts of energy.

To understand the behavior of a link, consider the bracing shown in Fig. 4.23 subjected to reversal of horizontal loads due to a severe earthquake. Note that the connections between the column and beams are moment-connected to achieve brace action. The force in the brace is transmitted to the beam as a horizontal force inducing axial stresses and as a vertical force inducing shear stresses in the beam web. Of more concern in the design of the link (which is defined as the length

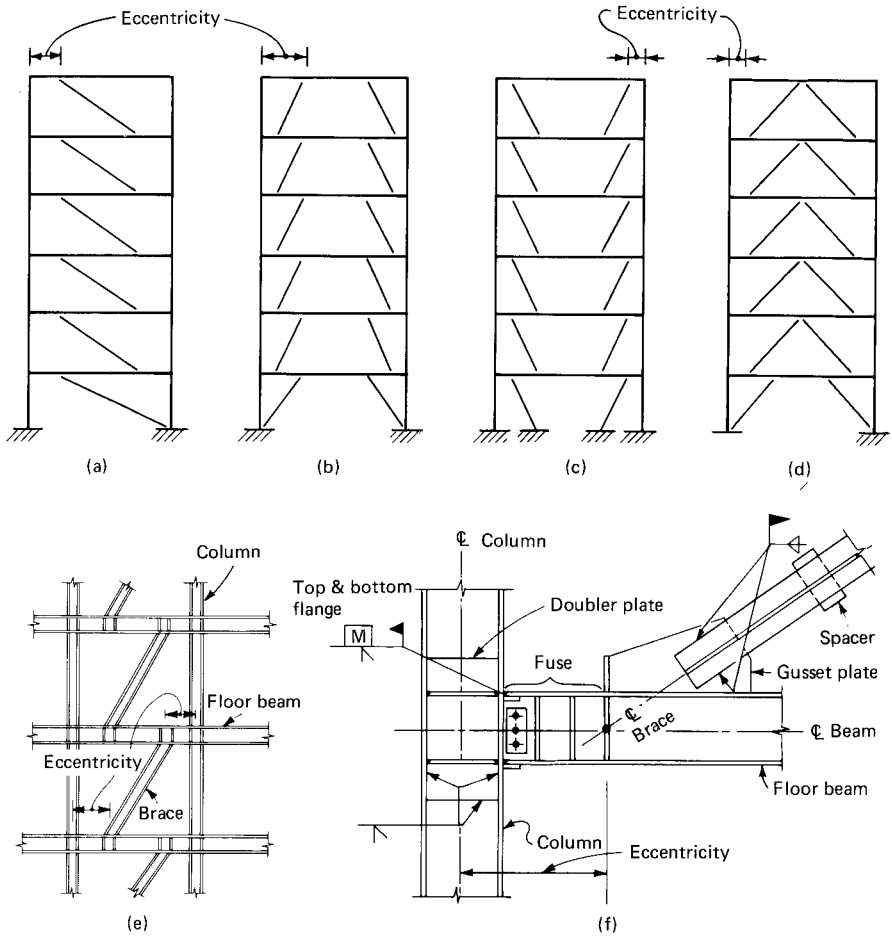

Figure 4.23 Eccentric bracing system. (*a* to *d*) Common types of bracing; (*e*) schematic elevation; (*f*) schematic detail.

of the beam between the column and the brace, Fig. 4.23) are the cyclic shear forces induced in the beam. Assuming that the beam and its moment connections to the columns have a large bending capacity, the mechanism of failure is by shear yielding of the beam web. The link connection to the brace must be designed to develop the plastic shear capacity of the beam without inducing web buckling. This is achieved by providing adequate stiffeners in the link beam to inhibit the web buckling phenomenon. Experiments conducted at the University of California at Berkeley have shown that shear links without the benefit of web stiffeners are not capable of sustaining cyclic loading and that their load-carrying capacity significantly deteriorates because of the lateral buckling of the web. Also, the experiments have shown that

stiffeners on one side of the web are sufficient to inhibit the web buckling. Although fitted stiffeners are not required from the point of view of web shear, it is a good practice to fit the stiffeners between the top and bottom flanges of the beam to inhibit the lateral torsional buckling of the beam.

4.6.4 Essential features of the link

Whether or not a beam develops plastic moment hinges at the ends or a shear yield hinge at its connection to the brace is a function of the length of the link. Making the lengths of links too short imposes an undue ductility demand on the links. Links longer than twice the beam depth tend to develop plastic hinges at the ends. As the length of the link increases, its behavior changes from that of a plastic shear hinge to one of a moment hinge. In considering the collapse mechanism of the system, links can be identified either as a short or long. The short link experiences a moderate rotation, while the long one is subjected to relatively larger rotations. There are no established rules to determine the length of the links. When the link is small, the collapse mechanism of the beam takes place in the form of a plastic shear hinge. The structure is relatively rigid and the elastic deflections tend to approach those of a concentrically braced frame. A large link, on the other hand, gives rise to familiar plastic hinges at the ends of the link. The deformation of the link adds considerably to the deflection of the frame, resulting in a relatively flexible frame. In either case, whether the link is small or large, it is essential that the link meet the ductility requirements. The web stiffener requirements progressively decrease as the length of the link increases. Whether the link is designed as a shear or moment link, it is still necessary to brace the beam flanges at the columns to prevent lateral-torsional buckling. The axial forces developed in the link must also be considered in the design.

It is good practice to make the links as long as practical without reducing the elastic deflection characteristics. A length of about two times the beam depth or five times the flange width of the beam is usually considered optimum. For links with moderate lengths of between two to four times the beam depth, the same requirements as for a plastic-shear-developing hinge can be used. Because plastic moment hinges develop, fitted stiffeners are required to develop the full capacity of the flanges.

The cyclic shear yielding is an excellent energy dissipation mechanism because large cyclic deflections can take place without failure or deterioration in the hysteretic behavior. This is because yielding occurs over a large segment of the beam web and is followed by a cyclic diagonal field. The web buckles after yielding in shear, but the tension field takes over the load-carrying mechanism to prevent failure,

resulting in a hysteretic loop having a large area representing good energy dissipation.

4.6.5 Analysis and design considerations

A moment-balancing technique is conveniently used for preliminary sizing of members in the eccentric bracing. The method in essence consists of starting with a set of statically admissible bending moments in the frame and distributing the moments to various members until the desired mechanism is reached. Equilibrium is maintained at each cycle of moment distribution, somewhat similar to the elastic moment distribution.

After the completion of plastic moment distribution, the various members are designed. In order to force the formation of a hinge in the beam web, the plastic moment capacity of the beam should exceed the beam shear yield capacity. In calculating the plastic moment capacity of the beam, the contribution due to the web portion of the beam is neglected because the web is assumed to have yielded. First the beam is selected for its shear capacity and then designed to assure that plastic hinges form at both ends of the eccentric beam element by requiring the moment capacity to be slightly larger than the shear capacity. As in other earthquake-resistant designs, the column should be selected by using the weak beam–strong column concept to assure that plastic hinges are formed in the beams and not in the columns. If the plastic moment of the beam selected is larger than that required by design, the column should be designed in an equally conservative manner. It is even more important to assure that the braces are prevented from buckling. This is achieved by designing the braces to withstand forces somewhat larger than those given by the analysis.

This conservatism in the design of braces is necessary to implicitly take into account the fact that the actual beam designed is likely to have additional capacity due to factors such as (1) beam strain hardening, (2) actual yield stress being more than the theoretical value, (3) interaction of floor slabs with beams tending to increase the plastic moment capacity. The brace-to-beam connection can be designed either as a welded or bolted connection. The bolts are designed as friction bolts and checked for bearing capacity because of the likelihood of slippage in the event of a large earthquake force. The beam-to-column connection is designed as a moment connection by welding the flanges of the beam to the column with full-penetration welds. Bolted friction connection augmented with fillet welds of a single-side shear plate is used to develop the high shear forces in the eccentric beam element. Lateral support is needed at the top and bottom flanges of the beam to prevent lateral torsion and weak axis bending.

The plastic moment distribution serves as a preliminary design only and therefore it is necessary to check the results by a linear elastic analysis. The elastic design of an eccentrically braced frame is no more difficult than the design of a concentrically braced frame, especially in view of the availability of computer programs. The results serve as a check on the serviceability criteria as well as a working stress check of the preliminary design. If adjustments in member sizes are required by the working stress analysis, it is necessary to go back and check the inelastic behavior to assure that the beam retains its weak link feature.

The design of beams and columns in the inelastic range is reasonably straightforward except for the design of the eccentric beam element. The beam length between the column and brace (the link element) is designed to carry the moment plus axial force while the remaining beam length outside of the brace is designed to carry the shear stresses. The behavior of the entire frame depends to a large extent on the behavior of shear link in the inelastic range. However, at present there exists no theoretical study or large body of test data describing the shear yielding of beam webs under cyclic loading. The only recourse open to the designer appears to be to determine the required stiffener along a link based on the satisfactory performance of a limited number of test frames which used small beams. Extrapolation of the test behavior done on frame models can be applied to prototype structures by introducing a stiffener to create equivalent unsupported panels.

4.6.6 Deflection considerations

The lateral deflection of an eccentrically braced frame can be estimated as the sum of three components: (1) deflection due to elongation of the brace; (2) deflection due to axial strain in the columns, usually referred to as the chord drift; and (3) the deflection due to deformation of the eccentric element. Because the braces and columns are designed to remain elastic even under severe earthquakes, their deflections are very nearly constant when the frame is plastic. The beam, which is designed for much heavier forces than in a corresponding concentrically braced frame, has a large stiffness and therefore is likely to contribute little to the deflection under elastic condition. During severe earthquakes, when the beam is plastic, its contribution to frame deflection in a properly proportioned system is relatively small. Therefore, an eccentrically braced frame is not an unreasonably flexible system as compared to a concentric frame.

4.6.7 Horizontal force factor *K*

The value of horizontal force factor K that is required for calculating the equivalent seismic forces to be used in the design of eccentric frame

is somewhat debatable and is a matter of seismic code interpretation. When properly detailed, moment connections are capable of undergoing large deformations and are therefore considered ductile. Building codes in general recognize the ductility characteristics of moment frames by giving preferential treatment to structures that depend on moment-resisting frames for their resistance to lateral forces generated by earthquakes. When a smaller value of $K = 0.8$ rather than 1.0 is used in the analysis, many seismic codes require that 100 percent of the lateral forces be resisted in the bracing. Normally the eccentric bracing is employed together with other types of bracing to resist seismic forces and the eccentric bracing resists but a relatively small portion of seismic forces. If it can be demonstrated that by ignoring the eccentric bracing the seismic story shears resisted by the conventional moment frames are more than those required by the code, then a case can be made for using $K = 0.8$ in the design of the eccentric brace. Most codes accept a reduced horizontal force factor since at extreme lateral loads caused during a major earthquake these frames behave in a ductile manner.

4.6.8 Conclusions

The steel buildings designed using the concept of eccentric bracing are lighter than the equivalent moment-resisting frames and, while retaining the elastic stiffness of concentrically braced frames, are more ductile. In summary the eccentric bracing system has the following characteristics:

1. Provides a stiff structural system that satisfies the serviceability requirements without imposing undue penalty on the weight of structural steel.
2. Eccentric beam elements, although yielding in shear, act as fuses to dissipate excess energy during a severe earthquake.
3. Premature failure of an eccentric beam element does not bring about the collapse of the structure because the structure continues to retain most of its strength and stiffness.

4.7 Interacting System of Braced and Rigid Frames

4.7.1 Introduction

Even for buildings in the range of 10 to 15 stories, unreasonably heavy columns result if wind bracing is confined to the building service core because the available depth for bracing is usually limited. In addition, high uplift forces occurring at the bottom of core columns can present

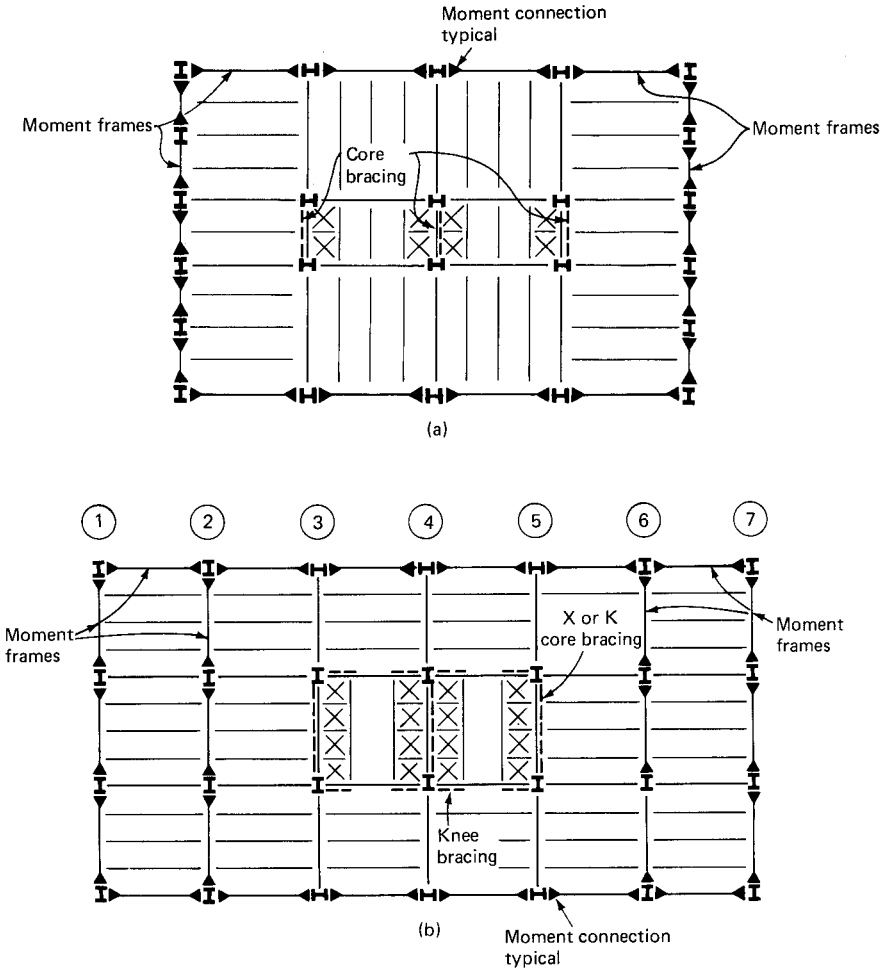

Figure 4.24 Schematic plans showing interacting braced and rigid frames. (*a*) Braced core and perimeter frames; (*b*) braced core and interior and exterior frames.

foundation problems. In such instances an economical structural solution can be arrived at by creating rigid frames to act in conjunction with the core bracing system. Although deep girders and moment connections are required for frame action, rigid frames are often preferred because they are least objectionable from the interior space planning point of view. Although each building has its own set of criteria, many times architecturally it may not be objectionable to use deep spandrels and additional columns on the building facade because the additional columns will not interfere with the space planning and the depth of spandrels may not present any undue problems for

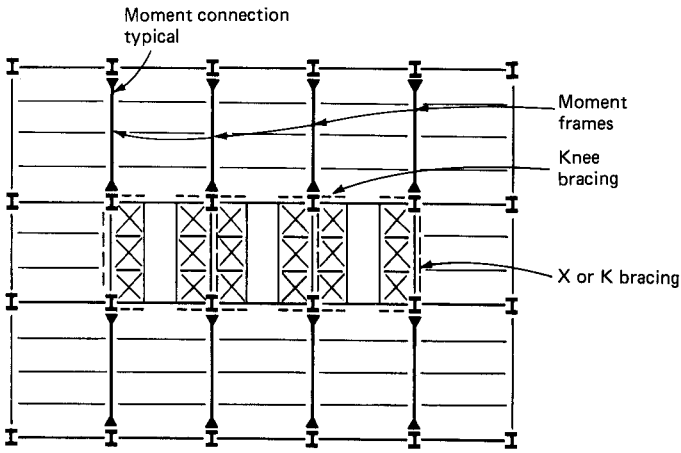

(c)

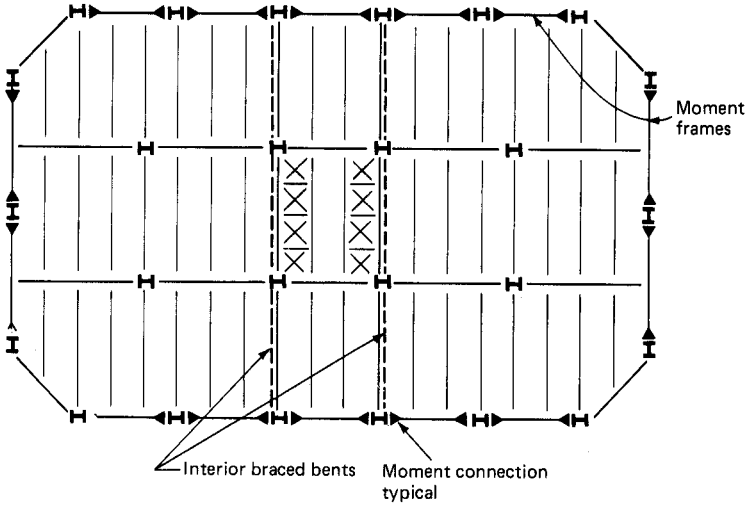

(d)

Figure 4.24 (*Continued*) (*c*) Braced core and interior frames; (*d*) full-width interior bracing and exterior frames.

passage of air conditioning ducts. A typical floor plan of a building that uses this concept is shown in Fig. 4.24*a*.

As an alternative to perimeter frames, a set of interior frames can be made to act in conjunction with the core bracings. Such an arrangement is shown in Fig. 4.24*b* in which frames on grid lines 1, 2, 6, and 7 participate with core bracings on lines 3, 4, and 5. Yet another option

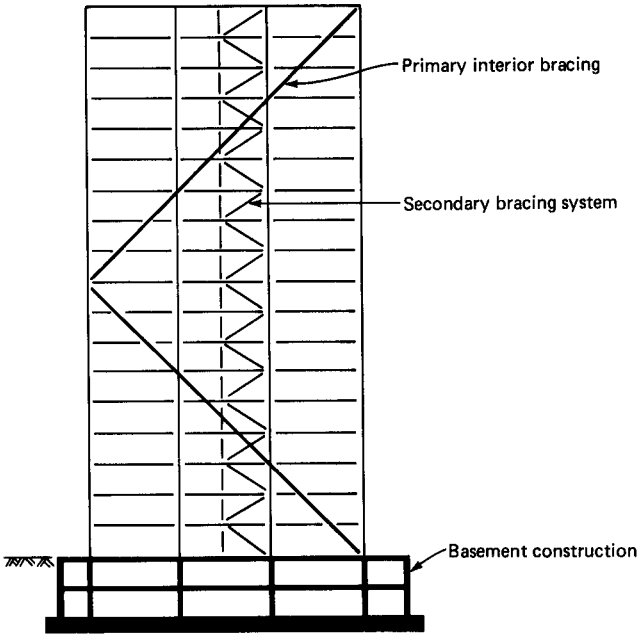

(e)

Figure 4.24 (*Continued*) (*e*) Transverse cross section showing primary interior bracing, secondary bracing, and basement construction.

is to moment-connect the girders between the braced core and perimeter columns as shown in Fig. 4.24*c*.

For very slender buildings with height-to-width ratios in excess of 5, it becomes uneconomical to use an interacting system of moment frames and braces whose depths are limited by the depths of building cores. An economical structural solution is to spread the bracing to the full width of the building along the facades if such a system does not compromise the architecture of the building. If it does, then a possible solution is to move the full-depth bracing to the interior of the building. Such a bracing concept is shown in Fig. 4.24*d*, in which moment frames located at the building facade interact with two interior-braced bents. These bents stretched out for the full width of the building form giant K braces, resisting overturning and shear forces by developing predominantly axial forces. A transverse cross section of the building is shown in Fig. 4.24*e*, wherein a secondary system of braces required to transfer the lateral loads to the panel points of the K braces is also indicated. The diagonals of the K braces running through the interior of the building result in sloping columns whose presence has to be acknowledged architecturally as a trade-off for structural efficiency of the system.

All of the above four bracing systems and any number of their variations can be used either singly or in combination and can be made to interact with moment-connected frames. The magnitude of their interaction can be controlled by varying the relative stiffness of various structural elements to achieve an economical structural system.

4.7.2 Physical behavior

If the lateral deflection patterns of braced and unbraced frames are similar, the wind loads can be distributed between the two systems according to their relative stiffness. However, in normally proportioned buildings the unbraced and braced frames deform with their own characteristic shapes, necessitating that we study their behavior as a unit instead of individually.

Insofar as the lateral-load-resisting function of tall buildings is concerned, unbraced and braced frames can be considered as two distinct types. The basis of classification is the mode of deformation of the unit when subjected to lateral loading. The deflection characteristics of a braced frame are similar to those of a cantilever beam. Near the bottom the vertical truss is very stiff, and therefore the floor-to-floor deflections will be less than half the values near the top. Near the top the floor-to-floor deflections increase rapidly mainly due to the cumulative effect of chord drift. The column strains at the bottom of the building produce a deflection at the top, and since this same effect occurs at every floor, the resulting drift at the top is cumulative. The chord drift problem encountered in practice is very difficult to control and normally requires structural steel quantities well in excess of those required for gravity needs.

Unbraced or rigid frames deform in a predominantly shear mode with the relative story deflections, depending on the magnitude of shear applied at each story level. Although near the bottom the story deflections are somewhat larger and near the top somewhat smaller as compared to the braced frames, the floor-to-floor deflections can be considered more nearly uniform. This combination of different deflection patterns between braced and rigid frames is very helpful in producing stiff structures.

The difference in behavior between braced and unbraced frames results in a nonuniform interacting force between these elements when these are connected by a system of floor slabs.

Figure 4.25 shows the typical deformation patterns anticipated by braced and unbraced frames when subjected separately to lateral loads. Also shown are the horizontal interaction forces developed when both elements are connected by floor slabs that enforce compatibility of later deformation at the floor levels. The braced frame acts as a

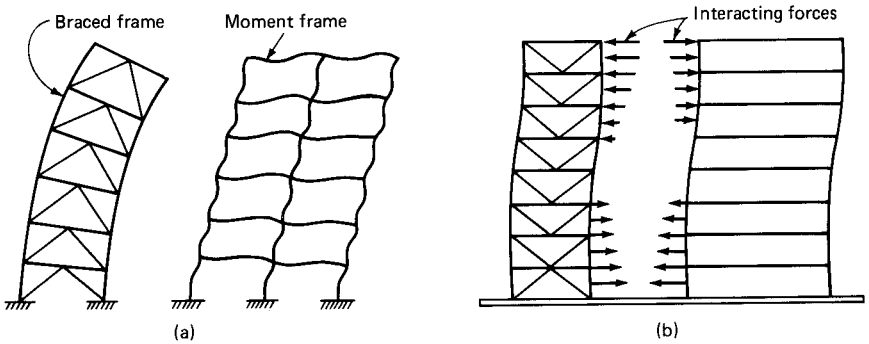

Figure 4.25 Interaction between braced and unbraced frames. (*a*) Characteristic deformation shapes; (*b*) variation of shear forces resulting from interaction.

vertical cantilever beam, bending as such, with the slope of the deflection greatest at the top of the building, indicating that in this region the braced frame contributes the least to the lateral stiffness.

The rigid frame has a shear mode deformation, with the slope of deformation greater at the base of the structure where the maximum shear is acting. Because of the different lateral deflection characteristics of the two elements, the frame tends to pull back the brace in the upper portion of the building and push it forward in the lower portion. As a result, the frame participates more effectively in the upper portion of the building where the wind shears are relatively less. The braced frame carries most of the shear in the lower portion of the building. Thus, because of the difference in the deflection characteristics of a rigid and braced frame, the two systems help each other a great deal. The frame tends to reduce the lateral deflection of the trussed core at the top, while the trussed core supports the frame near the base. A typical variation of shears carried by each element in such a system under lateral load is shown in Fig. 4.25*b*. It is significant to note that the total shear carried by the unbraced frame at the top stories can exceed the applied story shear at these levels. Clearly, distributing the applied shears to the different resisting elements in proportion to their relative stiffness can lead to grossly erroneous results.

When stiff cores are used to brace a building, it may be acceptable to disregard the lateral stiffness of the frame and assume that the horizontal load is carried entirely by the core system. However, if the frame is capable of making a significant contribution to the lateral stiffness, it is necessary to assess the distribution of load that occurs throughout its height with heavy interactions near the top and bottom. Heavy interacting forces also occur whenever significant stiffness changes take place in the height of the building.

Although the framed part of a high-rise structure is usually more flexible in comparison to the braced part, as the number of stories increases, its interaction with the braced frame becomes more significant, contributing greatly to the lateral resistance of the building. Therefore, when the frame part is fairly rigid by itself, its interaction with the braced portion of the building can result in a considerably more rigid and efficient design.

4.8 Outrigger and Belt Truss Systems

4.8.1 Introduction

Innovative structural schemes are continuously being sought in the design of high-rise structures with the intention of limiting the wind drift to acceptable limits without paying a high premium in steel tonnage. The savings in steel tonnage and cost can be dramatic in high-rise buildings if certain techniques are employed to utilize the full capacities of the structural elements. Various wind-bracing techniques have been developed to this end; this section deals with one such system, namely, the belt truss system, also known as the core-outrigger system.

A simple analytical model is developed to explain the essential behavior of the system, and a method of analysis is presented for obtaining optimum combination of belt truss locations which minimizes wind drift of buildings.

4.8.2 Physical behavior

A traditional approach to wind bracing for medium high-rise structures is to provide trussed bracing at the core or around stair wells and to supplement the lateral resistance by providing moment-connected frames at other convenient plan locations. But when buildings are taller than 500 ft (152.4 m) or so, the core, if kept consistent with the vertical transportation and mechanical requirements, does not have adequate stiffness to keep the wind drift down to acceptable limits.

A relatively new concept which has evolved within the past two decades is the technique of using a cap truss on a braced core combined with exterior columns. In this system columns are tied to the cap truss through a system of outrigger and belt trusses. Therefore in addition to the traditional function of supporting gravity loads, the columns restrain the lateral movement of the building. When the building is subjected to lateral forces, tie-down action of the cap truss restrains the bending of the core by introducing a point of inflection in its deflection curve. This reversal in curvature reduces the lateral movement at the top. The belt trusses function as horizontal fascia stiffeners and engage

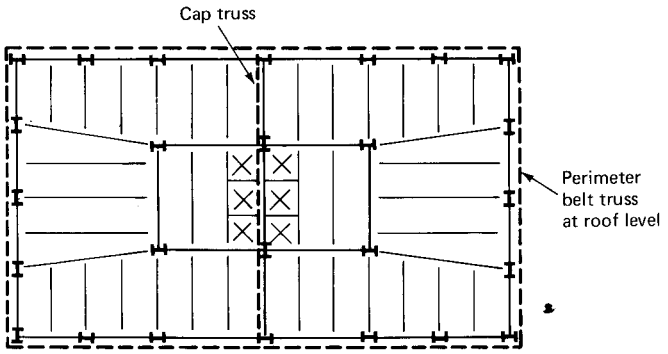

Figure 4.26 Building floor plan showing cap and belt trusses.

the exterior columns, which are not directly connected to the outrigger trusses. A general improvement of up to 25 to 30 percent in stiffness can be realized in contrast to the same system without such trusses because instead of individual columns acting as tiedowns, all the facade columns participate in resisting the lateral loads.

The cap and belt truss system illustrates the important role that can be played by a core and pin-connected columns on the exterior of the building. It permits an open facade design with sound overall structural scheme. The system, in addition to being efficient in resisting the lateral loads, also offers the additional benefit of equalizing the differential shortening of exterior columns resulting from temperature and the axial load imbalance between the core and exterior columns. Placement of a rigid truss at the top of the building eliminates differential movement between interior and exterior columns by providing compressive restraint for exterior columns in expansion and tension restraint when columns are in compression.

The behavior of the cap and belt truss system is explained with reference to Fig. 4.26, which shows the typical floor plan of a core-braced building. Assuming that only the core provides lateral bracing, the behavior of a braced core would be similar to that of a free cantilever; but when the core is coupled to the exterior columns through a system of cap and belt trusses, the core is no longer free to rotate at the top as a free cantilever. The outrigger arms, in trying to rotate with the core, are restrained from doing so by the exterior columns.

The rotation of the truss is restrained by lines of exterior columns; the windward columns are stretched by the rotation of the cap truss and are subjected to tension, while the leeward columns are compressed by this rotation and are therefore subjected to compression. These tensile and compressive forces produce partial reversal of

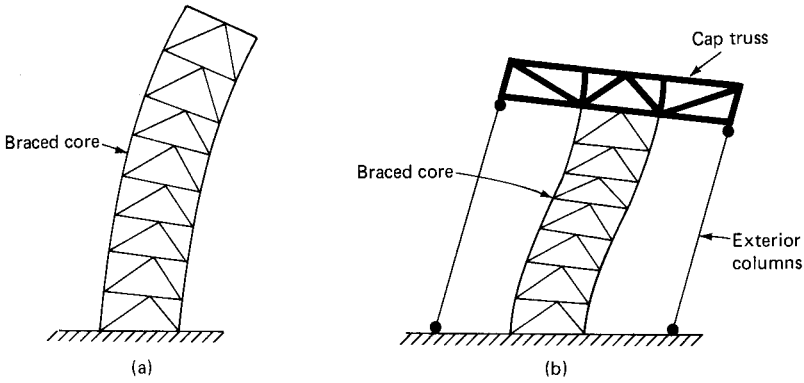

Figure 4.27 (*a*) Cantilever deflection of core; (*b*) reversed curvature induced by cap and belt trusses.

rotation of the braced core. The system no longer acts as a pure cantilever because it is restrained at the top as well as at the bottom. The resulting deflection is a flat S curve with a point of inflection, as shown in Fig. 4.27. The net effect of the coupling action is to reduce the bending moments of the core and thereby reduce deflections. The amount of reduction in drift depends on the relative stiffness of the core, cap truss, and size of tiedowns.

4.8.3 Method of analysis

It is generally recognized that a three-dimensional analysis is necessary if full advantage is to be taken of the special interaction among different elements of the complete structure. Although such an analysis has come within reach as a normal structural design procedure, its use as an optimization tool may not be desirable in view of the expense and time required. Herein, a method based on simplifying assumptions is presented for determining optimum location of a belt truss. For purposes of illustration, consider a high-rise structure in which the perimeter columns are tied to the core at one level. The assumed plan dimensions of the building and the arrangement of the core, outrigger, and belt trusses are shown in Fig. 4.28. A wind load of an intensity increasing linearly with the height of the building is assumed to act on the long face. The building is assumed to be 50 stories high. The following assumptions are made in the analysis:

1. The outrigger arms are connected to the columns in such a way that only axial forces are induced in the exterior columns.
2. The core walls in line with the outriggers are heavily braced so that the rotation of the core due to bracing deformations is negligible.

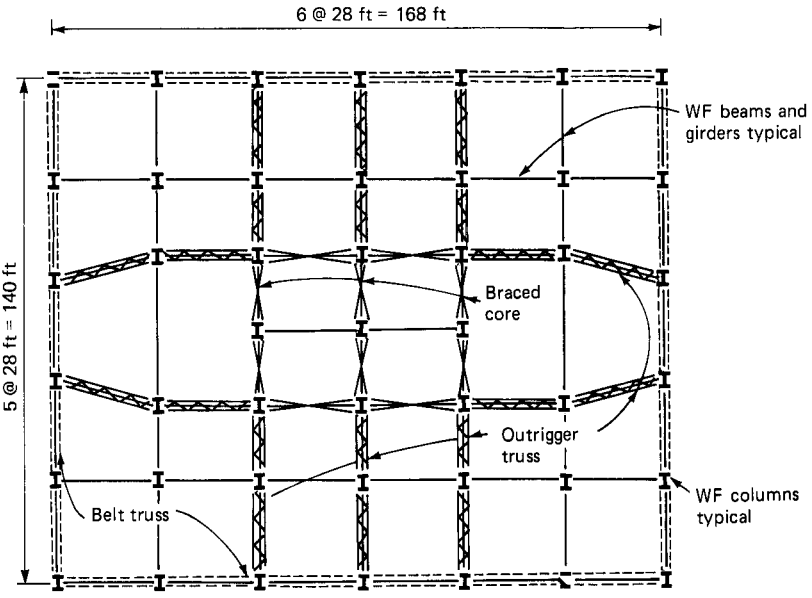

Figure 4.28 Belt truss structure framing plan.

3. The girder-to-column connections in all the other frames are pinned; thus, the braced core acting in conjunction with the perimeter columns provides total resistance to the wind load.
4. The belt truss is infinitely rigid and wraps around the full perimeter of the building.
5. The axial stiffness of the perimeter columns and the moment of inertia of the core decrease linearly with height of the structure.
6. The core is fully fixed at the base.

With these assumptions, the analytical model for the example problem reduces to a tied cantilever. Here, the core and outrigger deformations are dependent primarily on the flexural energy changes, while the columns can only store direct force energy and their deformation will be dependent only upon this energy form. Either of the two classical methods (stiffness or flexibility) can be employed to obtain the optimum location of the belt truss. Before this is attempted, let us consider qualitatively how the location of the belt truss influences the magnitude of the wind drift. Assume that the belt and outrigger trusses are located anywhere along the height of the structure and that the wind load and the member properties of the perimeter columns and the core remain constant for the full height. Figure 4.29 shows the analytical

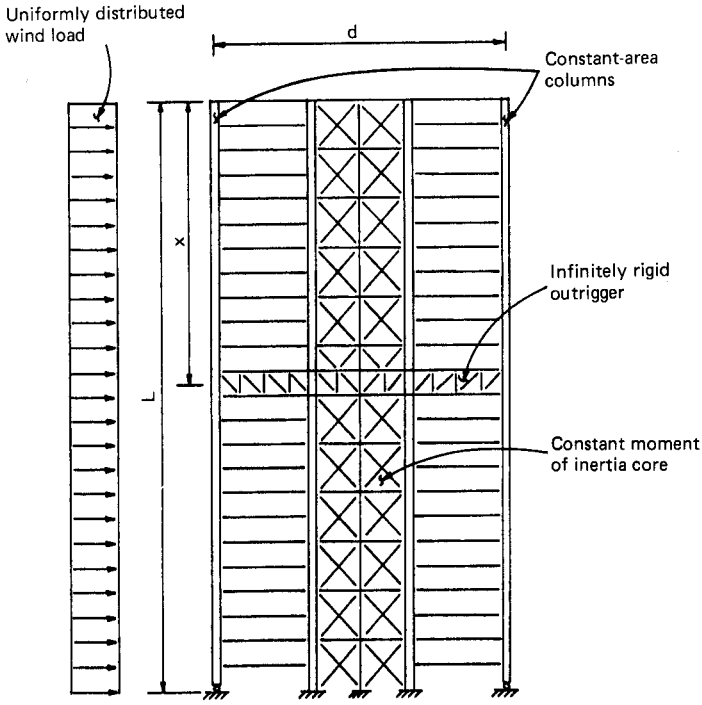

Figure 4.29 Simplified analytical model for single-outrigger system.

model incorporating the aforementioned assumptions. Consider the deflection of the tied cantilever, which is given by the algebraic sum of the deflections of the free cantilever under external load and the deflection due to the restraint of the outrigger and columns. The effect of the outrigger and columns can be looked upon as being similar to that of a moment-resisting spring whose stiffness depends on its location.

Before we attempt to formulate the problem for a closed-form solution, it is useful to study the behavior of the restrained cantilever for a few specific locations of the spring. Figure 4.30*a* through *d* shows the analytical model with springs located at top, at three-quarters of the height, at midheight, and at quarter points along the height.

Case 1 (Fig. 4.30*a*), spring at $Z = L$. The rotation compatibility condition at $Z = L$ can be written as

$$\theta_W - \theta_S = \theta_L \tag{4.5}$$

where θ_W = rotation of the cantilever at $Z = L$ due to a uniform lateral load W, in radians

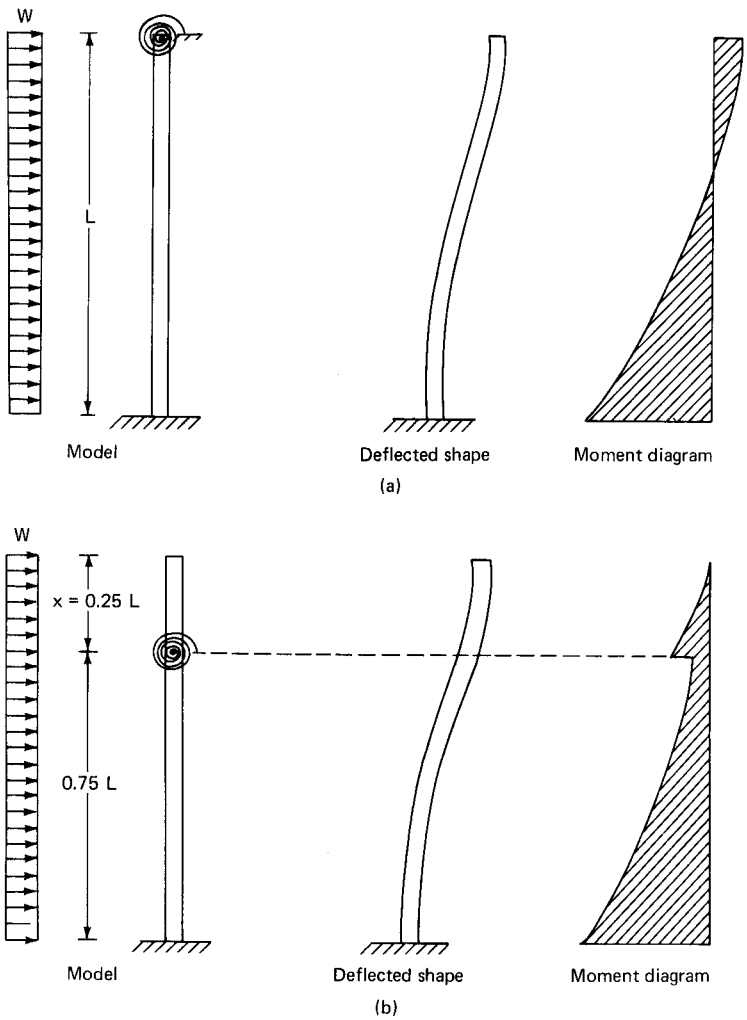

Figure 4.30 Behavior of tied cantilever. (*a*) Restraining spring at $x = 0$; (*b*) restraining spring at $x = 0.25L$.

θ_S = rotation due to spring restraint located at $Z = L$, in radians. The negative sign indicates that the rotation of the cantilever due to the spring stiffness acts in a direction opposite to the rotation due to external load.

θ_L = final rotation of the cantilever at $Z = L$, in radians.

For a cantilever with uniform moment of inertia I and modulus of elasticity E subjected to uniform horizontal load W,

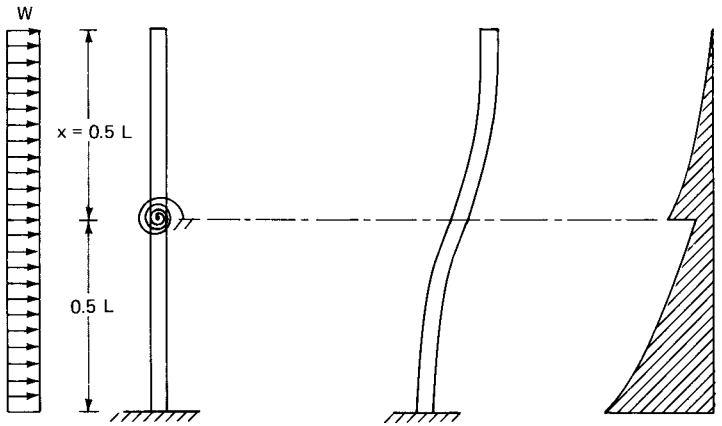

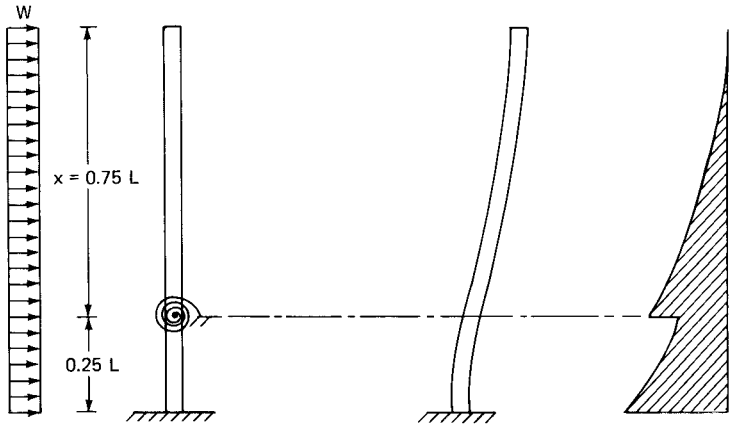

Figure 4.30 (*Continued*) (*c*) Restraining spring at $x = 0.5L$; (*d*) restraining spring at $x = 0.75L$.

$$\theta_W = \frac{WL^3}{6EI} \tag{4.6}$$

If M_1 and K_1 represent the moment and stiffness of the spring located at $Z = L$, Eq. (4.5) can be rewritten thus:

$$\frac{WL^3}{6EI} - \frac{M_1 L}{EI} = \frac{M_1}{K_1} \tag{4.7}$$

and

$$M_1 = \frac{WL^3}{1/K_1 + L/EI} \tag{4.8}$$

The resulting drift Δ_1 at the building top can be obtained by superposing the deflection of the cantilever due to external uniform load W and the deflection due to the moment induced by the spring, thus

$$\Delta_1 = \Delta_{\text{load}} - \Delta_{\text{spring}} \tag{4.9}$$

$$= \frac{WL^4}{8EI} - \frac{M_1 L^2}{2EI}$$

$$= \frac{L^2}{2EI}\left(\frac{WL^2}{4} - M_1\right) \tag{4.10}$$

Case 2 (Fig. 4.30*b*), spring at $Z = 3L/4$. The general expression for lateral deflection y for a uniform cantilever subjected to a uniform lateral load is given by

$$y = \frac{W}{24EI}(x^4 - 4L^3x + 3L^4) \tag{4.11}$$

Note that x is measured from the top.

Differentiating with respect to x, the general expression for slope of the cantilever is given by

$$\frac{dy}{dx} = \frac{W}{6EI}(x^3 - L^3) \tag{4.12}$$

The slope at the spring location is given by substituting $Z = 3L/4$, i.e., $x = L/4$ in Eq. (4.12). Thus

$$\frac{dy}{dx}\left(\text{at } z = \frac{3L}{4}\right) = \frac{W}{6EI}\left(\frac{L^3}{64} - L^3\right)$$

$$= \frac{WL^3}{6EI} \times \frac{63}{64} \tag{4.13}$$

Using the notation M_2 and K_2 to represent the moment and stiffness of spring at $Z = 3L/4$, the compatibility equation at location 2 can be written thus

$$\frac{WL^3}{6EI}\left(\frac{63}{64}\right) - \frac{M_2}{EI}\left(\frac{3L}{4}\right) = \frac{M_2}{K_2} \tag{4.14}$$

Noting that $K_2 = 4K_1/3$, the expression for M_2 can be written thus

$$M_2 = \left(\frac{WL^3/6EI}{1/K_1 + L/EI}\right)\frac{63/64}{3/4} = \left(\frac{WL^3/6EI}{1/K_1 + L/EI}\right) 1.31 \tag{4.15}$$

Noting that the terms in the parenthesis represent M_1, Eq. (4.15) can be expressed in terms of M_1

$$M_2 = 1.31\, M_1$$

The drift is given by the relation

$$\Delta_2 = \frac{WL^4}{8EI} - \frac{M_2 3L}{4EI}\left(L - \frac{3L}{8}\right) \tag{4.16}$$

or

$$\Delta_2 = \frac{L^2}{2EI}\left(\frac{WL^2}{4} - 1.23M_1\right) \tag{4.17}$$

Case 3 (Fig. 4.30*c*), spring at $Z = L/2$. The rotation at $Z = L/2$ due to external load W can be shown to be equal to $7WL^3/48EI$, giving the rotation compatibility equation

$$\frac{7WL^3}{48EI} - \frac{M_3 L}{2EI} = \frac{M_3}{K_3} \tag{4.18}$$

where M_3 and K_3 represent the moment and stiffness of the spring at $Z = L/2$. Noting that $K_3 = 2K_1$, the expression for M_3 works out as

$$M_3 = \left(\frac{WL^3/6EI}{1/K_1 + L/EI}\right) \times \frac{7}{4} \tag{4.19}$$

Since the expression in the parentheses is equal to M_1, M_3 can be expressed in terms of M_1

$$M_3 = 1.75M_1 \tag{4.20}$$

The drift is given by the equation

$$\Delta_3 = \frac{WL^4}{8EI} - \frac{M_3 L}{2EI}\left(L - \frac{L}{4}\right) \tag{4.21}$$

or

$$\Delta_3 = \frac{L^2}{2EI}\left(\frac{WL^2}{4} - 1.31M_1\right) \tag{4.22}$$

Case 4 (Fig. 4.30*d*) spring at $Z = L/4$. The rotation at $Z = L/4$ due to uniform lateral load can be shown to be equal to $WL^3/6EI[(37/64)]$, giving the rotation compatibility equation

$$\frac{WL^3}{6EI}\left(\frac{37}{64}\right) - \frac{M_4 L}{4EI} = \frac{M_4}{K_4} \tag{4.23}$$

where M_4 and K_4 represent the moment and stiffness of the spring at $Z = L/4$. Noting that $K_4 = 4K_1$, M_4 in Eq. (4.23) can be expressed in terms of M_1.

$$M_4 = 2.3\, M_1 \tag{4.24}$$

The drift for this case is given by the expression

$$\Delta_4 = \frac{WL^4}{8EI} - \frac{M_4 L}{4EI}\left(L - \frac{L}{8}\right) \tag{4.25}$$

or

$$\Delta_4 = \frac{L^2}{2EI}\left(\frac{WL^2}{4} - M_1\right) \tag{4.26}$$

Equations (4.10), (4.14), (4.22), and (4.26) give the building drift for four different locations of the belt and outrigger trusses.

The value of K_1 which corresponds to stiffness of the spring when it is located at $Z = L$ can be derived as follows. A unit rotation given to the core at the top results in extension and compression of all perimeter columns, the magnitudes of which are given by their respective distances from the center of gravity of the core. The resulting force multiplied by the lever arm gives the value for stiffness K_1. Thus, if K_1 is measured in kips and the distance in feet, K_1 has units of kip-feet. The force p in each exterior column is given by the relation $p = AE\delta/L$; since by definition δ corresponds to column

extension or compression due to unit rotation of the core, $\delta = d/2$, where d is the distance between the exterior columns. Therefore,

$$p = \frac{AE}{L}\left(\frac{d}{2}\right) \tag{4.27}$$

and its contribution to the stiffness K_1 is given by the relation

$$\begin{aligned} K_i &= p_i d \\ &= \frac{A_i E}{L}\frac{d^2}{2} \end{aligned} \tag{4.28}$$

The total contribution of all exterior columns on the long faces is given by the summation relation

$$K_1 = \sum_{i=1}^{n} K_i = \frac{d^2 E}{2L}\sum_{i=1}^{n} A_i \tag{4.29}$$

The contribution of the columns on the short faces can be worked out in a similar manner.

4.8.4 Optimum location for a single truss

From the previous illustration it can be noted that for a given building, the magnitude of beneficial effect of tying down the exterior columns to the core is a function of two distinct characteristics, the stiffness of the equivalent spring and the magnitude of the rotation of cantilever at the spring location due to external loads.

The stiffness of the equivalent spring, for example, is at a minimum when located at the top and a maximum when at the bottom. The strain energy that can be stored in the spring is a function of stiffness and the rotation of the cantilever at its location. The rotation of the free cantilever for the assumed wind load varies parabolically from a maximum value at the top to zero at the bottom. Therefore, from the point of view of spring stiffness alone it is desirable to locate the outrigger at the bottom, whereas from a consideration of rotation, the converse is true. It is obvious that the optimum location is somewhere in between.

For the simplified structure shown in Fig. 4.29, assuming the outrigger to be infinitely rigid, a closed-form solution for the optimum location can be derived by the principles of calculus. First, we write the compatibility equation for the rotation at x, which is the location of the outrigger measured from the top as shown in Fig. 4.29.

$$\frac{W}{6EI}(x^3 - L^3) - \frac{M_x}{EI}(L - x) = \frac{M_x}{K_x} \tag{4.30}$$

where W = intensity of the wind load per unit height of the structure
M_x = moment at x, the outrigger and column restraint
K_x = spring stiffness at x equal to $AE/(L-x) \cdot d^2/2$
E = modulus of elasticity of the core
I = moment of inertia of the core
A = area of the perimeter columns
L = height of the building
x = location of truss measured from top
d = distance out-to-out of columns

Next, obtain the deflection at the top of the structure due to M_x:

$$Y_M = \frac{M_x(L - x)(L + x)}{2EI} \tag{4.31}$$

From our definition, the optimum location of the belt truss is that location for which the deflection Y_M is a maximum. This is obtained by differentiating Eq. (4.31) with respect to x and equating to zero. Thus,

$$\frac{d}{dx}\left[\frac{W(x^3 - L^3)(L + x)}{12(EI)^2\,(1/AE + 1/EI)}\right] = 0 \tag{4.32}$$

$$4x^3 + 3x^2L - L^3 = 0 \tag{4.33}$$

giving the optimum location at $x = 0.455L$. If the flexibility of the outrigger is taken into account, even for the overly simplified model, the corresponding equation for the solution of x becomes too involved to be solved by hand. Extension of the solution to two or more outrigger trusses further complicates the solution, thus necessitating a formulation suitable for a computer. This is considered next.

4.8.5 Systems with two or more stiffening trusses

A necessary step to counter wind overturning problems in tall structures is to engage the perimeter of the building to resist the lateral loads. For buildings in the 40- to 60-story range, it is possible to resist lateral loads without increasing the structural steel weight to unreasonably high levels by formulating structural systems that only partly develop pure cantilever action. They can be looked upon as medium-

efficiency equivalent tubular structures. These systems are more efficient than braced frames or a system of interacting braced and rigid frames. Introduction of outrigger and belt trusses to an otherwise nominally efficient frame makes it a very efficient system, increasing its application from about 40 stories to as many as 60 stories or so.

At times bracing required for buildings may not have an adequate span-to-depth ratio; the depth available for the vertical bracing system may be limited. One solution for controlling the building drift is to increase the column areas to an unreasonably high value. However, the resulting high uplift forces can present foundation anchoring problems. In such instances the technique of introducing outrigger and belt trusses can be very effective in enhancing the efficiency of shallow bracing systems, especially when two or more stiffening trusses are employed along the height of a building. The purpose of providing more than one truss is to increase the strength and stiffness of the system over and above the beneficial effect of a single truss, and to this end additional trusses are mobilized at two or three floor levels to provide stiff points of resistance. At these levels, stiff outrigger arms are used to activate a perimeter truss, which in turn enforces the participation of the exterior columns in resisting wind loads. The structural system is shown schematically in Fig. 4.31.

The building can have one, two, or on very rare occasions, three belt trusses. The more trusses used, the better the integration of the core and facade columns. The outrigger trusses can be placed at locations within the building where the diagonal bracing will not interfere with the building's function. Usually outriggers are confined to mechanical levels where they are least objectionable. In many parts of North America air conditioning and heating for tall buildings is provided by installing large mechanical units at every 20th floor or so. On a 60-story building, for example, the 20th, the 40th, and the roof levels may be dedicated as mechanical floors. In such buildings, it may not be architecturally objectionable to run outrigger trusses on each side of the core through the building space. Thus the mechanical floors usually occurring at the one-third, one-half, or three-quarter height of the building are convenient locations to be most effective as truss floors. If a diagonal truss along the building perimeter is architecturally unacceptable, a less efficient Vierendeel truss can be incorporated at the perimeter to function as a belt truss.

At each trussed level the system is restrained from rotation. The partial fixity of the outrigger truss pulls the moment diagram back at these levels; consequently, the bending moment at the base of the building is further reduced because of the greater translation of lateral forces to axial forces. As in the case of single truss, for a given number of exterior columns and relative stiffness of various components of the

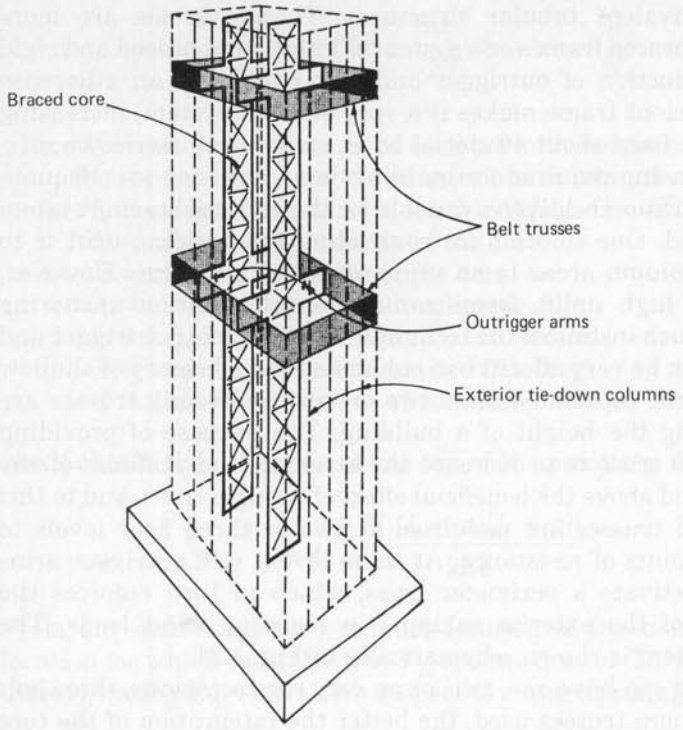

Figure 4.31 Schematic elevation of two outrigger and belt truss system.

structure, the amount of drift reduction is influenced considerably by the locations at which the outrigger and belt trusses are attached to the perimeter columns. The importance of choosing the optimum locations for two truss systems is considered next.

4.8.6 Optimum locations for two trusses

As discussed previously, by making certain simplifying assumptions it is relatively easy to obtain a closed-form solution which gives the optimum location for a single truss system. The oversimplifications are necessary to demonstrate the qualitative relationship between the truss location and the magnitude of lateral sway. In a real building the simplifying assumptions are violated to various degrees. Determination of optimum location of a single truss without incorporating the simplification becomes too cumbersome to formulate for hand computations. The problem gets even more complicated when optimization of two or more truss locations is attempted by hand computations, thus necessitating a computer solution.

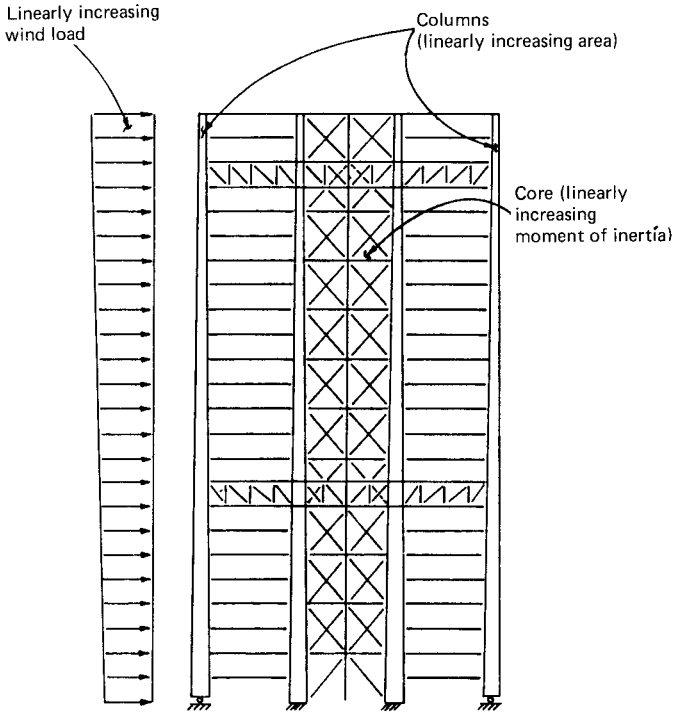

Figure 4.32 Analytical model.

Computer solution. The analytical model is shown in Fig. 4.32. A flexibility approach has been employed for the solution. The method is briefly explained with reference to the example problem. The moments at the outrigger locations are chosen as the unknown arbitrary constants M_1 and M_2, and the structure is released by removing the rotational restraints, making it statically determinate, so that the effect of any loading can be easily calculated. The flexibility coefficients f_{11} and f_{22} are calculated by using integrals of the form

$$\int \frac{m_i m_j}{EI}\, ds + K \int \frac{s_i s_j}{GA}\, ds + \int \frac{n_i n_j ds}{EA} \tag{4.34}$$

where m, s, and n represent the moment, shear force, and the axial load distribution on the statically determinate system due to the application of a unit moment at the location and in the direction of the arbitrary constants. E, G, I, and A are the familiar notations for material and member properties of the element of the structure for which the integral is being calculated. Note that different forms of energy are significant in different members.

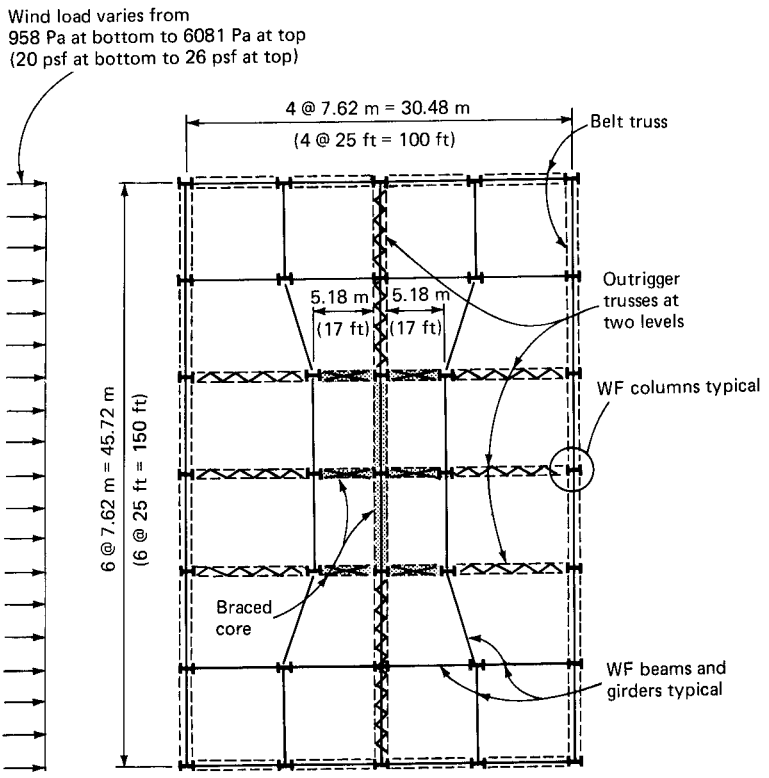

Figure 4.33 Example problem: schematic plan.

Next, the compatibility equations for the rotations at the truss locations are set up and the magnitudes of the arbitrary constants M_1 and M_2 obtained. The tip deflection for the structure is obtained by superposition of the solutions for the external load and for the moments M_1 and M_2. A single solution to the problem is trivial and may easily be carried out by hand calculations. A computer solution is necessary, however, since the object of the exercise is to seek an optimum combination of the truss locations to minimize the wind drift, requiring many solutions for different truss locations. A computer program was written for this purpose and computations were carried out for a 46-story example structure shown in Fig. 4.33. The results of the analysis are given in the form of graphs in Fig. 4.34.

Explanation of graphs. The magnitudes of the top floor deflection of the structure for three assumed modes of resistance have been presented in a nondimensional form in Fig. 4.34. The vertical ordinate with the value of the deflection parameter equal to 1 represents the top floor

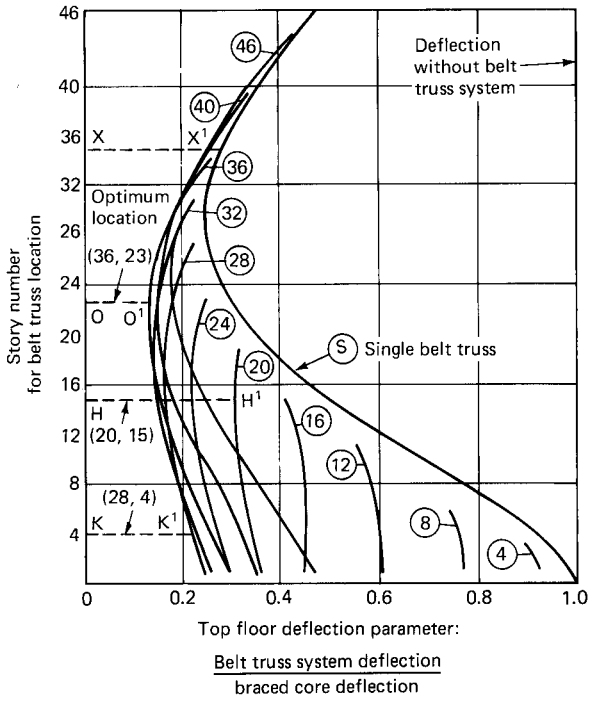

Figure 4.34 Graph for optimum belt truss locations.

deflection, obtained by assuming that there are no belt trusses. The resistance is provided by the cantilever action of the braced core alone. The curve designated as S represents the deflection, assuming that a single belt truss located anywhere along the height of the structure is acting in conjunction with the braced core. The deflection for a particular location of the truss is obtained by the horizontal distance between the curve S and the vertical axis measured at the floor level (e.g., distance XX′ multiplied by the cantilever deflection gives the top floor deflection for the location of the belt truss at floor 35). It is seen that the wind drift is quite sensitive to the truss location. The most favorable location is at floor 27; the resulting deflection is reduced to less than a third of the pure cantilever deflection.

The curves designated as 4, 8, . . . , 46 represent the top floor deflections obtained by assuming that there are two belt trusses located anywhere along the height of the structure. To obtain each curve, the location of the upper outrigger was considered fixed in relation to the building height, while the location of the lower outrigger was moved in single-story increments, starting from the first floor to the floor immediately below the top outrigger.

The number designations of the curves represent the floor number at which the upper outrigger is located. The second outrigger location is given on the vertical axis. The horizontal distance between the curve and the vertical axis is the top deflection parameter for the particular combination of truss locations given by the curve designation and the vertical ordinate. For example, let us assume that the deflection at top is desired for the combination (20, 15), the numbers 20 and 15 being the floors at which the upper and lower outriggers are located. The procedure is to select the curve with the designation 20 and to draw a horizontal line from the vertical ordinate at 15 to this curve. The required top deflection parameter is the horizontal distance between the vertical axis and the curve 20 (distance HH′ in Fig. 4.34). Similarly, distance KK′ gives the deflection parameter for the combination (28, 4). It is seen from Fig. 4.34 that the relative location of the trusses has a significant effect on controlling the wind drift. Furthermore, it is evident that a deflection very nearly equal to the optimum solution can be obtained for a number of combinations. For the example problem, a deflection parameter of 0.15, which differs negligibly from the optimum value of 0.13, is achieved by the combinations (40, 23), (32, 23), etc. The effectiveness of the belt truss system is self-evident from the figure.

4.8.7 Example projects

Figure 4.35*a* and *b* shows photographs of The First Wisconsin Center, a 42-story, 1.3-million-square-foot (120,770-m^2) bank and office building which utilizes the concept of belt and outrigger system of lateral bracing. The building rises 601 ft (183 m) from a two-level glass-enclosed plaza and sports three belt trusses located at bottom, middle, and top of the building. The belt truss at the bottom serves as a transfer truss, eliminating every other exterior column. Outrigger trusses are used at the top and middle of the building to engage the braced core to the exterior columns. Mechanical levels are located at the trussed floors. The architecture and engineering for the project were by the Chicago office of Skidmore, Owings & Merrill.

As a second example of practical application of outrigger trusses, Fig. 4.35*c* shows a schematic partial elevation of wind bracing system used in One Houston Center. The building, consisting of 48 stories, rises to a height of 681 ft (207.5 m) above grade. To minimize the building drift, two-story-deep outrigger trusses tie the perimeter columns to the K-braced core between the 33rd and 35th levels. Three outrigger trusses on each side of the core run through the building space. Use of these outrigger trusses helped in reducing the drift to less than 1/460 of the building height. The structural engineering for the project was by the Houston office of Walter P. Moore & Associates. A

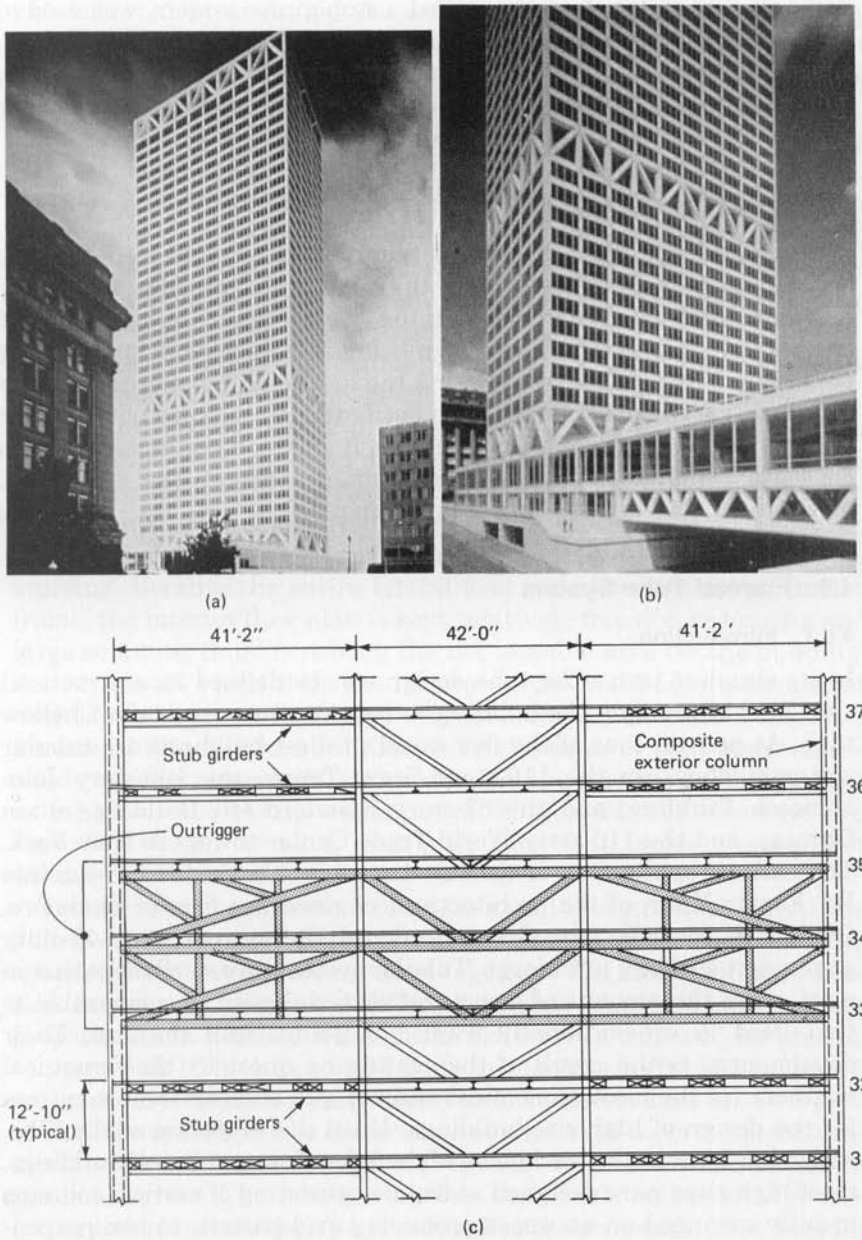

Figure 4.35 (*a* and *b*) Photographs of First Wisconsin Center, Milwaukee. A system of outriggers and belt trusses interacting with moment frames constitutes the lateral bracing system (Architect/Engineer, Skidmore, Owings & Merrill, Chicago); (*c*) schematic framing elevation of outrigger truss for One Houston Center project (Structural engineers, Walter P. Moore and Associates).

novel system of floor framing, called a stub girder system, was used to frame typical bays measuring 41 ft 2 in by 30 ft (12.54 m by 9.14 m). This unique system of floor framing, which is discussed in Chap. 9, attempts to reduce the building cost by simultaneously minimizing structural steel tonnage and floor-to-floor height.

4.8.8 Concluding remarks

Although the analysis presented herein is based on certain simplifying assumptions, it is believed that the results do provide sufficiently accurate information for determining the optimum location of belt trusses in high-rise structures. Significant reductions in wind drift can be obtained by judiciously selecting the locations. Furthermore, since solutions very nearly equal to the optimum solution are obtained for various combinations of truss locations, it should be relatively easy to choose a combination that satisfies simultaneously the structural, mechanical, and architectural requirements.

4.9 Framed Tube System

4.9.1 Introduction

In its simplest terms the tube design can be defined as a structural system that prompts the building to behave as an equivalent hollow tube. At present four of the five world's tallest buildings are tubular systems. They are the 110-story Sears Tower, the 100-story John Hancock Building, and the 83-story Standard Oil Building, all in Chicago, and the 110-story World Trade Center towers in New York. The earliest application of the tubular concept is credited to the late Dr. Fazlur Khan of the architectural engineering firm of Skidmore, Owings & Merrill, who first introduced the system in a 43-story apartment building in Chicago. Tubular systems are so efficient that in most cases the amount of structural material used is comparable to that used in conventionally framed buildings half the size. Their development is the result of the continuing quest by the structural engineer for the most economical and yet safe and serviceable system for the design of high-rise buildings. Until the evolution of the tube, which has become the workhorse of the lateral system in tall buildings, most high rises were designed as frames consisting of vertical columns usually arranged on an uncompromising grid pattern in two perpendicular directions, with beams and girders spanning between the columns. Lateral loads were resisted by various girder-to-column connections, supplemented if required by vertical shear walls or trusses located within the service core of the building, or by various types of knee braces. Further improvement in the structural economy

was achieved by engaging the exterior frames with core trusses by tying the two systems through belt and outrigger trusses. The belt trusses, as the name implies, encircled the building perimeter, and the outriggers, strategically located at various levels, forced the participation of exterior columns in resisting the lateral loads. The resulting partial tubular behavior extended the range of application of the frame and core truss systems, but the radical departure in structural action occurred only when the structure on the perimeter was modified to behave as a three-dimensional cantilever. This concept led to the exploitation of the maximum plan dimensions, greatly enhancing the efficiency of the structural systems.

The introduction of the tubular system for resisting lateral loads has brought about a revolution in the design of high-rise buildings. All recent high-rise buildings in excess of 50 to 60 stories employ the tubular concept in one form or another. In essence the system strives to create a rigid wall-like structure around the building exterior. In a framed tube this is achieved by a closely spaced column and deep spandrel arrangement placed around the entire perimeter of the building. Because the entire lateral load is resisted by the perimeter frame, the interior floor plan is kept relatively free of core bracing and large columns, thus increasing the net leasable area for the building. As a trade-off, views from the interior of the building are somewhat limited by the presence of large exterior columns. Maximum efficiency for lateral strength and stiffness using the exterior wall alone as the wind-resisting element is achieved by making the entire building act as a hollow tube cantilevering out of the ground. The structure can then be thought of as a cantilever tube with holes punched for windows.

The necessary requirement to create a wall-like structure is columns placed on the exterior relatively close to each other and to use deep spandrel beams to tie the columns together. The structural optimization reduces to examining different column spacings and member proportions. In practice the tubular behavior is achieved by placing columns 5 to 10 ft (1.52 to 3.05 m) to as much as 15 ft (4.57 m) apart, with spandrel depth varying from 3 to 5 ft (0.90 to 1.52 m).

The tube system can be constructed of reinforced concrete, structural steel, or a combination of the two, termed composite construction, in various degrees. The tube has become the workhorse of the high-rise construction system because it minimizes the structural premium for lateral strength and stiffness, simultaneously accommodating recent trends in architectural forms.

The method of achieving the tubular behavior by using columns on close centers connected by a deep spandrel is by far the most used system because rectangular windows can be accommodated in this

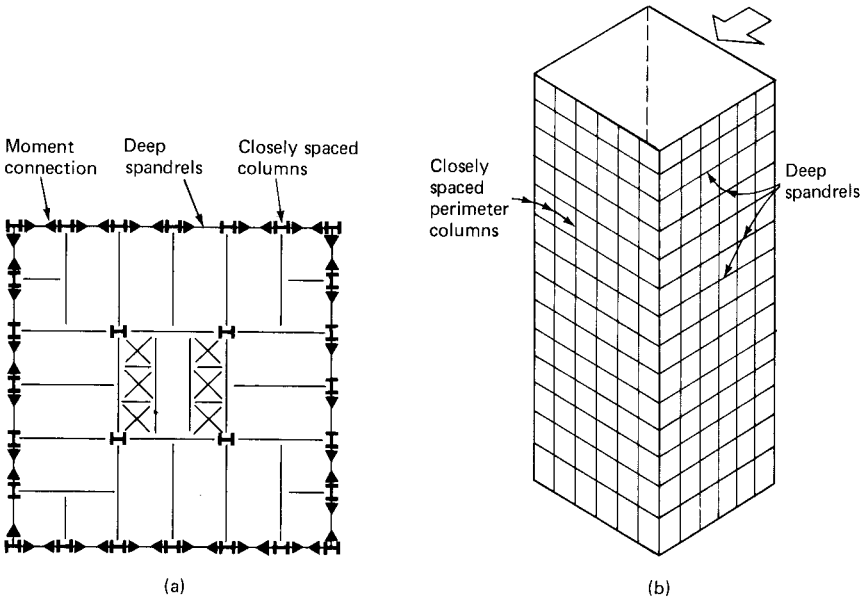

Figure 4.36 Framed tube building. (*a*) Schematic plan; (*b*) isometric view.

design. A somewhat different approach that permits larger spacing of columns is called the braced tube concept. It sports diagonal or K-type bracing on the periphery of the building.

Another version of the braced tube is the method of infilling window penetrations in a systematic pattern to achieve the same effect as diagonal or K-type bracing. Yet another is to use two or more tubes tied together to form a bundled tube. Lastly, the idea of an interior braced tube presents yet another alternate to achieve tubular action. In this section a description of the framed tube system is undertaken; other systems are explained in later sections.

4.9.2 Framed tube behavior

To understand the behavior of a framed tube, consider a square-shaped 50-story building as shown in Fig. 4.36 consisting of closely spaced exterior columns. Assuming that the interior columns are designed for gravity loading only, their contribution to lateral load resistance is negligible. The floor system, as in other types of lateral bracing systems, is considered as a rigid diaphragm and is assumed to distribute the wind load to various elements according to their stiffness. Its contribution to lateral resistance in terms of its out-of-plane action is considered negligible. The system resisting the lateral load thus comprises only the perimeter columns and moment-connected

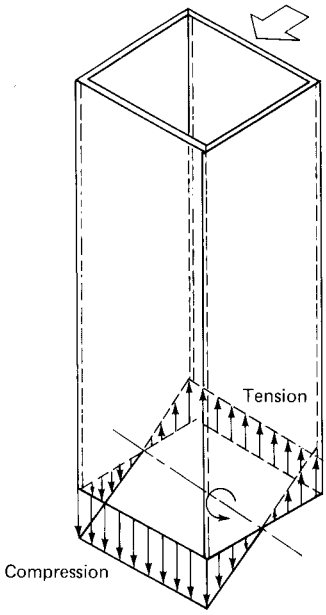

Figure 4.37 Axial stress distribution in square hollow tube.

spandrel beams. In a well-proportioned tube, the primary resistance to lateral load is provided by the overall bending of the tube, which introduces tensile and compressive forces in the tube's windward and leeward faces. The discrete columns and spandrels on the perimeter can be considered mathematically equivalent to a continuous wall element. The mathematical model is therefore equivalent to a square hollow tube which, when subjected to lateral forces, behaves as a cantilever responding predominantly in a bending mode. The stress distribution is as shown in Fig. 4.37. From this analogy, it is easy to visualize the behavior of the tube buildings having plan forms other than square. Examples of stress distribution for rectangular, circular, and triangular shapes are shown in Fig. 4.38*a* to *c*. The discovery of tubular behavior has allowed considerable freedom for manipulating the plan form of buildings without reducing the structural efficiency. The rigorous organizations of orthogonal bay spacing required with other types of lateral bracing systems are no longer necessary. Almost overnight a new system was created which by its very nature allowed considerable latitude in the shaping of the building forms. The only discipline essential for tubular behavior is that the structure be continuous around the building exterior and be of a closed form. The efficiency of the system is directly related to the geometry of the shape, such as the overall depth-to-width ratio and the height-to-width ratio.

Figure 4.39 shows some of the free-form tubular configurations that

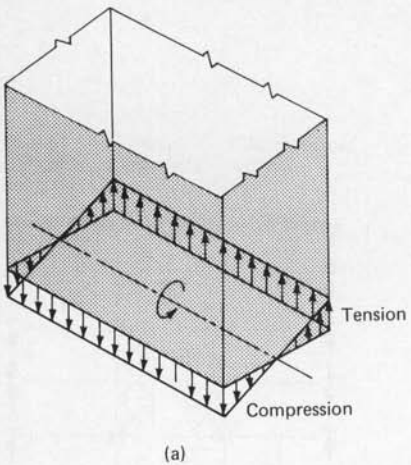

(a)

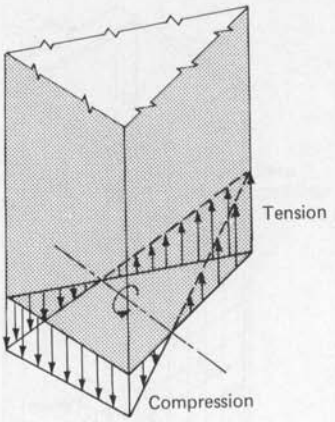

(b)

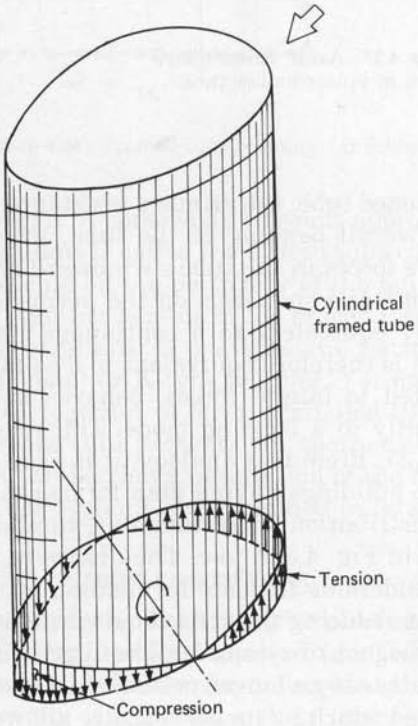

(c)

Figure 4.38 Axial stress distribution in columns resulting from lateral loads. (*a*) Rectangular tube; (*b*) triangular tube; (*c*) circular tube.

have been successfully used in the design of high rises. Although in simplistic terms the behavior of the tube can be compared to that of a hollow cantilever, in reality its response to lateral loads is in a mode that resembles the overall action of the cantilever bending due to shortening of leeward columns and elongation of windward columns

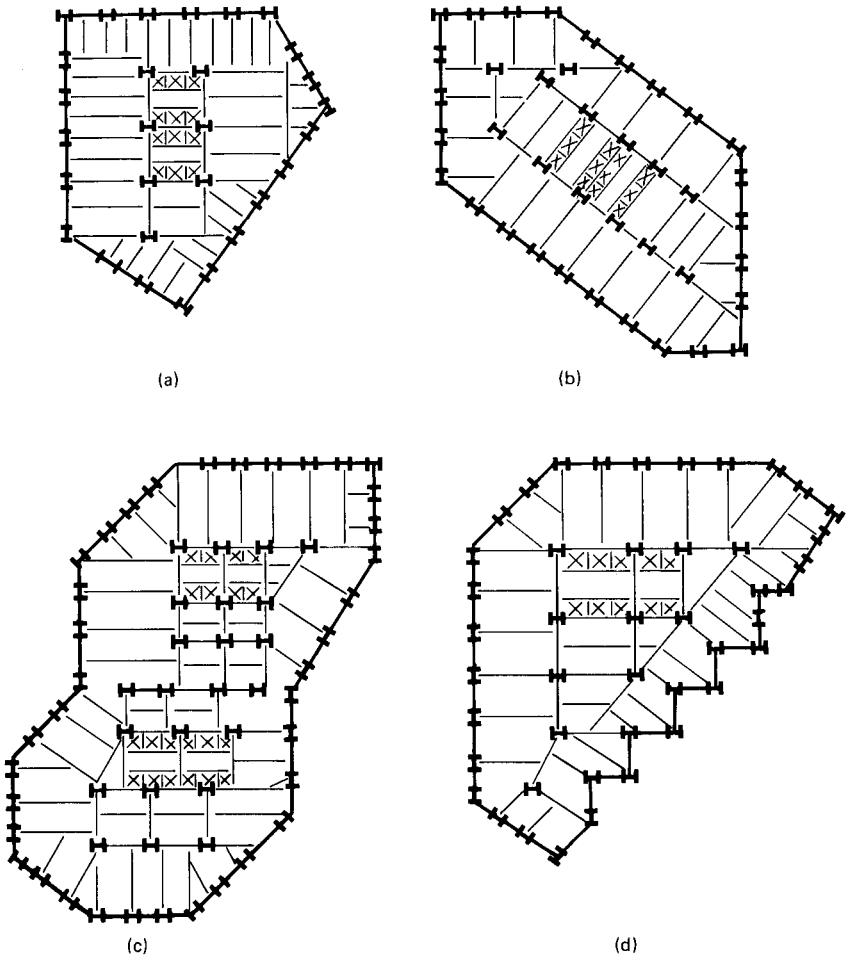

Figure 4.39 Free-form tubular configurations.

plus a shear deformation brought about by the local bending of columns and spandrels. The underlying principle behind an efficient tube system is to design a bracing system that eliminates or minimizes the shear type of deformation so that the tower as a whole bends essentially as a cantilever. Such a system results in considerable savings in material for any predetermined acceptable total wind drift. Braced frames located in the plane of exterior walls provide one of the most efficient systems for carrying lateral loads because the system essentially eliminates the shear type of deformation. A framed tube can be made to approach the efficiency of a braced tube if the material is distributed continuously around the perimeter. In this context a very efficient framed tube structure can be visualized as a tall chimney

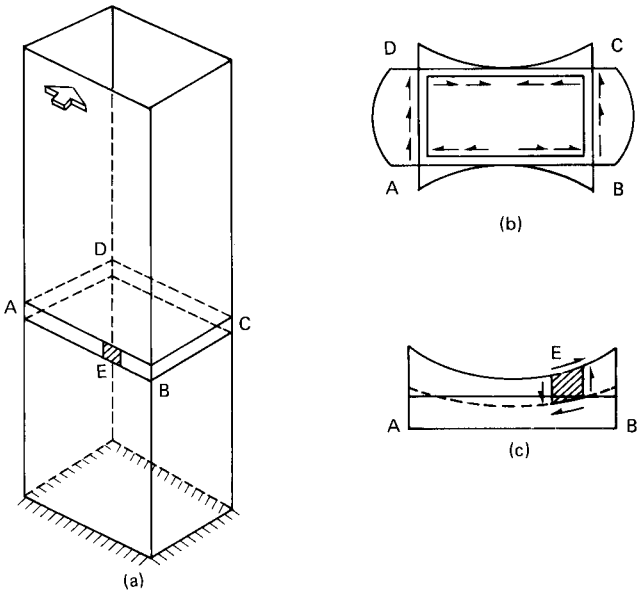

Figure 4.40 Shear lag effects in tube structures. (*a*) Cantilever tube subjected to lateral loads; (*b*) shear stress distribution; (*c*) distortion of flange element caused by shear stresses.

with punched openings for windows. In general, columns placed transverse to the wind direction function as compression and tension flanges of a box beam, while frames parallel to the wind direction function as webs.

4.9.3 Shear lag phenomenon

A perfect tube for a tall building behaves as a true cantilever, resisting all the lateral forces in the exterior walls. The closest structure to a perfect tube is one that consists of a system of perimeter walls without any discontinuities. A hollow box structure represents such a system, as shown in Fig. 4.40*a*. Consider the behavior of this structure when subjected to lateral loads. In order to fix ideas, assume the hollow box represents a 50-story steel building with a typical floor-to-floor height of 13 ft (3.94 m), giving a total height of 650 ft (198 m) for 50 stories. Assume the building is square, with a plan dimension of 110 by 110 ft (33.5 by 33.5 m). It is fairly well known to structural engineers that for a 50-story steel building the unit quantity of structural steel, including that required for gravity, is in the range of 22 to 24 psf (1053 to 1149 Pa) of the gross area of the building. Conservatively, assume for the example building shown in Fig. 4.40 that 24 psf (1149 Pa) of structural steel is available for the lateral bracing of the building. The most

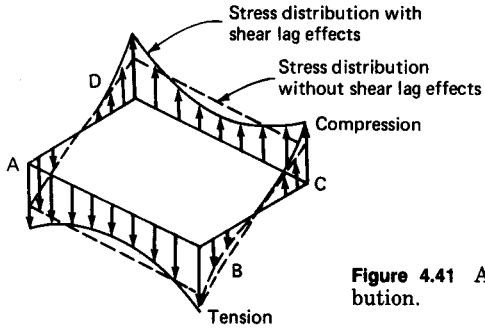

Figure 4.41 Axial stress distribution.

efficient manner of using this material with regard to lateral loads is to utilize it as a bearing wall located on the periphery of the building. It can be shown by simple calculations that the equivalent thickness of the steel bearing wall works out to 15 in.

Total steel available for bracing

$$= 24 \times 110 \times 110 \times 50 = 14{,}520{,}000 \text{ lb } (64{,}585 \text{ kN})$$

Area of perimeter wall

$$= 4 \times 110 \times 650 = 286{,}000 \text{ ft}^2 \ (26{,}569 \text{ m}^2)$$

Equivalent thickness of wall

$$= 14{,}520{,}000/286{,}000 \times 3.4 = 15 \text{ in } (381 \text{ mm})$$

In comparison to the plan dimensions of the building, it is seen that the 15-in (381-mm) dimension for the wall is relatively small, giving a length-to-thickness ratio of 1:88. Because of this characteristic, the structure has a tendency to behave like a thin-walled beam. In a thin-walled beam the shear stresses and strains are much larger than those in a solid beam and often result in large shearing deformations with a significant effect on the distribution of bending stresses. Because of the resulting large shear strains, the usual assumption used in engineers' bending theory is violated. This assumption, which states that plane sections before bending remain as plane sections after bending over the entire cross section, is known as the *Bernoulli hypothesis* and forms the basis for derivation of many useful mathematical relations used in engineering mechanics. However, in thin-walled structures the large shearing strains cause the plane of the section to distort. For the hollow box structure, the element E on the flange face distorts as shown in Fig. 4.40*c*. The final outcome due to the cumulative effect of distortion of all such elements is that under lateral load, the originally flat plane of the cross section distorts as shown in Fig. 4.41. Because of these distortions, the simple stress distribution

given by the engineers' theory of bending is no longer applicable. The bending stresses are no longer proportional to the distance from the neutral axis of the section. The stress at the center of the flanges "lags" behind the stresses near the web because of the lack of shear stiffness of the wall panel. This phenomenon is known as shear lag and plays a very important role in the design of tubular high-rise structures. The bending stresses in the webs are also affected in a similar manner.

In order to better appreciate the shear lag phenomenon, let us take a closer look at our hypothetical high-rise building. In a normally proportioned steel building, the usual method of framing for gravity loads necessitates that interior columns be located in and around the core to maintain the span of floor beams in the economical range of 35 to 45 ft (10.6 to 13.64 m). The interior gravity columns and floor beams amount to about one-third of the total steel required for the building. For the example building, the effective unit quantity of steel available for the bearing wall is therefore equal to 16 psf (766 Pa), effectively reducing the equivalent thickness of the tube wall to 10 in (254 mm), with a proportional increase in the shear strain. The departure of bending stress distribution from those predicted on the basis of plane sections becomes even more severe. A high-rise building in practice has to accommodate penetrations in the exterior wall for obvious reasons. The efficiency and integrity of the bearing wall are further reduced because of these penetrations in almost direct proportion to the mass taken out of the tube walls. Several structural formulations are in vogue which strive to achieve tubular action with a minimum of shear lag effect and yet accommodate the window penetrations. One method is just to punch holes in the exterior solid walls at regular intervals. Indeed, such a concept, wherein circular penetrations are provided for windows in the exterior tube walls, has been used on a 50-story, 600-ft (183-m) office tower in Hong Kong. The exterior wall thickness of this building tapers from the base to roof from 15 to 6 in (381 to 152 mm).

4.9.4 Irregularly shaped tubes

The buildings of the 1950s and 1960s were rectangular prismatic forms. These have now evolved into nonprismatic and curvilinear shapes prompted by a change in aesthetics and the stringent requirements placed on the plan forms by leasing considerations. In many instances these shapes have been exploited to highlight the verticality of the building, bringing visual interest. The tubular system, which was the workhorse of the simple prismatic buildings of the 1960s, is adaptable to many of the new forms and responds well to the plan modulations. These continually evolving trends are variously termed

postmodernist or *neorationalist* and tend toward irregular shapes that make use of the inherent characteristics of the tube system for fulfilling the structural requirements of arbitrary building forms. Plan configurations for tall buildings therefore need not be confined to regular shapes like the first generation of high rises. Because the framed tube system achieves strength and stiffness with rigid beam-column frame action, any reasonable arrangement of plan accommodating the beam and column elements around the building periphery can be achieved without serious loss in efficiency. However, sharp changes in the plane of tubular face result in a less efficient tube action because the shear flow must pass around corners solely through axial shortening of columns.

Although it is not essential to configure the plan form of tall buildings as rectangular, square, circular, or other regular shapes, it is necessary for any free-form shape to be compact and of a closed profile to serve as an efficient tubular system. Compact plan forms can be defined in the structural sense as those shapes that possess an adequate number of column bays both in the web and in the flange portions of the tube system. This is usually achieved when the plan aspect ratio is not greater than 1.5 or so. Elongated shapes with plan aspect ratios well in excess of 1.5 may suffer three drawbacks: (1) the elongated plan shape, because of a large exposure area, acts like a large sail collecting large magnitudes of wind loads; (2) these large forces present structural design problems because the frames on the narrow faces of the building most usually are not adequate to provide the required shear resistance; (3) efficient tube action is difficult to achieve in elongated shapes because the shear lag phenomenon is more pronounced. These problems are not unique to free-form shapes and apply equally to elongated rectangular shapes.

Because of the relatively long length of the flange frame, the shear in the spandrel beam at locations away from the corner lags considerably behind its value at the web frame. Fewer flange columns participate in resisting the overturning moment, thereby decreasing the efficiency of the system considerably.

4.9.5 Tube systems with column offsets

In the quest for creating new forms motivated either by site restrictions or by a desire to shape buildings that stand out in a forest of skyscrapers, the architect often comes up with building shapes that require offsetting different portions of an otherwise regular shape. Consider, for example, the plan forms shown in Fig. 4.42. In Fig. 4.42*a* the basic geometry is obtained by offsetting two quarter circles at the center. The plan form in Fig. 4.42*b* is obtained by displacing an elongated rectangle with semicircular ends. Other similar plan shapes

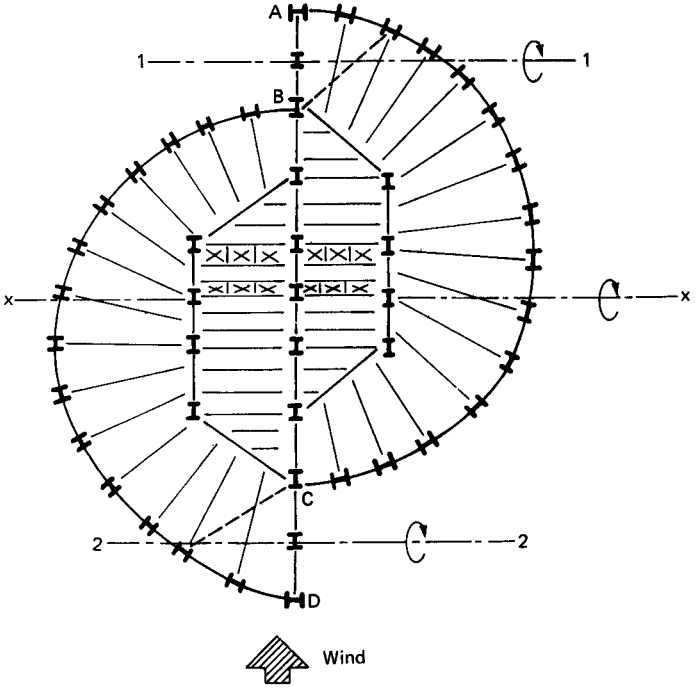

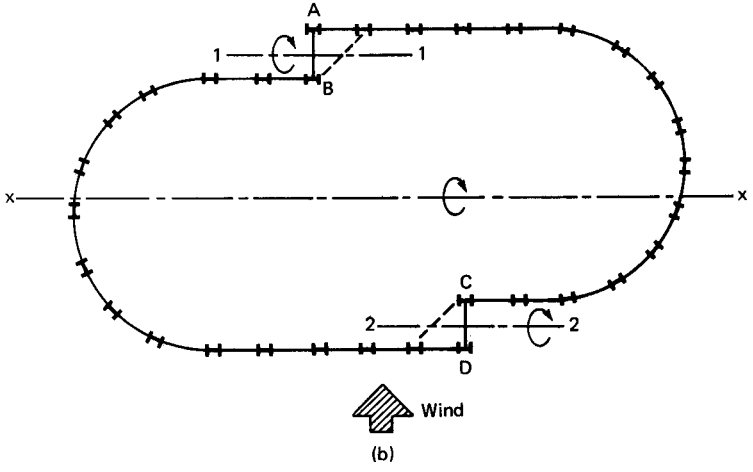

Figure 4.42 Offset tubes. (*a*) Semicircular tubes; (*b*) rectangular tube with semicircular sides.

are in vogue; the architectural motivation behind the shape is that the offsets help to emphasize the verticality of the building and, of course, allow for more corner offices. From a structural sense, these shapes can still be considered as tube forms as long as the rhythm of closely spaced columns and deep spandrel is maintained at the perimeter. However, at locations of offsets, the stresses in columns are somewhat altered by the so-called frame action between the columns at the reentrant corners. This phenomenon is similar to the stress concentration experienced by bodies at locations where the shape changes occur abruptly. The vertical stresses in the columns are made up of two distinct actions. One action results in axial stresses due to the overall bending of the tube; the second action is the local frame action between the columns at the faces of the offset. The total stress in the column at the offsets is obtained by superposing the two actions. This is explained further with respect to Fig. 4.42

To get the idea across, assume that the tube structures shown in Fig. 4.42*a* and *b* are perfect tubes and the shear lag due to spandrel and column bending and the joint rotations are negligible. Consider wind acting on the broad face producing bending about the x-x axis. Due to the wind load, columns A and B, which are on the leeward side of the tube, are subjected to compression, whereas columns C and D, which are on the windward side, are subjected to tension. Portions AB and DC of the tube are subjected to a secondary bending action about axes 1-1 and 2-2, as shown in Fig. 4.42. Columns adjacent to these portions experience additional axial stresses by virtue of the structural continuity along the building faces. Columns A and B, while bending about the axis 1-1, are subjected to compression and tension, respectively. The secondary bending, therefore, has a tendency to increase the compressive stresses in column A while decreasing the same for column B. The resulting load on column B may either be compression or tension, depending upon the geometrical layout of the tube and the relative stiffness between various elements. A similar behavior is observed along the offset face CD.

The total overturning moment is resisted by two distinct actions of the tube. The primary action is the tube action brought about by the closely spaced columns and moment-connected spandrel beams. The secondary resistance is provided by the portal frame action of the columns along the two offset faces which tend to bend about the local neutral axes 1-1 and 2-2 of frames AB and CD. The terms primary and secondary are used herein to distinguish the two actions and do not necessarily mean that one is more predominant than the other. For example, it is easy to see that the bending of columns AB and CD about axes 1-1 and 2-2 will be the domineering resistance, if we assume that these columns are connected by a stiff diagonal bracing, and that the

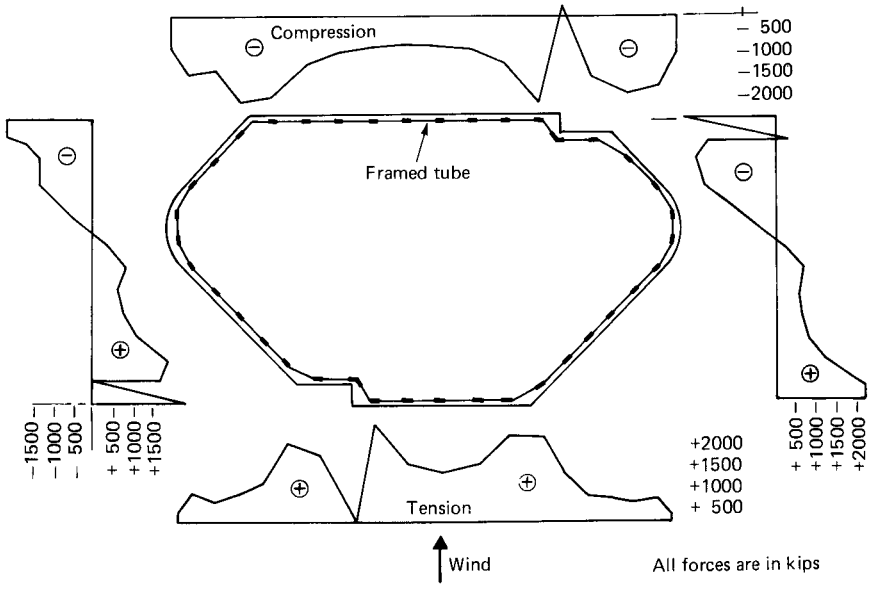

Figure 4.43 Axial force distribution.

spandrels elsewhere on the tube are relatively limber. This analytical model produces bending about axes 1-1 and 2-2 as the major resistance, while the overall bending of the tube about the axis x-x may not yield significant resistance.

Figure 4.43 shows the computed axial forces obtained on a 42-story tube building with column offsets. It can be clearly seen that the distribution of stresses along the windward and leeward columns is a combination of the two actions mentioned earlier. A method of minimizing the secondary bending would be to achieve a gradual transition in the layout of the structural columns and spandrels at the offset faces. Instead of rigidly following the architectural envelope with a rhythmic structural layout at the periphery of the building, it may be advantageous to eliminate columns A and D and continue the tube action through interior girders as shown schematically by dotted lines in Fig. 4.43. This system gives an opportunity to eliminate some corner columns, making the floor plan more desirable from the point of view of space planning.

4.9.6 Column transfers in tube buildings

The tube design, with its characteristic closely spaced columns on the exterior, although very efficient from the structural point of view, presents certain architectural problems at the base. For example,

especially with the current architectural trend of creating identity to the building at the street level, it is common to have grand entrances to the building. Closely spaced frame tubes, which typically have columns from 10 to 15 ft (3.05 to 4.58 m) on center, need a structural solution that terminates some columns and yet does not penalize the structural system as a whole. Another instance that commonly requires elimination of ground-level columns is the requirement of providing loading docks to the building. Wide-open spaces at ground level are often desired by the owners and developers, especially when the lower levels of the building are designed as retail spaces. Functionally open space at ground level below the building may be required for reasons such as car parking. Below-ground construction of high rises normally extends to the limits of the property lines, and when this whole area is used for parking it may require elimination of at least some of the building columns.

There exist a number of solutions for transfer of columns at ground level, and chief among them are the transfer girder and transfer truss techniques. Depending upon the desired architectural treatment, other methods such as arch action may also be workable alternatives. Although in comparison to a truss, steel plate girders require more steel, they have the advantage of providing a stiffer system within specified depth and deflection limits. In a framed tube with closely spaced columns and deep spandrels, removal of certain perimeter columns can be accomplished with very little structural premium by invoking the vierendeel truss action of the whole facade frame. It may be necessary to use temporary supports at the base of truncated columns until such time as a sufficient number of spandrels are erected in the facade to carry the dead load and construction loads without overstressing the members. A schematic view of the shoring that can be employed in a medium high rise of about 30 stories is shown in Fig. 4.44. The shoring consists of two steel columns that are braced horizontally and diagonally. Steel plates are used at the base of temporary shoring forms which rest on a sand bed contained in a steel enclosure. Shims are used between the bottoms of girders and tops of temporary columns to compensate for any irregularities or settling of sand. When the steel frame is complete, sand is released from the boxes to load the transfer girder. If shoring is provided at more than one location, the rate of loading on the girder can be controlled by manipulating the quantity of sand removed from the steel box.

In cases where the transfer is too severe and requires removal of a large number of columns, one- or two-story-deep transfer trusses may provide the optimum solution. This solution requires active coordination between the architect and engineer because diagonals on the exterior may present some architectural problems.

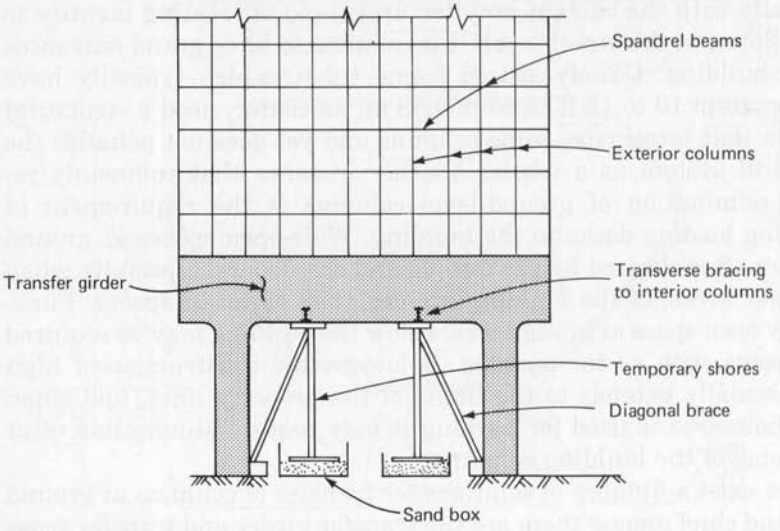

Figure 4.44 Temporary shoring of transfer girder.

Steel girders and vierendeel or diagonalized perimeter trusses provide a method of collecting axial gravity and wind loads from closely spaced columns and channeling them to a few selected columns below the transfer girder. However, removal of columns, unless confined to only a few members, often presents structural problems in terms of resistance to wind shear, requiring introduction of additional vertical elements between the foundation and the transfer level. Normally this is achieved within the building core by using braced frames or reinforced concrete shear walls. Sometimes the shear resistance of concrete walls is supplemented by steel plates designed to act compositely with the walls through welded shear studs. A heavy diaphragm is required at the transfer level to deliver the shear forces from the tube columns to the core walls. Normally, below ground level it is possible to carry the large shear forces to the basement walls by transferring the load back from the core walls to the basement walls, again through the diaphragm action of the floor.

For purposes of illustration, consider the tube structure shown in Fig. 4.45, consisting of closely spaced columns and deep spandrels. Assume that for architectural reasons it is required to eliminate all columns below the second floor except four columns located at the center of each face. The overturning moment due to lateral loads can be replaced by a system of axial compressive and tensile forces in the tube columns as shown in Fig. 4.46. Normally it is uneconomical to transfer the total wind shear to just a few columns below the transfer level. Shear walls or braced frames located around stairs and elevators

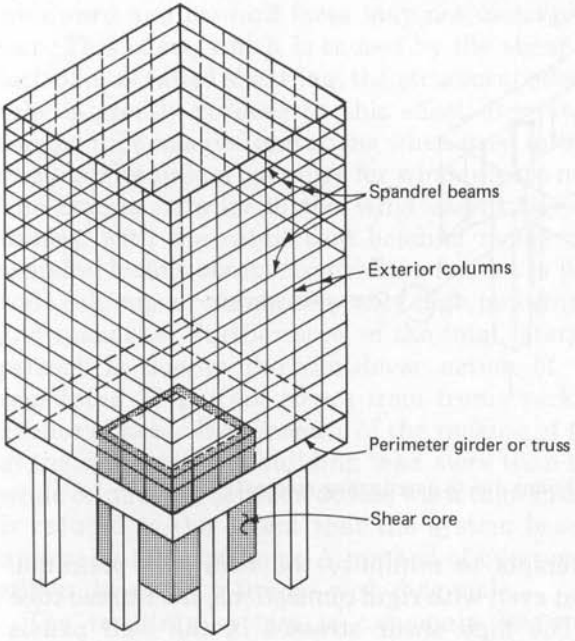

Figure 4.45 Column transfer in tube structures.

provide an excellent system for resisting shear forces. In Fig. 4.47, the shear force at the transfer level is distributed between the four columns and the core located at the center of the building. Note that the interior core terminates at the transfer level and, therefore, is not subjected to bending moment at this level. However, it collects large amounts of shear because, in comparison to columns, its shear resistance is typically very large. A load path is thus required for transferring the large magnitude of shear at the transfer level. In a steel-framed building this is normally achieved by providing diagonal bracing in the plane of the transfer floor. In concrete buildings the solution normally requires additional concrete and reinforcement in the slab system.

4.10 Trussed Tube System

The stiffness and strength of the framed tube reside in the rigidity of the connections between closely spaced columns and steel spandrels that require welded or high-strength bolted connections at the joints. The fabrication and erection costs of these tight joints may present a drawback to its use, although the concept of shop-fabricated "tree sections" consisting of two- or three-story-high column sections and

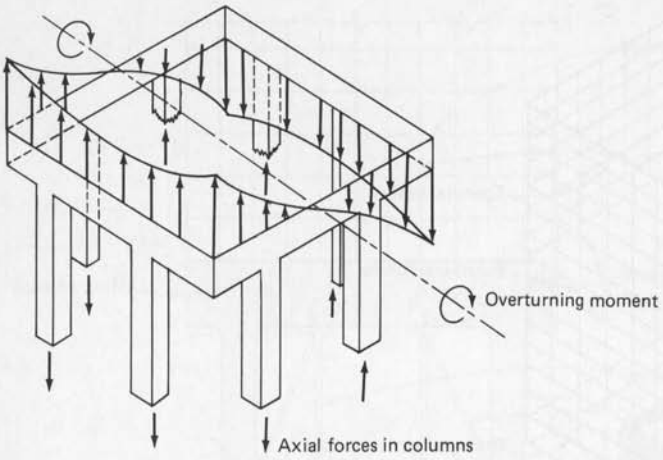

Figure 4.46 Axial forces in columns due to overturning moment.

bay-wide spandrels attempts to minimize the field cost premium. Another drawback is that even with rigid connections, the framed tube is somewhat flexible. The high shear stresses in the wall panels parallel to the wind cannot be transferred effectively around the corners of the tube to the sides perpendicular to the wind. For maximum efficiency, the tube should respond to lateral loads with the purity of a cantilever with compression and tension forces spread uniformly across the windward and leeward faces. The framed tube, however, behaves like a thin-walled tube with openings provided for the windows. The shear forces tend to diminish as they travel around the corners, with the result that the columns in the middle of the

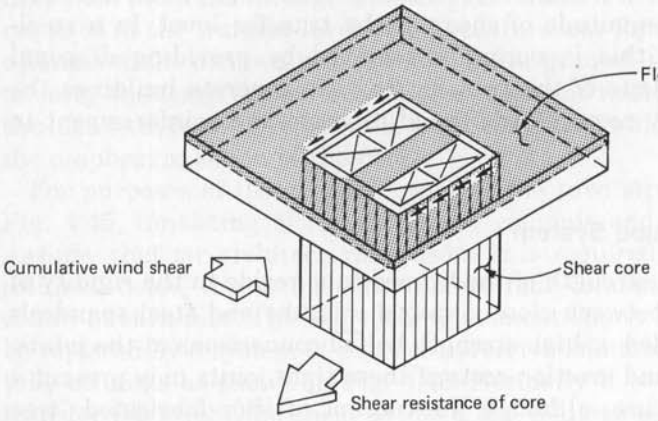

Figure 4.47 Shear transfer through floor diaphragm.

windward and leeward faces may not undergo compression and tension. This effect, which is caused by the shear stiffness or rather the lack of it, is called shear lag; the structural effectiveness of the framed tube is greatly reduced by this effect. Because of these reasons the framed tube has its limitations when used in buildings taller than 50 or 60 stories unless openings for windows are made relatively narrow. The frames parallel to the wind essentially act as multibay rigid frames, with the result that bending moments in the columns and spandrel beams become controlling factors in design, requiring either wide columns or an unacceptably high percentage of steel in columns and spandrels. Furthermore, of the total lateral sway, only about 25 percent is due to the cantilever action of the framed tube; the remaining 75 percent comes from frame racking as a direct consequence of shear lag. Because of the racking of the frame, the columns at the corners of the building take more than their share of the load, while columns in between do less work than in an ideal tube. Efficiency is reduced to the extent that the system becomes uneconomical for unusually tall buildings. A method of overcoming this problem is to stiffen the exterior frames with diagonals.

The resulting system is commonly known as column diagonal trussed tube. The most effective trussed tube action can be obtained by replacing the vertical columns with closely spaced diagonals in both directions. However, this creates problems in terms of window wall details because of the large number of joints between the diagonals. Moreover, the diagonals are less efficient than the vertical columns in transmitting gravity loads to the ground. The so-called column diagonal or braced tube presents an efficient compromise. In this system the exterior columns are spaced apart but are made to act together as a tube by the widely spaced diagonals. At levels where the diagonals meet at corners of the building, it is necessary to provide a large tie to limit the horizontal stretching of the floors and to make the diagonals function more efficiently as inclined columns. The shear is now primarily absorbed by the diagonals and not by the spandrels. The diagonals carry the lateral forces in predominantly axial action, reducing shear lag and thus providing for nearly pure cantilever behavior. The diagonals, together with the spandrel beam, create a wall-like rigidity against lateral loads.

An example of a trussed tube structural system is shown in Fig. 4.48*a*, a 56-story office building in downtown Dallas. Designed by structural engineers Ellisor & Tanner, Inc., the building consists of 1.9 million square feet (174,437 m^2) of office space and rises to a height of 710 ft (216 m) above grade. Exterior columns are spaced at 25 ft (7.62 m) on center with a floor-to-floor height of 12 ft, 6 in (3.81 m) to facilitate intersection of diagonals with columns and spandrels. There

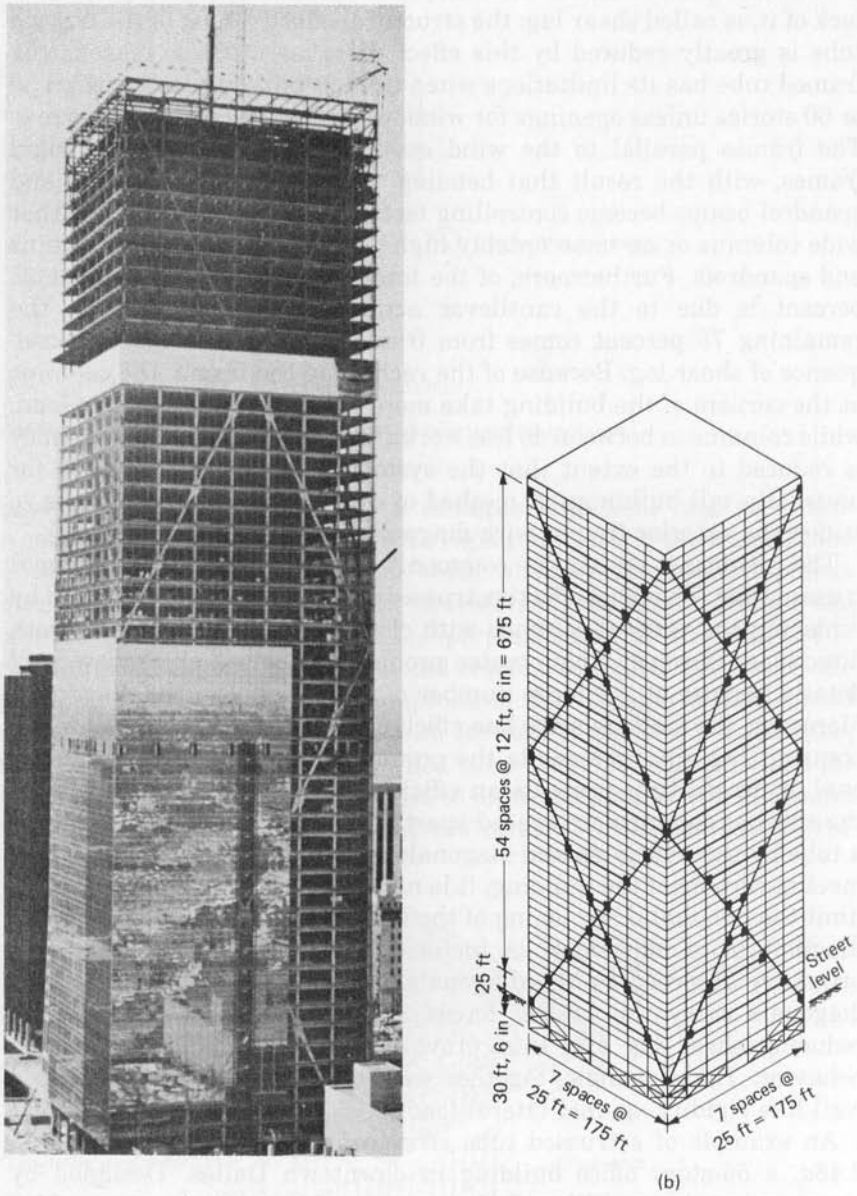

Figure 4.48 (*a*) First International Plaza, a 56-story trussed tube office building (Architects, Hellmuth, Obata, Kassabaum, Inc.; structural engineers, Ellisor & Tanner, Inc.); (*b*) schematic bracing of the building.

are two X braces, each 28 stories tall, on each of the four sides, as shown in Fig. 4.48*b*. The diagonal bracing, in addition to carrying the wind loads, helps to distribute gravity loads along the exterior columns on each side of the building. The vertical bracing is located within the glass line to minimize problems associated with fireproofing the exterior structure and the effects of temperature on exposed steel. All members in the primary exterior framing—beams, columns, and diagonals—were fabricated from high-strength W14 shapes except for a few near the bottom which were built-up shapes. W14 shapes were selected because of the wide range of available sections and because all shapes had the same nominal inside dimension between flanges, thus facilitating the connection details. The gusset plates used to connect the diagonals, columns, and beams are approximately 10 ft (3.0 m) wide and 12 ft (3.65 m) tall. The diagonals, which were fabricated four stories in length, were field-welded with full-penetration welds at one end and were high-strength-bolted through splice plates at the other end. The welded connection at one end reduced gusset and splice material, while the bolted connection at the other end provided the necessary tolerances for erection. Corner gusset assemblies were required where diagonal bracing met at the corners of the building. These were fabricated from four plates, two in each of the two directions. The four plates were joined by electroslag welds and were stress-relieved after fabrication.

Perhaps the most notable example of this structural system is the John Hancock Center in Chicago (Fig. 4.49) designed by the Chicago office of Skidmore, Owings & Merrill. The building is 100 stories with a rectangular plan that tapers from the ground level to the top. The diagonals are placed at 45° angles to each other, forming enormous X braces on each side. The diagonals serve multiple functions, acting as inclined columns to resist some of the gravity load, absorbing most of the wind shear, and stiffening the tube so that it mimics the behavior of a solid tube. This unique design, combined with the use of high-strength steel, enabled the engineers to achieve a 100-story building with only 29.7 psf (1422 Pa) of steel as compared to 42.2 psf (2020.5 Pa) for the 102-story Empire State Building. Many variations of this basic scheme, as given in the following two examples, have been used to date to provide wind bracing for tall buildings.

1. For the CitiCorp Center in New York, structural engineer William J. LeMessurier incorporated giant triangular trusses into the exterior facade of the building. These facade trusses collect about half the gravity loads and resist the entire wind loads on the building. The loads collected on the facade are channeled into four massive columns at the base. Because the shear resistance of the giant trusses is no

Figure 4.49 The John Hancock Tower in Chicago is an outstanding example of a steel building with exterior braced tube.

longer available below the transfer level, a central core is designed to resist wind shears. Diagonal bracing is employed in the plane of the transfer floor to achieve shear load transmission from the tubular frame to the core. The structural system is shown schematically in Fig. 4.50.

2. Recently, structural engineer Leslie E. Robertson devised a megaspace frame structural system to frame Asia's tallest building, the Bank of China Tower in Hong Kong. The prism-shaped building, designed by the architectural firm of I. M. Pei and Partners, rises to a height of 76 stories. A brief description of the structural system, which is condensed from an article in the August, 1986, *ASCE Civil Engineering Journal*, follows. The building is divided into four quadrants in plan and rises out of a granite-clad base. Each quadrant rises to a different height, and only one out of the four reaches the full 76 stories. The bracing system provided for the tower is at once an ingenious and economic solution and uses a system of space trusses to resist both lateral loads and almost the entire weight of the building. From the top quadrant down, the gravity load is systematically transferred out to the building corner columns. Transverse trusses wrap around the building at various levels and help in transferring the load to the corner columns. At the 25th floor, the column at the center of four quadrants is transferred to the four corners by the space truss system, providing an uninterrupted 158-ft (48-m) clear span for the banking lobby. To achieve continuity between different truss members of the

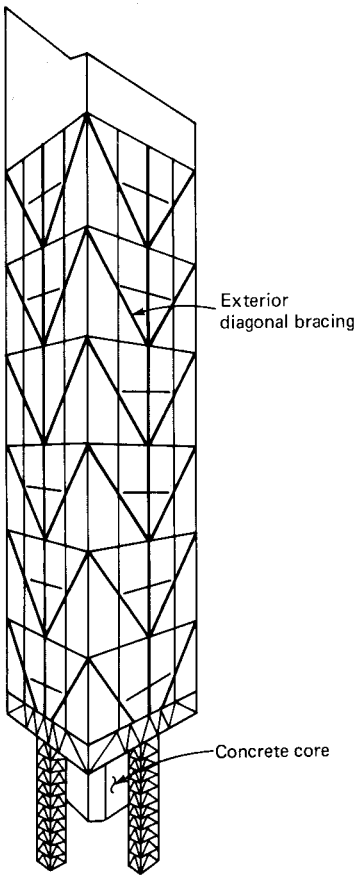

Figure 4.50 Schematic framing of CitiCorp Center, New York (Structural engineers, Le Messurier Associates).

space frame, instead of complex three-dimensional connections requiring expensive weldments, the members are made to act as a single unit by encasing them in steel-reinforced concrete columns. The concrete encasement surrounding the steel columns acts as a shear transfer mechanism and also counteracts eccentricities in the truss system. The lateral loads are thus carried down to the fourth story through the space truss system and corner columns. At the fourth floor, shear forces are transferred to a system of interior composite core walls through $\frac{1}{2}$-in (12-mm) thick steel plate diaphragms acting compositely with the concrete slab. Although much of the shear force collected by the interior core walls is transferred to the 3-ft (0.9-m) thick slurry walls at the perimeter, the core walls are continued to the foundation to serve the dual function of resisting shear and of forming walls for the bank vault. The corner columns, which continue to the foundation, resist the overturning moments. The foundation for the building

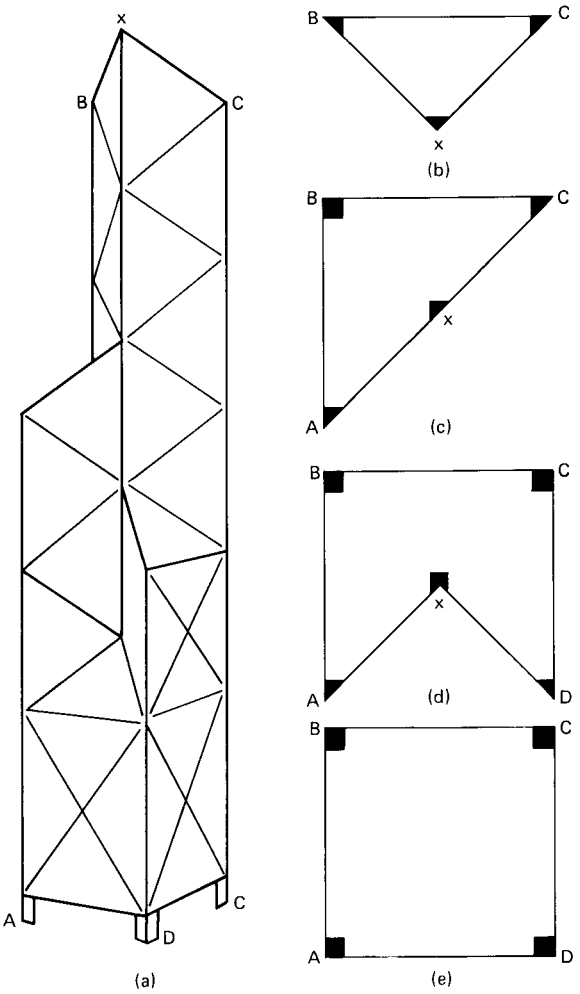

Figure 4.51 Schematic framing of Bank of China Tower (Structural engineers, Robertson & Associates, P.C.). (*a*) Elevation; (*b–e*) floor plans at various heights.

consists of caissons at bedrock. Some of the caissons are as large as 30 ft (9.1 m) in diameter. A schematic representation of floor plans, together with the bracing concept, is shown in Fig. 4.51.

4.11 Cellular Tube Structures

A cellular or bundled tube building can be thought of as a structure resulting from a conglomeration of two or more independent tube

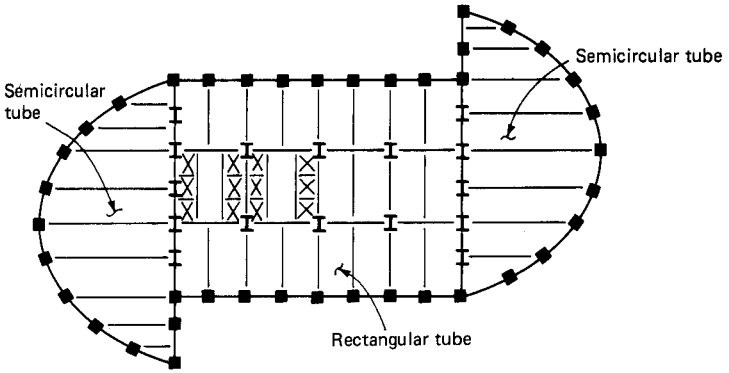

Figure 4.52 Bundled tube.

structures made to act in concert with each other. This union between adjacent tubes can be achieved by bundling the tubes together as shown in Fig. 4.52. Because the bundled tube design is derived from the layout of individual tubes, it is possible to achieve a variety of floor configurations by simply terminating a tube at any desired level. In the simple case of two tubes, the corresponding plan shapes are as shown schematically in Fig. 4.53. Figure 4.54 shows the diversity in plan forms that can be achieved in a three-cell bundled tube. In order for a structure to behave as a bundled tube it is not necessary that the adjacent tubes be of similar shape. A bundled tube consisting of a square and a triangular cell would respond, in a conceptual sense, in a manner similar to two square or two triangular cells.

A distinct advantage of the modular or bundled tube concept is that the individual tubes can be assembled in any configuration and terminated at any level without loss of structural integrity. This feature enables the architect to create setbacks with a variety of shapes and sizes. The disadvantage, however, is that the floors are divided into tight cells by a series of columns that run across the building width.

The structural principle behind the modular concept is that the interior rows of columns and spandrels act as internal webs of a huge cantilever beam in resisting shear forces, thus minimizing the shear lag effect. Without the beneficial effect of these internal diaphragms, most of the exterior columns toward the center of the building will be of little use in resisting the overturning moment. Because of their relative distance from the web frames, even with very stiff spandrels shear lag effects in the exterior columns are quite pronounced. The modular system can be seen as an extension of the perimeter tubular system with stiffened interior frames in both directions. The interior frames of the cell parallel to the wind resist shear forces, in a manner

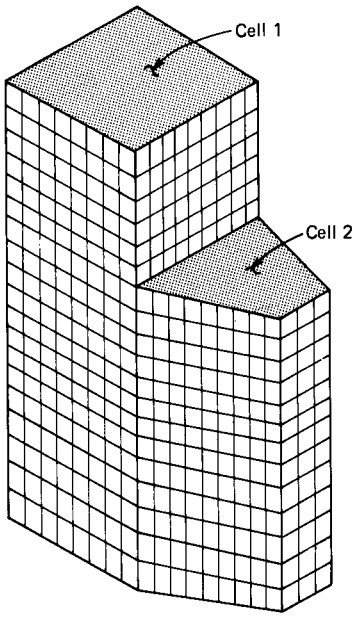

Figure 4.53 Two-celled tube.

similar to the two end frames generating peak axial stresses at points of intersection of the web frames with the flange frames. The internal diaphragms tend to distribute the axial stresses equally along the flange frames. Shear lag effects may be still present, but the deviation from the ideal tube behavior is considerably less than if there were no internal frames. Each tube acts independently, and the shear lag diagram drapes from a peak at the corners to lesser and lesser heights at the center of each tube as shown in Fig. 4.55.

In addition to reducing the shear lag effect, the interior frames contribute to the bending strength of the system. Because more frames are provided for resisting the lateral loads, the column spacings can be increased while maintaining the efficiency of the structure. The ultimate structure with maximum efficiency for lateral loads would appear to be bundled tube with diagonals in the walls.

The bundled tube system has been instrumental in making possible irregular building forms which may be required by site constraints and building massing considerations. It ties together an irregularly shaped building and offers considerable freedom in varying the shape of the building along the height. The decrease in shear lag effect improves the bending behavior and torsion and warping behavior of the building. In general, the cellular form has an inherent advantage in resisting torsional excitations over a single perimeter-framed tube.

An outstanding example of the bundled tube concept is seen in the

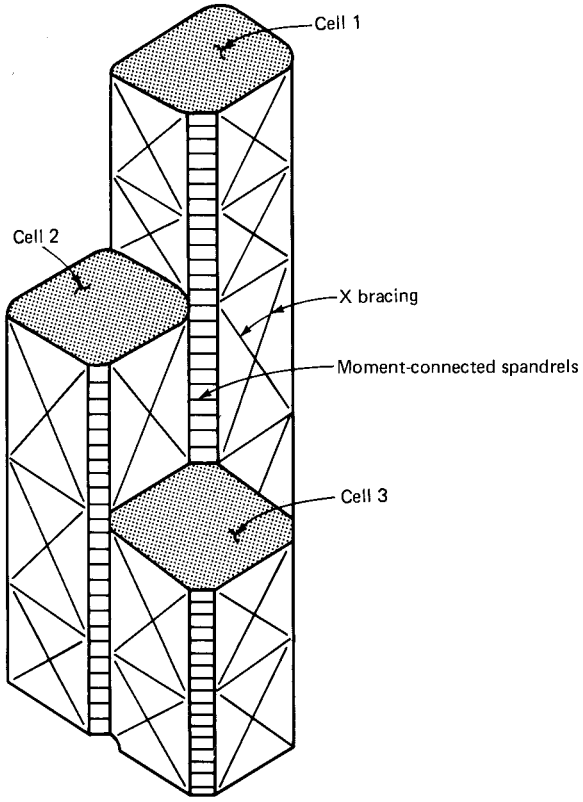

Figure 4.54 Three-celled tube.

1454-ft (443.5-m) Sears Tower, the world's tallest building. The structural solution was to organize the building plan as a series of square modules. The interior columns in the square module add shear strength at intermediate points, minimizing the shear lag effect. The structure thus tends to behave with the purity of a single cantilever in resisting lateral loads. The Sears Tower covers a base of 225 by 225 ft (68.6 by 68.6 m), made up of an assemblage of nine modules, each 75 ft square (22.9 m) with columns 15 ft (4.57 m) apart. The tubes terminate at different heights as shown in Fig. 4.56.

The nine bundled tubes of the Sears Tower are arranged in a 3 by 3 matrix at the base. Two corner tubes drop off at the 15th floor, two more at the 66th floor. Out of the five remaining tubes, three terminate at the 90th floor and only two rise to the full 1454 ft (443.5 m). The arrangement, in addition to providing a variety of floor plans, has the structural advantage of reducing mass in the upper floors, a significant advantage in earthquake-prone regions. Also, wind sway is reduced by

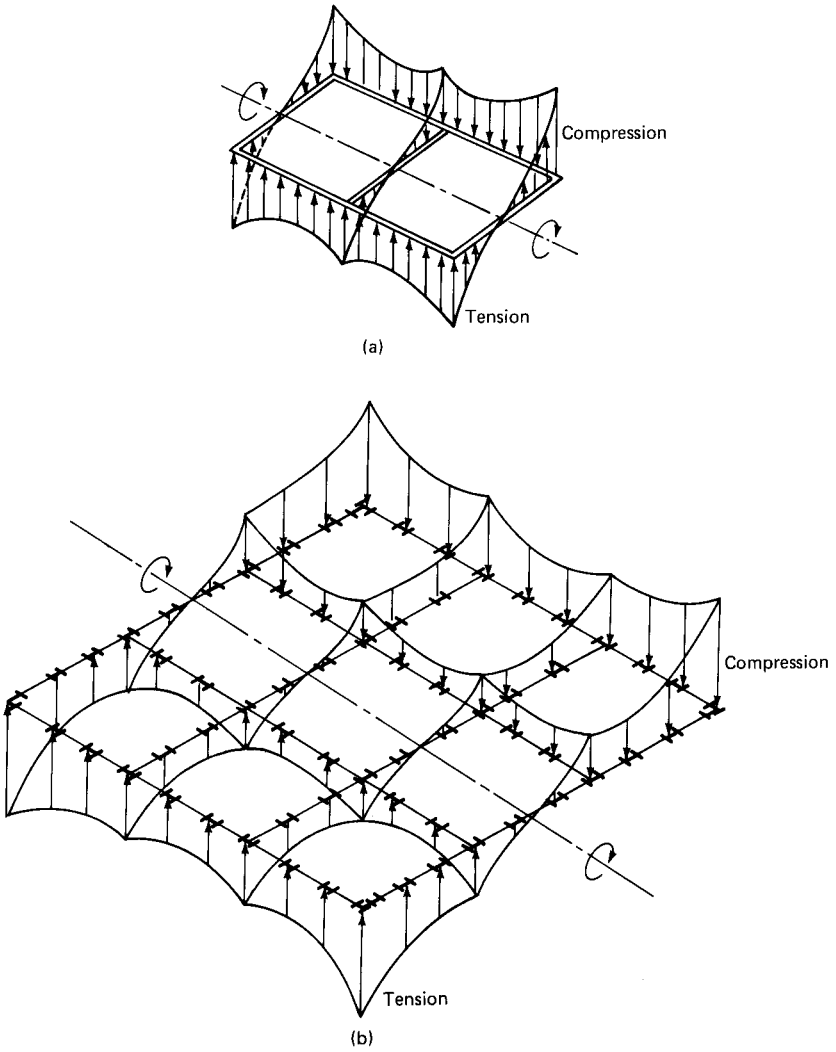

Figure 4.55 Shear lag in cellular tubes. (*a*) Two-celled tube; (*b*) nine-celled tube.

virtue of less exposed surface areas. The undulations created at the top of the building have another beneficial effect of reducing vortex shedding because of turbulence created at the upper levels.

To achieve the structural action of a bundled tube it is not necessary to have closely spaced columns dividing the building plan into secondary cells. In many buildings it is possible to achieve an equivalent action, though not as efficient as that with closely spaced columns, by inserting a minimum number of columns between the windward and leeward faces of the tube to reduce the shear lag. An outstanding

example of this application can be seen in the 695-ft (211.83-m) office building called Four Allen Center in downtown Houston. In plan, the building is an elongated rectangle with semicircular ends with overall dimensions of approximately 110 by 260 ft (33.5 by 79.25 m) as shown in Fig. 4.56*b* and *c*. The tower is remarkably slender, with a height-to-width ratio in excess of 6.0. The elongated shape of the tower creates a striking knife-edged silhouette on the skyline. Although the columns are spaced at a reasonably close interval of 15 ft (4.57 m) along the entire perimeter, which is normally sufficient to achieve a framed tube solution for a building of this height, it was clear from the analysis that a pure framed tube was impractical because of the high plan-aspect ratio. The extent of shear lag was too severe to allow a single perimeter tube solution to be economical. Structural engineers Ellisor & Tanner devised a modified bundled tube by introducing interior cross frames, effectively subdividing the plan into a four-celled grid as shown in Fig. 4.56*b*. These cross frames were formed by horizontal tree beams interacting with diagonal trusses. A tree-column element consists of short vertical stub columns attached to the girders at middistance between the exterior and core columns. This in effect creates a Vierendeel truss action between the core and exterior columns, greatly increasing the shear stiffness of the system. Connections between the stub columns are designed to carry no axial forces and therefore the columns are not required to go all the way to the foundation. A schematic elevation of the framing is shown in Fig. 4.56*c*.

4.12 Ultimate High-Efficiency Structures

It is interesting to recall that there have been no quantum leaps in the height of tall buildings that are being built today as compared to the buildings built during the 1930s and 1940s. For example, the Empire State Building scraped the sky at 1,250 ft (381 m), which is not a small feat by any stretch of the imagination. The success of this awe-inspiring building and other similar buildings of the era is credited to the holding-down power of the heavy exterior stone cladding and the masonry partitions that were in vogue during that period. Modern high-rise technology has largely replaced the heavy cladding and interior masonry systems with relatively lightweight counterparts. The holding-down power of these systems is no longer present in modern construction. Let us examine how we can employ the relatively lightweight materials to help in providing resistance to the lateral loads. The tube system, with its characteristic deployment of the columns at the building perimeter, certainly provides the much-required separation between the windward and leeward faces of the

(a)

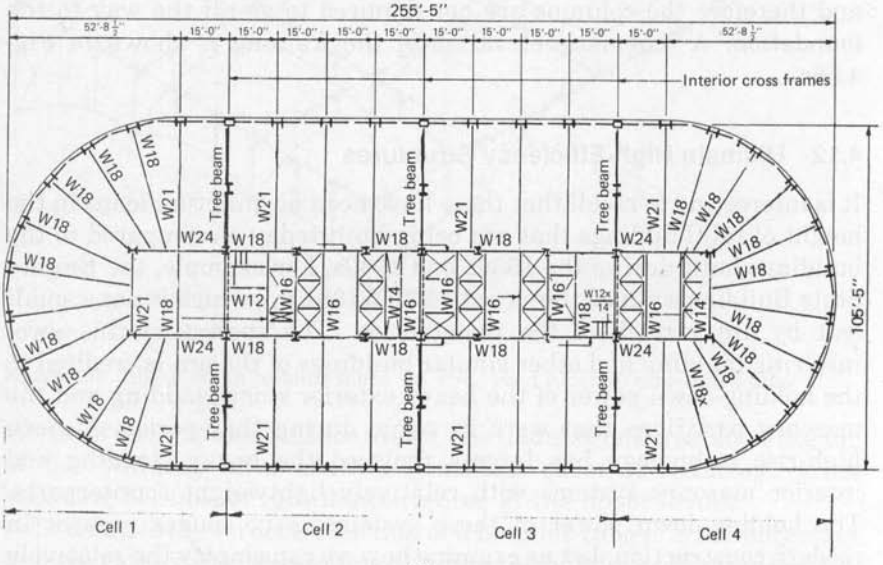

(b)

Figure 4.56 (*a*) Sears Tower, a 110-story office building in Chicago (Architects and engineers, Skidmore, Owings & Merrill, Chicago); (*b*) Four Allen Center building, Houston, Texas (Architects, Lloyd Jones and Fillpot; engineers, Ellisor & Tanner, Inc.).

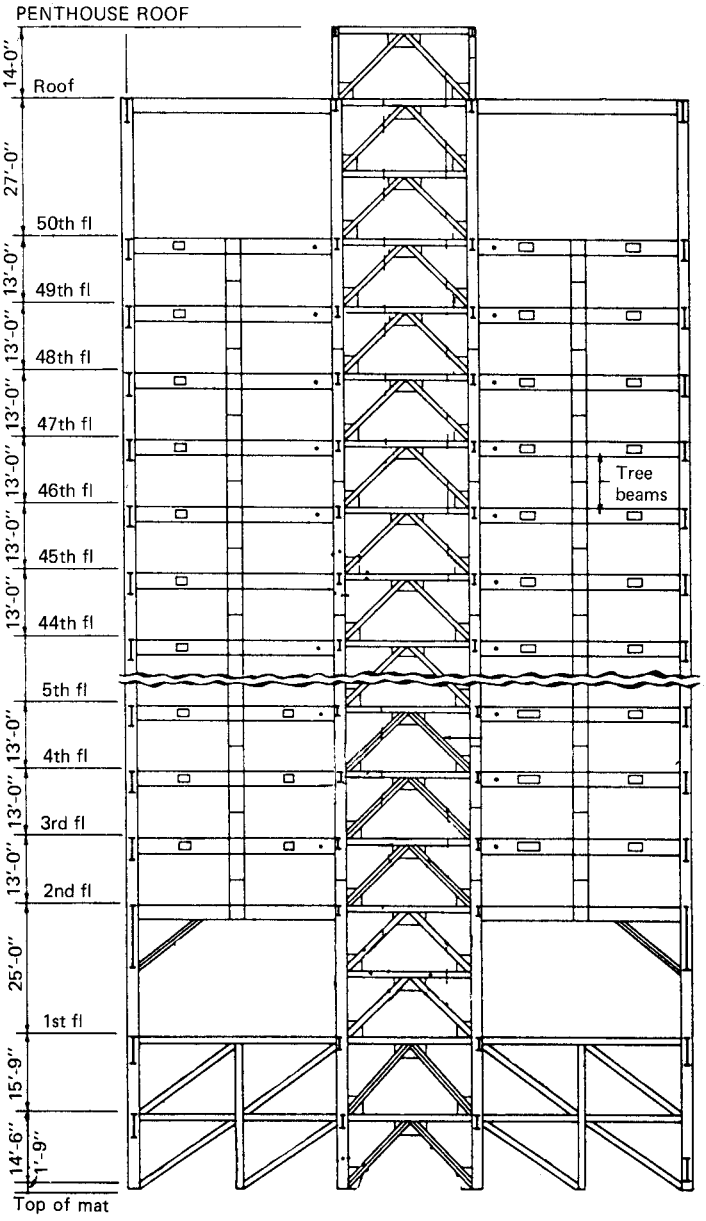

(c)

Figure 4.56 (*Continued*) (c) Building section.

building for resisting the overturning moments. However, since the exterior columns, especially in a framed tube, are placed relatively close to each other, their tributary areas for collection of gravity loads are rather small. Therefore, the beneficial effect of gravity load in counteracting the tensile forces of the columns is somewhat limited, first because of the relatively light materials used in current construction practice, and second by the limited tributary area for the exterior columns. If somehow we could induce more gravity loads into these columns, would not the efficiency of the system be improved? This is precisely the idea behind the ultimate high-efficiency structures first envisioned by the master builder Dr. Fazlur Khan. The main premise behind the ultimate high-efficiency structure is to transfer as much gravity load as practicable to the columns resisting the overturning moments. Note that this idea is routinely used by engineers when they are confronted with high uplift forces while designing interior-core-braced buildings with limited separation between the leeward and windward columns. They would normally rearrange the floor framing to achieve more flow of gravity loads into the wind columns or may choose to eliminate certain interior columns altogether in order to collect more gravity loads on the wind columns. A similar approach is possible in a tube building—eliminate as many interior columns as possible, perhaps all of the interior columns, and collect the total weight of the building on the exterior columns. This way the holding-down power of gravity loads is put to use in the most efficient manner. It must be recognized that there is a certain amount of trade-off in the floor framing system because it is economically prohibitive to clear-span the floor members using traditional approaches. Accommodation has to be made to achieve the transfer of entire building load into the exterior columns without paying a significant premium. This is considered next.

Consider a tube building with closely spaced exterior columns and deep spandrels. Imagine that all the interior columns are eliminated completely, leaving a column-free volume inside. Within this basic configuration it is possible to provide a system of transfer floor trusses at approximately every 15th floor, corresponding to the levels at which the low, low-mid, high-mid, and high-rise elevators terminate. The trusses could be designed as one- or two-story-deep vierendeel trusses spanning in two directions for the full width and length of the building. Where appropriate, the transfer levels could be made into skylobbies or other forms of common areas. The trusses then can support interior columns within the zones between two trusses. Any type of conventional structural steel framing such as composite rolled beams, haunch girders, or stub girders can be employed to span the distance from the core columns and the exterior of the building. Since the interior

columns carry gravity loads from a limited number of floors, their sizes will be substantially smaller than in a conventional system in which they would rise from foundation level to the building top. Another advantage is that the columns within any particular zone bounded by two transfer levels may be located at will to suit the interior space planning desired for specific occupancies. This in itself may be reason enough to consider this system because of the tremendous flexibility offered in the layout of columns for mixed development use. For instance, in the space planned for office use, the interior columns may be located at about 40 ft (12.20 m) on center, parking levels could have columns at 60 ft (18.28 m), and so on. For major tenants willing to lease the full block of floors between two transfer levels, columns can be arranged to suit their particular needs. Column transfers within the zones can be achieved with little structural difficulty because (1) the loads to be transferred are relatively small, and (2) it is possible to hang the upper six floors or so in one zone from the transfer girder, creating opportunities to have some floors entirely column free. In fact, the floor framing options are limited only by the imagination of the designer. The principal structural advantage is, of course, that total dead and live load from every floor is transferred only to the exterior columns, thereby increasing the structural capacity of the system to withstand lateral loading. Undoubtedly there would be some premium in the tonnage of steel for the trusses and their associated fabrication and erection costs. However, the premium spread over the total square footage of the building is likely to be small.

It is, of course, necessary to tie the windward and the leeward columns of the tube with a structural system capable of resisting the shear forces caused by the lateral loads. This can be achieved with a system of deep spandrel beams when the perimeter columns are closely spaced, or with a system of diagonal bracing when the columns are spaced apart as in a trussed tube system. Dr. Fazlur Khan has shown that by progressively shifting the exterior columns to the corners of a rectangular trussed tube, the efficiency of the system can be greatly improved. An ultimate structure for a rectangular building, then, will have just four corner columns interconnected by massive diagonals as shown in Fig. 4.57.

The efficiency of a building to resist lateral loads can be increased further by using interior bracing with a structural system in which the total gravity load of the building is made to bear on a limited number of exterior columns. To increase the uplift capacity, interior columns are eliminated within the building envelope. However, to achieve an economical floor system, it is necessary to use columns in the core area without unduly interfering with the leasing requirements. Therefore, a structural system is needed for transferring the loads from the

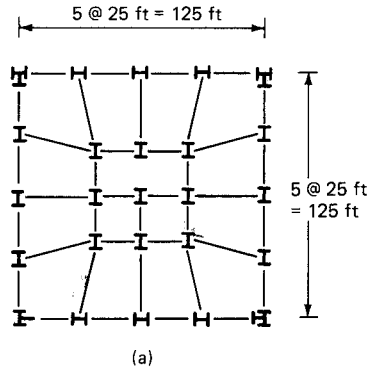

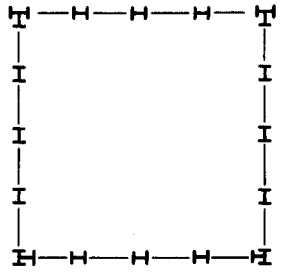

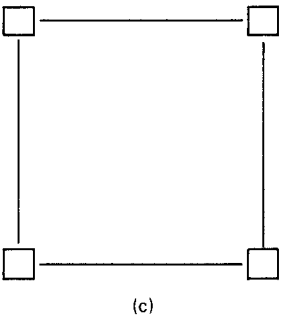

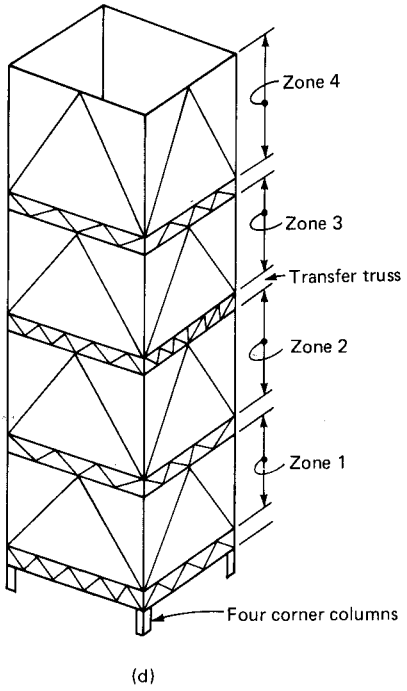

Figure 4.57 Floor plans. (*a*) Conventional framing with interior and exterior columns extending to the foundation; (*b*) exterior columns extend to foundation; interior columns are supported by transfer trusses; (*c*) floor plan for ultimate high rise; only four corner columns extend to the foundation; interior columns supported by transfer trusses; (*d*) Khan's concept of the ultimate high-rise building.

interior columns to the building envelope. If this system can simultaneously work as a shear-resisting element, then the need for closely spaced columns or diagonal bracing on the perimeter can be eliminated. In other words a system of interior bracing that performs the dual function of channeling the loads from the interior columns to the exterior while at the same time functions as a shear element between the windward and leeward columns is likely to be the optimum system. From a pure structural point of view, such a system is highly desirable.

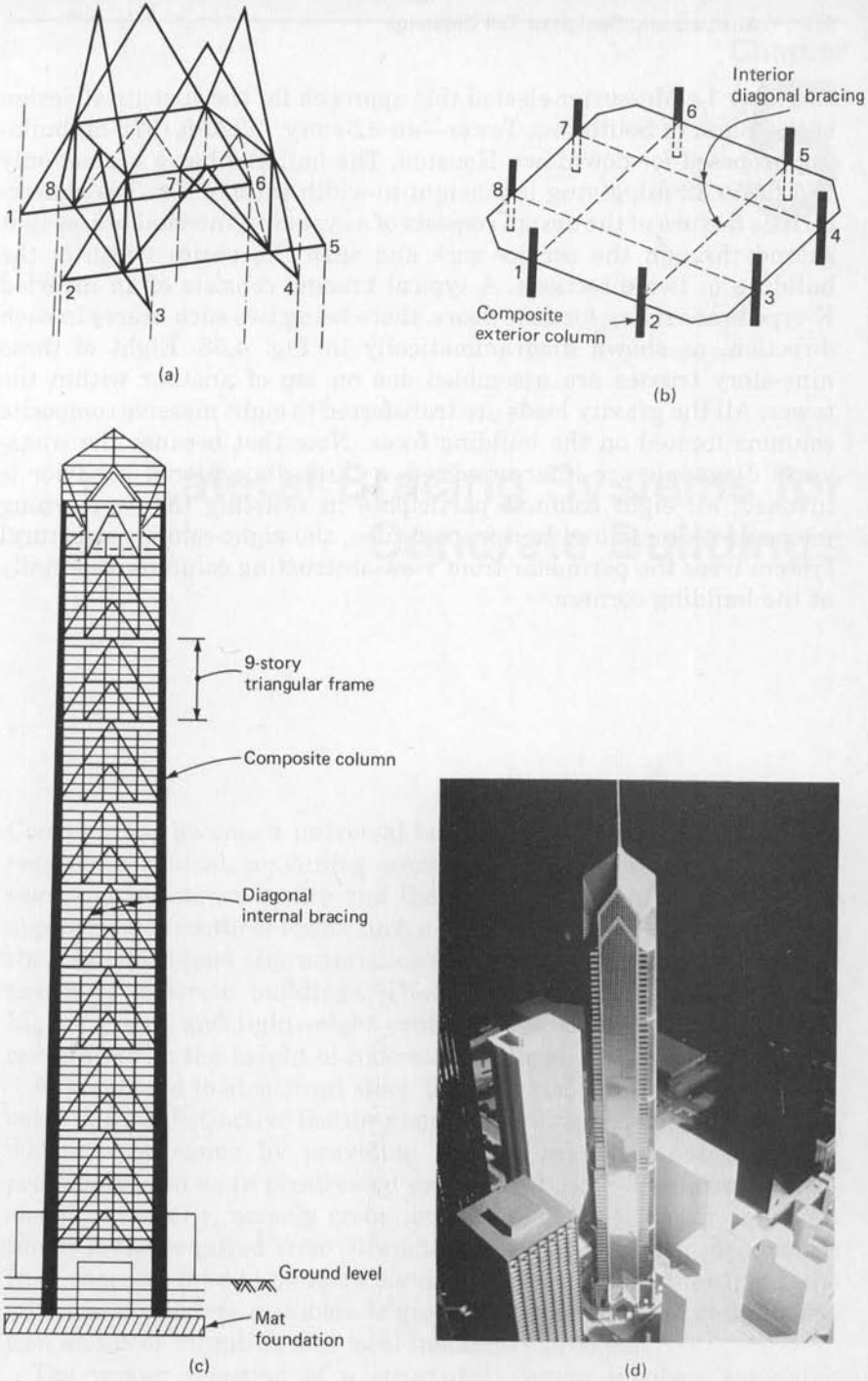

Fig. 4.58 Bank of Southwest Tower (Structural engineers, Le Messurier Associates and Walter P. Moore Associates, architects Murphy/Jahn and Lloyd Jones and Fillpot). (*a*) Schematic representation of interior diagonal bracing; (*b*) schematic plan; (*c*) schematic section; (*d*) photograph of model. (*Photo courtesy of Malcolm Stewart, Century Development Corporation.*)

Engineer Le Messurier elected this approach for the structural design of the Bank of Southwest Tower—an 82-story, 1,220-ft (372-m) building proposed for downtown Houston. The building has a base of only 165 ft (50.32 m), giving it a height-to-width ratio of 7.4. The characteristic feature of the design consists of a system of internal braces that extend through the service core and span the entire width of the building in two directions. A typical bracing consists of an inverted K-type brace rising for nine floors, there being two such braces in each direction, as shown diagrammatically in Fig. 4.58. Eight of these nine-story trusses are assembled one on top of another within the tower. All the gravity loads are transferred to eight massive composite columns located on the building faces. Note that because the transverse diagonals are interconnected, a three-dimensional behavior is invoked; all eight columns participate in resisting the overturning moment. As compared to a framed tube, the eight-column structural system frees the perimeter from view-obstructing columns, especially at the building corners.

Chapter

5

Lateral Bracing Systems for Concrete Buildings

Concrete has become a universal building material because in many respects it is ideal, combining economy, versatility of form and function, and resistance to fire and the ravages of time. With the more appropriate structural forms such as shear walls and tube structures, the high dead-load characteristics are no longer a limitation on the height of concrete buildings. The advent of superplasticizers and high-strength and lightweight concrete has removed all economical constraints on the height of concrete buildings.

As compared to structural steel, the material properties of concrete exhibit some distinctive features such as (1) low resistance to tension, which is overcome by providing tension reinforcement or initial precompression as in prestressed concrete; (2) time-dependent dimensional variations, namely creep and shrinkage; (3) larger cross-sectional areas required from strength considerations. The dead loads from concrete tend to be more significant, but on the other hand, the stiffness of concrete members is greater, minimizing the sway deflection and floor vibration and local instability problems.

The proper selection of a structural system involves satisfying conflicting centers of interest required by different disciplines. The owner is concerned with obtaining a building that maximizes leasa-

bility. The architect is anxious for a functional and aesthetic design. There are special needs imposed by mechanical, electrical, and elevator consultants. In addition to satisfying these varying demands, the structural system should also be compatible with the specialized talents and building techniques common to the given locale. If not, it may be perceived by the contractors as a difficult system, making it expensive because of their unfamiliarity with it.

Although a number of structural solutions are possible, it is important to consider the following features in the selection of a concrete system for a high-rise building.

1. It is well known that the cost of form work has a significant effect on the total cost of concrete construction. Therefore, the structural system should minimize this cost by the use of repetition of form work.
2. Where poor soil conditions exist, the cost of foundations should be minimized by reducing the weight of structure. Lightweight aggregates should be employed where available.
3. It is well known that short spans are more economical than large spans. However, in tall office buildings the leasability of the buildings most often dictates clear spans in the range of 30 to 40 ft (9.14 to 12.19 m). Use of haunch girders and other techniques such as posttensioning which give the desired span without unduly increasing the building height must be considered.
4. Experience of local contractors and available construction methods are also factors that need to be considered in the selection of a system. The most efficient design will minimize the structural cost when all other factors are constant. The general objective in most building systems is to minimize the material quantities, which in most cases leads to a solution very close to the optimum.

One of the most important tasks for the engineer is to assist the owner or developer to choose the best construction material for the framing of the building. The construction material selected has a significant impact on the initial cost of the project, speed of construction and early return on investment, cost of energy, and cost of maintenance. The following factors have contributed significantly to the cost-competitiveness of reinforced concrete for tall buildings.

1. New advances in concrete forming techniques such as flying forms, tunnel forms, slip forms, and gang forms.
2. Use of faster concrete-placing equipment such as concrete pumps.
3. The inherent fire resistance of concrete, which eliminates the need for fireproofing materials.

4. Minimum thickness of floor system, which reduces the floor-to-floor height, thereby reducing the amount of materials needed to enclose the building.
5. Grade 60 and 75 ksi (413.7 and 517 MPa) mild steel reinforcement in combination with high-strength concrete results in the use of smaller and fewer columns, thereby maximizing rentable floor space.
6. Advent of superplasticizers to increase the workability and the strength of concrete. Normal water reducers are capable of lowering water requirements by about 10 to 15 percent. Incorporating larger amounts to produce higher water reductions results in undesirable effects on setting, air content, bleeding, segregation, and hardening characteristics. Superplasticizers are chemically different from normal water reducers and are capable of reducing water content by about 30 percent.
7. The capacity of concrete to be molded into controlled shapes and configurations offers an opportunity to create dramatic and aesthetically pleasing shapes.
8. Buildings framed with pan joist or other types of construction with a uniform structural depth make it possible to use a simpler mechanical distribution system.
9. Exterior shear walls, columns, and spandrels can be formed with textured finform liners to achieve architectural finish without additional treatment or painting.

Analogous to steel or composite construction, concrete offers a wide range of structural systems suitable for high-rise buildings. There are perhaps as many structural concepts as there are engineers, making it awkward if not impossible to either define all the concepts or to classify them into distinct categories. However, for purposes of presentation, it is convenient to group the most common systems into separate categories, each with an applicable height range as shown in Fig. 5.1. Although the height range for each group is logical for normally proportioned buildings, the appropriateness of each system can only be judged when all other factors influencing the lateral load behavior are taken into account. Such factors include building geometry, severity of exposure to wind, seismicity of the region, ductility of the frame, and limits imposed on the size of the structural members. Many tall buildings may efficiently utilize a few or many of the systems depending upon the individual requirement of the building. Oftentimes, systems combining the characteristics of two or more systems can be employed to fulfill the specific project requirement. The multitude of

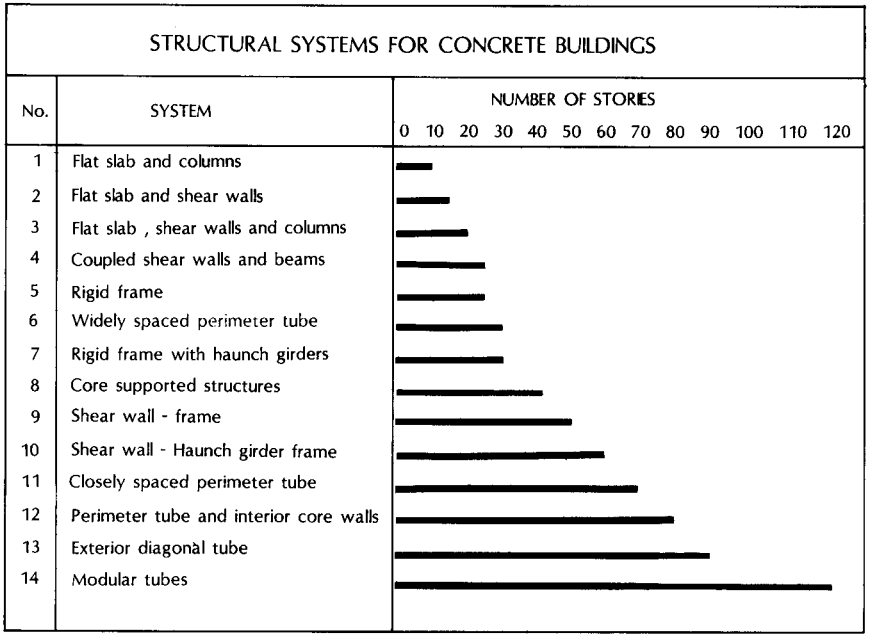

Figure 5.1 Structural systems for concrete buildings.

systems available presents an opportunity for an experienced engineer to come up with a structural system that will serve its optimum function in the overall sense of the project. Although the selection of a system requires knowledge of both horizontal and lateral systems, the material presented in this chapter emphasizes the requirements of lateral systems only. Gravity systems are covered separately in Chap. 8. Figure 5.1 shows 14 different categories of structural systems, starting with the most elementary system consisting of floor slabs and columns. At the other end of the spectrum is the bundled tube system, which is appropriate for very tall buildings and for buildings with a large plan aspect ratio. Certain categories of systems such as staggered truss and belt truss systems and those that employ the concept of megastructures are not included because their structural actions have been covered in Chap. 4. Their application to concrete buildings has been well demonstrated, as, for example, the "Australia Square" tower in Sydney, a 46-story, 590-ft (180-m) concrete building that employs the concept of engaging the perimeter columns with the core as the major wind-resisting system. Almost all of the systems described in Chap. 4 are equally applicable to concrete buildings. Therefore, proper selection of a system can only be made when the engineer has an appreciation of the basic systems described not only in this chapter,

but elsewhere throughout this work. A brief description of the major systems shown in Fig. 5.1 follows.

5.1 Frame Action of Column and Slab Systems

Concrete floors in tall buildings often consist of a two-way floor system such as a flat plate, flat slab, or a waffle system. In a flat-plate system the floor consists of a concrete slab of uniform thickness which frames directly into columns. Two-way flat slabs make use of either capitals in columns or drop panels in slab or both, requiring less concrete than a flat plate because extra concrete is provided only at the columns where the shears and moments are greatest. The waffle slab system is obtained by using rows of joists at right angles to each other; the joists are commonly formed by using square domes. The domes are omitted around the columns to increase the moment and shear capacity of the slab. Any of the three systems can be used to function as an integral part of the wind-resisting systems for buildings in the 10- to 20-story range.

Consider the plan form shown in Fig. 5.2 consisting of a flat slab system spanning between rectangular columns. The floor slab distributes the lateral load to the various resisting elements mainly through the forces in its own plane. The actual in-plane deformation of the floors seldom has an effect on this distribution. Therefore, the assumption that the floor slabs are fully rigid can be used in almost all analyses without meaningful loss in accuracy. The out-of-plane bending of the slab, however, has a significant effect on the behavior of the entire system.

The concept of an "effective width" is usually used in the analysis of such buildings subjected to lateral loads. Although physically no beam exists between the columns, for analytical purposes it is convenient to consider a certain width of slab behaving as a beam between the columns when the lateral loads are considered. The effective width factor is dependent on various parameters, such as column aspect ratios, distance between the columns, and thickness of the slab. Assuming that one can determine the effective width, the lateral resistance of the system is analytically equivalent to a rigid frame consisting of columns and equivalent beams interconnected to the columns. Medium-rise office buildings in the range of 10 to 15 stories and high-rise 15- to 25-story apartments, because they have more columns, can be designed by using the concept of effective width. Frame action can be developed by using a portion of the slab as a shallow beam continuous with the columns.

Lateral analysis can be carried out by idealizing the structure as a

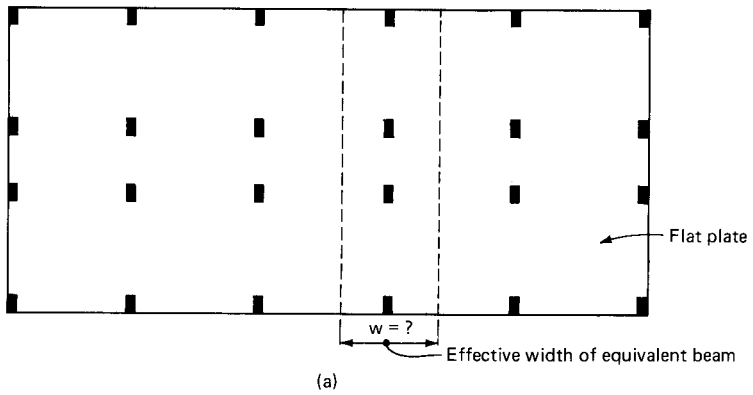

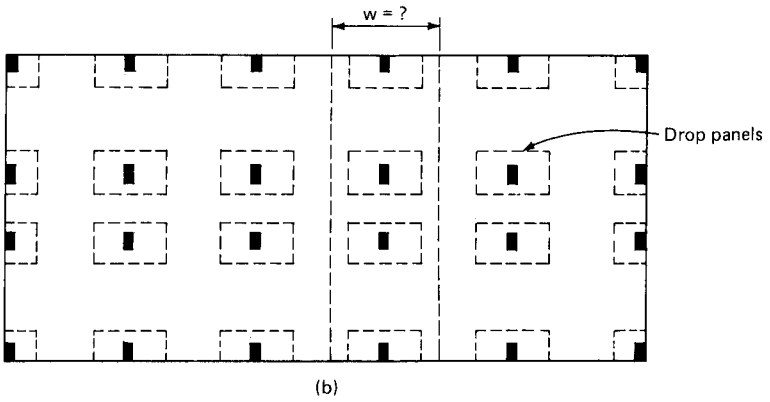

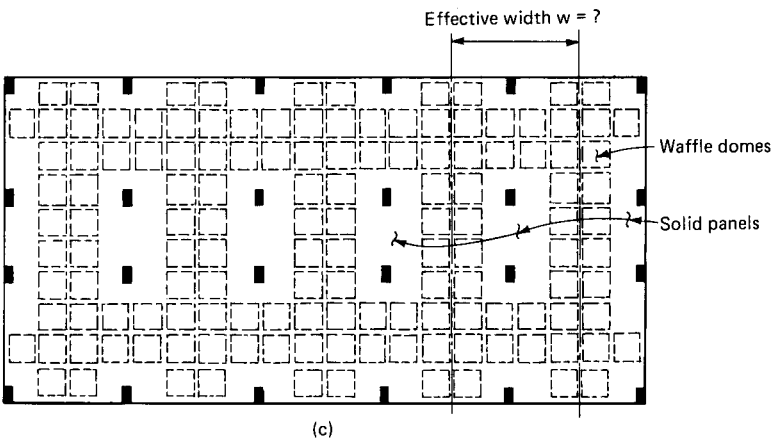

Figure 5.2 Lateral systems using slab and columns. (*a*) Flat plate; (*b*) flat slab with drop panels; (*c*) two-way waffle system.

series of linked plane frames. This assumption is reasonable for the flexural action of the slab if the parallel frames are more or less similar so that torsion effects do not produce significant irregularities in the distribution of forces. If the irregularities in the framing of the building are too severe, a three-dimensional analysis can be done to capture the torsional effects.

The lateral analysis of column and slab system is, therefore, no more difficult than that for an assemblage of horizontal and vertical elements. However, the designer faces a special problem when the horizontal connecting system consists of flat plate, flat slab, or waffle system. This is because there is a nagging question as to what width of the slabs will be effective as a connecting beam. Many factors affect the complex behavior of wall and slab systems and research conducted so far indicates that values less than the full width, equal to the full width, and greater than the full width are all valid under different circumstances. Analytical and experimental studies relating to the problem of effective slab width have considered the panel–column-width ratio as the principal variable and have indicated effective slab width ratios ranging from 0.5 to greater than unity, the effective width increasing for increasing values of column–panel width ratios. However, other parameters such as the slab span–width ratio, the relative dimensions of the column with respect to the longitudinal and transverse spans of the slabs, and the distribution of reinforcement in the slab all have a significant influence on the effective width of slab.

The building code requirements for reinforced concrete design as given in the American Concrete Institute (ACI) code provide two specific procedures for flat slab structures, (1) the direct design method, and (2) the equivalent frame method. The ACI code also allows any procedure that satisfies the conditions of equilibrium and geometric compatibility. In the equivalent frame method, a concept of equivalent column is specified in the code. This is intended to permit an increase in the positive slab moment under pattern loading because the column restrains the slab only along a portion of its width. The equivalent column also reduces the moment at the exterior columns under gravity loading. By decreasing the column stiffness, the ACI method increases the slab distribution factors and thereby achieves reduction in the slab moment at the columns.

The ACI allows the use of the full width of slab bounded transversely by adjacent panel centerlines in the analysis of the system for both gravity and lateral loads, as long as the lateral load analysis takes into account the effect of cracking and reinforcement on the stiffness of frame numbers.

The ACI equivalent frame method, which incorporates the concept of equivalent column, can be used for gravity analysis without meaning-

ful loss of accuracy. Since the code does not specifically prohibit the method for lateral load analysis, there is a temptation to use a similar procedure for lateral analysis also. This procedure may be legally acceptable (or acceptable from the point of view of the ACI code), but it may lead to a design that is too flexible.

However, it is generally agreed among engineers that the concept of equivalent column using the full width of the slab gives incorrect results when used for lateral load analysis. The ACI method tends to overestimate the slab stiffness and underestimate the column stiffness, compounding the error in estimating the distribution of moments due to lateral loads.

The shortcomings of the ACI method can be overcome by determining the equivalent stiffness on the basis of a finite-element or grid analysis. The stiffness thus obtained is appropriate for analysis of slabs subjected to either horizontal or vertical load in contrast to the equivalent column approach, which, as mentioned previously, is reasonably correct for gravity analysis but grossly inappropriate for lateral load analysis.

It is difficult to specify for what number of stories or slenderness ratio of the building a complete finite-element or grid analysis of the slab is required because of the many factors involved. For buildings taller than 10 stories or so, it behooves the engineer to overcome the temptation to use the simplified code approach. Equivalent beam stiffness as obtained through a slab analysis is more appropriate for taller buildings.

Of particular concern in flat plate and flat slab structures is the problem of stress concentration at the column-slab joint where, especially under lateral load, nonlinear behavior is initiated through concrete cracking and steel yielding. Shear reinforcement at the column-slab joint is especially necessary to improve the joint behavior and avoid early stiffness deterioration under lateral cyclic loading. Note that two-way slab systems without beams are not permitted by the ACI code in regions of high seismic risk (zones 3 and 4). Their use in regions of moderate seismic risk (zone 2) is permitted subject to certain requirements, mainly relating to reinforcement placement in the column strip. Since the requirements are too detailed to be mentioned here, the reader is referred to Section A.9.6 of the ACI code for further information.

5.2 Flat Slab and Shear Walls

Frame action obtained by the interaction of slabs and columns is not adequate to give the required lateral stiffness for buildings taller than about 15 to 20 stories. The advantages of beamless flat ceilings could

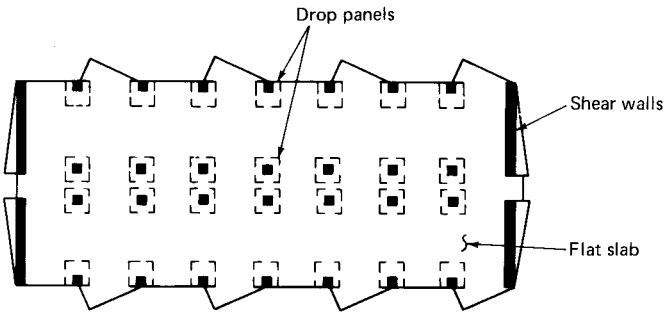

Figure 5.3 Shear wall flat slab system.

still be achieved in taller buildings by strategically locating shear walls to function as the main lateral-load-resisting element. The walls can be either planar, open sections, or closed sections around elevator and stair cores. Figure 5.3 shows the plan of a tall building in which planar shear walls are located at the ends of the building. The layout in general may not always be in a simple orthogonal orientation. Skewed and irregular layouts of shear walls require three-dimensional analysis for determining the distribution of lateral loads. The shear wall in essence behaves as a deep and slender cantilever. When no major openings are present, stresses in and deflections of walls can be determined using simple bending theory. Complicated shapes are analyzed as outlined in Sec. 10.7.

5.3 Flat Slab, Shear Walls, and Columns

The applicable height range of slab and shear wall systems can be increased marginally by including the frame action of column and slabs. The system is best suited for apartments, condominiums, and hotel layouts and is identical to the system described in the previous section. The difference is only in the analysis in that the frame action of column and slabs is also taken into account in the lateral load analysis. Whether this action is significant or not is a function of relative stiffness of various elements. In most apartment or hotel layouts, the frame resistance to overturning moments is no more than 10 to 20 percent of the resistance offered by the shear walls. Many engineers, therefore, ignore the frame action altogether by designing the shear walls to carry the total lateral loads. However, in keeping with the current trend of taking advantage of all structural actions, it is advisable to include the frame action in the analysis.

5.4. Coupled Shear Walls

When two or more shear walls are interconnected by a system of beams or slabs, it is well known that the total stiffness of the system exceeds the summation of the individual wall stiffnesses. This is because the connecting slab or beam restrains the individual cantilever action of each wall by forcing the system to work as composite section. Where shear walls are compatible with other functional requirements and are of sufficient length, such walls can economically resist lateral forces up to 30 to 40 stories. However, planar shear walls are efficient lateral load carriers only in their plane. Therefore, it is necessary to provide walls in two orthogonal directions. However, in long and narrow buildings sometimes it is possible to resist wind loads in the short direction by the frame action of columns and slabs because first, the area of the building exposed to the wind in the short direction is small, and second, because the building is long, usually a sufficiently large number of columns exists in that direction. The layout of walls and columns should take into consideration the torsional effects.

Walls around elevators, stairs, and utility shafts offer an excellent means of resisting both lateral and gravity loads without requiring undue compromises in the leasability of buildings. Closed- and partially closed-section shear walls are efficient in resisting torsion, bending moments, and shear forces in all directions, especially when sufficient strength and stiffness are provided around door openings and other penetrations through these core walls. This is discussed in greater detail in Chap. 10.

5.5. Rigid Frame

Cast-in-place concrete buildings have the inherent advantage of providing continuity at the various joints. The girders, which are supported directly by the columns, can be considered rigid with the columns; such a girder-column arrangement can be thought of as a portal frame. However, girders that carry shear and bending moments due to lateral loads often require additional construction depth, necessitating increases in the overall height of the building. With the increased use of haunch girders and slab-band construction which attempt to minimize the floor-to-floor heights, this method of construction is being superseded.

The design and detailing of joints where girders frame into building columns should be given particular attention, especially when buildings are designed to resist seismic forces. The column region within the depth of the girder is subjected to large shear forces. Horizontal ties must be included to avoid uncontrolled diagonal cracking and disintegration of concrete. The ACI code includes detailed special provisions

that apply to reinforced concrete structures to be built in regions of moderate risk (zone 2), and high risk (zones 3 and 4). The underlying principle is to have a structural system which can respond to overloads without critical loss of strength. Specific code requirements are too detailed to be presented here. The ACI code and commentary will provide the necessary guidance for engineers designing buildings in zones of high seismic risk.

Rigid-frame systems for resisting lateral and vertical loads have long been accepted as a standard means of designing buildings because they make use of the stiffness in the beams and columns that are required in any case to carry the gravity loads. In general, rigid frames are not as stiff as shear wall construction and are considered more ductile and less susceptible to catastrophic earthquake failures when compared to shear wall structures.

As discussed in Chap. 4, a rigid frame is characterized by its flexibility, which is created by flexure of individual beams and columns and the rotation at their joints. The strength and stiffness of the frame is proportional to the beam and column size and inversely proportional to the column spacing. Internally located frames are not very popular in tall buildings because the leasing requirements of most buildings limit the number of interior columns available for frame action. The floor beams are generally of long spans and are limited in depth. However, frames located at the building exterior do not necessarily have these disadvantages. An efficient frame action can be developed by providing closely spaced columns and deep beams at the building exterior.

5.6 Widely Spaced Perimeter Tube

A tube system in the usual building terminology suggests a system of closely spaced columns 8 to 15 ft on center (2.43 to 4.57 m) tied together with a relatively deep spandrel. No one column spacing is applicable to all structures because of the many variables. In certain building layouts it is possible to achieve tube action with relatively widely spaced columns interconnected with a deep spandrel. An example of such a layout for a 28-story building is shown in Fig. 5.4. Lateral resistance is provided by the perimeter frame, consisting of columns spaced at 25-ft (7.62-m) centers and a deep spandrel.

5.7 Rigid Frame with Haunch Girders

One of the drawbacks of rigid frame systems is the excessive depth of girder that is necessary to make the rigid frame economical. Rigid frames, when located at the perimeter, often can use deep spandrels

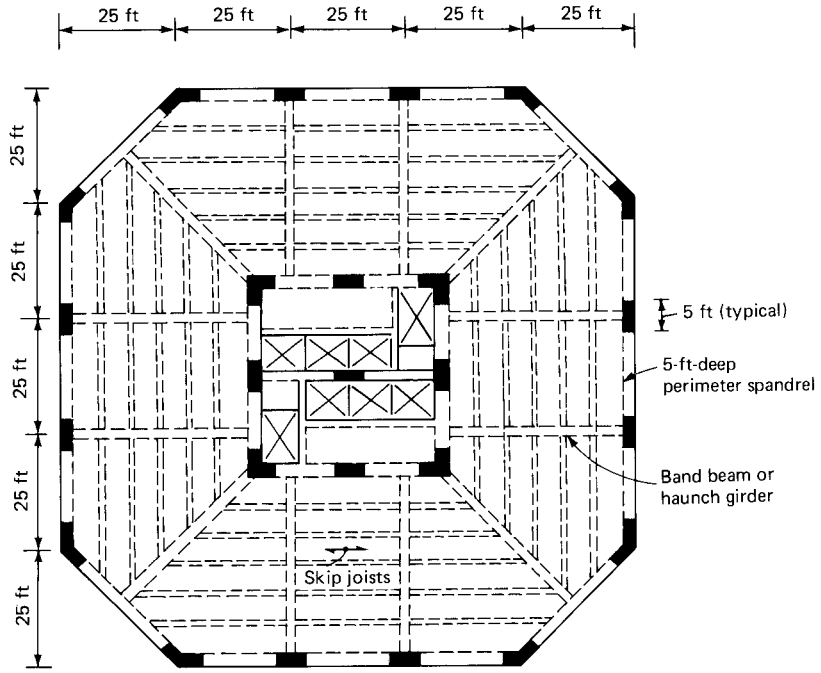

Figure 5.4 Tube building with widely spaced perimeter columns.

without adversely affecting the floor-to-floor height of the building. Also it may be architecturally acceptable to use relatively closely spaced columns at the exterior.

Office buildings usually are laid out with a lease depth of about 40 ft (12.19 m) without any interior columns between the core and the exterior. To make such a large span economical requires a girder of about 3 ft (0.91 m) in depth. This requirement clearly impacts the floor-to-floor height and often is unacceptable because of additional cost of curtain wall and the heating and cooling loads due to extra volume of the building. A haunch girder, which consists of a girder of variable depth, gives the required stiffness for lateral loads without having to increase the floor-to-floor height. This is achieved by making the girder flush with the floor system, thus providing ample beamless space at midbay for passage of mechanical ducts.

Girders with haunches on either end are ideal for resisting lateral loads, but certain types of column layouts may limit the haunches to one end of the girder. Such an arrangement of single-end haunch girder is shown for a 28-story building in Fig. 5.5. To keep the skip-joist framing simple, the girders are framed into the spandrel

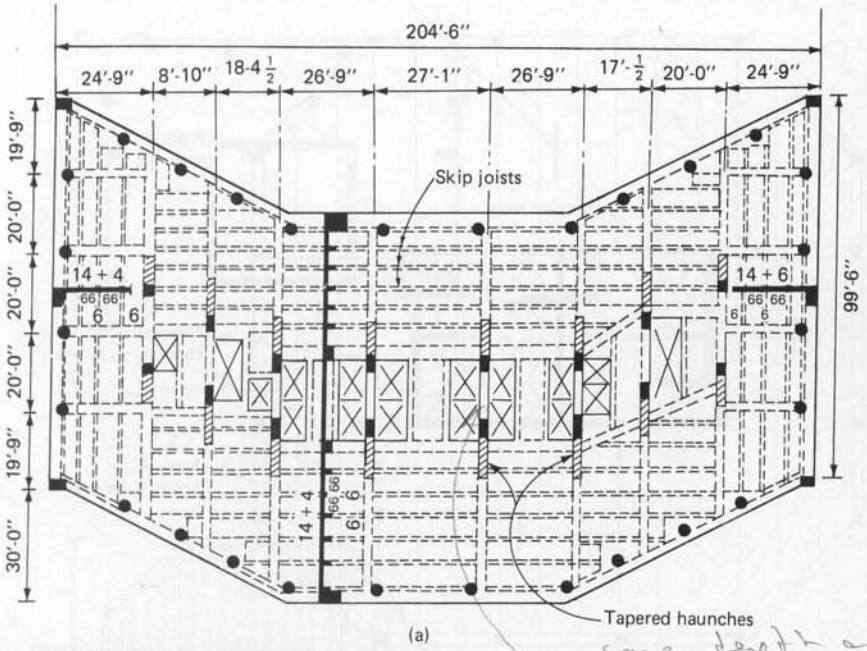

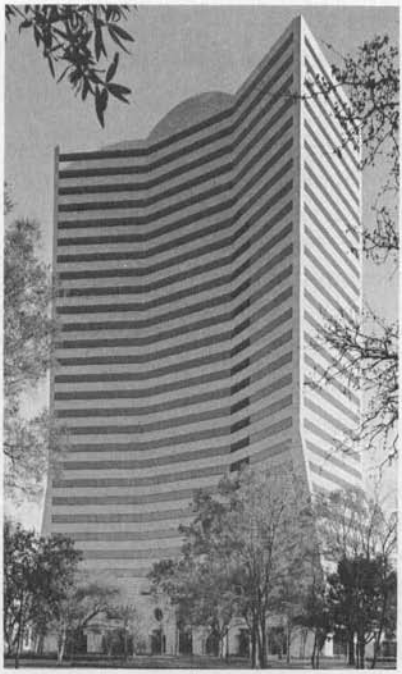

(b)

Figure 5.5 A 28-story haunch girder building. (*a*) Typical floor plan; (*b*) photograph of Five Post Oak Building, a 28-story concrete office building in Houston. (Architects, Morris-Aubry Associates; structural engineers, Walter P. Moore Associates) *(Photograph © Richard Payne AIA, 1987. Reproduced with permission.)*

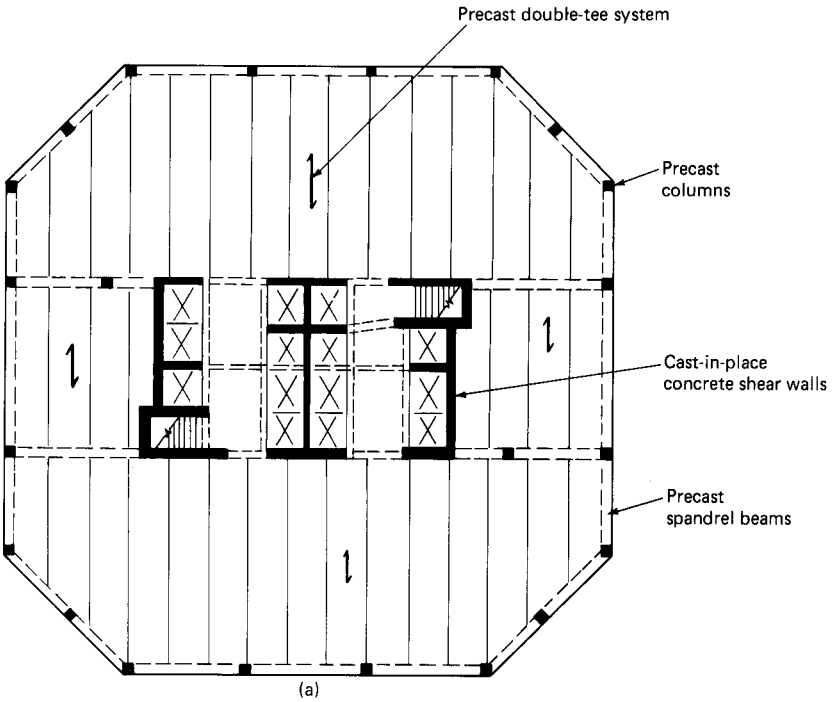

Figure 5.6 Examples of shear core buildings. (*a*) Cast-in-place shear walls with precast surround.

without haunches at the exterior end. A haunch depth girder is used between the core columns, as shown in Fig. 5.5. The additional depth of these girders between the core columns did not affect the mechanical distribution and therefore did not require increases in floor-to-floor height. A 9-ft (2.74-m) ceiling was accomplished with a 12-ft, 10-in (3.91-m) floor-to-floor height.

5.8 Core-Supported Structures

One of the most frequent uses of shear walls is in the form of rectangular box-shaped cores around stairs, elevators, and other shafts. This is not surprising because this arrangement makes use of vertical enclosures that are required around the cores. Arrangement of internal cores is especially suitable for office buildings because it frees the lease space outside of the core from massive vertical elements. The walls around the core can be considered as a spatial system capable of transmitting both the vertical and gravity loads to the foundation. The advantage of core structures is that being spatial structures, they are capable of resisting all types of loads: vertical forces, shear forces, and

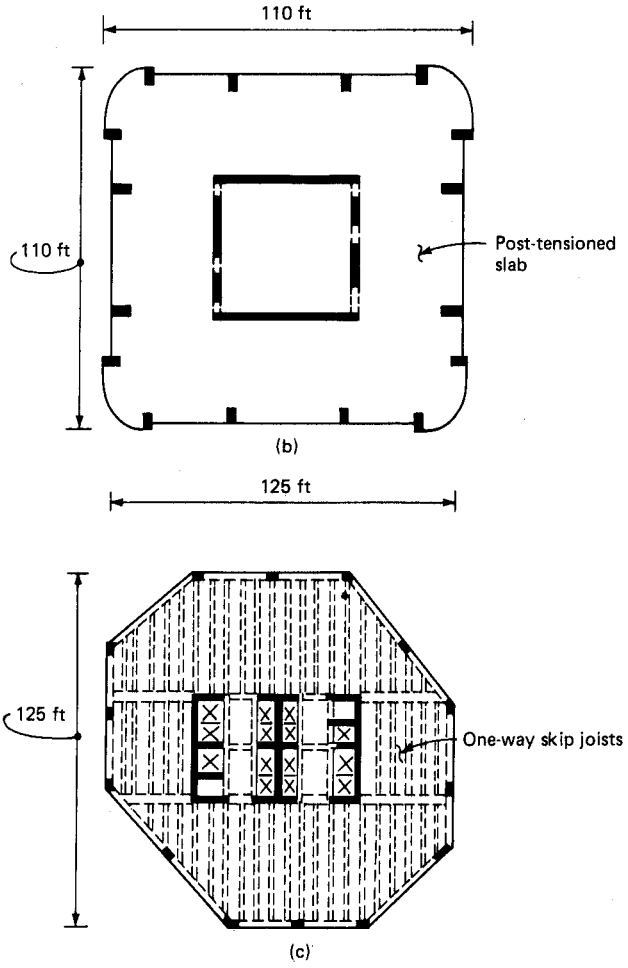

Figure 5.6 (*Continued*) (*b*) Shear walls with posttensioned flat plate; (*c*) shear walls with one-way joist system.

bending moments in all directions, as well as torsion, especially when adequate stiffness and strength are provided between flanges of open sections. The relative location of the cores can be different for different buildings and may consist of single or multiple cores. The shape of the core to a large extent is governed by the elevator and stair layout and variations in layout of shear walls could occur from a single rectangular box core to a complicated arrangement of planar shear walls. Other vertical structural elements surrounding the core may consist of either cast-in-place or precast concrete or structural steel columns. In a precast or steel surround system, it is more than likely that the stiffness of the core will overwhelm the stiffness of other vertical

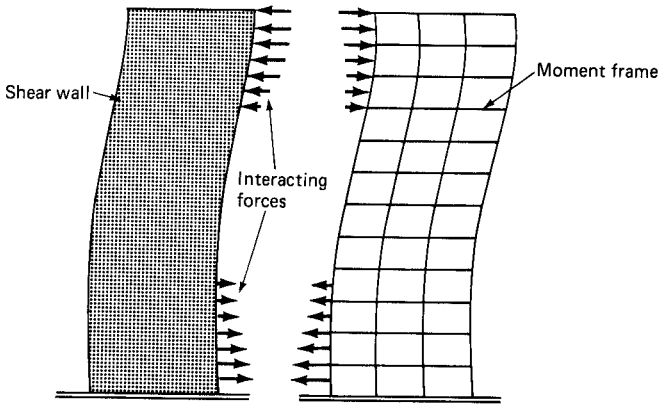

Figure 5.7 Shear wall–frame interaction.

elements. Even in a cast-in-place system, unless the exterior frame consists of relatively closely spaced columns and a deep spandrel, it is justifiable to ignore the resistance of other vertical members and to design the core system for the entire lateral load. Figure 5.6*a* through *c* shows some of the core arrangements used in tall buildings.

5.9 Shear Wall-Frame Interaction

Without question this system is one of the most, if not the most, popular system for resisting lateral loads. The system has been used for buildings as low as 10 stories to as high as 50-story or even taller buildings. With the advent of haunch girders, the applicability of the system could easily be extended to buildings in the 70- to 80-story range.

The interaction of frame and shear walls has been understood for quite some time; the classical mode of the interaction between a prismatic shear wall and a moment frame is shown in Fig. 5.7; the frame basically deflects in a so-called shear mode while the shear wall predominantly responds by bending as a cantilever. Compatibility of horizontal deflection introduces interaction between the two systems which tends to impose a reverse curvature in the deflection pattern of the system. It is not always easy to differentiate between the two modes of deformation. For example, under lateral loads a frame consisting of closely spaced columns and deep beams tends to behave more like a shear wall responding predominantly in a bending mode. Similarly, a shear wall weakened by a row or rows of openings may tend to act more like a frame by deflecting in a shear mode. The combined structural action, therefore, depends on the relative rigidities of different elements used in the makeup of the lateral-load-resisting system.

The distribution of total wind shear to the individual shear walls and frames as given by the simple interaction diagram is valid only if one of the following two conditions is satisfied.

1. Each shear wall and frame must have constant stiffness properties throughout the height of the building.
2. If stiffness properties vary over the height, the relative stiffness of each wall and frame must remain unchanged throughout the height of the building.

Architectural and other functional reasons frequently influence the configuration of each wall and frame. It is rarely possible in a practical structure to conform to the above requirements. In a contemporary high-rise building one can very rarely have the luxury of maintaining the geometry of walls and frames the same over the full height of the building. Core walls are routinely stopped at levels corresponding to the elevator dropoffs. Columns are made smaller as they go up the building. Building geometry very rarely remains the same for the full height. Because of the abrupt changes in the stiffness of walls and frames combined with the changes in the geometry of the building itself, the simple interaction model shown in Fig. 5.7 does not even come close to predicting the actual behavior of the building structure. With the availability of computers and commercial two- and three-dimensional programs, this no longer is a limitation. It is within reach of everyday engineering practice to capture the essential behavior of the shear wall frame system.

As a first example, consider the framing plan of a high-rise building shown in Fig. 5.8*a*. The building is somewhat unusual in that it exhibits almost perfect symmetry in two directions and maintains a reasonably constant stiffness throughout its height. Therefore, in a qualitative sense, interaction between the frames and shear walls should be similar to that shown in Fig. 5.7. A brief description of the building and a qualitative explanation of the distribution of lateral loads among the various interacting elements is considered next.

The building is 25 stories tall and consists of four levels of basement below grade. The floor framing consists of 6-in-wide by 20-in-deep (152.4- by 508-mm) skip joist framing between haunch girders which span the distance of 35 ft, 6 in (10.82 m) between the shear walls and the exterior of the building. Haunch girders are 42 in wide by 20 in deep (1.06 by 0.5 m) for the exterior, 28 ft, 6 in (8.67 m) with a haunch at the interior which tapers from a pan depth of 20 to 33 in (0.5 to 0.84 m). Four shear walls of dimensions 1 ft, 6 in by 19 ft, 6 in (0.45 by 5.96 m) rise for the full height from a 5-ft (1.52-m) deep mat foundation. The exterior columns vary from 38 by 34 in (965 by 864 mm) at the bottom

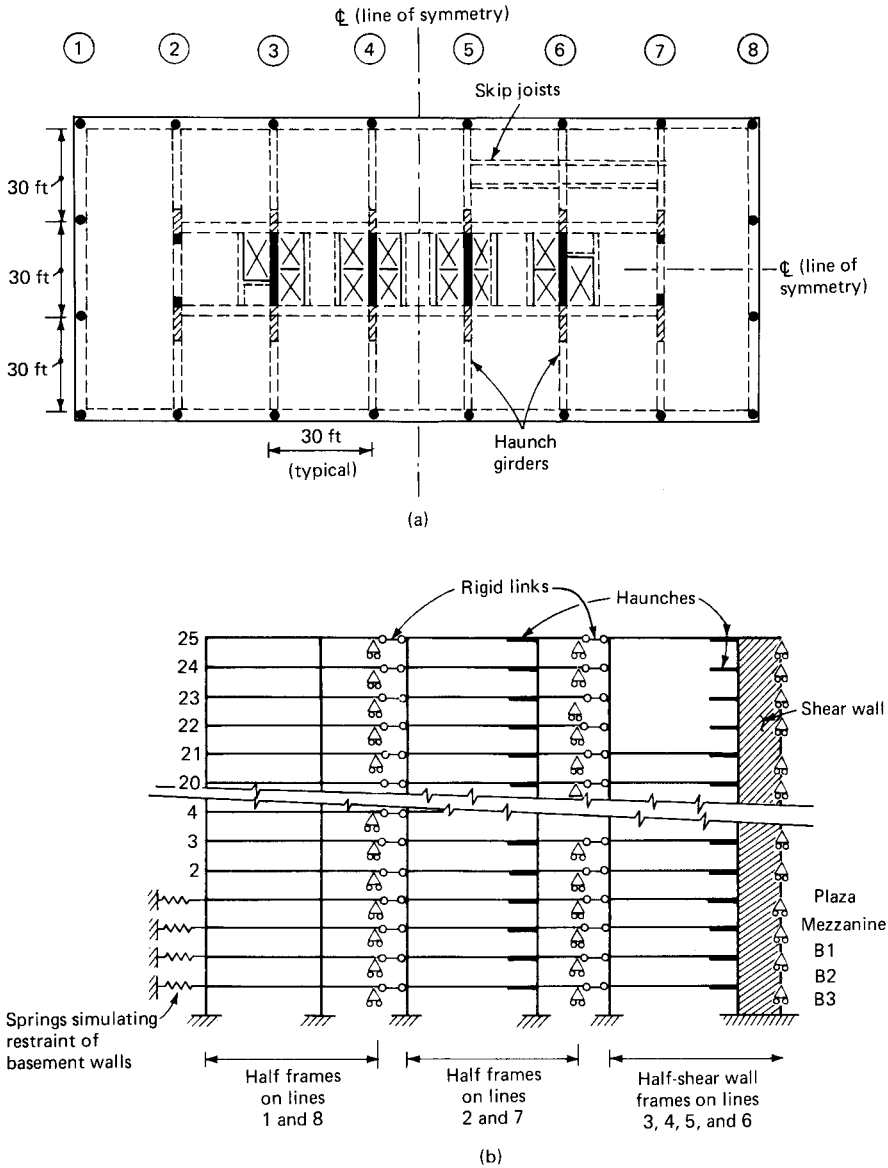

Figure 5.8 Practical example of shear wall–frame interaction. (*a*) Typical floor plan; (*b*) analytical two-dimensional model for wind on long face;

to 38 by 24 in (965 by 610 mm) at the top. Note that the width of haunch girder is made deliberately larger than the width of exterior column to facilitate flying of forms. However, with the increased use of flying forms with built-in hinges at the ends, this is no longer a necessity; the width of haunch girders can be made consistent with the

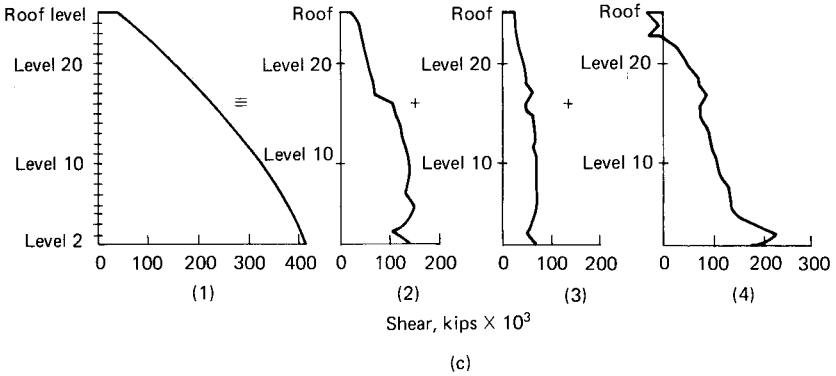

(c)

Figure 5.8 (*Continued*) (*c*) distribution of lateral loads: (1) applied lateral loads, (2) lateral loads resisted by end frames, (3) lateral loads resisted by interior frames, (4) lateral loads resisted by shear wall frames.

structural requirements without undue concern for the width of flying of forms.

The lateral load resistance in the short direction of the building is provided by a combination of three types of frames: (1) two exterior frames along grids 1 and 8, (2) two haunch girder frames along grids 2 and 7, and (3) four shear wall–haunch girder frames along grids 3 through 6. The lateral load resistance in the long direction is provided primarily by frame action of the exterior columns and spandrels along the broad faces.

For purposes of structural analysis, the building is considered symmetrical about the two centerlines as shown in Fig. 5.8*a*. The lateral load analysis can be carried out by lumping together similar frames and using only one-half the building in the computer model. This is shown in Fig. 5.8*b* for a two-dimensional computer model for the analysis of wind on the broad face. In the model only three equivalent frames are used to represent the lateral load resistance of eight frames present in the building and only one-half of each frame is used to simulate the structural action of a full frame. The latter simplification is achieved by restraining the vertical displacement at the end of each frame as shown in Fig. 5.8*b*. Note lateral spring restraints at the basement levels B1, B2, B3, and at the plaza are used to stimulate the lateral restraint of the basement walls and soil structure interaction. The rigid links shown in Fig. 5.8*b* between the individual frames simulate the diaphragm action of the floor slab by maintaining the lateral displacements of each frame the same at each level.

The purpose of the example is to show qualitatively the nature of interaction that exists between shear walls and frames in a building without abrupt changes in the stiffness of either element. We will not

burden the reader with an avalanche of computer results, but will limit the presentation to the distribution of horizontal shear in various frames. Part 1 of Fig. 5.8*c* shows the diagram of cumulative shear forces applied vertically along the broad face of the building. The distribution of the shear forces among the three types of frames is indicated in parts 2 to 4 of Fig. 5.8*c*. Note the reversal in the direction of the shear force at the top of shear wall-frame in part 4 of Fig. 5.8*c*, which indicates that the shear wall–frame combination has a tendency to behave as a propped cantilever, not unlike the behavior observed in the simplified shear wall–frame interaction model shown in Fig. 5.7. This is not surprising because although the practical example consists of a combination of three different types of frames, in essence the structural system can be considered as a single shear wall acting in combination with a frame. There are no sudden changes in the stiffness of walls or frames along the building height contributing to its departure from the fundamental behavior.

The example shown in Fig. 5.8 (although it is taken from the analysis of a real building) has very little in common with the usual types of structural systems that structural engineers are called upon to design. It is a rare event indeed to be commissioned to design a building that is symmetrical and has no significant structural discontinuity over its height. More usually, there is an asymmetry in the plan layout of various lateral and vertical load-resisting elements. Abrupt stiffness changes occur because either some of the shear walls or frames drop off or the building shape is changed vertically in response to massing and vertical sight line considerations. The reality of present-day architecture precludes generalization of even qualitative comments regarding the interaction between shear walls and frames that could be applied to a practical building. The structural engineer has very little choice but to use two- and three-dimensional analysis for determining the distribution of load among various elements. Standard interaction diagrams that were helpful in assigning the lateral loads to simple shear wall and frame systems have limited application and are therefore generally not used in practice and will not be discussed here.

As a second example, let us consider a contemporary high-rise building which has asymmetrical floor plans and abrupt variation in stiffness of shear walls and frames throughout its height. Figure 5.9 shows an artist's rendering and a computer-drawn perspective of a twin-tower high-rise office development called The Lone Star Towers, scheduled for construction in Dallas, Texas. The first phase of the complex consists of a four-level, 1600-car below-grade parking structure and a 1,000,000-ft^2 (92,903-m^2) office space. The building is 655 ft tall (200 m) and consists of 50 stories above grade. A variety of floor

(a)

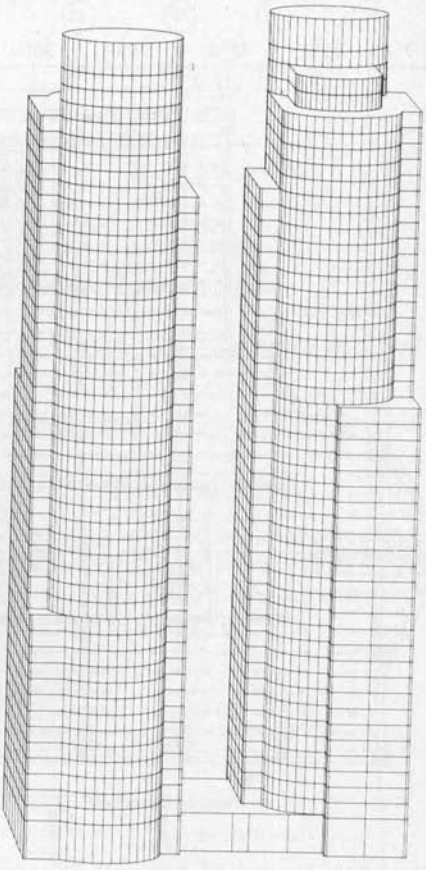

(b)

Figure 5.9 (*a*) Artist's rendering and (*b*) computer-drawn perspective of Lone Star Towers, Dallas. Interacting shear walls and haunch girder frames provide resistance to lateral loads. (Owner/developer, metropolitan/harbord joint venture; architects, Fujikawa Johnson & Associates, Inc., and Fisher and Spillman, Inc.; structural engineers, Ellisor & Tanner, Inc.) (*CAD view is courtesy of Heinz Winkler.*)

plans are accommodated between the second and the roof levels, resulting in a number of setbacks as shown in Fig. 5.10, with a major transfer of columns at level 40 (Fig. 5.10*d*). The floor plan, which is essentially rectangular at the second floor, progressively transforms into a circular shape at the uppermost levels. Figure 5.10*a* through *f* shows the framing plans at various levels. The resistance to lateral load is provided by a system of I- and C-shaped shear walls interacting with haunch girder frames. The floor framing is of lightweight concrete consisting of 6-in (152.4-mm) wide skip joists at 6-ft, 6-in (1.98-m) centers. The 20-in (508-mm) depth of haunch girders at midspan

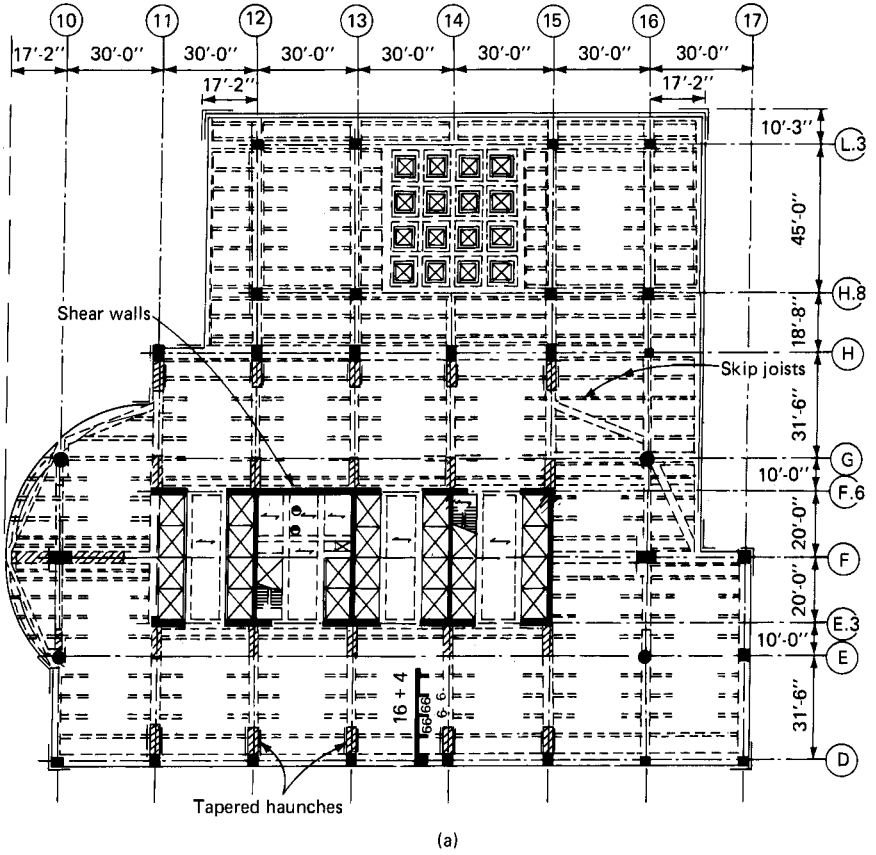

(a)

Figure 5.10 Example of shear wall–frame interaction in a 50-story building. (*a*) Levels 2 through 14 floor plan;

matches that of pan joist construction. Tapered haunches are used at both ends of girders and vary from a depth of 20 in (508 mm) at midbay to a depth of 2 ft, 9 in (0.84 m) at the face of columns and shear walls. High-strength normal-weight concrete of up to 10 ksi (68.95 MPa) is used in the design of columns and shear walls. The shear walls around low, mid, mid-low, mid-high, and high-rise elevators are either terminated or made smaller in their dimensions at various levels corresponding to the zoning of the vertical transportation. The analytical model necessarily resulted in a system of shear walls and frames which were asymmetrical not only with respect to the plan dimensions but also varied in stiffness over the building height. The final lateral load analysis was accomplished by using a three-dimensional computer model which included each and every structural member. The results were, however, verified by comparing the results with those of (1) a

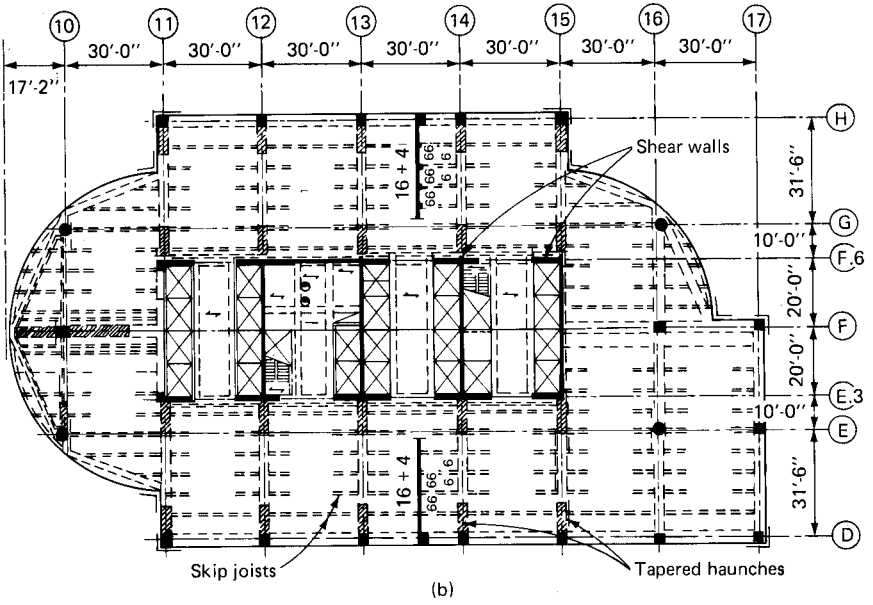

(b)

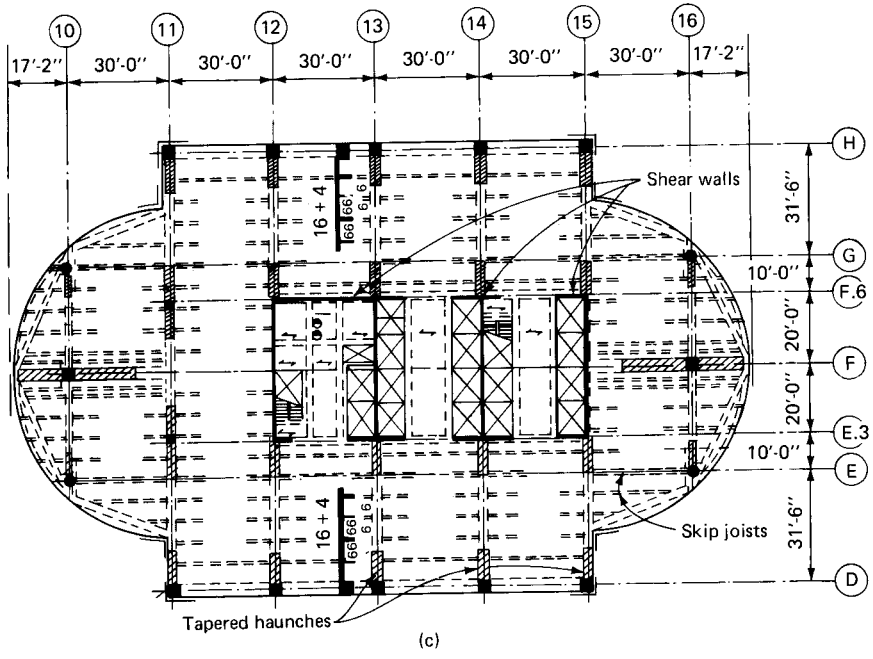

(c)

Figure 5.10 (*Continued*) (*b*) levels 15 through 26 floor plan; (*c*) levels 27 through 39 floor plan;

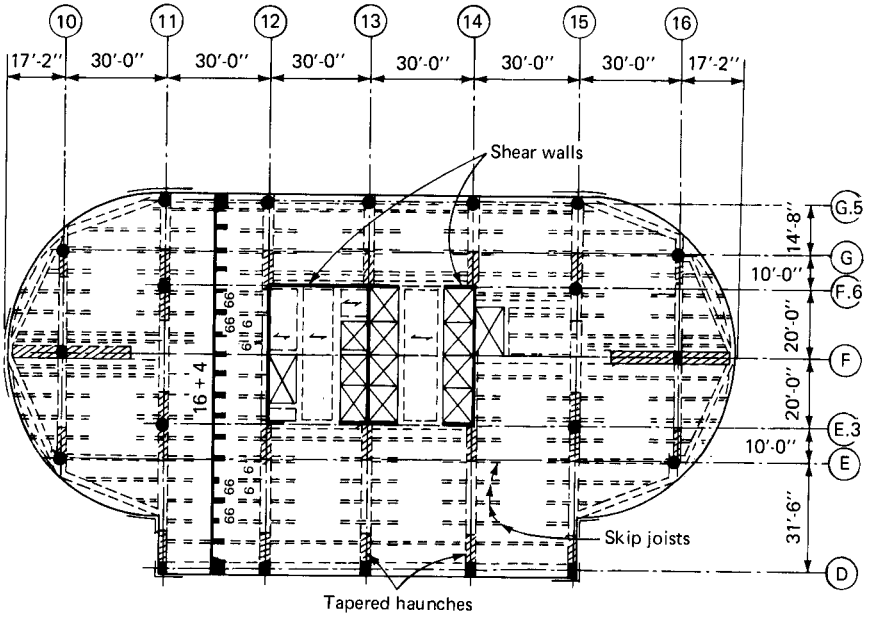

(d)

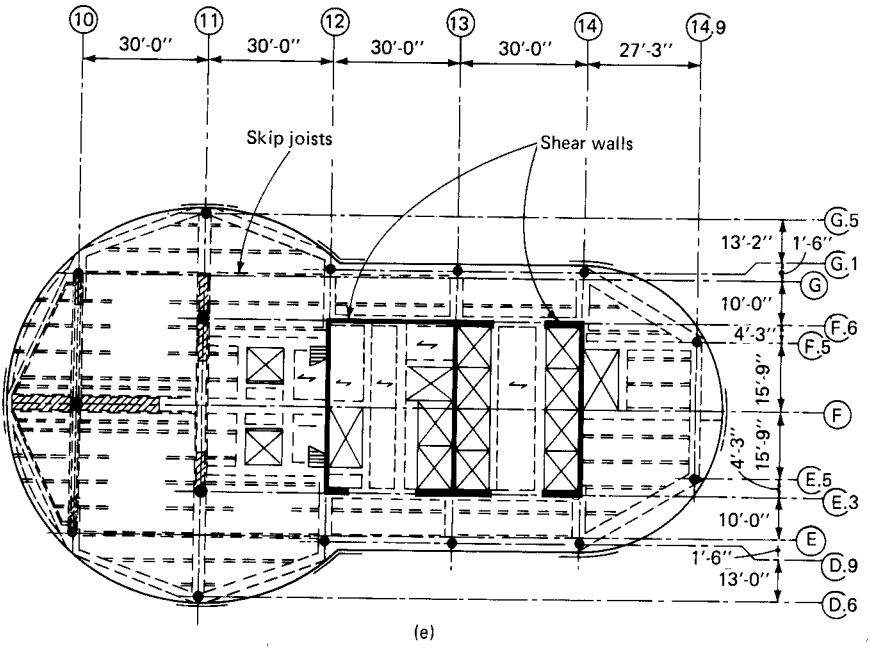

(e)

Figure 5.10 (*Continued*) (*d*) levels 40 through 47 floor plan; (*e*) levels 48 and 49 floor plan;

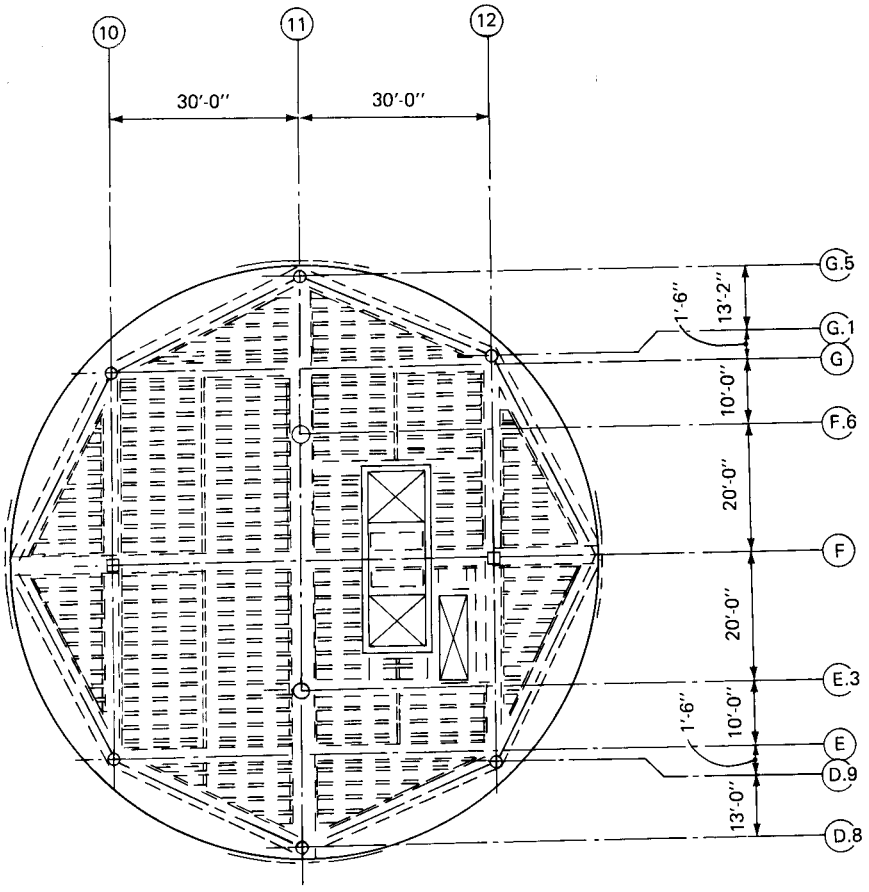

(f)

Figure 5.10 (*Continued*) (*f*) levels 50 and 51 floor plan.

relatively simpler three-dimensional model in which every other floor was lumped and (2) an equivalent shear wall and frame which represented the lateral stiffness of the building in the short direction. The agreement between the various computer results was within acceptable limits.

Figure 5.10*g* shows the distribution of horizontal shear forces among various lateral-load-resisting elements for wind loads acting on the broad face of the building. The lateral loads in the shear wall frames are shown by the curves designated as 12, 13, 14, and 15, which correspond to their locations on the grid lines shown in Fig. 5.10*a* through *f*. The shear forces in the frames are shown by curves designated as 10, 11, 16, 17, and 18. The results shown are from an

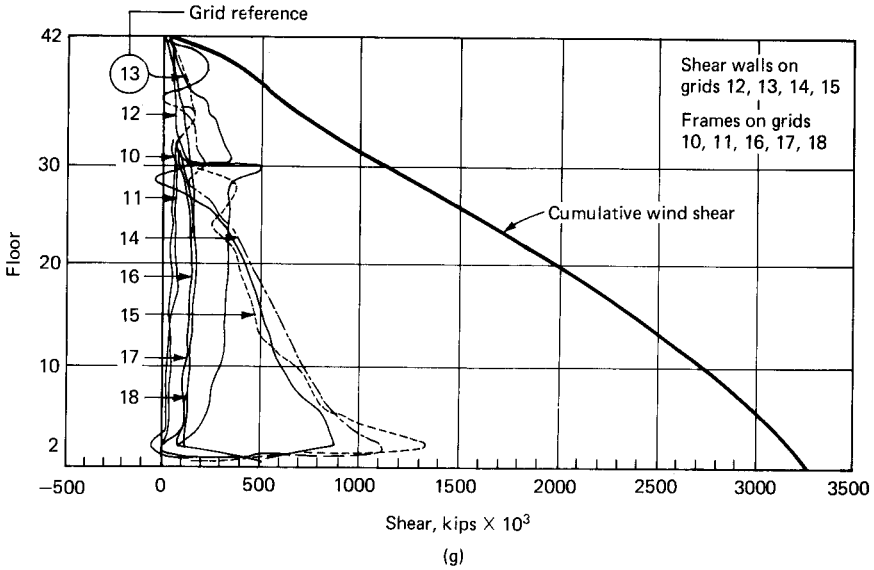

Figure 5.10 (*Continued*) (*g*) distribution of lateral loads.

earlier version of the tower, which consisted of 42 floors with slight modifications to the floor plans shown in Fig. 5.10.

The purpose of presenting limited results of the analysis is to show qualitatively how the distribution of transverse shear in a practical building is considerably different than in a structure with regularly placed, full-height shear walls and frames of fairly uniform stiffness. The large difference in the pattern of transverse shear distribution occurs for two reasons. First, the structure is complex, with stiffness varying significantly over the height. Second, the mathematical assumption of a rigid diaphragm that is commonly used in the modeling of the floor slab tends to bring about sharp shear transfers at levels where the stiffness of the building changes abruptly. Although it is possible to smooth out the harsh distribution and sudden reversals of transverse shear by modeling the floor slab as a flexible diaphragm by using finite elements, such a complex modeling technique will have little effect on the final shear wall design. Its effect on the design of the diaphragm, however, can be significant.

5.10 Frame Tube Structures

The tube concept is an efficient framing system for tall slender buildings. In this system, the perimeter of the building consists of closely spaced columns connected by a relatively deep spandrel. The resulting system works as a giant vertical cantilever and is very

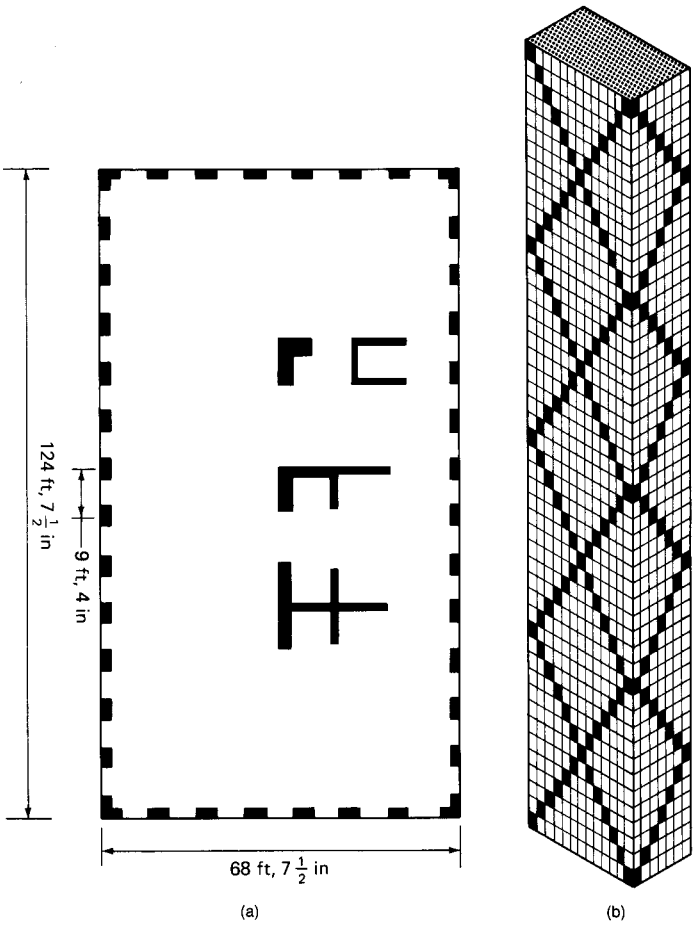

Figure 5.11 Exterior braced tube. (*a*) Plan; (*b*) schematic elevation. (Architects, Skidmore, Owings and Merrill; engineers, Robert Rosenwasser Associates.)

efficient because of the large separation between the windward and leeward columns. The tube concept in itself does not guarantee that the system satisfies stiffness and vibration limitations. The "chord" drift caused by the axial displacement of the columns and the "web" drift brought about by the shear and bending deformations of the spandrels and columns may vary considerably depending upon the geometric and elastic properties of the tube. For example, if the plan aspect ratio is large, say much in excess of 1:1.5, it is likely that a supplemental lateral bracing is necessary to satisfy drift limitations. The number of stories that can be achieved economically by using the tube system depends on a number of factors such as spacing and size of columns, depth of perimeter spandrels, and plan aspect ratio of the

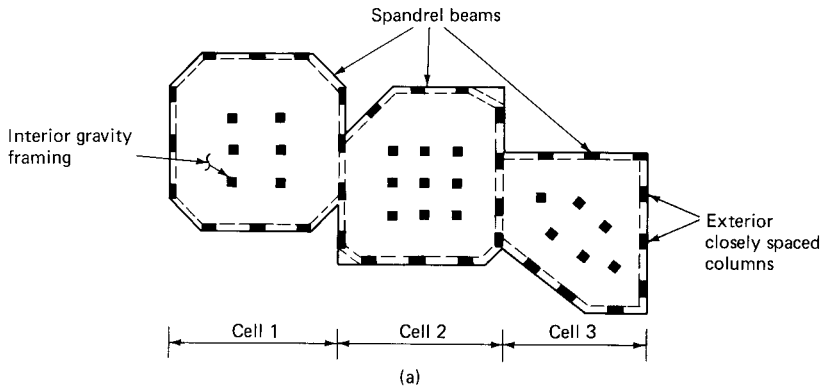

Figure 5.12 Bundled tube. (*a*) Schematic plan;

building. The system should be given serious consideration for buildings taller than about 40 stories. Other aspects of frame tube behavior will not be discussed here since they were already covered in Chap. 4.

5.11 Exterior Diagonal Tube

Master builder Fazlur Khan of Skidmore, Owings & Merrill envisioned as early as 1972 that it was possible to build high rises in concrete rivaling in height those in structural steel. His quest to find a structural solution for eliminating the shear lag phenomenon led him to the diagonal tube concept. A brilliant manifestation of this principle in steel construction is seen in the John Hancock Tower in Chicago. Applying similar principles, Khan visualized a concrete version of the diagonal truss tube consisting of exterior columns spaced at about 10-ft (3.04-m) centers with blocked out windows at each floor to create a diagonal pattern on the facade. The diagonals could then be designed to carry the shear forces, thus eliminating bending in the tube columns and girders. Although Khan enunciated the principle in the 1970s, the idea had to wait almost 15 years to find its way to a real building. Currently, two high rises have been built using this approach. The first is a 50-story office structure located on Third Ave. in New York and the second is a mixed-use building located on Michigan Ave. in Chicago. The structural system for the building in New York consists of a combination of a framed and trussed tube interacting with a system of interior core walls. All the three subsystems, namely, the framed tube, trussed tube, and shear walls, are designed to carry both lateral and vertical loads. The building is 570 ft (173.73 m) high with an unusually high height-to-width ratio of 8:1. The diagonals created by filling in the windows serve a dual function. First, they increase the efficiency of the tube by diminishing the shear lag, and second they

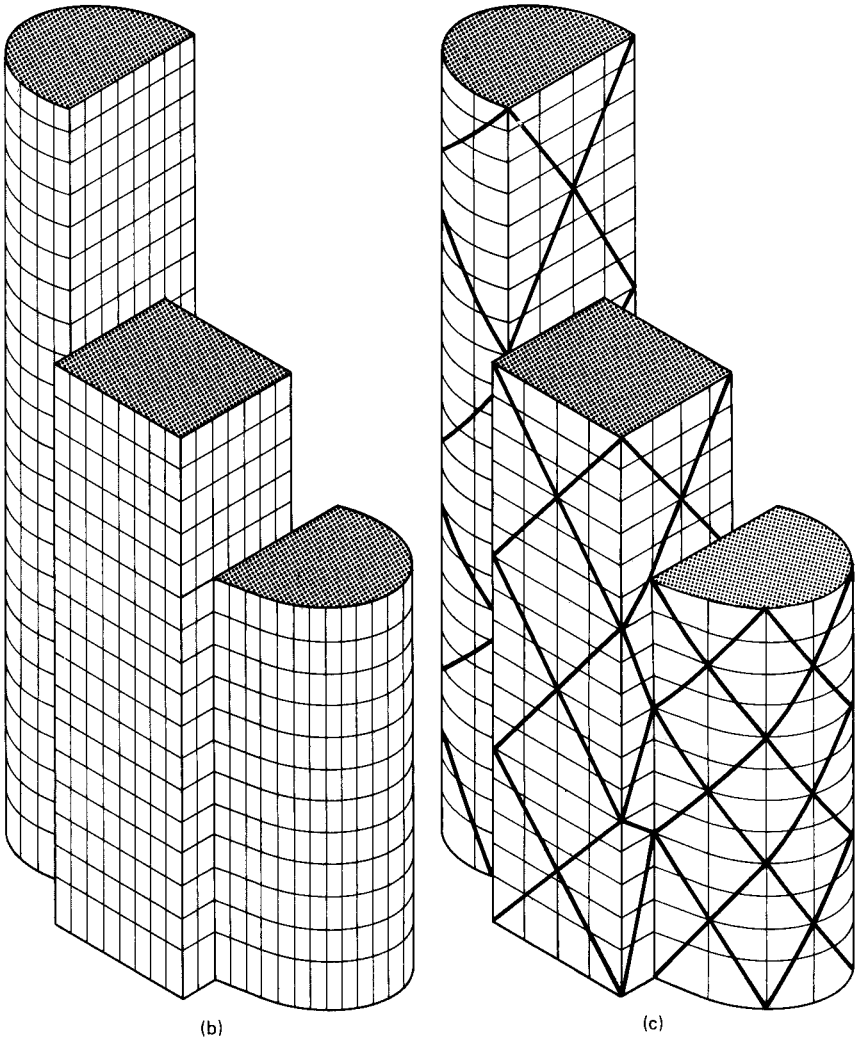

Figure 5.12 (*Continued*) (*b*) Framed bundled tube; (*c*) diagonally braced bundled tube.

reduce the differential shortening of exterior columns by redistributing the gravity loads. A stiffer, much more efficient structure is realized with the addition of diagonals. The idea of diagonally bracing this structure was suggested by Fazlur Khan to the firm of Robert Rosenwasser Associates, who executed the structural design for the building. Schematic elevation and floor plan of the building are shown in Fig. 5.11.

The Chicago version of the braced concrete tube is a 60-story multiuse project. The building rises in two tubular segments above a flared base. According to the designers, diagonal bracing was used primarily to allow maximum flexibility in the interior layout needed for mixed uses. In contrast to the building in New York, which has polished granite as cladding, the Chicago building sports exposed concrete framing and bracing.

5.12 Modular or Bundled Tube

The concept of bundled tube in concrete high rises is similar to that discussed in Chap. 4 under steel systems. The underlying principle is to connect two or more individual tubes in a bundle with the object of decreasing the shear lag effects. Figure 5.12*a* shows a schematic plan of a bundled tube structure. Two versions are possible using either framed or diagonally braced tubes as shown in Fig. 5.12*b* and *c*. A mixture of the two is, of course, possible.

Chapter

6

Lateral Systems for Composite Construction

6.1 Introduction

In a broad sense almost all high-rise buildings are of composite construction because it is very rare indeed, if not impossible, to construct a functional building using a single material. For example, concrete is invariably required to provide a flat surface in an otherwise all steel building. Similarly, in a large sense, use of mild and posttensioned steels has made concrete buildings composite. Likewise, almost all steel buildings built recently have used composite metal deck and composite floor beams of one type or another for carrying gravity loads. Although composite systems are more commonly used for carrying gravity loads than lateral loads, we will not dwell on the gravity systems in this chapter. Only the overall composite design techniques for lateral systems wherein two or more distinctly different subsystems are called upon to resist lateral loads are considered in this chapter. Composite gravity systems are dealt with separately in Chapter 9.

For tall buildings the economics of concrete versus steel could go either way, necessitating the cost comparison for each project to determine which is more economical. Apartment houses and hotels are an exception because they tend to be concrete-framed buildings, and in such buildings the underside of the concrete floor slab can be used as

finished ceiling. Unlike office buildings, the air conditioning duct work required in a hotel or condominium is relatively simple and thus there is no need for hung ceilings. On the other hand, an office building can be made of either steel or reinforced concrete; the choice, although it depends to a great extent on the in-place cost of the frame, is nevertheless influenced by the speed of construction. If the building can be constructed faster with a particular material and can bring a return on the investment sooner, the speed of construction necessarily enters the cost equation. The choice of the frame, in other words, is based not on its cost alone but on the speed of construction as well. Both steel and concrete possess advantages and disadvantages as structural materials. It follows, therefore, that an ideal structural system is one that overcomes the disadvantages and exploits the advantages of both materials in a unified structural system.

Structural steel is well suited for providing the generally column-free lease space required in contemporary high-rise office buildings. Using high-strength structural steel, building cores enclosing the services can be efficiently condensed without unduly disrupting the leasability of floor space. Also, because of its light weight, steel construction imposes less severe foundation requirements and goes up faster. Minimizing the building weight might be a consideration where the soil conditions are poor, requiring special and costly foundation systems. Also readily apparent as an advantage of steel construction, is the use of steel decking for floor construction, offering a more flexible system for wiring a building than a solid concrete slab, making it easy to change wiring to meet the requirements of new tenants. Also a steel frame is simpler to modify to meet the changing needs of tenants over the life of the building. With steel framing it is less expensive to increase the load capacity of the floor framing system or cut holes in the floor to install stairways, atriums, etc. The owner is interested in keeping the building economically viable long enough to make the investment worthwhile. Therefore, adaptability to renovation and rehabilitation is an important factor.

At the same time, concrete buildings possess their own advantages as a result of recent innovations. Chief among them are the advent of superplasticizers and high-strength concretes, which have made possible the construction of a reinforced concrete frame for a tall office building without columns getting cumbersomely large. Floor framing techniques have progressed from flat slab construction to skip joist and haunch girder systems, resulting in an increase in the spanability of concrete floor systems. Lateral bracing systems have been developed that rival those of steel systems. The advantages of concrete framing are low material cost, moldability, insulating and fire-resisting quality, and most of all, its inherent stiffness. However, in relation to steel

construction, concrete construction is slow, which is a major disadvantage in light of today's ever-higher field labor costs. If the value of time is excluded from the cost picture, concrete is likely to be the most economical material for high-rise buildings.

The two basic building types, concrete and steel framing, evolved independently of each other, and buildings were conceived either as a pure structural steel or as reinforced concrete. Up until the 1960s, engineers were trained to think of tall buildings either in steel or concrete. Fazlur Khan broke this barrier in 1969 by blending steel and concrete into a single system that he used on a relatively short 20-story building. The building's frame essentially used structural steel with the exterior columns and spandrels encased in concrete to provide lateral resistance for the building.

Structural steel was used primarily for its strength, speed of construction, and flexibility in interior space planning, whereas reinforced concrete was used on the exterior for its fireproofing, moldability, and stiffness characteristics. Simply stated, the earlier composite system was a steel frame stabilized by reinforced concrete.

The understanding of the relative economics of steel and concrete has resulted in growing use of combinations of these materials. Designers have overcome the steel versus concrete hangup and have come up with many innovative combinations. As already stated, the major advantages of steel are its speed of construction, a high strength-to-weight ratio, and the relative ease with which complex arrangements such as truss and space frames can be fabricated. The high strength of steel leads to compact columns and low foundation loads. Concrete, on the other hand, is more economical for providing axial or shear rigidity in structural systems. The optimum combination for a very tall building will combine the economy of concrete for carrying axial loads and provide rigidity under lateral loads with the speed of steel erection.

The term *composite system* has taken on numerous meanings in recent years because of the several different combinations that have resulted from mixing and matching steel and concrete. As used here, the term means any and all combinations of steel and reinforced concrete elements and is considered synonymous with other definitions such as mixed systems and hybrid systems. The term is generally used to encompass both gravity- and lateral-load-resisting elements. Besides the economy of the materials, composite buildings have the advantage of speed of construction by virtue of the vertical separation of the structural construction activity. Inherent stiffness of concrete is used to more easily control building drift under lateral loads and perception of motion by the occupants at the upper levels. The required strength is obtained by judicious use of structural steel. The combina-

tion of concrete and steel frequently results in building systems that are more economical than either all steel or all concrete systems.

Since the advent of the first composite system, engineers have not hesitated to use a whole range of combinations by selecting appropriate material for each part of the structure so as to capitalize on the advantages of both materials. Needless to say, there are many composite systems, making distinct categorization a nearly impossible task.

The different composite systems that are currently in vogue for high-rise construction can best be understood by referring to several examples, some taken from actual structures built within the past decade. This format helps to keep the discussion simple without having to categorize the complete spectrum of composite construction. Design assumptions and theory associated with each system are briefly discussed to highlight the validity of certain combinations.

6.2 Composite Elements

In order to get a broad picture of composite schemes that are popular for high-rise office buildings, it is instructive to consider the different elements of the buildings that lend themselves to composite construction. These are (1) slab systems; (2) beams, girders, and spandrels; (3) columns; and (4) shear walls.

6.2.1 Slab systems

Use of high-strength light-gauge metal decks with embossments in their ribs to achieve composite action with structural concrete has become almost a standard method of construction for high-rise buildings in North America. This is understandable because in a typical concrete building it is the forming and placing of concrete for the floor that takes up most time requiring much labor just for material handling. Substituting structural steel beams and metal deck greatly simplifies the construction process.

6.2.2 Beams, girders, and spandrels

A typical moment frame in a steel building consists of steel columns and girders along grid lines and invariably a composite metal deck with a concrete topping as the floor system. If the lateral-load-resisting element is a full or partial tube, the system consists of closely spaced columns and deep spandrels. As pointed out in Chap. 4, the stiffness of the frame to a large extent depends upon the stiffness of the girder. Any increase in girder stiffness is likely to result in substantial increase of the frame stiffness because normally in a nontubular

building the relative stiffness of the column is usually much larger than the beam stiffness because of its shorter length. To achieve savings in gravity design and create better deflection characteristics, steel buildings normally employ composite beams with the use of welded shear connectors. Some engineers do not specify shear connectors for moment-connected beams and use only the properties of the steel section for computing the stiffness and strength of the frame. However, since shear connectors are being used on the job anyway, it is worthwhile to investigate the use of composite moment-connected beams as part of the moment frame. The stiffness of composite beams in a typical steel building is at least 40 to 50 percent more than a steel beam in the positive region. However, for lateral loads, moment-connected beams respond by bending in double curvature. Since concrete is ineffective in tension, the composite properties can be counted on only in the positive moment region, resulting in a beam with two distinct moments of inertia. Although design rules are not well established, a rational method can be used to achieve potential savings in structural steel.

6.2.3 Columns

A frequently used item in composite design is the composite column, which can be defined as a vertical element in which longitudinal and horizontal reinforcing bars are arranged around a steel column. Concrete is then placed around the steel core to provide a composite column. The steel section, reinforcing bar, and concrete all act together to resist the bending moments, shear, and axial forces. One can imagine the composite column as a section with reinforced bars by replacing the steel section with additional mild steel reinforcement of the same volume.

Most frequently the steel column is designed to carry the dead load and construction load of a limited number of stories during construction. The idea is to combine the erection speed of structural steel with the economy of reinforced concrete in compression. A composite column of this type will result in considerable economy in the use of structural steel. A disadvantage of a composite column is the difficulty in building interior columns. Usually interior columns have steel beams framing into them on all four sides, which complicates the placement of mild steel reinforcement around the steel columns and placing and removal of column forms. Exterior columns, on the other hand, are open-faced, and for that reason are easier to composite. Hinges on form work allow the form to wrap around steel columns and then unwrap after concrete is poured and set. Once unwrapped, form work is jumped to the next floor and the cycle is repeated. The

development of jump forms is the key reason for favorable economics of exterior composite construction.

As mentioned in Chap. 4, the response of a structural system is made up of contributions from column shortening and bending and shear deformations of columns and girders. The column-shortening effect, or the so-called chord drift of the system, increases in importance as buildings become taller and more slender. The major problem is to provide sufficient rigidity in the columns to limit the chord drift. Use of composite columns with a large concrete envelope results in a substantial reduction in the building drift because of the high axial stiffness of concrete columns as compared to steel columns.

6.2.4 Shear walls

Shear walls in high-rise construction can be conveniently used around the cores for enclosing the building services. The walls are usually C or I shapes interconnected with coupling beams. In one version of composite construction, the interconnecting link beam is made of structural steel as shown in Fig. 6.1. Steel erection columns are used at the intersection of web and flanges of the shear wall. The steel link beam is shear-connected to steel columns and the required moment capacity is obtained by welding shear studs to the top and bottom flanges of the beam as shown schematically in Fig. 6.2.

As noted in Chap. 4, shear walls are sometimes called upon to resist large shear forces that result from the transfer of major wind-resisting elements, such as tube columns or X braces. A composite shear wall consisting of stiffened steel plates and reinforced concrete may be conveniently used for resisting high shear stresses. The steel plate and the concrete wall are made to act compositely by the use of shear studs as shown in Fig. 6.3.

6.3 Composite Systems

Even with the cacophony of composite systems in use today, for purposes of presentation it is convenient to classify the major systems into the following categories.

1. Shear wall systems
2. Shear wall–frame interacting systems
3. Tube systems
4. Vertically mixed systems

A brief description of each follows.

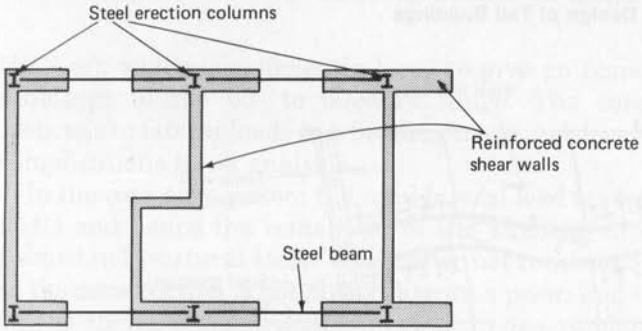

(a)

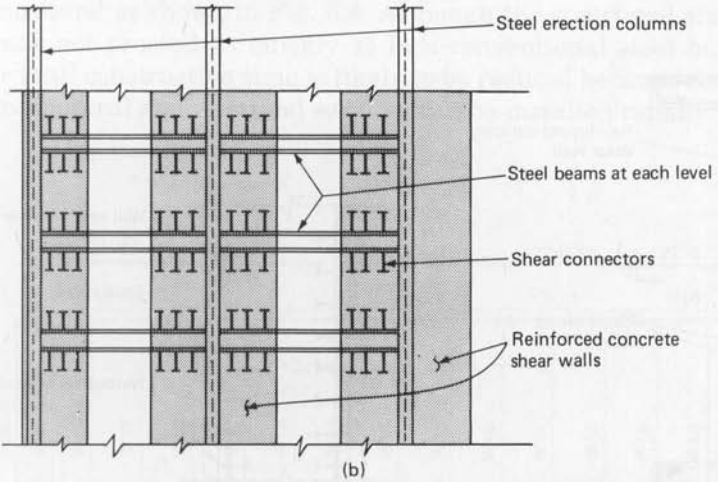

(b)

(c)

Figure 6.1 Composite shear wall with steel beams. (*a*) Plan; (*b*) elevations; (*c*) photograph (note that steel beams run both parallel and perpendicular to shear wall).

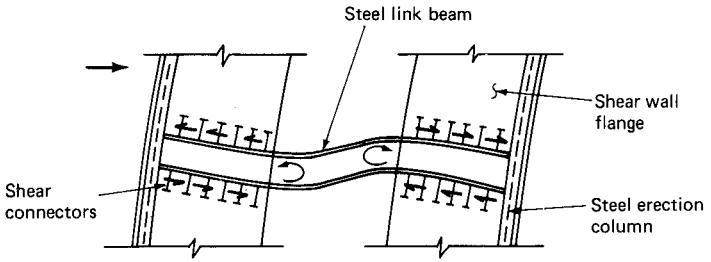

Figure 6.2 Moment transfer between steel beam and concrete wall.

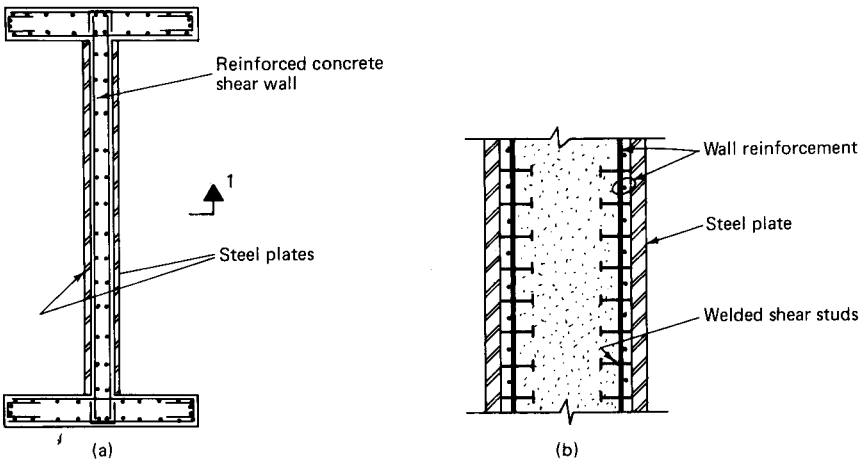

Figure 6.3 Composite shear wall with steel plates. (*a*) Plan; (*b*) section 2.

6.3.1 Shear wall systems

Core walls enclosing building services such as elevators, mechanical and electric rooms, and stairs have been used extensively to resist lateral loads in tall concrete buildings. Simple forms such as C and I shapes around elevators interconnected with coupling or link beams are used extensively. Their popularity as a lateral-load-resisting element has once again come to the forefront because of the current trend in architecture which appears to favor lean vertical elements around the perimeter. Earlier applications of this system were limited to buildings in the 30- to 40-story range, but with the advent of superplasticizers and high-strength concrete, it is now possible to use this system for taller buildings in the 50- to 60-story range. The range of application is mostly a function of available depth of core. Buildings using four-deep elevators provide a core depth of approximately 40 ft.

(12.2 m), which is sufficiently large to give an economical system for buildings in the 50- to 60-story range. The shear core basically responds to lateral loads in a bending mode and does not present undue complications in its analysis.

In the core-only system the total lateral load is resisted by the shear walls and hence the remainder of the building can be conveniently framed in structural steel. Whether or not concrete or steel comes first in the construction is not always known a priori and is often influenced by the choice of construction method. In one version, concrete core is cast first by using jump or slip forms, followed by erection of the steel surround as shown in Fig. 6.4. Although the structural steel framing may not proceed as quickly as in a conventional steel building, the overall construction time is likely to be reduced because elevators and mechanical and electrical services can be installed rapidly in the core

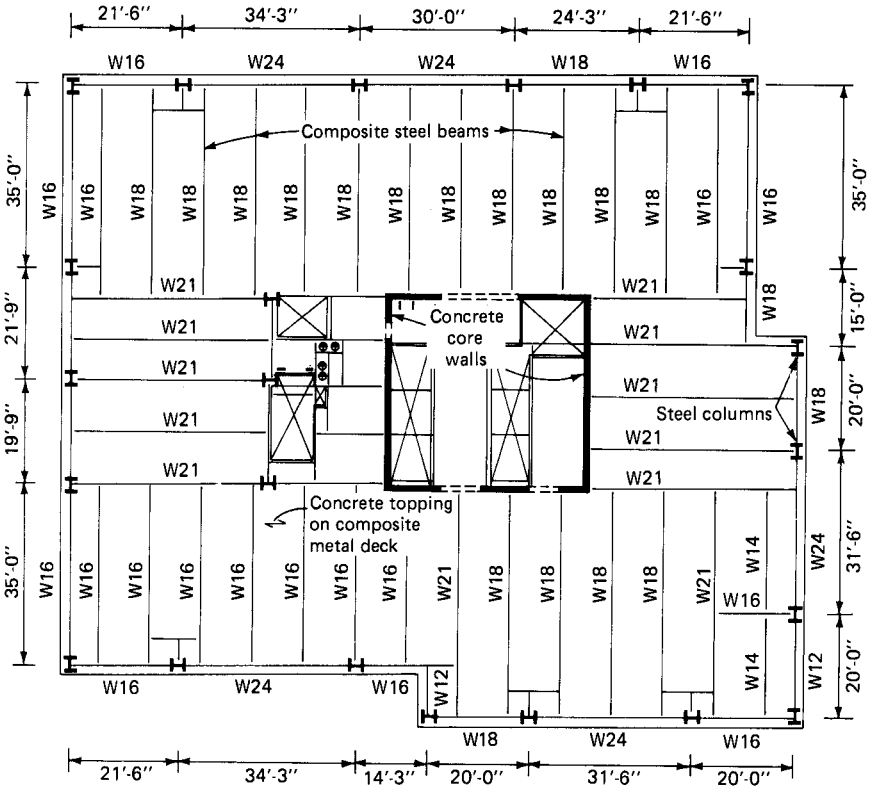

Figure 6.4 Typical floor plan of core structure with steel surround. (Courtesy of Steve Ball and Heinz Winkles of Ellisor & Tanner, Inc.)

while construction outside the core proceeds. In another version, steel erection columns are used within the shear walls to serve as erection columns and steel erection proceeds as in a conventional steel building. After the steel erection has reached a reasonable level, concreting of core starts using conventional forming techniques. In order to facilitate faster jumping of forms to the next higher level, temporary openings are left in the floor slab around the shear walls.

The structural behavior of this system is no different than a concrete building with shear walls designed to take all the lateral forces. However, it behooves the engineer to recognize the absence of torsional stiffness, so readily present in concrete construction, in core-only composite buildings. It is advisable to provide some moment frames or other form of bracing around the building perimeter to counteract torsional effects.

If all the lateral loads are resisted by concrete shear walls, the steel surround is designed as a simple framing for gravity loads only. Since there are no moment connections involving welding or heavy bolting, the erection of steel proceeds much faster. The only nonstandard connection is between the shear walls and floor beams. Various techniques have been developed for this connection, chief among them, the embedded plate and pocket details, as shown in Fig. 6.5*a*. The floor construction invariably consists of composite metal deck with a structural concrete topping. This system has the advantage of keeping the steel fabrication and erection simple. Since columns carry only gravity loads, high-strength steel can be employed with the attendant savings. Interior as well as exterior columns can be made small, increasing the space-planning potential. However, buildings in seismic zones need to be designed with certain moment frames to provide the required ductility.

The floor within the core can be constructed either with cast-in-place beams and slabs or structural steel framing, steel decking, and concrete fill. At the connection between the floor slabs, both within and outside of the core shear keys are provided in the core walls to transmit lateral diaphragm forces from the floor system to the core. Although several options are available for connecting the steel beams to the concrete core, a weld plate detail shown in Fig. 6.5*a* is most popular, especially so in a slip-formed construction. During slip-form operation, the weld plates are set at the required locations, with the outer surface of the plate set flush with the wall surface. Anchorage of the weld plate is achieved by shear connectors welded to the inner surfaces, sometimes supplemented with a top-bent steel bar to resist high tensile forces. The shear connectors and steel bar ultimately become embedded in the core wall. It is a good practice to oversize the plates to allow for placement tolerance. Experience with slip-formed composite buildings indicates that it is prudent to overdesign these connections to compensate for misalignment of cores. Subsequent to the installation

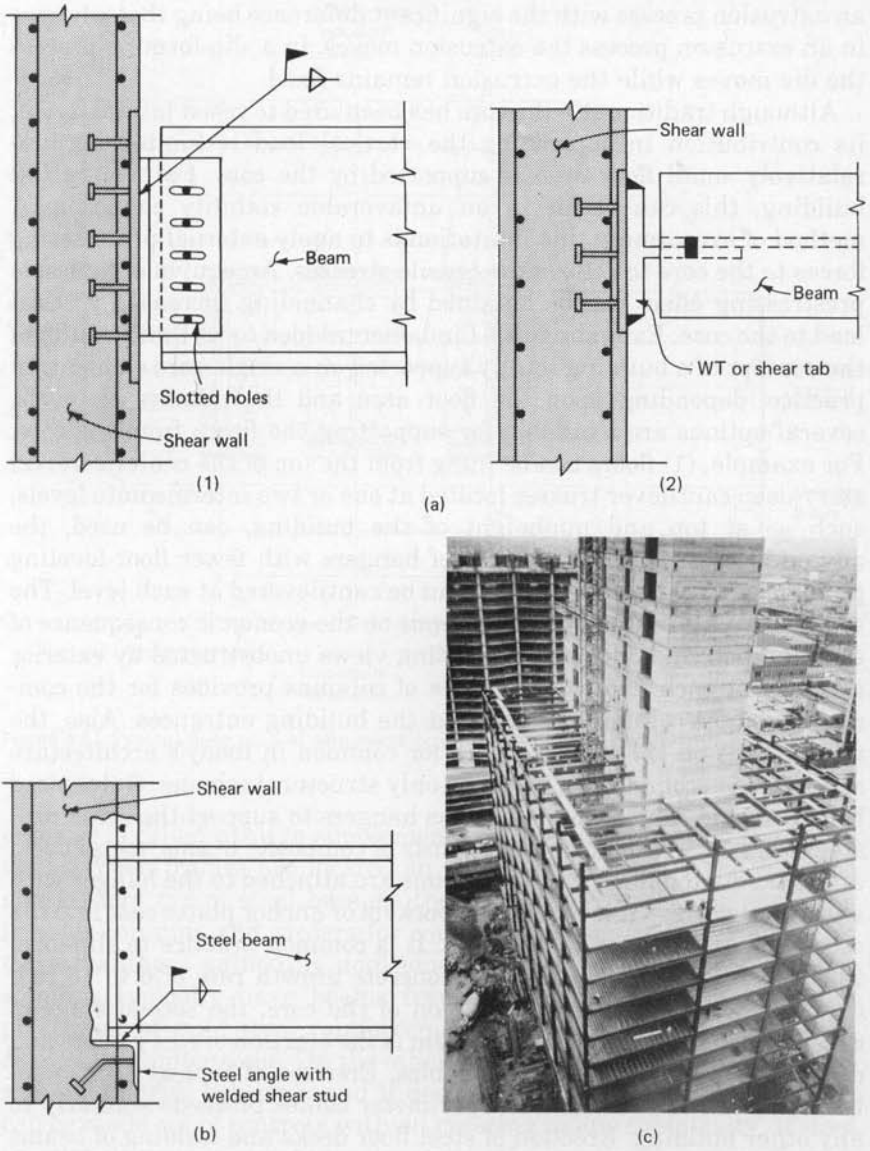

Figure 6.5 Beam to shear wall connection. (*a*) Embedded plate detail: (1) elevation; (2) plan; (*b*) pocket detail; (*c*) Photograph of composite building with shear core and steel surround.

of weld plates, structural tee or shear tab connections with slotted holes are field-welded to the plate. Slotted holes are used for bolting of steel beams to provide additional tolerance for erection.

Slip forming is a special construction technique that uses a mechanized moving platform system. The process of slip forming is similar to

an extrusion process with the significant difference being that whereas in an extrusion process the extrusion moves, in a slip-forming process the die moves while the extrusion remains fixed.

Although traditionally the core has been used to resist lateral forces, its contribution in supporting the vertical load is limited because relatively small floor area is supported by the core. For a very tall building, this can result in an unfavorable stability condition. A method of overcoming this limitation is to apply external prestressing forces to the core to relieve the tensile stresses. An equivalent passive prestressing effect can be obtained by channeling increased vertical load to the core. Extending this fundamental idea to its limit results in the concept of a building totally supported on a single-core element. In practice, depending upon the floor area and the number of levels, several options are available for supporting the floors from the core. For example, (1) floors can be hung from the top of the center core; (2) story-deep cantilever trusses located at one or two intermediate levels, such as at top and midheight of the building, can be used, the advantage being reduced length of hangers with fewer floor-leveling problems; or (3) the floor system can be cantilevered at each level. The selection of a suitable system depends on the economic consequence of each method. In addition to providing views unobstructed by exterior columns at each floor, the absence of columns provides for the commonly sought column-free space at the building entrances. Also, the undulations on the building exterior common in today's architecture are easy to accommodate in a core-only structural scheme. Galvanized bridge-strand cables can be used as hangers to support the structural steel framing which normally consists of composite beams, metal deck, and concrete topping. The floor beams are attached to the hanger with simple supports, while at the core pockets or anchor plates cast into the core walls provide for the support. It is common practice to slip-form the center core with an average concrete growth rate of 6 to 18 in/h (152 to 457mm/h). After completion of the core, the second stage of construction in the hung-floor system is the erection of roof girders and draping of the floor-supporting cables. Erection of typical floor members between the core and the perimeter cables proceeds similarly to any other building. Erection of steel floor decks and welding of beams for composite action follows by placement of concrete topping. Because the elongation of the cable due to cumulative floor loads can be substantial, it is necessary to compensate for this effect properly.

6.3.2 Shear wall–frame interaction

This system has applications in buildings which do not have cores sufficiently large to resist the total lateral loads; interaction of shear walls with other moment frames located in the interior or at the

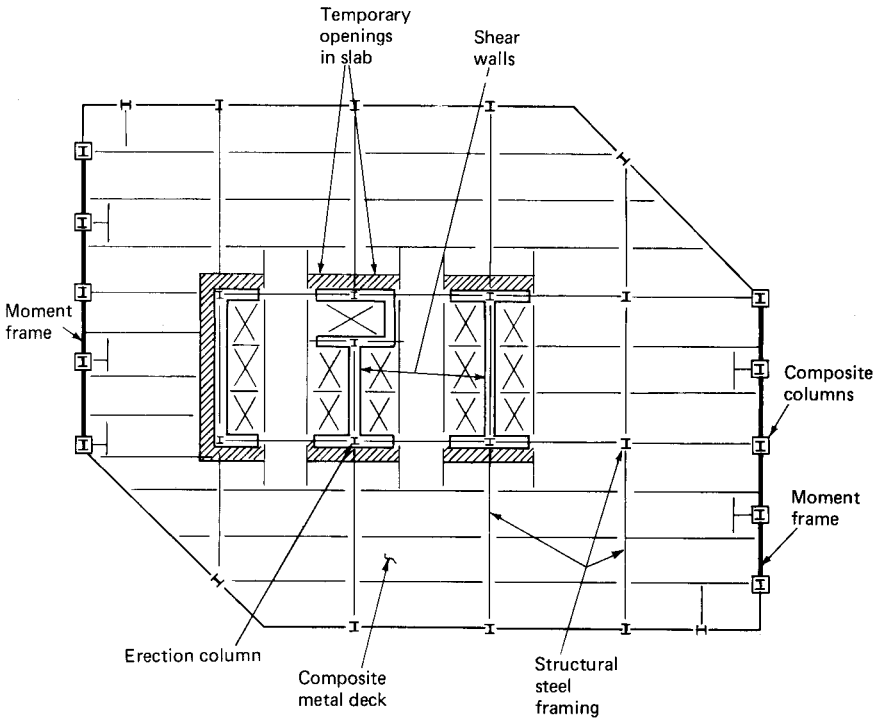

Figure 6.6 Typical floor plan of composite building using shear wall–frame interaction.

exterior is called upon to supplement the lateral stiffness of the shear walls. When frames are located on the interior, usually the columns and girders are of steel because the cost of form work for enclosing interior columns and girders for composite construction far outstrips the advantages gained by additional stiffness of the frame. Interior columns typically have beams framing in four directions, making placement of mild steel reinforcement and form work around them extremely cumbersome. On the other hand, it is relatively easy to form around exterior columns, and if desired, even the exterior spandrels can be made out of concrete without creating undue complexity. If steel erection precedes concrete construction, it is usually more cost effective to use steel beams as interconnecting link beams between the shear walls. A schematic plan of a building using this system is shown in Fig. 6.6.

6.3.3 Tube systems

A framing system used extensively in Louisiana and Texas is known as the composite concrete tube. It makes use of the well-known virtues

of tube system with the speed of steel construction. As in concrete and steel systems, closely spaced columns around the perimeter and deep spandrels form the backbone of the system. Two versions are currently popular: one system uses composite columns and concrete spandrels and the other uses structural steel spandrels in place of concrete spandrels. A small steel section can be used as a steel spandrel in the former scheme to stabilize the steel columns. However, in the design of the concrete spandrel, its contribution of the strength and stiffness is generally neglected because of its relatively small size. Schematic plan and sections for the two versions of tubular system are shown in Figs. 6.7 and 6.8.

In either system, the speed of construction, rivaling that of an all-steel building, is maintained by building a steel skeleton first with interior steel columns, steel floor framing, and light exterior columns. Usually the steel frame is erected some 10 to 12 stories ahead of the perimeter concrete tube. The key to the success of this type of construction lies in the rigidity of closely spaced exterior columns, which, together with deep spandrels, results in an exterior facade that behaves more like a bearing wall with punched windows than a moment frame.

6.3.4 Vertically mixed systems

Mixed-use buildings, wherein two or more types of occupancies are provided in a single building by vertically stacking different amenities, are popular. For example, the lower levels of a building may house parking; the middle levels, office floors; and the top levels, residential units, such as apartments and hotel rooms. Since different types of occupancies economically favor different types of construction, it seems logical to use mixed construction vertically along the building height. As mentioned earlier, beamless flat ceilings are preferred in residential occupancies because of the minimum finish required underneath the slab. Also, the large spans of the order of 40 ft (12.2 m) required for optimum lease space for office buildings are too large for apartments. Additional columns can be introduced without unduly affecting the architectural layout of residential units. The decrease in span combined with the beamlessness of flat-plate construction gives the engineer an opportunity to use concrete in the upper levels.

In certain types of buildings, use of concrete for the lower levels and structural steel for the upper levels may provide the optimum solution. Shown in Fig. 6.9 is a scheme which uses concrete for the lower levels and structural steel for the upper floors. The bracing for the concrete portion of the building is provided by the shear walls, while the braced steel core provides the lateral stability for the upper levels. A sug-

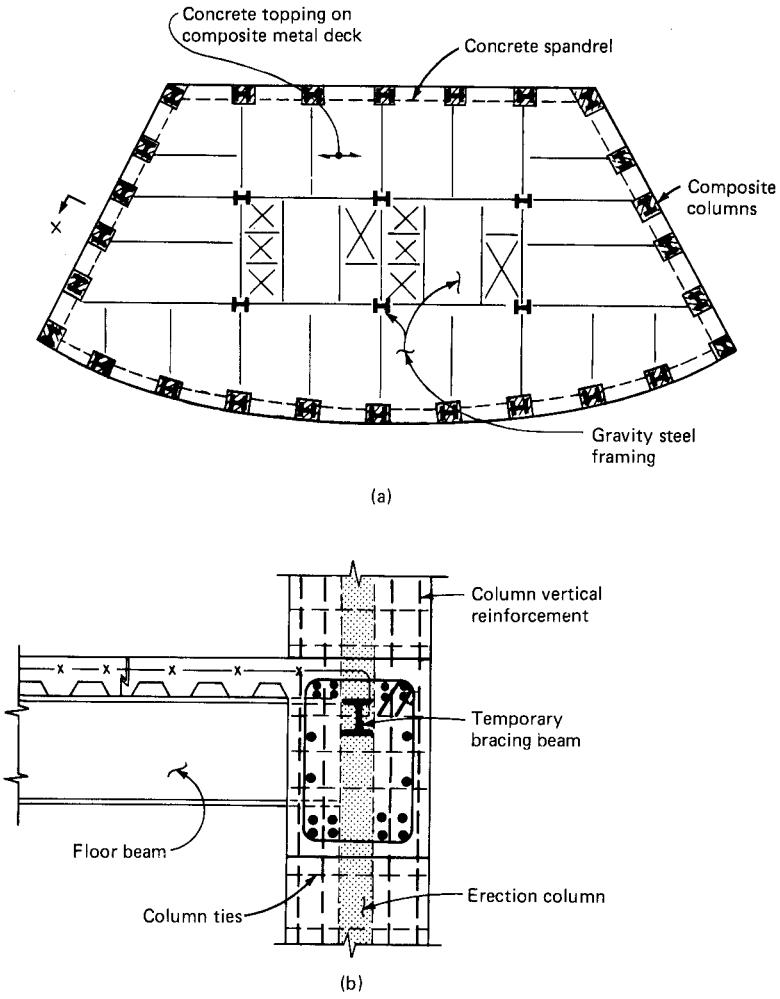

Figure 6.7 Composite tube with concrete spandrels. (*a*) Typical floor plan; (*b*) typical exterior cross section.

gested technique of transferring steel columns onto a concrete wall consists of embedding a steel column for one or two levels below the transfer level. Shear studs shop-welded to the embedded steel column provide for the transfer of axial loads from steel column to the concrete walls.

6.4 Case Histories

The remainder of this chapter gives brief case histories of three variations of composite systems that have been successfully used in

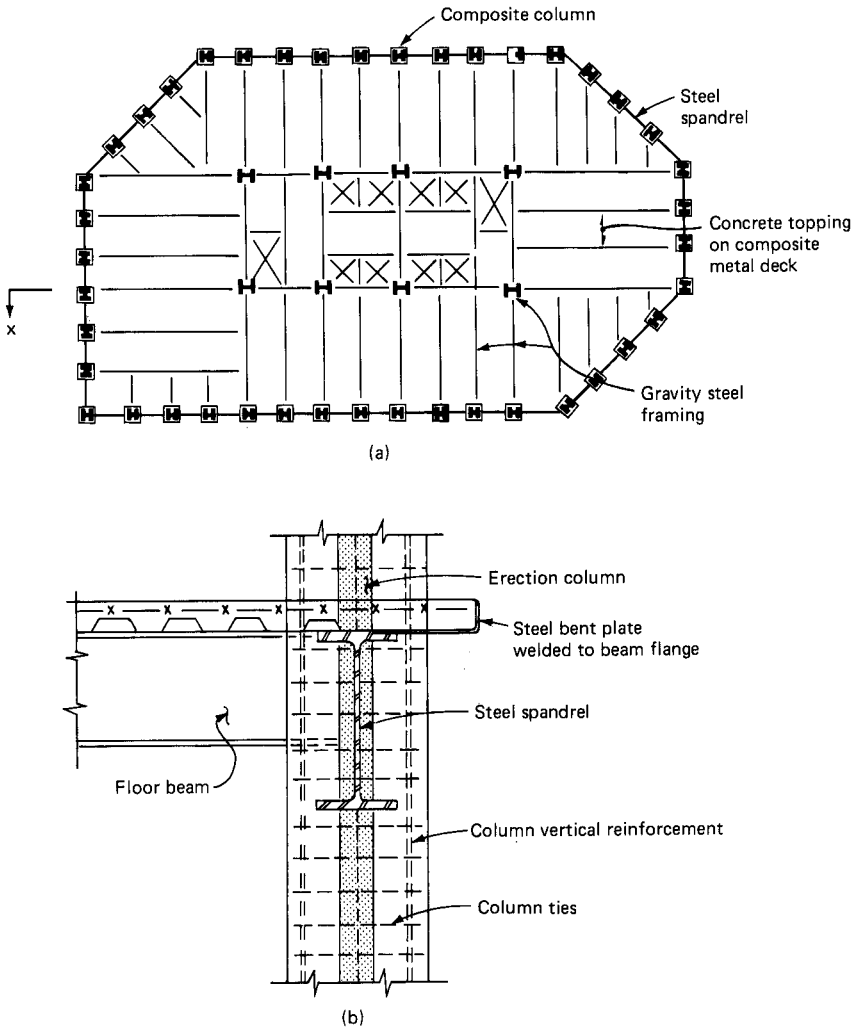

Figure 6.8 Composite tube with steel spandrels. (*a*) Typical floor plan; (*b*) typical exterior cross section.

high-rise buildings in Houston, Texas. The author was the principal engineer for these projects with the structural firm of Walter P. Moore and Associates. The projects demonstrate the underlying structural philosophy in bringing together steel and reinforced concrete to benefit from the advantages of both materials: the inherent stiffness and economy of concrete and the speed of construction of the conventional steel building. The first is an interacting system of composite shear walls and composite frames; the second is a tubular system with composite exterior columns and steel spandrel beams; and the third

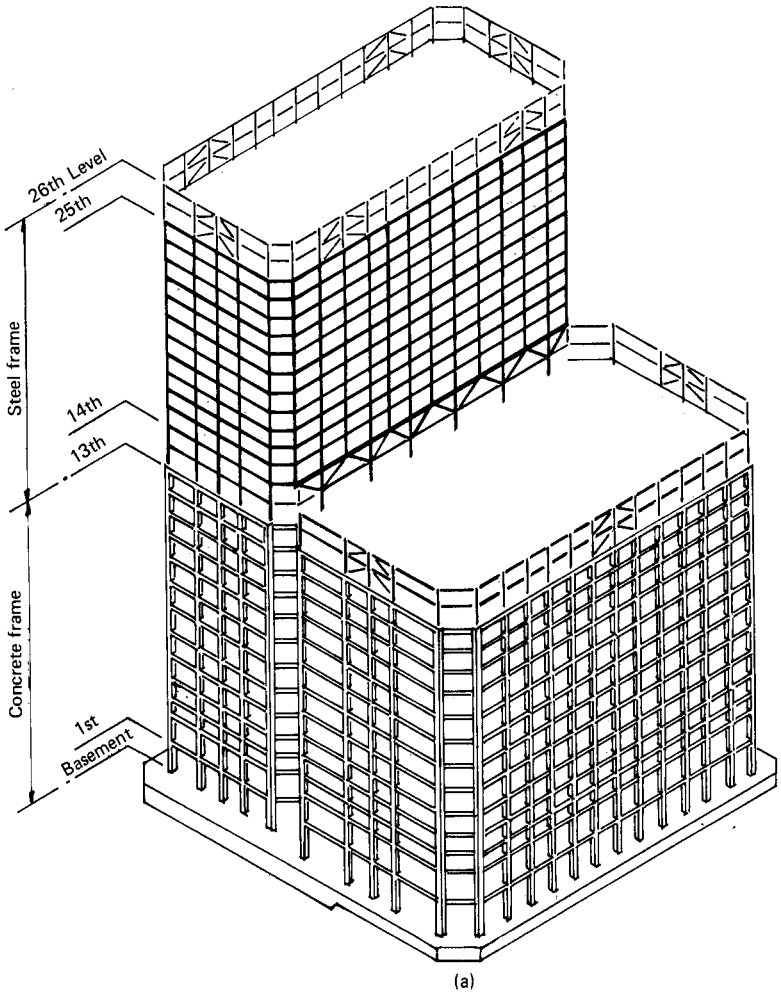

Figure 6.9 Vertically mixed system. (*a*) Schematic perimeter framing.

variation is conventional concrete construction with a composite steel floor-framing system inside of the concrete core.

6.4.1 Composite shear walls and frames

The building called the First City Tower consists of a base structure extending one level below the plaza, covering an entire downtown Houston block. A tower extension through 49 stories gives 1.4 million square feet (130,000 m^2) of office space (Fig. 6.10). The building is a parallelogram in plan and is positioned on the site to create views. Among the architecturally distinctive features of First City Tower are

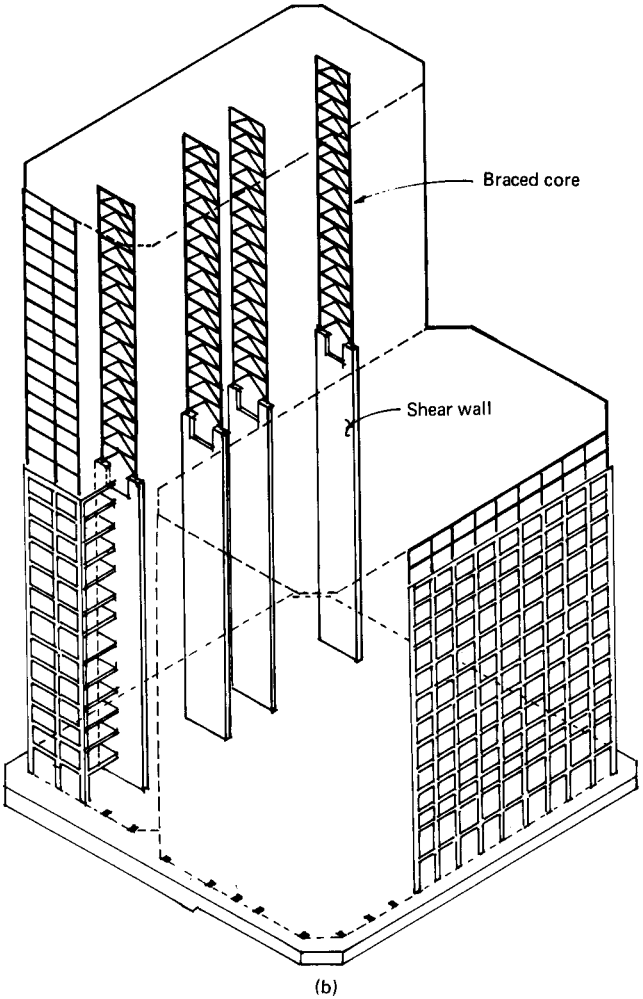

Figure 6.9 *(Continued) (b)* Schematic bracing concept.

the four 11-story-high indentations in the facade where the glass panels open the building for viewing. These "vision strips" rise in staggered formation along the height of the two long faces. They not only provide optimum positioning for elevator banks containing 27 high-speed cabs, they also make for dynamic views of Houston from the elevator lobbies.

Structural anatomy. In common with most other projects, First City Tower went through a design metamorphosis. The architecturally acceptable column locations for an earlier scheme are shown in Fig.

Figure 6.10 First City Tower (Architects, Morris & Aubry; Engineers, Walter P. Moore and Associates; contractor: W. S. Bellows Construction Corp.) (*Photograph © Richard Payne AIA 1987. Reproduced with permission.*)

6.11 and consist of closely spaced columns on the two short faces and around the corners. The north facade was planned to have the vision strips, which ruled out the possibility of closely spaced columns on that face. Architecturally, it was acceptable to continue closely spaced

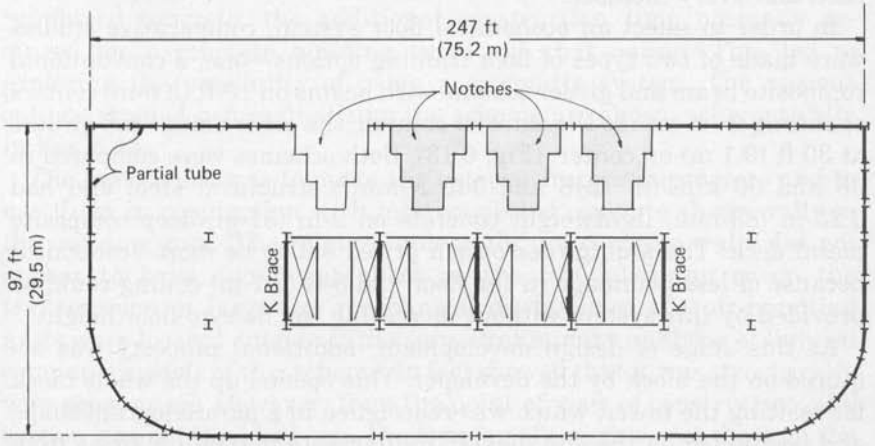

Figure 6.11 Plan of an earlier scheme for First City Tower.

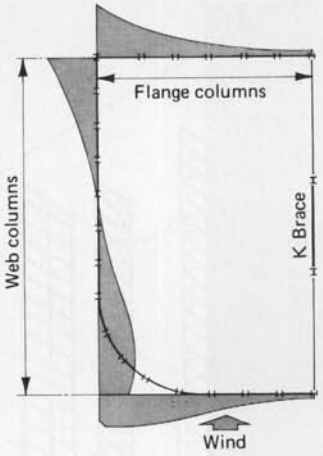

Figure 6.12 Braced core–partial tube interaction: schematic representation of axial stresses in exterior columns.

columns on the south face, but this was ruled out structurally because of asymmetry and associated problems of torsion.

Analysis of a partial framed tube concept using closely spaced exterior columns and moment-connected exterior spandrels indicated that partial tube action alone was not sufficient to carry the wind loads. Addition of K braces at the building core resulted in a shear truss–frame interaction system. In comparison to a plane frame, a partial framed tube that interacts with the braced core is more efficient because in addition to the web columns, the columns on the flanges of the tube also participate in resisting the lateral loads as shown in Fig. 6.12. The feasibility of applying this structural system to First City Tower was verified using preliminary planar analyses and a three-dimensional computer analysis of one-half of the building representing each and every member.

In order to select an economical floor system, comparative studies were made of two types of floor framing options—one, a conventional composite beam and girder scheme with beams on 10-ft (3.0-m) centers spanning from core to the exterior column, the other using stub girders at 30 ft (9.1 m) on center. (Fig. 6.13). Both schemes were compared in 36 and 50 kips/in^2 (248 and 345 N/mm^2) structural steel and had 3.25-in (83-mm) lightweight concrete on 2-in (51-m) deep composite metal deck. The stub girder option priced out to be more economical because of less poundage in the floor and 9-ft (2.7-m) ceiling could be provided by this system without increasing the floor-to-floor height.

At this stage of design development, additional property was acquired on the block by the developer. This opened up the whole block for resiting the tower, which was redesigned in a parallelogram shape and positioned on the site diagonally to create maximum views from

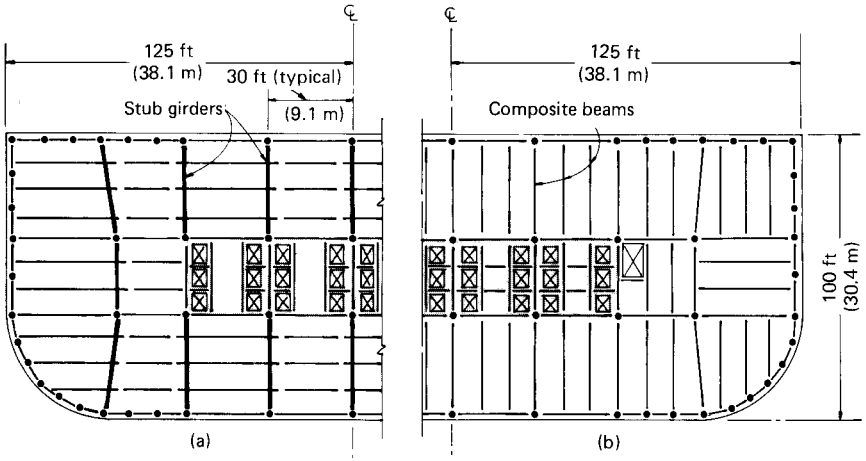

Figure 6.13 Floor framing options. (*a*) Stub girder scheme; (*b*) composite beam scheme.

the building. The vision strips were now planned on two faces of the building, and the floor plans were laid out on a new module of 3 ft 4 in (1.0 m), giving no more than eight columns on the two short faces and a large bay spacing of 30 to 47 ft (9 to 14.3 m) between columns on the long faces. The partial framed tube action, which was very efficient in resisting the lateral load in the earlier scheme, is completely absent in the new scheme. Although shear truss–frame interaction is still applicable between the exterior frames and the braced cores, it was clear from the preliminary designs that the structural premium associated in making this scheme work in steel would be too high.

The next step was to look at a structural system that would incorporate reinforced concrete members for resisting the lateral loads. Although it is possible to design the lateral system entirely in reinforced concrete, the additional construction time normally required for a concrete building ruled out that option. This led to exploring the possibility of using a composite system. The various options studied before finalizing the scheme are shown schematically in Fig. 6.14.

The first choice was to make the exterior frames in concrete and to use them in conjunction with interconnected concrete shear walls in the building core. The relative inflexibility of concrete walls did not appear to have significant effect on the core planning or on the transmission of large-size mechanical ducts, since the air-handling units were located outside of the core. Preliminary analysis of lumped computer models of this scheme, in fact showed that it was structurally very economical. However, from the point of view of construction, the system was not the ideal one. The forming of concrete spandrels on the

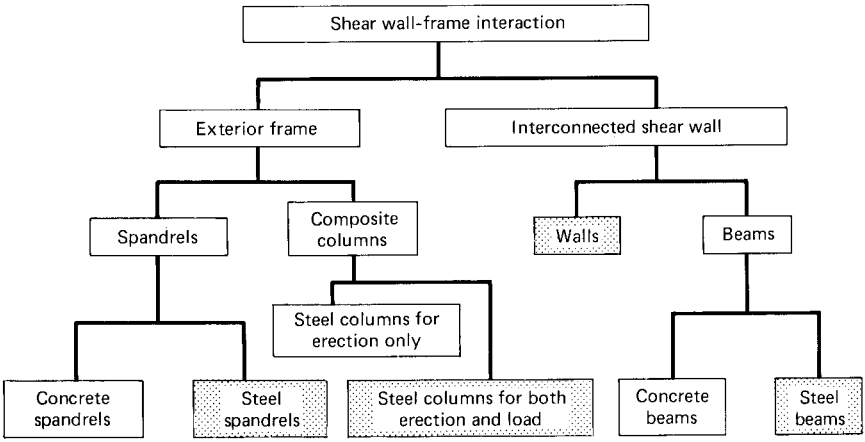

Figure 6.14 Composite scheme options.

short faces and link beams in the shear walls would have required additional material-hoisting equipment and would have slowed down the construction schedule. As an alternative, steel wide-flange beams were proposed at these locations and accepted by the design team as the most economical scheme. A floor-framing study similar to one done on the previous scheme convincingly established the economical advantage of the stub girder system over the conventional composite beam framing. This was used for about 80 percent of floor area as shown in Fig. 6.15. The large size of ducts that occur adjacent to the mechanical rooms precluded the use of stub girders in bays adjacent to the air-handling units. Composite beams with large penetrations were used in these areas. Thus, the final scheme adopted has the following composite components, as shown schematically in Fig. 6.16.

1. Composite floor-framing system, consisting of steel beams and concrete slab on formed steel deck interconnected with shear studs to act together as a unit.

2. Composite stub girder system, consisting of rolled steel beams connected to floor slab with a series of stubs welded to the beam. This system minimizes overall space requirements by combining the space for mechanical ductwork in the design of the structural system and will be discussed in greater detail in Chap. 9.

3. Composite columns consisting of steel rolled shapes embedded in reinforced concrete columns (Fig. 6.17).

4. Composite frame consisting of composite columns and moment-connected steel beams (Fig. 6.16).

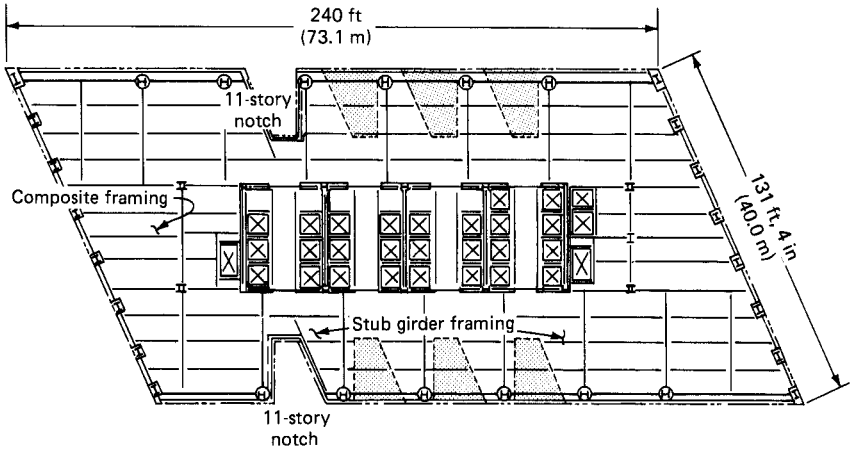

Figure 6.15 Composite floor-framing plan.

5. Composite shear walls consisting of a series of I- and C-shaped reinforced concrete shear walls interconnected with steel link beams (Fig. 6.16).

6. Composite construction that allows the initial growth of steel followed by the pouring of concrete to form composite columns and shear walls as shown schematically in Fig. 6.19.

Design. Figure 6.17 shows the arrangement of vertical reinforcement and structural steel core column for composite vertical framing elements. Typically, the embedded steel columns vary from a W14 by 370 lb/ft (455 by 418 mm, 551 kg/m) member at the bottom to a W14 by 68 lb/ft (356 by 254 mm, 101 kg/m) member at the top. For rectangular

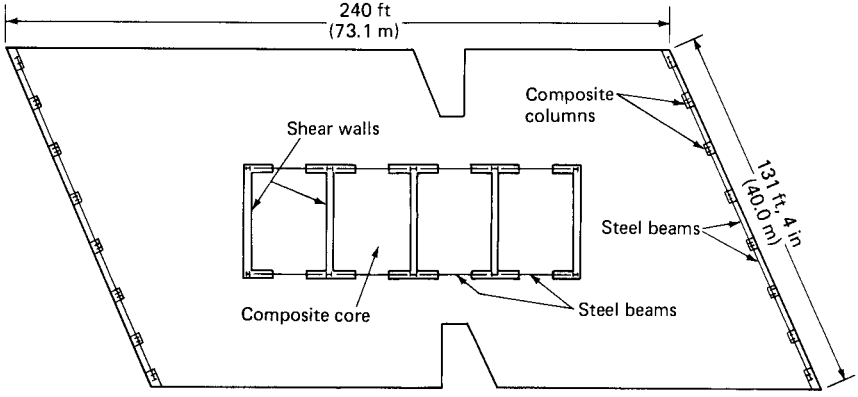

Figure 6.16 Composite elements.

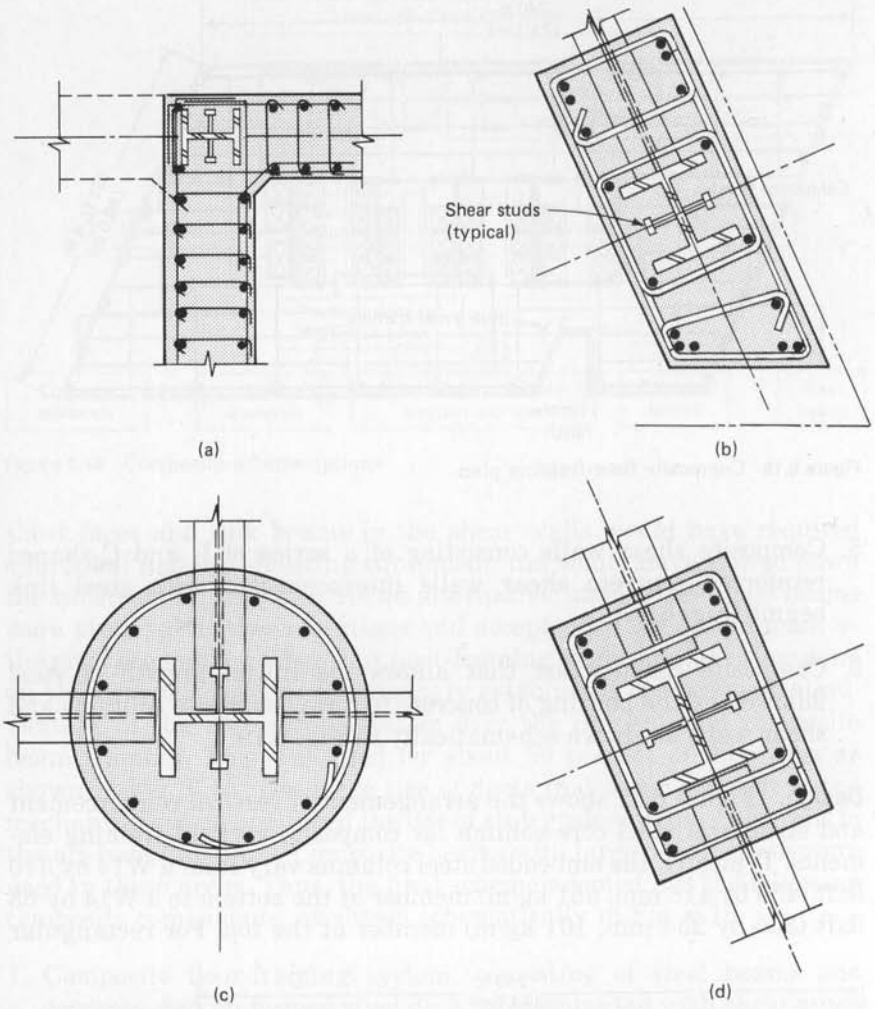

Figure 6.17 Composite vertical systems. (*a*) Composite shear wall; (*b*) composite corner column; (*c*) typical circular column on long faces; (*d*) typical exterior column on short faces.

columns, width of the concrete envelope is maintained for full height, while the depth of column into the building is reduced in the upper floors.

The vertical reinforcement in the columns varied from #18 bars (57 mm in diameter) at the bottom to #7 bars (22 mm in diameter) at the top. Open ties are used throughout to facilitate placement of column reinforcement. Mechanical tension splices are used for wind columns on the short faces, and compression mechanical splices are used for the gravity columns on the long faces. Shear studs shop-welded to the webs

Figure 6.17 *(Continued). (e)* Reinforcement placement in exterior composite column.

of steel columns are used to achieve load transfer from concrete to steel.

Figure 6.17*a* shows the arrangement of reinforcement and erection column embedded in the shear wall. Typically, a W10 by 72 lb/ft (267 by 257 mm, 107 kg/m) steel column is embedded at each shear wall corner. The ties enclosing the vertical reinforcement are needed if 1 percent or more reinforcement is required for compression in the walls. Typically, the ties are used in the shear walls up to level 6 only.

Figure 6.18 shows a typical connection detail between concrete shear wall and a typical interconnecting beam. The beam to embedded steel column connection is a typical bolted shear connection. Moment capacity required at the face of the shear wall is developed by means of shear transfer mechanism between the concrete and shop-welded studs at the top and bottom flanges of the beam. The stiffener plate, set flush with the wall face, has no structural purpose but helps in simplifying shear wall forming around the beam. A conventional moment connection was used between the core columns and beams at levels where the shear walls were dropped.

Composite construction. In terms of construction, as mentioned many times over, concrete buildings are slower to erect than steel buildings, especially when the steel members are preordered. The speed of construction has a significant effect on the financing charges associated with office buildings built on a speculative basis. The composite

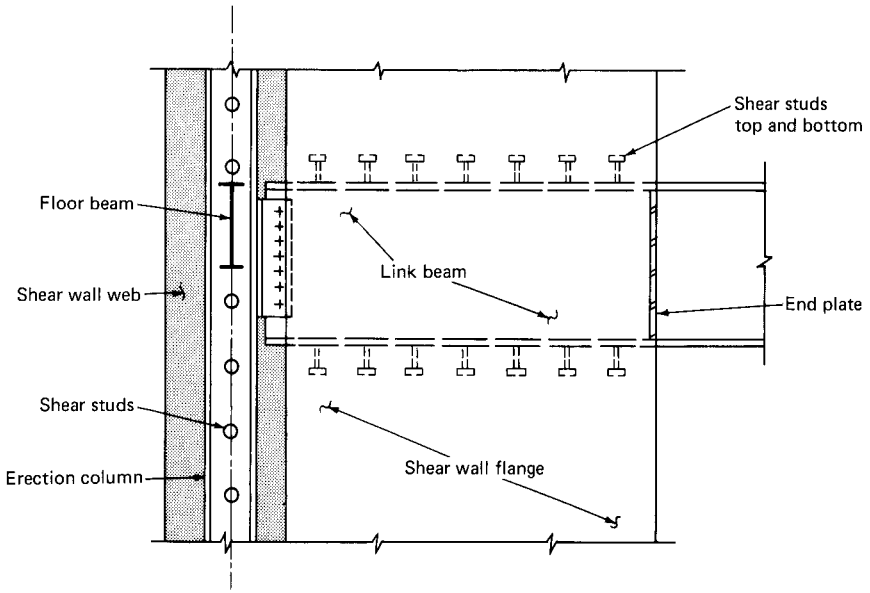

Figure 6.18 Arrangement of link beam in shear wall.

system attempts to combine the merits of concrete stiffness and speed of steel construction. It aspires to get a lighter structural system that has the inherent stiffness of concrete and the speed of construction of a conventional steel frame.

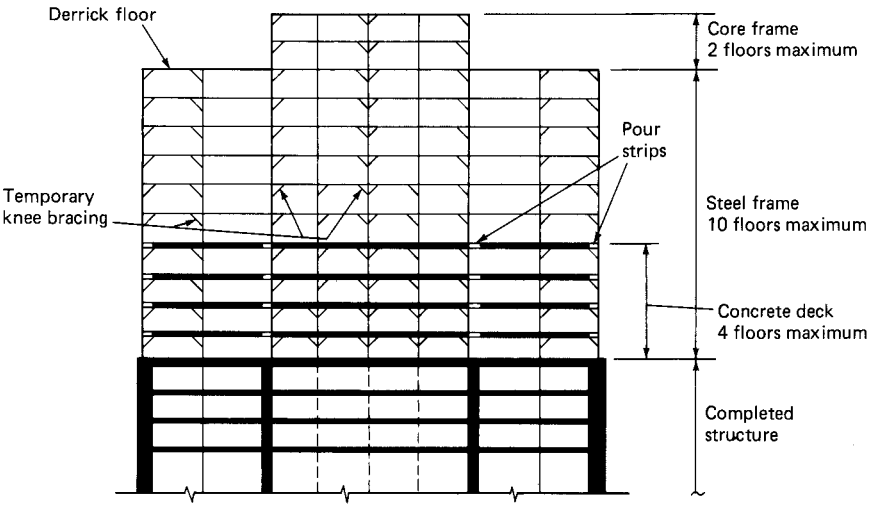

Figure 6.19 General construction sequence in composite structures.

Needless to say, this method of construction requires a high degree of proper construction sequencing. The basic idea of composite construction is to let the construction of the steel frame advance to a predetermined number of stories first and then to envelop the column with concrete, as shown schematically in Fig. 6.19. The step-by-step process is as follows. After completion of the foundation system, the steel frame erection is started using standard procedures and AISC tolerances. Since the general idea is not to wait for the concreting of shear walls for steel erection, small steel columns are utilized for vertical support at the intersection of shear wall web and flanges. In order to limit their size, heavy steel sections are embedded in the exterior columns. The erection of exterior spandrels, stub girder, and purlins proceeds as in a conventional steel frame.

The size of the interior steel columns embedded within the shear walls depends on the maximum separation of the derrick floor from the level to which concrete shear walls have been completed. For this project, the criterion was set at a maximum of 10 floors. This was established during the early phase of design with proper coordination from the steel erector and the general contractor. Metal deck installation and welding of spandrels on the short faces follow closely behind steel erection. Diaphragm action of the deck is established by welding metal deck to beam flanges and by the installation of shear studs welded through the deck. Concrete topping is placed on metal deck several floors above the concreted portion, with the exception of pour strips around the shear walls and exterior columns.

The completed floor slab serves as a platform to transport concrete from material hoist to shear walls and exterior columns. The reinforcing steel for exterior columns and shear walls is tied into position several floors high with story-high bar lengths. The form work is then placed around the reinforcing cage.

Concrete is hoisted through the material hoist at the exterior of the building and then buggied over the concrete slab to the required location. Columns and walls below the floor are concreted by pouring concrete through the pour strips left around the shear walls and columns. Metal deck in the pour strip around the shear walls is cut to provide room for hoisting of shear wall forms. The forms are hoisted to the floor above through these temporary openings.

As a next step, the shear walls above the floors are poured and integration between floor slab diaphragm and shear walls is completed by concreting the pour strips. The various stages of the shear wall construction sequence are shown schematically in Fig. 6.20.

With proper sequencing of different trades, the construction of concrete shear walls and columns can proceed at a pace equal to the overall speed of a conventional steel building. Typically for First City

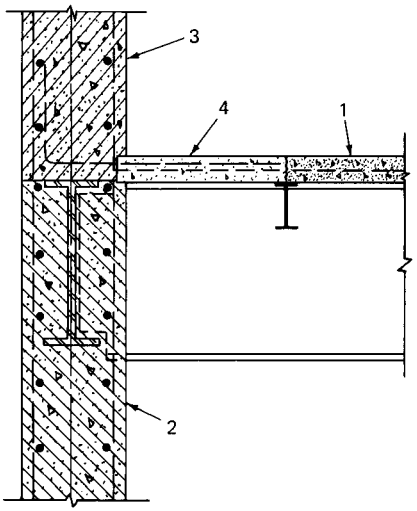

Figure 6.20 Shear wall construction sequence. (1) Concrete topping over composite metal deck is poured on several levels; (2) shear walls below the lowest concreted floors are poured; (3) shear wall form work is raised to the next floor through temporary floor openings in metal deck and walls on the next floor are poured; (4) temporary openings are filled around shear walls to establish diaphragm action.

Tower, steel erection proceeded at the rate of two floors per week, with concreting of shear walls and columns following closely behind at the same rate.

Temporary bracing. In a pure steel or concrete building, the resistance to wind loads is provided as the structure is built. There is no measurable lag between the levels at which the construction is proceeding and the level at which the building lateral resistance is established. For example, in a steel building moment connections or braces are connected between steel columns immediately behind the erection of the steel frame in order to provide resistance and stability to lateral loads. Monolithic casting of concrete beams and columns and other elements, such as shear walls, automatically provides the required stability. However, for a composite building, final resistance to stability does not become available until after the concrete has been poured and cured around erection columns. Since the level at which the steel framing is erected is deliberately made sufficiently high above the concreted level, there exists in composite construction a distinct need for considering bracing during the erection process. Steel cables traditionally used in steel buildings to plumb and stabilize the structure are often inadequate, requiring a more positive method of lateral stability. This was done for the First City Tower project by providing supplementary knee bracing around the building perimeter and also in the building core. The braces at the perimeter were later removed, while those in the core were left in place to become embedded in the composite shear walls since they did not interfere with the architecture of the building.

Figure 6.21 The America Tower, a 42-story composite building in Houston, Texas. Closely spaced exterior composite columns and moment-connected spandrel beams constitute a tube for resisting lateral loads. Note climbing form work on the exterior for composite exterior columns.

6.4.2 Composite tube system

In this system a concrete exterior tube consisting of closely spaced columns and deep spandrels forms the essential wind-bracing system. Fast erection of the steel frame is achieved by using light structural columns around the perimeter. Interior columns and floor framing are identical to gravity-framed steel construction.

A somewhat new technique, as mentioned earlier, adapts a variation of this concept. This system does away with the concreting of the spandrels; instead, steel spandrels are employed in conjunction with composite columns to resist the lateral loads (Fig. 6.21). This is the system used on a 42-story building called America Tower.

The America Tower project consists of 1 million square feet (92,858 m^2) of office space and is elliptical in plan with offsets on the long faces to highlight the verticality of the building and provide more corner offices. The exterior facade is designed with a curtain wall of alternating glass and precast panels. Figure 6.22*a* and *b* shows the architectural plan and a photograph of the building.

Structural anatomy. The salient structural features are given in Table 6.1. A framed tube consisting of closely spaced exterior columns and spandrels was chosen as the proper structural solution. Initially, a spacing of 10 ft (3.0 m) for the exterior column was considered for the project. Five tube systems were comparatively priced. These were (1) composite tube, consisting of composite columns and concrete span-

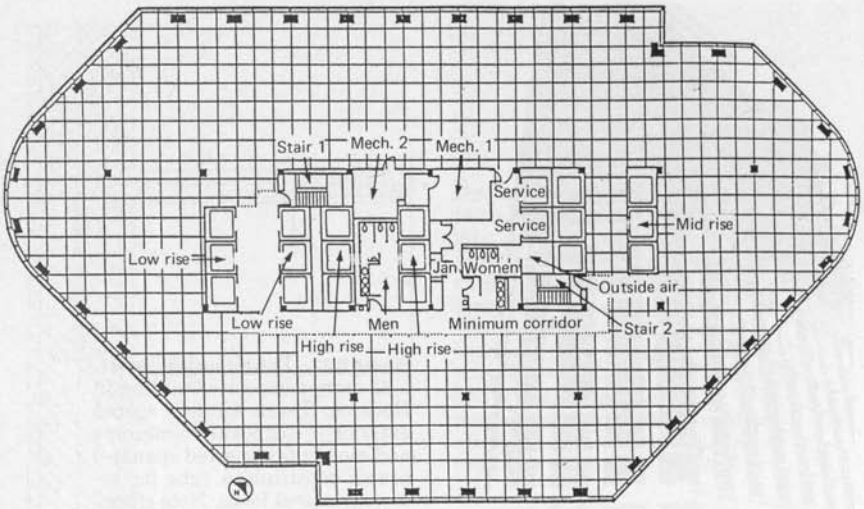

(a)

(b)

Figure 6.22 (*a*) America Tower architectural floor plan; (*b*) photograph of America Tower (Architects, Lloyd Jones and Fillpot; structural engineers, Walter P. Moore and Associates; contractor, W. S. Bellows Construction Corp.)

TABLE 6.1 America Tower: Structural Features

Height above mat	619 ft 7 in (188.85 m)
Width	125 ft 4 in (38.2 m)
Height/width ratio	4.94
Interior columns	W14 rolled steel sections
Floor framing	W18 composite beams span 41 ft (12.45 m)
Exterior columns	42 by 27 in (1.07 by 0.68 m) composite columns.
Spandrels	W36, W33, W30 steel shapes
Mat	6-ft (1.83-m) thick

drels, (2) steel tube with straight spandrels, (3) steel tube with tapered spandrels, (4) mixed tube, consisting of exterior composite columns and steel spandrels, and (5) steel and mixed tube combination. In addition to these, two options each for floor framing and metal deck construction were studied for a total of 18 alternate solutions. The relative cost index for each of these schemes, including the effect of interest rate charges, is given in Table 6.2. The composite tube system gave the most economical system with regard to material and labor costs. However, with the additional construction time of two months and the associated interim finance charges, this scheme turned out to be

TABLE 6.2 America Tower: Comparative Study Table

	System				
	Tube system				
Scheme no.	Columns	Spandrels	Floor system	Metal deck depth, in	Relative cost index
1	S	SS	WF beams	2	1.025
2	S	SS	WF beams	3	1.046
3	S	TS	WF beams	2	1.000
4	S	TS	WF beams	3	1.020
5	S	SS	Trusses	2	1.113
6	S	SS	Trusses	3	1.133
7	S	TS	Trusses	2	1.090
8	S	TS	Trusses	3	1.108
9	FC	SS	WF beams	2	1.027
10	FC	SS	WF beams	3	1.047
11	FC	SS	Trusses	2	1.114
12	FC	SS	Trusses	3	1.135
13	CT	SS	WF beams	2	1.021
14	CT	SS	WF beams	3	1.041
15	CT	SS	Trusses	2	1.108
16	CT	SS	Trusses	3	1.129
17	FC	C	WF beams	2	1.120
18	FC	C	WF beams	3	1.140

Note: S = Steel columns full height, SS = straight steel spandrels, TS = tapered steel spandrels, FC = full-height composite columns, CT = composite columns above level 3 and steel columns below level 3, C = concrete spandrels.

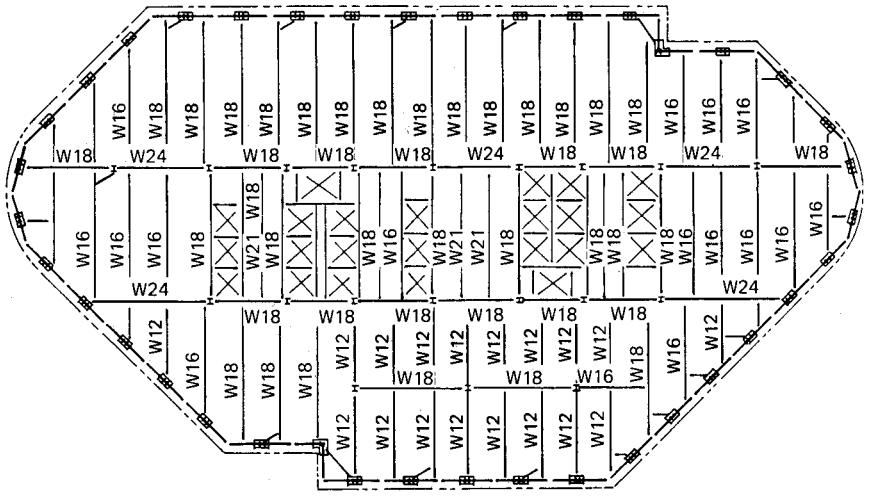

Figure 6.23 Floor framing plan with 10-ft beam spacings, 2-in deck + $3\frac{1}{4}$-in slab.

uneconomical. Schemes 1, 2, 3, 4, 9, and 13 came to within 3 percent of each other. However, because the mixed tube construction had a good track record for the contractor, it was chosen as the final scheme.

At this stage of the project, the exterior column spacing was changed to 15 ft (4.57 m). The additional structural premium associated with this change was assumed constant for all the schemes and no further studies were made for the tube system. However, floor framing studies were made for 10- and 15-ft (3.0- and 4.57-m) beam spacings as shown in Figs. 6.23 and 6.24. Table 6.3 lists various items used in the comparative study including some nonstructural items such as fireproofing.

Construction. As is common with most tube buildings, the system used for America Tower is the so-called prefabricated tree column system. (Fig. 6.25). A typical tree column consists of a two-story column and two levels of spandrels. The major difference in the mixed tube construction is that the column sizes are small compared to an all-steel scheme, resulting in savings in the fabrication and erection of steel members.

Another feature that has resulted in considerable savings is the use of a hybrid tubular frame on the perimeter of the building. Composite columns used in the typical levels (floors 3 through roof) are integrated into pure structural steel columns at the second level. This marriage of steel columns to composite columns simplified the construction of the exterior columns at nontypical lower levels. Although the savings in the structural cost for this scheme appeared to be only marginal from

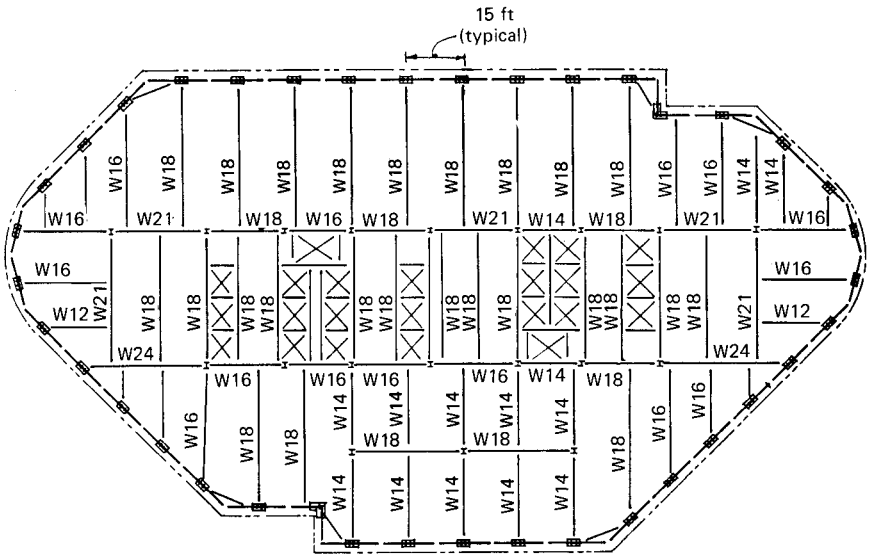

Figure 6.24 Floor framing plan with 15-ft beam spacings, 3-in deck + $3\frac{1}{4}$-in slab.

the comparative study, the contractor elected to use this scheme because his recent job experience on another similar high-rise project had proved that a hybrid frame is more economical than a full-height composite scheme. Figure 6.26 shows a detail of intersection of composite column with a steel column. The resistance to lateral loads during the erection of the tower was provided by the tube action of the erection columns and spandrel beams. The columns, which were sized for 12 floors of construction gravity loads, were found to be adequate for providing resistance to lateral loads. Additional welds between the erection column and the spandrel and stiffeners were necessary in order to develop the bending capacity of the columns.

TABLE 6.3 America Tower Floor Framing Cost Comparison Study

	15-ft spacing	10-ft spacing
Beams	3.57 psf (171 Pa)	4.06 (194 Pa)
Concrete	0.396 ft^3 (0.011 m^3)	0.354 ft^3 (0.01 m^3)
Shear studs	0.087	0.116
Metal deck	3-in—16-gauge (76.2 mm)	2-in—18 gauge (50.8 mm)
Welded wire fabric	6 × 6 W2.1 × W2.1 0.030 psf (1.44 Pa)	6 × 6 W1.4 × 1.4 0.021 psf (1.0 Pa)
Fireproofing	$0.60	$0.85

Conclusion: 15-ft spacing is more economical. All quantities are per square foot of floor framing.

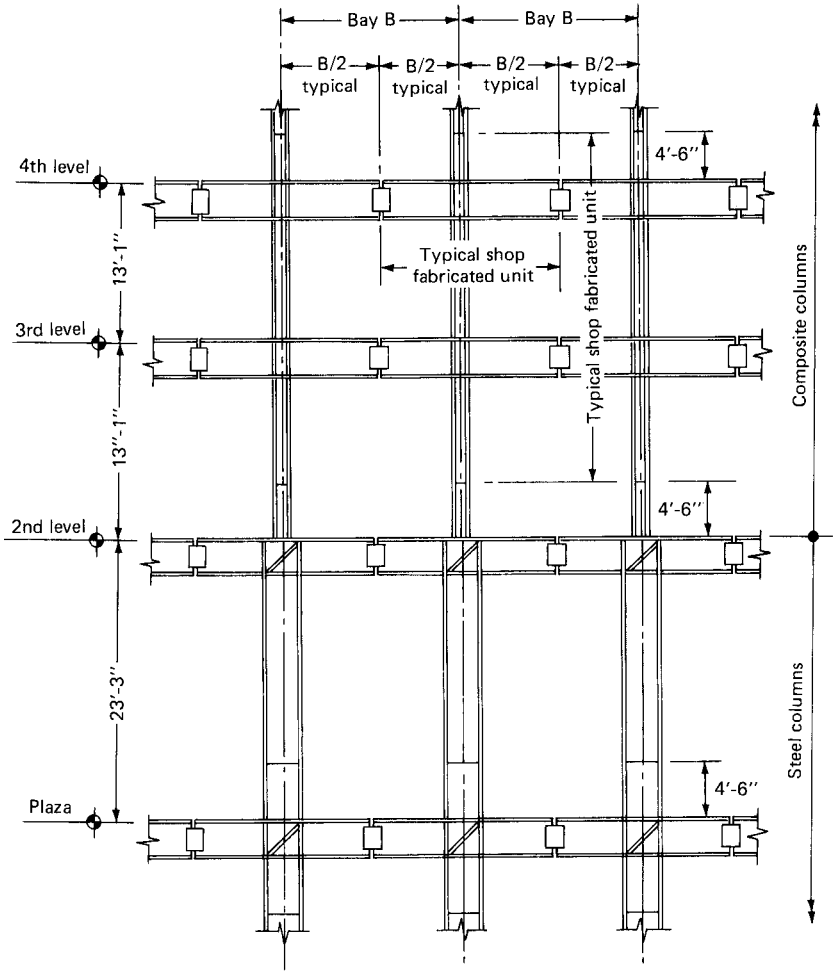

Figure 6.25 Typical frame fabrication unit.

6.4.3 Conventional concrete system with partial steel floor framing

The Huntingdon in River Oaks, Houston, is a 34-story condominium project (Fig. 6.27) with living units in the tower, resident parking on three floors under the building, and a landscaped plaza featuring amenities such as a heated swimming pool, spa, pool-side room, etc. Construction consists of a poured-in-place concrete structure with a white precast exterior. Windows are dual-pane tinted glass with operable vents.

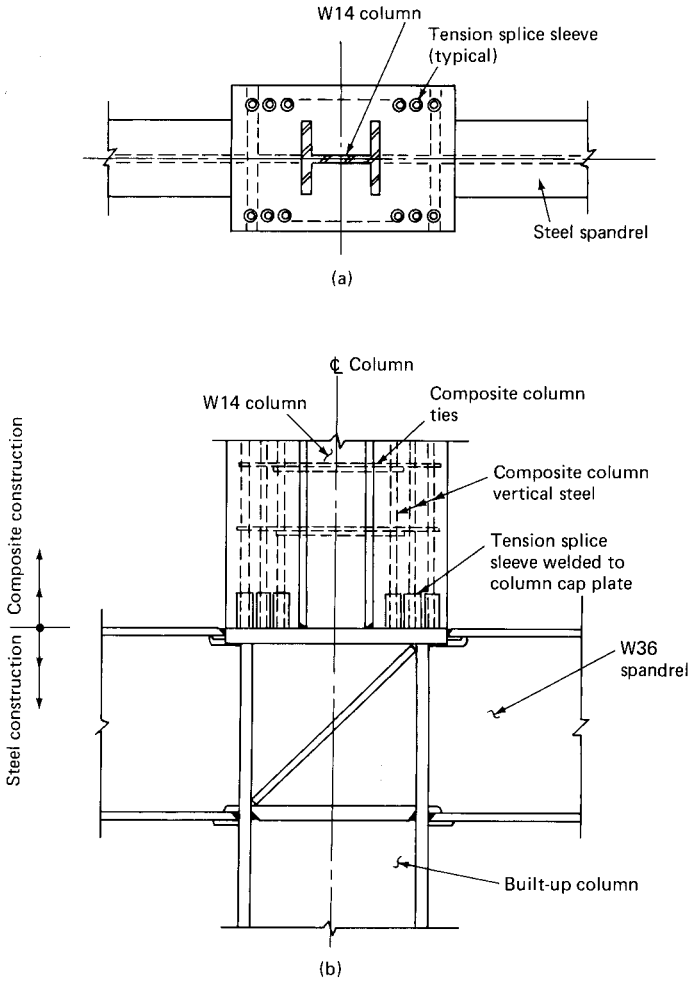

Figure 6.26 Composite column–steel column connection detail. (*a*) Plan; (*b*) elevation.

Structural anatomy. The building is essentially symmetrical in plan with a rectangular dimension of 142 ft 6 in by 106 ft 6 in (43.5 by 32.5 m) and is 490 ft (149.5 m) tall. The architectural design called for column-free space between the core and exterior of the building. The desired elevation dictated that exterior columns be spaced at 20-ft (6.1-m) centers around the building except at the corners. Columns were not permissible at the corners because each home has a balcony offering views in two directions. With this layout of exterior columns it was not possible to develop the tube action to resist the lateral loads because of lack of continuity of structural resistance around the

Figure 6.27 The Huntingdon. (Architects, Talbot Wilson & Associates; structural engineers, Walter P. Moore and Associates; contractor, W. S. Bellows Construction Corp.)

corners. A preliminary analysis was performed on a structural system that consisted of 24-in (610-mm) deep pan joists for floor system and an interacting system of shear wall and end frames for lateral loads. The analysis indicated that the system could be designed for strength without too much of a premium in material quantities, but the calculated lateral deflection under Houston hurricane wind code was too large for the occupancy of the building. Addition of stiffening elements without introducing more columns was necessary to maintain reasonable size of structural members and to reduce the deflection values.

The addition of girders between the core and exterior at each column line as shown in Fig. 6.28 was the answer. In comparison to the pan joist floor system, these girders are very stiff and help in mobilizing the exterior columns to resist the wind loads. The resulting structural system consisting of the core, end frames, and exterior columns reduced the deflection to well within the drift limitations.

Haunch girders. A framing system employing girders of constant depth criss-crossing the interior space between the core and the exterior often presents nonstructural problems because it limits the

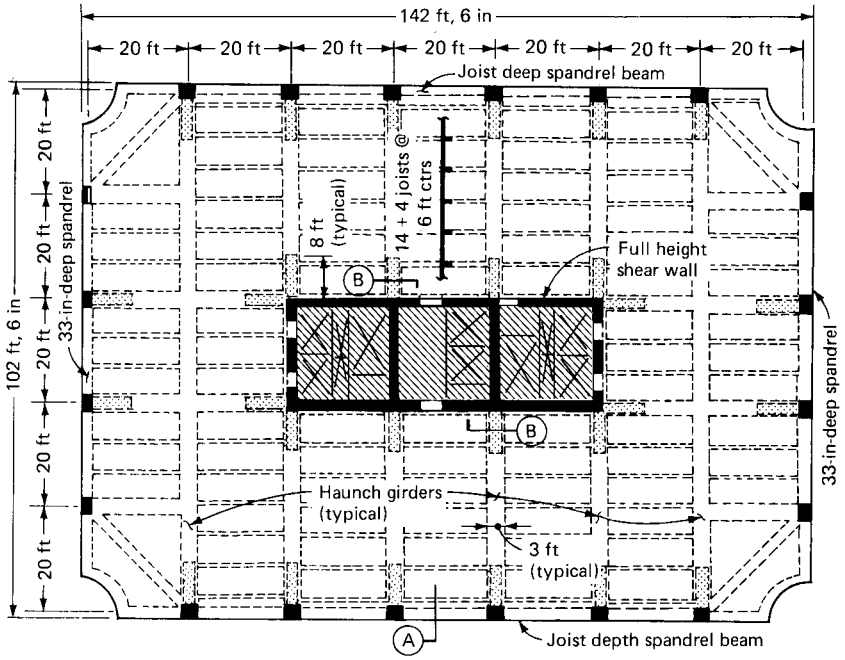

Figure 6.28 Typical floor framing plan: haunch girder scheme.

space available for passage of air conditioning ducts. A system known as the haunch girder system, with wide acceptance in many parts of North America, alleviates nonstructural problems without making undue compromises in the structure. The basic system consists of a girder of variable depth as shown in Figs. 6.29 and 6.30. The use of shallow depth at the center facilitates the passage of mechanical ducts and eliminates the need to raise the floor-to-floor height. Material quantity comparisons for gravity loads indicated that haunch girder framing is very economical.

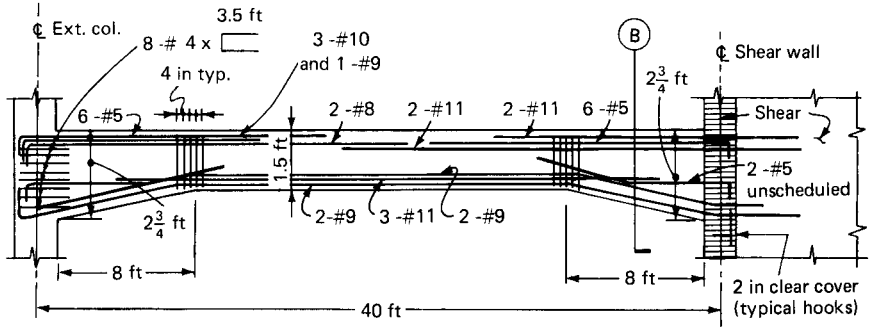

Figure 6.29 Haunch girder elevation and reinforcement.

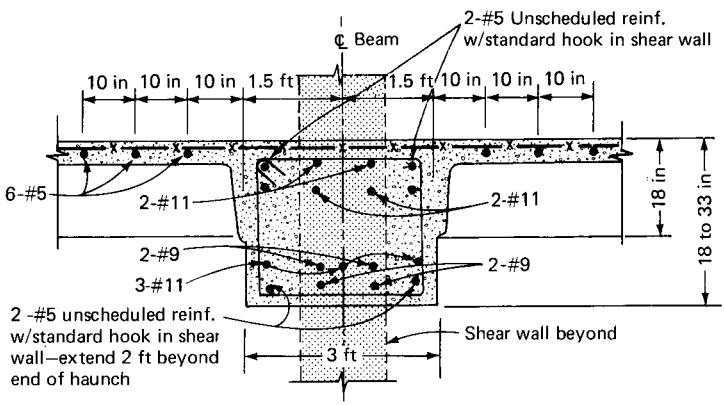

Figure 6.30 Haunch girder section.

Additional comparison for lateral load design indicated even more savings from the reduced floor-to-floor height.

Flying forms. For the in situ construction to be competitive with other forms of construction, such as precast concrete or steel, it is imperative that the forming for the floor system should lend itself to repeated uses in a multistory frame. One-way joist system using flange-type steel pans is a reusable system that is currently popular in almost all high-rise buildings in North America. Wide pans in two common sizes of 53- and 66-in (1346- and 1676-mm) widths have become a standard, replacing the 30-in (762-mm) pans.

A conventional method of concrete joist construction is to nail the flanges of pans on a formed solid decking built on adjustable shores. When concrete has gained sufficient strength, shores are removed and pans stripped and stored in an area to await reuse until shoring and wooden decking are erected for the next floor. This method of forming is labor-intensive and also time consuming, particularly when joists of different lengths are used.

A method of forming that fully utilizes the opportunity for repetition offered in multistory construction is a system known as flying form system. In this system joist pan forms are attached to slab, creating a system of deck surface, adjustable jack, and supporting framework. For stripping, the form is lowered by jack, slipped out of the slab, and lifted to the next floor for reuse as one rigid structure, resulting in economy of handling and placing.

The floor framing used in the Huntingdon project lent itself to the use of flying forms. To further simplify the form work, the width of haunch girders was kept slightly larger than the maximum width of the exterior column.

Mixed-floor construction. The architectural requirement for the project dictated that typical floors be constructed at two different elevations with a 2-ft 6-in (762-mm) drop occurring at the outline of the interior core. This design allows flexibility to the buyers in locating wet areas, whereas the common areas such as the service and passenger elevator lobbies and stair landings are kept higher because of predetermined finish. Forming of a poured-in-place concrete slab at two different elevations on either side of the core would have been somewhat complicated. This required taking a fresh look at the framing of slab inside the core.

When compared to an office building, the vertical transportation requirements for a condominium are relatively small. The core size dictated by the elevator and mechanical requirements for this project worked out to 50 by 20 ft (15.2 by 6.1 m). The elevator lobbies normally required in an office building are eliminated in the core arrangement because the elevators open on each floor directly to a private foyer serving a maximum of two homes, making it possible to have a very small core. The floor area that is enveloped within the core is very small. This, combined with the problem of a raised floor inside the core, made possible the use of a steel floor framing with composite deck, unwittingly creating yet another variation to the many types of mixed construction currently in vogue for tall buildings.

Pockets were provided in the shear wall to receive the steel beams in the core. Shelf angles were quick-bolted to the walls in areas where supports for the metal deck were required. This idea of using conventional steel framing on the inside of the core facilitated the construction of shear walls and the floor framing independent of the framing inside the core. Typically, the construction of shear walls and concrete framing proceeded at the rate of one floor a week and at times the turnaround was reduced to 4 days. The steel framing in the core was deliberately left to lag behind the concrete framing so that the ironworkers could work without interfering with other trades.

The absence of diaphragm within the core required that the forces in the slab be transferred to the shear wall at the exterior of the core only. This was achieved by providing dowels and shear keys from the wall to the floor slab.

6.4.4 Conclusion

Compositing of steel members and the use of hybrid construction offers substantial savings in the building cost of high-rise structures. A broad range of construction techniques is at the structural engineer's disposal in the search for economical structural systems.

Chapter

7

Gravity Systems for Steel Buildings

7.1 Introduction

In comparison to all other materials employed in the construction of buildings, steel, other than its somewhat unusual ability to resist compression and tension without being overly bulky, has many other properties that have made it one of the most common building materials in use today. Chief among these characteristics are high strength, ease of erection, and uniformity and ductility. Although structural steel components need fireproofing to meet the fire codes, the invention of a sprayed-on cementitious coating mixture has replaced the earlier, more expensive practice of embedding steel members in poured-in-place concrete, thus greatly improving the economy of steel structures. Steel, because of its high ratio of strength to unit weight or volume, allows structures to be designed for smaller dead loads and larger spans. Various aspects of steel construction such as fabrication, transportation, and field assembly must be considered during the design stages to achieve the most satisfactory and economical result. Greatest economy will be realized when there is as much duplication of the various units and parts as possible. Structures in which every bay and every span are even slightly different will result in increased costs of shop drawing and fabrication and probably of

erection. Although not entirely correct, a consideration that takes precedence over other items when designing steel structures is the idea that a savings in weight of steel necessarily yields a savings in overall cost. This is understandable, since steel, both fabricated and plain, tends to be bid in a healthy competitive market on a price per ton basis.

Modern high-rise buildings typically demand clear spans in the range of 35 to 42 ft (10.66 to 12.8m). For these relatively long spans, the weight of steel becomes a major consideration. This in turn has led to the development of high-strength steels which justify their increased cost by the savings they permit in the lighter members.

There are basically three groups of structural steel available for use in bridges and buildings.

1. Carbon steels: ASTM-A36 and A529
2. High-strength, low-alloy steels: ASTM-A440, A441, A572, A242, and A588
3. Heat-treated low-alloy steels: ASTM-A514

In the A572 category six grades of steel: 42, 45, 50, 55, 60, and 65 are available for structural use. The grade numbers correspond to the minimum yield point in kilopounds per square inch of the specified steel. Carbon steel is available in 36 and 42 grades, while the A514 group consists of tempered steels with specified yield points ranging from 90 to 100 ksi (620.5 to 689.5 MPa).

The most commonly available type and grade of structural steel shapes in stock is grade 36, comprising approximately 75 percent of U.S. production of structural shapes. Until about a decade ago, it was a routine and economical choice because of availability for early delivery and maximum competition among bidders. Although low-alloy, high-strength steels are available with yield points ranging from 40 to 65 ksi (276 to 448 MPa), the most common choice where high-strength steel is desired is ASTM-A572 grade 50.

For comparative purposes, the practical choice of grade for floor framing members usually narrows down to grade 36 versus grade 50. Both of these steels are readily usable in bolted and welded construction without any modification as long as the welding procedures are suitable for the type of steel and the intended use. Preliminary calculations of typical beam and girder tonnages in the two grades of steel for a typical floor of a high-rise building are not difficult. The only additional data required for an economical choice of grade are the cost differentials per erected ton of grade 50 versus grade 36 steel, which can be obtained from local fabricators and erectors. However, experience in the U.S. market indicates that the use of A-572 grade 50 is invariably economical because of the lighter members possible with

the higher yield stress unless considerations of local buckling, instability, deflection, and vibration penalize the allowable stress.

Assuming that a basic structural system has been selected in the overall context of the architectural and mechanical requirements, the value of structural analysis and design refinements and the selection of the type and grade of steel can only be measured by savings in the cost of steel frame itself. A widely recognized index for comparison of design efficiency is the unit weight of steel, obtained by dividing the total tonnage by the gross area of the building. This index as a measure of either design efficiency or even the cost of steel frame is strictly applicable when all of the variables of cost and tonnage are identical, a condition very unlikely to occur in practice. In spite of this well-known drawback, the unit weight of steel is an index of vital interest recognized by engineers, owners, and contractors alike, perhaps because it is the only convenient one available. It is easily computed and encompasses fewer uncertainties than cost per unit of area.

Steel buildings in the United States are designed as per the American Institute of Steel Construction (AISC) specifications, which were first published in 1923. The specifications are revised periodically to keep pace with new research findings and availability of new materials. Steel construction for buildings is commonly referred to as steel skeleton framing, signifying that a majority of the members consist of linear structural elements such as beams and columns. With the exception of concrete that is used for foundations, basement walls, and as topping for floor systems, a high-rise can be built entirely by using hot-rolled and built-up steel sections. The building components are assembled in the fabricating shop and erected at the site by skilled laborers called iron workers. In skeleton framing all loadings on the structure are supported by the steel work. Interior partitions and curtain walls are also supported on the skeleton, which therefore resists all the gravity loading. Skeleton framing is normally erected in two-story increments, each increment being called a *tier*. Light-gauge steel decking is most often used in modern office buildings as a permanent form, thus eliminating costly form work needed for concrete slabs.

The rules for the design of structural steel members subject to any one, or combination of, stress conditions due to bending, shearing, axial tension, axial compression, and web crippling are given in the AISC specifications. Although members can be designed by plastic theory based on their ultimate strength, elastic theory is usually used in the design of high-rise buildings. The design is based on allowable unit stresses, usually those given in the AISC specifications and local building codes. In many structural systems the floor elements, such as

girders and spandrels, also participate in resisting the lateral loads. The design process for such elements is conveniently treated by superimposing the gravity and lateral load effects and designing for the 33 percent increase for the combined effect allowed for in most codes.

The functional needs of occupancy invariably dictate that floors be relatively flat. In a steel building this is most often achieved by horizontal subsystems consisting of beams, girders, spandrels, and trusses over which spans a light-gauge metal deck. Concrete topping over the metal deck completes the floor systems. In this chapter a brief description of some of the elements normally employed in the framing of steel buildings is given. We first describe gravity loads, followed by a description of metal deck, steel beams, joists, and finally columns. The description of metal deck is somewhat limited in this chapter because most usually metal deck is employed as a composite member, which we cover in greater detail in Chap. 9.

7.2 Loads

As a result of gravity, the weight of the building itself imposes loads on the structure called dead loads, which remain constant for the life of the building unless, of course, the building undergoes major renovation, such as replacement of exterior cladding or addition of new floors. Occupancy loads also impose gravitational effects, which vary because of the changing occupancy of the floors. These are called live loads and include the effect of people and furniture. Unlike dead loads, live loads cannot be accurately predicted but can only be estimated. These are dictated by building codes based on structure type and occupancy, thus relieving the engineer of the burden of estimating these loads. Since the nature of occupancy is known, the applicable live loads are used in the design. However, in evaluating the capacity of an existing floor system, it is becoming increasingly common to calculate the actual live load on floors based on the tenant layouts, with due regard to the location of heavy loads such as computers, filing systems, and book stacks.

Gravity loads on buildings are of two kinds: (1) static and (2) dynamic. Static load is considered permanent, whereas the dynamic load is time-dependent. The weight of every element within the structure is a static load. The static load includes weights of load-bearing elements, beams, slabs, columns, walls, ceiling, floor and wall finishes, sprinkler systems, light fixtures, sheet metal ducts, permanent partitions, exterior cladding, cooling towers, central plants, pump rooms, thermal storage tanks, and other mechanical equipment. The actual weight of the structural elements is perhaps one of the most

accurately calculable, but even here the allowable construction tolerances, especially in cast-in-place construction, may introduce appreciable errors in the calculated loads.

Although their effect is similar to dead loads and essentially static, live loads are less accurately predictable and subject to greater variation. Most often in North America a value of 50 psf (2394 Pa) for live load plus 20 psf (958 Pa) for partition allowance is used in the design of speculative office buildings. Sometimes if tenants' requirements are known prior to the design of the building, allowance is made for expected usage of heavier loads such as book stacks, filing cabinets, and computers and business machines. It is becoming increasingly common in certain cities of the United States to design an area 20 ft (6.0 m) or so deep adjacent to the exterior of the building for the minimum 50 plus 20 psf (2394 plus 958 Pa) load, while the interior space is designed for a heavier load such as 100 psf (4788 Pa). The rationale is that the space adjacent to the building exterior invariably consists of office space with light furniture, whereas heavily loaded areas such as storage and computer rooms are tucked away from the exterior closer to the building core.

When a typical speculative office building is planned, the nature of tenant layout is not known, although it is common practice to study the floor plans for single- and multitenant occupancies from the architectural point of view. Architectural drawings hypothetically delineate various spaces as lease space, corridors and lobbies, etc., which may turn out to be entirely different from the final layout. Therefore, it is almost impossible to accurately predict the live-load conditions to which a structure will be subjected. The loads given in the codes are based on experience, survey analysis, and previous successful history for various occupancies.

The loads given in the code tables have built-in empirical safety factors to account for maximum possible loading conditions and are given in the form of equivalent uniform loads and prescribed concentrated loads. Although there is a common understanding among engineers that the values given in the codes are rather conservative, invariably the design is done to the standards given in the codes applicable to the particular occupancy. However, when the actual layout and height of partitions are known, an attempt is made to justify a lower partition load. This is done more to justify the load-carrying capacity of an existing framing than to take advantage of the reduction in the design of a new facility.

Concentrated loads indicate possible single-load action at critical locations and are in addition to the uniform distributed load. It is perhaps obvious that the chances of having the full occupancy load simultaneously on every square foot of a large area in a building are

next to zero. The larger the area under consideration, the less is the potential for having full occupancy load. This probability aspect is taken into consideration in the codes by allowing the use of live-load reduction factors. However, recent failures of long-span structures have brought to light the necessity of taking extra precautions, especially in the detailing of connections to account for extraordinary situations, such as people crowding because of ceremonies, parties, fire drills, etc.

Construction loads are caused by building construction techniques, requiring stockpiling of materials on relatively small areas. Construction materials, such as dry walls and glass lights for curtain wall are usually stacked on each floor. Theoretically, the structure can be loaded to its full design load (live load plus partition load) once the materials have reached their design strengths. Some engineers, however, limit the loads from stockpiling of materials to the design live load only without including the partition load. The partition load of 20 psf (957 Pa) is considered equivalent to the incidental loading due to equipment and persons used to shift the load around the floor areas.

7.3 Metal Deck Systems

The primary function of a floor system is to collect and distribute gravity loads to vertical elements such as columns and walls and occasionally to tension members such as hangers. This is accomplished by the out-of-plane bending action of the floor system. Another structural function the floor system is often called upon to fulfill is to transmit the lateral loads to various lateral-load-resisting systems. This action is called the diaphragm action. In addition to these two structural actions, other nonstructural functions of the floor system are (1) to support nonstructural components such as finish materials in the ceiling and floor, piping, ducts, wiring, lighting, and sprinklers; (2) to provide protection from damage that may be caused by fire; and (3) to provide resistance to transmission of sound. In this section we will consider the bending and diaphragm action of floor systems commonly used in steel buildings.

7.3.1 Bending behavior

Corrugated high-strength, light-gauge, cold-rolled steel deck can serve as a permanent base for concrete floors in conventional steel buildings. It provides a strong, efficient structural section for forming slabs and also provides an immediate working surface for other trades while protecting workers on lower levels.

The deck is used as a permanent centering. It is formed from light-gauge cold-rolled steel to a corrugated rib pattern of various

depths and pitch varying from about $\frac{9}{16}$ to $\frac{15}{16}$ in (14.2 to 23.8 mm) in depth and a pitch of about $2\frac{1}{2}$ to $4\frac{1}{2}$ in (63.5 to 114.3 mm). The deck is erected with ribs perpendicular to purlins and welded to the supporting structures. The deck can be designed either for shored or unshored conditions. When the deck is galvanized, it is normal practice to assume that it carries the dead load of the slab permanently; the reinforcement in the slab is designed for superimposed loads only. Most usually the thickness of concrete above the deck is $2\frac{1}{2}$ and 3 in (63.5 to 76.2 mm) in buildings using joist systems. Reinforcement in the slab normally consists of welded wire fabric and is calculated on the basis of continuous spans, assuming that it is placed at the middepth of the slab. For slabs over 3 in (76.2 mm) the welded wire fabric is draped over bolsters to provide a $\frac{3}{4}$-in (19-mm) top cover at the supports.

The metal deck is designed as a form to support the load of wet weight of concrete plus a construction load of workers usually at 20 psf (957 Pa). The entire live load is supported by the reinforced concrete slab after it has cured to design strength. Intermediate shoring of deck is normally omitted by selecting a proper gauge of the material. The slab is designed in accordance with ACI code, with welded wire mesh either draped over supports or placed at the middle depth of slab. Concrete admixtures containing calcium chloride should not be used over metal deck. Care should be exercised during pouring operations not to allow heavy concentrated loads or equipment to be placed on steel forms. Some metal decks can be used for composite beam construction with the bottom of the flute wide enough to accommodate $1\frac{1}{4}$-in (38.1-mm) ferrules, which are standard in the industry for $\frac{3}{4}$-inch (19.0-mm) diameter studs. Fusion welding is generally the most economical and efficient method for attaching steel deck to structural supports. Welds are made from the top side of the deck. Normally the welds to supports are $\frac{1}{2}$-in (12.7-mm) diameter puddle welds or an elongated weld having an equal perimeter. Puddle welds are similar to plug welds, except that no prepunched hole exists prior to welding. The welding heat is sufficient to penetrate the panel and permit fusion to the supporting structure.

7.3.2 Diaphragm behavior

The lateral loads, such as wind loads, that act on the face of a building are distributed to various lateral-load-resisting elements through the so-called horizontal diaphragm action of the floor slabs and roof. Steel floor and roof deck panels properly designed and attached to the building's structural framing members furnish an effective bracing system. As a bracing system, the diaphragm transmits horizontal loads to shear-resisting elements such as vertical shear walls, mo-

ment-resisting frames, and braced bents. The structural behavior of a horizontal diaphragm can be compared to a steel wide flange beam turned on its side. The steel floor panel forms the web, while the perimeter structural members of the building constitute its flanges. The wind loads on the building face are transferred as in-plane loads to the diaphragm by the bending action of window mullions and other portions of the curtain wall support system.

The quality of welds between the deck and the structural support is critical in the design of the diaphragm, as are the connections between the seams of adjacent panels and between the deck and the boundary elements. Puddle welds are made by using a welding rod to burn through the steel deck panel and to contact the flange of the support member. The crater thus formed is filled with weld rod material. The quality of welding to a great extent depends on the ability of the welder to consistently produce welds of structural strength.

The use of trench header ducts greatly diminishes the diaphragm continuity, especially if placed in areas of high shear stresses. When trench headers are used, the deck should be investigated for shear capacity without concrete. To restore its capacity, additional welding may be required. In general, the diaphragm must be designed for lateral loads in both the transverse and longitudinal directions, and like all beams must be designed to resist both shear and bending.

Horizontal diaphragms can be classified according to their tendency to deflect under load. Composite metal deck systems with structural concrete topping behave similarly to a concrete slab and deflect very little under lateral loads and are therefore classified as rigid diaphragms. However, rigidity is a relative term, and whether a floor system can be considered rigid or flexible is a function of the stiffness of the floor system as compared to the stiffness of the lateral-load-resisting elements. It is conceivable that in a narrow building consisting of braced cores or shear walls, the diaphragm is relatively flexible as compared to the braced core or shear wall. In general, in high-rise building design, it is common practice to consider the diaphragm as rigid, unless the plan aspect ratio of the building is greater than 3 to 1 or so.

The horizontal shear at any level is distributed to various vertical elements of the lateral-force-resisting system, such as shear walls, braces, and moment frames, in proportion to their rigidities, considering the rigidity of the diaphragm. For illustration purposes, diaphragms can be conveniently classified into three groups of relative flexibility: rigid, semirigid, and flexible. No diaphragm is infinitely rigid nor any load-carrying diaphragm infinitely flexible.

A rigid diaphragm (Fig. 7.1) is assumed to distribute horizontal forces to the vertical-load-resisting elements in proportion to their

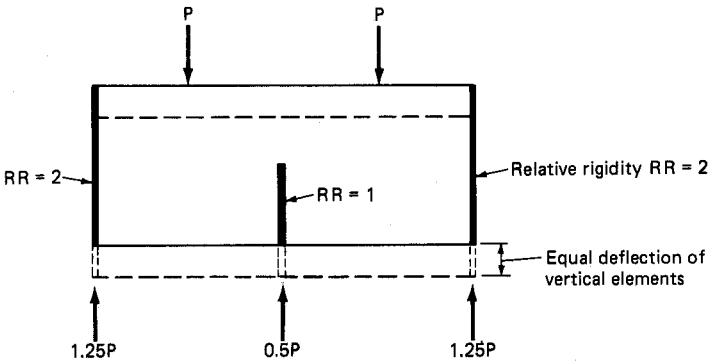

Figure 7.1 Rigid diaphragm.

relative rigidities. In other words, under symmetrical loading a rigid diaphragm will cause each vertical element to deflect an equal amount. Therefore, a vertical element with high relative rigidity will resist a greater proportion of the lateral force than an element with lower rigidity.

The behavior of a flexible diaphragm (Fig. 7.2) can be considered similar to that of a continuous beam or series of beams spanning between supports. The vertical resisting elements are considered nonyielding because their relative stiffness as compared to that of the diaphragm is very large. Thus a flexible diaphragm is considered to distribute the lateral forces to the vertical resisting elements on a tributary load basis and therefore is not capable of distributing torsional loads.

Semirigid diaphragms (Fig. 7.3) are those that have significant

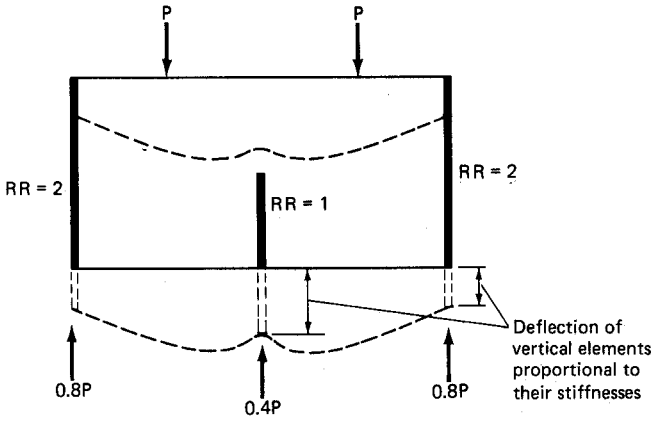

Figure 7.2 Flexible diaphragm.

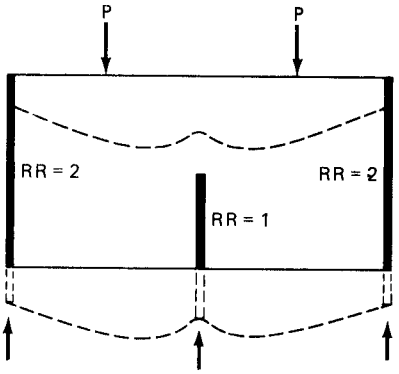

Figure 7.3 Semirigid diaphragm. *Note*: Support reactions are a function of relative stiffness of diaphragm.

deflection under load but at the same time possess sufficient stiffness to distribute a portion of their load to vertical elements in proportion to the rigidities of the vertical resisting elements. Their action is analogous to a beam on yielding supports. The support reactions, which are the loads resisted by the vertical elements, are a function of not only the stiffness of the vertical elements but also the stiffness of the diaphragm itself. Although theoretical considerations demand that all building floor slabs be analyzed as semirigid diaphragms, a rigorous analysis is very time consuming and frequently unjustified by the results. At best the results are no better than the assumptions that must be made. Many fine designs of tall buildings have been accomplished using the rigid slab assumption; however, in long and narrow buildings it is prudent to design lateral-load-resisting elements based on reasonable limits by bracketing the likely range of reactions and deflections.

In most buildings it is economical to use the roof and floor systems as diaphragms. This results in the greatest economy, since these are required anyway for carrying the vertical loads and to provide fire resistance compatible with the governing codes. A number of features of diaphragm design must be examined in detail. Chief among these are

1. The span of the diaphragm; if the vertical resisting elements of approximately equal stiffness are equally spaced, the diaphragm connecting these elements need only be nominally stiff, since each vertical element carries its tributary loads. If the diaphragm has to span from one end to the other end of the building, consideration should be given for the selection of horizontal steel bracing.
2. In the seismic design of tall buildings, use of a rigid diaphragm is almost mandatory to distribute the horizontal forces and torsion in proportion to the relative rigidities of the vertical resisting ele-

ments. A relatively flexible diaphragm will permit portions of the building to vibrate out of phase with the rest of the structure, creating undesirable effects.

3. Diaphragms can be designed as deep beams, with the deck and slab carrying the shear, and the flanges, such as spandrel beams at the edges, resisting bending moments. Metal deck will require details for joining the units to each other and to their supports to distribute shear forces. Boundary members that are designed to resist direct tensile and compressive forces must have adequate splices at points of discontinuity. For example, spandrel beams acting as flanges of the diaphragm require a splice design at the column for transferring tensile and compressive forces.
4. Diaphragms with cutouts and openings for elevators, stairs, atriums, etc., should be analyzed similarly to a plate girder with web openings.
5. Particular attention is required for the detail of connections when the length of contact between the vertical resisting element and the diaphragm is limited.

7.4 Open-Web Joist System

Open-web joists have been in use as floor and roof framing members since the early 1920s. The first joist used in 1923 was a warran truss type with top and bottom chords of round bars and a web formed from single continuous bent bar. Since then, many types of joists have been developed, primarily to provide an economical floor and roof system. Their capacities and sizes are standardized and they are delivered to the site completely fabricated. They are made in standard depths from 8 to 30 in (0.2 to 0.76 m) for the H series and 18 to 48 in (0.46 to 1.2 m) for LH series, and 52 to 72 in (1.32 to 1.84 m) for the DLH series. Recently K series have been introduced which are more economical than H series. Open-web joists are manufactured utilizing hot-rolled or cold-formed steel. They are designed according to the standards set by the Steel Joist Institute (SJI), primarily as simply supported uniformly loaded trusses. The top chord is assumed to be continuously braced by a floor or roof deck. The bottom chord is designed as an axially loaded tension member. The web members are designed to resist both the vertical and horizontal shear. Either diagonal or horizontal bridging is used to stabilize the joists. The number of rows of bridging required is a function of the clear span of the joist and the chord size. Typically three to five rows may be required for the 30- to 40-ft (9.15- to 12.2-m) span range normally required for office buildings.

The reasons for providing bridging in open-web joist construction are

(1) to provide stability for the joists during construction; (2) to maintain alignment of the joists at locations as specified by the engineer; (3) to control the slenderness ratio of tension bottom chord to below 240 (although this limitation is not essential for the structural integrity of tension members, it is adhered to in practice to maintain a certain minimum stiffness of the members to prevent undesirable lateral movements); and (4) to provide lateral stability for compression diagonals.

Although other types of floor decks, such as precast concrete, gypsum, wood, or other materials capable of supporting the load can be used, in high-rise buildings concrete topping on metal deck is typical. The load tables published by the SJI are based on uniform conditions. They can be used in selecting joists for gravity loads that can be expressed in terms of load per unit length of joist. Partitions, heavy pipes, and other elements running perpendicular to the joist and mechanical units mounted on joists should be treated as a concentrated load. In such cases the joist should be designed for the full combination uniform load and concentrated load.

In everyday engineering practice, the engineer is relieved of the burden of designing the joists per se and selects the standard type and size required for the span and load conditions. Joists are manufactured with 50-ksi (344.75-MPa) steel for the chords and 36- or 50-ksi (248.2- and 344.75-MPa) steel for web members at supplier's option. Chords of joists used for floor members are essentially parallel. Top chords are designed for uniform loads and are assumed either simply supported between or continuous over the panel points.

It is normal practice to design the compression diagonals of an open-web joist with an effective length factor of $K = 1$ on the premise that the transverse flexural stiffness of the bottom tension chord coupled with the resistance of tension diagonals and bottom chord braces provides adequate stiffness. It behooves the engineer to verify that adequate bracing exists in unusual conditions with high stresses in the compression diagonals.

In some North American locations, it is becoming more common to use open-web joists to support the roof system. Even when the remainder of the building is of concrete construction, consideration is given to framing elevator, stairs, and mechanical penthouse roofs by using open-web joists. It is necessary in such cases to check the uplift capacity of the joists because of the vertical suction forces induced by wind loads. In keeping up with the current architectural trend, many buildings sport fancy roofs which, when framed with joists, require due consideration of uplift forces. The net uplift force on roof joists is the gross uplift force due to wind, less the dead load of the roof system tributary to the joist, including the weight of the joist. If adequate dead

load exists on the system in excess of the gross uplift load, no further consideration is necessary. If not, the design of the joist should be reviewed for reversal of stresses, such as compression of the bottom chord. Lateral bracing required to stabilize the bottom chord can be provided by (1) additional bridging, (2) rearranging the bridging provided for the normal loading, or (3) increasing the size of the bottom chord. The web system may also undergo stress reversal. Therefore, all components of the joists must be checked for stress reversal. As in other wind design, a 33 percent increase in allowable stresses is allowed, as long as the required section is not less than that required for dead and live load combination.

Buildings of low height in the 1- to 10-story range stand a good chance of being more economically built in steel than concrete because there may not be enough repetitions of the form work to make concrete economical. When these buildings are constructed in steel, most often the system consists of structural steel columns and beams with open-web joists spanning from beam to beam. Metal deck is laid on top of the joists with a 3-in (76-mm) concrete floor slab poured on the deck itself. Open-web joists are economical because they make use of structural steel more efficiently than do typical wide-flange sections. To support a given area, a joist costs less than a comparable beam. Although buildings with open-web joists are perfectly safe in the eyes of some developers, bar-joist-framed buildings are least prestigious and, therefore, are not used for certain sectors of the rental market. Developers consider such buildings to have less solid feeling because the floor tends to transmit more sound and vibrations than a concrete building. In their eyes, a step up from open-web joist systems is a steel building with steel columns, steel girders, and beams made to act compositely with a concrete floor system. A further step up from the standpoint of stiffness, vibration, and sound transmission is a concrete frame building. However, a commercially acceptable floor system with open joists is achievable for high-rise structures provided proper evaluation is made for stiffness, vibration, and sound transmission characteristics of the floor system.

Form work for high-rise building floors with open-web joists usually consists of a decking of corrugated steel sheets placed on top of the joists to act as a permanent form. The sheets are produced in various material thicknesses and depths especially for this purpose and are marketed in North America under various trade names. The design recommendations for this type of deck are given in the Steel Deck Institute (SDI) *Specifications and Commentaries*. The following is a brief summary of the salient features of SDI specifications.

The material for the manufacture of steel deck shall conform to ASTM A611 or A446 with a minimum yield strength F_y of 33 ksi (227.5

MPa) with an allowable bending stress limited to $0.6F_y$ but not exceeding 36 ksi (248.2 MPa). The actual thickness of the deck supplied shall not be less than 0.95 percent of the design thickness.

When unshored galvanized metal deck is used to support concrete slab, the weight of the slab is considered to be carried permanently by the deck. The minimum galvanizing required for permanent load-carrying function should comply with ASTM-A525 G60, which means that a minimum of $\frac{3}{4}$ oz of galvanizing is required per square foot of deck. When uncoated or painted deck is used to support a reinforced concrete slab, the form is considered temporary and the reinforcement is designed for both the weight of the slab and other dead and live loads. Reinforcement is determined by conventional reinforced concrete procedures as recommended by ACI 318-83, using either the working stress or ultimate strength method. The minimum thickness of concrete above the top rib of deck shall not be less than $1\frac{1}{2}$ in (38 mm). The design of the metal deck itself should comply with the ASCE *Specifications for the Design of Cold Formed Steel Structural Members.* The bending stresses in the deck should not exceed 36 ksi or $0.6F_y$ under dead load of wet concrete and deck and construction loads. For purposes of stress calculation, the construction load may be assumed to be equal to 20 psf (957.6 Pa) of uniformly distributed load or 150-lb (667.2-N) concentrated load acting at midspan on a one-foot (0.3-m) width of deck. The allowable deflection is limited to $L/180$ or 3/4 in (19 mm) where L is the span of deck; when the deck thickness is less than 0.028 in (0.71 mm), welding washers are required to achieve adequate connection between the deck and structural steel. For spans greater than 5 ft (1.52 mm) side laps at middle or at 3-ft (0.91-m) centers, whichever is smaller, are required. Mechanical fasteners satisfying the design criteria can be used as anchoring devices.

7.5 Wide-Flange Beams

Wide-flange rolled structural shapes constitute the most common types of flexural members used in steel buildings to support transverse loads. These are used as beams, girders, and spandrels and can be designed as simply supported, fixed-ended, or partially fixed. They can be proportioned for shears and moments determined by elastic analysis using allowable stresses. Designs using plastic theory for factored loads, although allowed in the AISC code, have not come about as a general office procedure and will not be discussed here. It is not the intent of this work to present the whole array of elaborate adjustments to allowable bending stresses as required by the AISC specifications. Only the highlights of design aspects are considered.

7.5.1 Bending

According to AISC specifications, under usual conditions the allowable bending stress $F_b = 0.66F_y$, where F_y is the yield strength of steel. Almost all beams are designed to bend about their major axis and are required to be laterally braced within certain intervals to resist lateral torsional buckling. Lateral supports for flexural members are required because the compression flange behaves in a manner similar to a column and tends to buckle in the absence of lateral supports. Metal decking welded to the beam top flange at sufficiently close intervals constitutes lateral bracing, as do cross beams framing into the sides of the beam if adequate connection is made to the beam top flange. Assuming adequate lateral bracing, the design of a steel beam boils down to the selection of a bending member having a section modulus equal to or slightly larger than the calculated value.

7.5.2 Shear

Steel beams used in floor framing most often are wide-flange shapes possessing an axis of symmetry about the plane of bending. Such members are designed for shear assuming (1) the contribution of flanges to the shear capacity is negligible, and (2) the parabolic variation of shear stress in the web is replaced by an average stress on the gross area of the web. With these assumptions, for purposes of calculating the shear stresses, symmetrical shapes can be reduced to an equivalent rectangle with dimensions $t_w d$ where t_w is the thickness of web and d is the beam depth. The calculated shear stress $f_v = v/t_w d$ should not exceed the allowable shear stress $F_v = 0.40\,F_y$. Shear stress is very rarely a factor in the design of beams subjected to uniformly distributed loads imposed in typical office floors. However, it should be checked for beams with very short spans and for beams with heavy concentrated loads near the supports.

7.5.3 Deflections

Steel beams are usually cambered for dead load deflections when such deflections are in excess of 0.75 in (19 mm). The maximum camber should be limited to about 2.5 in (63.5 mm) because of floor-leveling problems during concreting operations. The allowable live load deflection is a function of the type of ceiling suspended from the beams, and for plastered ceilings it should not exceed 1/360 of the span. The AISC commentary recommends that the depth-to-span ratio of fully stressed beams in floors be not less than $F_y/800{,}000$, and, if subject to shock and vibration, not less than $F_y/650{,}000$. However, it should be pointed out that commercially acceptable floor systems can be designed with lesser

depths provided the vibration characteristics are adequately considered in the design.

7.6 Columns

The gravity loads collected by the floor and roof system are transferred to vertical subsystems consisting of columns which in turn carry the vertical loads to the foundation. A vertical subsystem designed as part of a lateral load system is called upon to carry the horizontal loads also to the foundation. In this section we are concerned with columns that are designed to carry vertical loads only, it being assumed that there exists an independent structural system for resisting lateral loads. The design of such a column primarily carrying vertical loads reverts to selecting a steel section with calculated compressive stresses below or equal to the allowable stresses given in the AISC specifications. An effective length factor of $K = 1$ is used in the design. Although the steel sections rolled in the United States are quite heavy, for buildings in excess of 40 stories or so, it becomes necessary to use built-up shapes or to use cover plates on heavy rolled shapes. A few examples of gravity columns used in the lower floors of high-rise buildings are given in Fig. 7.4.

When a straight column is subjected to a bending stress as well as a compressive stress, the member behaves as a beam-column and starts to deflect laterally at an axial load much smaller in magnitude than the load that can be supported by a column subjected to axial stresses only. As the load is gradually increased, the deflection increases at a much faster rate because of the increased eccentricity of the load.

AISC specifications give comprehensive rules for the elastic design of columns subjected to known axial loads and bending moments. The first step is to calculate the effective length of the column, which is expressed as K times the actual length. An "alignment chart" is provided to evaluate K when the elastic rotational restraints are known. The restraints offered by the beams at the ends of the column are expressed in terms of a quantity G, which is the ratio of stiffness of columns to the stiffness of beams at the location of beams. For columns in frames which are free to sway, the designer is cautioned that the effective length can exceed twice the length of the column.

The next step is to check the safety of the column by the use of interaction formulas. In recognition of the fact that moment magnification is negligible when axial loads are small, a simple relation applicable only when $f_a/F_a \leq 0.15$ is given. For bending in one plane only, this equation is of the form

$$\frac{f_a}{F_a} + \frac{f_b}{F_b} \geqslant 1.0$$

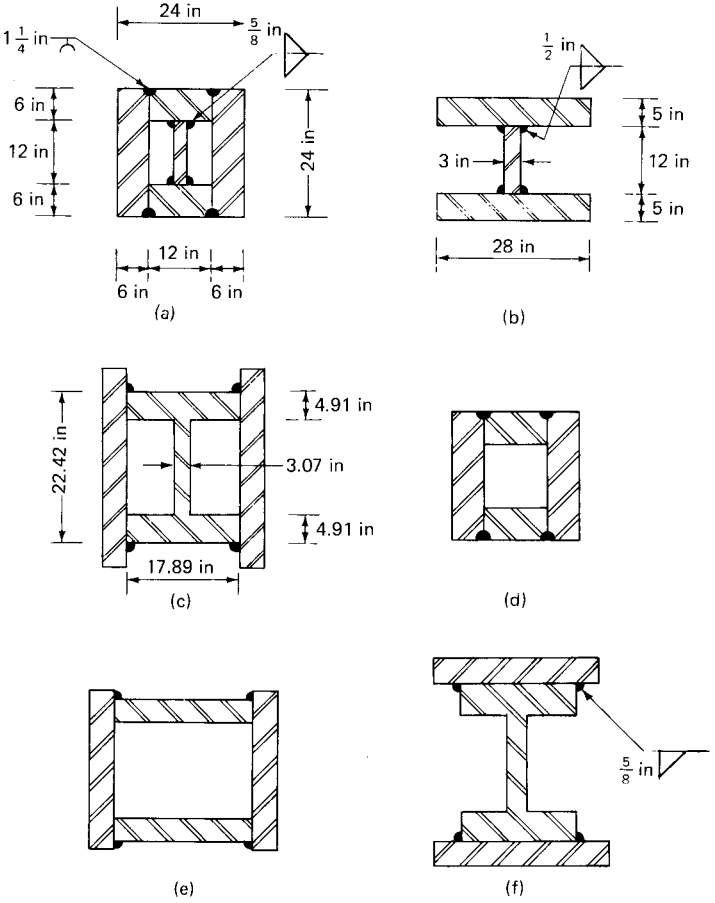

Figure 7.4 Examples of gravity columns.

where F_a = allowable axial stress in the absence of bending
F_b = allowable bending stress in the absence of axial load
f_a, f_b = axial and bending stresses at working loads

When the axial stress is not small, a more comprehensive interaction formula is used

$$\frac{f_a}{F_a} + \frac{f_b}{F_b}\left(\frac{C_m}{1 - f_a/F'_e}\right) \not> 1.0 \tag{7.1}$$

where F_a, F_b, f_a, and f_b have the same meaning as before; C_m is a coefficient that allows for the variable location of the critical section in the length of the column, and F'_e is the elastic critical stress calculated

by taking into account any end restraints, divided by a safety factor of 23/12.

The expression $[C_m/1-(f_a/F'_e)]$ is an amplification factor by which the bending stress f_b is multiplied to account for the destabilizing effect of axial load. Equation (7.1) is intended to check the combination of axial stress and amplified bending stress when the critical location is not close to the ends of the member. The amplification factor is considered inappropriate for cases where the largest bending stress occurs at one end; the following additional check is required for such cases:

$$\frac{f_a}{0.6\,F_y} + \frac{f_b}{F_b} \gtrless 1.0$$

where F_y = yield stress. Similar relations, which include two expressions for bending stresses in the x and y directions, are used for columns subjected to compressive loads and biaxial bending.

Today, with the availability of computer programs which can take into account the effect of secondary moments or the so-called p-Δ effect, it is no longer necessary to use the moment magnification terms given in the AISC interaction equations. The increases in the column and girder moments due to the p-Δ effect can be accounted for directly in the design, thus satisfying the requirement that general stability be provided for the structure as a whole and for each compression element. This is examined further in Chap. 11.

Chapter

8

Gravity Systems in Concrete Buildings

In the previous chapter we discussed that almost all types of floor systems in steel buildings utilize light-gauge steel deck as a permanent form, and in composite construction as positive reinforcement as well. In contrast to steel framing, concrete floor systems are cast upon temporary form work or centering of lumber, plywood, or panels that are removed when the concrete has reached enough strength to support its own weight combined with any likely superimposed loads. This necessary procedure dictates that form work be simple to erect and remove and be repetitive to achieve maximum economy. Although in general floor systems for high-rise buildings are the same as for their lower brethren, there are several characteristics which intensify themselves in the case of high-rise buildings. For example, floor systems in high-rise buildings are duplicated many times over, necessitating optimum solutions in their design because:

1. Savings that might otherwise be insignificant for a single floor may add up to a considerable sum when multiplied by the large number of repetitions
2. Dead load of the floor system has a major impact on the design of vertical-load-bearing elements

The desire to minimize dead loads is not unique to concrete floor systems but is of greater significance because the weight of the

concrete floor system tends to be heavier than steel floor systems and therefore has a greater impact on the design of vertical elements and foundation system. Another consideration is the impact of floor depth on the floor-to-floor height and thus the total height of the building. Thus it is important to design a floor system that is relatively lightweight without being too deep.

One of the necessary features of cast-in-place concrete construction for tall buildings is the large demand for job-site labor. Form work, reinforcing steel, and the placing of concrete are the three aspects that demand the most labor. The opportunity for repetition in the use of forms is almost a necessity for economical construction of cast-in-place high-rise buildings. Types of forms which can be used repetitively are "ganged" together and are collectively referred to as *gang forms*. These forms are carried forward, or up the building, in large units, often combining column, beam, and slab elements in a large piece of form work. Where the layout of the building frame is maintained constant for several stories or for the whole structure, these result in economy of handling and placing. "Slip" forming is another type of economical repetitive forming. "Flying" forms for flat work are another type that can be built and handled to place concrete for large floor areas. For example, in a conventional construction method called the stick method, plywood sheets are nailed to a formed solid decking built on adjustable shores. When concrete has attained sufficient strength, the shores are removed and the plywood sheets are stripped, and if undamaged, they are stored for reuse when shoring and wooden decking are erected for the next floor. This method of forming is labor-intensive and also time consuming. If the floor-to-floor cycle is delayed one day because of it, the construction time of a tall building can be lengthened by two months or so. The flying form system makes maximum use of repetition in multistory construction. In this system, floor forms are attached to a unit consisting of deck surface, adjustable jack, and supporting frame work. For stripping, the form is lowered by the jack, slipped out of the slab, and shifted to the next floor for use as one rigid structure, resulting in economy of handling and placing. In this chapter a brief description of some of the common types of floor systems is given followed by a description of principles and applications of posttensioning techniques.

8.1 Floor Systems

8.1.1 Flat plates

Concrete slabs are often used to carry the loads directly to vertical systems such as walls and columns without the use of beams or girders.

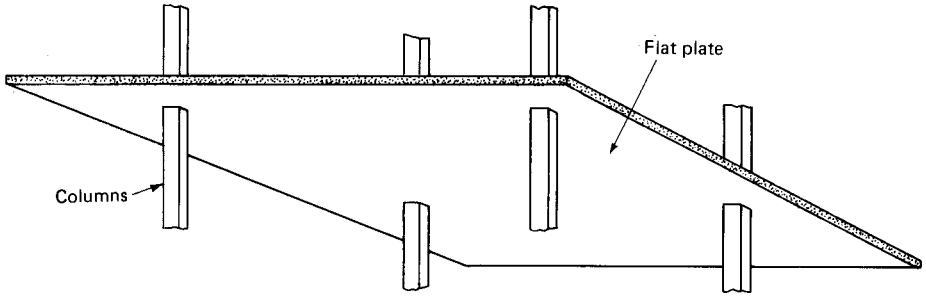

Figure 8.1 Flat plate system.

Such a system is called flat-plate system (Fig. 8.1) and is used where spans are not large and loads are not heavy as in apartment and hotel buildings.

Flat plate is the term used for a slab system that spans to columns without any column flares or drop panels. Although column patterns are usually in a rectanglar grid, flat plates can be used with irregularly spaced column layouts. Flat plates have been successfully built using columns in triangular grid patterns and other numerous variations.

8.1.2 Flat slabs

The flat slab (Fig. 8.2) is also a two-way system of beamless construction but incorporates a thickened slab region at the columns and walls. In addition to the thickened slab, the system can have flared columns; both the thickened slab and the column flares, which are referred to as drop panels and column capitals, respectively, reduce shear and negative bending stresses around the columns.

A flat slab system with a beamless ceiling allows minimum structural depth, providing for maximum flexibility in the arrangement of

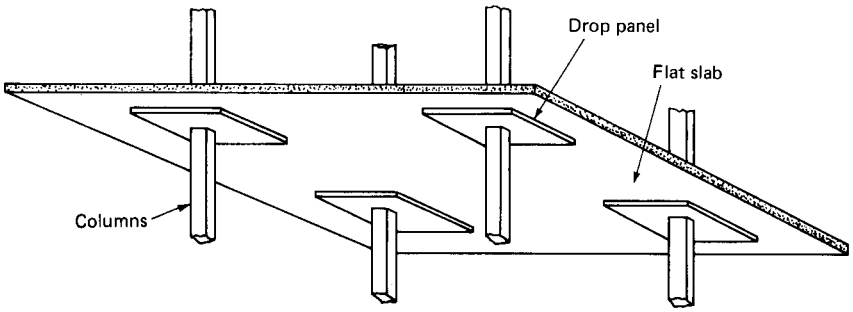

Figure 8.2 Flat slab system.

air conditioning ducts and light fixtures. For residential designs, the slab can serve as a ceiling for floor below and therefore is more economical. Since there are no beams in a flat slab or plate system, the slab itself replaces the action of the beams by bending in two orthogonal directions. Therefore, the slab has to be designed to transmit the full load in each direction, carrying the entire load in shear and in bending.

The limitations on span are dependent upon the use of column capitals or drop panels on top of the columns. The criterion for thickness of the slab is usually the punching shear around the columns. In high-rise buildings these slabs are generally 5- to 10-in (127- to 254-mm) thick and are used to span from 15 to 25 ft (4.56 to 7.6 m) in each direction.

8.1.3 Waffle system

The two-way joist or the waffle system (Fig. 8.3) is closely related to flat slab system. To reduce the dead load of solid slab construction, metal or fiberglass domes are used in the form work in a rectilinear pattern as shown in Fig. 8.1. Domes are omitted near the columns resulting in solid slab to resist the bending and shear stresses better in these critical areas.

In contrast to a joist system which carries the floor load in one-way action along its length, a waffle system carries the load simultaneously in both directions because the joists are constructed to form a two-way grid. The system is therefore more suitable for approximately square bays than rectangular bays. The overall behavior and moment distribution of a waffle system are similar to those of a flat slab. However, the waffle is more efficient for spans in the 30- to 40-ft (9.1- to 12.2-m) range because it has the luxury of greater overall depth than a flat slab without the penalty of added dead weight.

8.1.4 One-Way Concrete Ribbed Slabs

This system is also referred to as the one-way joist system and constitutes one of the most popular systems for high-rise building construction in North America. The system is based on the well-founded premise that since the concrete in a solid slab below the neutral axis is well in excess of what is required for shear, much of it can be eliminated by forming voids. The resulting system is shown in Fig. 8.4. The voids between the joists can be made with removable forms of steel, wood, plastic, or other material. The joists are designed as one-way T beams for the full-moment tributary to its width. However, in calculating the shear capacity, the ACI code allows for a 10 percent increase in the allowable shear stress of concrete. It is

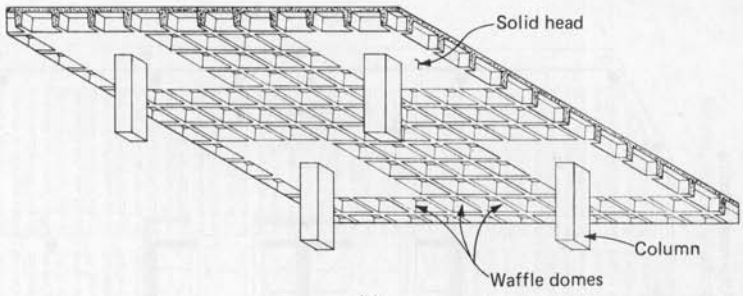

(a)

(b)

Figure 8.3 (*a*) Waffle system; (*b*) waffle slab construction. Note elimination of domes at column to achieve greater punching shear capacity.

standard practice to use distribution ribs at approximately 10-ft (3.0-m) centers for joists with spans greater than 20 ft (6 m). In the design of floors using joists, it is important to conform to the standard forms available in the locality. Maintaining beams, spandrels, and other floor framing members the same depth as joists throughout the project makes for maximum economy of form work and should be investigated if undue penalty is not imposed on the girder and beam designs.

8.1.5 Skip joist system

Another type of joist system called the skip joist system is finding more and more application in high-rise floor framing. Instead of the stan-

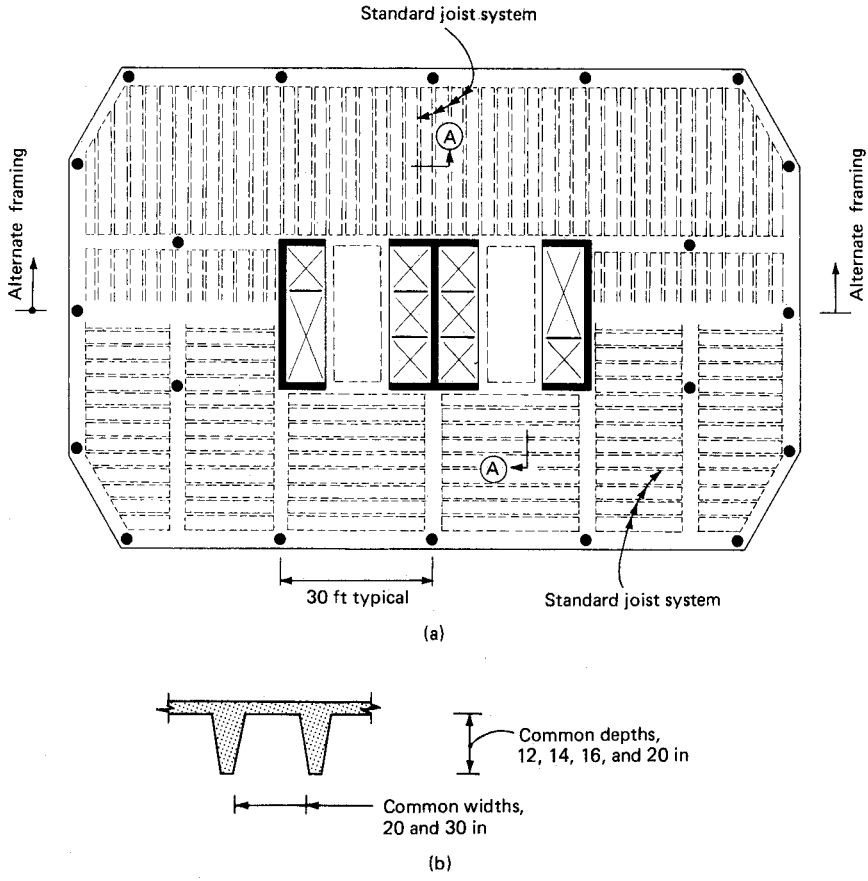

Figure 8.4 One-way joist system. (*a*) Building plan; (*b*) section A.

dard 3-ft (0.91-m) spacing, skip joists are spaced usually 5 ft and 6 ft 6 in (1.52 and 1.98 m) apart using 53- and 66-in (1346- and 1676-mm) pans. The system is frugal in its demand for concrete. The joists are designed as beams without making use of 10 percent increase in the shear capacity allowed for standard joists in the code. Also the system is normally designed without distribution ribs thus requiring even less concrete. The spacing of vertical shores can be larger than in the standard pan layout and consequently the form work is more economical. Figure 8.5 shows a typical layout of skip joist system.

The fire rating of the floor system is normally specified by the governing building codes. The most usual method of obtaining the rating is to provide a slab that will meet the code without the use of sprayed-on fireproofing. In the United States, normally the slab

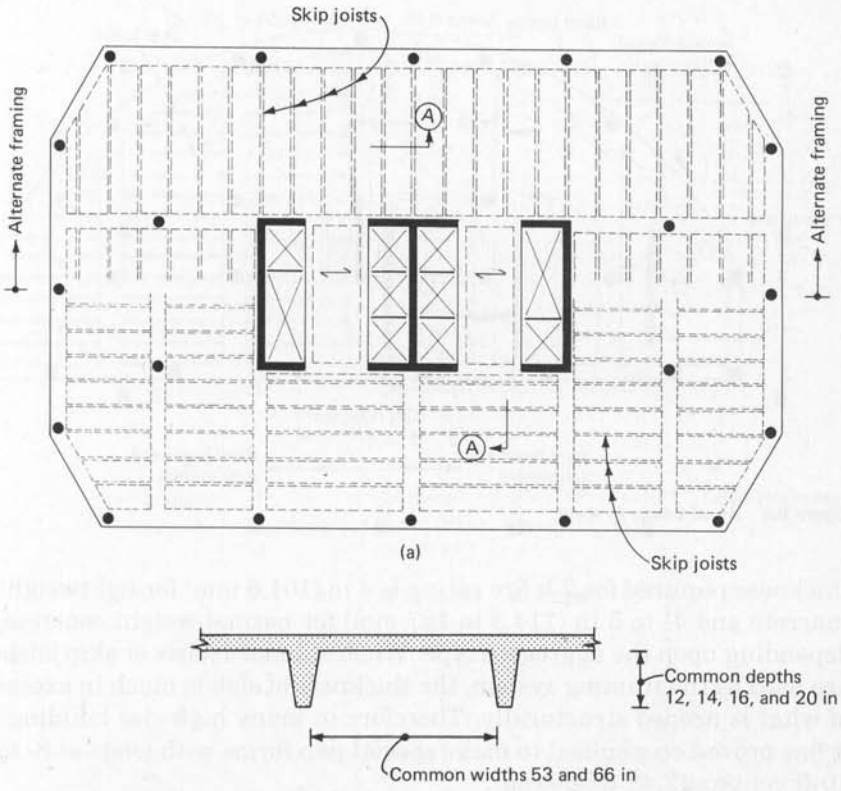

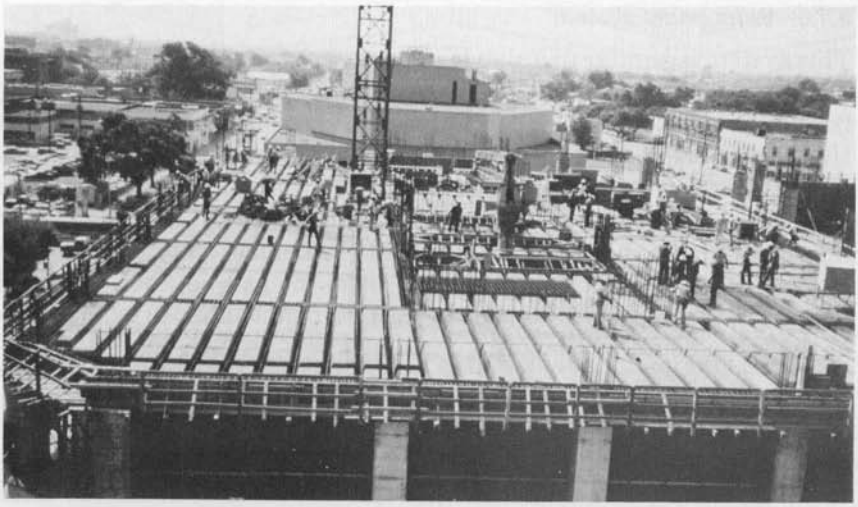

(c)

Figure 8.5 Skip joist system. (*a*) Building plan; (*b*) section A; (*c*) photograph.

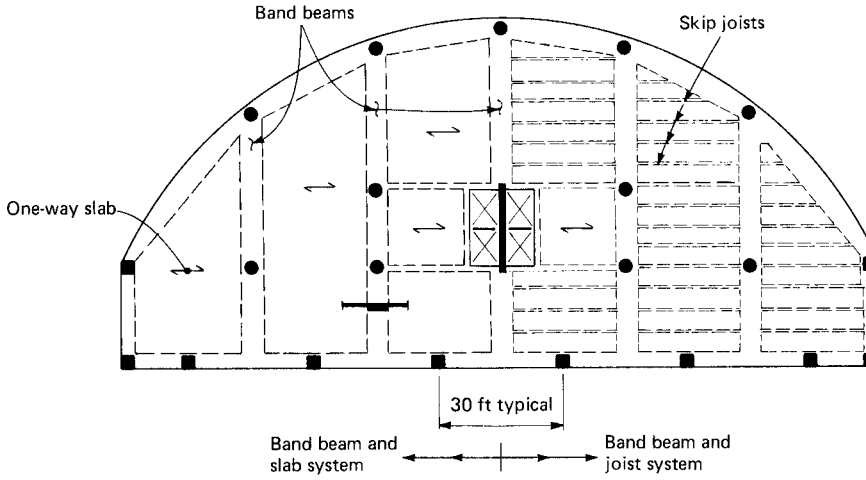

Figure 8.6 Band beam system.

thickness required for 2-h fire rating is 4 in (101.6 mm) for lightweight concrete and $4\frac{1}{2}$ to 5 in (114.3 to 127 mm) for normal-weight concrete, depending upon the aggregate type. When standard joists or skip joists are used as the framing system, the thickness of slab is much in excess of what is needed structurally. Therefore in many high-rise buildings it has proved economical to make special pan forms with joists at 8- to 10-ft centers (2.43 to 3.04 m).

8.1.6 Band beam system

This system is similar to a slab beam system but uses wide and shallow beams and is being increasingly used in floor systems in which the floor-to-floor height is critical. Figure 8.6 shows a schematic layout of this system. Note that it is not necessary to line the band beams with either the exterior or interior columns. The slab in between the band beams is designed as a member with varying moment of inertia to take into account the increased thickness at the beams. Another variation of the scheme uses standard or skip joists to span between the band beams. In terms of form work it is most economical to use band beams of the same depth as the joists.

8.1.7 Haunch girder and joist system

A floor framing system employing girders of constant depth criss-crossing the interior space between the core and the exterior often presents nonstructural problems because it limits the space available for the passage of air conditioning ducts. The haunch girder system is

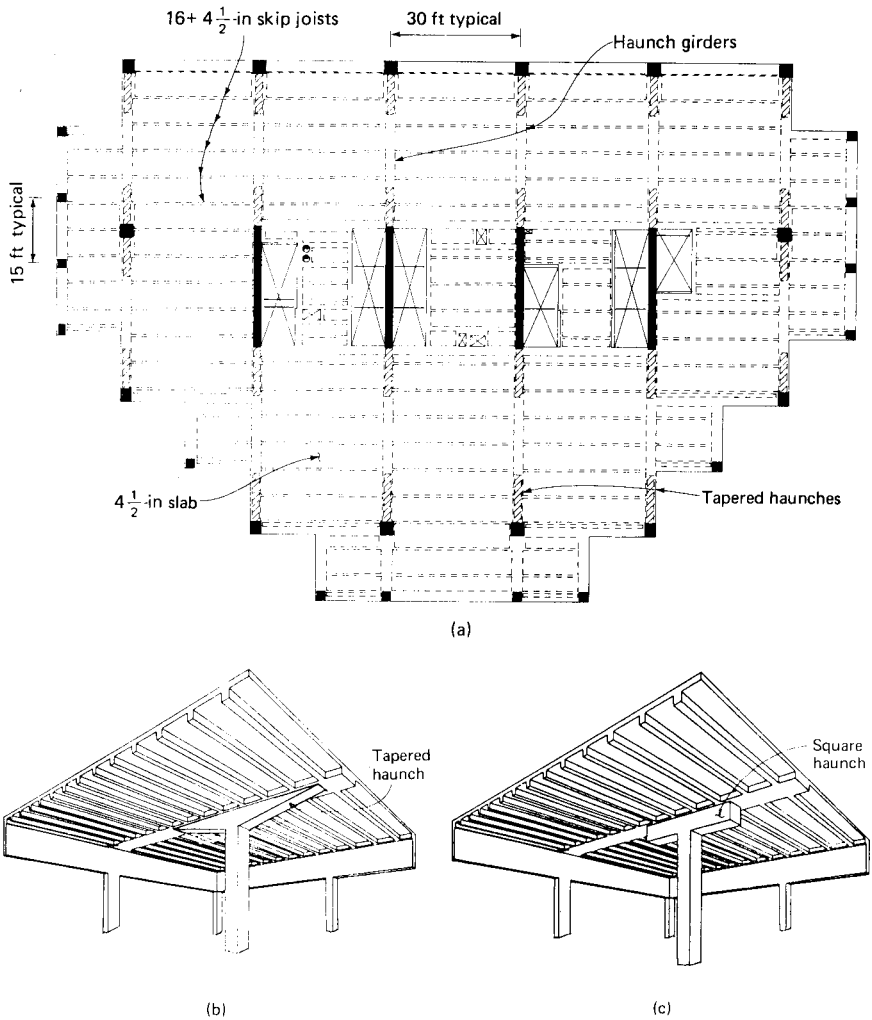

Figure 8.7 (*a*) Haunch girder and joist system; (*b*) perspective view of tapered haunch girder and skip joist system; (*c*) perspective view of square haunch girder and skip joist system.

widely accepted in certain parts of North America and alleviates nonstructural problems without making undue compromises in the structure. The basic system shown in Fig. 8.7*a* consists of a girder of variable depth. The use of shallow depth at the center facilitates the passage of mechanical ducts and eliminates the need to raise the floor-to-floor height. Two types of haunch girder construction are in vogue. One uses a tapered haunch (Fig. 8.7*b*) and the other a square haunch (Fig. 8.7*c*).

8.1.8 Beam and slab system

This system consists of a continuous slab supported by integrally cast beams generally spaced at 10 to 20 ft (3.04 to 6.08 m) on center. The thickness of the slab is generally selected from structural considerations and is usually much in excess of that required for fire rating. The system has broad application and is generally limited by the depth available in the ceiling space for the beam stem. This system is "heavy-duty" and is often used for framing nontypical floors such as ground floor and plaza levels, which are typically subjected to heavier superimposed loads due to landscape and other architectural features.

8.2 Prestressed Concrete Systems

Although mild-steel-reinforced concrete is well suited for the construction of high-rise floor systems, it requires considerable depth to work efficiently, especially in the 35- to 40-ft (10.66- to 12.2-m) span range normally required in modern office buildings. For example, to keep the long-term creep deflection to within acceptable limits, span-to-depth ratios of two-way flat slab and one-way beam or joist systems are limited to about 1/30 to 1/35 and 1/15 to 1/20, respectively. The relatively short span capability of flat slab system limits its application to high-rise multiple-unit residential buildings which can accommodate relatively closely spaced columns within fixed and frequent partition layouts. When used for office layouts, the flat slab system becomes too heavy, imposing undue structural penalty, especially in difficult foundation conditions. The one-way joist system, especially with skip joists, although relatively lightweight, requires about 20 to 24 in (508 to 610 mm) of structural depth for a 35- to 40-ft (10.66- to 12.2-m) span range. By using prestressing it is possible to overcome the aforementioned shortcomings of conventionally reinforced concrete. Prestressing can thus be looked upon as an aid to boost the span range of conventionally reinforced floor systems by about 30 to 40 percent. This is the primary reason for the dramatic increase in the use of prestressing for cast-in-place high-rise construction. Some of the particular advantages of prestressed concrete as compared to normal reinforced concrete structures are:

1. Prestressed concrete members are generally crack-free and are, therefore, more durable.
2. Smaller sections can be used because a larger depth of compression block is available in flexure.
3. Prestress concrete is resilient. Cracks due to overloading completely close and deformations are recovered soon after the removal of overload.

4. Fatigue strength (though not a design consideration in normal high-rise design) is considerably more than that of conventionally reinforced concrete because tendons are subjected to smaller variations in stress limits due to repeated loadings.
5. Prestressed concrete members are generally crack-free and, therefore, are stiffer than conventional concrete members.
6. The structural members are almost self-tested for material and workmanship during stressing operations, thereby safeguarding against unexpected poor performance in service.
7. Prestressing is more manipulable since it is a system wherein additional force is introduced in the system; the magnitude, location, and technique of introduction of such an additional force system is left to the designer, who can tailor the design according to the particular conditions.

Major motivation for the use of prestressed concrete comes from the reduced structural depth, which translates into lower floor-to-floor height, reduction in the area of curtain wall, and the reduction in building volume, with a consequent reduction in heating and cooling loads.

From the point of economy it is fairly well known that little or no savings are obtained in posttensioned systems by using relatively small quantities of high-strength strands instead of rather substantial quantities of mild steel in conventional system. This is because the savings in mild steel reinforcement quantities are just about offset by the higher unit cost of prestressing steel. The real cost savings, however, come from the reduction in the quantity of concrete combined with the nonstructural savings resulting from reduced floor-to-floor height. Although from an initial cost consideration a posttension scheme may be least expensive, it is necessary to include other considerations. These include, but are not limited to, characteristics such as behavior of floor members in resisting lateral loads, ease with which openings in floors for future tenants are accommodated, etc. In this section a brief outline of prestressed concrete as applied to high-rise floor systems is given followed by some practical examples.

8.2.1 Methods of prestressing

Centuries ago humans discovered the underlying principle of prestressing by using tightened metal bands or rope around wooden planks to form barrels. They may not have had the dubious pleasure of figuring out the exact nature and magnitude of stresses, but they knew intuitively that the stronger the bands, the better the chance for containing liquids in the wooden barrels. It was not until the 1880s

that a similar principle was applied to reinforced concrete slab with the idea of counterbalancing the tensile stresses in concrete. Intentional compressive stress in concrete was created to overcome the tensile stresses developed from external loads. These early attempts at prestressing did not meet with great success because the amount of prestressing that could be imposed via conventional steel was limited by the strength of the steel itself. Even at low pressures, it was hard to maintain the prestress because creep and shrinkage of concrete would destroy the prestress in the course of time.

The eminent French engineer Eugene Freyssinet is credited as the forefather of prestressing as we know it today. He is regarded as the first to establish the use of high-tensile-strength steel to assure that even after creep and shrinkage losses there remained adequate prestress to counteract the external loads.

Current methods of prestressing concrete members can be studied under two groups, (1) pretensioning and (2) posttensioning. In pretensioning, the tendons are stressed to a predetermined amount and then, while the stress is maintained in the tendons, concrete is placed around the tendons. After the concrete has hardened, the tendons are released to impart prestress into the concrete member.

In posttensioning, the tendons, which may consist of steel wires, strands, or bars, are tensioned and anchored against the concrete after it has hardened. The tensioning is accomplished by hydraulic jacks. Tendons most usually remain permanently unbonded to concrete and are shipped to the site greased and wrapped in plastic tubes to achieve complete separation. The tendons are placed directly in the forms, usually in a sequence compatible with the mild steel reinforcement, and after the concrete has reached 75 percent of the design strength, the tendons are stressed. The elongations measured at the site are compared against the calculated values, and if satisfactory, the tendons projecting beyond the concrete face are cut off. Form work is removed after posttensioning of tendons, but the concrete is backshored immediately to prevent overloading of members due to shoring of floors above and construction load.

Posttensioning can be accomplished by using high-strength strands, wires, or bars as prestressing tendons. In North America the use of strands by far leads the other two types of tendons. Posttension construction can either be bonded or unbonded depending upon whether tendon ducts are filled with a mortar grout after stressing (bonded) or whether the tendons are greased and covered in plastic (unbonded).

For high-rise construction, unbonded construction predominates because it eliminates the need for grouting. Posttensioned members in a multistory construction such as an apartment or an office building

consist of slab, joists, beams, and girders, which contain a large number of small tendons. Grouting each of the multitude of tendons is a time consuming and expensive operation. Therefore, unbonded posttension construction using strands is popular in the North American high-rise construction industry.

8.2.2 Materials

Posttensioning steel. The basic requirement of steel used in posttensioning is that the loss of tension in the steel due to shrinkage and creep of concrete and the effects of steel relaxation should be a relatively small portion of the total prestress in order to obtain an economical design. In a practical prestressed structure, the loss of prestress generally varies from a low of 15 ksi (103.4 MPa) to a high of 50 ksi (344.7 MPa). If a mild steel having a yield point of 60 ksi (413.7 MPa) is employed in prestressed concrete with an initial prestress of, say, 40 ksi, it is very likely that most of the prestress, if not the entire prestress, is lost because of shrinkage and creep losses. It is clear that to limit the prestress losses to a small percentage of about 20 percent, the initial stress in the steel must be in excess of 200 ksi (1379 MPa). Therefore, high-strength steel is invariably used in prestressed concrete construction.

Although in general high-strength steel is produced by alloying with elements such as carbon, manganese, and silicon, prestressing steel obtains its high tensile strength by virtue of the process of cold-drawing, in which high-strength steel bars are drawn through a series of progressively smaller dyes. During this process, the crystallography of the steel is improved, because cold-drawing tends to realign the crystals.

The high-strength steel used in North American prestress work is available in three basic forms: (1) uncoated stress-relieved wires, (2) uncoated stress-relieved strands, and (3) uncoated high-strength steel bars. Stress-relieved wires and high-strength steel bars are not generally used for posttensioning of high-rise floor systems and therefore are not considered here. The interested reader can find descriptions of these materials in standard textbooks on prestressed concrete.

High-strength strands are fabricated in factories by helically twisting a group of six wires around a slightly larger center wire by a mechanical process called stranding. The resulting seven-wire strands are stress-relieved by subjecting them to a continuous heat treatment to produce the required mechanical properties.

ASTM specification A416 specifies two grades of steel, 250 and 270 ksi (1724 and 1862 MPa), the higher-strength strand being more commonly used in the building industry. For calculation of elongation,

a modulus of elasticity of 27500 ksi (189,610 MPa) is used for posttensioning strands. In order to prevent the use of brittle steel which would result in failure pattern similar to that of an overreinforced beam, ASTM A-416 specifies that the prestressing strand should have a minimum elongation of 3.5 percent at rupture.

A special type of strand called a low-relaxation strand is increasingly being used because it has a very low loss due to relaxation, usually about 20 to 25 percent of that for stress-relieved strand. In effect less posttensioning steel is required, but the cost of low-relaxation strand is relatively more because of the special process used in manufacture.

Corrosion of unbonded posttensioned strand is a possibility and can be prevented by using galvanized strands. This is not, however, a practice in North America because (1) various anchorage devices in use for posttensioned systems are not suitable for use with galvanized strand because of low coefficient of friction, (2) damage can result to the strand because the heavy bite of the anchoring system can ruin the galvanizing, (3) galvanized strands are more expensive.

A little understood, and infrequent occurrence that is of great concern in engineering is the so-called stress corrosion which occurs in highly stressed strands. The reason for the phenomenon is little known, but chemicals such as chlorides, sulfides, and nitrates are known to start this type of corrosion under certain conditions. It is also known that high-strength steels exposed to hydrogen ions are susceptible to failure because of loss in ductility and tensile strength. This phenomenon is called *hydrogen embrittlement* and is best counteracted by confining the strands in an environment having a pH value greater than 8.

Concrete. Concretes having 28-day cylinder strength of 5000 to 6000 psi (34 to 41 MPa) are commonly employed in the prestress industry. This relatively high-strength concrete is desirable, for the following reasons. First, commercial anchorages are designed on the basis of high-strength concrete to prevent failure of concrete during the application of prestressing. Second, such concretes possess higher resistance to tension, shear, bond, and bearing and are desirable for prestressed structures which are typically under higher stresses than ordinary reinforced concrete. Third, concrete of high compressive strength is less liable to shrink. Its higher modulus of elasticity and smaller creep result in smaller loss of prestress in steel.

In a reinforced concrete member subjected to bending the critical sections are limited to certain portions of the cross section such as at the center of spans and at supports to resist the maximum bending

moments and shear forces. In comparison, a prestressed member is subjected to high stresses more or less throughout the whole span for the entire section. For example, during prestressing the bottom fibers are under high compression at the transfer of prestress, whereas top fibers are likely to be compressed under external loads. Hence it is more important to obtain concrete of consistent strength in prestress application than in conventionally reinforced members.

Posttensioned concrete is looked upon by engineers as a self-testing system because if the concrete is not crushed under the application of prestress it should be able to withstand subsequent loadings in view of the strength gain with age. In general practice, however, it is not the 28-day strength that dictates the mix design but rather the strength of concrete at the transfer of prestress. Construction schedules on high-rise projects require that posttensioning be done as early as possible to facilitate early removal of forms for reuse in higher floors. It is usual to specify that the minimum strength of concrete at transfer be 70 to 75 percent of the 28-day strength. Assuming the stressing operation takes place on the fourth day or so, it is more than likely that the expected 28-day strength is much more than the specified strength. For example, assume that the design specifies a 28-day compressive strength of 5000 psi (34.47 MPa). The minimum strength required at transfer of prestress is 70 to 75 percent of 5000, approximately equal to 4000 psi (27.6 MPa) at 4 days. This requirement would normally yield a concrete of 28-day strength of about 6000 psi (41.37 MPa), which is well in excess of the design strength. This rather wasted strength is unnecessary and can be avoided in a negotiated contract by tailoring the mix design and using the higher strength in the actual design of members.

Although high early strength (Type III) portland cement is well-suited in posttension work because of its ability to gain the required strength for stressing relatively early, it is not generally used because of higher cost. Invariably, Type I cement conforming to ASTM C-150 is employed in buildings.

The use of admixtures and flyash is considered a good practice where job conditions can be improved thereby. However, use of calcium chlorides or other chlorides is prohibited since the chloride ion may result in stress corrosion of prestressing tendons.

A slump of between 3 to 5 in (76 to 127 mm) has been found from experience to give good results. The aggregate used in the manufacture of normal concrete members is usually satisfactory in prestressed concrete, including lightweight aggregates. However, care must be exercised in estimating the volume changes so that a reasonable amount of prestress losses is calculated. Lightweight aggregates man-

ufactured by expanding clay or shale have been used to a significant extent in posttensioned buildings. Lightweight aggregates that are not crushed after burning maintain their coating and therefore absorb less water. Such aggregates have drying and shrinkage characteristics similar to the normal-weight aggregates, although the available test reports are somewhat conflicting. The size of aggregate, whether lightweight or normal weight, has a more profound effect on shrinkage. Larger aggregates offer more resistance to shrinkage and also require less water to achieve the same consistency, resulting in as much as 40 percent reduction in shrinkage when the aggregate size is increased from say $\frac{3}{4}$ to $1\frac{1}{2}$ in (19 to 38 mm). It is generally agreed that both shrinkage and creep are more a function of the cement paste than the type of aggregate. Lightweight aggregate has been gaining in application to prestressed construction since about 1955 and has a good track record. It befits the engineer to consider its application for high-rise structures.

8.2.3 Design

The design of posttensioned members involves the following steps:

1. determination of the size of the concrete member
2. establishing the profile of and the prestressing force in the strands
3. checking the section for ultimate capacity in bending and shear
4. verifying the serviceability characteristics, primarily in terms of stresses and long-term deflections

It is well known that the depth of a member depends on many variables such as magnitude of the design loads, shape of the cross section, available clearance, span length, and allowable deflections. The deflections of prestressed members tend to be small because under service loads they are usually uncracked and are much stiffer than nonprestressed members of the same cross section. Also, the prestressing force creates deflections which are opposite to those produced by external loads. The final deflections, therefore, are a function of tendon profile and the magnitude of prestress. Appreciating this fact, the ACI code does not specify minimum depth requirements to control the deflections of prestressed members. However, as a rough guide, the suggested span-to-depth ratios given in Table 8.1 can be used to establish the depth of continuous flexural members subjected to building floor loads. Another way of looking at the suggested span-to-depth ratios is to consider, in effect, that prestressing increases the

TABLE 8.1 Approximate Span Depth Ratios for Posttensioned Systems

Floor system	Simple spans	Continuous spans	Cantilever spans
One-way solid slabs	40–48	42–50	14–16
Two-way flat slabs	36–45	40–48	13–15
Wide band beams	26–30	30–35	10–12
One-way joists	20–28	24–30	8–10
Beams	18–22	20–25	7–8
Girders	14–20	16–24	5–8

Note: The above values are intended as a preliminary guide for the design of building floors subjected to a uniformly distributed superimposed live load of 50 to 100 psf (2394 to 4788 Pa). For the final design, it is necessary to investigate for possible effects of camber, deflections, vibrations, and damping. The designer should verify that adequate clearance exists for proper placement of posttensioning anchors.

span range by about 30 to 40 percent over and above the values normally used in nonprestressed concrete construction.

The profile of posttension strands is established in accordance with the types and distribution of loads with due regard to the clear cover requirements for fire resistance and for corrosion protection. Clear spacing between tendons must be sufficient to permit easy placing of concrete. For maximum economy, the tendon should be located at an eccentricity to the center of gravity of the concrete section producing a maximum counteracting effect to the external loads. For members subjected to uniformly distributed loads a simple parabolic profile is ideal, but in continuous structures parabolic segments forming a smooth reversed curve at the support are more practical. The effect is to shift the point of contraflexure away from the supports. This reverse curvature modifies the load imposed by posttensioning from those assumed using a parabolic profile between tendons.

The design of a simple span posttensioned member is rather trivial and can be accomplished with hand calculations. In continuous or indeterminate posttensioned members, the moments due to posttensioning are not directly proportional to the tendon eccentricity because the support deflection due to posttensioning is resisted by the supports. These restraints introduce moments called the secondary moments. The name is a misnomer because it does not mean that its values are negligible or necessarily smaller than the primary moments.

The initial posttension force immediately after transfer is less than the jacking force because of (1) slippage of anchors, (2) frictional losses along tendon profile, and (3) elastic shortening of concrete. The force is reduced further over a period of months or even years due to change in the length of concrete member resulting from shrinkage and creep of concrete and relaxation of the highly stressed steel. The effective prestress is the force in the tendon after all the losses have taken place.

For routine designs, empirical expressions yield sufficiently accurate results, but in cases with unusual member geometry, tendon profile, and construction methods it may be necessary to make refined calculations of losses.

In North America it is usually sufficient to specify effective force in tendons and the general profile of the tendons. The posttension contractor submits the calculations of prestress losses for the engineer's review. Therefore, the engineer is spared the drudgery of calculating these prestress losses. The posttension design of a statically determinate structure is trivial and can be accomplished with little difficulty by hand. The floor framing systems normally encountered in practice are invariably statically indeterminate and are most usually designed by resorting to computer solutions. Commercially available programs are used extensively, as are in-house programs written for that purpose. Most programs appear to use the concept of load balancing.

In the load-balancing method, prestressing is seen as an attempt to balance a certain portion of the external loads on the member by inducing a counteracting load due to posttensioning. This method, first developed by T. Y. Lin, enjoys the position of favorite design tool among engineers and has the advantage that its application to statically indeterminate systems could be visualized just as easily as for statically determinate structures. Also, the procedure gives a simple method of calculating deflections. The deflections are simply computed by considering only that portion of the external load that is not balanced by the prestress. If the effective prestress completely balances the sustained loading, the posttensioned member will not undergo any deflection and will remain horizontal irrespective of the modulus of rigidity or flexural creep of concrete.

In the load-balancing approach, the analysis of a prestressed member is reduced to the analysis of a nonprestressed element subjected to the load differential. Since the analysis is performed with only the unbalanced portion of the external load, the inaccuracies in the method of analysis become relatively insignificant. Often, approximate method is all that is necessary for the final design. The load balancing method can be conveniently applied to multiple-span beams and slabs. The prestressing force need not be the same in all the spans. The load in each span can be balanced by choosing a suitable prestress and a suitable profile. For spans requiring higher prestressing forces, additional tendons can be added.

A question that usually arises is how much of the external load is to be balanced. The answer, however, is not simple. Balancing all the dead load often results in too much prestressing force, leading to

uneconomical design. On the other hand, there are situations in which the live load is significantly heavier than the dead load, making it more economical to prestress not only for full dead loads but also for a significant portion of the live load. However, in the design of floor framing systems, the prestressing force is normally selected to balance about 80 to 100 percent of the dead load and, occasionally, a small portion of the live load. This condition generally leads to an ideal condition with the structure having little or no deflection under dead loads.

Limiting the maximum tensile and compressive stresses permitted in concrete does not in itself assure that the prestressed member has an adequate factor of safety against flexural failure. Therefore, its nominal bending strength is computed in a procedure similar to that of a reinforced concrete beam. Underreinforced beams are assumed to have reached the failure load when the concrete strain reaches a value of 0.003. Since the yield point of prestressing steel is not well defined, empirical relations based on tests are used in evaluating the strain and hence the stress in tendons.

The shear reinforcement in posttensioned members is designed in a manner almost identical to that of nonprestressed concrete members, with due consideration for the longitudinal stresses induced by the posttensioned tendons. Another feature unique to the design of posttensioned members is the high stresses at the vicinity of anchors. Prestressing force is transferred to the concrete by anchoring the tendons with the aid of anchorages. Large stresses are developed at the anchorages, which have to be dealt with properly by providing well-positioned and sized reinforcement in the region of high stresses. At the cross section of a beam sufficiently far away (usually 2 to 3 times the larger cross-sectional dimension of the beam) from the end zones, the axial and bending stresses in the beam due to an eccentric prestressing force are given by the usual P/A and Mc/I relations. But in the vicinity of the application of the large forces, the stresses are distributed in a complex manner. Of importance are the transverse tensile forces generated at the end blocks for which reinforcement is to be provided. The bursting tensile stress has a maximum value along the axis of the force. Its distribution depends on the location of bearing area and its relative proportion with respect to the areas of the end face.

Because of the indeterminate nature and intensity of the stresses, the design of reinforcement for the end block is primarily based on empirical expressions for internal forces. Reinforcement is designed to carry the tensile stresses created in the end block by the tendon reactions and usually consists of closely spaced stirrups together with horizontal bars.

8.2.4 Practical examples

In today's high-rise market, more and more posttensioned structural systems are becoming available. A multitude of schemes may present themselves as final contenders, giving an opportunity to the engineer to compare the costs and intrinsic advantages and disadvantages of the various systems. After the engineers have satisfied themselves that future tenant improvements do not seriously affect the earning power of the building by requiring extensive modifications, they can then proceed to zero in on the most appropriate structural systems. It is beyond the scope of this work to chronicle in detail the design aspects of structural systems consisting of beam and slab, flat plate, flat slab, girder and joists, and their other various combinations. However, a brief description of these systems with two practical examples follows.

Simply stated, slab and beam in a posttensioned system are comprised of one-way slabs supported on an orthogonal grid system of beams. The system is popular for garages with beam spans in range of 50 to 60 ft (15.2 to 18.25 m) spaced at 20 to 30 ft (6.0 to 9.14 m).

Condominiums and apartment buildings are economical if a structural system with a flat ceiling is used for floor construction. A posttensioned flat plate presents one such system for buildings with column spacings in the range of 20 to 30 ft (6.09 to 9.14 m). The form work is simple and lends itself to quick construction. The resulting flat plate system has good acoustical characteristics while maintaining a minimum floor-to-floor height. A flat slab with drop panels, which can be considered as an extension of the flat plate system, is suitable for office buildings with clear spans in the range of 35 to 45 ft (10.6 to 13.7 m). In such systems it may be economical to use long and narrow shear heads to accommodate flying forms. Posttensioned joists clear spanning between the core and building exterior offer an alternative method for framing office buildings.

As in reinforced concrete and structural steel construction, the use of posttensioned concrete is only limited by the imagination and ingenuity of the engineer and the relative economics of various construction materials and labor at the bid time. Certain rules of thumb for span-to-depth ratios and the average value of posttensioning stresses in structural members are useful in conceptual design. The depth for slabs usually works out between $L/40$ and $L/50$, while for joists it is between $L/25$ and $L/35$. Beams can be much shallower, with a depth in the range of $L/20$ and $L/30$. Band beams offer perhaps the least depth without using as much concrete as in flat slab construction. Although a span-to-depth ratio approaching 35 is adequate from strength and serviceability points of view, it is necessary to make sure that ade-

quate room exists for proper detailing of anchorages. Detailing of beam-column intersection of shallow band beams should be carefully developed to avoid conflicts between the posttensioning tendon, anchorage, and main vertical column reinforcement. Bundling of column vertical bars may be required to relieve reinforcement congestion. Adequate clearance must be provided to permit access by stressing equipment.

Another practical rule of thumb normally used in posttensioned structures is the compression stress level induced in the members due to posttensioning. A minimum compression level of 125 and 150 psi (862 and 1034 KPa) is a practical economical range for slabs while a range of 250 to 300 psi (1724 to 2068 KPa) has been found to be adequate for beams. Compression stresses as high as 500 psi (3447 KPa) have been used successfully in band-beam systems.

As a first example, the framing plan for a two-way flat plate office building is shown in Fig. 8.8. In the typical exterior panel, the primary tendons are $\frac{1}{2}$-in diameter (12.7-mm) strands which are banded in the north-south direction. Unbanded tendons run from left to right across the building width. Additional tendons are used in the end panels to allow for the increased moments due to lack of continuity at one end. Figure 8.8 also shows placement of nonprestressed reinforcement in the floor system.

As a second example, Fig. 8.9 shows the framing plan for an office building with posttensioned band-beam–slab system. Shallow beams which are only 16-in (0.40-m) deep span across two exterior bays of

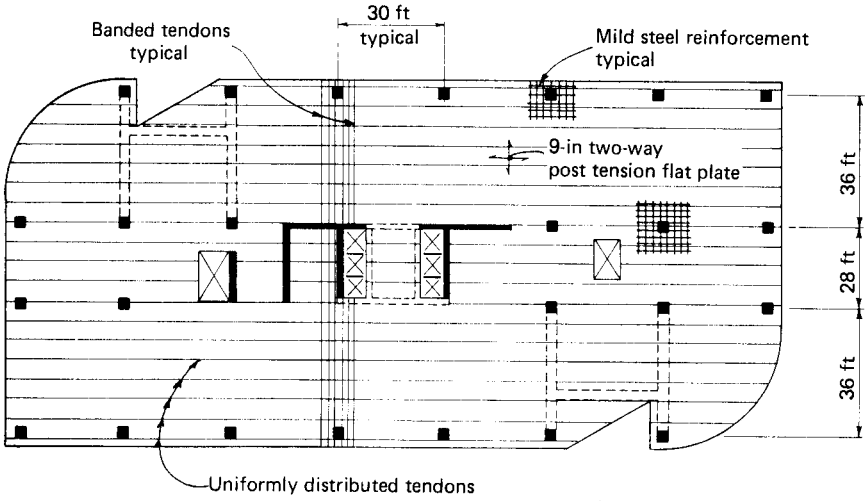

Figure 8.8 Typical floor plan of two-way posttensioned slab system.

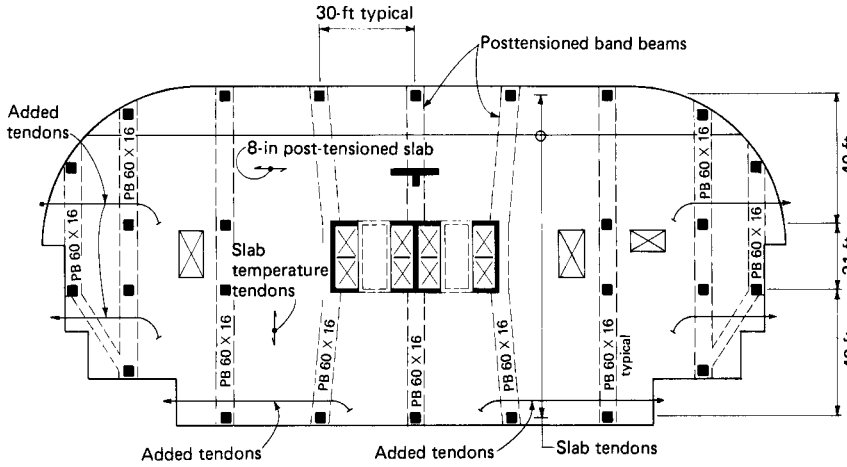

Figure 8.9 Typical floor plan of posttensioned band beam and slab system.

40 ft (12.19 m) and an interior bay of 21 ft (6.38 m). Posttensioned slabs which are 8-in (203-mm) deep span between the band beams, which are typically spaced at 30 ft (9.14 m) on center. In the design of the slab additional beam depth is considered as a haunch at each end. Primary tendons for the slab run across the building width, while the temperature tendons are placed in the north-south direction between the beams.

Chapter

9

Composite Gravity Systems

Gravity systems used in composite construction can be broadly classified into horizontal and vertical types. Composite metal deck is a very popular surface element often used in conjunction with other composite horizontal members, such as composite prismatic and haunched beams, composite trusses, and finally a relatively new system called composite stub girders. The vertical element most often used is the composite column, which uses a wide-flange steel section within a concrete envelope. In this chapter a brief description of each of these elements with particular emphasis on the practical aspects of their design and application to high-rise structures is given.

9.1 Composite Metal Decks

9.1.1 General considerations

In steel buildings the most common floor system consists of a deck element supported on regularly spaced beams, joists, or trusses which are in turn supported by other beams or framed directly into columns. The deck element is made of cold-formed steel sheets and is available in an extensive choice of depths, profiles, and thicknesses and is applicable to a wide range of projects and structural designs. For floor construction, metal deck is available most commonly in $1\frac{1}{2}$-, 2-, and 3-in (38-, 51-, and 76-mm) depths and with rib spacings of 6, $7\frac{1}{2}$, 8, 9, and 12 in (152, 190, 208, 228, and 305 mm). During fabrication, cold-formed steel sheets are

given special shapes, embossments, and indentations to achieve maximum efficiency as bending members. This results in a high strength-to-weight ratio, reducing delivery, erection, and structural framing costs. Composite metal deck can be thought of as a double-duty element; it acts not only as a permanent form but also as the positive bending reinforcement for the structural concrete. Prior to concreting, when suitably fastened to the steel members, composite metal deck provides a platform for the work of the various trades. After the concrete has hardened, the steel deck and the concrete are interlocked by the surface bond and the unique shape of the deck.

The span limitation for a composite metal deck is a function of depth of deck, the material thickness, and the number of spans on which the deck is laid as a continuous member. The floor deck can be considered as a surface member which, in addition to resisting the loads, also provides a useful surface. In the case of composite metal deck, the deck constitutes a slab form during construction and the positive slab reinforcement in the finished structures.

Metal deck is produced from steel sheets by a fully mechanized, high-speed cold-rolling process. Although it is possible to produce shapes up to $\frac{1}{2}$-in (12.7-mm) and even $\frac{3}{4}$-in (19-mm) thick by cold forming, cold-formed steel construction is generally restricted to plates and sheets weighing from 0.5 psf (24 Pa) to a maximum of 9 psf (431 Pa).

Composite metal deck is manufactured with deformations specifically designed in to produce composite action under flexure between the metal deck and the concrete slab to be placed over the deck. Considerable variety of sheet steel is available for the production of composite metal deck. For most high-rise applications, unshored construction is a preferred practice. Deck thickness and profile are normally selected to fulfill this criterion, which in most cases is adequate to carry the superimposed office floor loads.

The most common method of designing a composite slab is to design it as a simply supported reinforced concrete slab with the steel acting as positive reinforcement. The slab is theoretically assumed to crack over each supporting beam. The welded wire fabric normally provided as temperature reinforcement does not provide enough area for continuity in all but very small spans of the order of 3 to 5 ft (0.91 to 1.52 m). Even when the area of the mesh is adequate for continuity, many engineers hesitate to use it as negative steel because during concrete placement operation it is very difficult to maintain proper cover to the negative steel in spite of elaborate chairing and other devices. Some engineers caught in the fever of providing the most economical structure assume that they have taken care of this problem by putting the burden on the contractor by specifying that contractor should take

adequate precautions to maintain proper cover to the mesh at the support. This, of course, turns a blind eye to current field practices and should be avoided. Mild steel reinforcement or a heavy mesh over the supports only without the need of draping is a better detail achievable in the field.

Twenty years ago, composite steel beam construction did not use metal deck, and encasement of both column and steel beams with concrete was primarily done to obtain the required fire rating because labor and materials were relatively inexpensive in those days. Today this method is very uneconomical because of the temporary form work required for the entire floor area and is limited to renovation and remodeling of buildings where upgrading the capacity of the old construction is required to support heavier loads. However, in certain parts of North America, for instance on the east coast, slender girders with studded top flanges are sometimes used with wood-formed flat slabs.

The Steel Deck Institute (SDI), which is regarded as the industry standard by the metal deck manufacturers, has published a manual which encompasses the design of composite decks, form decks, and roof decks. A brief description of the SDI specifications with practical comments is given in the following sections.

9.1.2 SDI specifications

The steel used for the fabrication of composite metal deck shall have a minimum yield point of 33 ksi (227.5 MPa). The specified yield point is the primary criterion for strength under static loading because the allowable unit stresses are expressed in terms of it. The tensile strength is of secondary importance because fatigue strength and brittle fracture, which relate to tensile strength rather than yield point, are rarely of consequence; metal deck is rarely subjected to repetitive loads and the characteristic thinness invariably precludes the development of brittle fracture. Ductility is, of course, required to allow the material to be cold-formed to relatively complicated shapes without cracking and to provide stress relief by plastic yielding in localized regions subjected to stress concentration.

Considerable variations in thickness of metal deck may occur because of rolling tolerances. Therefore, SDI stipulates that the delivered thickness of bare steel without the finish such as phosphotising and galvanizing shall be not less than 95 percent of the design thickness. The increase in the stiffness of deck due to galvanizing is not relied upon in the design of metal deck.

Considerable debate exists in the engineering community whether the metal deck used inside of a building which is not directly exposed

to weather needs galvanizing or not. SDI does not mandate any particular type of finish, and the appropriate finish is left to the discretion of the engineer with the recommendation that due consideration be given to the environment to which the structure is subjected. However, SDI in its commentary recommends a galvanized coa ting conforming to ASTM A-525 G.60 requiring a minimum galvanizing of 0.75 ounce per square feet (2.24 Pa) of metal deck. Other salient features of SDI specifications are as follows:

1. Minimum compressive strength of concrete shall be 3.0 ksi (20.68 MPa). The compressive stress in concrete is limited as in the ACI code to $0.4f_c$ under the applied load for unshored construction and under the total dead and live loads for shored construction. The flexural or shear bond is to be based on ultimate strength analysis with a minimum safety factor of 2. The minimum temperature and shrinkage reinforcement in a composite slab is a function of the area of concrete, as in ordinary reinforced concrete slab, but only the concrete area above the metal deck need be considered in calculating the area of concrete.
2. The use of admixtures containing chloride salts is prohibited because salts can corrode the steel deck, virtually eliminating the slab reinforcement.
3. When designing the section as a form in bending, the section properties are to be calculated as per AISC *Specification for the Design of Cold-formed Steel Structural Members.*
4. Bending stress is limited to 0.6 times the yield strength of steel being used. An upper limit of 36.0 ksi (248.2 MPa) is imposed on the allowable stress. In addition to the weight of wet concrete and deck, allowance should be made for the construction live loads of 20 psf (958 Pa) of uniform load or a 150-lb (667-N) concentrated load to account for the weight of one person working on a 1-ft (305-mm) width of deck. Although it is common practice to allow for a 200-lb (890-N) point load as the equivalent load of a person, because of the temporary nature of this loading a 33 percent increase in the stress is allowed, which is equivalent to reducing the 200-lb (890-N) load by 25 percent. Clear spans are to be used in the moment calculations.
5. For calculating deflections, it is not necessary to consider the construction loads since the deck, which is designed to remain elastic, will rebound after the removal of construction loads. The calculated deflection based on the weight of concrete is limited to the smaller value $L/180$ or ¾-in (19-mm), in which L is the clear span of the deck. Deflections of composite slabs due to live loads of 50 to 80 psf (2394 to 3830 Pa) normally imposed in a high-rise building are seldom a design criterion and are usually less than $L/360$, where L is the span of deck.

Because the slab is assumed to have cracked at the supports, the deflections are best predicted by using the average of the cracked and uncracked moment of inertia using transformed sections. Note that when slabs are poured level to compensate for the deflection of metal deck, 15 percent or more concrete may be used than calculated using the slab's design thickness and area.

6. A minimum bearing of $1\frac{1}{2}$ in (38 mm) is specified for proper deck seating on supports.

7. A maximum average spacing of 12 in (305 mm) for puddle welds is specified to obtain proper anchorage to supporting members. The maximum spacing between adjacent welds is limited to 18 in (457 mm). Welding of decks with thickness less than 0.028 in (0.71 mm) is not practical because of the likelihood of burning off the sheet. Therefore, SDI stipulates use of welding washers when welding steel floor deck of less than 0.028 in (0.71 mm) in thickness. Stud welding through the metal deck to the steel top flange can be used instead of puddle welding to satisfy the minimum spacing requirements. However, since it is possible to get an uplift force on the deck before installation of studs, it is necessary to use a minimum number of puddle welds to prevent metal decks from being blown off buildings under construction during windstorms.

8. Mechanical fasteners which satisfy the anchorage criteria can be used in lieu of puddle welds.

9. Side laps with proper fasteners are required between two longitudinal pieces of deck to (a) prevent differential deflection, (b) provide sufficient diaphragm strength to maintain building alignment, and (c) sustain local construction loads without distortion or separation. The edges of metal deck shall be connected with ¾-in (19-mm) diameter fusion welds at a maximum spacing of 3 ft (0.9 m) throughout for simply supported spans. Button punching at 2 ft (0.61 m) on centers is an acceptable alternative to minimum fusion welding.

To function as form work, decks supporting cantilevers should be proportioned to satisfy the following criteria. (1) Dead load deflection should be limited to $L/90$ of overhang or 3/8 in (9.5 mm), whichever is smaller. (2) Steel stress should be limited to 26.7 ksi (184 MPa) for dead load plus 200-lb (890-N) concentrated load at outside edge of overhang, or steel stresses limited to 20.0 ksi (138 MPa) for dead load plus 20 psf (958 Pa) of additional load, whichever is more severe. (3) The deck should receive one fusion weld at the cantilever end, and the spacing of welds throughout the cantilever span should not exceed 12 in (0.30 m). Button punching can be used as an acceptable alternative to fusion welding.

9.2 Composite Beams

9.2.1 General considerations

During the last 20 years, steel beams which act compositely with floor slabs have been extensively used in building construction. Earlier versions of composite beam construction can be traced back to bridge building, which generally used wood-formed and -shored construction. Several systems of composite metal deck which are used as permanent form and also as reinforcement have been in vogue and have virtually replaced wood-formed systems. The reduced labor costs and speedier construction resulting from elimination of form work, combined with the facility to weld shear studs onto the beam flanges through the metal deck, have been the basic elements in its universal adaptation.

It has been well established that concrete slabs and steel beams act as one unit when joined together to resist horizontal shear. In high-rise steel construction, the slab usually takes the form of fluted metal deck with structural concrete topping, and the beams are usually rolled-steel sections. The required interaction between the two is achieved by providing resistance to horizontal shear by welding shear connectors to the beam top flange. Such a combination of two distinctly different materials results in a significant increase in the strength and stiffness of the bending member.

Two types of composite construction are recognized by the AISC specifications: (1) fully encased steel beams, and (2) steel beams with shear connectors. In fully encased steel beams, the natural bond between concrete and steel interface is considered sufficient to provide the resistance to horizontal shear provided that (1) the concrete thickness is 2 in (50.8 mm) or more on the beam sides and soffit with the top of the beam at least 1½ in (38 mm) below the top and 2 in (50.8 mm) above the bottom of the slab; (2) the encasement is cast integrally with the slab and has adequate mesh or other reinforcing steel throughout the whole depth and across the soffit of the beam to prevent spalling of concrete.

Design of encased beams can be accomplished by two methods. In the first method for unshored construction, the stresses are computed by assuming that the steel beam alone resists all the dead load applied prior to hardening of concrete. The superimposed dead and live loads applied after hardening of concrete are assumed to be resisted by composite action. In addition to providing the composite action, the concrete encasement is assumed to restrain the steel beam from both local and lateral torsional buckling. Therefore an allowable of stress of $0.66F_y$, instead of $0.60F_y$ can be used when the analysis is based on the properties of transformed section. Thus for positive bending moments we get

$$f_b = \frac{M_D}{S_s} + \frac{M_L}{S_{tr}} \leq 0.66F_y$$

where f_b = computed stress in the bottom flange for positive bending moment
M_D = dead-load bending moment
M_L = superimposed dead- and live-load bending moment
S_s = section modulus of the steel section referred to its bottom flange
S_{tr} = section modulus of the transformed section referred to its bottom flange.

The second method of design for encased beams is a recognition of a common engineering practice where it is desired to eliminate the calculation of composite section properties. This provision permits a higher stress of $0.76F_y$ in steel when the steel beam alone is designed to resist all loads. Thus

$$f_b = \frac{M_D + M_L}{S_s} \leq 0.76F_y$$

The second type of composite steel beam, namely, composite beams with shear connectors, is by far the more popular in the construction of buildings in North America. Invariably composite action is achieved by providing shear connectors between steel top flange and concrete topping on metal deck because encasing beams with concrete would result in expensive form work. Before considering the AISC design provisions for composite beams with formed metal deck, it is instructive to consider some practical aspects of their construction and qualitative behavior.

Composite sections have greater stiffness than the summation of the individual stiffness of slab and beam and, therefore, can carry larger loads or similar loads with appreciably smaller deflection and are less prone to transient vibrations. Composite action results in an overall reduction of floor depth, and for high-rise buildings, the ultimate savings in curtain walls, electrical wiring, mechanical ductwork, interior walls, plumbing, etc., can be considerable. The savings in exterior curtain wall or other type of facade treatment alone is often sufficient to warrant use of composite beams.

Composite beams can be designed either for shored or unshored construction. For shored construction, the cost of shoring required at sufficiently close intervals to prevent the beam from sagging should be evaluated in relation to the savings achieved by the use of lighter beams. For unshored construction, steel is designed to support alone

the wet weight of concrete and construction loads. The steel beam, therefore, is heavier than in shored construction.

In composite floor construction, the top flanges of the steel girder or beam are attached to the concrete floor by the use of suitable shear connectors. These allow the slabs to act with the steel and form a composite beam having greater strength and rigidity. The concrete slab becomes part of the compression flange of this composite element. As a result, the neutral axis of the section shifts upward, making the bottom flange of the beam more effective in tension. Such an arrangement offers the possibility of reducing beam cross sections and weight.

Since the concrete already serves as part of the floor system, the only additional cost will be that of the shear connectors. In addition to transmitting the horizontal shear forces from the slab into beam, making both beam and slab act as a unit, the shear connector provides anchorage for the slab and prevents any tendency for it to rotate independently of the beam. It also helps in the collection and distribution of diaphragm shear from one element to the other.

The stud shear connector is a short length of round steel bar welded to the steel beam at one end and having an anchorage provided in the form of a round head at the other end. The most common diameters are $\frac{1}{2}$, $\frac{5}{8}$, and $\frac{3}{4}$ in (12, 16, and 19 mm). The length is dependent on the depth of metal deck and should extend at least $1\frac{1}{2}$ in (38 mm) above the top of the deck. The welding of studs typically reduces their length by about $\frac{3}{16}$ in (5 mm). The upset head thickness of the study is usually $\frac{3}{8}$ or $\frac{1}{2}$ in (9 or 12 mm), and the diameter $\frac{1}{2}$-in (12-mm) larger than the stud diameter. The studs are normally welded to the beam with an automatic welding gun, and when properly executed, the welds are stronger than the steel studs. Studs located on the side of the trough toward the beam support are more effective than studs located toward the beam centerline. The larger volume of concrete between the stud and the pushing side of the trough helps in the development of a larger failure cone in concrete, thus increasing the horizontal shear resistance of the system.

The length of stud has a definite effect on the amount of shear that can be resisted by the stud. As the length of the stud increases, so does the size of the shear cone, with a consequent increase in the shear value. The shear capacity of the stud also depends on the profile of the metal deck. To get a qualitative idea, consider the two types of metal decks shown in Figs. 9.1 and 9.2. The deck in Fig. 9.1 has a narrow hump compared to the one in Fig. 9.2. When subjected to a horizontal shear load V, the concrete and the metal deck tend to behave as a portal frame. The concrete in the troughs can be thought of as columns, with the concrete over the humps acting as beams. A narrow hump results in an equivalent beam of smaller span when compared to the

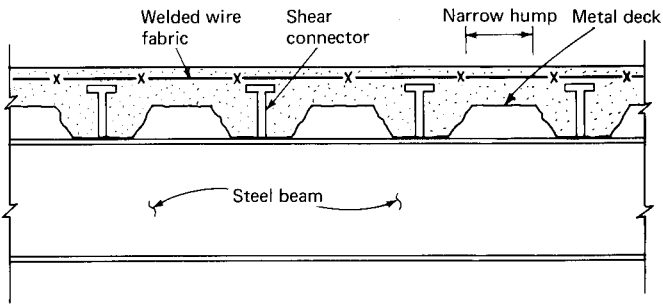

Figure 9.1 Composite beam with narrow hump metal deck.

one with a wider hump, meaning that a deck profile with the widest trough and narrowest hump will yield the highest connector strengths. Figure 9.2*b* shows a simplified analytical model of composite metal deck subjected to horizontal shear. A qualitative feel for the behavior of the deck can be obtained by considering the deck and concrete topping as a series of portal frames. However, other considerations such as volume of concrete, section modulus, and the stiffness of deck also influence the shear strength of the connector.

Metal decks for composite construction are available in the United States in three depths, $1\frac{1}{2}$ in (38 mm), 2 in (51 mm), and 3 in (76 mm). The earlier types of metal deck did not have embossments, and the interlocking between concrete and metal deck was achieved by welding reinforcement transverse to the beam. Later developments of metal deck introduced embossments to engage concrete and metal deck and dispensed with the transverse-welded reinforcement.

The spans utilizing composite metal deck are generally in the range of 8 to 15 ft (2.4 to 4.6 m).

In floor systems using $1\frac{1}{2}$-in (38-mm) decks, the electrical and telephone services are generally provided by the so-called poke-through system, which is simply punching through the slab at various locations and passing the under-floor ducts through them. A deeper deck is required if the power distribution system is to be integrated as part of the structural slab; as a result, 2- and 3-in (51- and 76-mm) metal decks were developed. Experiments have shown that there is very little loss of composite beam stiffness due to the ribbed configuration of the metal deck in the depth range of $1\frac{1}{2}$ to 3 in (38 to 76 mm). As long as the ratio of width to depth of the metal deck is at least 1.75, the entire capacity of the shear stud can be developed similar to beams with solid slabs. However, with deeper deck a substantial decrease in shear strength of the stud occurs, which is attributed to a different type of failure mechanism. Instead of the shear stud failure, the mode of failure is initiated by cracking of the concrete in the rib corners.

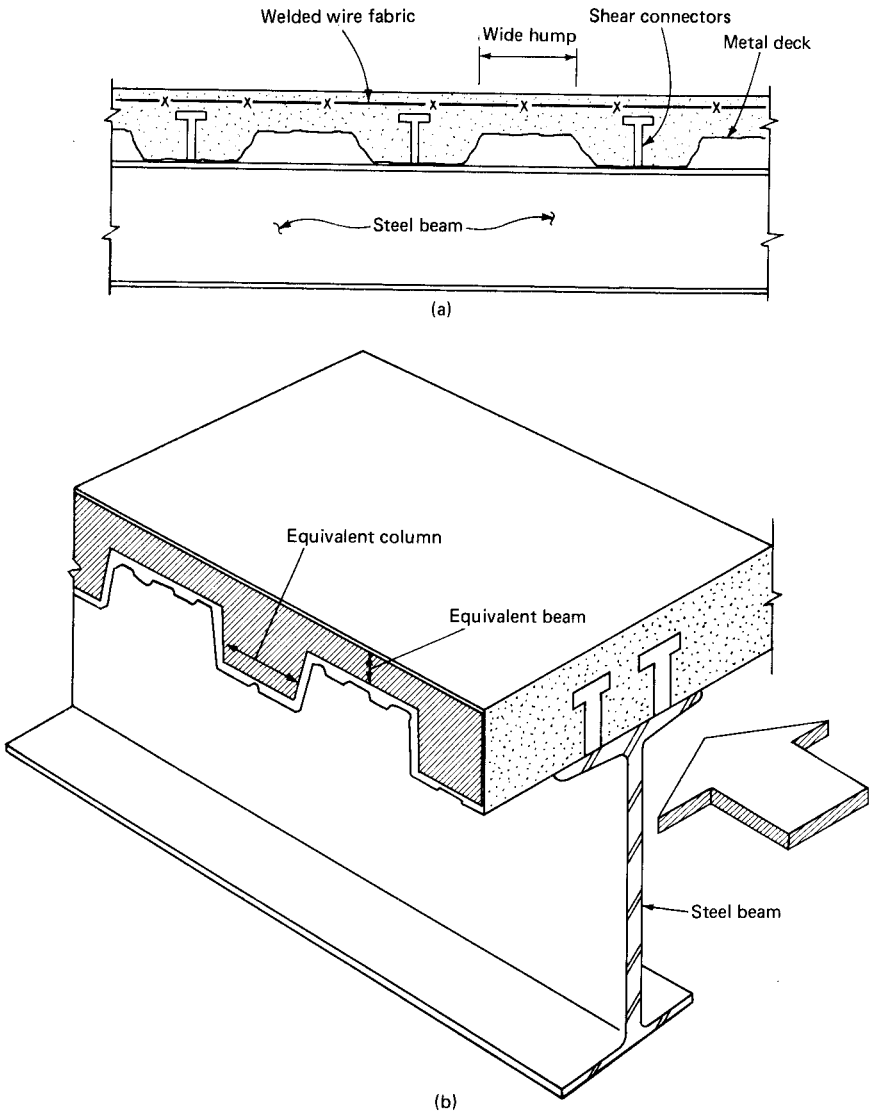

Figure 9.2 (*a*) Composite beam with wide hump metal deck; (*b*) simplified analytical model of composite metal deck subjected to horizontal shear.

Eventual failure takes place by separation of concrete from the metal deck. When more than one stud is used in a metal deck flute, a failure cone can develop over the shear stud group, resulting in lesser shear capacity per each stud. The shear stud strength is therefore closely related to the metal deck configuration and factors related to the surface area of the shear cone.

Often special details are required in composite design to achieve the optimum result. Openings interrupt slab continuity, affecting capacity of a composite beam. For example, beams adjacent to elevator and stair openings may have full effective width for part of their length and perhaps half that value adjacent to the openings. Elevator sill details normally require a recess in the slab for door installations, rendering the slab ineffective for part of the beam length. A similar problem occurs in the case of trench header ducts, which require elimination of concrete, as opposed to the standard header duct, which is completely encased in concrete. When the trench is parallel to the composite beam, its effect can easily be incorporated in the design by suitably modifying the effective width of compression flange. The effect of the trench being oriented perpendicular to the composite beam could range from negligible to severe depending upon its location. If the trench can be located in the region of minimum bending moment, such as near the supports in a simply supported beam, and if the required number of connectors could be placed between the trench and the point of maximum bending moment, its effect on the composite beam design is minimum. If, on the other hand, the trench must be placed in an area of high bending moment, its effect may be so severe as to require that the beam be designed as a noncomposite beam.

The slab thickness normally employed in high-rise construction with composite metal deck is usually governed by fire-rating-requirements rather than the thickness required by the bending capacity of the slab. In certain parts of the United States it may be economical to use the minimum thickness required for strength and to use sprayed-on or some other method of fireproofing to obtain the required ratings. Some major projects have used $2\frac{1}{2}$-in (63.5-mm) thick concrete on 3-in (76.2-mm) deep metal deck spanning as much as 15 ft (4.57 m). It goes without saying that a comparative study is necessary to zero in on the most economical scheme.

Negative moment sections can be designed such that (1) the steel beam alone resists the negative moment, or (2) the longitudinal reinforcement in the slab parallel to the beam acts compositely with the steel beam. In some instances it may be more economical to design the beam under the second assumption because longitudinal reinforcement, which is often provided to control the cracking of the slab, may also be structurally used. When the slab reinforcement is assumed to act compositely with the steel beam, shear connectors must be provided throughout the negative moment region.

Careful attention should be paid to the deflection characteristics of composite construction because the slender not-yet-composite shape deflects as wet concrete is placed on it. There are three ways to handle the deflection problem.

1. Use relatively heavy steel beams to limit the dead-load deflection and pour lens-shaped tapering slabs to obtain a nearly flat top. Although a reasonably flat surface results from this construction, the economic restraints of speculative office buildings do not usually permit the luxury of the added cost of additional concrete and heavier steel beams.
2. Camber the steel beam to compensate for the weight of steel beam and concrete. Place a constant thickness of slab by finishing the concrete to screeds set from the cambered steel. Continuous lateral bracing as provided by the metal deck is required to prevent the lateral torsion buckling of beam. If steel deck is not used, this system requires a substantial temporary bracing system to stabilize the beam during construction.
3. Camber and shore the steel beam. The beam is fabricated with a camber calculated to compensate for the deflection of the final cured composite section. Shores are placed to hold the steel at its curved position while the concrete is being poured. As in method 2, slab is finished to screeds set from cambered steel. Although methods 1 and 3 are occasionally used, the trend is to use method 2 because it is the least expensive, especially so when unshored metal deck is employed for floor construction.

9.2.2 AISC design specifications

The AISC specification that became effective on November 1, 1978, provides new design criteria for composite beams with formed metal deck. The specification is based on extensive research done to obtain working values of headed shear connectors when used with metal deck. Full-scale composite beam, push-off, and push-out tests have been used to verify the equations and variables introduced in the specification. The steel deck can be perpendicular or parallel to the steel beam as shown in Figs. 9.3 and 9.4. Including provisions for solid slab, there are three categories of composite beams with differing effective concrete areas.

1. *Solid Slab.* The total slab depth is effective in compression unless the neutral axis is above the top of the steel beam. In high-rise floor systems invariably the neutral axis of steel beams is below the slab, rendering the total slab depth effective in compression.
2. *Deck perpendicular to the beam.* The main requirements are
   a. Concrete below the top of steel decking shall be neglected in computations of section properties and in calculating the number of shear studs, but the concrete below the top flange of deck may be included for calculating the effective width.

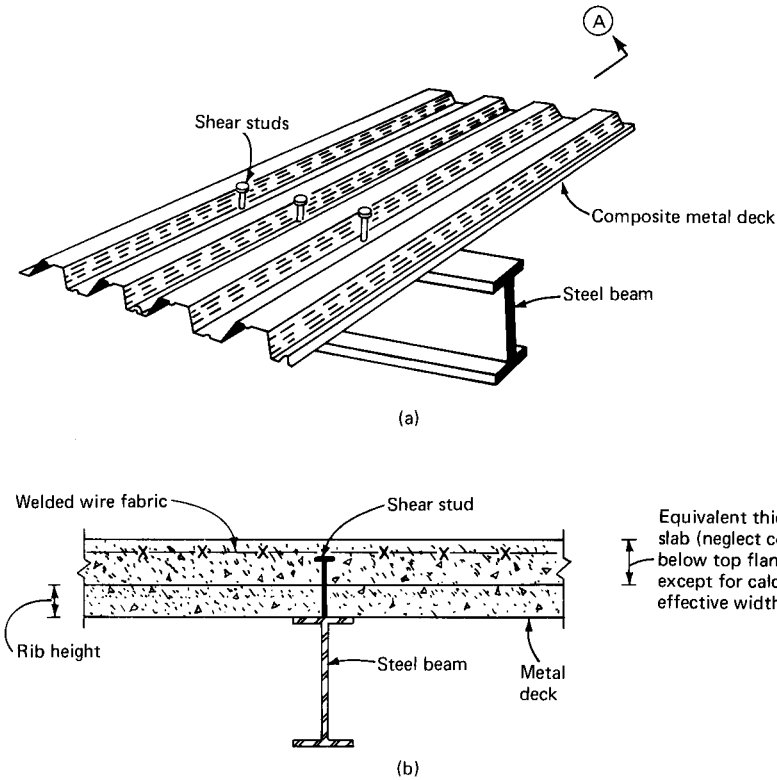

Figure 9.3 Composite beam with formed deck perpendicular to beam. (*a*) Schematic view; (*b*) section A showing equivalent thickness of slab.

b. The maximum spacing of stud shear connectors shall not exceed 32 in (813 mm) along the beam length.

c. The steel deck shall be anchored to the beam either by welding or by other means at a spacing not exceeding 16 in (406 mm).

d. A reduction factor as given by the AISC formula 1.11-3

$$\left(\frac{0.85}{\sqrt{N_r}}\right)\left(\frac{W_r}{h_r}\right)\left(\frac{H_s}{h_r} - 1\right) \leq 1.0$$

should be used for reducing the allowable horizontal shear capacity of stud connectors. In the above formula h_r is nominal rib height, in inches. H_s is length of stud connector after welding, in inches. An upper limit of $(h_r + 3)$ is placed on the length of shear connectors to be used in computations even when longer studs are installed in metal decks. N_r is the

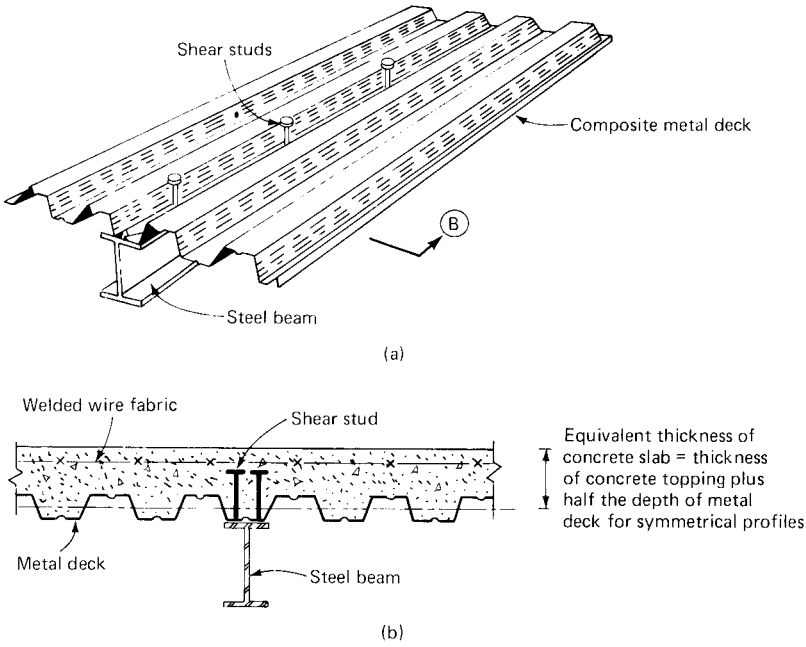

Figure 9.4 Composite beams with formed deck parallel to beam. (*a*) Schematic view; (*b*) section B showing equivalent thickness of slab.

number of studs in one rib. A maximum value of 3 can be used in computations although more than three studs may be installed. W_r is average width of concrete rib.

3. *Deck ribs parallel to the beam.*
   a. The major difference between perpendicular and parallel orientation of deck ribs is that when deck is parallel to beam, the concrete below the top of decking can be included in the calculations of section properties and must be included when calculating the number of shear studs.
   b. If steel deck ribs occur on supporting beam flanges, it is permissible to cut high-hat to form a concrete haunch.
   c. When nominal rib height is $1\frac{1}{2}$ in (38.1 mm) or greater, minimum average width of deck flute should not be less than 2 in for the first stud in the transverse row plus four stud diameters for each additional stud. This gives minimum average widths of 2 in (51 mm) for one stud, 2 in plus $4d$ for two studs, 2 in plus $8d$ for three studs, etc., where d is the diameter of stud. Note that if a metal deck cannot accommodate this width requirement, the deck can be split over the girder to form a haunch.
   d. A reduction factor as given by AISC formula 1.11-9

$$0.6\left(\frac{W_r}{h_r}\right)\left(\frac{H_s}{h_r} - 1.0\right) \leq 1.0$$

shall be used for reducing the allowable horizontal shear capacity of stud connectors.

4. Certain specific rules of ASCE applicable to formed steel deck construction are shown schematically in Fig. 9.5. More general comments regarding the rules follow:
   a. The deck rib height shall not exceed 3 in (76.5 mm).
   b. Rib average width shall not be less than 2 in (51 mm). If the deck profile is such that the width at the top of the steel deck is less than 2 in (51 mm), this minimum clear width shall be used in the calculation.
   c. The section properties do not change a great deal from deck running perpendicular to deck running parallel to the beam, but the change in the number of studs can be significant.
   d. The reduction formula for stud strength is based on rib geometry, number of studs per rib, and embedment length of the studs.
   e. The equation for calculating the partial section modulus makes the choice of heavier, stiffer beams with fewer studs economically more attractive.
   f. Higher shear values can be used in longer shear studs. Concrete cover over the top of the stud is not limited by the AISC specifications, but for practical reasons the author recommends a minimum of $\frac{1}{2}$ in (12.7 mm).
   g. Studs can be placed as close to the web of deck as needed for installation and to maintain the necessary spacing.
   h. Deck anchorages can be provided by the stud welds.
   i. Maximum diameter of shear connectors is limited to $\frac{3}{4}$ in (19 mm).
   j. After installation, the studs should extend a minimum of $1\frac{1}{2}$ in (38 mm) above the steel deck.
   k. Total slab thickness including the ribs is used in determining the effective width without regard to the orientation of the deck with respect to the beam axis.
   l. The slab thickness above the steel deck shall not be less than 2 in (51 mm).

For design purposes, a composite floor system is assumed to consist of a series of T beams, each made up of one steel beam and a portion of the concrete slab. The AISC specifies limits on the width of slab that

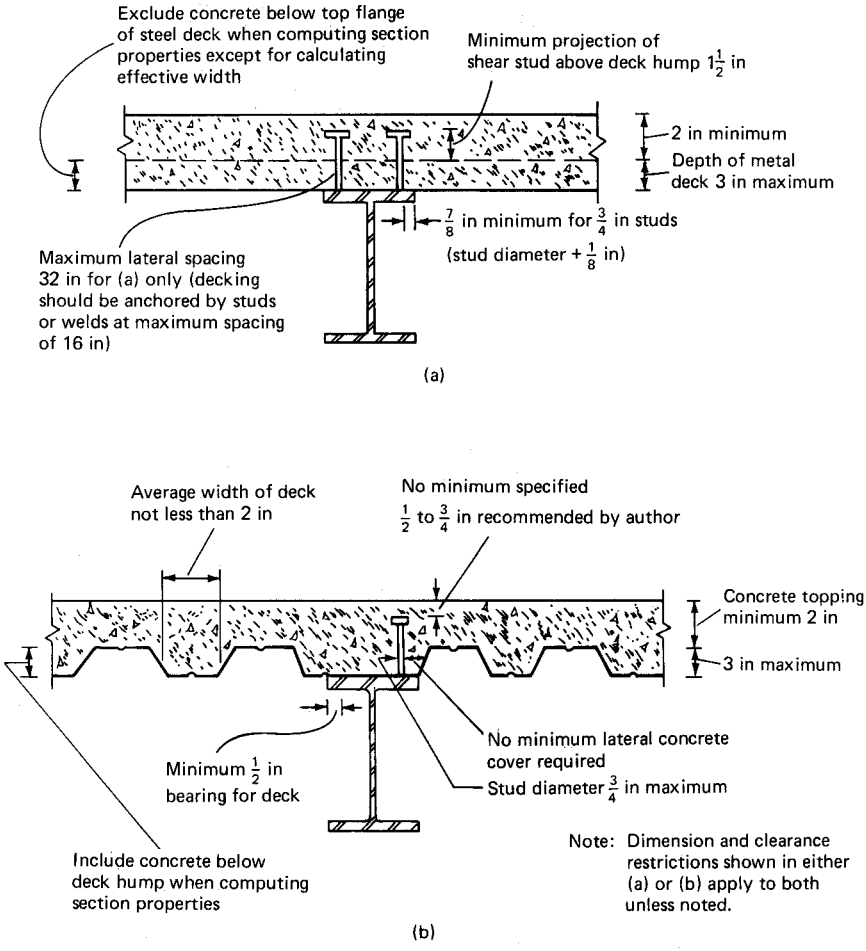

Figure 9.5 Composite beam with formed steel decking showing AISC requirements. (*a*) Deck perpendicular to beam; (*b*) deck parallel to beam.

can be considered effective in the composite action as shown in Fig. 9.6. When the slab extends on one side of the beam only, as in spandrel beams and beams adjacent to floor openings, the effective width naturally is less than when the slab extends on both sides of the beam. For slabs extending on both sides of the beam, the maximum effective flange width b may not exceed (1) one-fourth of the beam span L; (2) one-half the clear distances to adjacent beams on both sides plus b_f, the width of steel beam flange; or (3) 16 times the slab thickness t plus b_f. On the other hand, when the slab extends on only one side of the beam, the maximum effective width b may not exceed (1) one-twelfth of the beam span L, or (2) one-half the clear distance to the adjacent beam plus b_f, or (3) six times the slab thickness t plus b_f. Furthermore, the

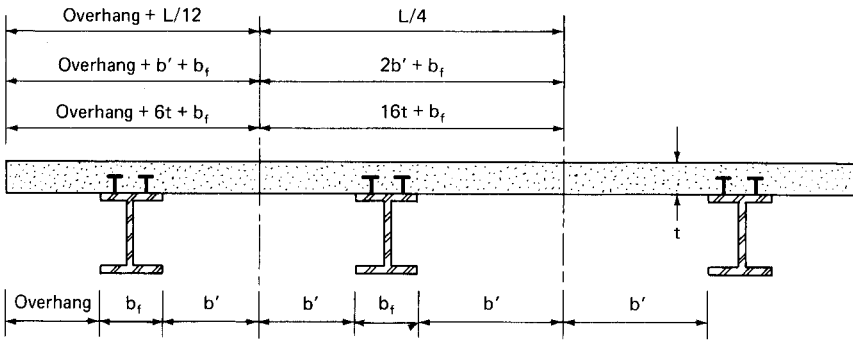

Figure 9.6 Effective width concept as defined in AISC specifications.

effective width on the outside of the steel section may not exceed the actual width of overhang, and the effective width on the inside must not extend beyond the centerline between the edge beam and the adjacent interior span.

The design of composite beams is usually achieved by the transformed area method, in which the available concrete effective area of the composite beam is transformed into an equivalent steel area. It is equally admissible to transform the steel area into an equivalent concrete area, but calculations are somewhat simplified by the former method. The method assumes transverse compatibility at the concrete and steel interface; the strain of both materials is the same at equal distances from the neutral axis. The unit stress in each material is equal to the strain times its modulus of elasticity. Because of strain compatibility, the stress in steel is given by n times the stress in concrete, where n is the modular ratio E_s/E_c. A unit area of steel is, therefore, mathematically equivalent to n times the concrete area. Therefore, the effective area of concrete $A_c = bt$ can be replaced by an equivalent steel area A_c/n.

Concrete is neither linearly elastic nor ductile and has a constantly changing slope with a sudden brittle failure. In spite of these characteristics, concrete can be considered as an elastic material within a stress strain range of up to 0.50 f_c' and the modulus of elasticity in pounds per square inch can be approximated by the relation $E_c = W_c^{1.5} \times 33\sqrt{f_c'}$, where W_c is the unit weight of concrete in pounds per cubic foot and f_c' is the compressive strength of concrete in pounds per square inch. The compressive strength f_c' of concrete normally used in floor construction is in the range of 3000 to 5000 psi (20.7 to 34.4 MPa) giving a range of E_c for normal weight concrete of $3.12 \times 10^6 < E_c < 4.03 \times 10^6$ psi ($21{,}512 < E_c < 27{,}787$ MPa), which can be compared to E_s of steel at 29×10^6 psi (199,955 MPa). The value of $n = E_s/E_c$, therefore, lies between 9.3 and 7.2 and is usually approximated to the

whole number in recognition of the great amount of error in the formula for E_c when compared to actual performance.

For strength calculations, the AISC specification uses the value of n for normal-weight concrete of the specified strength. For deflection computations, n depends not only on the specified strength but also the weight. Therefore, in computing deflections, especially for beams subjected to heavy sustained loads, it is necessary to account for the effects of creep. This is even more important in shored construction when the dead load of the concrete is resisted by the composite action. Creep effect is accounted for in computing deflections by using a higher modular ratio, n. A multiplication factor of 2 for creep effects appears to be adequate in building designs. Live loads are always resisted by the composite section. If the live loads are of short duration, the live load deflections are computed with the short-term modular ratio.

The transformed steel section can be conveniently considered as the original steel beam with an added cover plate to the top flange of thickness t and an equivalent width b/n. The properties of the transformed section are calculated by first locating the neutral axis and its transformed moment of inertia I_{tr}. The maximum stress in steel is expressed by

$$f_{bs} = \frac{MY_{tr}}{I_{tr}}$$

where M is the bending moment and Y_{tr} is the distance of the extreme bottom steel fibers from the neutral axis. The maximum bending stress for concrete is expressed by

$$f_{bc} = \frac{MC_t}{nI_{tr}}$$

where C_t is the distance from the neutral axis to the extreme concrete fibers and n is the modular ratio. The value

$$S_{tr} = \frac{I_{tr}}{Y_{tr}}$$

is called the transformed section modulus of the beam referred to the bottom flange.

For construction without temporary shores, the concrete stress is based upon the load applied after the concrete has reached 75 percent of the required strength. This stress is limited to 0.45 f_c', just as in working stress design of reinforced concrete beams.

According to the AISC, the total horizontal shear to be resisted between the point of maximum positive moment and point of zero moment is the smaller of the two values as determined by

$$V_h = \frac{0.85\, f'_c A_C}{2} + \frac{A'_s\, F_{yr}}{2}$$

$$V_h = \frac{A_{sr} F_r}{2}$$

where f'_c = specified compressive strength of concrete
A_c = actual area of effective concrete flange
A_s = area of steel beam

Note that the formula $V_h = 0.85 f'_c A_c/2$ assumes that there is no longitudinal reinforcing steel in the compression zone of composite beam. If the compressive zone is designed with mild steel reinforcement, the formula for horizontal shear is to be modified as follows:

$$V_h = \frac{0.85\, f'_c A_C}{2} + \frac{A'_s\, F_{yr}}{2}$$

where A'_s = area of the longitudinal compression steel
F_{yr} = yield stress of the reinforcing steel

AISC permits averaging of horizontal shear flow; that is, the total number of connectors between the point of maximum moment and that of zero moment must be sufficient to satisfy the total shear flow within that length. The shear connector formulas represent the horizontal shear at ultimate load divided by 2 to approximate conditions at working loads.

The number of shear connectors required for full composite action is determined by dividing the smaller value of V_h by the shear capacity of one connector. The number of connectors obtained represents the shear connectors required between the point of maximum positive moment and point of zero moment. For example, in a simply supported, uniformly loaded beam this represents half the span; and in a simply supported beam with two equidistant concentrated loads, this represents the distance between the point load to the support point. The total number of connectors required for the entire span is thus double the number obtained as above.

A composite beam subject to negative bending moment suffers tensile stresses in the concrete zone and loses much of its advantage. However, when reinforcement is placed parallel to the beam within the

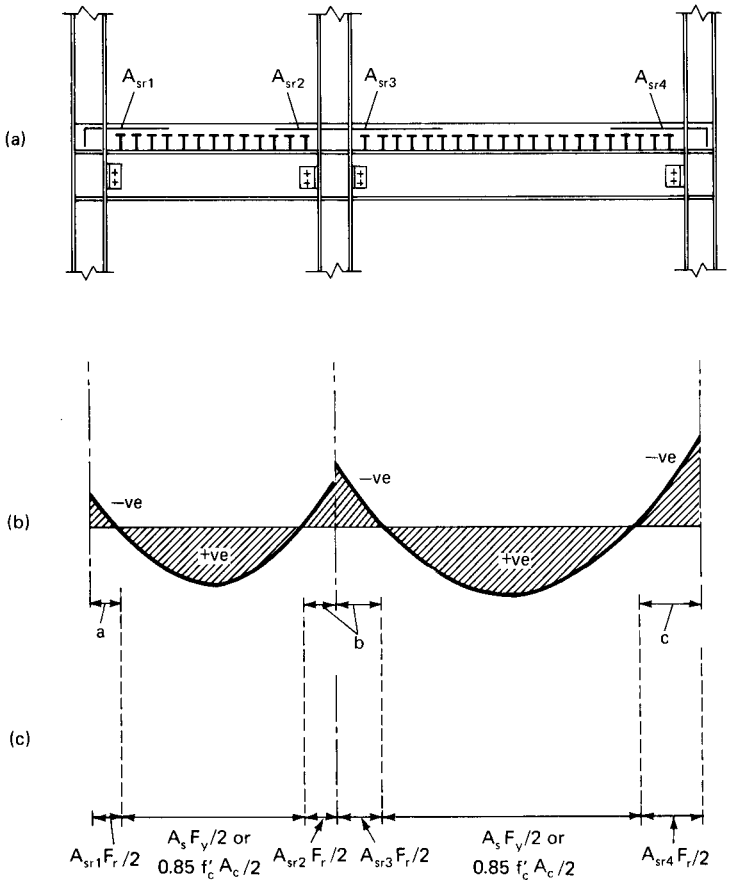

Figure 9.7 Continuous composite beam subjected to uniformly distributed load. (*a*) Elevation; (*b*) moment diagram; (*c*) horizontal shear to be resisted by shear studs in positive and negative moment regions.

effective width of slab and anchored adequately to develop the tensile forces, the advantage of continuous composite construction is restored. The steel used in the tensile zone is included in computing the property of the composite section. Similarly, when the compressive stress in concrete subject to positive moment exceeds the allowable stress, it is permissible to use compressive steel in the effective width zone.

Consider a continuous composite beam shown in Fig. 9.7. The total horizontal shear to be resisted by shear connectors between an interior support and each adjacent point of contraflexure (regions *a*, *b*, and *c* in Fig. 9.7) is given as

$$V_h = \frac{A_{sr}F_r}{2}$$

where A_{sr} = area of reinforcing steel provided at the interior support within the effective flange width
F_r = yield stress of the reinforcing steel

The AISC permits uniform spacing of connectors between the points of maximum positive moment and the point of zero moment. Also, the connectors required in the region of negative bending can be uniformly distributed between the point of maximum moment and each point of zero moment. For concentrated loads, the number of shear connectors N_2 required between any concentrated load and the nearest point of zero moment must be determined by AISC formula

$$N_2 = \frac{N_1[(M\beta/M_{\max}) - 1]}{\beta - 1}$$

where M = moment at concentrated load point (less than the maximum moment)
N_1 = number of connectors required between point of maximum moment and point of zero moment
β = ratio of transformed section modulus to steel section modulus

This relation is schematically shown in Fig. 9.8.

In the design of composite beams for high-rise buildings, it is often unnecessary to develop the full composite action. A partial composite action with fewer studs is all that may be necessary to achieve the required composite action. AISC permits the design of less than 100 percent composite beams by introducing the concept of effective section modulus as determined by the relation

$$S_{\text{eff}} = S_S + \left(\frac{V_h'}{V_h}\right)^{1/2} (S_{tr} - S_S)$$

where S_s is the section modulus of steel beam alone, and V_h' is the shear capacity provided by the connections, which is obtained by multiplying the number of connectors used and the shear capacity of one connector. When the required transformed section modulus S_{tr} is less than the available, transposing the above equation gives the horizontal shear force to be carried by shear connectors to satisfy the required section modulus. Thus

$$V_h' = V_h \left(\frac{S_{\text{reqd}} - S_S}{S_{\text{avail}} - S_S}\right)^2$$

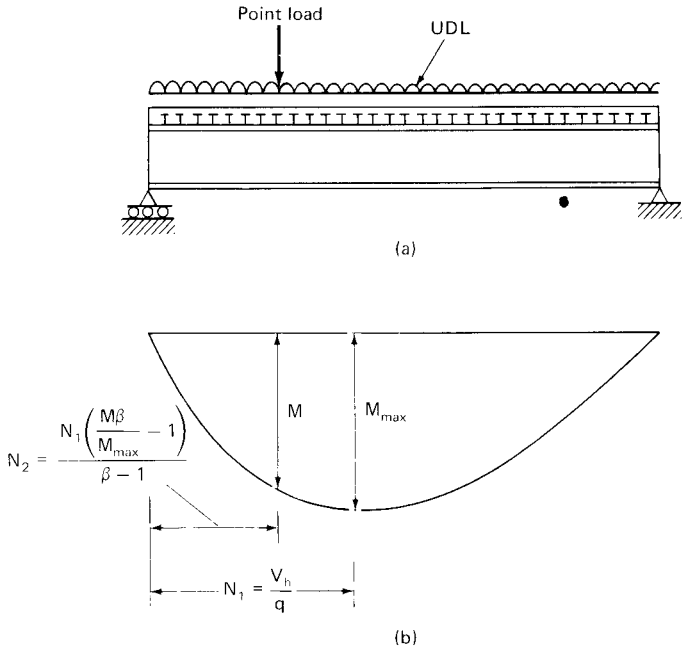

Figure 9.8 Shear connector requirements for composite beams subjected to concentrated loads. (*a*) Schematic loading diagram; (*b*) shear connector requirements.

AISC stipulates that a minimum requirement of V_h' be not less than $0.25V_h$ to prevent excessive slip and loss in beam stiffness. This minimum requirement does not apply if shear studs are used for reasons other than increasing the flexural capacity, such as increase in stiffness of beams or to increase the diaphragm action.

The AISC specification gives three criteria for stud placement: (1) a minimum center-to-center spacing of six stud diameters between the studs in the longitudinal direction, (2) minimum spacing of four stud diameters in the transverse direction, and (3) maximum spacing in the longitudinal direction of 32 in (813 mm). Note that if stud spacing exceeds 16 in (406.4 mm), a plug weld between the studs is required to resist uplift forces.

If the required bending capacity is provided by the steel beam alone without depending upon the composite action, the maximum spacing requirement of 32 in (813 mm) need not be met. Other criteria such as studs required to generate diaphragm action or an increase in frame stiffness may influence the spacing of the studs.

The recommended sequence for installing studs when deck is perpendicular to beam is as follows:

- Deck ribs at 6 in (153 mm) on center: Start at beam ends and place a single stud at every fourth flute, working toward the center of beam. If studs remain, fill in empty ribs, again starting at beam ends and working toward the center without exceeding 30 in (762 mm) for stud spacing.
- Deck ribs at 12 in (305 mm) on center: Start at beam ends and place a single stud in every other flute working toward the center of beam. If studs remain, fill in empty ribs, again starting at beam ends and working toward the center of beam without exceeding 24 in (610 mm) for stud spacing.
- If the number of studs is more than the number of ribs, place a double or triple row as needed, always starting from beam ends and working toward the beam center. In general, if studs cannot be uniformly spaced, the greatest number of studs should occur at the ends.

The recommended sequence for installing studs when deck is parallel to the girder is as follows. Start at the girder ends by placing the first stud at approximately 12 in (305 mm) from the centerline of support and work toward the center of girder with uniform spaces between the studs. If double row of studs is required, it is a good practice to place them in a staggered pattern rather than side by side.

The allowable shear load for stud connectors is influenced by several factors when used in metal deck construction. As in solid slabs, the strength and type of concrete, whether regular or lightweight, determines the allowable horizontal loads. The rib geometry of metal deck and the height of the stud above metal deck (when deck is parallel to the girder) are other factors influencing the allowable horizontal loads. For girders, the wider the rib opening and the greater the penetration of the stud above the deck, the more closely the allowable horizontal shear load will approach the published AISC value for studs in solid concrete slab.

9.3 Composite Haunch Girders

Composite haunch girders, although not often used as a floor framing system, merit mention because they strive to minimize the floor-to-floor height without requiring complicated fabrication. Figure 9.9 shows a schematic floor plan in which composite haunch girders frame between exterior columns and interior core framing. The haunch girder shown in Fig. 9.9 consists of a shallow steel beam, 10 to 12 in (254 to 305 mm) deep for spans in the 35- to 40-ft (10.6- to 12.19-m) range. At each end of the shallow beam is a triangular haunch formed by a diagonal cut along a relatively deep wide-flange beam usually 24

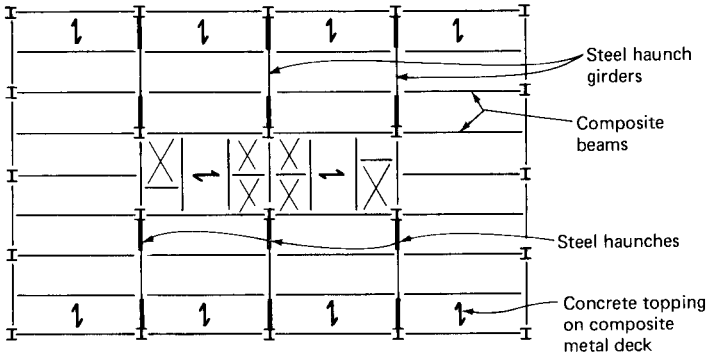

Figure 9.9 Schematic floor plan showing haunch girders.

to 27 in (610 or 686 mm) deep. The haunch is welded to the shallow beam and to the columns at each end of the girder. In this manner the last 8 or 9 ft (2.4 or 2.7 m) of the haunch girder at either end flares out toward the column with a depth changing from about 10 or 12 in (254 or 305 mm) at the center to about 27 in (686 mm) at the ends. The system has proved practical in certain applications because it uses less steel and provides greater flexibility for mechanical ducts, which can be placed anywhere under the shallow central span. The reduction in floor-to-floor height further cuts the costs of exterior cladding and heating and cooling loads. The system, however, is not common because although it uses less steel and reduces the building envelope for the same number of floors, it requires more labor for fabrication of haunches.

Another variation of the same concept is shown in Fig. 9.10. In this scheme, as in the previous scheme, the depth of the girder is reduced to the same depth as the filler beams, permitting horizontal transfer of ductwork without increasing story height. Nontapered haunches are used at each end to obtain the required stiffness and strength. The square haunch girder can thus be fabricated as three separate units, one shallow rolled section in the center and two deep rolled sections, one at each end. Another method of fabricating the girder is to notch the bottom portion of a deep girder at midspan and reweld the flange to the web. The method requires more steel but comparatively less fabrication work.

In comparison to shallow girders, haunch girders are significantly stiffer and, therefore, can be employed in resisting lateral loads. The combined action of dead, live, and wind loads often results in a moment diagram as shown in Fig. 9.11. Concrete in certain portions of the girder is subjected to tension, rendering the composite action ineffective. A schematic moment of inertia diagram that can be used in the

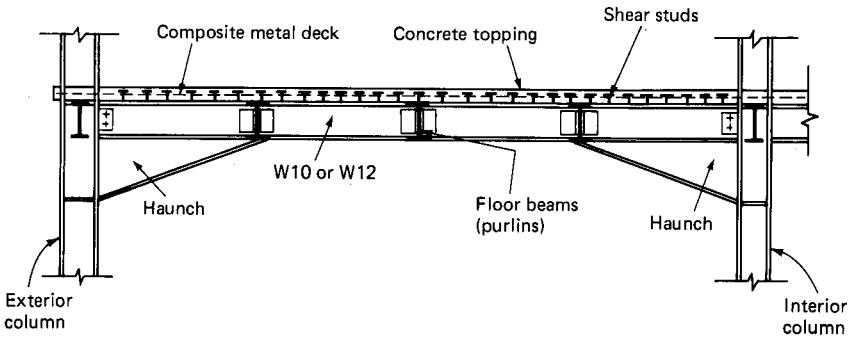

Figure 9.10 Composite girder with tapered haunch.

frame analysis is shown in Fig. 9.10*b*. As an alternate to a beam with variable moment of inertia, a prismatic beam with an equivalent moment of inertia can be used in the analysis.

9.4 Composite Trusses

Figure 9.12 shows a floor framing plan which uses composite trusses. In order to keep the fabrication simple, the top and bottom chords consist of T sections to which double-angle web members are welded directly without the use of gusset plates. The top chord of the truss is made to act compositely with the floor system by the use of welded shear studs. The space between the diagonal webs is used for the passage of air-conditioning ducts. In cases where the space is not sufficient, one or two web members can be welded vertically between the chords to form a Vierendeel panel.

9.5 Composite Stub Girders

9.5.1 General considerations

In the design and construction of high rises, maximum flexibility is achieved if structural, mechanical, electrical, and plumbing trades have their own designated layers in the ceiling. This can be achieved in a conventional floor framing system by placing HVAC ducts, lights, and other fixtures under the beams. In some instances where deep girders are used, penetrations are made in the girder webs to accommodate the ducts. Usually the typical span between the core and exterior of the building is about 40 ft (12.2 m), requiring 18- to 21-in (457- to 533-mm) deep beams acting compositely with the floor slab. Usual requirements of HVAC ducts, lights, sprinklers, and ceiling construction result in depths of 4 to 4.25 ft (1.21 to 1.3 m) between the ceiling and top of floor slab. The depth-of-ceiling sandwich can,

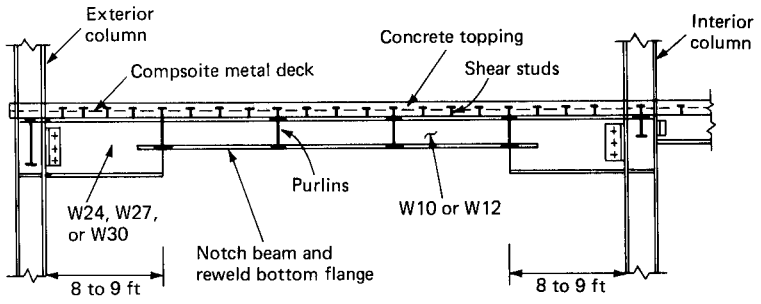

(a)

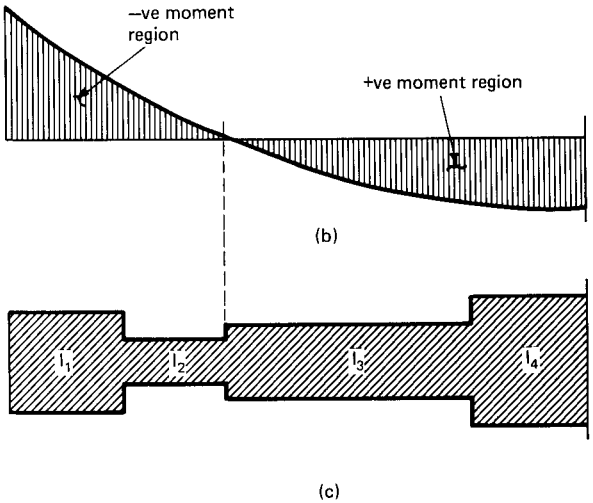

(c)

I_1 = Moment of inertia of unnotched steel section
I_2 = Moment of inertia of notched steel section
I_3 = Moment of inertia of composite notched section
I_4 = Moment of inertia of composite unnotched section

Figure 9.11 Composite girder with square haunch. (*a*) Schematic elevation; (*b*) combined gravity and wind moment diagram; (*c*) schematic moment-of-inertia diagram.

however, be decreased at a substantial penalty either by introducing penetrations in deep beams or by using a shallower, less economical beam depth.

The stub girder system, invented by engineer Dr. Joseph Caloco, attempts to eliminate some of these problems while at the same time reducing the total steel weight. It is a novel composite design which increases the economic range for composite beams and provides space for mechanical ducts without any increase in the floor-to-ceiling

depths. The key components of the system are short stub beams welded at intervals to the top flange of a steel beam. Sufficient space is left between stub beams to accommodate continuous steel beams and mechanical ducts. The floor system is completed by placing a concrete slab on steel decking spanning between the floor beams. A plan of a stub girder system is schematically shown in Fig. 9.13*a*. The system consists of a series of girders spaced from about 25 to 35 ft (7.62 to 10.7 m) on center and spanning between the core and the exterior of the building. The stub girder consists of a high-strength wide-flange beam with stub pieces shop-welded onto the top flange of the wide-flange beam. Floor beams are placed over the girder between stub girders, with spacing varying anywhere from 8 to 10 ft (2.44 to 3.05 m).

Although the lease depth in office buildings is normally around 40 to 42 ft (12.20 to 12.8 m), the centerline location of the column relative to the exterior face of the curtain wall may vary by as much as 2 to 3 ft (0.61 to 0.91 m), depending upon architectural requirements. In some buildings the exterior face of the column is held flush with the back of the curtain wall and in certain other buildings it is placed 1 to 2 ft (0.3 to 0.6 m) from the back face of the curtain wall. This results in a stub girder span of about 38 to 40 ft (11.6 to 12.2 m), giving a spacing of 8 to 10 ft (2.44 to 3.05 m) for the floor beams. The floor beams are designed for continuity and are spliced usually 3 to 4 ft (0.92 to 1.22 m) from the centerline of the stub girder. The system is completed by placing metal deck over the steel beams and an appropriate thickness of concrete over the metal deck. Composite action between the concrete and the stub girder is achieved by providing shear connectors. The floor deck with the concrete on top acts compositely with the stub beams welded to the main girder. Stub girder systems effectively provide adequate stiffness, as well as excellent provision for distribution of electrical and mechanical distribution systems at an economical price.

Structurally, the behavior of stub girders is akin to a Vierendeel truss; the concrete slab serves as the compression chord, the full-length girder serves as the high-strength steel bottom tension chord, and the steel stubs serve as vertical shear members. This assemblage of different elements using concrete and steel attempts to optimize the material strengths of all elements and, therefore, results in cost savings. Less steel is required for the floor framing. From the overall system consideration, the structure allows installation of mechanical system within the structural envelope, thus reducing floor-to-floor heights; the mechanical ducts run through and not under the floor structure. There are openings between the concrete slab and the girder through which air conditioning ducts, pipes and communication equipment run without the need of penetrating the girders. The cost

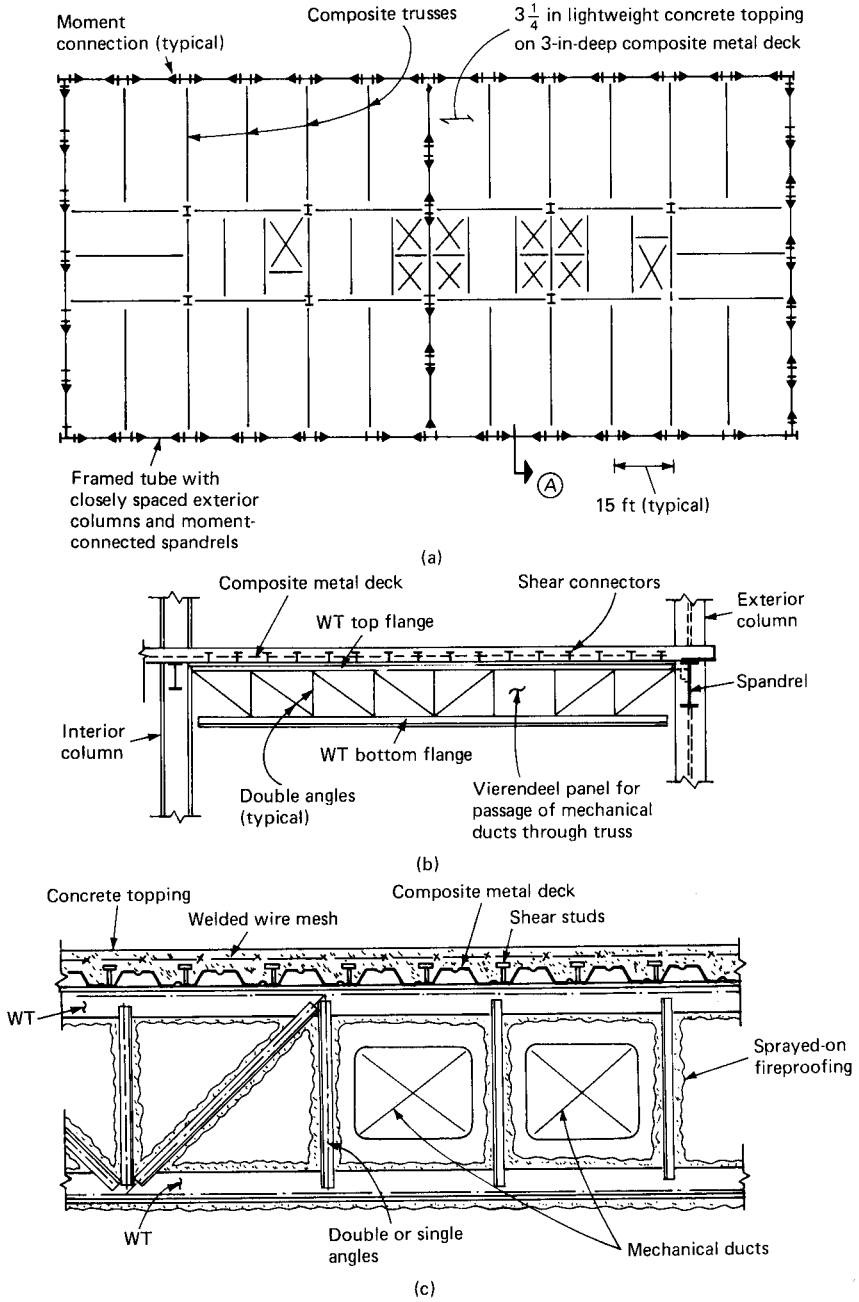

Figure 9.12 Composite truss. (*a*) Framing plan; (*b*) elevation of truss, section A; (*c*) detail of truss.

(d)

Figure 9.12 *(Continued)* *(d)* Photograph of composite truss and metal deck framing.

reductions are normally attributed to the following factors: (1) Reduction required in the steel girders due to the greater depth available for bending resistance, and (2) reduction in the weight of floor beams due to continuity. On an average, these factors could be counted on to bring down the weight of floor framing by 1.5 to 2 psf (71.8 to 95.76 Pa). The savings are valid for large spans of 30 to 45 ft (9.15 to 13.72 m) only. For spans less than 30 ft (9.15 m), the additional cost of fabrication of stub girders outweighs the advantages. For spans larger than 45 ft (13.72 m), there have not been enough practical cases to make meaningful economic comparisons. A reduction of normally 3 in (76.2 mm) in most cases, and as much as 6 to 8 in (152.4 to 203.2 mm) in some unusual cases, in the total attic space between the top of the slab and bottom of the ceiling could be achieved. As a result, floor-to-floor height is reduced, effecting considerable savings in the exterior cladding of the building.

A stub girder requires a more complicated analysis than a conventional composite girder. The slab, deck, and the steel beam act together as a Vierendeel system, the slab and beam developing axial loads in addition to bending moments. In addition, shear forces are also developed in the various elements. Since there is no guidance printed in steel specifications in a design standard format, modeling techniques vary from one design firm to another and sometimes among engineers within the same office. Fortunately, the essential structural action is easy to formulate and the different modeling techniques usually tend to lead to the same final design.

A reason for nonacceptance of stub girders in certain parts of North

America is that the system is perceived as being somewhat expensive in terms of HVAC ductwork. The ducts must change levels to cross the girders and require more bends, adding to the cost. Also there are additional fabrication costs because of additional welding. Finally, a rather important construction-related consideration is that stub girders must be shored to support the weight of concrete until the concrete reaches its full strength. In a multistory building, this means shoring not only underneath the stub girder that is being concreted, but also a certain number of levels, usually three, below the concreting level.

Stub girder framing is most suited for steel-framed office buildings with a minimum width of 100 ft (30.5 m) and spans from core to the exterior wall of 35 to 45 ft (10.67 to 13.72 m). The premium in steel fabrication is not justified when the span is less than 30 ft (9.2 m). The system is not a cost saver for short spans.

9.5.2 Stub Girder Behavior and Analysis

The primary action of the stub girders is essentially similar to that of a Vierendeel truss; the bending moments are resisted by tension and compression forces in the bottom and top chord of the truss and the shearing stresses are resisted by the stub pieces welded onto the bottom continuous wide-flange beam. The bottom chord of this truss is manifested in the steel wide-flange beam, and since steel is good in resisting tensile forces, it makes an excellent material for carrying these loads. The compression forces are carried by the concrete slab. Usually a width of concrete slab which varies from 6 to 7 ft (1.83 to 2.13 m) is effective, and additional reinforcement is normally required to supplement the compression capacity of the concrete. The shear forces are resisted by the stub pieces, which are connected to the concrete slab through shear connectors and to the steel beam by welding.

Because the truss is a Vierendeel truss as opposed to a diagonalized truss, bending of top and bottom chords and the vertical members constitutes a significant structural action. Therefore, it is necessary to consider the interaction between axial loads and bending stresses in the design of both the top and bottom chords of the truss. Another way of looking at the structural behavior of the stub girder, though somewhat simplistic, is to consider the stub girder as a beam of varying moment of inertia. A simply supported beam model with variable moment of inertia is a statically determinate structure. Therefore, the bending stresses in the steel beam and the concrete slab can be easily calculated by the relation $f = M/S$, where f is the bending stress, M is the bending moment, and S is the section modulus. The deflection is obtained by integration of M/EI diagram. Design of stub girders using a nonprismatic beam as an analytical model is not used

in practice because the analysis does not give the various forces and moments required in the design. Invariably the model used is a simulated Vierendeel truss. Even then, the design of stub girder has not come about as a routine office design and is not covered in design specifications. Therefore, it will be presented in this section somewhat elaborately. To make the presentation more meaningful, a specific example with numerical values will be given.

Figure 9.13*a* shows a typical floor plan of a hypothetical office building. The stub girders are designated in the plan as SG1, SG2, etc. Consider a typical stub girder SG1, spanning the full distance of 40 ft (12. 19 m) between the exterior and interior of the building. Figure 9.13*b* shows the elevation of the stub girder and the length of the stub pieces welded to the bottom beam. The deck system consists of a 2-in (51-mm) deep 19-gauge composite metal deck with a $3\frac{1}{4}$-in (82.5-mm) lightweight structural concrete topping. A welded wire fabric is used as crack control reinforcement in the concrete slab. The first step in the analysis is to model the stub girder as an equivalent Vierendeel truss. This is shown in Fig. 9.14*a*. A 14-in (356-mm) deep steel beam is assumed as the continuous bottom chord of the truss. The slab and the steel beam are modeled as the continuous top and bottom chords of the truss. Note that the line elements representing these members are placed at the neutral axes of the slab and beam, respectively, as shown in Fig. 9.14*b*.

The vertical stub pieces can be modeled as a series of line elements between the top and the bottom chords of the truss. Other techniques for representing stub pieces are possible, and slight variations do occur in the results depending upon the type and the number of elements used to represent the stub pieces. Some engineers employ a combination of vertical and diagonal beam elements to represent the bending and shear resistance of the stub pieces, respectively. Others employ only vertical elements possessing both bending and shear resistance. The results do vary from one analytical model to another, but they are not considered significant enough to affect the design. Since the finite width of the stub is represented by a discrete number of elements, it should be expected that all reasonable representations converge to the same solution as the number of elements is increased. Early computer solutions of stub pieces did not attempt to model the rigid regions between the neutral axes of the horizontal beam and slab elements and the stub pieces. This had the effect of underestimating the stiffness of the stub girders. The current practice is, however, to include the rigid zone effect in the computer model by using a vertical element with artificially large bending and shear properties as compared to the properties of other elements. Normally a value which is about 1000 times the properties of the largest real member will suffice to capture

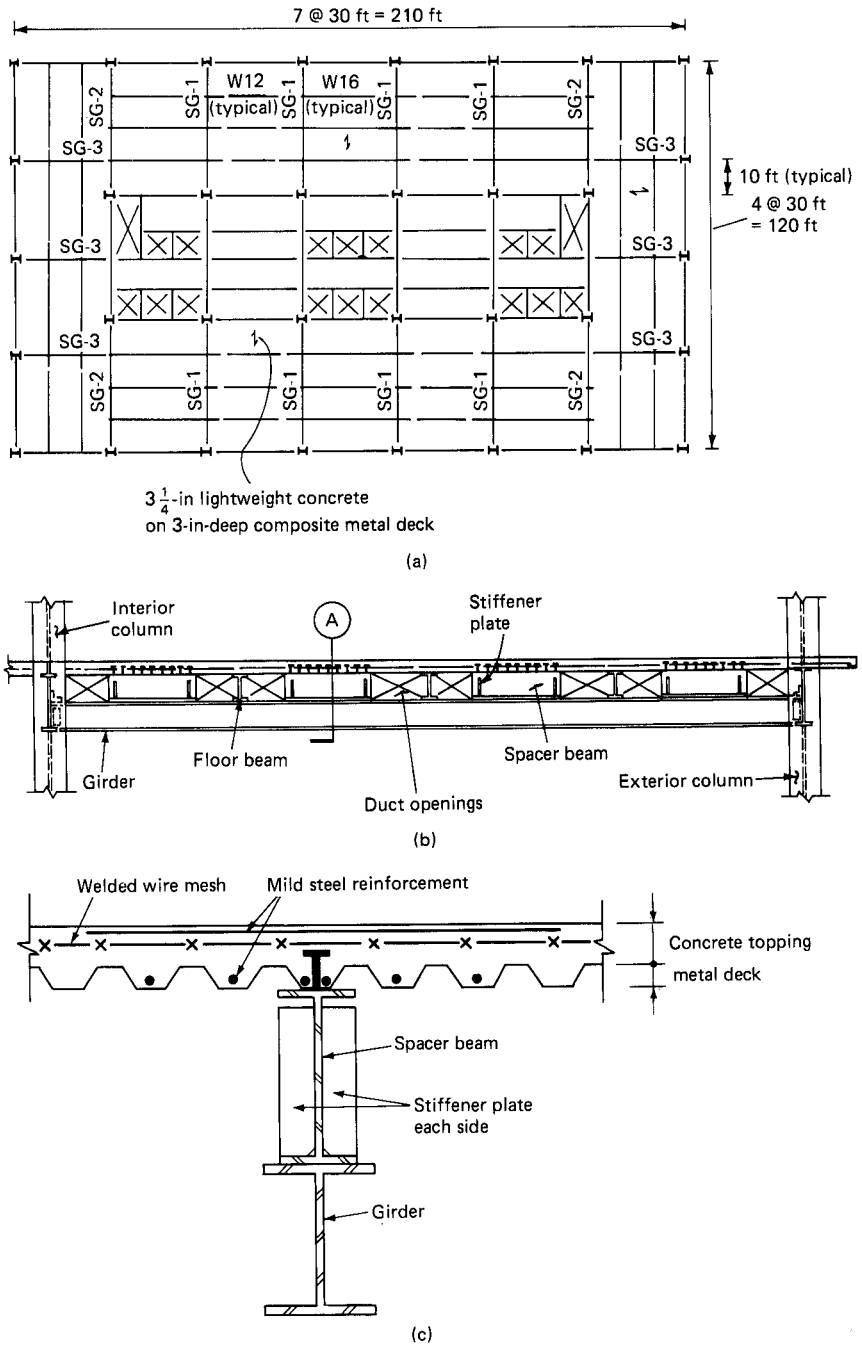

Figure 9.13 Stub girder framing (*a*) framing plan; (*b*) elevation of stub girder SG-1; (*c*) section A through stub girder.

(d)

Figure 13 *(Continued)* *(d)* Photograph of stub girder framing.

the rigid zone effect without unduly introducing round-off errors in computer solutions.

The floor beam that cantilevers off the bottom chord is represented as a line element. Since the bending stiffness of the beam web in the plane of the stub girder is relatively small compared to other members, it makes very little difference in the design whether a rigid region is incorporated or not in this member.

The various steps required for modeling the stub girder can be summarized as follows:

1. *Top chord of Vierendeel truss.* As shown in Fig. 9.15, the top chord consists of an equivalent transformed area of the concrete section. This is obtained by finding the effective width of concrete slab and dividing it by the modular ration $n = E_s/E_c$. In calculating the transformed properties of the concrete slab, advantage can be taken by including the steel area of longitudinal bars which are invariably required from strength requirements. For strength calculations, the use of modulus of elasticity of normal-weight concrete is permissible even for lightweight concrete slabs in composite construction. However, the usual design practice is to use the lower value of n for lightweight concrete slabs both for deflection and strength calculations. The moment of inertia I_t of the top chord is obtained by multiplying the unit value of I of composite slab, given in the deck catalog, by the effective width of slab.

2. *Bottom chord.* The properties of the steel section are directly used for the bottom chord properties.

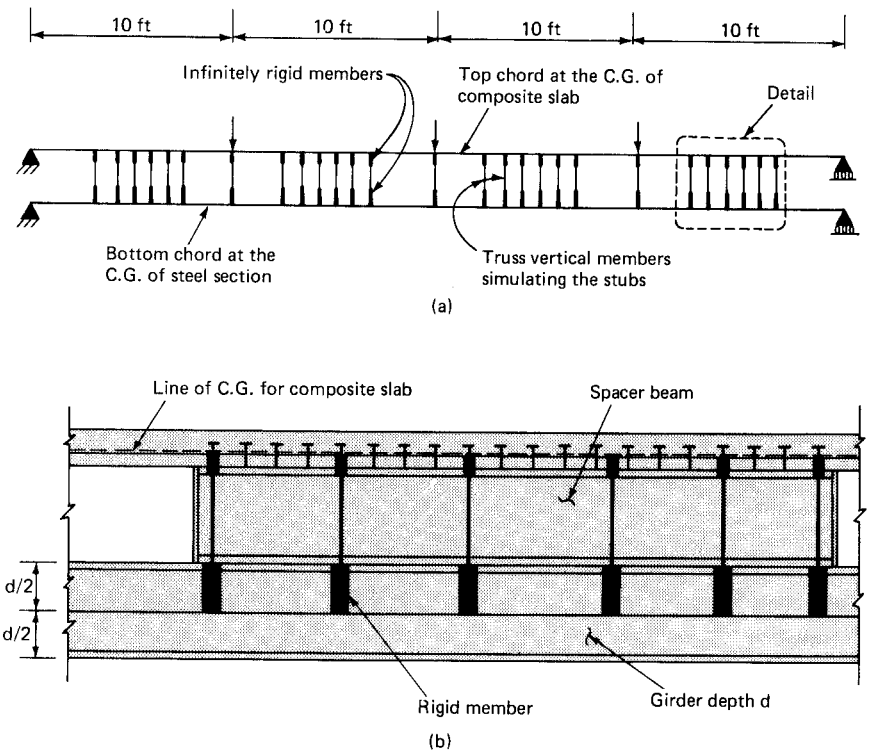

Figure 9.14 (*a*) Elevation of Vierendeel truss analytical model; (*b*) partial detail of analytical model superimposed on stub girder.

3. *Stub pieces.* The area of the web of the stub piece and its moment of inertia in the plane of bending of the stub girder are calculated and apportioned to a finite number of vertical elements that represent the stubs. In common with other finite-element solutions, it is to be expected that the more elements employed to represent the stub pieces, the better will be the accuracy of the solution. As a minimum, the author recommends one vertical element for 1 ft (0.3 m) of stub width. The segments of the vertical elements between the top and bottom flanges of the stub and the neutral axes of the top and bottom chords are treated as rigid arms with comparatively large values for area and moment of inertia. Stiffener plates used at the ends of stubs can be incorporated in calculating the moment of inertia of the stubs.

To get a better feel for the design, an example follows:

Example A $3\frac{1}{4}$-in (82.55-mm) lightweight, 3-ksi (20.7 MPa) concrete topping is to be used on 3-in (76.2-mm) deep 18-gauge composite metal deck with

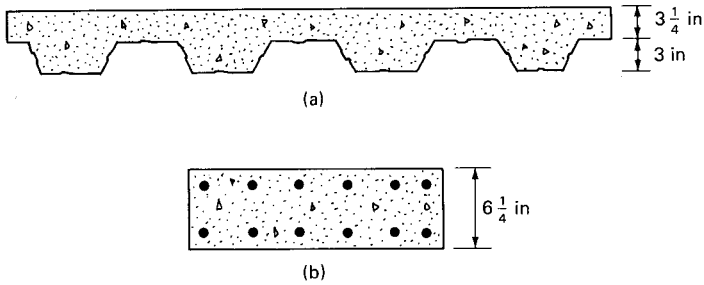

Figure 9.15 Equivalent slab section.

nominal welded wire fabric reinforcement, with spans between steel purlins at 10-ft (3.05-m) centers. W14 × 53 (356 mm × 773 N/m), 50-ksi (344.75-MPa) structural steel beam is proposed for the bottom continuous chord of stub girder. Exterior and interior stub pieces consist of W16 × 26 (406 mm × 379 N/m), 36-ksi (248.3-MPa) steel beams with $6\frac{1}{2}$- and $3\frac{1}{2}$-ft (1.98- and 1.07-m) lengths, respectively. It is required to model the stub girder as a Vierendeel truss to design and check various elements under the AISC and ACI specifications.

As a first step, we compute the equivalent properties of (1) top chord, (2) bottom chord, and (3) stub pieces for setting up the computer model.

1. *Top chord.* The concrete slab extends on both sides of the stub girder. The effective width of concrete flange needs to be determined by considering three values:

$$b = 16t + b$$

$$b = L/4$$

b = distance between stub girders

For the example, the least value of effective width for the top chord is

$$16t + b = 16\,(1.5 + 3.25) + 5 = 81 \text{ in} = 6.75 \text{ ft } (2.06 \text{ m})$$

Area A of transformed section using $n = 14$

$$A = (3.25 + 1.5) \times \frac{81}{14} = 27.48 \text{ in}^2\ (17732 \text{ mm}^2)$$

Equivalent moment of inertia I_e is the value of I for the particular metal deck and slab thickness usually given in the product catalog, multiplied by the effective width of compression chord. Assuming that the moment of inertia of $3\frac{1}{4}$-in (82.55-mm) slab on 3-in (76.2-mm) composite deck is 5.82 in^4/ft, we get

$$I = 5.82 \times 6.75 = 39.3 \text{ in}^4\ (0.0164 \times 10^{-3} \text{ m}^4).$$

2. *Bottom chord.* W14 × 53 steel wide-flange beam has the following section properties.

$$A = 15.3 \text{ in}^2\ (9872 \text{ mm}^2) \quad I = 541 \text{ in}^4\ (0.225 \times 10^{-3} \text{ m}^4)$$

Shear area A_v = depth of web × web thickness

$$= 13.92 \times 0.37 = 5.15 \text{ in}^2\ (3323 \text{ mm}^2)$$

3*a*. Exterior stub piece W16 × 26, 6$\frac{1}{2}$ ft (1.98 m) long

$$\text{Area} = 78 \times 0.25 = 19.5 \text{ in}^2 \ (12581 \text{ mm}^2)$$

Moment of inertia in the plane of stub girder

$$I = \frac{bh^3}{12} = \frac{0.25 \times 78^3}{12} = 9886 \text{ in}^4 \ (4.12 \times 10^{-3} \text{ m}^4)$$

We divide the area and moment of inertia of the stub piece into the six members which are used in the computer model to stimulate the stub piece. Therefore, the area of each vertical member is 19.5/6 = 3.25 in^2 (2097 mm^2), and the moment of inertia I is 9886/6 = 1648 in^4 (0.686×10^{-3} m^4).

3*b*. Interior stub piece W16 × 26, 3$\frac{1}{2}$ ft (1.07 m) long.

$$A = 42 \times 0.25 = 10.5 \text{ in}^2 \ (6775 \text{ mm}^2)$$

$$I = \frac{0.25 \times 42^3}{12} = 1543.5 \text{ in}^4 \ (0.642 \times 10^{-3} \text{ m}^4)$$

Since three vertical members are used to stimulate the interior stub piece, we divide the area and moment of inertia values by 3 to get the equivalent values for the computer model.

$$A = \frac{10.5}{3} = 3.5 \text{ in}^2 \ (2258 \text{ mm}^2)$$

$$I = \frac{1543.5}{3} = 514.3 \text{ in}^4 \ (0.214 \times 10^{-3} \text{ m}^4)$$

The next step is to set up the model of the equivalent Vierendeel truss to obtain a computer solution for axial load, bending moment, and shear forces in all the members. The adequacy of each member under the action of combined forces is checked using the ACI and AISC procedures. A brief description of the procedure follows.

Bottom chord. Assume that the maximum axial tension and bending moment obtained from the computer run are T = 265 kips (1178.8 kN) and M = 90 kft (122.0 kN · m), respectively. Check the W14 × 53 for combined tension and moment thus

$$f_a = \frac{265}{15.3} = 17.2 \text{ ksi } (118.6 \text{ MPa})$$

$$f_b = \frac{90 \times 12}{77.8} = 13.75 \text{ ksi } (94.8 \text{ MPa})$$

$$F_a = 0.6 F_y = 0.6 \times 50 = 30 \text{ ksi } (206.8 \text{ MPa})$$

$$\frac{d}{t} = \frac{13.92}{0.37} = 37.62 > \frac{257}{\sqrt{F_y}} = 36.3$$

$$\therefore F_b = 0.60\,F_y = 30 \text{ ksi (206.8 MPa)}$$

$$\frac{f_a}{F_a} + \frac{f_b}{F_b} = \frac{17.2}{30} + \frac{13.75}{30} = 1.03$$

This is very nearly equal to 1.0, and therefore is OK.

Top chord. The top chord of the Vierendeel truss is subjected to compression and bending moment and therefore is designed as a reinforced concrete column subjected to compressive forces and bending. In the opinion of the author any rational method that does not violate the spirit of the ACI code can be used in the design of the equivalent beam or column. One procedure is to neglect the contribution of metal deck and design the slab section as an equivalent column. For purposes of calculation of moment magnification factor, the column can be conservatively assumed to have an effective length of 10 ft (3.04 m), which is equal to the distance between the purlins.

For the example problem, assume that the computer results for axial compression and bending moment at critical sections are 250 kips (1112.0 kN) and 10 kft (13.56 kN · m), respectively.

We now proceed to design the equivalent section of the compression chord shown in Fig. 9.15 as a reinforced concrete column subject to axial loads and bending moment. First calculate the slenderness ratio Kl_u/r by conservatively ignoring the restraint offered to the slab at the interface of stub pieces. The assumption that the equivalent column is hinged at the purlins gives a value of 1.0 for effective length factor K. The unsupported length l_u of the equivalent column can be considered equal to 10 ft (3.05 m), which is the distance between the purlins. The radius of gyration for the equivalent rectangular column is 0.3 times the overall dimension in the direction of bending, i.e., $0.3 \times 6.25 = 1.875$ in (47.62 mm).

The slenderness ratio

$$\frac{Kl_u}{r} = \frac{1 \times 10 \times 12}{1.875} = 64.0$$

Since this ratio is greater than 22, it is necessary to consider slenderness effects in the design of column. The moment magnification procedure will be used to take into account the slenderness effects. A conservative approximation will be made by assuming that the value for the coefficient C_m (which relates the actual moment diagram to an equivalent moment diagram) is 1.0.

Since the axial load P and moment M obtained from the computer analysis are working stress values, these are converted to ultimate values by multiplying them with an average load factor of 1.5. Therefore,

$$P_u = 1.5 \times 260 = 390 \text{ kips (1735 kN)}$$

$$M_u = 1.5 \times 10 = 15 \text{ kft (20.34 kN· m)}$$

The critical load P_c is given by the relation

$$P_C = \frac{\pi^2 E_C I}{(k l_u)^2}$$

For the example problem, we have

$$E_C = W_C^{1.5} \times 33\sqrt{f'_C} = 110^{1.5} \times 33\sqrt{3000} = 2085 \text{ ksi } (14378 \text{ MPa})$$

$$I = \frac{40.5 \times 6.25^3}{12} = 824 \text{ in}^4 \ (0.343 \times 10^{-3} \text{ in}^4)$$

Substituting, we get

$$P_C = \frac{3.14^2 \times 2085 \times 824}{(10 \times 12)^2} = 1176 \text{ kips } (5230 \text{ kN})$$

The moment magnification factor is given by

$$\delta_1 = \frac{C_m}{1 - (P_u/\phi P_C)}$$

$$= \frac{1}{1 - (390/0.7 \times 1176)} = 1.90$$

Therefore, design $M_u = 15 \times 1.9 = 28.5$ kft (38.65 kN · m).

The equivalent column is designed for $P_u = 390$ kips (1735 kN) and $M_u = 28.5$ kft (38.65 kN · m). The required reinforcement is obtained by using a procedure conforming to the ACI code. For the present example, ten #5 longitudinal reinforcement is found to be adequate to carry the design axial load and bending moment.

Computation of number of shear studs. The shear studs between the stud pieces and the concrete slab form the backbone of composite stub girders. Their design is similar to composite beam design for which the shear connector formulas represent the horizontal shear at ultimate load divided by 2 to approximate conditions at working loads. The total horizontal shear to be taken by the connectors between the point of maximum moment and each end of stub girder is the smaller of the values obtained from the following equations:

$$V_h = \frac{0.85 f'_C A_C}{2}$$

or

$$V_h = \frac{A_S f_y}{2}$$

For the example problem, it is found that a value of $V_h = 458$ kips (2037 kN) obtained from the first equation governs the design. Using a value of 9.5 kips (42.26 kN) as the allowable shear load, the number of shear studs $N = 458/9.5 = 48.2 \approx 50$, giving 32 and 18 shear connectors at the exterior and interior stubs.

Check exterior stub W16 × 26, $6\frac{1}{2}$ ft (1.98 m) long The design check is performed for shear and bending stresses per the AISC specifications. The

summation of shear forces at the six members in the computer model corresponding to the exterior stub gives the design shear. The design moment for the stub is obtained by multiplying the accumulated shear by the height of stub. Assume for the example problem that the accumulated shear = 210 kips (934 kN). The design moment then is 210 × 16/12 or 280 kft (380 KN · m). The shear stress is 210/78 × 25 or 10.76 ksi (74.25 MPa). The allowable shear stress is $0.4 \times F_y$ = 0.4 × 36 = 14.4 ksi (99.3 MPa). Therefore, the stub is okay for shear force.

To check the bending stresses, we calculate the moment of inertia and section modulus of the stub by including the contribution of the stiffener plates at the ends of stub. Without burdening the presentation with trivial calculations, let us assume that the section modulus of the stub piece and stiffener plate is equal to 300 in^3 (4.92 × 10^6 mm^3). The bending stress

$$f_b = \frac{280 \times 12}{300} = 11.2 \text{ ksi (77.3 MPa)}$$

This stress is checked against the allowable stresses per the AISC specifications.

A similar procedure is used to check the bending and shear stresses in the interior stub.

9.5.3 Moment-connected stub girder

The stub girder system, due to its large overall depth of approximately 3 ft (0.92 m), has a very large moment of inertia and can be used as part of a wind-resisting system. The model used for analysis is a Vierendeel truss, where the concrete slab and the bottom steel beam are simulated as linear elements and each stub piece is divided into several vertical elements. The gravity and wind load shear forces and moments are introduced as load cases, and the combined axial forces and moments in each section of the stub girder are obtained. All parts of the stub girder are checked for combined axial forces, shear, and moments as per the AISC and ACI codes. The controlling section for the slab is generally at the end of the first stub piece furthermost from the column. Particular care is required to transfer the moment at the column girder interfaces. In cases where wind moments are small, moment transfer can take place between the slab and the bottom steel beam. The slab needs to be attached to the column either by long deformed wire anchors or by reinforcing bars welded to the column. If deformed anchors are used, reinforcing bars are generally used alongside the studs to transfer the forces past the end of the studs. For relatively large moments, the solution is to extend the first stub piece to the column face. The top flange of the stub piece and the bottom flange of the W14 girder are welded to the column as in a typical moment connection. The design of the connection is, therefore, identical to that of any other beam-and-column moment connection. The girder system should be checked along its full length for the critical combination of gravity and wind load forces. Depending upon the

magnitude of reversal of stresses due to wind load, bracing of the bottom chord may well be necessary.

9.5.4 Strengthening of stub girder. Strengthening of existing stub girders for tenant-imposed higher loads is more expensive than in conventional composite construction. A speculative type of investment building is usually designed for imposed loads of 50 psf (2.4 kN/m^2) plus 20 psf (0.96 kN/m^2) as partition allowance. If the tenant needs higher imposed loads as, for example, for storage or for a library, strengthening of local framing is required. The bottom girder, which is in tension and bending, is relatively easy to reinforce by welding additional plates or angles to the existing steel member. Reinforcing the top chord of the stub girder, which is in compression and bending, is somewhat tricky. Addition of structural steel angles by adding expansion anchors to the underside of metal deck and welding of additional stub pieces to reduce the effective length of compression chord, which acts like a column, have been used in practice with good results. From the point of view of ultimate load behavior, it is acceptable to strengthen the bottom chord to resist to total load without the truss action. However, it is important to check the lateral bracing requirements for the top flange of the continuous bottom chord.

9.6 Composite Columns

Reinforced concrete columns used everyday in concrete building construction can be considered as composite columns under the broad definition of the term because mild steel reinforcement and concrete are, after all, two distinctly different materials. However, the term "composite column" in the building industry is taken to represent a unique form of construction in which structural steel is made to interact compositely with concrete. The structural steel section can be a tubular section filled with structural concrete or it could be a steel wide-flange section used as a core with a concrete surround.

Historically, in a manner somewhat similar to the composite beams, composite columns evolved from the concrete encasement of structural steel shapes primarily intended as fire protection. Although the increase in strength and stiffness of the steel members due to concrete used as fireproofing was intuitively known, it was not until the 1940s that methods to actually incorporate the increases were developed. In fact, in the earlier days the design of the steel column was penalized by considering the weight of concrete as an additional dead load on the steel column. Later developments took account of the increased radius of gyration because of the concrete encasement and allowed for some

reduction in the amount of structural steel. In some earlier designs the concrete encasement was ignored from the viewpoint of strength considerations, but the additional stiffness of concrete was included in calculating the lateral deflections of frame comprising the composite columns.

After the development of sprayed-on contact fireproofing in the 1950s and 1960s, concrete protection of structural steel in the United States was no longer an economical proposition. The high form-work cost of concrete could not be justified as a means of fireproofing and was relegated to special applications requiring resistance to the weather, such as in buildings exposed to salt environment near seacoasts, and for surface toughness, such as parking and loading dock columns required to resist impact of vehicular traffic.

Over the last 15 years or so, the use of encased structural steel columns has found applications in buildings varying from as low as 10 stories to as high as 70-story or even taller buildings. These columns have been incorporated in an overall construction known as the composite system, which has successfully captured the essential advantages normally associated with steel and concrete construction: The speed of steel with the stiffness and moldability of concrete. Concrete columns with very small steel-core columns used as erection columns were perhaps the earliest applications. Later much heavier columns were used, serving the dual purpose for both steel erection and load resistance. The heavier steel columns were used essentially to limit the size of composite vertical elements. With the advent of high-strength concretes, use of larger steel-core columns to make them more space effective may no longer be an overriding consideration.

Another version of composite columns used sparingly in construction consists of exterior columns with a composite steel plate or precast cladding exterior. Yet another version popular in some countries uses laced columns fabricated from light structural shapes such as angles, T sections, and channels. The concrete enclosure provides both fireproofing qualities and also imparts additional stiffness to the light structural shapes, inhibiting their local buckling tendencies. Additional conventional reinforcement can be accommodated in the concrete encasement, as in conventionally reinforced concrete columns.

The ACI building code encompasses the design of all types of composite columns under one unified method using the same general principles as for conventionally reinforced concrete columns. Concrete-filled pipe columns, structural steel cores with or without additional longitudinal reinforcement for design purposes, are considered as composite columns without reference to classifications.

In essence, the ACI procedure is based on an ultimate concrete strain of 0.3 percent with the plane sections remaining plane during bending.

As in conventionally reinforced concrete members, the tensile stress in concrete is disregarded. Either a parabolic or an equivalent uniform concrete strain can be assumed in the compression zone. The axial load assigned to the concrete portion of the composite column is required to be developed by direct bearing through studs, lugs, plates, or reinforcing bars welded to the structural steel plate prior to casting of concrete. In other words, the code requires a positive method for the transfer of axial load between the steel core and the concrete surround for strength calculations. For calculation of stiffness, however, merely wrapping the concrete around the steel core would suffice. Axial loads induced in the concrete section of the composite column due to bending of columns need not be transferred in direct bearing.

Composite columns with longitudinal reinforcements normally make up for a large percentage of the cross section. When such a column is subjected to sustained loads, the load transfer from the concrete to steel due to creep is not a significant factor. Any reduction in the stiffness of the column due to premature yield of steel is negligible. Accordingly, the code stipulates that only the EI of the concrete be reduced for sustained load effects.

A cast-in-place spirally reinforced composite column is rare because of the practical difficulties involved in tying the spirals around an already erected steel core. In cases where it is used, its design is governed by the same procedures as for conventional concrete columns with spiral reinforcement.

Tied composite columns are required to have more lateral ties than needed for ordinary reinforced concrete columns. In fact, the ACI code stipulates twice as many ties, but this is based on somewhat questionable assumptions. First, it assumes that concrete that is laterally contained by the ties is thin. Second, it assumes that the concrete has a tendency to spall out from the smooth faces of the steel core. To prevent this separation, the lateral ties are specified to be vertically spaced no more than half the least dimension of the composite member. The ACI code does not permit the use of longitudinal bars in the evaluation of stiffness of columns on the premise that the longitudinal bars are rendered ineffective because of separation of concrete at high strains. They may, however, be included in the calculation of strength. Finally, the yield strength of the steel core is limited to 52 ksi (359 MPa) to correspond to the yielding strain of concrete of 0.0018.

The practical approach to the design of composite columns is to assume that the steel wide-flange section behaves as a reinforcing steel. With this assumption, interaction diagrams can be generated for various combinations of concrete column size, structural steel shape, and reinforcing steel. Figure 9.16 shows an interaction diagram generated for a 36 by 36-in (915 by 915-mm) column with twelve #18

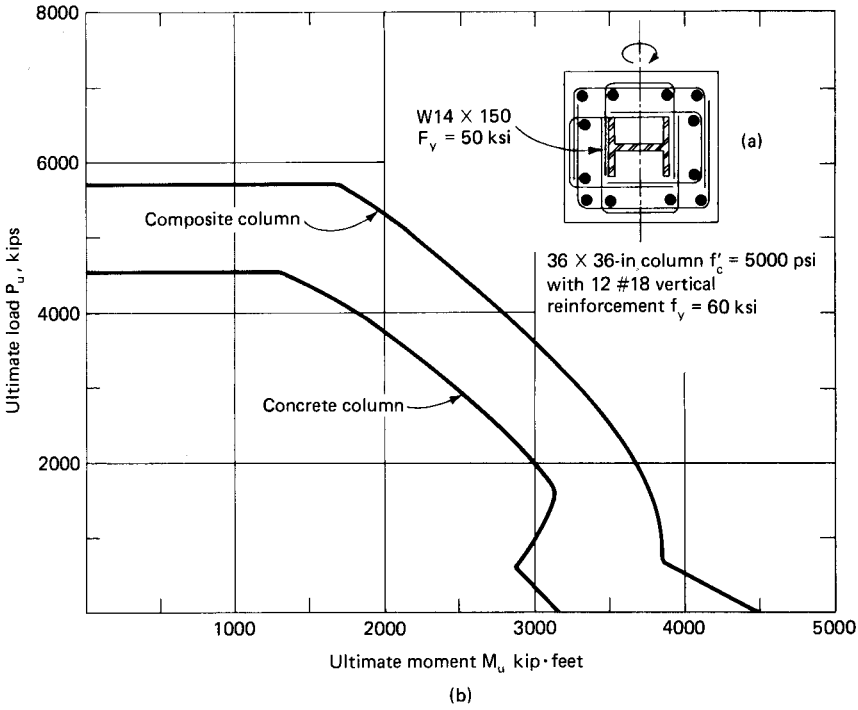

Figure 9.16 Comparison of interaction diagrams. (*a*) Column detail; (*b*) load moment interaction diagram.

(57-mm diameter) reinforcing bars and a heavy, W14 × 150 (378 mm × 394-mm × 2188-N/m) structural steel shape. For comparison purposes, the interaction diagram for the same concrete column without the embedded structural steel shape is given. It can be seen that large increases in column capacity occur when structural steel shapes are added within the envelope of concrete. Construction and detailing aspects of composite columns will not be discussed here since they have been already covered in Chap. 6.

Chapter

10

Structural Analysis and Design

10.1 Introduction

In nature the structures of organisms differ according to their size. For example, the bone structure of a large animal such as an elephant is radically different from that of a dog or mosquito. However, until about the middle of the seventeenth century, scientists believed that it was possible to build larger structures simply by duplicating the form and proportion of a smaller one. The prevailing opinion was that if the ratios between structural elements in the larger structure were made identical to the ratios in the smaller structure, the two structures would behave in a similar manner. In 1638, Galileo refuted this principle by citing examples from animate and inanimate structures, thus formulating the idea of an ultimate size for structures. He clearly recognized the effect of self-weight, or gravity, loads on the efficiency of structures. These principles have since been extended, and engineers have come to recognize that different scales require different types of structures. For example, in the field of bridge engineering it is well known that for maximum efficiency each type of bridge structure has an upper and lower span limit.

The built-up plate girder scheme for a steel bridge structure, for example, may be economical for continuous spans up to about 800 ft (243.8 m), whereas for spans from 1000 to 1200 ft (305 to 366 m) a truss system may be the best solution. Finally, very large spans in the range

of the present maximum of 4200 ft (1,281 m) with predictable limits in the range of 10,000 ft (3,048 m) would require a totally different system, such as a cable suspension structure, to make the project economically feasible. Similarly, structural engineering of tall buildings requires the use of different systems for different building heights. Each system, therefore, has an economical height range, beyond which a different system is required. What these systems and their range are are somewhat imprecise because a lot depends on the demands imposed on the structure. However, a knowledge of different structural systems, their approximate range of application, and the premium that would result in extending their range is almost indispensable for a successful solution of a tall building project because engineers, like other human beings, are creatures of habit with a strong temptation to repeat concepts that were used successfully on earlier, similar projects. This is understandable because not only are the methods of analysis well established but also it makes good business sense. Fortunately, at least in the design of high-rise structures, the engineer is not subject to this boredom and stagnation. Thanks to the architects who are coming up with an array of new forms and daring concepts, building heights are increasing and their slenderness ratios are challenging the engineer. Architects and owners are assisted by a stream of experts who look at the bottom line and who demand more efficient plans with maximum rentable areas. No longer can the engineer get away with proposing one or two structural solutions. Even though the proposed systems may make the most sense from the structural engineering point of view, they may not be the most efficient from the space planning point of view. It will benefit the structural engineer to remember that there are more ways than one to solve a design problem. The engineer should consider it a challenge to look at alternative schemes and to think through a series of conceptual designs that apply existing knowledge to new applications. The engineer should consider the merits and demerits of each scheme not only from structural cost but also the overall sense of the project. During the preliminary stage the engineer should not be overly concerned with the details, but should allow for sufficient load paths in the structure to obey the inescapable laws of nature. Eventually, it will be necessary to subject the concept to analysis—a mathematical technique usually prescribed by detailed regulations contained in the codes. Although there is a temptation to follow the code blindly, limiting the need for making judgment calls, the engineer should be aware that code requirements are decided by a majority vote in a committee. It is likely that the views of a wise member of the committee might not have prevailed. There are risks in blindly following codes or arbitrarily increasing code requirements with the

mistaken assurance that the code is a minimum requirement and anything done beyond its specifications is making the structure better. Analysis is the easy part because today we can analyze almost any structure with computers. Design is the hard part—it is the conceptualization of something that never was.

As compared to a theoretical problem which usually has only one correct answer, a practical problem has more than one solution. It takes experience and a certain amount of knowledge of material costs and construction methods to assert that one design is superior to another. In today's professional environment, the engineer is called upon to complete a piece of design work, usually with limited information and under time and budget pressure. The engineer is required to come up with designs that should be structurally safe, reasonably economical, and most of all practical to build.

Simply defined, structural analysis is a mathematical process by which the engineer verifies the adequacy of the structure with respect to its strength and stiffness. It is not always possible or necessary to obtain rigorous mathematical solutions for building engineering problems. In fact, rigorous analytical solutions can be obtained only for certain simplified cases. High-rise structural problems, like most other practical engineering problems, involve complex material property, loading, and boundary conditions. The engineers introduce assumptions and idealizations deemed necessary to make the problem mathematically manageable, but still capable of providing sufficiently accurate solutions and satisfactory results from the point of view of safety and economy. They establish a link between the real physical system and the mathematically feasible solution by providing an analytical model which is the symbolic designation for the substitute idealized system, including all the assumptions imposed on physical problems. Modeling techniques, therefore, can be defined as a way to reduce, synthesize, and properly represent the structural system.

The basic principles and mathematical relationships used in the design and analysis of tall buildings are not unique to this type of construction. Virtually all of the fundamental relationships are based on the normal assumptions of elastic design which form the backbone of the study of the strength of materials. Although the form of certain relationships is somewhat modified, their application to the analysis and design of high-rise buildings will not impose undue difficulty.

Two major types of problems are encountered by the engineer engaged in the design of tall buildings: (1) review of a set of completed working drawings, and (2) the actual design, starting from the preliminary stages. The review of a completed design consists of the determination of the stresses and deflections under appropriate conditions of loading in order to confirm their compliance with the design criteria

and applicable codes. The strength of a member under all loading conditions, bending, shear, torsion, axial, and bond must be determined to equal or exceed the minimum strength requirements. It should be apparent that in order to review the design, the dimensions and material properties of all structural elements that are used in the makeup of the tall building, together with a knowledge of the loads to which the structure is subjected, must be known.

The task of checking the work of another engineer is done to ensure that the design satisfies the safety requirements as specified in the applicable codes. Although there is no uniform procedure for carrying out this work, a balance must be maintained between checking for safety compliance and the avoidance of malicious damage to the reputation of another engineer. The check should be carried out in a climate of mutual understanding. The checker must recognize that he or she has no duty to comment on the choice of design, only on its validity and its satisfactory compliance with applicable codes. It is a mistake to concentrate on the minute accuracy of the calculations when time can be saved by assessing the soundness of the structure.

The design of a building, on the other hand, consists of selecting and proportioning member sizes in which the stresses do not exceed the permissible values under any combination of loads. The design also includes the study of the deformation characteristics to assure that the building meets applicable serviceability criteria. In common with other types of design, member sizes in a tall building are arrived at from a trial-and-error procedure. In the design of a member, several adjustments of the trial section are normally required before a satisfactory solution is found. Of course, it is just as important to adjust members that are found to be excessively conservative.

At the schematic stages of architectural design, overall options associated with different space forms of the building are thought through with due consideration given to the basic relationship of the building to the available site, environmental conditions, intended use of the building, and other performance criteria. The architectural task at this stage is to organize and orient various space components such as service cores, stairs, elevator cores, and mechanical rooms. These are arranged around the typical floor plan configuration, with the understanding that if it works around a typical floor, it is relatively easy to force the arrangement to work at other nontypical levels. The various components are organized around the typical floor to achieve maximum efficiency, measured in terms of the gross to net leaseable floor space. A structural appraisal is made of the general geometry of the building, especially the height-to-width ratio, function of the structure, whether it is a single-use or multiuse project, whether there is a basement, parking, or other requirements that may necessitate

transfer of large vertical elements, limitations on layout and sizes of structural members, head room and span requirements. The process of preparing structural system alternatives starts simultaneously with due regard to choice of construction materials, availability of building materials, and local workmanship. Generally speaking, the economy of a structure depends to a great extent upon the design criteria and framing layout adopted, but to a far lesser extent upon the detailed design of structural members. Although the decision on the framing may be somewhat subjective, it should have the backing of at least some preliminary economic comparison. While the analytical phase of structural engineering is based on physical sciences, designing remains essentially an art for which knowledge of structural analysis, imagination, judgment, and experience are prerequisites.

It is difficult, if not impossible, to outline the thought process that would go through a structural engineer's mind when he or she conceptualizes the structure at the schematic level. It is very likely that more than one solution may present itself at this stage, and proper guidance to the architect may require knowledge of relative cost and construction procedures on the part of the structural engineer. The point is that one does not really make a lot of calculations or hard-line drawings at this stage, but guides the architect with enough confidence obtained through experience. What is needed is a thorough knowledge of the structural systems to augment the creative thinking of the architect by concentrating on the design evolution of the whole rather than becoming entangled in premature consideration of consequential details of the parts. The key to successful application of structural design ideas at schematic stages of architectural design rests in being able to look at the big picture first without getting bogged down by the details.

Although for optimum results a comprehensive interactive approach between architectural and engineering fields is necessary, there is a growing tendency for the architect to initiate a space-form scheme and then to have the engineer find a way to technically implement the form. This idea appears to stem from the premise that building forms, like pure art, need to be developed without the restriction imposed by engineering disciplines. The results have often been very daring and interesting building forms.

This chapter assumes that the architect has first established the building in conceptual terms, the overall space form, etc. It assumes that feasibility of basic scheme options has been studied, as well as the major subsystem requirements implied by the scheme. In other words, the properties of major subsystems have been worked out, but only enough to verify the inherent compatibility of their basic form relationships and behavioral interaction.

With these assumptions, an attempt is made in this chapter to give

an overview of the basics of structural analysis and design of tall buildings. Preliminary hand calculations that are normally used for evaluating the feasibility of a particular system are considered first; these consist of portal and cantilever methods for determining forces and moments in, and deflection of, building frames. Framed tube structures, which can be considered as equivalent portal frames, are considered next, followed by approximate nonrigorous computer solutions which use lumping techniques (Sec. 10.3) and then by partial computer models in Sec. 10.4. Section 10.5 deals with general computer analysis techniques with a brief description of stiffness analysis procedures. Effects of rigid diaphragm and joints on the results of the analysis are touched upon.

This is followed by discussion of special techniques suitable for the analysis of planar shear walls in Sec. 10.6. Randomly distributed shear walls and planar coupled shear walls which can be analyzed either by modeling them as wide columns or as a system connected by a continuous shear medium are considered, with special emphasis on the determination of effective width of interconnecting slabs. Section 10.7 deals with the essential formulation of finite element techniques for the solution of plane stress problems for shear walls and plate bending problems for slab systems.

Section 10.8 deals at length with the warping behavior of open-section shear walls and interior-braced steel structures. The method presented therein allows an open-section core and its warping action to be analyzed by a computer program. The core structure is considered as a column element with a seventh degree of freedom $d\theta/dz$ at each node to represent warping. The analysis progresses sequentially from particular structural systems with single cores, to twin cores, to multiple cores, and finally to the most general case of a combination of any number of open and planar shear walls. The procedure presented serves as an alternate method for the analysis of shear wall structures without requiring representation of shear walls by finite elements.

Section 10.9 presents a general procedure for capturing the essential behavior of shear wall and floor system by using relatively simple computer programs.

As can be seen, the chapter makes an ambitious attempt to present as wide an analysis field as possible with special reference to warping torsion of open sections. Numerical examples and design recommendations are inserted throughout the text to make the presentation more meaningful, to break the monotony of the theory, and to hold the reader's attention.

The principal aim of the chapter is to strengthen the bond between the analytical and design aspects of tall buildings, and in doing so to provide a concise summary of the basic principles behind the formu-

lation of the analytical problem. It is hoped that by following and understanding this background the designer will be assisted in the task of dealing with the safety and serviceability aspects of tall buildings, and above all by grasping the essentials, the engineer will be better equipped to anticipate problems in novel designs not covered by existing systems.

10.2 Preliminary Hand Calculations

Even in today's high-tech computer-oriented world with all its sophisticated design capability, there still is a need to undertake approximate analysis of structures. First, it provides a basis for selecting preliminary member sizes because the design of a structure, no matter how simple or complex, begins with a tentative selection of members. With the preliminary sizes, an analysis is made to determine if design criteria are met. If not, an analysis of the modified structure is made to improve its agreement with the requirements, and the process is continued until a design is obtained within the limits of acceptability. Starting the process with the best possible selections of members results in a rapid convergence of the iterative process to the desired solution.

Second, because of the ever-increasing cost of labor and building materials, it is almost mandatory for the structural engineer to compare several designs before choosing the one most likely to be the best from the points of view of structural economy and how well it minimizes the premium required by the mechanical, electrical, and curtain wall systems. Of the myriad structural systems which present themselves as possibilities, only two or three schemes may be worthy of further refinement requiring full-blown computer solutions. Approximate methods are all that may be required to logically arrive at cost figures and to sort out the few final contenders from among the innumerable possibilities. It is very time consuming, costly, and indeed unnecessary to undertake a complete sophisticated analysis for all the possible schemes. Preliminary designs are therefore very useful in weeding out the weak solutions.

Sophisticated computer analyses are indispensable in reducing the number of inaccuracies caused by hand analysis techniques and are being used routinely in everyday engineering practice. Although such computer analyses may intimidate the structural engineer by virtue of their unbelievable amount of documentation and output, the prudent engineer will always verify the reasonableness of the computer analysis by using approximate hand-calculated values for forces, moments, and deflections. Approximate analysis is, therefore, a powerful tool in providing the engineer with (1) a basis for preliminary sizing of members, (2) an orderly method for evaluating several schemes to

select the most likely one for further study, and (3) methods for obtaining approximate values of forces, moments, and deflections to check on the validity of the computer solutions.

Having established the need for preliminary analysis techniques, what then are the techniques available for the structural engineer? The techniques are many and range from sophisticated solutions satisfying both compatibility and equilibrium conditions requiring lengthy calculations to simple ones based on considerations of equilibrium alone. The moment distribution technique discovered by Hardy Cross in 1935 is still very popular in the preliminary sizing of continuous beams subjected to gravity loads. Gravity analysis of continuous beams subjected to uniform loads in which hinges are assumed at distances of 0.2 and 0.1 of the spans from the end of interior and exterior bays may be considered as an example of an approximate analysis based on considerations of equilibrium alone. In this section we will consider the analysis of structural systems subjected to lateral loads only, it being assumed that the reader is familiar with approximate methods of gravity analysis.

In the lateral load analysis of buildings, wind and earthquake forces are treated as equivalent static loads and are reduced to a series of horizontal concentrated loads applied to the building at each floor level. Portal and cantilever methods offer quick ways of analysis of a rigid bent with unknown sizes. The idea behind both these methods of analysis is based on the well-observed characteristic of portal frames, namely that the points of contraflexure in beams and columns tend to form near the center of each column and girder segment. For purposes of analysis, the inflection points are assumed to occur exactly at the center of each member.

In the portal method, a wind bent is treated as a series of consecutive single-bay portal frames in the determination of axial stresses in the columns due to overturning effect. Interior columns are considered as part of two such portals, and the direct compression arising from the overturning effect on the leeward column of one portal is offset by the direct tension arising from the overturning effect on the windward column of the adjacent portal. If the widths of different portals are unequal, the distribution of wind shear resisted by each portal can be assumed proportional to the aisle widths to maintain the interior column free of direct stress. Alternately, the column shears can be assumed to be unaffected by aisle widths resulting in axial stresses in the interior columns. With the shears in each column known and the points of contraflexure preestablished, the moments in beams and columns are determined. Simple statics will yield axial and shear forces in beams and columns.

In the cantilever method, as the name implies, the building is

analyzed as a cantilever standing on end fixed at the ground level. The overturning moment is assumed to be resisted by the axial compression of all columns on the leeward side of the neutral axis and tension on all columns on the windward side of the neutral axis. The neutral axis for the cantilever frame is determined as the centroid of the areas of the columns in the bent, and the axial forces in the columns due to overturning are assumed to be proportional to their distances from the neutral axis. As in the portal method, the points of inflection are assumed to occur at midheight of columns and midspan of girders. From the known axial forces in columns and the locations of the points of contraflexure, moments in columns and girders are obtained. These two methods are considered in some detail in the sections that follow. Applications of the methods for manual calculations of deflection of frames and tube structures are illustrated by example problems.

10.2.1 Portal method

In this method it is assumed that (1) points of contraflexure are located at midpoints of girders and columns, and (2) the shear in columns is distributed in a rational manner. Under the second category, some engineers assume that the shear in exterior columns equals one-half the shear in an interior column, while some assume that the shear is distributed in proportion to the tributary bay width. For unequal bays, the former assumption results in direct stresses in the interior columns equal to the difference in girder shears on either side of the column. The latter assumption keeps the interior columns free from direct stresses.

We will now consider the application of the portal method to a 30-story frame shown in Fig. 10.1, consisting of two equal exterior bays and a smaller interior bay. Table 10.1 lists the lateral loads assumed in the analysis. The procedure is as follows. Distribute the accumulated story shears to each column in proportion to the aisle widths to keep the interior columns free of direct stresses. Calculate the moments in the top and bottom of each column as a product of the known shear in the column and one-half the story height. Next, starting at the upper left corner of the frame, write the girder moments where the column and girder moments are the same. Since the points of contraflexure are assumed at the center of girder, the moments at each end are equal but opposite in sign. Determine the girder shears by the relation that shear multiplied by half of span length equals girder end moment. Next the direct stresses at the exterior columns are written directly from girder shears. The results for the example frame are shown in Fig. 10.2.

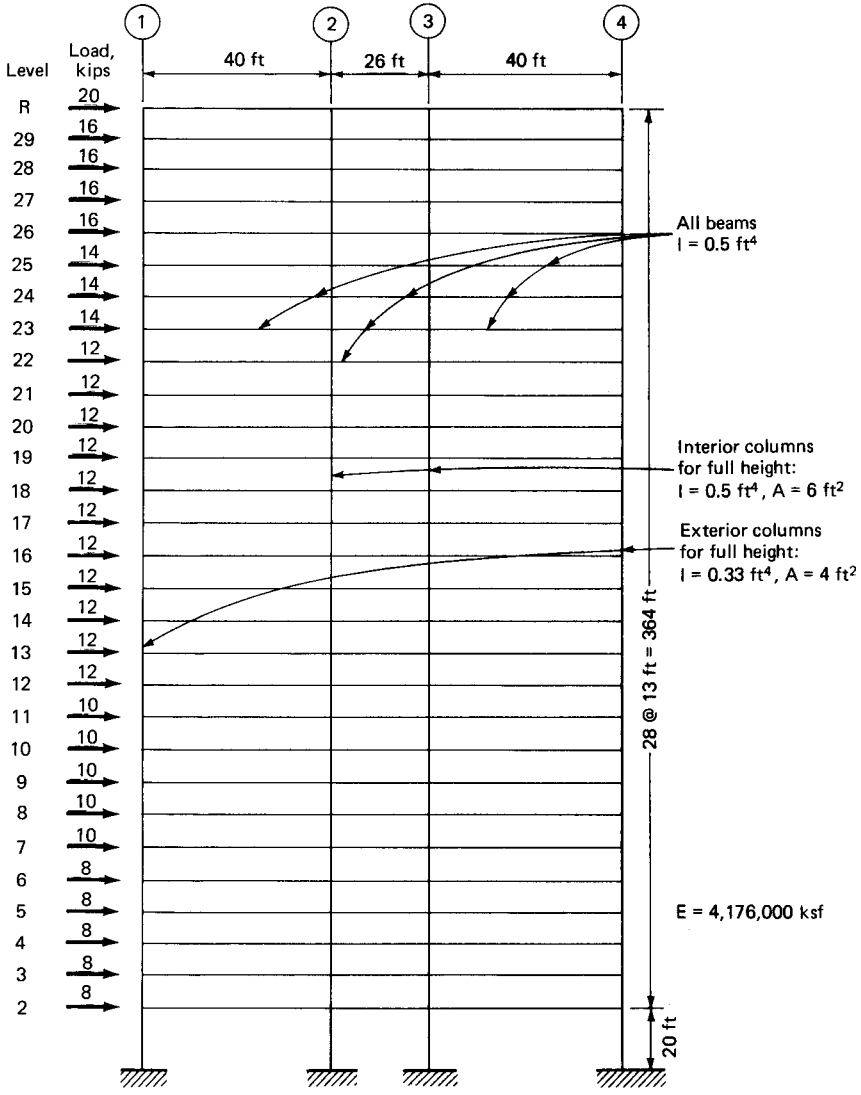

Figure 10.1 Example frame; dimensions and properties.

10.2.2 Cantilever method

The frame analysis for horizontal loads by the so-called cantilever method is obtained by assuming that (1) inflection points, i.e., hinges, form at midspan of each beam and at midheight of each column; and (2) the unit direct stresses in the columns vary as the distance from the frame centroidal axis. It is usually further assumed that all columns in a story are of equal area. In this case the total column forces will vary

TABLE 10.1 Lateral loads for 30-story building shown in Fig. 10.1.

Level	Story shear, kips	Accumulated shear, kips	Level	Story shear, kips	Accumulated shear, kips
R	20	20	15	12	222
29	16	36	14	12	234
28	16	52	13	12	246
27	16	68	12	12	258
26	16	84	11	10	268
25	14	98	10	10	278
24	14	112	9	10	288
23	14	126	8	10	298
22	12	138	7	10	308
21	12	150	6	8	316
20	12	162	5	8	324
19	12	174	4	8	332
18	12	186	3	8	340
17	12	198	2	8	348
16	12	210			

Note: 1 kip = 4.448 kN.

as the distance from the center of gravity of the bent. Using these assumptions the frame is rendered statically determinate and the direct forces, shears, and moments are determined by equilibrium considerations. The application of the method to an example frame will now be considered. To get a comparison with the results of the portal method, we shall apply the cantilever method to the three-bay portal frame (Fig. 10.1) analyzed in the previous section.

The first assumption locates the points of contraflexure. Shown in Fig. 10.3A, part 1 is a free-body diagram of the top story above the points of contraflexure in the columns. The frame axis of rotation is located at the center of gravity of the columns, which for the example problem coincides with the line of symmetry of the frame. The column axial forces for the top story are obtained by equating the moment of the column reactions about the frame axis to the moment of the wind forces taken about a horizontal plane through the assumed hinges of the top floor. These are also shown in Fig. 10.3A, part 1.

In a similar manner the axial forces in the columns of other stories are computed by passing a section through the points of contraflexure of columns of each story and considering the moment equilibrium of the frame above the section (Fig. 10.3A, parts 2–4).

After the column axial forces are found, the girder shears are determined at once. For example, in Fig. 10.3A, part 3, the tension in the exterior windward column at the fifteenth level is 210.72 kips (937.28 kN). Tension in the same column at the fourteenth level is 187.08 kips (832.13 kN). Therefore, by the relation that the summation

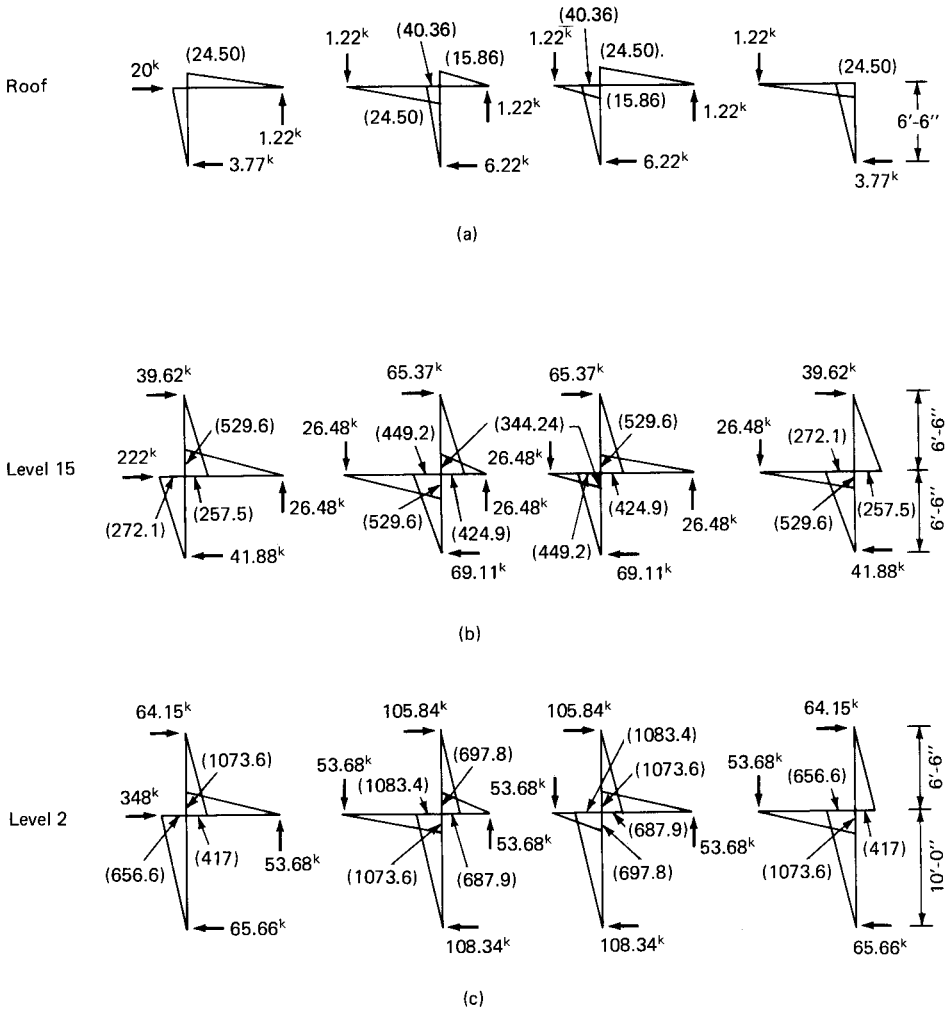

Figure 10.2 Portal method. (*a*) Moments and forces at roof level; (*b*) moments and forces at level 15; (*c*) moments and forces at level 2. *Note:* All moments are in kip·ft and forces in kips.

of the axial forces in the columns and the girder shear is equal to 0 at the joint where the fifteenth-story girder joins the exterior windward column, the girder shear is 210.72 − 187.08 = 23.64 kips (105.15 kN). Figure 10.3A, part 3, shows the method of obtaining this and the remaining shears for the fifteenth-level girder.

With the girder shears known, the girder moments follow directly. These equal the shear in the girder times one-half the span length. The study of the various joints will show that from the relation that $\Sigma M =$

0 at any joint, the sum of column moments must equal the sum of girder moments. Using this principle, the moments in the columns at the roof are obtained from roof girder moments (Fig. 10.3A, part 1). Since the points of contraflexure in the columns are at midheight, the column moments above the 29th level have the same value as at the roof level (Fig. 10.3A, part 2). Moments in the columns below the 29th level are obtained from the relation $\Sigma M = 0$, and in a similar manner column moments in other floors are found. The column shears are obtained by dividing column moments by half the height of columns. As a check, observe that the shear in the columns of any level equals the sum of the horizontal external loads above that level. The moments and forces obtained by using the above procedure for the example problem are shown in Fig. 10.3A.

In order that a feel can be developed for the accuracy of the foregoing approximate procedures, the bent in Fig. 10.1 has been analyzed by a plane-frame computer analysis and the results shown in Fig. 10.3B. As may be expected, the computer results vary considerably from either of the two methods. Chief among the reasons for the discrepancy are (1) points of contraflexure in the lower stories are not at the midpoints, and (2) the shears are greater in exterior girders than in the interior girders of that floor.

Before the advent of computers, it was common practice to use the portal or cantilever method with some modifications for the final design of structures. The modifications consisted of a number of assumptions. Chief among them are:

1. Locate point of contraflexure in exterior girders at 0.55 of their length.
2. Locate the points of contraflexure in the bottom-story columns at 0.6 height from the base, in top-story columns at 0.65 height from the top.
3. Use of rather complicated rules to divide the story shears among columns.

These approximations are no longer popular since the approximate methods are very rarely used in the final analysis of the structures.

10.2.3 Lateral stiffness of frames

The lateral displacement of one floor relative to the floor below results from a combination of bending and shear deformation of the bent. The bending deformation or the chord drift, as it is sometimes called, is a consequence of axial deformation of the columns alone and is independent of the size, type, location, and arrangement of the web system. The shear deformation is due to the rotation of the joints in the frame, which causes bending of columns and girders of the frame. For

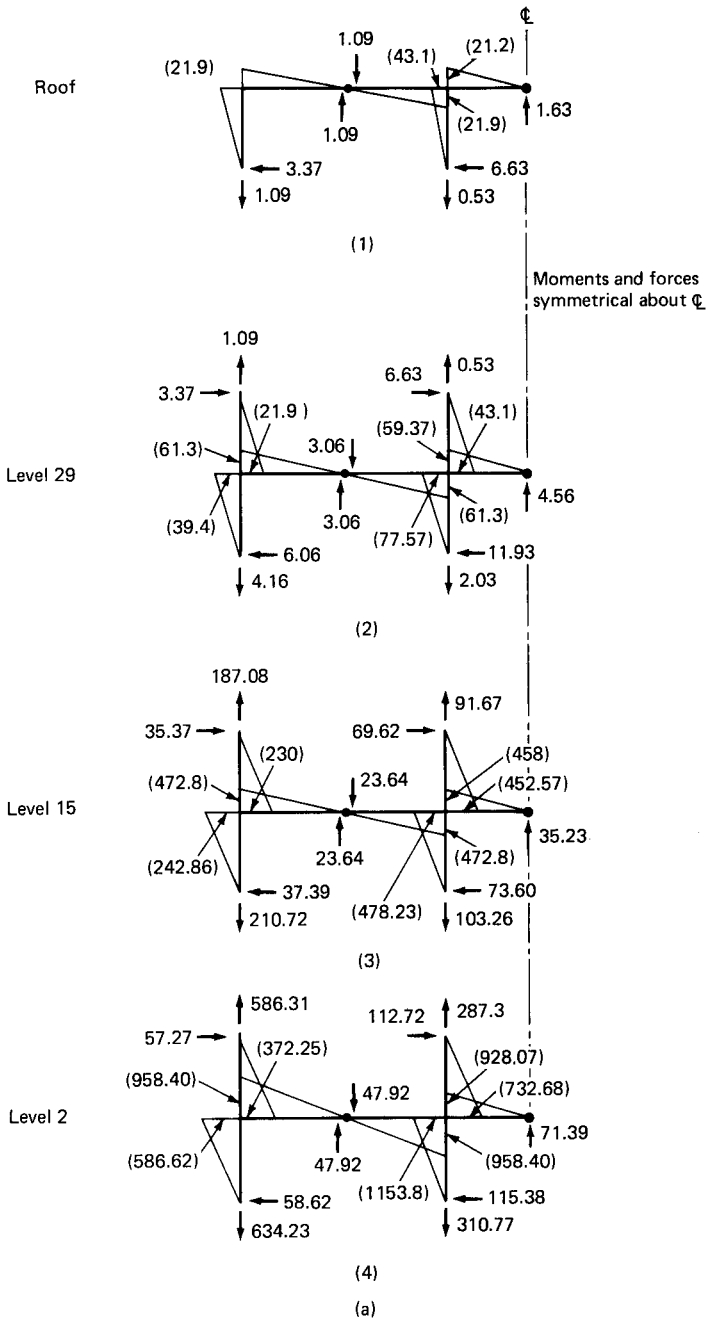

Figure 10.3A Cantilever method. (1) Moments and forces at roof level; (2) moments and forces at level 29; (3) moments and forces at level 15; (4) moments and forces at level 2. *Note:* All moments are in kip·ft and forces in kips.

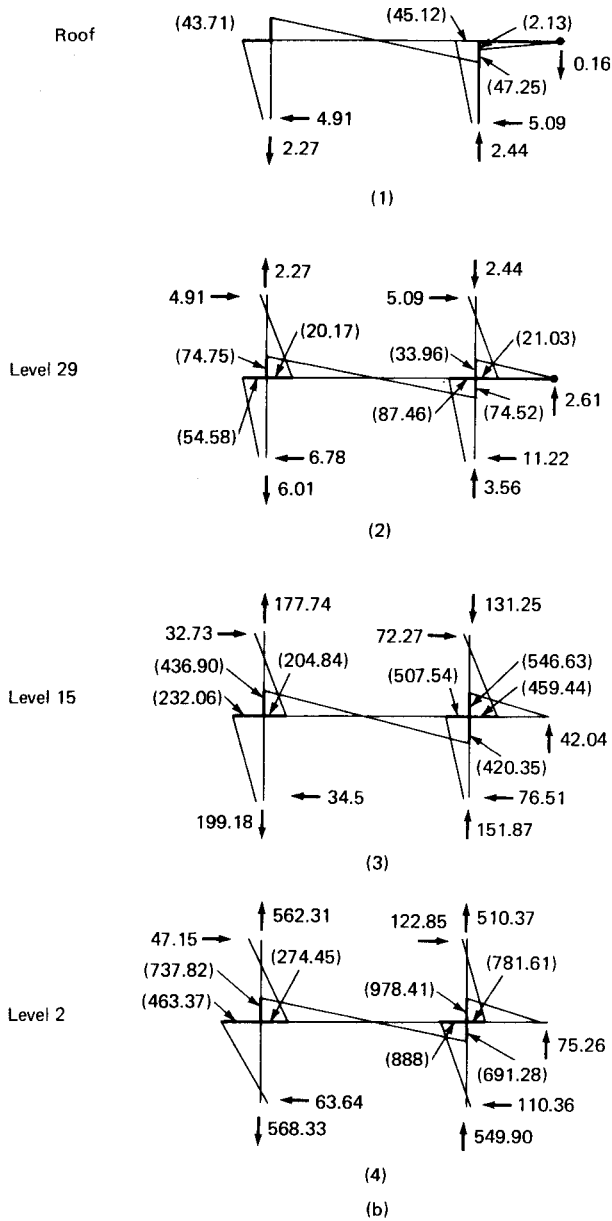

Figure 10.3B Computer elastic analysis: Moments and forces at (1) roof level; (2) level 29; (3) level 15; (4) level 2. *Note:* All moments are in kip·ft and forces are in kips.

relatively short frames with height-to-width ratios less than 3, the deflection due to axial shortening of columns can be neglected and the deflection of the frame can be assumed to be entirely due to joint rotations. Its contribution to deflection can, however, be obtained by considering the frame as a cantilever with an equivalent moment of inertia $I = 2ad^2$ where a is the area of exterior column and d is half the base of the portal frame. For taller frames, it is prudent to consider the axial deformation of the interior columns; the equivalent moment of inertia is determined by the relation $I = \Sigma_1^n a_1 d_1^2$, where $a_1, a_2, \ldots, a_n$ represent the areas of the columns and $d_1, d_2, \ldots, d_n$ represent their corresponding distances from the natural axis of the frame. To derive the equations for the shear deformations, let us consider a portal frame subjected to lateral shear forces as shown in Fig. 10.4. We isolate a representative portion of the frame consisting of a typical floor and column segments between the points of contraflexure above and below the floor as shown in the figure. We will now consider the shear deformation which is due to bending of columns and girders of the representative segment. First we consider the contribution of columns by assuming the girders to be infinitely rigid; then we consider the girder contribution by assuming the columns to be infinitely rigid.

Deflection due to column rotations. Consider the free-body diagram of a typical story bounded between the points of contraflexure in the columns above and below the ith level as shown in Fig. 10.5. When the number of stories is large, it is reasonable to assume that the shears in the columns above and below the floor do not differ appreciably. If the floor girders are rigid, the lateral deflection $\Delta_1/2$ of each column would be equal to the sum of the deflections of the two cantilevers of length $h/2$ under the action of wind shears V (Fig. 10.5).

$$\frac{\Delta_1}{2} = \frac{V\left(\frac{h}{2}\right)^3}{3EI_c} \quad \text{or} \quad \Delta_1 = \frac{Vh^3}{12EI_c} \tag{10.1}$$

giving for all columns $\Delta_1 = Vh^3/12\,E\,\Sigma\,I_c$.

Deflection due to girder rotations. Next consider the columns as rigid, giving rise to rotations of the girders as shown in Fig. 10.6*a*. Each girder undergoes a rotation equal to θ at each end giving rise to an internal moment of $12EI\theta/L$ for each girder. The total internal moment is given by the summation of such terms for each girder. Thus the total internal moment due to girder rotation is $12E\theta\,\Sigma(I_{bi}/L_i)$. The external moment due to wind shears V is given by $V \times h$. Equating external

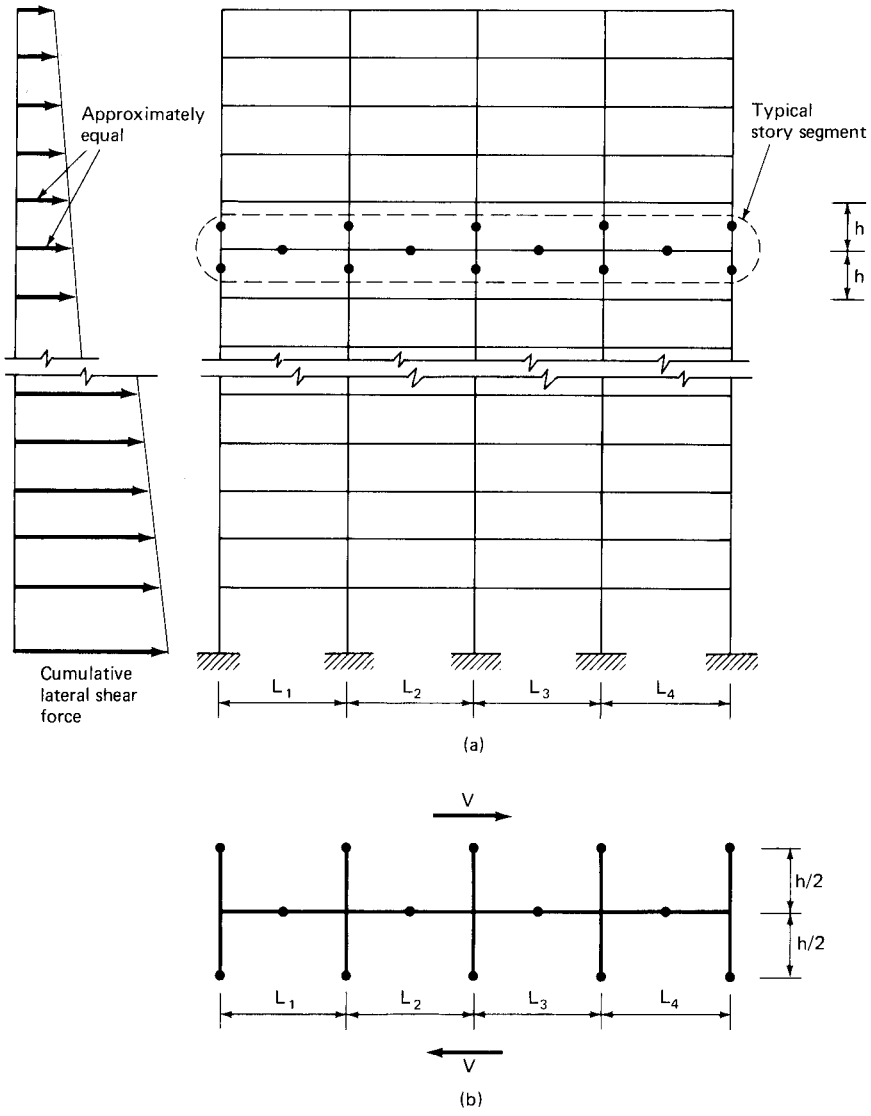

Figure 10.4 Deflection of portal frame. (*a*) Frame subjected to lateral loads; (*b*) typical story segment.

moment to internal moment and noting that θ produces a displacement $\Delta_2 = \theta\, h$, we get

$$\Delta_2 = \frac{Vh^2}{12E\Sigma(I_{bi}/L_i)} \tag{10.2}$$

The total frame shear deflection Δ_s is given by

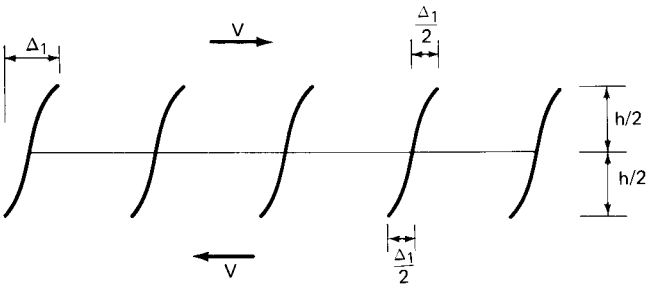

Figure 10.5 Lateral deflection of typical story due to bending of columns.

$$\Delta_s = \Delta_1 + \Delta_2 = \frac{Vh^2}{12}\left\{\frac{h}{(\Sigma EI)_{\text{col}}} + \frac{1}{[\Sigma(EI/L)]_{\text{beam}}}\right\} \tag{10.3}$$

The deflection for the total number of stories is obtained by the summation of the deflections for each story.

An example of deflection calculations using the above procedure follows. To keep the presentation simple, we will consider the same example frame that was used for calculating moment and forces by the portal and cantilever methods (refer back to Fig. 10.1).

Deflection calculations for frame shown in Fig. 10.1.

Cantilever deflection. The neutral axis for the frame lies on the line of symmetry. The moment of inertia of the frame about the neutral axis is given by $I = 2(a_1d_1^2 + a_2d_2^2)$ where a_1 and a_2 are the areas of the exterior and interior columns and d_1 and d_2 their distance from the neutral axis. Substituting $a_1 = 4$ ft^2 and $a_2 = 6$ ft^2, $d_1 = 53$ ft and $d_2 = 13$ ft, we get $I = 2(4 \times 53^2 + 6 \times 13^2) = 24{,}500$ ft^4 (211.46 m^4).

For purposes of deflection calculation, we can assume that the frame is subjected to a uniformly distributed horizontal load = 12/13 = 0.9231*k/ft*. The cantilever deflection at the top is given by

$$\Delta_{\text{cant}} = \frac{wl^4}{8EI} = \frac{0.9231 \times 384^4}{8 \times 4{,}176{,}000 \times 24{,}500} = 0.0245 \text{ ft } (7.47 \text{ mm})$$

Shear deflection due to column rotations. This is given by

$$\Delta_1 = \frac{Vh^3}{12E \Sigma I_c}$$

For the example problem, the moments of inertia for the exterior and interior columns are, respectively, equal to 0.33 ft^4 and 0.5 ft^4, giving

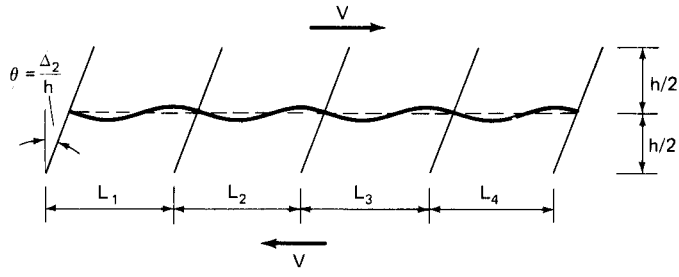

(a)

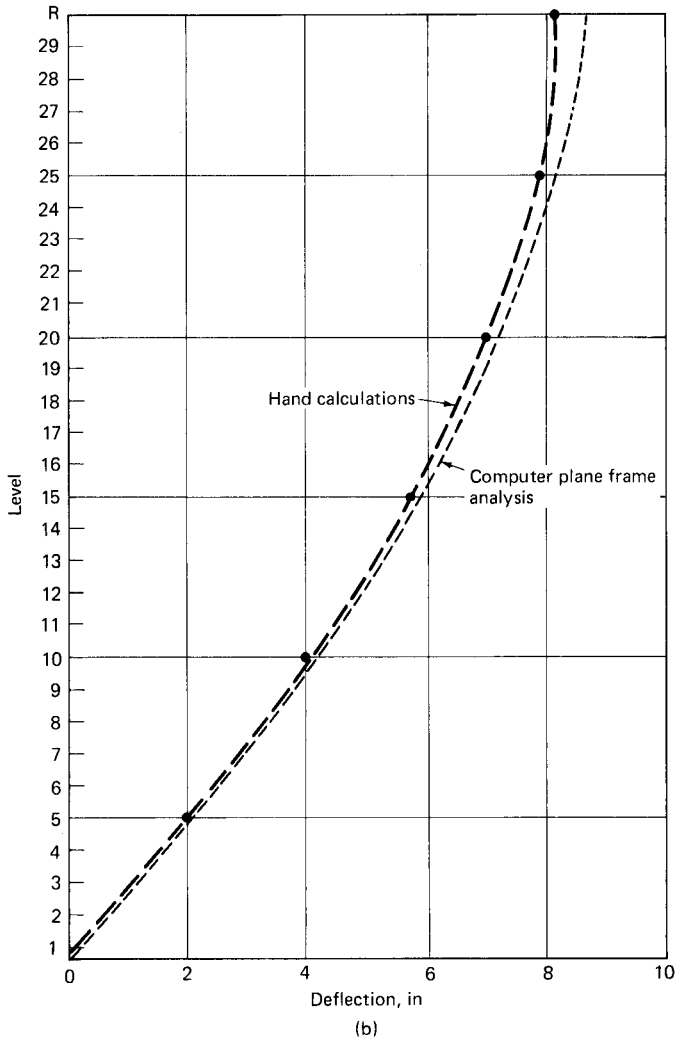

(b)

Figure 10.6 (*a*) Lateral deflection of typical story due to bending of girders; (*b*) deflection comparison (30-story frame).

$\Sigma I_c = 2 \times 0.33 + 2 \times 0.5 = 1.66$ ft^4. Using an average cumulative shear value of $V = 210$ kips and $h = 13$ ft,

$$\Delta_1 = \frac{210 \times 13^3}{12 \times 4{,}176{,}000 \times 1.66} = 0.0056 \text{ ft } (1.70 \text{ mm})$$

Shear deflection due to girder rotations. This is given by

$$\Delta_2 = \frac{Vh^2}{12E\ \Sigma(I/L)}$$

For the example problem, $\Sigma I/L$ of girders = 0.5/40 + 0.5/26 + 0.5/40 = 0.0442 ft, giving

$$\Delta_2 = \frac{210 \times 13^2}{12 \times 4{,}176{,}000 \times 0.0442} = 0.016 \text{ ft/floor } (4.87 \text{ mm/floor})$$

The total shear deflection $\Delta_s = \Delta_1 + \Delta_2 = 0.0056 + 0.016 = 0.0216$ ft/floor (6.58 mm/floor). The shear deflection at top of 30 stories is given by $30 \times 0.0216 = 0.648$ ft. Therefore total deflection at top due to chord drift and shear deformation is 0.0245 + 0.648 = 0.6725 ft (204.97 mm). A comparison of floor-by-floor deflections obtained by using the above approach with those of a computer plane frame analysis is given in Fig. 10.6*b*. The appropriateness of the method for preliminary design is obvious.

Another method with the objective of simplifying the numerical work involved in the calculation of frame deflection consists of representing the columns and beams as a single cantilever column bestowed with an equivalent flexural stiffness of I_e and shear stiffness of A_e to simulate the cantilever and shear modes of bending of the frame. The method is best explained with reference to Fig. 10.7 which shows a 19-story, three-bay unsymmetrical portal frame with columns of varying moments of inertia. We first locate x, the distance of frame axis of bending from the windward column by equating moments of individual column areas to the moment of total area about the windward column. Using the values given in Fig. 10.7, we get,

$$4 \times 30 + 6 \times 50 + 6 \times 90 = (4 + 6 + 6 + 4)\, x$$

giving

$$x = 48 \text{ ft } (14.63 \text{ m})$$

from the windward column.

Calculate the moment of inertia of the frame about its axis of bending by the relation $I = \Sigma\, Ax^2$. Since the areas of the columns change at four locations, the corresponding four values of frame moment of inertia from the top work out equal to 21,120 ft^4, 42,240 ft^4, 63,360 ft^4, and 84,480^4 ft, respectively (182.3 m^4, 364.6 m^4, 546.86 m^4, 729.15 m^4).

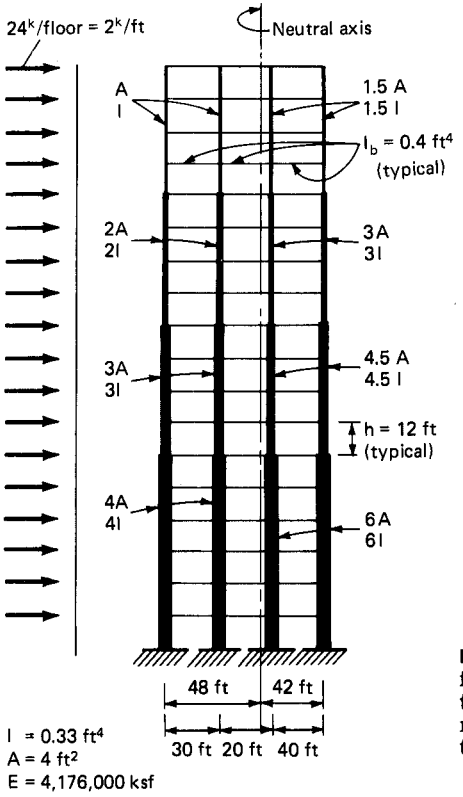

Figure 10.7 Example portal frame for deflection calculations. Note the variation of column areas and moments of inertia at four locations.

Figure 10.8 shows the equivalent cantilever with varying moments of inertia. If the beams were infinitely rigid, the deflection calculated for the cantilever would have represented the total lateral deflection of the frame. Since in reality the beams are flexible, the deflection of the cantilever is increased by the racking component, which is equivalent to the shear deformation of the cantilever. This was shown equal to

$$\Delta_s = \frac{Vh^2}{12}\left[\frac{h}{(EI/h)_{\text{col}}} + \frac{1}{(EI/L)_{\text{beam}}}\right] \tag{10.4}$$

Defining story stiffness as the deflection per unit of horizontal shear, the equivalent story stiffness is given by the relation

$$\frac{V}{\Delta_s} = \frac{12}{h^2\{1/(\Sigma\, EI)_{\text{col}} + 1/[\Sigma(EI/L)]_{\text{beam}}\}} \tag{10.5}$$

An equivalent shear area for the cantilever is worked out as follows. Consider the shear deformation of the cantilever for unit height h

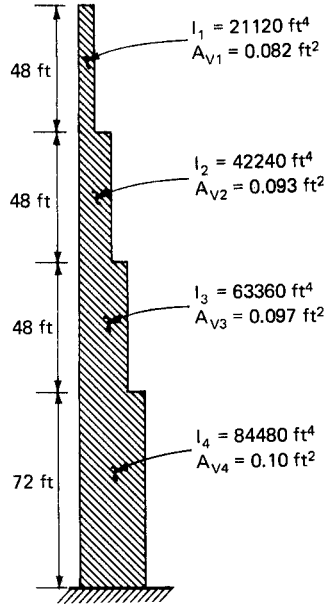

Figure 10.8 Equivalent cantilever representing the portal frame.

subjected to horizontal forces V as shown in Fig. 10.9. The shear deflection Δ_s is given by

$$\Delta_s = \frac{Vh}{GA_v} \tag{10.6}$$

The story stiffness Δ_s/h works out equal to $0.4\,EA_v/h$ in which it is assumed that $G = 0.4E$. Equating story stiffness relations of Eq. (10.5) and (10.6), we get

$$\frac{0.4\,EA_v}{h} = \frac{12}{h^2\{1/(\Sigma E_c I)_{\text{col}} + 1/[\Sigma(E_b I/L)]_{\text{beam}}\}}$$

Assuming E is constant for beams and columns, i.e., $E_c = E_b = E$, we get

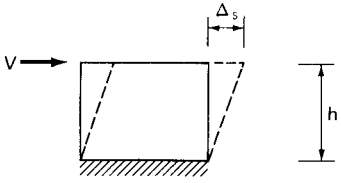

Figure 10.9 Shear deformation of a cantilever of unit height.

$$A_v = \frac{30}{h\{1/(\Sigma I)_{\text{col}} + 1/[\Sigma(I/L)]_{\text{beam}}\}} \tag{10.7}$$

Using the numerical values shown in Fig. 10.7, the equivalent shear areas at four vertical locations work out, respectively, equal to 0.082 ft^2, 0.093 ft^2, 0.097 ft^2, and 0.1 ft^2 (0.0076 m^2, 0.0086 m^2, 0.0090 m^2, 0.0093 m^2) from the top. These values are shown schematically in Fig. 10.8.

The deflection of the equivalent cantilever of varying moment of inertia can be obtained either by long-hand methods such as virtual work or by using a relatively simple stick computer model. In keeping with the approximate nature of analysis, reasonable results can be obtained by assuming average properties for the equivalent cantilever. The average values for I and A for the example problem work out equal to 56,320 ft^4 and 0.093 ft^2 (486 m^4 and 0.0086 m^2), respectively. Using a value of 216 kips for the average cumulative shear V, we get a total top deflection of 0.319 ft (94 mm) as compared to a value of 0.28 ft (82.3 mm) obtained from a stick computer model and a value of 0.24 ft (73 mm) as obtained from a plane frame analysis. Comparison of deflections are shown in Fig. 10.10.

The analysis presented thus far is based on the centerline dimensions, which in general overestimate the deflection. Although all structural members have finite widths, it is unnecessary, especially in view of the approximate nature of the analysis, to be overly concerned about the effect of joint widths on the stiffness of the structure. However, in those cases in which the dimensions of the members are large in comparison to story height and girder spans, it is possible to incorporate the effect of joints by assuming that no member deformation occurs within the joint. An approximate expression for the equivalent shear area for the equivalent column can be shown to be:

$$A_v = \frac{30}{h^2\{h\alpha_1{}^3/(\Sigma I)_{\text{col}} + \alpha_2{}^3/(\Sigma(I/L)]_{\text{beam}}\}} \tag{10.8}$$

where α_1 = the average ratio of clear height to center to center heights of columns (Fig. 10.11)

α_2 = the average of the ratio of the clear span to the centerline spans of girders (Fig. 10.11).

Analytical and experimental investigations have shown that an analysis based on rigid offset lengths to the outer face of supports overestimates the stiffness of the structure. The analysis should therefore include some method for compensating the deformations that do exist in the panel zones. A rigid zone reduction factor can be used to

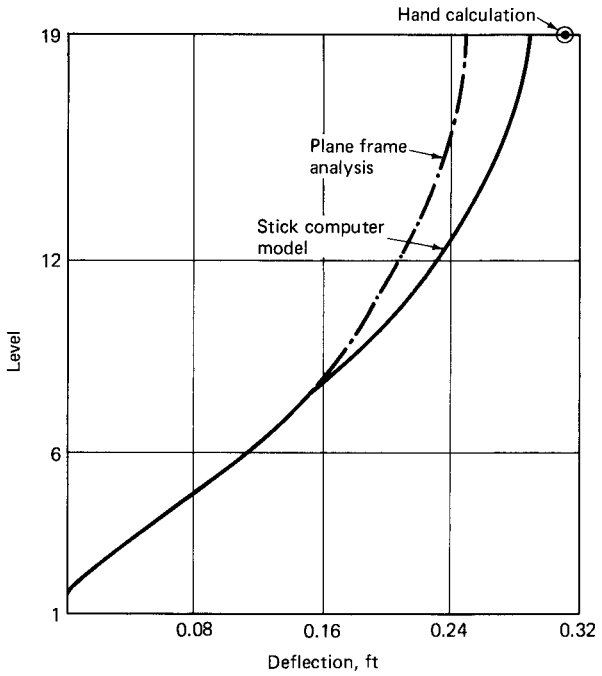

Figure 10.10 Deflection results.

reduce the lengths of rigid offsets—a method similar to that employed in many commercial computer programs. Arbitrary reductions are assigned to joint sizes in an effort to compensate for the joint deformation.

The underlying principle in both the portal and cantilever methods

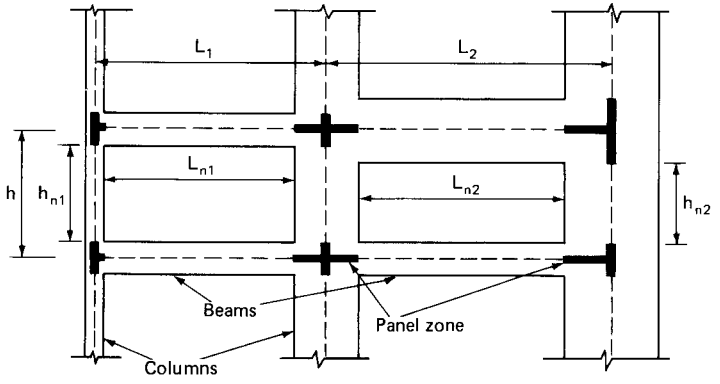

Figure 10.11 Typical beam-column joint with infinitely rigid panel zone.

is the assumption that the point of contraflexure is located at mid-height and midspan of columns and girders. Rigorous computer analyses almost invariably show that the fundamental assumption is violated in various degrees, especially at the top and bottom floors of a tall building. It is possible, however, to improve the results of the approximate analyses by assuming locations for points of contraflexure at locations representative of what is commonly found from computer analysis.

For example, it is fairly well known that the actual points of contraflexure in portal frames at the lower floors, especially at the first story, occur at a location closer to about $h/3$ below the second floor. Expressions for equivalent shear stiffness for the first story can be shown to work out:

$$A_v = \frac{20}{h\{1/(\Sigma\, EI)_{\text{col}} + 1/5[\Sigma(EI/L)_{\text{beam}}]\}} \tag{10.9}$$

Further refinement of the analysis is generally considered unnecessary in view of the approximate nature of the analysis and the availability of computer techniques.

10.2.4 Framed tube structures

As mentioned earlier, the framed tube system in its simplest form consists of closely spaced exterior columns tied at each floor level by relatively deep spandrels. The behavior of the tube is in essence similar to that of a hollow perforated tube. The overturning moment under lateral load is resisted by compression and tension in the columns while the shear is resisted by bending of columns and beams primarily in the two sides of the building parallel to the direction of the lateral load. The bending moments in the beams and columns of these frames, which are called the web frames, can be evaluated using either of the two approximate procedures, namely the portal or the cantilever analysis. It is perhaps more accurate to use the cantilever method because tube systems are predominantly used for very tall buildings in the 40- to 80-story range in which the axial forces in the columns play a dominant role. The moments in spandrels and columns as well as the racking components of the tube deflection can be evaluated by using the cantilever method.

As mentioned earlier, because of the continuity of closely spaced columns and spandrels around the corners of the building, the flange frames are coaxed into resisting the overturning moment. Whether or not all the flange columns, or only a portion thereof, contribute to the bending resistance is a function of shear rigidity of the tube. A device normally used in approximate analysis is to reduce the tube config-

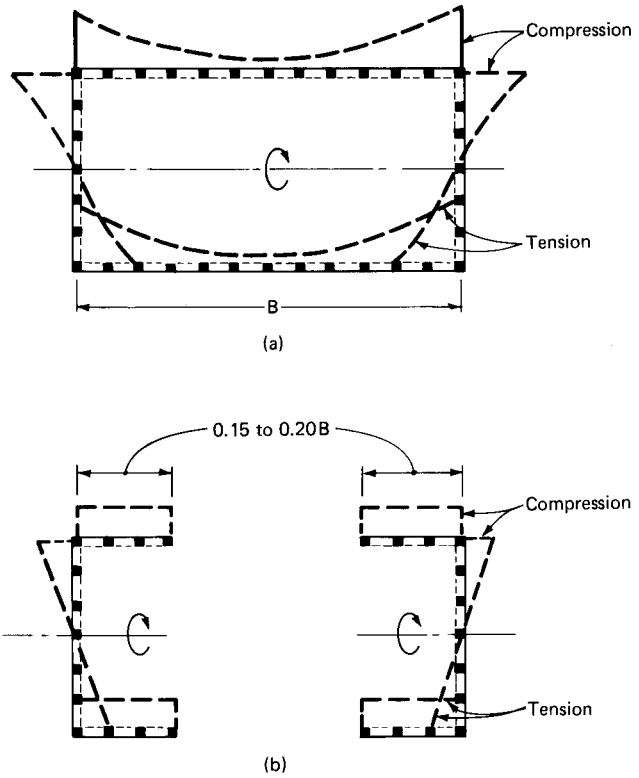

Figure 10.12 Framed tube. (*a*) Axial stress distribution with shear lag effects; (*b*) axial stress distribution in equivalent channels without shear lag effect.

uration into two equivalent channels as shown in Fig. 10.12. The determination of width of channel flange is subjected to engineering judgment and is usually limited to 15 to 20 percent of the width of the building. It is a function of the shear lag across the windward and leeward sides of the tube and the aforementioned rules of thumb give results sufficiently accurate for preliminary sizing of the tube system.

Shown in Fig. 10.13 is the plan of a framed tube system delineating portions of the columns in the leeward and windward sides that were assumed to be part of the equivalent channel flanges. The axial forces were obtained on the basis of equivalent structure, as shown in Fig. 10.13. Shown in Fig. 10.14 are the axial forces obtained from a three-dimensional computer analysis.

An equivalent column approach, as shown in the previous section, can be used to obtain approximate deflection values. In calculating the moment of inertia of the frame it is only necessary to include the

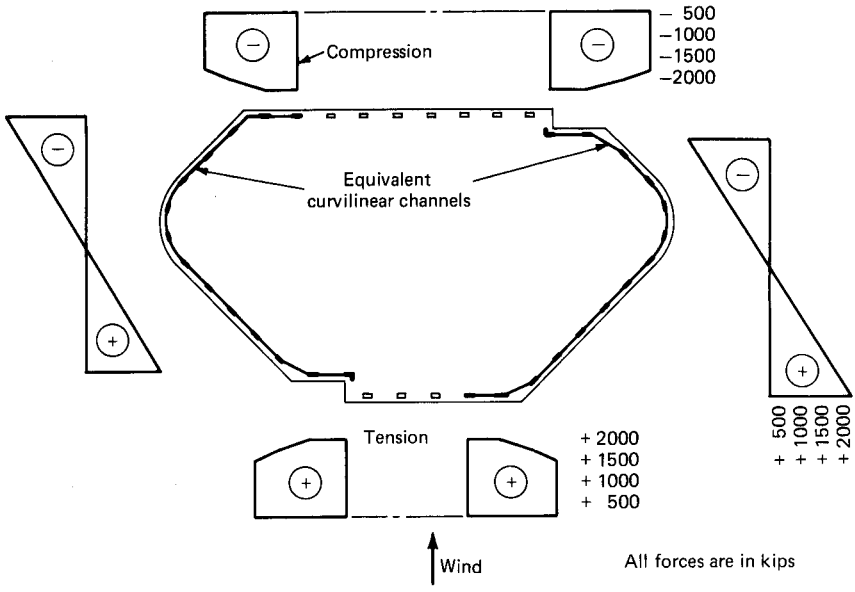

Figure 10.13 Axial forces in columns assuming two equivalent curvilinear channels.

contribution of equivalent flange columns on the windward and leeward sides of the tube.

10.3 Lumping Techniques

Historically, engineers have used lumping techniques to reduce the size of analytical models for computer analysis. The reduction in size was necessitated because, even with large-capacity computers, there just was no economical way of solving very tall buildings with large numbers of joints. Before the academically minded engineer raises his or her eyebrows in surprise, it is well to bear in mind that many notable buildings have been analyzed using lumping techniques and they have been performing successfully over the years. Therefore, although the speed and capacity of modern mainframe computers are so vast as not to require lumping, introduction of desktop computers with relatively less capacity has once again required lumped computer modeling techniques. It is important to realize that as long as the essential features of the building are captured in the model, it makes very little difference whether a lumped or a full model is used for the analysis. Of course, there will be differences between the results of the two models, especially in regard to the stress resultants. The order of magnitude of the differences can even be scary to some engineers, but it is essential to appreciate that similar differences may be encoun-

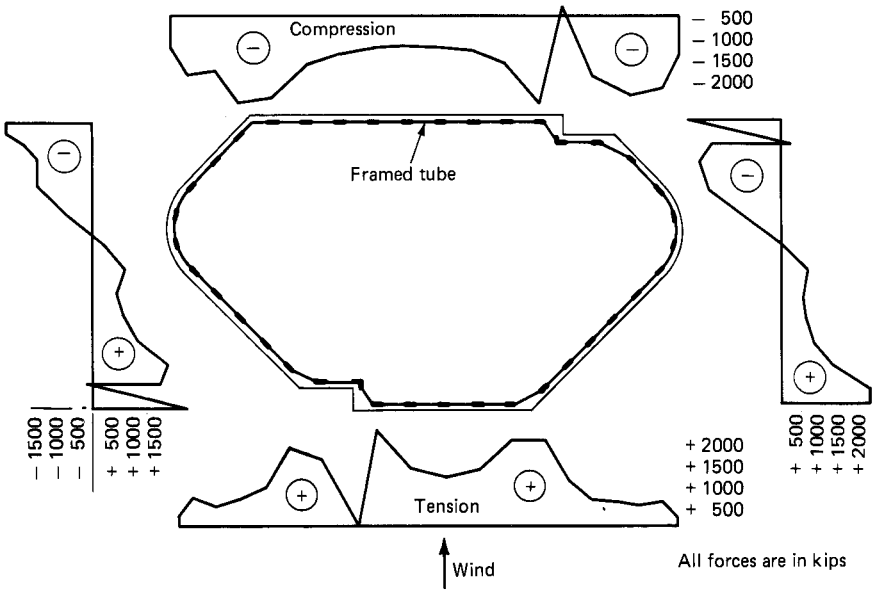

Figure 10.14 Axial forces in columns from three-dimensional analysis of framed tube.

tered, for example, between an analysis that accounts for the flexibility of floor diaphragm, and another that ignores its effect. The intent of the above argument is not to promote indiscriminate use of lumping techniques, but to remind academically minded young engineers that lumping techniques have been and continue to be used as design tools. It goes without saying that a great amount of intuition and judgment are necessary ingredients behind a successful lumping procedure.

Analysis of tall buildings is a highly complex and indeterminate problem. Even with the availability of large-capacity high-speed computers, certain simplifying assumptions are necessary for all but the simplest of structures. In deriving an equivalent structure, engineers have always tried to capture the essential behavior of the actual building. One such behavior commonly observed in rigid frames is that the points of contraflexure occur at the midspan and midheight of beams and columns, respectively. While it is true that in the lower and upper few stories the point of contraflexure does not remain in the midstory or at mid span of beams, in the typical stories which constitute a major portion of a tall building, it is reasonable to assume that the point of inflection is at the midheight and midspan of columns and beams. It is, therefore, possible to lump the typical floors without losing meaningful accuracy. This is explained with reference to Fig. 10.15. The prototype frame, consisting of a 30-story, three-bay frame,

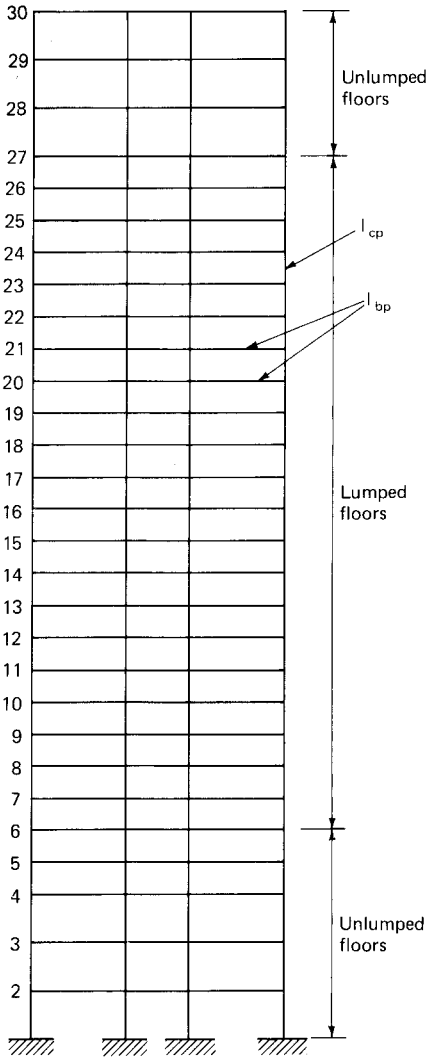

Figure 10.15 Prototype of unlumped frame.

is to be modeled as a lumped frame. Generally, in a high-rise building the floor-to-floor heights at the bottom and top few levels are different from typical floor-to-floor heights. Also as noted before, the points of contraflexure for beams and columns in these floors are at somewhat different locations than for those at typical floors. It makes good sense to limit the lumping to the intermediate typical floors, as shown in Fig. 10.16. For purposes of illustration let us assume that two floors of the prototype are to be considered equivalent to a single floor of the lumped model.

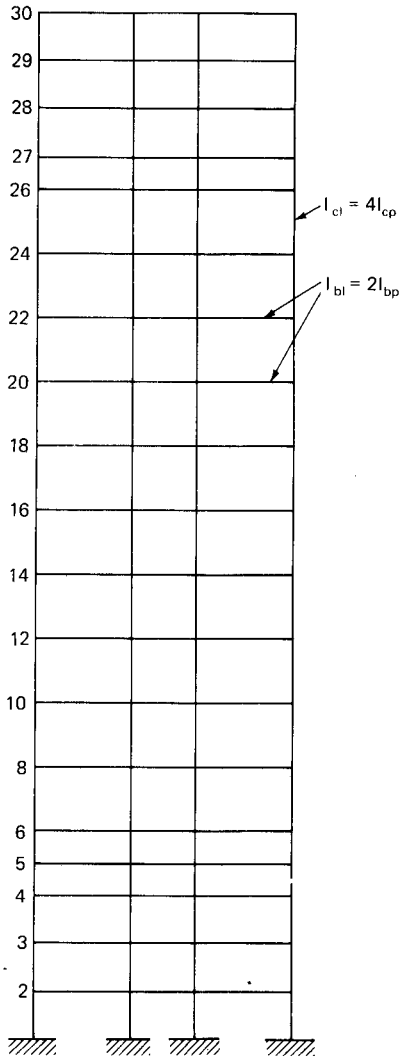

Figure 10.16 Lumped model.

The behavior of a rigid frame, as mentioned many times over, is a combination of the cantilever and shear racking modes. The cantilever behavior is a function of the location and axial stiffness of the columns only and does not depend on the arrangement of beams. Therefore, to maintain the cantilever behavior intact between the prototype and the lumped model, the areas and location of the columns are kept the same in both unlumped and lumped models; the lumped model column occupies the equivalent position of the prototype column with the actual prototype column areas.

The equivalence of the raking component between the two models is maintained by keeping the ratio of column and girder stiffness factors the same between the two. Since two floors of the actual model are lumped into one floor, the moment of inertia and area of the girder in the lumped model should be twice their values in the prototype model. If n floors are lumped into one floor, the corresponding properties will be n times the prototype values. To keep the explanation simple, it is useful to introduce the following notations.

I_{cp} = moment of inertia of column in the unlumped model (prototype)
I_{cl} = moment of inertia of the column in the lumped model
L = length of girder which is the same in both models
h_{cp} = height of column in the unlumped model (prototype)
h_{cl} = height of column in the lumped model

In the present example, two stories are lumped together. Therefore, ratio of $h_{cl}/h_{cp} = 2.0$. In general, this ratio can be considered as n, where n is the model ratio. Equating stiffness ratios of column and beams between the two models gives

$$\frac{I_{cp}/h_{cp}}{I_{bp}/L} = \frac{I_{cl}/h_{cl}}{I_{bl}/L} \tag{10.10}$$

which simplifies to

$$I_{cl} = I_{cp}\left(\frac{h_{cl}}{h_{cp}}\right)\left(\frac{I_{bl}}{I_{bp}}\right) \tag{10.11}$$

Since in the example the ratio of the heights of prototype and model columns is 2.0 and the moment of inertia of the model beam is twice that of the prototype, we get

$$I_{cl} = I_{cp}(2)^2 \tag{10.12}$$

In the general case, the moment of inertia of the lumped model column works out to be n^2 times the prototype value. Lumping of nontypical floors can also be accomplished by assuming locations of point of contraflexure at, say, one-third the height for the lower stories and by using the principle of virtual work to equate the deflection properties. However, since the mathematical expressions get unwieldy, this procedure is not done in general practice.

Discrepancies always exist in all but the simplest of structures between the unlumped and lumped models, especially at regions of abrupt change in stiffnesses and geometry. Although such deviations

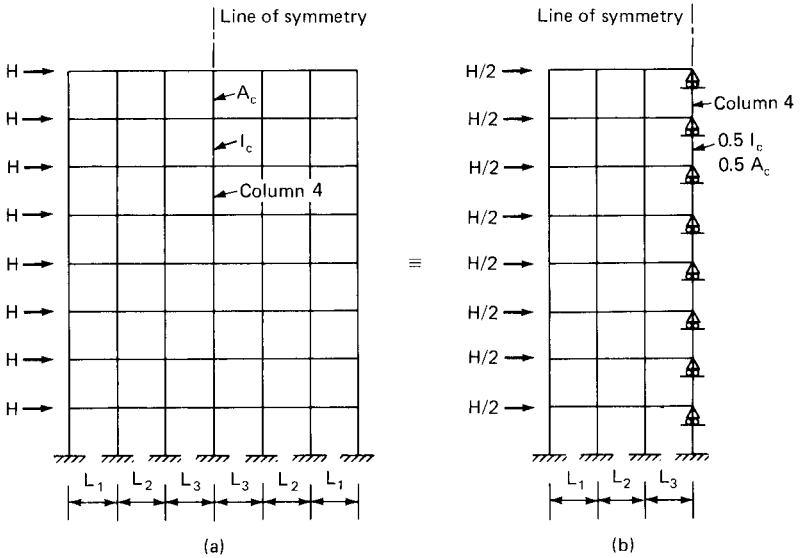

Figure 10.17 Symmetrical frame with even number of bays. (*a*) Full model; (*b*) partial model.

may be high locally, in general the overall behavior is kept unaltered. The application of lumped models to the final design of structures with radically varying member properties, geometry, and abrupt changes in stiffness requires the skilled judgment of the engineer.

10.4 Partial Computer Models

With the advent of microcomputers, which have less storage capacity than mainframe computers, the need to model structures taking into consideration symmetry conditions is once again receiving considerable attention in design offices. Not all buildings, especially those built over the past 10 years, exhibit geometric symmetry, but a considerable number of them can be treated as symmetrical, at least for preliminary assessment of member properties. Modeling techniques using symmetric characteristics of structure are rather elementary, but a brief description is given here to acquaint the beginner with the method.

Consider a plane frame with an even number of bays subjected to lateral loads as shown in Fig. 10.17. The frame is symmetrical about column 4, and therefore computationally it is more efficient to analyze only one-half of the frame. It is only necessary to reduce the geometric properties of column 4 by 50 percent and to introduce appropriate kinematic boundary conditions at the centerline of the column. For the cantilever bending action of the frame due to lateral loads, the neutral axis can be considered to pass through the centerline of column 4. To

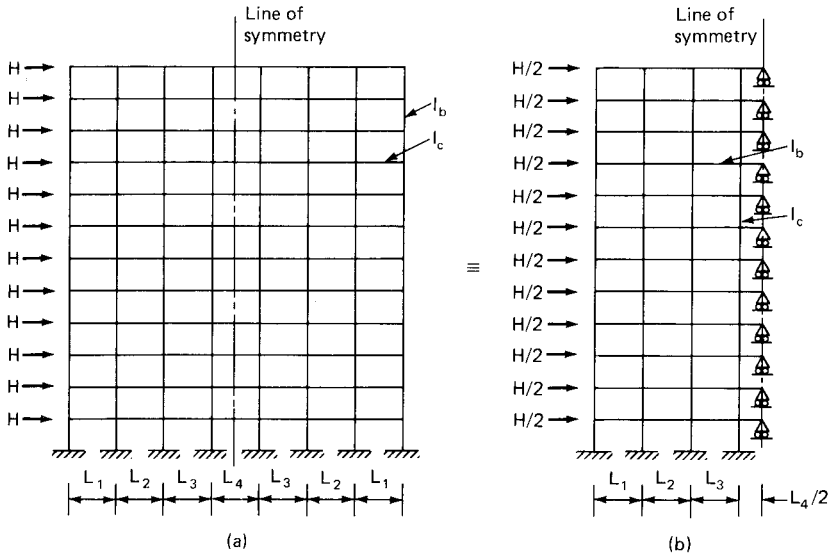

Figure 10.18 Symmetrical frame with odd number of bays. (*a*) Full model; (*b*) partial model.

reproduce this effect in the half model, it is only necessary to restrain the axial deformation of column 4 at each floor. Since only one-half the frame is analyzed, the model is subjected to half the horizontal loads as shown schematically in Fig. 10.17*b*. Other symmetrical structures involving shear walls and braced frames can be analyzed using a similar procedure.

The procedure for analyzing a symmetrical structure with an odd number of bays is similar to the previous procedure and is shown in Figs. 10.18 and 10.19. The only difference is that the neutral axis for frame bending action passes through the center of beam spans. This affect is duplicated in the half model as before by introducing fictitious vertical supports at the midspan of beams. Only one-half of the lateral loads is applied to the model as in the previous cases.

A symmetrical tube structure can be analyzed by considering only a quarter of the model. In addition to the aforementioned boundary conditions, it is necessary to assure that the three-dimensional model does not twist due to the application of horizontal loads.

A tube is a three-dimensional structure, and as such responds by bending about both its principle axes and rotation about a vertical axis. In analyzing a quarter or half model, it is necessary to restrain the transverse bending and rotation of the tube. The kinematic restraints that preclude transverse movement and rotation of the model are shown in Fig. 10.19.

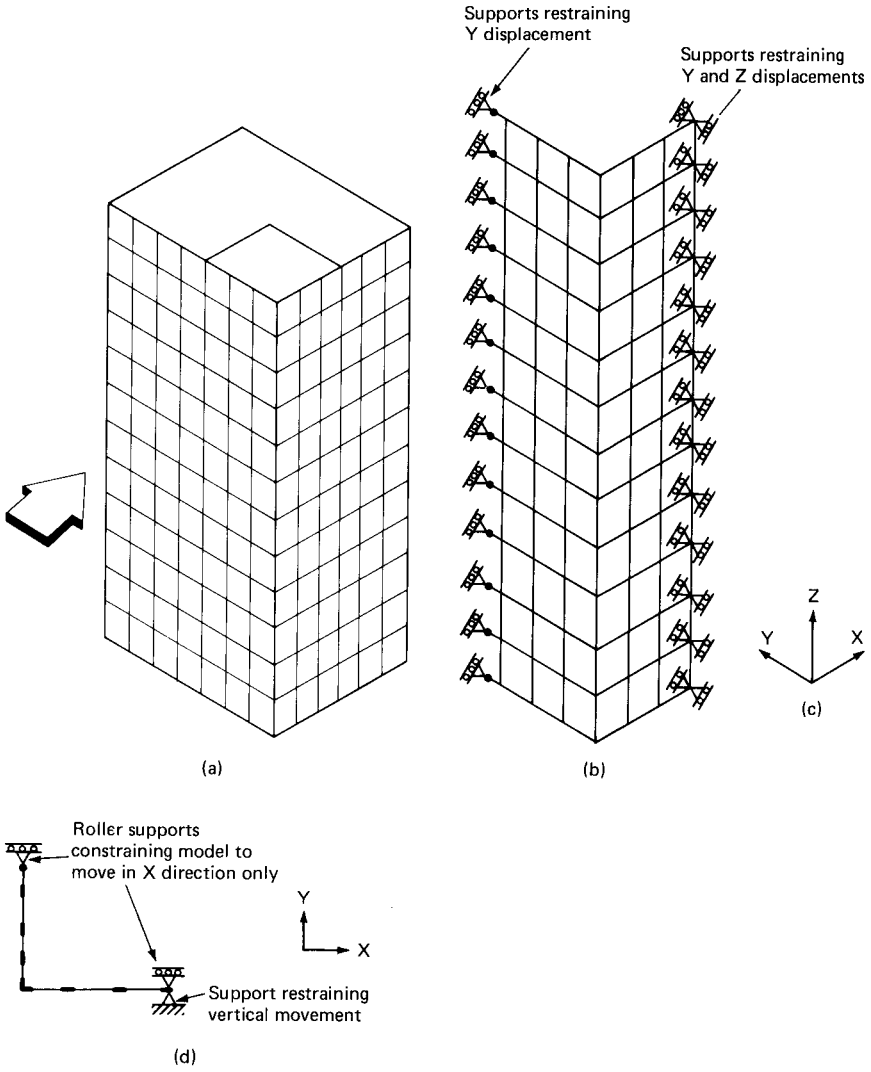

Figure 10.19 Partial analytical model for framed tube. (*a*) Full tube model; (*b*) partial model; (*c*) coordinate axes system; (*d*) plan of partial model.

10.5 General Computer Analysis Techniques

Today the availability of large-capacity computer programs capable of providing static and dynamic solutions of linear elastic structures is overwhelming. Numerous programs are made available by commercial networks to provide "exact" analyses of large-scale buildings.

Linear elastic analyses of two- or three-dimensional structures are achieved by modeling prototype structures as assemblages of line members and panels. The line members may have axial, flexural, shearing, and torsional properties, while the panels may carry in-plane direct and shear stresses in addition to out-of-plane stress resultants. The analysis method employed is a matrix formulation of the stiffness or displacement type. In a general three-dimensional program, the coefficients which relate the applied loading to six generalized displacements at the joint are calculated, and a set of linear simultaneous equations is set up for each loading. Solutions of these equations result in the displacements of the joints, which are then used to calculate internal loads and stresses in the structural elements. Most available computer programs enable the engineer to specify characteristics of problems, perform analyses, reduce and combine results, and output any information stored within the system. Some programs also include member design capabilities according to certain specifications. Analytical solutions can be obtained for both framed structures and continuous mechanics problems. High-rise buildings are mostly analyzed as two- or three-dimensional structures composed of relatively slender linear members which can be mathematically represented by properties along a centroidal axis. Surface systems such as slabs and walls are treated as an assemblage of finite elements in some special problems. Many programs allow for mixing of different element types and are useful in idealizing problems of complex shape. External influences which may result from forces, temperature effects, and fabrication errors can be considered in the design.

Generation options are available for convenience of inputting large amounts of data. Many programs have plotting capabilities for the undeformed and deformed shape of the structure for verification of the model geometry and the structural behavior of the system. The library of elements consists of elements from the basic linear element to the most sophisticated three-dimensional elements. Boundary elements in the form of spring supports can be incorporated. Loading options include gravity, thermal, and prestress conditions in addition to the usual nodal loading consisting of either specified forces or displacements.

Among the dynamic analysis options, two of the most useful ones are eigenvalue analysis and response spectrum analysis. Seismic analysis by the response spectrum approach requires the undamped free vibration mode shapes and frequencies of the system. The response spectrum analysis is obtained by solving the dynamic equilibrium equations by using the modal superposition method.

Data preparation involves defining the basic geometric dimensions of the structure by establishing joints or nodes on the structure. The

physical behavior of the structure is imparted to the model by connecting the nodes with structural elements. The model geometry in the most general case is defined in a three-dimensional global coordinate system. Although in some programs translational and rotational springs may be introduced to elastically restrain any and all the six degrees of freedom, in high-rise building analysis applications it is more useful to have an option that facilitates elastic restraint for the whole building. For example, the elastic restraint of the basement wall in resisting the lateral displacements and rotations at the ground level can be conveniently represented by restraining that level with elastic springs.

The stiffness analysis procedure in computer analysis is a linear, elastic small displacement analysis using the well-known displacement procedure. In some structures introduction of hinges, rollers, etc., makes certain force components zero. The user can specify releases to provide this capability in most programs. Most programs assume prismatic members with symmetric and uniform cross section. Members with varying cross sections are described by specifying rigid joints at points of section change.

A brief outline of the theoretical basis and the method of analysis fundamental to direct stiffness analysis program is as follows. As the first step, the actual system is idealized as an assemblage of discrete structural members interconnected at a finite number of joints called *nodes*. The structure is idealized in such a way as to retain the essential response of the real system.

Next, the member stiffness relations between coordinates and joint forces are set up. Individual member stiffnesses are most usually derived in a coordinate system that is intrinsic to the member itself such as the longitudinal axis of the beam and the axis of principal moments of inertia. For purposes of adding the individual member contribution to the equilibrium equations governing the complete structural system, it is convenient to express the member equations in a set of coordinates that is common to all members in the system. This coordinate system is called the global coordinate system and is also used to define the joint coordinates of the structure. After this transformation, the formation of complete structural stiffness matrix proceeds using direct addition at each joint in the system. The resulting set of equations, appropriately modified for displacement boundary conditions, represents the global equilibrium equations for the discretized structure. The solution of the equilibrium equations results in displacement components at each joint arising from the loads applied to the system. The internal stresses are calculated for each member from the displacement and member stiffness of each member.

In its simplest terms, computer modeling of high-rise buildings

consists of an assemblage of vertical frame systems interconnected by horizontal floor members. The vertical frames may consist of braced frames, shear walls, etc. The effects of bending, axial, and shear deformations are included in the stiffness formulations. Most usually the columns are assumed to be supported at the foundation by nonyielding supports. However, there may be conditions requiring consideration of the vertical and rotational flexibility of the foundation system. A method that is convenient for this purpose is the creation of a hypothetical column below the foundation of the building. By manipulating the stiffness properties of the hypothetical column, it is possible to simulate the desired restraint conditions of the foundation.

Lateral analysis of structures is most usually based on the assumption that floor slabs are rigid diaphragms, thus reducing the computational effort required to solve a three-dimensional model, especially in dynamic analysis, wherein the dynamic degrees of freedom are reduced to a maximum of three per floor. This assumption is generally valid for most buildings, more so for buildings with conventional moment frames. However, the validity of the assumption is somewhat questionable for narrow buildings and for buildings with lateral resisting elements whose stiffnesses are very nearly equal to the stiffness of the floor slab itself. In such buildings the flexibility of the slab significantly affects the lateral distribution of forces among the various lateral-load-resisting elements, making it different from the distribution derived from the rigid diaphragm assumption. The effect is very pronounced in irregularly shaped buildings with major discontinuity in lateral-load-resisting elements or with diaphragms carrying major shear transfers. It is prudent in the analysis of such buildings to study the effect of flexible diaphragm to smooth out sharp shear transfers and to eliminate obviously invalid results. Thus great care and engineering judgment are warranted in applying one of the most common analysis assumptions made today.

A structure in general is composed of frames and walls disposed in a manner most efficient from leasing considerations and is, therefore, subjected to three-dimensional behavior as a whole, even though the frames and walls are two-dimensional by themselves. Any form of asymmetry either in the structural disposition or the external loading results in torsion, generating considerable interaction between the various elements. Only a complete three-dimensional analysis is capable of accurately predicting the behavior of such systems.

Although engineers have recognized for a long time that structural members have finite dimensions, before the advent of the tube system with its rhythm of closely spaced columns and deep spandrel beams, it mattered very little if the centerline dimensions of the beams and

columns were used in the formulation of element stiffnesses. With the increased use of deep spandrels and closely spaced columns, an analysis based on centerline dimensions of members can overestimate the deflections to such an extent as to rule out certain systems that would have otherwise worked had the rigidity of the joint been taken into account. Current programs give an option to the engineer to formulate the stiffness of members by using clear heights and spans. However, since no joint is perfectly rigid, many programs attempt to simulate the panel deformation characteristics of joints by arbitrarily considering only a certain portion of the joint to be rigid.

10.6 Special Techniques for Planar Shear Walls

Shear wall systems are now widely accepted as a rational and economical part of multistory construction. Although often a matter of choice for buildings up to 15 or 20 stories, for taller nontubular buildings the use of shear walls in one form or another becomes necessary for economic reasons. It would be futile to attempt to classify all the current shear wall structural concepts into distinct categories because of the innumerable variations that are possible with these systems. Instead, this section attempts to summarize the behavior of planar forms of shear walls starting with the most elementary system to interconnected combinations that are encountered in practice.

Randomly distributed shear walls are considered first, followed by a detail treatment of coupled shear walls. Two methods, (1) the continuous medium technique which is suitable for hand calculations, and (2) the wide-column analogy suitable for computer formulations, are considered. The concept of effective width of interconnecting slab and its determination by finite element techniques are discussed. Suggestions are made for idealizing practical problems using commercially available standard computer programs. Design recommendations are touched on where appropriate.

10.6.1 Randomly distributed planar shear walls

The most elementary shape in which a shear wall is employed in a tall building is a planar shear wall without openings. The layout of such shapes may vary from a simple orthogonal orientation, requiring only hand calculations for determining the distribution of wind shears, to a random distribution necessitating a three-dimensional analysis. In either case the behavior of the shear wall is essentially similar to a deep, slender cantilever beam. The calculation of stresses and deflection in a single shear wall without openings involves simple bending

theory only. The distribution of lateral forces among individual walls is best accomplished by a three-dimensional computer analysis to account for changes in wall thickness and different wall orientations that normally occur in practice. Commercially available computer programs that consider the floor system as a rigid diaphragm are excellent for this purpose and are being used as an everyday tool in design offices. Figure 10.20 shows a plan layout that is best analyzed by using a three-dimensional computer analysis to obtain the distribution of wind moments in the walls. The selection of reinforcement in shear walls subjected to bending moment and axial loads can be approached in three ways. One method, as shown in Fig. 10.20*b*, is to obtain an elastic stress distribution in the wall, assuming that the total length of wall contributes in resisting the bending stresses. The distribution of axial stresses (tension and compression) are obtained by superposition of wind and gravity loads for the three ultimate load combinations as specified in the ACI code. The next step is to divide the shear wall into small segments and design each segment as a column, if the controlling stress is compression, or as a tie member if tension controls. This procedure yields an even distribution of reinforcement for the full length of wall, but may require placement of confining ties around the vertical reinforcement in a large portion of wall. Another method is to assume that the overturning moment is resisted by finite lengths of wall located at the extremities and to design reinforcement in these zones to carry the axial forces. This procedure yields somewhat heavy reinforcement at the ends, which may require the use of bundled bars and mechanical splices. Because the intermediate section of wall between these zones is minimally reinforced requiring no confining ties, this approach is sometimes preferred from the detailing point of view.

The third approach is to obtain the reinforcement directly for a given set of ultimate axial load and moment capacities, as is normally done in the design of columns. A direct solution of vertical reinforcement for given values of moment and axial loads is too cumbersome to attempt manually because of the considerable complexity of behavior of eccentrically loaded shear walls. This behavior ranges from concentric compression to the other extreme of simple bending without any axial loads. Between these two ranges the behavior varies considerably, depending on whether crushing of concrete or yielding of reinforcement controls the design. However, it is relatively easy to determine the possible load combinations for given arrangements and amounts of reinforcement, particularly with the aid of computers. The results of such an interaction diagram for compression versus bending can then be used to select the required reinforcement at any level along the full height of the wall.

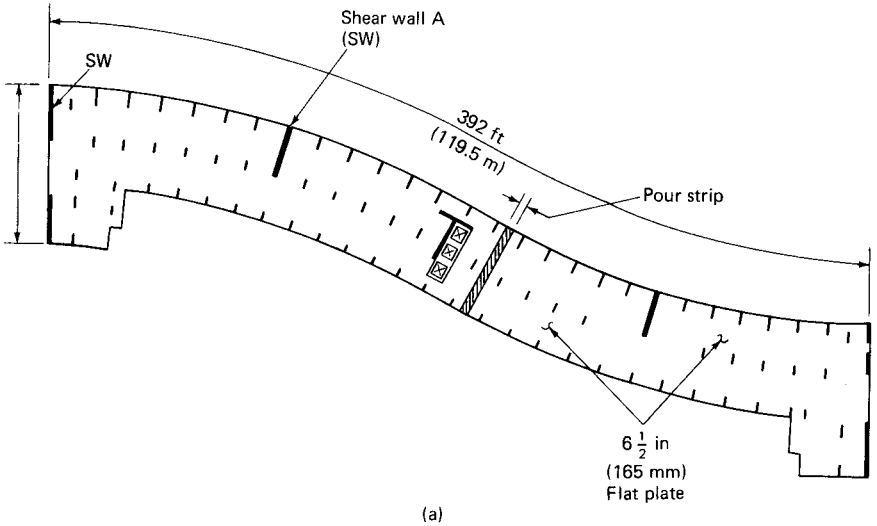

(a)

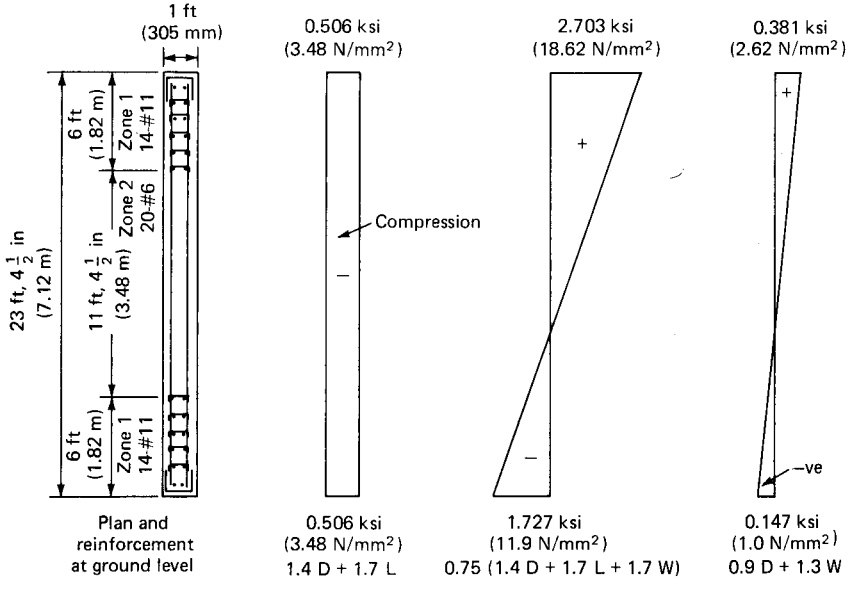

Note: #11 bar = 35.8 mm dia.
6 bar = 19.05 mm dia.

(b)

Figure 10.20 Twelve-story condominium project example. (*a*) Typical floor plan; (*b*) axial stresses in shear wall *A*.

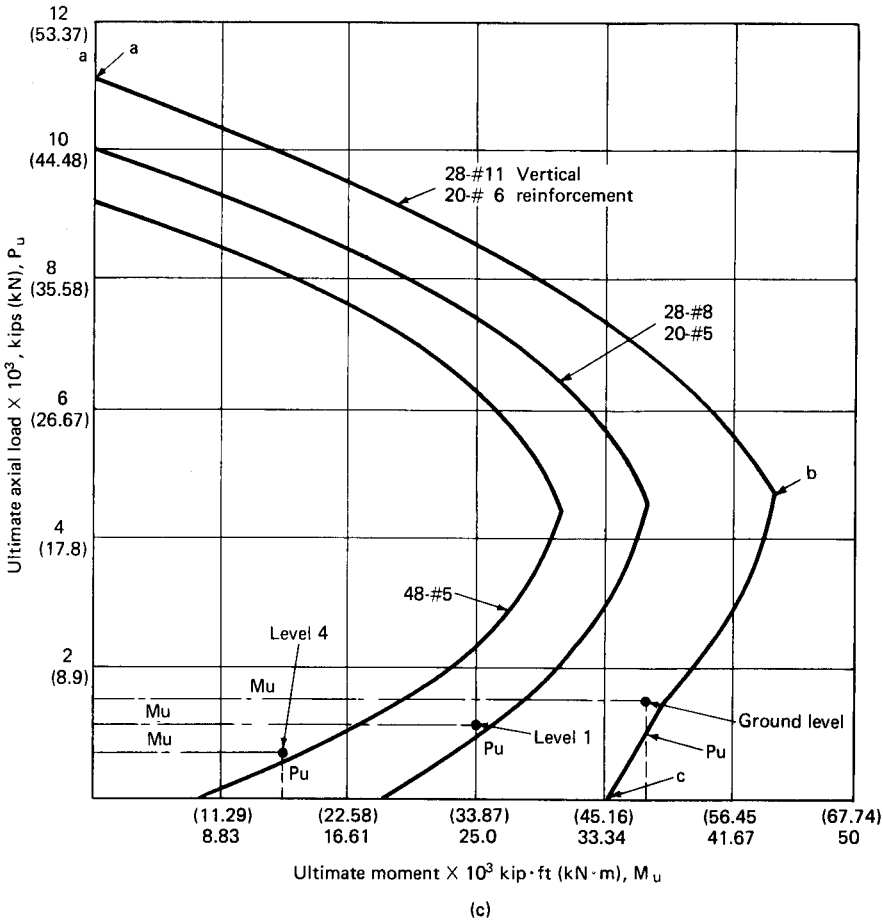

(c)

Figure 10.20 *(Continued).* (*c*) Interaction diagram for shear wall A for different vertical reinforcement.

For a given rectangular cross section and reinforcement, an interaction diagram has the general shape shown in Fig. 10.20*c* plotted with ultimate axial loads on the ordinate and ultimate moments on the abscissa. Any point on the curve represents a pair of values P_u and M_u, corresponding to the ultimate axial load and moment which, according to the ultimate theory, are just large enough to cause the member to fail.

The point A on the curve represents the value for concentric ultimate axial load. The portion AB is the range in which failure is initiated by crushing of concrete. The point B corresponds to the balanced condition at which the concrete will reach the limiting strain of 0.003 while the steel in the tension side simultaneously reaches its yield stress. The portion BC represents the range in which the failure

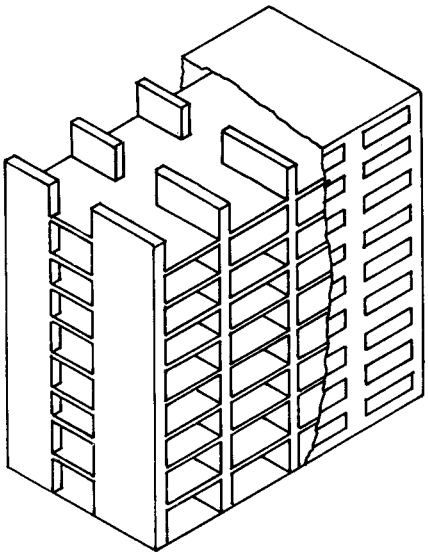

Figure 10.21 Shear wall–slab structure.

is initiated by the yielding of tension steel. Note that in this region, the larger the axial load, the larger the moment capacity, quite the reverse to the behavior in the region AB. Finally, the endpoint C refers to the moment capacity of the members in simple bending.

The vertical reinforcement in the tensile zone of shear walls requires larger lap lengths or other mechanical splices to transfer the tensile stresses, which are more expensive than conventional compressive splices.

Therefore, an ideal situation is to size the shear wall such that little or no tensile forces are developed or to limit the tension force to the tension capacity of compression lap splices. This is very seldom achieved in practice because usually the length of wall is limited for architectural reasons, and it is not always possible to induce a great amount of gravity load into walls. Tensile stresses per se are not a problem as long as the foundation is designed for uplift forces and the laps or other mechanical splices in the reinforcement are able to develop tensile forces.

10.6.2 Coupled shear walls

Frequently, vertical rows of doors or windows occur within the shear wall, dividing it into two walls coupled by beams at each floor. This is usually referred to as a coupled shear wall. Another system popular in apartment and hotel buildings in the 20- to 30-story range is the cross-wall system. This system, as shown in Fig. 10.21, consists of a

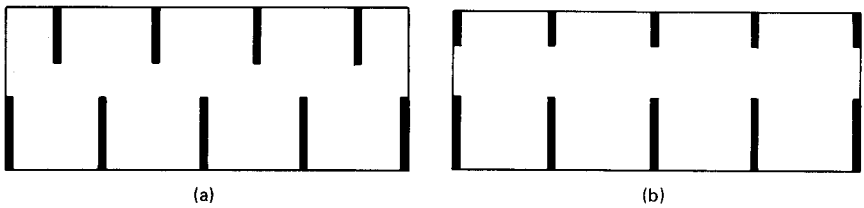

Figure 10.22 Coupled shear walls. (*a*) Staggered shear walls; (*b*) walls in line with each other.

continuous one-way slab spanning between load-bearing reinforced concrete walls, which resist both horizontal and vertical loads. The shear walls are either staggered in plan or placed in line with each other, as shown in Fig. 10.22. From the point of view of structural analysis, the behavior of the coupled and cross-wall systems of walls is very similar. Invariably, the connection between the horizontal floor system and the walls is a moment connection because of the monolithic nature of concrete construction. Also, in a shear wall system the width of wall that is in contact with the floor system is much larger than in a conventional moment-connected frame, resulting in a high degree of interaction between the horizontal and the vertical elements. Take, for example, the rotation θ at the center of gravity of the shear wall, as shown in Fig. 10.23. In having to comply with the deformed shape of the wall, the floor system undergoes not only a rotation, but a corresponding vertical displacement at all locations except at the center of gravity of the wall. Add to this the two-dimensional behavior of the floor system, especially in a flat slab or waffle construction. It is obvious that the combined effects of the slabs are too large to be ignored in all but very preliminary analysis.

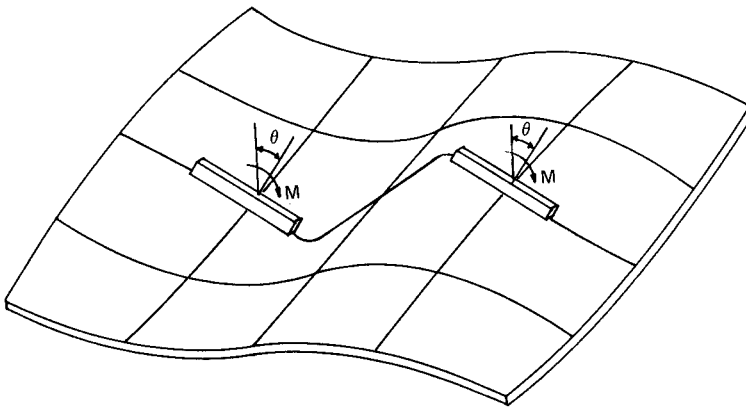

Figure 10.23 Displacement compatibility between slab and walls.

Two approaches are possible for the analysis of shear walls with regular series of openings. The first, commonly known as the continuous medium technique, uses an analogous structure in which the discrete beams are replaced by a continuous medium of the same stiffness. By assuming a fixed point of contraflexure in the middle of the connecting system, conditions of compatibility and equilibrium yield differential equations of the second order, making possible a closed mathematical solution. This is considered next.

Continuous medium method. In the past two decades a great deal of research and development of the so-called continuous medium method, or continuum method, for the analysis of coupled shear wall structures has been carried out both in the universities and by practicing engineers. A number of papers which have added considerably to the understanding of the basic behavior of coupled shear wall structures have been published by Coull and Choudhury (Ref. 56), Rosman (Ref. 57), Qadeer and Stafford-Smith (Ref. 58), and others.

The underlying principle of the method is to replace the effect of individual beams or slabs which interconnect the walls at each floor by a continuously distributed reaction. In deriving the differential equation, certain assumptions are made. As in the portal and cantilever methods of analysis, the points of contraflexure in the beams are assumed to occur at midspan of the beams. The walls are assumed to deform equally in the horizontal direction and therefore resist the lateral loads in proportion to their stiffness.

Briefly, the analysis procedure is as follows. The individual connecting beams of finite stiffness I_b are replaced by an imaginary continuous connection or laminae. The equivalent stiffness for a story height $h = I_b/h$ giving a stiffness of $I_b\ dx/h$ for a height dx. When the wall is subjected to horizontal loading, the walls deflect, inducing vertical shear forces in the laminae. The system is made statically determinate by inducing a cut along the center of beams which is assumed to lie on the points of contraflexure. The displacement at each wall is determined and, by considering the compatibility of deformation of the laminae, a second-order differential equation with the vertical shear force as a variable is established. The solution of this differential equation for the appropriate boundary conditions, of which fixed base is most common, leads to an equation for the integral shear T from which the moments and axial loads in the walls can be established. Once the distribution of T has been established, the shear force in the connecting beam at any level is obtained as the difference between the values of integral shear T at levels $h/2$ above and below the beam. At any level x the bending moment in each wall can be established by superposition of the moment due to external lateral loads and a

counteracting moment due to eccentricity of integral shear force from the center of gravity of the wall. The deflected form of the structure can then be established by integrating the moment curvature relationships.

The following notations are used in the development of the analysis.

A_1	Area of wall 1
A_2	Area of wall 2
I_1	Moment of inertia of wall 1
I_2	Moment of inertia of wall 2
H	Total height of wall
h	Story height
I_b'	Moment of inertia of interconnecting beam
l	Distance between centroids of walls 1 and 2
T	Integral shear force or sum of the laminae shears above a given level
q_n	Shear force in the laminae
w	Uniformly distributed lateral load
E	Modulus of elasticity assumed constant for the system
b	Width of opening
A_b	Area of connecting beam
I	$I_1 + I_2$
A	$A_1 + A_2$
G	Shear modulus
I_b	Moment of inertia of connecting beam reduced to take into account the effect of shear deformation in the beam. This is given by the relation:

$$I_b = \frac{I_b'}{1 + 2.4\,(d/b)^3(1 + \nu)}$$

d	depth of interconnecting beam
ν	Poisson's ratio
α, β, and μ	Parameters given by the following relations

$$\alpha^2 = \frac{12\,I_b}{hb^3}\left[\frac{l^2}{I} + \frac{A}{A_1A_2}\right]$$

$$\beta = \frac{6\,wlI_b}{Ib^3h}$$

$$\mu = 1 + \frac{AI}{A_1A_2l^2}$$

Figure 10.24*a* shows a pierced shear wall subjected to a uniformly distributed horizontal load of intensity w. In Fig. 10.24*b* the wall is imagined cut along the centerlines of the connecting beams and the tie

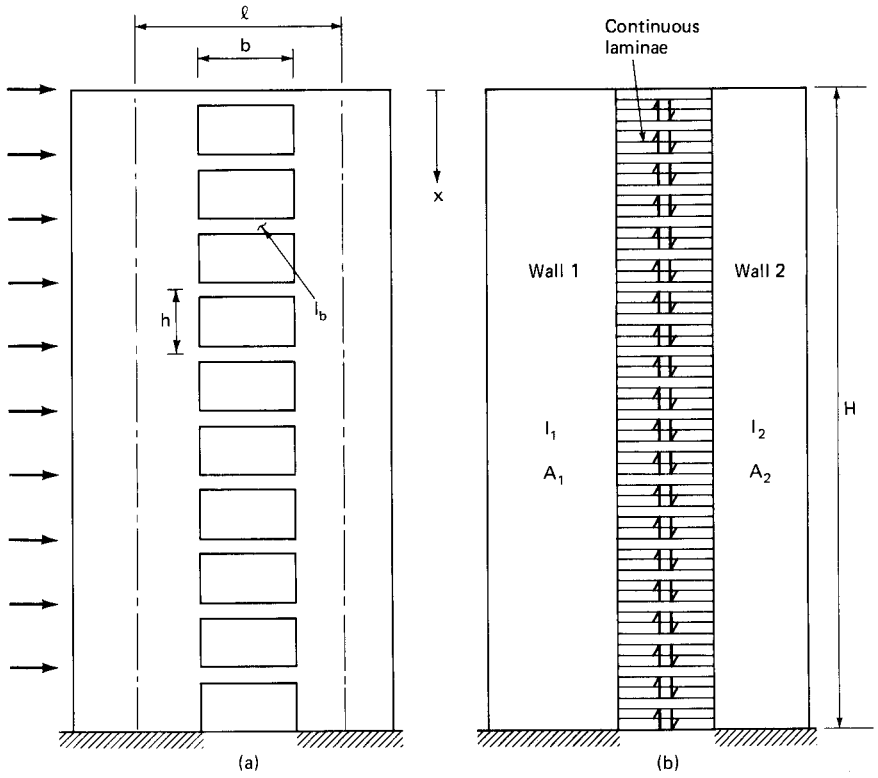

Figure 10.24 Analysis of coupled shear wall by continuous medium technique. (*a*) Interconnected shear walls; (*b*) replacement of discrete beams by a continuous medium.

beams are replaced by an imaginary equivalent continuous laminae. The shearing force T acting along the vertical axis of the wall is determined by considering the relative displacement of each wall.

Figure 10.24*c* shows an experimental setup for testing a coupled shear wall subjected to horizontal load.

Under lateral loads the two ends of beam at the cuts experience a vertical displacement consisting of contributions δ, δ_2, δ_3, and δ_4 as shown in Fig. 10.25.

The relative displacement δ_1 due to bending of each wall element (Fig. 10.25*a*) is given by

$$\delta_1 = l\frac{dy}{dx}$$

The shear force $T = qh$ acting at each floor level at the center of connecting beams will cause a relative displacement δ_2 (Fig. 10.25*b*) due to bending of these beams. This is given by

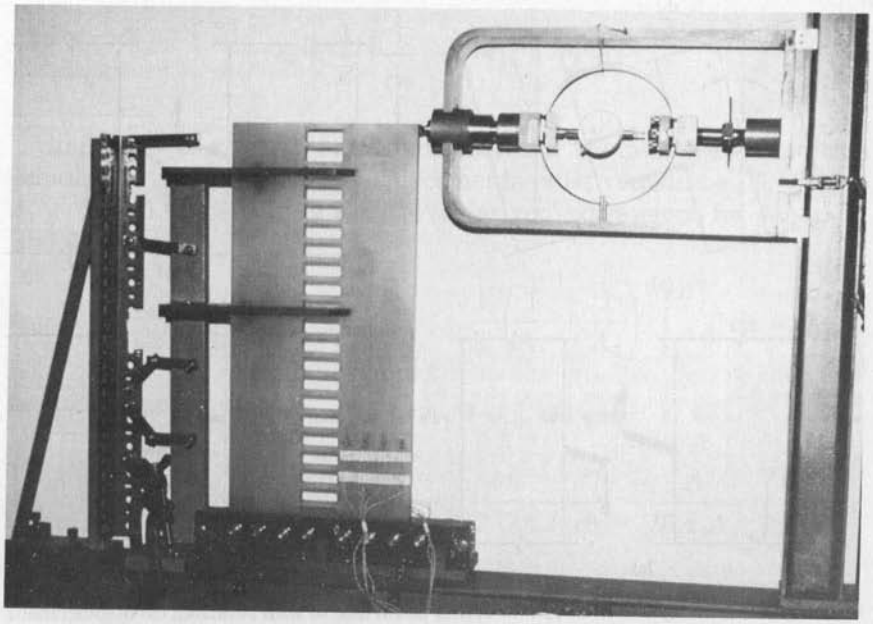

Figure 24 (*Continued*). (*c*) Experimental setup for coupled shear wall model.

$$\delta_2 = \frac{qb^3h}{12EI_b'}$$

The same shear force causes a shear deformation δ_3 (Fig. 10.25*c*) in the beam given by

$$\delta_3 = \frac{qbh}{GA_b'}$$

For rectangular sections effective cross-sectional shear area A_b' *can be considered* $= A_b/1.2$. Therefore,

$$\delta_3 = \frac{1.2\ qbh}{GA_b}$$

The displacement δ_4 (Fig. 10.25*d*) is the relative displacement of the two wall elements due to the axial deformation of the walls caused by T acting as a vertical load on the wall elements. This is determined as follows. The axial force in wall at any height is

$$T = \int_0^x q\ dx$$

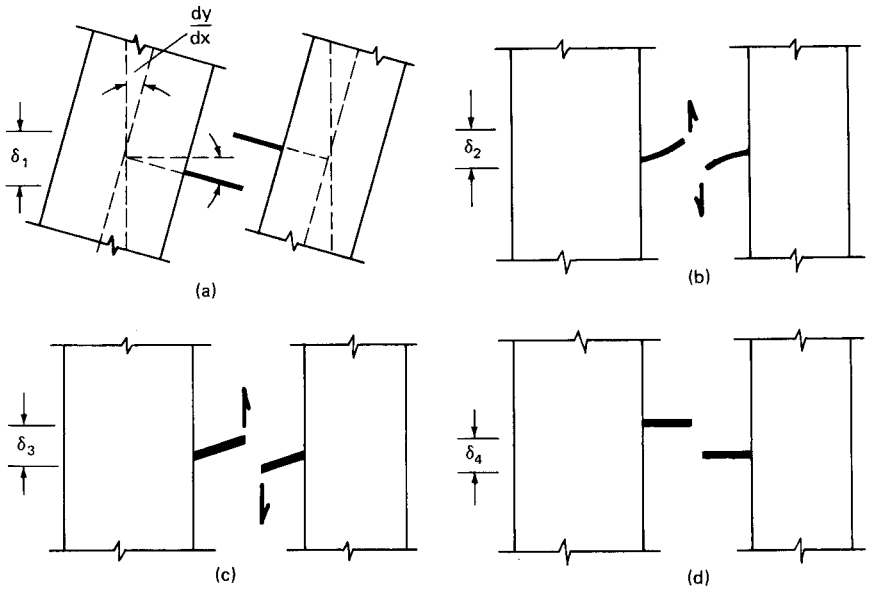

Figure 10.25 (*a*) Displacement of connecting beam due to wall rotation; (*b*) displacement of connecting beam due to beam bending; (*c*) displacement of connecting beam due to beam shear deflection; (*d*) displacement of connecting beam due to axial tension and compression in shear walls.

and therefore

$$q = \frac{dT}{dx}$$

The strain in wall 1 due to axial loads is equal to

$$\frac{\text{stress}}{E} = \frac{\text{force}}{E \times \text{area}} = \frac{T}{EA_1}$$

Therefore total increase in length for wall 1 is

$$\int_x^H \frac{T}{A_1 E}\, dx$$

Similarly, total axial shortening for wall 2 is

$$\int_x^H \frac{T}{A_2 E}\, dx$$

Therefore, relative displacement is

$$\delta_4 = \frac{1}{E}\left(\frac{1}{A_1} + \frac{1}{A_2}\right)\int_x^H T\,dx$$

Since the two walls are connected, the compatibility condition stipulates that the relative displacements must vanish, i.e., $\delta_1 + \delta_2 + \delta_3 + \delta_4 = 0$. Substituting the above-derived expressions for δ_1, δ_2, δ_3, and δ_4, we get

$$l\frac{dy}{dx} + \frac{b^3hq}{12EI_b'} + \frac{qhb}{1.2\,GA_b} + \frac{1}{E}\left(\frac{1}{A_1} + \frac{1}{A_2}\right)\int_x^H T\,dx = 0$$

Substituting $q = dT/dx$ and $A = A_1 + A_2$, we get

$$\frac{dy}{dx} = -\frac{b^3h}{12\,lEI_b'}\frac{dT}{dx} - \frac{bh}{1.2\,GA_bl}\frac{dT}{dx} - \frac{A}{lEA_1A_2}\int_x^H T\,dx$$

Differentiating with respect to x, we get

$$EI\frac{d^2y}{dx^2} = -\frac{b^3hI}{12lI_b'}\frac{d^2T}{dx^2} - \frac{2bhI}{1.2\,lA_b}\frac{d^2T}{dx^2} - \frac{IAT}{lA_1A_2} \qquad (10.13a)$$

The first two terms on the right-hand side of the above equation, which pertain to the bending and shear deflection of the beam, can be combined into a single term by reducing the moment of inertia of the beam to include the effect of shear deformation. The reduced moment of inertia I_b is given by the relation

$$I_b = \frac{I_b'}{1 + 2.4\,(d/b)^3\,(1 + \nu)}$$

Using this relation Eq. (10.13b) reduces to

$$EI\frac{d^2y}{dx^2} = -\frac{b^3hI}{12I_bl}\frac{d^2T}{dx^2} - \frac{AI}{lA_1A_2}T \qquad (10.13b)$$

The total applied moment M_x at any point x is given by

$$M_x = \frac{wx^2}{2}$$

Hence equation of statistical equilibrium is arrived at as follows. The applied moment less moment due to T acting at an eccentricity l is

$$EI\frac{d^2y}{dx^2} = \frac{wx^2}{2} - Tl \tag{10.13c}$$

From Eqs. (10.13*b* and *c*) the following governing second-order differential equation is derived:

$$\frac{d^2T}{dx^2} - \alpha^2 T = -\beta^2 x^2 \tag{10.13d}$$

where

$$\alpha^2 = \frac{12\,I_b}{hb^3}\left[\frac{l^2}{I} + \frac{A}{A_1A_2}\right]$$

$$\beta = \frac{6\,wlI_b}{hb^3I}$$

The solution of Eq. (10.13*d*) gives

$$T = c_1 \sinh \alpha x + c_2 \cosh \alpha x + \frac{\beta}{\alpha^2}\left(x^2 + \frac{2}{\alpha^2}\right) \tag{10.14a}$$

where c_1 and c_2 are constants of integration.

To eliminate these constants we introduce boundary conditions. Most commonly, the boundary condition at the base of shear walls where $x = H$ is to assume a rigid foundation which permits no deformation. The deformation at the cut ends of the laminae is zero and hence $q = 0$ or $dT/dx = 0$ at $x = H$. At top of walls where $x = 0$ the wall is free; therefore, the integral of shear force must vanish, i.e, $T = 0$ at $x = 0$. Substituting the boundary conditions in Eq. (10.14*a*) we get

$$T = \frac{2\beta}{\alpha^4}\left\{1 + \frac{\sinh \alpha - \alpha H}{\cosh \alpha H}\sinh \alpha x - \cosh \alpha x + \frac{\alpha^2 x^2}{2}\right\} \tag{10.14b}$$

Once the distribution of force T has been obtained, the shear force in any coupling beam may be determined as the difference in values of T at levels $h/2$ above and below that level. The bending moment in the beam is obtained by the product of shear force and half the clear span of beam. Since the walls are assumed to deflect equally, the bending moments are proportional to their stiffness. Therefore, the bending moments in walls 1 and 2 are given by

$$M_1 = \left(\frac{wx^2}{2} - Tl\right)\frac{I_1}{I}$$

$$M_2 = \left(\frac{wx^2}{2} - Tl\right)\frac{I_2}{I}$$

The general expression for deflection y at any point x can be obtained by integrating Eq. (10.13*c*) twice and substituting appropriate boundary conditions. Assuming the foundation for the walls to be rigid, the boundary conditions are

$$y = 0 \quad \text{and} \quad \frac{dy}{dx} = 0 \quad \text{at } x = H$$

Although interstory drifts are important, most usually in preliminary analysis the maximum deflection at top is of prime interest. This is given by the following expression:

$$y_{\max} = \frac{wH^4}{2EI}\left[0.25\left(1 - \frac{1}{\mu}\right) - \frac{2}{\mu}\left\{\frac{\alpha H \sinh \alpha H - \cosh \alpha H + 1}{(\alpha H)^4 \cosh \alpha H} - \frac{1}{2(\alpha H)^2}\right\}\right] \tag{10.15}$$

where

$$\mu = 1 + \frac{AI}{A_1 A_2 l^2}$$

To analyze a system of coupled shear walls by this method requires laborious calculations. Several researchers have proposed simplifications of this procedure. Of particular interest is the one proposed by Coull and Choudhury (Ref. 56). In this method, the stress distribution in coupled shear walls is obtained as a combination of two distinct actions: (1) walls acting together as a single composite cantilever with the neutral axis located at the centroid of the two elements, and (2) walls acting as independent cantilevers bending about their own neutral axes. Semigraphical methods are presented for rapidly evaluating maximum stresses and deflections in any system of coupled shear walls subjected to a variety of loading cases. The interested reader is referred to Ref. 56 for further details of this method.

Wide-column analogy. Simply stated, a shear wall is a column whose characteristic dimension is large compared to the overall dimensions of

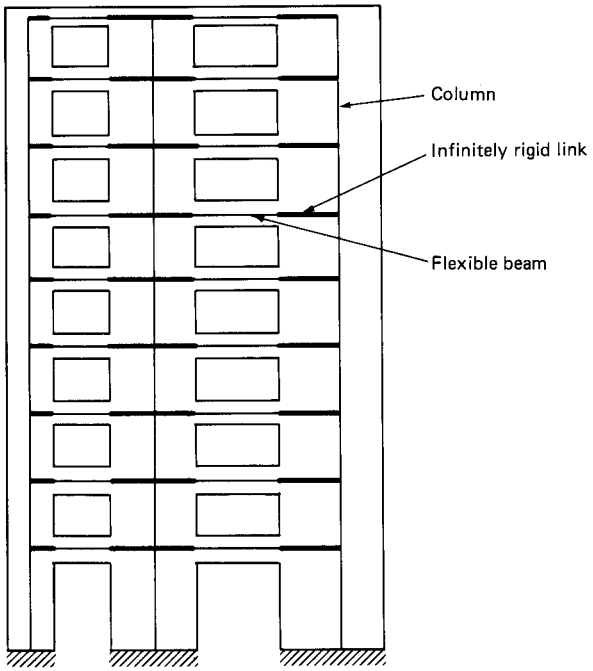

Figure 10.26 Wide column frame.

the frame. A shear wall–beam system in effect has rigid zone dimensions much larger than in a beam-column system, thus necessitating that finite dimensions of the member be considered in order to properly reflect the behavior of the system.

The earliest investigations of shear walls used the concept of equivalent frame, and today this method is still one of the most popular methods for the solution of practical problems. In essence the method considers walls and beams as interconnected line elements, the aggregate behavior being simulated by an equivalent frame as shown in Fig. 10.26. In comparison to a plane frame consisting of columns of normal proportions, the wide-column frame, as the name implies, attempts to capture the additional stiffness of the system due to the relatively large widths of shear walls. Referring to Fig. 10.26, it is seen that the rotation of the wall at its center of gravity produces not only a rotation at the end of the connecting beam but also a vertical displacement. This effect is accounted for in the wide-column frame by considering that portion of the beam between the center of gravity of the wall and the intersection of beam and wall to be infinitely rigid (Fig. 10.26). This methodology is similar to the rigid panel zone concept that is being incorporated into more and more analysis

programs in an effort to make the analytical model as close to the real structure as possible.

The wide-column analogy is very popular in design offices because the analysis can take into account such items as nonuniform floor heights, varying beam or slab stiffnesses, varying wall geometry, loading conditions, elastic support at bases, etc.

An occurrence that is all too familiar to the structural engineer is to find that the moment and shear forces in the connecting beam are much too large to be accommodated in the available depth. If the engineer assumes that the walls are connected solely by beams and ignores the existence of surrounding slab, he or she has very little choice but to use two or even three layers of reinforcement for bending resistance and very heavy multiple-leg stirrups for shear forces in the link beam. Assigning certain flexibility to the beam-wall joint will relieve some congestion of reinforcement, but substituting a steel lintel beam may be a solution in certain isolated cases.

The analysis of a pair of shear walls connected through intermediate floor slabs theoretically follows the same procedure as for a pierced shear wall. Mathematically, it is necessary to define only a hypothetical beam that has the same stiffness as the interconnecting slab, or find an "effective width" for the slab that gives the same stiffness as the pseudo beam. However, our understanding of the stiffness of the slab connecting different forms of shear wall is far from complete. Model experiments and research work have shown that various effective widths of slab are applicable under various conditions, the value ranging from five times the slab thickness to well over the full width of the distance between the centerlines of the slab on each side of the wall. The system stiffness is very sensitive to slab stiffness, except for very high and very low slab stiffness values. Therefore, it is important to determine accurately the stiffness of the connecting medium. Many researchers have tackled this problem and tried to come up with a recommended effective width concept for slabs. However, in practice, shear walls come in all shapes and sizes and usually fall outside the scope of study done by the researchers.

Shear walls are often formed in rectangular or box shapes around elevator and stair openings. The adjacent vertical element interconnected through the slab may be a wide column or perhaps even another box section. It is therefore impossible to cover all practical cases in terms of design charts. The engineers have no choice but to study each problem on an individual basis and arrive at their own values for effective widths.

It is a formidable problem if the engineers have to work out an analytical solution every time they are faced with an interconnected shear wall problem. They would spend half their lifetimes (and many

times over the allotted budget) before arriving at even an approximate solution because of the mathematical difficulties involved. Slab bending analysis problems are not the only type that defy analytical solutions. A similar limitation of analytical techniques is encountered in dealing with shear walls with sudden changes in width and for those with nonuniform openings. Contrary to the wish of structural engineers, the shapes and sizes of structural elements and their disposition to each other do not always follow well-defined mathematical rules. It is necessary in most cases to approximate the geometry and loading conditions to obtain practical solutions. Even with such simplified models it is not cost effective to obtain closed-form analytical solutions. A method of solution known as the *finite element* technique is being increasingly used for the solution of such problems.

Although the finite element method is based on the idea of discretization, the technique recognizes the structure as a continuous body and provides solutions not only at a finite number of discrete points but also at all other locations in the structure. One of the most important advantages of the finite element method is the ease with which boundary conditions can be incorporated into the technique. Kinematic boundary conditions in terms of displacements and rotations are easily introduced into the assembled equations without requiring special techniques. The method can accommodate complex geometry and boundary conditions. The technique is quite general and can be applied systematically to solve a wide range of structural engineering problems. Several structural analysis packages which can be applied to diversified categories of structural problems are available for use not only on mainframe computers but also on personal computers, making it possible for the engineer to develop solutions to complicated problems without having to become familiar with the mathematical aspects of the technique. It is possible to interpret the results in terms of the physical behavior of the structure, making this method particularly useful to practicing engineers. Nevertheless, the engineer must be aware of the mathematical foundations of the technique, the assumptions used in the formulation, and the possibilities of numerical difficulties inherent in the technique, in order to interpret and temper the results by proper engineering judgment. There probably is a tendency among structural engineers to be intimidated by the large volume of solution information generated by this method and to think of the particular solution as the most accurate. Nothing could be further from the truth. By changing, for example, the element size, shape, or the type, it is entirely possible to obtain results which may show that critical areas exist at locations much different than those obtained by the previous solution. In structural engineering practice, seeking solutions with elements of different size, shape, or type for the

same problem to verify if the solution is converging has not come about as a routine custom. For example, at the time of this writing, no fewer than 12 types of elements are available for the solution of plate bending problems alone. It is not the intent nor it is within the scope of this work to familiarize the practicing engineer with all the different types of elements. The intent is only to review the fundamentals.

Cases in structural problems appear in which it is necessary to approximate the geometry of the structure. Many problems of this nature have no closed-form solutions because of their complicated geometry and cannot be used to verify the adequacy of the finite element approximations. However, generally it is believed that useful structural engineering solutions can be obtained with these approximate solutions provided sufficient care and reason guided by experience are exercised in discretizing the body. Therefore, an understanding of the nature of finite element formulation is necessary to appreciate both the power and limitations of the method. An attempt will be made in the following sections to acquaint the readers with the essentials of the technique and to explain in somewhat greater detail the common types of elements they might encounter in the design of high-rise structures.

10.7 Finite Element Analysis

A structure such as a building frame can be considered as an assemblage of linear members or elements, each element being unidimensional, with its cross-sectional dimensions very small relative to its length. A surface structure such as a thin slab or shell, on the other hand, can be considered as made up of a network of two-dimensional elements. These elements differ from the beam elements because both their width and length are significant when compared to their thickness. A third category of structures such as a thick container vessel, a dam, or a massive concrete foundation can be thought of as an assemblage of solid three-dimensional elements. All the three dimensions, namely, the length, width, and thickness, need to be considered in the analysis. Before the advent of digital computers it was necessary, at least from the point of view of structural analysis, to pigeonhole a structure into a distinct category. With the use of digital computer analysis it is no longer a requirement to distinguish between these elements in the usual sense. The whole structure can be treated as an assembly of structural elements of different types. It is only necessary for the engineer to discretize the structure into proper categories in order to gain computational economy.

Before the advent of finite element methods, the technique of structural analysis consisted of studying an assemblage of construc-

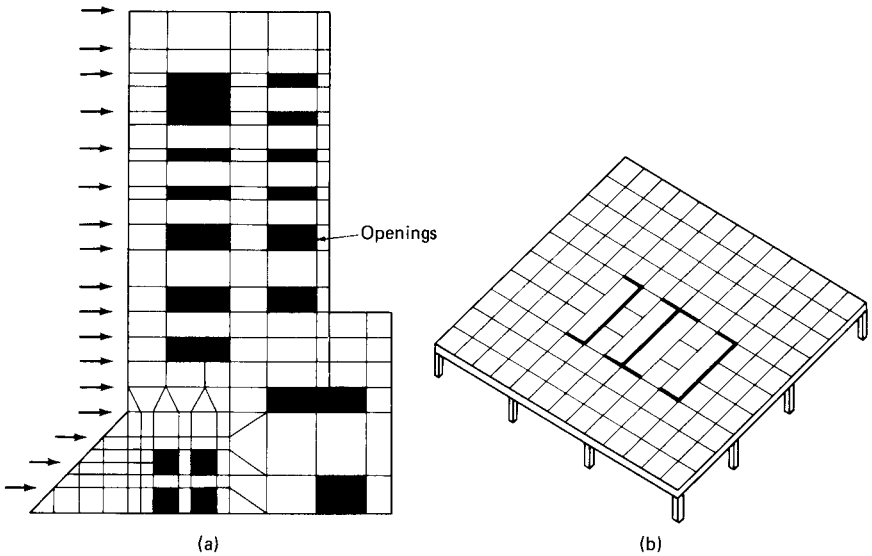

Figure 10.27 Finite element idealizations. (*a*) Shear wall with arbitrary openings; (*b*) floor slab.

tion elements of the kind represented by beams and columns. The physical behavior of these linear elements was easy to understand and oftentimes the structure being assembled for the analysis closely resembled the actual structure, which consisted of actual beams and column elements that were physically assembled into one structure at the site. If the structure to be analyzed was a surface structure such as a slab, a common technique was to use a grid of intersecting beams to represent the mathematical models. Each beam represented the properties of an equivalent width of slab and the analysis gave results at the intersection of beams.

The finite element technique can be thought of as a method of analysis which endeavors to better describe the physical behavior of a surface element. Figure 10.27 shows the finite element idealizations for a shear wall and a slab. The triangular, rectangular, and quadrilateral regions for the shear wall model and the rectangular regions for the plate are called the *finite elements*, while the discrete points where the elements are connected are called the *nodes*. A *mesh* defines an arrangement of nodes and elements.

The method, which was originally developed as a tool for structural analysis because of its versatility, is being increasingly used in other fields of engineering such as heat conduction, hydrodynamics, and soil mechanics. The advent of high-speed computers and the increasing emphasis on numerical methods have thrust this method of analysis into the forefront of many engineering disciplines. In structural

engineering, it is not always possible or desirable to obtain exact analytical solutions for many problems. Analytical solutions which are available for a number of engineering problems are almost always based on simplifying assumptions regarding load application and boundary conditions. There are many instances where these assumptions are not satisfied, forcing engineers to resort to numerical methods that provide approximate but satisfactory solutions. In contrast to an analytical solution which gives the values of the unknown quantity at any location, the numerical method yields values only at a discrete number of points in the body. It is necessary, therefore, to identify these points in the body at which the approximate values of the unknown are sought. This process of choosing only a certain number of points on the body is termed discretization in finite element terminology. The structure is discretized into an equivalent system of smaller units which, when assembled together, represent the original structure. As an alternative to solving this problem for the entire body in one operation, solutions are sought for each surrogate unit and are combined to obtain the solution for the original structure. The analysis is considerably simplified, but typically results in a vast amount of data, allowing only computer methods for the solution of the problem. The finite element method possesses certain characteristics that take advantage of special computer techniques in that it can be systematically programmed to take into account complicated loadings and boundary conditions.

Because of these reasons the finite element method has been applied to a wide variety of structural engineering problems. To mention a few, we have plane strain analysis for gravity dams; plane stress analysis of plates and walls with openings and bending of deep beams; plate bending analysis for floor and bridge slabs, hulls, and aircraft, and spacecraft panels; three-dimensional stress analysis for nuclear containment vessels; shell elements for the analysis of arch dams, domes, fuel tanks, aerospace structures, and so on. In high-rise structural engineering two types of problems most often require application of finite element technique. These are (1) the plane stress problem and (2) the plate bending problem, as illustrated in the following sections.

Contrary to the wish of structural engineers, shear walls come in all shapes and sizes with openings arranged in a rather random fashion. Sometimes engineers refer to these walls as "Swiss cheese." In such cases as those shown in Fig. 10.28, finite element solution offers a practical approach because the idealization of the wall into plate elements is not affected by the location or relative shift in the position of the openings.

Note that even for walls with sudden changes in width and for those with nonuniform openings, it is still possible to use the wide-column

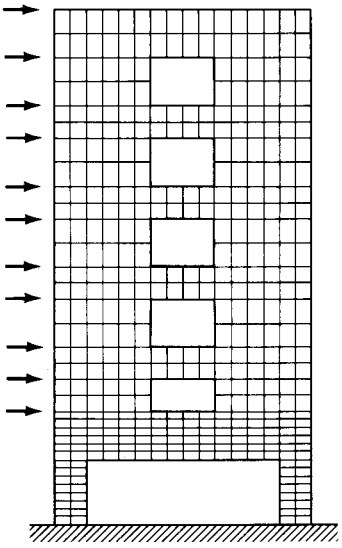

Figure 10.28 Shear wall with arbitrary openings. Finite element model.

analogy. It is only necessary to shift the centerline of the wall elements and to assume rigid members interconnecting the centerlines as shown in Fig. 10.29. This assumption in effect neglects the rotation of the walls at the offsets and therefore results in deflections that are slightly on the liberal side, i.e., the model deflections will be slightly less than the actual deflection of the structure. Since the equivalent frame method does not predict the exact stress distributions near the discon-

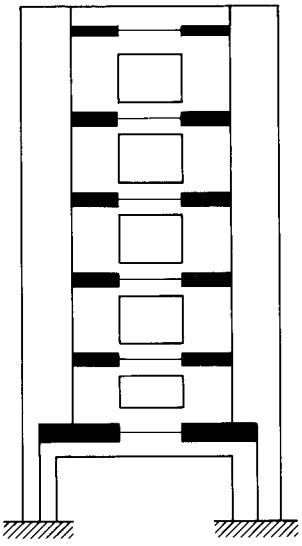

Figure 10.29 Wide-column model.

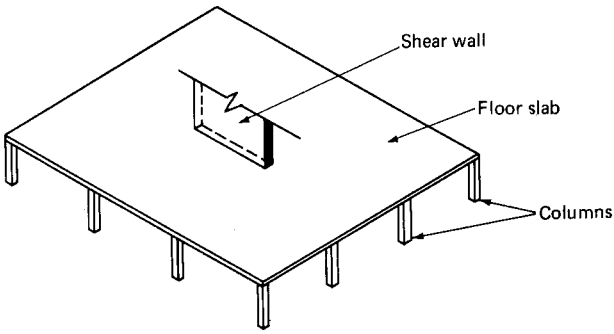

Figure 10.30 Floor slab supported by central core and perimeter columns.

tinuities, finite element techniques are often used to obtain solutions for such problems.

A planar shear wall loaded in its own plane is essentially a plane stress problem. Of the several types of elements available for the solution of the problem, rectangular and quadrilateral elements have found wider application.

The use of finite element analysis for plate bending problems is illustrated in Fig. 10.30. The slab is supported by columns at a distinct number of points around the perimeter and a wall at the center as shown in Fig. 10.30. Let us assume that we are interested in studying the behavior of the slab when it is subject to a bending action at the center that corresponds to the bending deformations of the central wall about its strong axis. The bending action can be schematically represented by a system of loads along the wall and column supports can be considered as equivalent elastic springs as shown in Fig. 10.31. Analytical methods that can be applied to practical problems as illustrated in Fig. 10.31 are just about nonexistent, requiring the application of a numerical procedure such as the finite element method.

10.7.1 Method of analysis

The finite element method essentially consists of

1. Idealization of the structure into an assemblage of discrete elements
2. Selection of displacement function
3. Evaluation of stiffness of each element from its geometric and elastic properties
4. Assembly of the overall stiffness matrix from individual element stiffness matrices

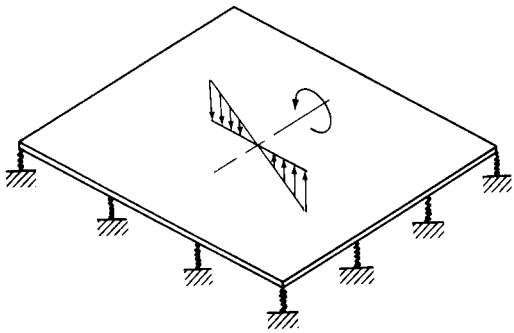

Figure 10.31 Analytical model.

5. Modification of the stiffness matrix to take into account the boundary conditions
6. Solution of resulting equilibrium equations to obtain nodal displacements
7. Calculation of stresses

The general description of the method can be detailed in a step-by-step procedure to describe the sequential process that is followed in setting up and solving a finite element problem. The method is similar to the displacement or the stiffness method familiar to most engineers.

Discretization of the structure. This is a process in which the structure being analyzed is subdivided into a system of finite elements. Depending on the type of structure, the element models can be line elements, two-dimensional plane stress or plane strain elements, flexural plate and shell elements, axisymmetric elements, general three-dimensional solid elements, etc. The element model and its stiffness characteristics are subjects of immense popularity with researchers, who have given us at least 30 types of elements for the general analysis of structures. It is not necessary for practicing engineers to evaluate the stiffness of element models because commercially available general-purpose programs have several such elements in their libraries.

The subdivision process is essentially a task that requires engineering judgment. During this process the engineer decides on the number, shape, size, and configurations of the elements with the purpose of simulating the structure as closely as possible. The principal objective of such a subdivision is to discretize the structure into sufficiently small elements such that their displacement can adequately reflect the true deflection pattern of the structure, keeping in mind at the same time that too fine a subdivision will lead to extra computational effort.

The underlying principle is to have an arrangement of finite elements that gives effective representation of the given structure for the particular problem considered. For the slab problem shown in Fig. 10.30, the finite element idealization is based on the premise that the stress gradients in the vicinity of the shear wall are likely to be steep compared with their values elsewhere in the slab. It is natural to subdivide this area into smaller elements and to use courser grids away from the regions of severe slab bending. This implies that for slabs subjected to other types of imposed loads or displacements it may be necessary to use an entirely new arrangement of finite elements. Based on the expected mode of deformation of the slab, the engineer must decide what number, size, and layout of finite element will best represent the structural behavior.

Figure 10.28 shows a shear wall subjected to horizontal loads. The most obvious locations for nodes or subdivision lines are the points at which loads are applied, where there is discontinuity in the geometry of the structure such as changes in shear wall thickness, and where the material properties change. From the point of view of data preparation, constructing regular mesh throughout the structure may be the easiest thing to do, but such a process is rarely satisfactory in structural engineering practice because most structures have distinct regions which are subjected to steep variations in stresses and strains. A finer mesh is necessary in regions where pronounced stress gradients are expected in order to obtain a reasonable solution. In the shear wall model it is reasonable to expect heavy stress concentrations between the openings; therefore, it is logical to subdivide this region into finer elements (refer back to Fig. 10.28).

In a sense, we can consider the finite elements as pieces of the actual structure if we recognize that the elements are connected to each other not only at the nodes but also at the sides. It is easy to see that if the pieces are held together only at the nodes, the structure is greatly weakened because the elements may separate along the mesh lines. Clearly, the actual structure does not perform this way, so a finite element must deform in certain restricted ways. In formulating this behavior, it is necessary to assure that adjacent elements do not behave as if sawcuts were placed between them until only wisps of material at the nodes hold the pieces together.

Selection of displacement models. One of the basic assumptions of the finite element method is introduced at this stage when the analyst chooses displacement functions to represent the actual distribution of the displacements. Usually in structural engineering problems, the displacement function is commonly assumed in a polynomial form with a limited number of terms. The displacement function in the form of a

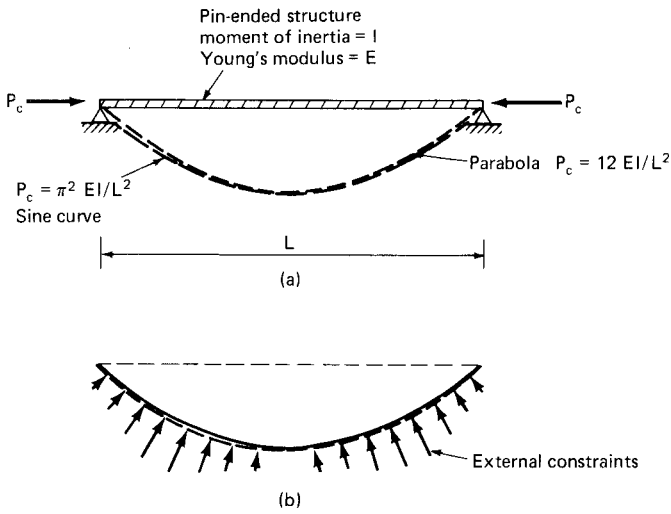

Figure 10.32 Pin-ended strut. (*a*) Buckling loads for assumed parobolic and sine curve; (*b*) schematic representation of external constraints required to force buckling curve from a sine curve to a parobolic curve.

polynomial has certain advantages over other types of functions such as trigonometric formulations. First, even though the polynomial selected for structural analysis purposes is of finite order (i.e., it contains a limited number of terms), it can approximate fairly closely the true displacements for each element. Second, it is relatively easy to carry out the mathematical manipulations such as differentiation and integration. Third, by choosing polynomials we are assured that the displacement variation within an element is continuous without any kinks or other discontinuities. Interelement compatibility is not generally satisfied completely, but solutions sufficiently accurate for purposes of structural design are obtainable even without full displacement compatibility between elements.

At this point it is convenient to discuss some general aspects of displacement function. First, any assumed displacement function constrains the structure to deflect in the assumed mode rather than the one it would adopt naturally. The stiffness values obtained by using such assumed displacement functions in general are too high. An insight into the physical interpretation of this phenomenon can be obtained by referring to Fig. 10.32, which shows a pin-ended strut subjected to axial load. An approximate method known as the Rayleigh-Ritz method can be used to obtain the buckling load of the strut. In this method the strut is assumed to deform in an assumed shape, and using energy principles it is possible to calculate an approximate value for the critical load. For example, assuming the displacement

function as a parabola, the critical load P_c works out equal to $12\,EI/L^2$ as compared to the correct value of $\pi^2 EI/L^2$ where E, I, and L are the elastic modulus, moment of inertia, and the length of the strut, respectively. The value calculated from the assumed parabolic displacement function is thus 22 percent too high. A better approximation is possible by assuming a displacement function that closely resembles the actual displacement. Indeed, by assuming a sine curve it is possible to obtain the exact value for the critical load $P_c = \pi^2 EI/L^2$.

Assuming a displacement function different from the actual displacement implies that external constraints are applied to the system to maintain equilibrium. The buckling load obtained, therefore, will be larger than the true buckling load for the strut.

This type of solution is said to have produced an upper bound value for the buckling load. The nearer the assumed curve to the actual curve, the nearer is the value of the estimated buckling load to the actual buckling load.

Because in finite element analysis we use assumed functions to describe the actual displacement pattern of an element, the computed stiffness coefficients and hence the stiffness of the structure tend to be larger than the actual stiffness of the structure. In other words, under a given load the actual structure deforms more than the simulated structure. Another point worthy of note is the displacement compatibility between adjacent elements. For example, the 12-term polynomial commonly employed for rectangular elements in plate bending problems does not yield a fully compatible displacement field between adjacent elements. The displacements, which include vertical displacements and two rotations, are completely compatible between adjacent elements only at the location of the nodes. Along a common boundary, out of the three generalized displacements, namely, the vertical displacement and the two types of rotations, only two are fully compatible between the interfaces. These are the vertical displacement and rotations parallel to the interface. The rotations normal to the interface in general are not compatible between two adjacent elements. This idea is shown schematically in Fig. 10.33*a* through *f*. Figure 10.33*a* shows a three-element idealization of a slab simply supported along two sides subjected to a central vertical load. The vertical displacement W of element A along the common boundary ab is completely compatible with those of element B, as are the rotations θ_x parallel to the line ab as shown in Fig. 10.33*c* and *d*. The slope θ_y across the common line in general is not the same for both the elements. In other words there is a discontinuity of displacement across ab as shown in Fig. 10.33*f*. The effect of this mathematical discontinuity upon the structure is to reduce its calculated stiffness. Thus, under a given load the simulated structure deforms more than

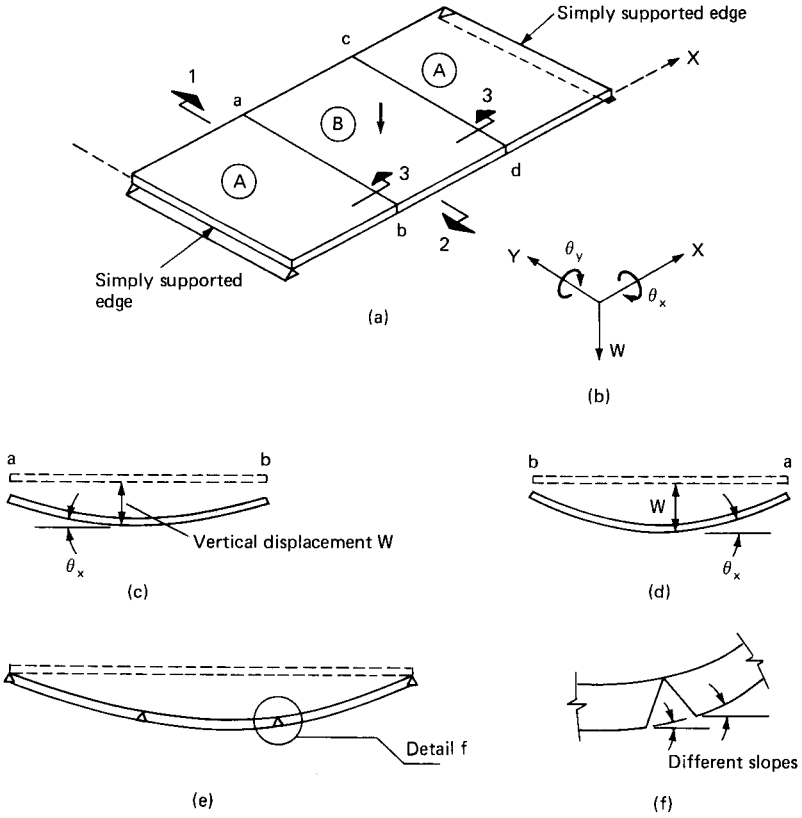

Figure 10.33 Displacement compatibility. (*a*) Finite element idealization; (*b*) coordinate axis system; (*c*) section 1; (*d*) section 2; (*e*) section 3; (*f*) detail at slope discontinuity.

the actual structure. Therefore, on the one hand we have the stiffening effect of the actual structure due to assumed polynomial functions, and on the other the reduction in stiffness because of nonconformity of the slopes across the finite element mesh. The two effects, therefore, tend to compensate each other, yielding results that are close enough for structural engineering purposes. Interelement compatibility criteria in finite element solutions is a subject of immense range and a full exposition with regard to the criteria for monotonic convergence, complete and conforming finite elements, and patch tests is beyond the scope of a single section in this book. What is attempted, therefore, is a review of the fundamentals with particular reference to the analysis of tall buildings.

Evaluation of element stiffness matrix. In the finite element technique, the problem of defining the stiffness properties of any structure reduces

basically to the evaluation of the stiffness of a typical element. The structure is assumed to be divided into a system of discrete elements which are interconnected only at the finite number of nodal points. The behavior of the complete structure is then found by evaluating the behavior of the individual finite elements and superposing them appropriately.

The stiffness properties for a simple element such as a linear beam element can be obtained in a number of ways by applying the methods of structural mechanics such as unit load method or moment-rotation diagram. However, in finite element analysis a versatile method commonly referred to as the Ritz or Galerkin method is used to establish the stiffness matrix of elements. The method has not received much coverage in textbooks on structural mechanics since it is not required for evaluating the stiffness matrix of determinate elements such as beam elements.

No attempt will be made in this work to present the stiffness relations for each type of finite element; the derivations can be found in textbooks on finite elements. The following is merely a summary of the procedure for determining the stiffness matrix $[K]$ of the element.

1. Express the internal displacements ν in terms of displacement function M; thus

$$\{\nu\} = [M]\{\alpha\} \tag{10.16}$$

2. Evaluate displacements at the nodes in terms of generalized coordinates thus

$$\{\nu\} = [A]\{\alpha\} \tag{10.17}$$

where the $[A]$ matrix is obtained by substituting coordinates of nodes in the matrix $[M]$.

3. Express the constants $\{\alpha\}$ in terms of $\{\nu\}$ thus

$$\{\alpha\} = [A^{-1}]\{\nu\} \tag{10.18}$$

4. Evaluate the strains ε in the element; thus

$$\{\varepsilon\} = [B]\{\alpha\} \tag{10.19}$$

where $[B]$ is obtained by differentiation of $[M]$

5. Find the stresses

$$\{\sigma\} = [D]\{\varepsilon\} = [D][B]\{\alpha\} \tag{10.20}$$

where $[D]$ is the stress-strain matrix.

6. Compute the stiffness of the element by the principle of virtual displacements as follows. If σ are selected as actual stresses and ε the virtual strains, then the elemental internal work

$$\begin{aligned} dw_i &= \{\varepsilon^{-T}\}[\sigma]\, dv \\ &= [\alpha]^{-T}[B]^T[D][B]\alpha\, dv \\ \therefore\ w &= \int_{\text{vol}} \partial w_i = \alpha^{-T}[\int_{\text{vol}}[B][D][B]\partial v]\alpha \end{aligned} \tag{10.21}$$

The external work $w_E = [\alpha]^{-T}\{\beta\}$, where $\{\beta\}$ are the forces corresponding to $[\alpha]^{-T}$. If $[\alpha]^{-T}$ is a unit matrix, the procedure is similar to introducing unit displacements one at a time and making all other displacements equal to zero. Equating the internal work to external work gives

$$[\alpha]^{-T}\{\beta\} = [\alpha]^{-T}[\int[B^T[D][B]dv]\alpha \tag{10.22}$$

Since $\alpha^{-T} = 1$,

$$\{\beta\} = [\int_{\text{vol}}[B][D][B]dv]\alpha \tag{10.23}$$

and since

$$[K] = \frac{\{B\}}{[\alpha]} \tag{10.24}$$

we get

$$[K] = \int_{\text{VOL}} [B]^T[D][B]\, dv \tag{10.25}$$

7. The stiffness $[K]$ in the required coordinates can then be obtained from transposition; thus $[K] = [A^{-1}]^T[K][A^{-1}]$. The end product of the above procedure is a stiffness matrix in which forces and moments at each node are expressed in terms of the geometry and the material properties of the element.

Assembly and solution of equations of equilibrium. This process consists of assembling the complete stiffness matrix for the total structure from the individual stiffness matrices and composing the overall global force system from the element nodal forces. In the direct stiffness technique, which is invariably used in structural analysis, the basis for an assembly method is that the displacements at the node common to adjacent elements should be the same for all elements interconnected at that node. The overall equilibrium relations between the total structure stiffness matrix, the total load, and nodal displacements are

expressed as a set of simultaneous equations of the form,

$$[K]\{\Delta\} = \{P\} \tag{10.26}$$

where $[K]$ = the overall stiffness matrix of the complete structure
$\{\Delta\}$ = the column matrix of nodal displacements
$\{P\}$ = the column matrix for the total load vector

The procedure is straightforward and is applicable to all types of problems since it is possible to add directly the individual loads and stiffnesses to locations in the overall stiffness matrices.

The mathematical process of deriving the equilibrium equations for the total structure from the equations of the individual elements can be thought of from the physical point of view as the construction of the total structure with individual elements joined together at preselected nodes such that all elements common to a particular node have the same displacement.

Introduction of boundary conditions. It is necessary to impose boundary conditions to the overall assembled stiffness matrix to remove the singularity of the matrix. The physical significance is that unless supports or kinematic constraints are imposed, the structure is free to experience unlimited rigid body motions. Boundary conditions can be thought of as restraints that arrest the rigid body motions.

Solution of equations. The equilibrium equations are modified for appropriate boundary conditions and then solved for unknown displacements. In linear structural analysis this is a relatively straightforward procedure which uses techniques of matrix algebra.

Computation of element stresses. By using the computed displacements, the nodal forces and hence the stresses at the nodes are calculated by multiplying the nodal displacements by the element stiffness matrix. Usually an average value of the nodal stresses is taken to provide the stress value for each element.

In conclusion, a detailed finite element analysis offers the best elastic solution for shear walls with complex patterns of openings. However, given the cost and time limitations of typical design projects, it is unlikely the engineer will have the luxury of studying the effect of local stress concentrations. Large elements may be adequate to describe the complex bending and shear behavior of pierlike shear walls, but they cannot come even close to the actual stress distributions near major stepbacks and complex sets of openings. No one modeling technique is adequate to give all the correct answers.

One method of obtaining a reasonable solution is to attempt a two-step procedure. In the first procedure the overall behavior is

duplicated as closely as possible by using the wide-column modeling technique. The second step consists of isolating the area in question and performing a finite element study by using a set of statically balanced forces obtained from the first state. In this manner it is possible to recognize the system's weak spots and detail them appropriately. It is imperative that the analyst review the underlying assumptions made in standard analysis programs. A successful application of computer analysis techniques to practical design problems requires a thorough understanding of each program and its limitations.

10.7.2 Practical example of a plane stress finite element solution

To break the monotony of rather theoretical work presented thus far, it is instructive to consider a practical application of the plane stress finite element problem. Recently the author had the opportunity to study the behavior of various structural systems suitable for a high-rise hotel project that was to consist of pairs of shear walls on either side of a double-loaded corridor. The building shown in Fig. 10.34 is

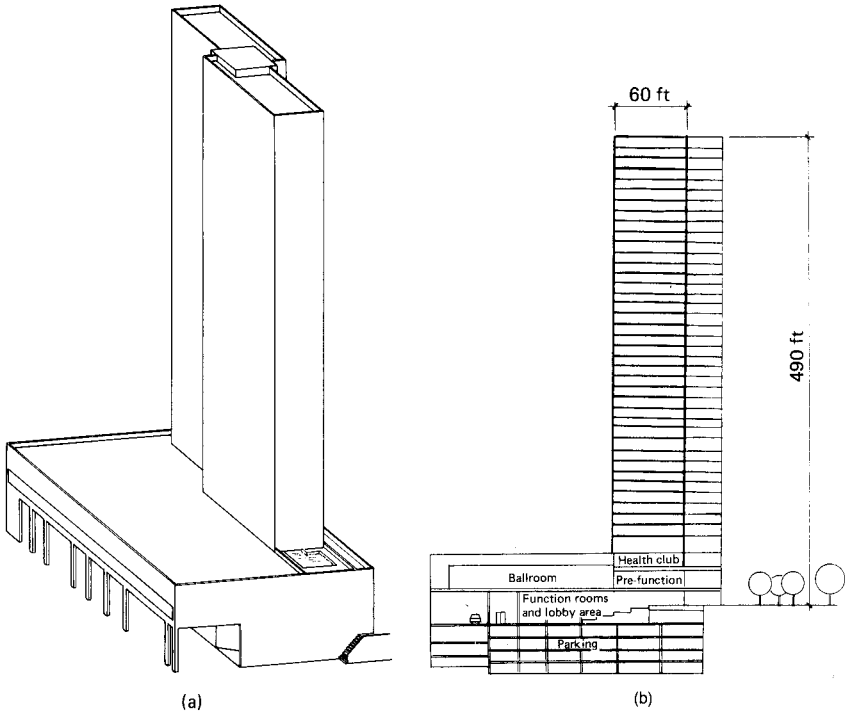

Figure 10.34 High-rise hotel project. (*a*) Isometric view; (*b*) schematic section.

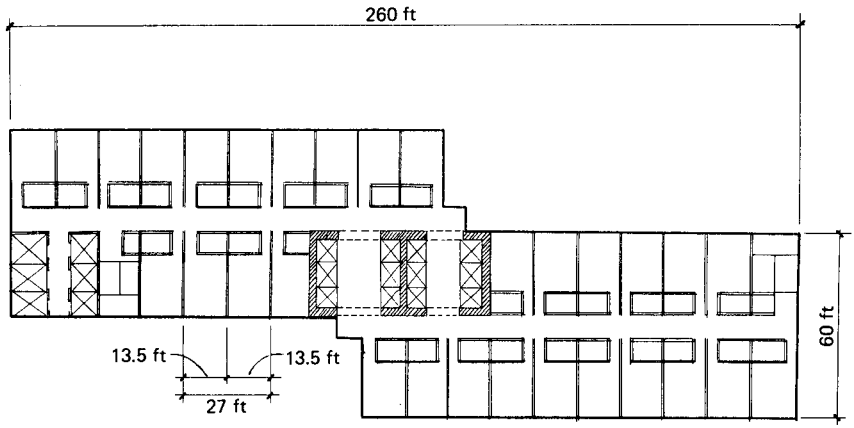

Figure 10.35 Typical hotel floor plan.

very slender, with a height-to-width ratio in excess of 8.0. The architectural layout of guest rooms and stairs and elevators is shown in Fig. 10.35. In common with other projects, several structural schemes were studied for this project. Figures 10.36 through 10.38 show various structural floor framing plans and the arrangement of shear walls found to be feasible for this project. The arrangement of shear walls in the first two schemes shown in Figs. 10.36 and 10.37 are identical. An attempt was made in these schemes to use a limited number of shear walls interconnected with rather a heavy floor system to achieve composite behavior. The scheme shown in Fig. 10.38 uses a large number of cross walls and attempts to minimize on the floor construction.

Another interesting feature of the project is that it was architecturally desirable to have a column-free space below the lowest guest room

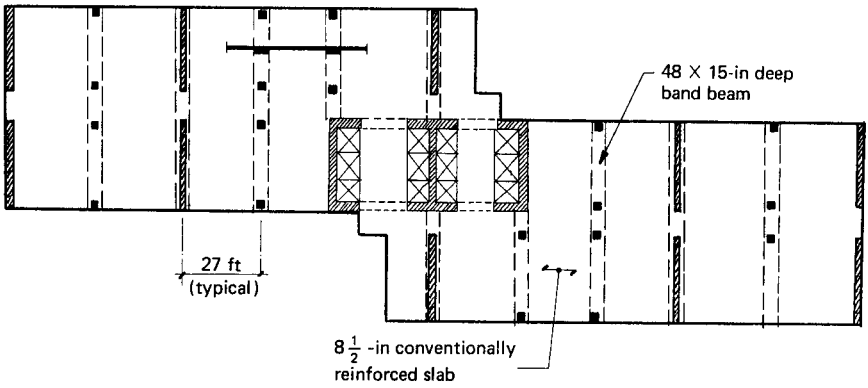

Figure 10.36 Shear walls with band beams.

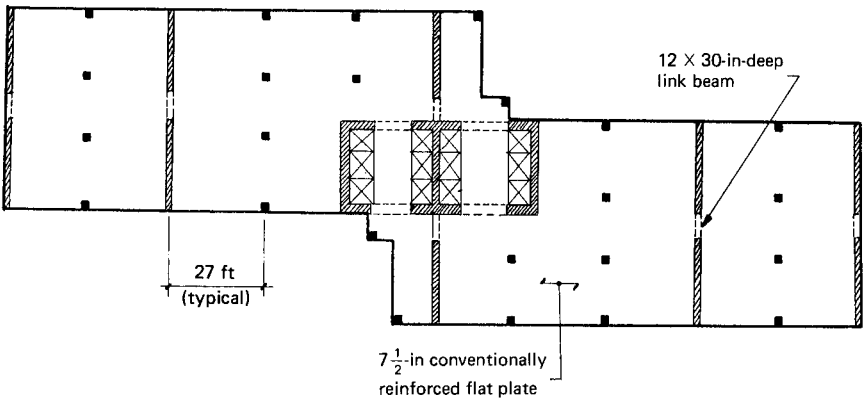

Figure 10.37 Shear walls with link beams.

floor to accommodate a health club, prefunction, and lobby areas. The resulting elevation of the shear wall is shown in Fig. 10.39. To study the lateral deflection characteristics of the building, a wide-column model of the shear wall was used. The centerlines of the wide columns were assumed at the center of wall elements interconnected with rigid arms as shown in Fig. 10.40. As mentioned earlier, this technique neglects the rotations of the walls at the offsets but was considered to be sufficiently accurate to predict the overall behavior of the building.

The distribution of stresses near the discontinuities, especially at the location of the wall offset, is impossible to predict with the equivalent frame method. The behavior of the transfer girder, which from elementary considerations appears to carry the entire height of the shear wall, is somewhat intriguing. A strength-of-material ap-

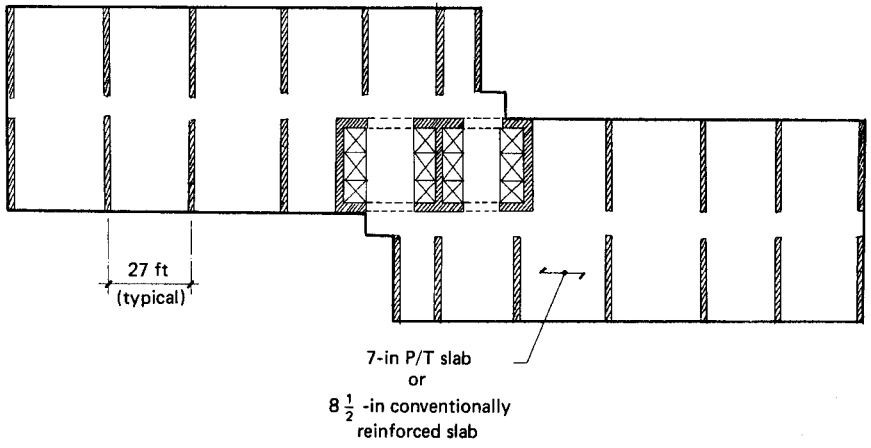

Figure 10.38 Cross wall and slab system.

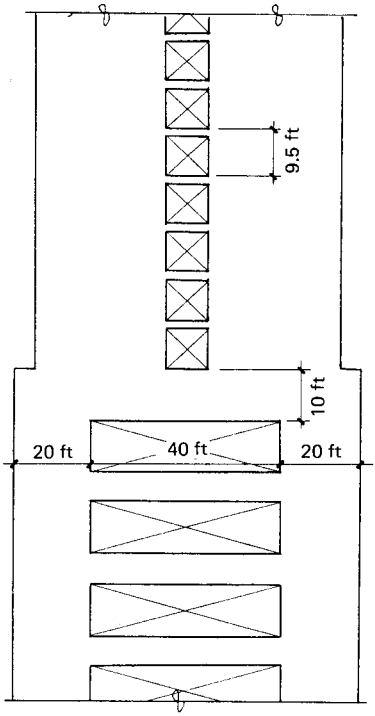

Figure 10.39 Wall elevation.

proach using an equilibrium model as shown in Fig. 10.41 appeared to indicate large tensile stresses in the girder. The wide-column frame technique showed compressive stresses of low magnitude in the same girder. A finite element solution obtained by using the analytical model shown in Fig. 10.42 indicated very high compressive stresses in the girder, pointing to distinct arch action.

10.8 Warping Torsion of Shear Wall Structures

Courses in structural mechanics deal at length with the subject of pure torsion of beams of solid cross sections and thin-walled closed sections which can be analyzed sufficiently accurately by using the classical St. Venant's torsion theory. This theory is restricted to twisting of bars whose cross sections warp freely and is based on the assumption that the effect of axial stresses which appear in the cross sections due to restraint of warping is of a local nature. However, it has long been established theoretically and experimentally that in the torsion of thin-walled open-section beams, axial stresses as well as tangential stresses appear in the cross sections. In general these are of such

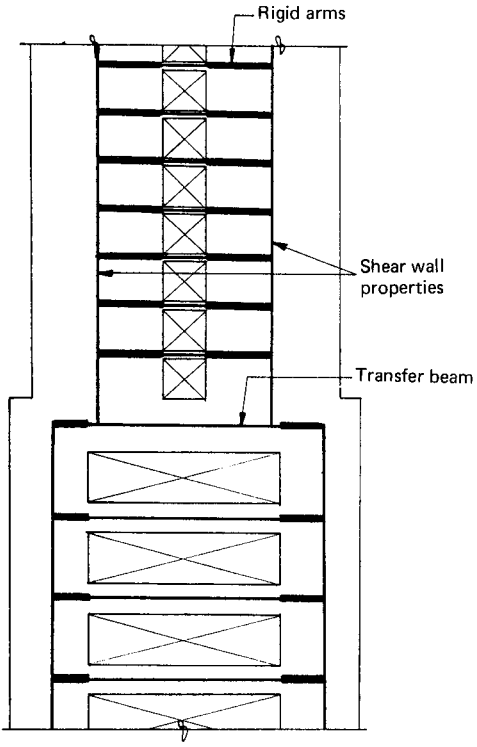

Figure 10.40 Wide-column model.

magnitude and character as to require a warping theory to adequately describe their behavior. Warping axial stresses and warping shear stresses which are critical in a torsionally loaded thin-walled member of open cross section are a consequence of restraint of warping of the cross section due to end restraints or variations in torque along the length of the member. The usual method of determining the warping stresses involves solution of the torsion differential equation. Torsion and warping stresses are functions of various order derivatives of the rotation with respect to the length. The purpose of this section is to introduce the warping concept to practicing engineers without an overabundance of differential equations and to review the methods available for the analysis and design of shear wall structures.

At the outset it is fair to say that in this day and age of computers it is not necessary to formulate the torsion problem in terms of the warping stress concept. Computer finite element methods are capable of capturing the essential behavior, but they require a large amount of data manipulation. Even with computer solutions it is necessary to have a basic concept of the warping phenomenon of open sections in order to verify the validity of computer solutions. This is the underly-

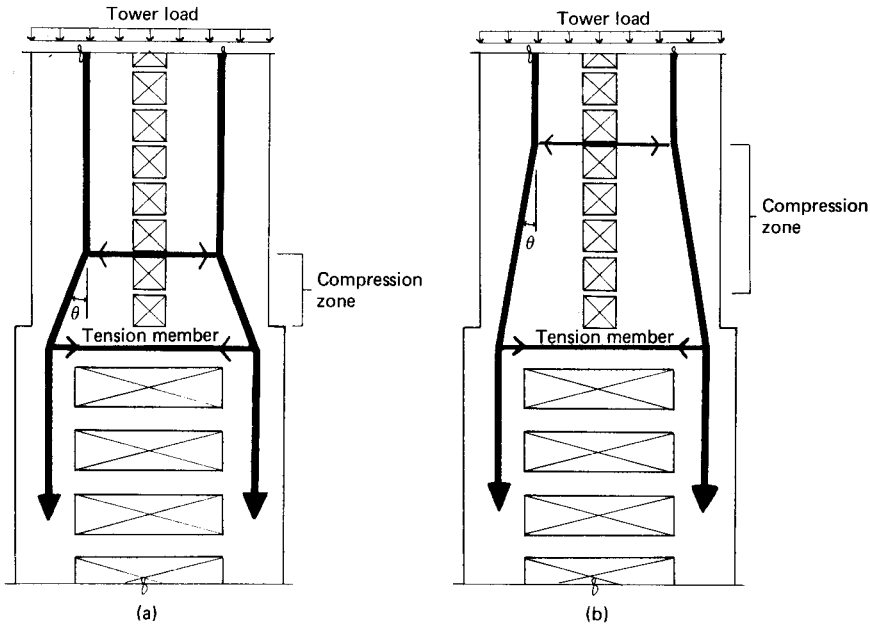

Figure 10.41 Strength of material approach. (*a*) Large transition angle θ; (*b*) small transition angle θ.

ing motivation for presenting this section in a somewhat detailed manner.

The section begins with a description of the behavior of open-section core by comparing it to a column of solid section. Torsion analysis of single-core structures is considered by treating the cantilever core as a column with a seventh degree of freedom $d\theta/dz$ at each end to represent the warping. Practical example and experimental investigations on model core structures are given. Torsion analysis of a steel core is presented by idealizing the core as an open section. A finite element technique for determining the warping stiffness of floor systems is given followed by a method which allows the core and its warping action to be analyzed by a computer stiffness program. The method of analysis for single core systems is gradually expanded to analyze shear wall systems consisting of twin cores, multiple cores, and finally any combination of open section and plan shear walls. At each stage, comparisons are made to show the effect of floor system on the magnitude of axial stresses induced by warping.

A good portion of the theoretical material presented in this section is taken from the author's doctoral research work conducted at the Southampton University, U.K. Although the examples considered are for buildings in the 10- to 20-story range, the results are nevertheless

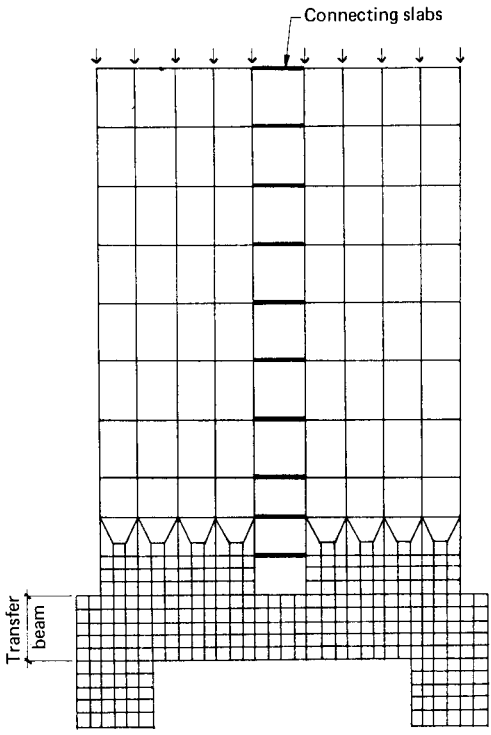

Figure 10.42 Finite element idealization.

useful in gaining an insight into the torsional behavior of tall buildings consisting of open-section shear walls.

A thin-walled structure can be defined as one which is made up of thin plates joined along their edges. A precise quantitative definition for the thinness is not easy to give, except to say that the wall thickness is small compared to other cross-sectional dimensions, which are in turn small compared with the overall length of the structure. Concrete shear walls of this type are extensively used in tall buildings which typically exhibit another characteristic, namely that the walls are open sections, meaning that they do not have closed sections as, for example, box girders.

Compared to closed sections, open-section shear walls possess very little torsional rigidity and, therefore, must be given special consideration in their analysis and design. In a shear wall the shear stresses and strains are relatively much larger than those in solid rectangular columns. When shear walls twist, there is a so-called warping of the cross section, and the usual assumption of bending theory, known as the Bernoulli hypothesis, which states that plane sections remain plane, is not generally satisfied under torsional loads. The term warping is defined as the out-of-plane distortion of the cross section of

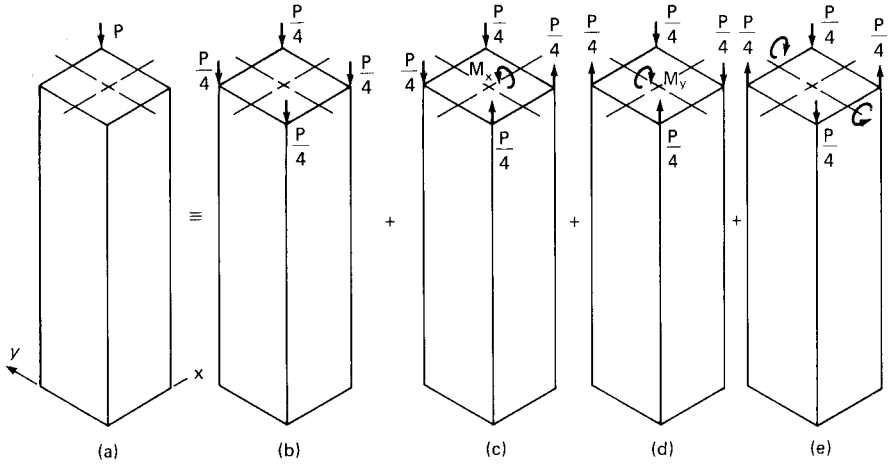

Figure 10.43 Cantilever column of solid cross section. (*a*) Vertical load at corner; (*b*) symmetrical axial loading; (*c*) bending about x axis; (*d*) bending about y axis; (*e*) self-equilibrating loads producing bimoment. *Note:* The resulting warping stresses are negligible.

the wall in the direction of longitudinal axis. Warping of shear walls is greatly inhibited by the interacting restraint offered by the floor slabs and the restraint of the foundations. As a result of this interaction, two types of warping stresses, namely direct stresses in the longitudinal direction and shear stresses in the tangential direction of walls are introduced.

Before attempting the derivation of warping torsion equations for a thin-walled open section, it is instructive to consider qualitatively the difference between its behavior and that of a solid section. A thin-walled beam differs from a beam of solid square section in the manner in which the stresses attenuate along its length. In order to demonstrate the difference in the behavior of these two structures, consider a square cantilever column loaded at that top corner by a vertical load P as shown in Fig. 10.43. The load can be replaced by four sets of loads acting at each corner, which together constitute a system of loads statically equivalent to the applied force P. The first set represents axial loading, the second and third sets represent bending moments about the x and y axes. The resulting axial and bending stresses can be computed by the usual engineer's theory of bending, which assumes that Bernoulli's hypothesis is valid. In the last loading case, the cross sections do not remain plane because the two pairs of loads on opposite faces of the column tend to twist the cross sections in opposing directions. This equal and opposite twisting of the cross section results in warping of the cross section. The last set of loads is, however, statically equivalent to zero and can be ignored by invoking St.

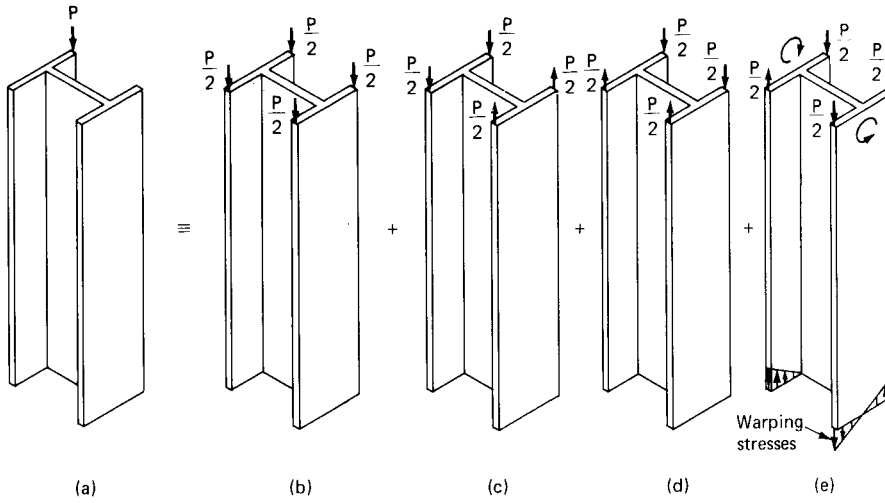

Figure 10.44 I-shaped cantilever column. (*a*) Vertical load at corner; (*b*) symmetrical axial loads; (*c*) bending about x axis; (*d*) bending about y axis; (*e*) self-equilibrating bimoment load. *Note:* Flanges bend in opposite directions producing significant warping stresses.

Venant's principle, which states that the perturbations imposed on a structure by a set of self-equilibrating system of forces affect the structure locally and will not appreciably affect parts of the structure away from the immediate region of applied forces. This statement simply means that the effect of self-equilibrating system of forces can be neglected in the analysis. The stresses caused by these forces attenuate rapidly toward zero and just about vanish at a distance equal to the characteristic dimension of the cross section. The stresses due to the self-equilibrating system of forces can be ignored throughout the whole length of the cantilever except at the very top region.

Now consider an I-shaped shear wall as shown in Fig. 10.44 which has the same overall dimensions as the column with the exception that it is composed of thin plates of thickness t. The first three sets of loads result in stress distributions which can be obtained as before by using the Bernoulli hypothesis. Although the fourth loading is self-equilibrating as before, its effect is far from local. The flanges, which are bending in opposite directions, do so as though they were independent of each other; the resistance offered by the interconnecting web is certainly not as strong as that offered by the mass of material of the solid column. The bending action of the flanges can be thought of as being brought about by equal and opposite horizontal forces parallel to the flanges. The compatibility condition between the web and flanges results in a twisting of the cross section as shown in Fig. 10.45.

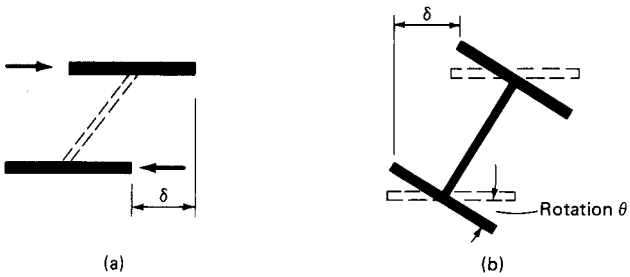

Figure 10.45 Plan section of I-shaped column. (*a*) Displacement of flanges due to bimoment load; (*b*) rotation due to geometric compatibility between flanges and web.

Although the cross section of each of the flanges remains plane, the wall as a whole is subjected to warping deformations. The restraint at the foundation prevents free warping at this end and sets up warping stresses.

The system of skew-symmetric loads which are equivalent to an internally balanced force system arising out of warping of cross section is termed a *bimoment* in thin-walled beam theory. Mathematically it can be construed as a generalized force corresponding to the warping displacement, just as moment and torsion are associated with rotation and twisting deformation, respectively. In the present example bimoment can be visualized as a pair of equal and opposite moments acting at a distance e from each other. Its magnitude is equal to M times e and has units of force times the square of the distance (1b · in^2, kip · ft^2, etc.).

It will be shown later that the warping stresses can be calculated by the relation

$$\sigma_\omega = \frac{B_\omega \omega_s}{I_\omega} \tag{10.27}$$

where B_ω = the bimoment, a term that represents the action of a set of self-equilibrating forces
ω_s = the warping function
I_ω = the warping moment of inertia

The three terms B_ω, ω_s, and I_ω are conceptually equivalent to the moment M, linear coordinate or x or y, and the moment of inertia I encountered in bending problems. Note the similarity between the bending stress as calculated by the familiar relation $\sigma_b = My/I$ and the warping stress formula

$$\sigma_\omega = \frac{B_\omega \omega_s}{I_\omega} \tag{10.28}$$

In open sections the magnitude of warping stresses can be very large and may even exceed the value of bending stress, depending upon the aspect ratios between the height, width, breadth, and thickness of the member. It is shown later that these stresses play a significant role in the design of open-section shear wall structures.

10.8.1 Torsion analysis of single cores

The cross sections of shear walls used for bracing tall buildings are frequently open and are characterized by the fact that their three dimensions, height, width, and thickness, are all of different orders of magnitude.

A central core with access openings can be considered as an example of this system. When such a core is subjected to torsion, it suffers warping displacements and may develop high axial stresses due to restraint at foundation. The St. Venant theory is inadequate for the analysis of such systems and a more appropriate theory which takes into account the axial stresses has to be applied when torsional loads are present.

The central-core-supported structure offers open floor plans free of columns except at the perimeter, allowing partitioning to be placed to suit the individual needs of occupants, with the elevators and other building services and stairs centralized within the core, which serves also as the main structural element for supporting the vertical and horizontal loads. The core invariably has openings for access into elevator lobbies and stairs; therefore, its cross section can be considered open. A further feature of the core is that its height, breadth, and thickness are dimensions of different orders of magnitude. For example, consider a 30-story building with a central core and perimeter columns as shown in Fig. 10.46. Assuming a 12-ft (3.66-m) floor-to-floor height and a 20 by 20 ft (6 by 6 m) core, with 15-in (381-mm) thick walls, the ratios of height to width and width to thickness work out to be rather large—18 and 16, respectively. These two features, namely the openness and the high ratios of characteristic dimensions of the core, prompt the core to behave as a thin-walled beam, causing warping deformation when subjected to torsion.

Torsion in high-rise buildings is usually the result of an eccentric disposal of the horizontal loading, from wind or earthquake, with respect to the center of reaction of the shear-resisting elements. This eccentricity can be caused by an orthogonally symmetrical core being offset horizontally from the center of area of the building elevation, but

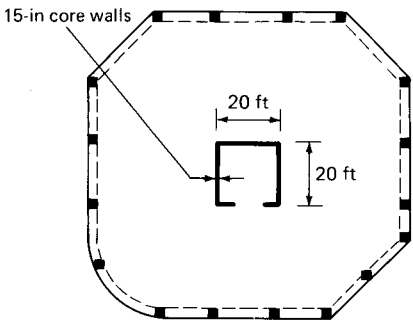

Figure 10.46 Plan of a 30-story building.

more often it is caused by asymmetry in the cross section of the core due to access openings.

A random examination of plans of high-rise buildings most often reveals that the structures exhibit one or the other type of asymmetry of the lateral-load-resisting elements. Even for perfectly symmetrical buildings, it is a good practice to consider some eccentricity of wind and seismic load because of their turbulent and variable natures. For seismic design many building codes such as the SEAOC and the UBC stipulate that buildings should be designed for an accidental torsion with a minimum eccentricity of 5 percent of the building width, even though there may not be any computed eccentricity of the loading because examination of buildings after earthquakes has revealed ample evidence of torsional damage to buildings.

Accidental wind torsion has also started receiving considerable attention in recent years. For example, the city of Houston building code stipulates that unless wind tunnel procedures are used in determining wind loads, the primary frame should be designed to resist a torsional moment caused by 50 percent of wind load acting on half of the windward and leeward faces, with the full wind loading acting on the remaining portions of the windward and leeward faces.

Many cases arise in practice where external constraints cause some sections of the core to remain plane. For example, heavy foundation at the base of the core prevents warping, giving rise to warping axial stresses. These stresses vary along the height and are accompanied by transverse shear stresses which also vary from section to section. The transverse shear stresses are in addition to tangential shear stresses caused by pure twisting and jointly resist the applied torque at any section. At the foundation, since the warping of the cross section is prevented, the shear stress distribution is solely due to transverse bending of the core. On the other hand, at the free end, since there are no applied loads other than the torque, the shear stress distribution corresponds to pure tangential stresses. Anywhere in between these two extremes, the shear stress distribution is obviously a combination

of both transverse and tangential stress distributions. A similar type of behavior is exhibited by the core without cross-sectional restraints when it is subjected to an axially varying torque.

A theory which can account for warping was developed by Vlasov; in what follows a brief derivation of the fundamental equation and a description of the method of solution is given, with a view to introducing the terminology. The following notation is used in the derivation of warping torsion equation.

M_1	Torsional moment due to constrained torsion shear stresses
M_2	Torsional moment due to St. Venant torsion shear stresses
M	Total torsional moment
z, s	Orthogonal system of coordinates
u	Longitudinal displacement due to warping along the z axis
v	Transverse displacement along the tangent to the profile
θ_z	Torsional rotation at z
ω_s	Sectorial area
$\sigma_{z,s}$	Longitudinal stress due to warping
ϵ	Strain
E	Modulus of elasticity of the material
G	Modulus of rigidity of the material
μ	Poisson's ratio of the material
γ	Shear strain
τ	Shear stress
t_s	Thickness of thin-walled beam
I_ω	Warping moment of inertia
m_z	Intensity of applied torque
B_z	Bimoment
l	Length of the beam
J	St. Venant torsion constant
k	Characteristic parameter, $l\sqrt{(1-\mu^2)GJ/EI_\omega}$
Z_z	Action matrix
G_0	Distribution matrix
Z_0	Initial boundary restraint matrix
C_1, C_2, C_3, C_4	Constants of integration

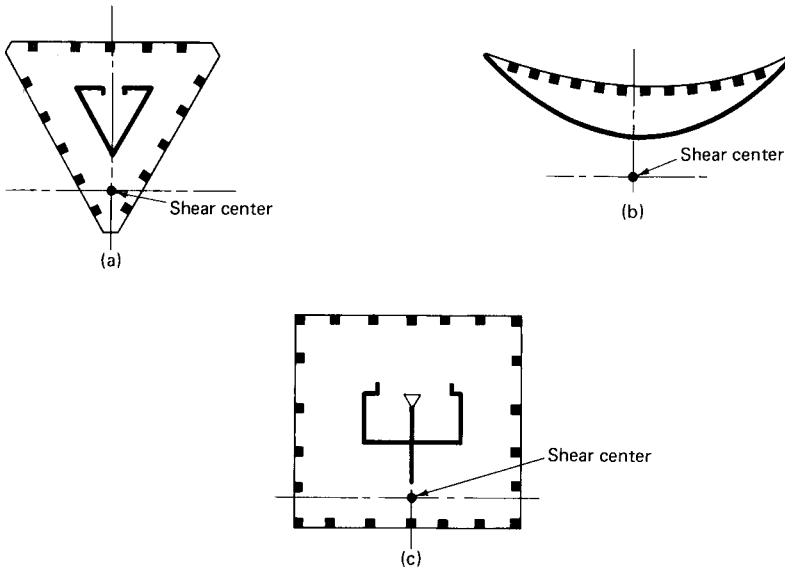

Figure 10.47 Example of core structures with eccentric disposal of shear center.

Constrained torsion equation. Consider the elementary core structures illustrated in Fig. 10.47. The conservative assumption is made that the out-of-plane stiffness of the floor slabs can be neglected, as also can the bending stiffness of any beams connecting the two return walls. A horizontal load distributed uniformly in the vertical direction and of unit intensity is taken to act in the direction of the x axis. The assumed loading is disposed eccentrically with respect to the shear center of the core, and therefore produces in addition to bending about the y axis, a twisting of the core about the z axis.

During twisting, the cross sections of the core undergo distortion, with different points on the cross section suffering different displacements along the longitudinal axis of the core. If this distortion or warping as it is called is not free to take place, longitudinal stresses directed along the z axis develop in the cross section. The foundation for a high-rise core is usually stiff and can be considered to restrain almost completely the vertical movement of the relatively light walls. The resulting axial stresses in general are not restricted to the vicinity of the foundation as assumed in St. Venant torsion theory.

In Vlasov theory two fundamental assumptions are made:

1. The cross section is completely rigid in the transverse direction.
2. The shear strain of the middle surface is negligible.

These two assumptions are almost completely satisfied in a practical core structure. The high in-plane stiffness of the floor slabs practically

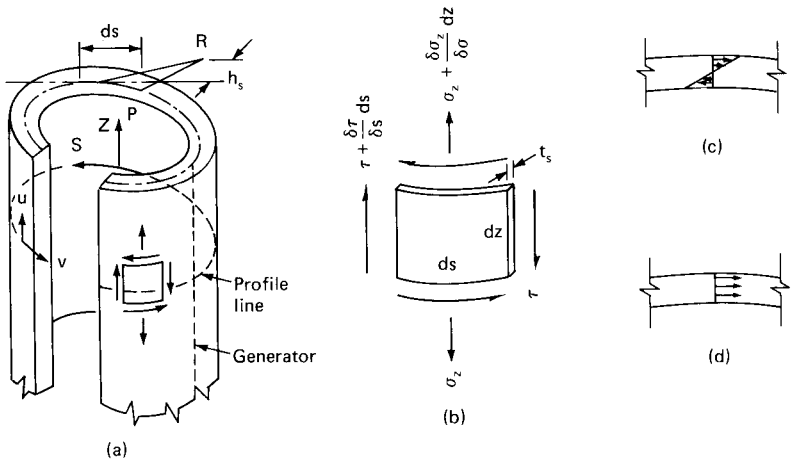

Figure 10.48 Open tube. (*a*) Coordinate system; (*b*) equilibrium of element *dz ds* on the middle surface; (*c*) St. Venant torsion shear stresses; (*d*) constrained torsion shear stresses.

prevents distortion of the core at frequent intervals along its length, and the second assumption is valid for all but very low buildings.

Consider an open tube shown in Fig. 10.48. An orthogonal system of coordinates *z,s* is chosen, consisting of a generator and the middle line of the profile (Fig. 10.48*a*). The origin for the coordinate *z* is taken at the base, and any generator is taken as the origin for the curvilinear coordinate *s*. Let θ_z be the angle of rotation of the profile at a distance *z* from the base. This rotation is in the *xy* plane and is measured with respect to any arbitrary center of rotation *R*.

Consider the displacements of any point *p* on the middle surface of the tube. The transverse displacement *v* in the direction of the tangent to the profile line is given by

$$v_{z,s} = \theta_z h_s \tag{10.29}$$

where h_s is the perpendicular distance from the tangent at *p* to the center of rotation *R* (Fig. 10.48). If $u_{z,s}$ is the longitudinal displacement along the generator, then considering the displacements at *p*, of an element *dz ds* (Fig. 10.48*b*), lying on the middle surface, the condition of zero shear strain is given by the relation

$$\gamma = \frac{\partial u}{\partial s} + \frac{\partial v}{\partial z} = 0$$

$$\frac{\partial u}{\partial s} + h_s \frac{d\theta}{dz} = 0 \tag{10.30}$$

Integrating,

$$u_{z,s} = -\int^{s} h_s \, ds \frac{d\theta}{dz} \tag{10.31}$$

The integral s is taken along the profile from an arbitrary point to the point p for which the longitudinal displacement is required. The product $h_s \, ds$ is equal to twice the area of the elementary triangle whose base and height are equal to ds and h_s, respectively, and is usually given the symbol $d\omega$.

$$u_{z,s} = -\int^{s} \frac{d\theta}{dz} \, d\omega \tag{10.32}$$

$$= -\frac{d\theta}{dz} \omega_s \tag{10.33}$$

Since the displacement $u_{z,s}$ changes along the distance z, the strain ε_z is given by

$$\varepsilon_z = \frac{\partial u}{\partial z} = -\frac{d^2\theta}{dz^2} \omega_s$$

Hence, corresponding stress $\sigma_{z,s}$ is

$$\sigma_{z,s} = \frac{E}{1 - \mu^2} \varepsilon_z$$

$$= \frac{E}{1 - \mu^2} \frac{d^2\theta}{dz^2} \omega_s \tag{10.34}$$

The origin of the coordinate s can now be found from the condition that there is no applied vertical load on the tube, i.e.,

$$\int_0^s \sigma_{z,s} \, t_s \, ds = 0 \tag{10.35}$$

where t_s is the thickness of the tube.

The longitudinal stresses $\sigma_{z,s}$ are accompanied by shear stresses and are found from the consideration of equilibrium of an element $t \, ds \, dz$ in the z direction (Fig. 10.48*b*)

$$t_s \frac{\partial \sigma}{\partial z} + \frac{\partial t_s \tau}{\partial s} = 0 \tag{10.36}$$

$$\tau = \frac{E}{1 - \mu^2} \frac{d^3\theta}{dz^3} \int_0^s \omega_s \, ds \tag{10.37}$$

Using now the condition of zero external shear forces, it may be deduced that the origin of the arbitrary center of rotation R is at the shear center. This determines completely the total stress distribution in terms of the derivatives of θ.

The torque M_1 carried by the membrane shear stresses (Fig. 10.48*d*) which accompany the longitudinal stresses is given by

$$M_1 = \int_0^s \tau t_s h_s \, ds = -\frac{E}{1 - \mu^2} \frac{d^3\theta}{dz^3} \int_0^s \omega_s^2 \, t_s \, ds \tag{10.38}$$

The quantity

$$\int_0^s \omega_s^2 \, t_s \, ds$$

is a structural constant, the so-called warping moment of inertia, and is usually denoted by I_ω.

Hence

$$M_1 = -\frac{-E}{1 - \mu^2} I_\omega \frac{d^3\theta}{dz^3} \tag{10.39}$$

The torque M_2 carried by St. Venant shear stresses (Fig. 10.48*c*) is given by

$$M_2 = GJ \frac{d\theta}{dz}$$

where GJ is the St. Venant torsional rigidity of the section.

The total torque $M = M_1 + M_2$ is then given by

$$M = \frac{-EI_\omega}{1 - \mu^2} \frac{d^3\theta}{dz^3} + GJ \frac{d\theta}{dz} \tag{10.40}$$

Differentiating with respect to z, Eq. (10.40) becomes

$$\frac{EI_\omega}{1 - \mu^2} \frac{d^4\theta}{dz^4} - GJ \frac{d^2\theta}{dz^2} = m_z \tag{10.41}$$

Using notation

$$k = l\sqrt{\frac{(1-\mu^2)GJ}{EI_\omega}}.$$

Eq. (10.41) can be written

$$\frac{d^4\theta}{dz^4} - \frac{k^2}{l^2}\frac{d^2\theta}{dz^2} = m_z \tag{10.42}$$

Equation (10.42) is the differential equation of constrained torsion and its solution yields the complete stress distribution.

Longitudinal stresses and bimoment. Consider the relation between the longitudinal stresses and warping,

$$\sigma_{z,s} = -\frac{E}{1-\mu^2}\frac{d^2\theta}{dz^2}\omega_s$$

Multiplying both sides of this equation by $\omega_s t_s$ and integrating over the whole profile gives

$$\int \sigma_{z,s}\omega_s t_s\, ds = -\frac{E}{1-\mu^2}\frac{d^2\theta}{dz^2}\int \omega_s^2\, t_s\, ds$$

and since

$$\int \omega_s^2\, t_s\, ds = I_\omega$$

$$\int \sigma_{z,s}\,\omega_s t_s\, ds = -\frac{E}{1-\mu^2}\frac{d^2\theta}{dz^2} I_\omega \tag{10.43}$$

The quantity

$$\int \sigma_{z,s}\,\omega_s t_s\, ds$$

is a generalized force called the bimoment and is represented by B_z. Thus

$$B_z = -\frac{EI_\omega}{1-\mu^2}\frac{d^2\theta}{dz^2}$$

From Eq. (10.34)

$$\frac{E}{1-\mu^2}\frac{d^2\theta}{dz^2} = \frac{\sigma_{z,s}}{\omega_s}$$

$$\therefore \sigma_{z,s} = \frac{B_z \omega_s}{I_\omega} \tag{10.44}$$

Hence the magnitude of bimoment at z and the distribution of the sectorial area over the profile completely determine the longitudinal stresses.

Solution of the differential equation. Using the notation $f_{(z)} = m(1-\mu^2)/EI_\omega$, Eq. (10.42) can be written as

$$\frac{d^4\theta}{dz^4} - \frac{k^2}{l^2}\frac{d^2\theta}{dz^2} - f_{(z)} = 0 \tag{10.45}$$

The solution is of the form,

$$\theta_{(z)} = C_1 + C_2 z + C_3 \sinh\frac{k}{l}z + C_4 \cosh\frac{k}{l}z + \bar{\theta}_z \tag{10.46}$$

Differentiating Eq. (10.46) and using Eqs. (10.40) and (10.44), equations for the displacements θ_z and θ_z' and the two forces B_z and M_z can be written thus,

$$\theta_z = C_1 + C_2 z + C_3 \sinh\frac{k}{l}z + C_4 \cosh\frac{k}{l}z + \bar{\theta}_z$$

$$\theta_z' = C_2 + C_3\frac{k}{l}\cosh\frac{k}{l}z + C_4\frac{k}{l}\sinh\frac{k}{l}z + \bar{\theta}'_z \tag{10.47}$$

$$B_z = -GJ\left[C_3 \sinh\frac{k}{l}z + C_4 \cosh\frac{k}{l}z + \frac{l^2}{k^2}\bar{\theta}'_z\right]$$

$$M_z = GJ\left[C_2 + \bar{\theta}'_z - \frac{l^2}{k^2}\bar{\theta}'''_z\right]$$

The constants C_1, C_2, C_3, and C_4 can be determined from the two boundary conditions at each end. However, calculations are greatly simplified if instead of the arbitrary constants C_1, C_2, C_3, and C_4,

displacement and force boundary conditions, in terms of θ, θ', B, and M, are used in Eqs. (10.47). If θ_0, θ'_0, B_0, and M_0 are the two sets of displacements and forces at the section $z = 0$, and if there are no applied forces, the constants C_1, C_2, C_3, and C_4 from Eq. (10.47) are given by

$$C_1 = \theta_0 + \frac{1}{GJ} B_0$$

$$C_2 = \frac{1}{GJ} M_0$$

$$C_3 = \frac{l}{k} \theta'_0 - \frac{l}{k} \frac{1}{GJ} M_0 \tag{10.48}$$

$$C_4 = \frac{-1}{GJ} B_0$$

Substituting these in Eqs. (10.47) and writing in matrix form the general equations for the four quantities, θ, θ', B, and M will be of the form

$$\begin{bmatrix} \theta_z \\ \theta'_z \\ \frac{B_z}{GJ} \\ \frac{M_z}{GJ} \end{bmatrix} = \begin{bmatrix} 1 & \frac{l}{k}\sinh\frac{k}{l}z & 1-\cosh\frac{k}{l}z & z-\frac{l}{k}\sinh\frac{k}{l}z \\ 0 & \cosh\frac{k}{l}z & \frac{-k}{l}\sinh\frac{k}{l}z & 1-\cosh\frac{k}{l}z \\ 0 & \frac{-l}{k}\sinh\frac{k}{l}z & \cosh\frac{k}{l}z & \frac{l}{k}\sinh\frac{k}{l}z \\ 0 & 0 & 0 & 1 \end{bmatrix} \begin{bmatrix} \theta_0 \\ \theta'_0 \\ \frac{B_0}{GJ} \\ \frac{M_0}{GJ} \end{bmatrix} \tag{10.49}$$

or in matrix notation, $Z_z = G_0 Z_0$, where Z_z is the action matrix, G_0 the distribution matrix, and Z_0 the initial boundary restraint matrix. If, in addition to the boundary restraints, concentrated forces and displacements are applied at any section $z = t$, then, using the principle of superposition, the expressions for the actions at any section $z (t \leq z \leq d)$ will be of the form

$$Z_{(z)} = G_{0(z)} Z_0 + G_{(z-t)} Z_t \tag{10.50}$$

Where $G_{(z-t)}$ is of the same form as $G_{0(z)}$, except that the argument $(z - t)$ replaces z, and z_t refers to the restraint matrix at $z = t$. The solution represented by Eq. (10.50) can easily be extended to other loading cases, such as several loads applied at various sections and distributed loads, by simple superposition and integration, respectively.

Calculation of rotation and stresses.

Sectorial properties. For the calculation of rotation and stresses, it is first necessary to determine the sectorial properties, namely, the function ω_s and the sectorial moment of inertia I_ω. These are readily calculated for the core by using the method well documented in Ref. 44. For the assumed dimensions of the core shown in Fig. 10.49*a*, the results for ω_s and I_ω are as indicated in Fig. 10.49*b* through *d* and as calculated in the following equation.

$$I_\omega = \int_0^s \omega^2 t\, ds = 2t\left[\frac{d^3e^2}{24} + \frac{d^2e^3}{12} + \frac{d^2(b-e)^3}{12} + \frac{c}{6}\left\{\frac{d}{2}(b-e)\cdot\left[\frac{3d}{2}(b-e) + c(b+e)\right] + \left[\frac{d}{2}(b-e) + c(b+e)\right]\cdot\left[\frac{3d}{2}(b-e) + 2c(b+e)\right]\right\}\right]$$

Boundary conditions. The horizontal loading on the core is replaced by a statically equivalent system of loads parallel to the x axis and acting along the shear center axis and a uniform twisting moment. The simple beam theory is used to analyze the effects of loads through the shear center axis.

The effect of the uniformly distributed twisting moment m_z is accounted for by considering the restraint vector at $z = t$ as $[0, 0, 0, m_z]$ and integrating the last column of the distribution matrix G_{z-t} of Eq. (10.50) between the limits 0 and l.

Assuming the core to be completely rigid at the base, the boundary conditions at the ends of the core are

$$\begin{aligned} &\text{Bottom:} \quad \theta_0 = 0 \quad \text{and} \quad \theta_0' = 0 \\ &\text{Top:} \quad B_l = 0 \quad \text{and} \quad M_l = 0 \end{aligned} \tag{10.51}$$

Using these boundary conditions in the general Eqs. (10.50), the expressions for the four quantities θ_z, θ_z', B_z, and M_z are written. The

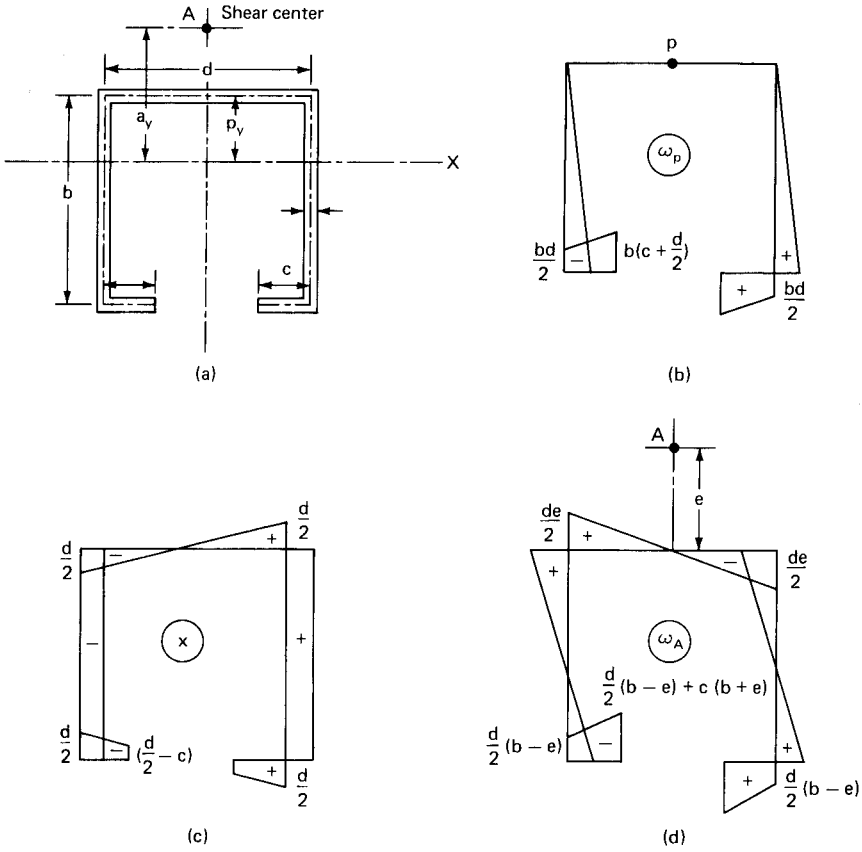

Figure 10.49 (*a*) Core dimensions; (*b*) diagram of sectorial areas ω with respect to arbitrary point P; (*c*) diagram of x coordinate; (*d*) principal sectorial areas ω.

two quantities θ_z and B_z which are a measure of deflection and stresses will be

$$\theta_z = \frac{-m}{GJ \cosh k}\left[\frac{-l^2}{k^2} - \frac{l^2}{k}\sinh k + z\left(l - \frac{z}{2}\right)\cosh k + \frac{l^2}{k^2}\cosh\frac{k}{l}z + \frac{l^2}{k^2}\cosh\frac{k}{l}z + \frac{l^2}{k}\sinh\frac{k}{l}(l-z)\right] \tag{10.52}$$

$$B_z = \frac{-ml^2}{k^2 \cosh k}\left[\cosh k - \cosh\frac{k}{l}z - \frac{k \sinh k}{l}(l-z)\right] \tag{10.53}$$

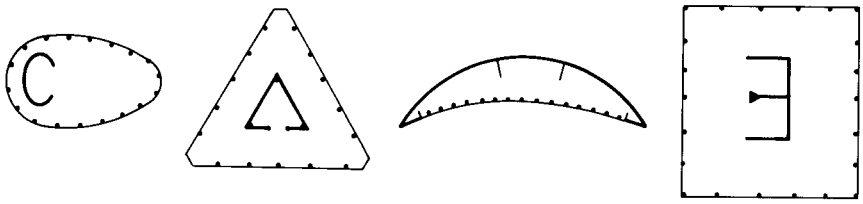

Figure 10.50 Examples of open-section shear wall structures.

Equations (10.52) and (10.53) are basic equations which are also applicable in the analysis of a wide variety of complex-shaped shear walls. Some examples of these are shown in Fig. 10.50. As long as the conditions of rigid base, rigid contour, and openness are satisfied, these equations, together with the sectorial properties, completely determine the variation of the longitudinal stresses and rotations.

Practical example. To show the order of magnitude of stresses under consideration, the results of an analysis made of the torsion and bending of a simple practical core are given. The assumed dimensions of and loading on the structure, the rotation, the variation of bimoment, and warping stresses at the base are indicated in Figs. 10.51*a* to *d*, respectively. The bending stresses due to the horizontal load are shown in Fig. 10.51*e* for purposes of comparison with the constrained torsion stresses. Figures 10.51*f* and *g* show the warping and bending stresses when the core is offset from the center of the building.

Experimental investigation. In order to verify the validity of the warping theory, a perspex model of a simple core was tested by the author at the University of Southampton, England. Figure 10.52 shows the torsion experimental model. The dimensions of the model, shown in Fig. 10.53, were chosen to represent to scale as practical a core structure as possible. It is seen that for a story height of 10 ft (3.04 m), which is typical for an apartment or a hotel building, the scale between a prototype building and the model works out to be 1:30. The model can therefore be considered to represent approximately to scale a 15-story building.

After considering various materials, such as araldite, sindanyo (asbesto cement), and aluminum, perspex was chosen as the most suitable in view of relatively low value of modulus of elasticity and the speed of construction in spite of its creeping properties. The creeping errors were minimized by taking readings at 2 minute intervals after each loading. The load was applied in four equal increments and was

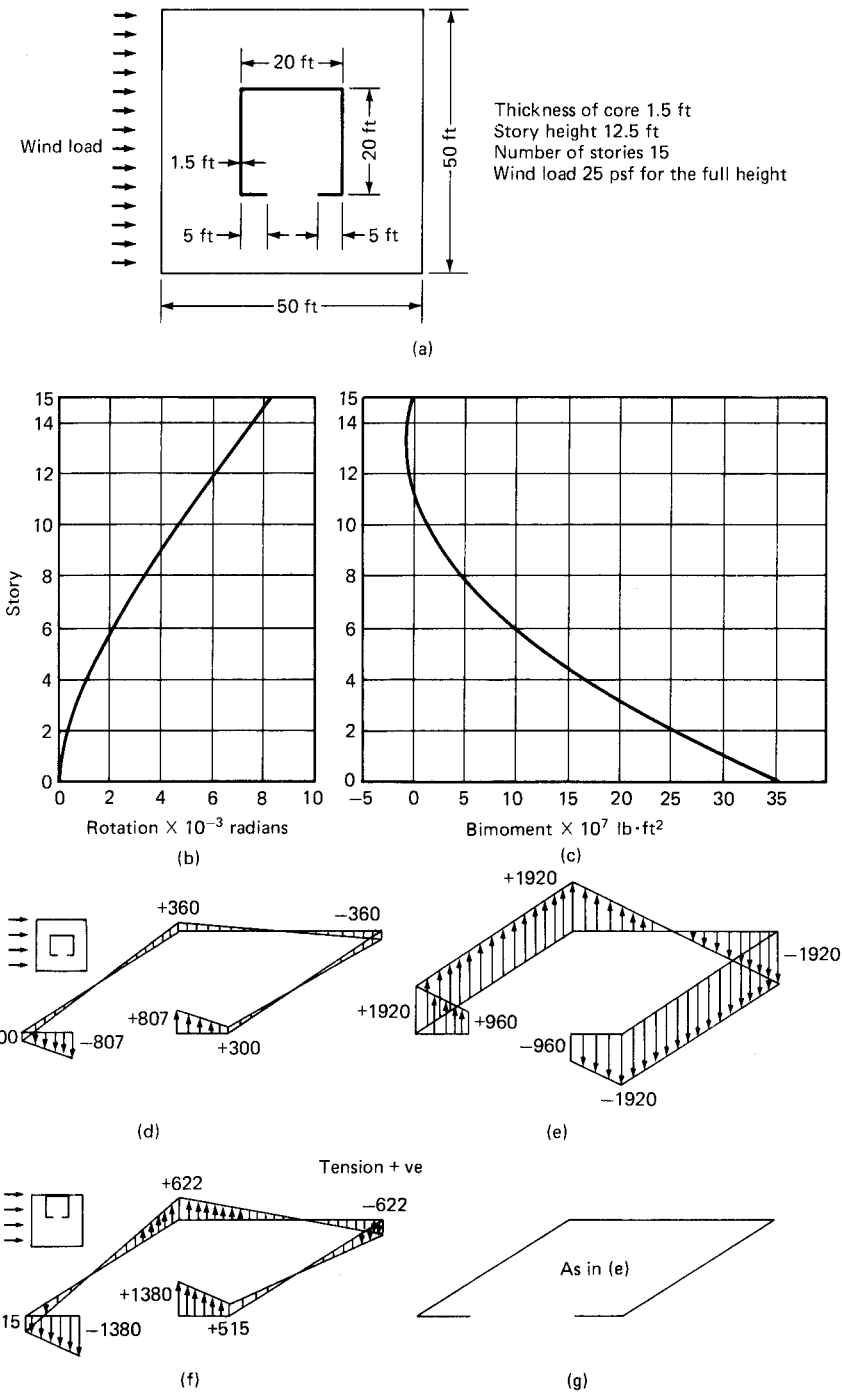

Figure 10.51 Example problem. (*a*) Dimensions and loading; (*b*) rotations; (*c*) bimoment variation; (*d*) warping stresses (core at center), in psi; (*e*) bending stresses, in psi; (*f*) warping stresses (offset core), in psi; (*g*) bending stresses.

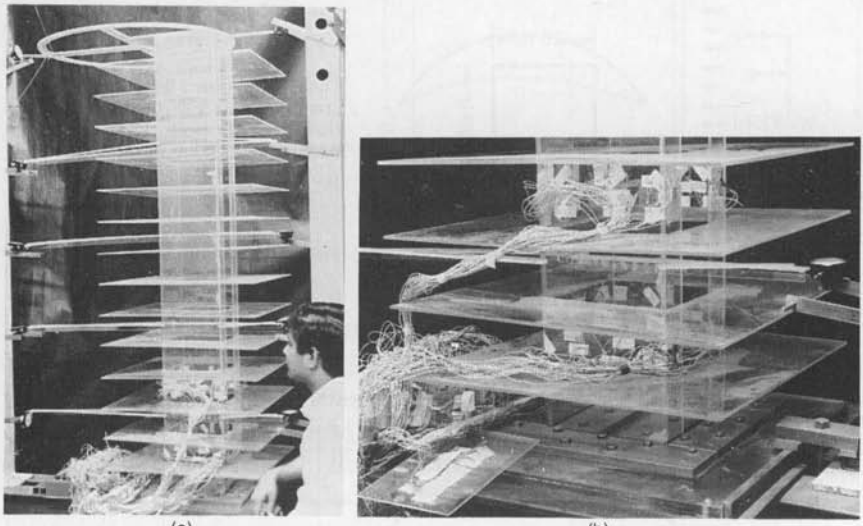

Figure 10.52 (*a*) Torsion experiment model of a high-rise core with cantilevering of floor slabs; (*b*) detail of model at base.

of such magnitude that the strains and deflections produced were large enough for accurate measurements, but were sufficiently small for creep effects to be ignored.

The model was tested under two load conditions.

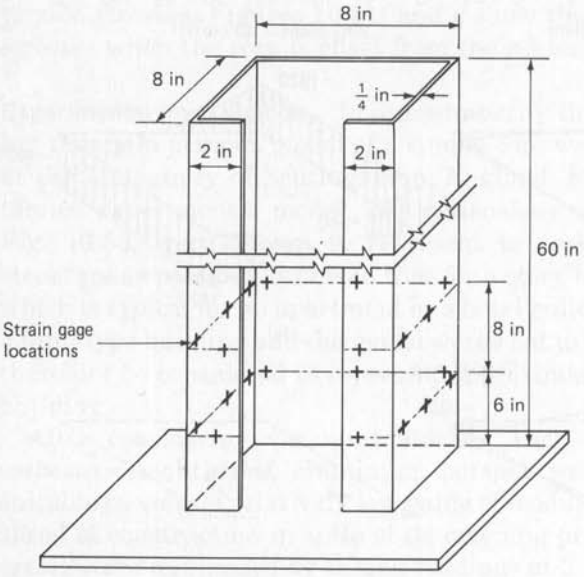

Figure 10.53 Model dimensions and strain gauge locations.

1. A horizontal point load at the top was applied by a screw jack through a proving ring. The load was positioned so that it produced both bending and torsion of the model. The experiments were conducted for different eccentricities of the load.
2. A pure twisting moment in the plane of the top floor was applied by means of dead weights, pulleys, and cords.

In an effort to achieve complete fixity at the base giving boundary conditions $\theta = 0$ and $\theta' = 0$, the model was fixed to a 0.5-in (1.25-cm) thick perspex baseplate by "sinking" the walls into the full depth of the plate and filling the central hole with a tight-fitting perspex sheet bonded into position. The base was then rigidly secured to a steel beam by suitable clamps.

Electrical-resistance strain gauges were attached to the model at locations shown in Fig. 10.53 and were selected to provide symmetry checks. For the point load experiments, strain gauges were present at only one level, while for the second load condition they were at two, as shown in Fig. 10.53. The dummy strain gauges were fixed on a separate piece of perspex of about the same thickness as the model. Rotations were calculated by measuring the deflections at the end of rigid arms fixed to the model at four levels. All experiments were repeated by reversing the load direction, and in each case a good symmetrical check on the results was obtained. The experiments were performed in a constant-temperature room to minimize the effects of temperature variation.

The value for the modulus of elasticity was obtained by conducting a simple bending test on a perspex beam of dimensions 0.25 by 1 by 12 in (6.35 by 25.4 by 305 mm). Two symmetrical loads were applied at the third-span positions, and from the deflections measured at the center of span, the value for E was calculated to be 425 kips/in^2 (2930 MPa) at a temperature of 70°F (21.1°C). The value for Poisson's ratio, being relatively less important, was taken as 0.35 from the manufacturer's handbook.

Discussion of results. Figure 10.54 shows the comparison of the theoretical stresses with the experimental values for various locations of the applied load on the model. In all cases the results were found to agree very closely with those predicted by the torsion theory (within 5 percent).

Figure 10.55 shows the comparison of the stresses for the applied torsion loading. The longitudinal variation of bimoment and the comparison of the rotations are shown in Figs. 10.56 and 10.57, respectively. It is seen that the measured stresses compare well with the theoretical predictions except at the intersection of the flanges and return walls. The discrepancy could be due to the very high stress gradient at these sections and lack of proper adhesion between the two

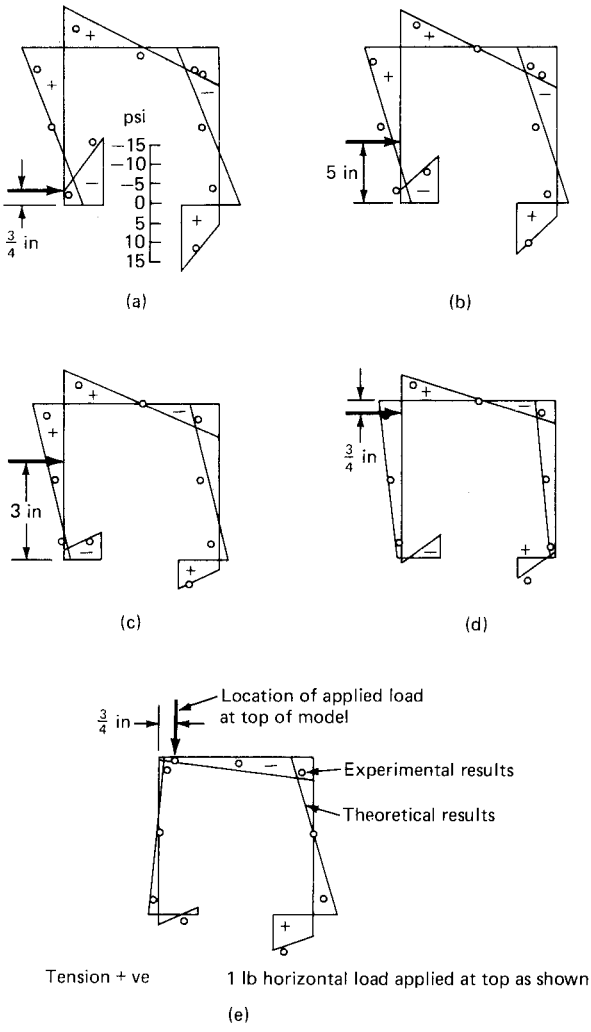

Figure 10.54 Comparison of stresses under applied horizontal load.

plates, which could have resulted in considerable reduction in the stress level.

Figure 10.56 shows that the rotations predicted by the torsion theory are in very good agreement with the experimental values. Comparing the stresses for the core (Fig. 10.51*d* through *g*), it is seen that the magnitude of the longitudinal stresses due to torsion are indeed alarming. Even allowing for the stiffness of other members such as columns, it is unlikely that the stresses will be reduced substantially unless, of course, the core is enclosed in a torsionally stiff tube

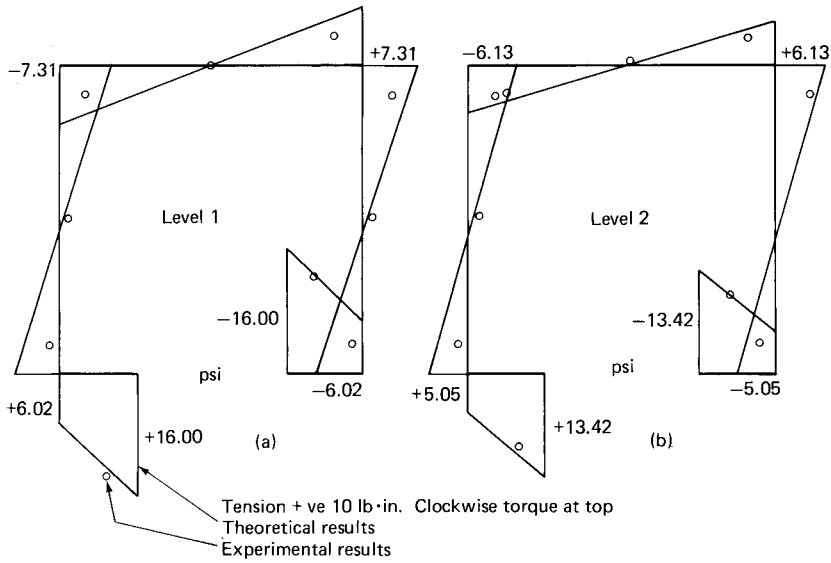

Figure 10.55 Comparison of stresses (in psi) under applied torsional load. (*a*) Stresses at level 1; (*b*) stresses at level 2.

structure. In the absence of such a stiff exterior shell, the need for a torsion analysis cannot be overemphasized.

Torsion analysis of cores in steel buildings. The behavior of braced cores in steel buildings can be predicted with sufficient accuracy by using the nonuniform torsion theory. For example, consider the typical floor plan of a 30-story steel building as shown in Fig. 10.58*a*. Assume that wind

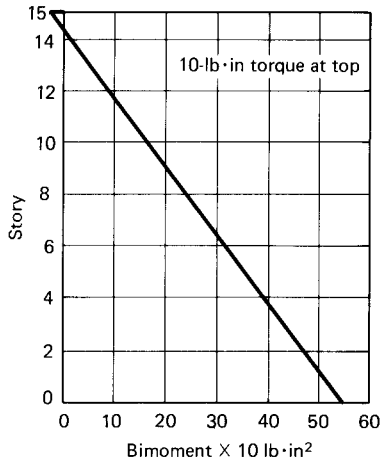

Figure 10.56 Variation of bimoment.

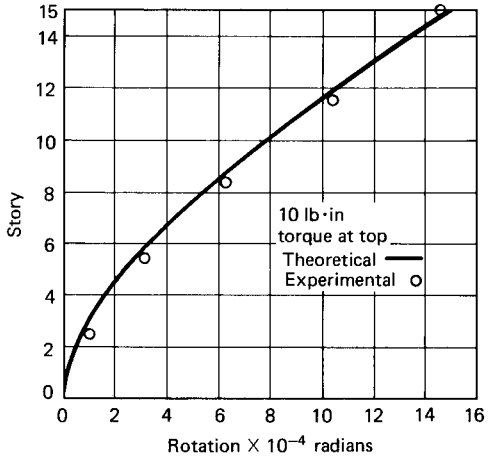

Figure 10.57 Comparison of rotations.

resistance is obtained by X-bracing the core all around except between two corridor columns as shown in Fig. 10.58*a*. Without the luxury of bracing all around its perimeter, the core loses much of its torsional resistance and behaves more like an open core as shown in Fig. 10.58*b*. In analyzing the core it will be assumed initially that the warping constraint of beam AB is negligible. These effects are considered later. In the analytical model, the braces can be considered as equivalent solid walls subjected only to shear forces. The normal forces can be assumed to be sustained by the columns alone, acting as vertical ribs. The idealized analytical model is shown in Fig. 10.58*c*. The differential equation of nonuniform torsion is of the form

$$\frac{d^4\theta}{dz^4} - \frac{k^2}{l^2}\frac{d^2\theta}{dz^2} = m_z \frac{1-\mu^2}{EI_\omega} \tag{10.54}$$

where θ = the rotation of the core at section z in the xy plane
k = the nondimensional parameter given by

$$k = l\sqrt{GJ/EI_\omega}$$

l = the height of the core
m_z = the intensity at z of the applied torque
μ = the Poisson's ratio
E = the modulus of elasticity
I_ω = the warping moment of inertia
J = the St. Venant's torsional moment of inertia of the braced core

For the case of no applied external forces, Eq. (10.54) has a solution of the form:

$$\theta_z = \theta_0 + \theta_0' \frac{l}{k} \sinh \frac{k}{l} z + \frac{B_0}{GJ} \left(1 - \cosh \frac{k}{l} z \right) + \frac{M_0}{GJ} \left(z - \frac{l}{k} \sinh \frac{k}{l} z \right) \tag{10.55}$$

where θ_0, θ_0', B_0 and M_0 are the rotation, warping, bimoment, and torque at the section $z = 0$.

In a high-rise core, the boundary conditions at the foundation level are $\theta_0 = 0$ and $\theta_0' = 0$. At the top, since there is no applied torque or bimoment, $M_l = 0$ and $B_l = 0$. Using these conditions in Eq. (10.55), we could write the expressions for the rotation θ_z and bimoment B_z at any section z. For the particular case of uniformly distributed twisting moment m_z, these expressions can be shown to be:

$$\theta_z = -\frac{m}{GJ \cosh k} \left[-\frac{l^2}{k^2} - \frac{l^2}{k} \sinh k + z \left(l - \frac{z}{2} \right) \cosh k + \frac{l^2}{k^2} \cosh \frac{k}{l} z + \frac{l^2}{k} \sinh \frac{k}{l} (l - z) \right] \tag{10.56}$$

$$B_z = -\frac{ml^2}{k^2 \cosh k} \left[\cosh k - \cosh \frac{k}{l} z - k \sinh \frac{k}{l} (l - z) \right] \tag{10.57}$$

Equations (10.56) and (10.57) are basic equations applicable to a wide variety of braced cores. These equations, together with the sectorial properties of the core, completely define the core rotations and axial stresses in the columns.

To show the order of the magnitude of axial forces induced in the columns, the results of torsion and bending analysis for the building shown in Fig. 10.58*a* are presented. A uniform wind load of 20 psf (97.64 kg/m^2) is assumed to act on the x face of the building for the full height. The diagram of principal sectorial coordinates and the sectorial moment of inertia for the core are given in Fig. 10.58*d*.

Conservatively, it will be assumed that the St. Venant's torsional stiffness of the core is small compared to the warping stiffness. The parameter k will be equal to zero, giving simple expressions for rotation and bimoment in the core. The bimoment B_0 at the base will

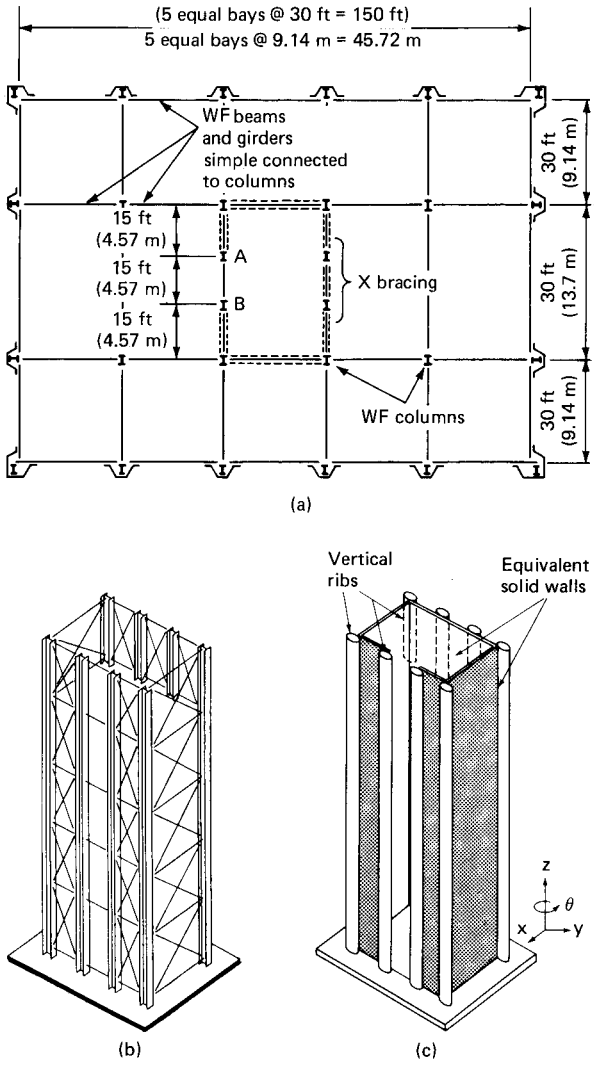

Figure 10.58 Example problem. (*a*) Typical floor plan; (*b*) asymmetrical bracing resulting in an open-section core; (*c*) analytical model for torsion analysis.

be $ml^2/2$ giving a value of 5.5×10^6 kft^2. The axial forces in the columns are calculated from the relation:

$$P_c = \frac{B_0 \omega_c^2 A_c}{I_\omega} \tag{10.58}$$

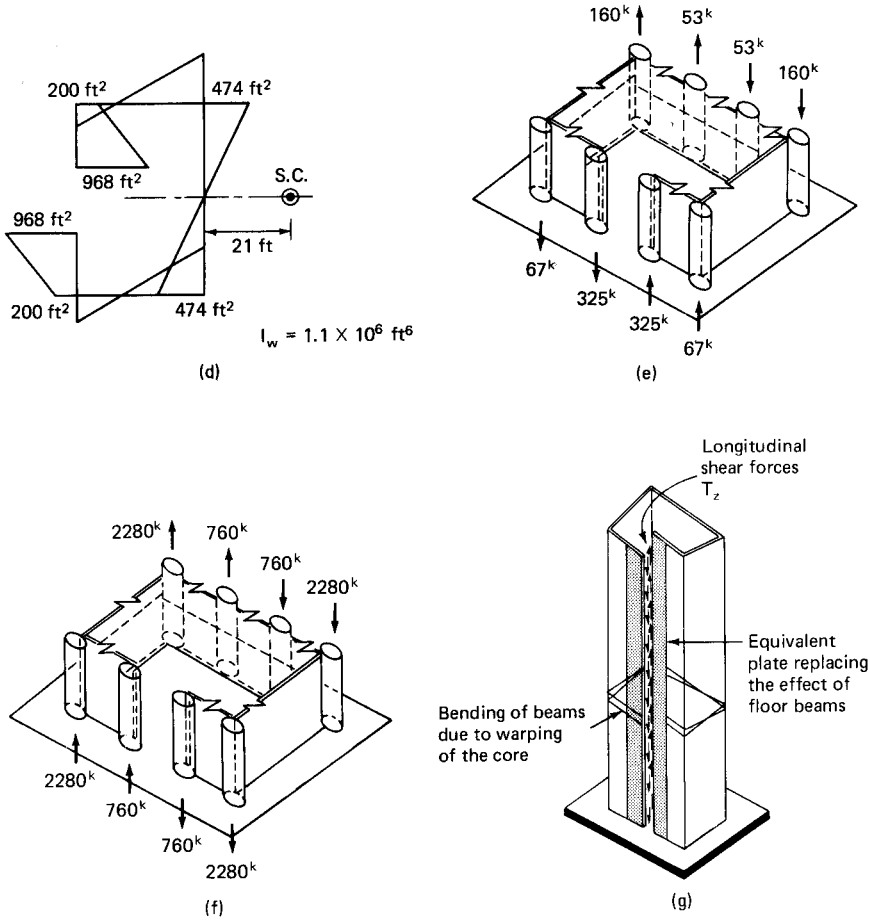

Figure 10.58 (*Continued*) (*d*) Diagram of principal sectorial coordinates; (*e*) axial forces in core columns due to torsion; (*f*) axial forces in core columns due to bending; (*g*) core warping constrained by floor beams.

where A_c is the area of the column under consideration. The calculated values for the example problem are shown in Fig. 10.58*e*. To allow comparison, the axial forces induced in the columns due to bending of the core are shown in Fig. 10.58*f*.

In practice, the unbraced face of a building core is not completely open; it is partially closed at each floor level by beams framing between the columns. The effect of the beams is to constrain the warping deformations of the core. At the same time, the beams themselves are subjected to large shear and bending moments in having to comply with the warping of the core as shown in Fig. 10.58*g*. One approach to the problem, which is explained later in this chapter, is to employ a stiffness method of analysis for the beam and core system by considering each

story segment of the core as a thin-walled beam element and by adding the effect of beams by incorporating the warping stiffness of the beam into the total stiffness of the core. Herein a different method analogous to the continuous connection technique, which can be carried out without the aid of a computer, is presented. Briefly, the procedure consists of replacing the effect of individual beams by a continuous plate equivalent in mechanical properties to the connecting beams.

The structure is rendered statically determinate by introducing an imaginary cut along a line bisecting the imaginary plate. The equilibrium equation is written for the core in terms of external transverse forces and equivalent shear forces applied along the cut edges of the plate. The compatibility condition for the relative displacement at the cut section leads to the differential equation for the core beam assembly. The detailed steps are as follows.

The equilibrium equation for nonuniform torsion of a thin-walled beam subjected to the action of external transverse loads and longitudinal shear forces applied along the edges can be shown to be

$$EI_{\omega} \frac{d^4\theta}{dz^4} - GJ \frac{d^2\theta}{dz^2} = m + \frac{dT}{dz} \Omega \tag{10.59}$$

where m = the external torsional moment at z
dT/dz = the derivative of the shear forces T_z at section z
Ω = twice the area of the enclosed contour between the core and the beam.

The vertical displacement $u_{z,s}$ which results from warping of the thin-walled beam is expressed according to the equation

$$u_{z,s} = -\frac{d\theta}{dz} \omega_s \tag{10.60}$$

where $d\theta/dz$ is the relative warping dependent upon the z coordinate and ω_s is the sectorial area which depends on the location of the point s on the contour.

The relative displacement at the cut section due to warping can be written thus

$$\delta_1 = -\frac{d\theta}{dz} (\omega_L - \omega_k)$$

or

$$\delta_1 = -\frac{\partial\theta}{\partial z} \Omega \tag{10.61}$$

The relative displacement δ_2 at the cut due to the flexibility of the beam under the application of a shear force $T_z h$ is given by

$$\delta_2 = \frac{T_z h}{G}\left(\frac{a^2 G}{12\,EI_b} + \frac{1.2}{A_b}\right) \tag{10.62}$$

where h = the story height
a = the beam length
I_b = moment of inertia of beam about the y axis
A_b = the area of the beam
E and G = the familiar material properties of the beam

For compatibility of displacement, we should have $\delta_1 + \delta_2 = 0$; i.e.,

$$\frac{d\theta}{dz}\Omega + \frac{T_z h}{G}\left(\frac{a^2 G}{12\,EI_b} + \frac{1.2}{A_b}\right) = 0 \tag{10.63}$$

Differentiating with respect to z, we have

$$\frac{d^2\theta}{dz^2}\Omega + \frac{dT}{dz}\frac{h}{G}\left(\frac{a^2 G}{12\,EI_b} + \frac{1.2}{A_b}\right) = 0 \tag{10.64}$$

Substituting for dt/dz in the equilibrium equation and using the notation

$$J_b = \frac{\Omega}{ah}\left\{\frac{a^2 G}{12\,EI_b} + \frac{1.2}{A_b}\right\} \tag{10.65}$$

we get

$$EI_\omega \frac{d^4\theta}{dz^4} - G(J + J_b)\frac{d^2\theta}{dz^2} = m_z \tag{10.66}$$

This equation is identical to Eq. (10.54). Therefore, the two solutions given in Eqs. (10.56) and (10.57) for the rotation and bimoment of the open core can also be used for the solution of the core and beam assembly. For this purpose, it is only necessary to replace St. Venant's torsional constant J by the sum $J + J_b$ as given by Eq. (10.66). The parameter k is now computed from the equation

$$k = l\sqrt{\frac{G(J + J_b)}{EI_\omega}} \tag{10.67}$$

The calculation of bimoment and axial forces follows the procedure outlined earlier.

For purposes of illustration, it is assumed in the problem that a W16 × 26 beam is moment-connected across the corridor columns. The values for J_b and k are found to be respectively equal to 55.38 ft^4 (0.478 m^4) and 19.5. Substituting the value of k in Eq. 10.57, the bimoment at the base is found to be equal to 60 percent of the value obtained for the open core. The resulting values of the column loads are also 60 percent of the values shown in Fig. 10.58*e*.

10.8.2 Interaction of core and floor systems

The interaction of floor slabs and planar shear wall systems subjected to lateral loads has been recognized for over two decades, and methods of analysis are now available which reasonably predict their behavior. The structural analysis and design of such systems is conveniently performed using techniques developed for beam-coupled shear wall systems. It is necessary, however, to assess the effective width of the slab that is assumed to act as a wide coupling beam or to establish the associated coupling stiffnesses for use in a computer stiffness program. Systematic studies using finite element, finite difference, and experimental techniques have been used to obtain useful information on coupling stiffness, effective width, and coupling stresses in uniformly spaced plane walls. However, comparatively little information is available for the structural analysis and design of slab-coupled tall core structures subjected to torsional loads, in spite of the fact that the interacting forces developed in a coupling slab of a core structure are substantially larger than those developed in a cross-wall system. In a cross-wall system the coupling beam or slab resists the independent cantilever action of the walls by developing shear and bending stresses. A slab surrounding a core by comparison is subjected to very high bending and twisting actions due to the warping deformation of the core walls. Guided by the available results for the cross-wall systems and the deformation pattern of the slab around a core, it is natural to expect substantial interacting forces around the core where the slab is rigidly connected to the core walls.

A versatile method of analysis that takes into account the interacting warping forces is necessary for predicting the behavior of such systems. The intermediate floor slabs surrounding a core have two distinct actions: one is to maintain the cross-sectional shape of the core

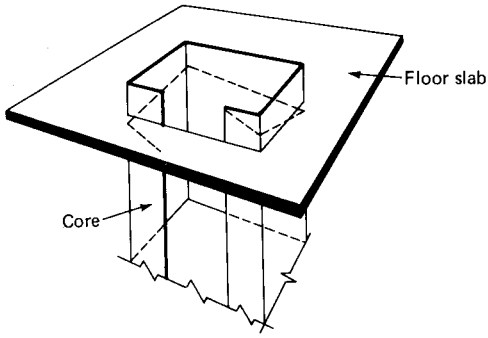

Figure 10.59 Warping deformation of core.

by preventing the transverse deformation, and the other is to restrain the longitudinal deformations of the core due to torsion. The torsion theory tacitly takes into consideration the in-plane action of the slabs by assuming the cross section of the core to be nondeformable. The out-of-plane stiffness of the slabs, which we will now refer to as *warping stiffness*, is usually ignored in the torsion theory, even though Vlasov's work deals with certain simple cases of internal diaphragm systems. These simple systems are, however, rare in practical core structures and invariably the floor slabs enclose the cores, thus giving rise to external diaphragm systems.

Such an external diaphragm system is shown in Fig. 10.59, in which the warping deformation of the core is also shown. It is seen from Fig. 10.60, which shows the deformation of the slab, that a high degree of restraint is offered by the out-of-plane bending and twisting of the floor slab in response to the warping deformation of the core. Even for a cantilever slab with free edges, the forces at the slab-core junction are likely to be high, indicating that for slabs connected to other vertical elements such as exterior columns, the interacting forces are even higher.

In this section we will consider the torsion analysis of a single-core system which takes into account the warping stiffness of the floor slab.

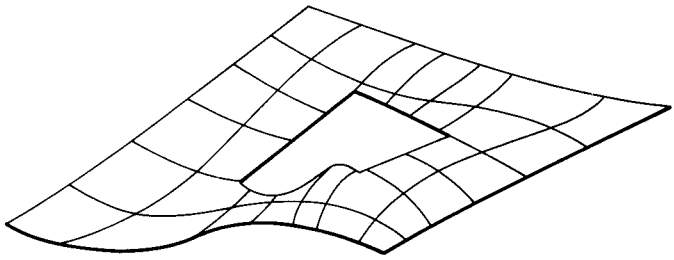

Figure 10.60 Warping deformation of floor slab.

A finite element method is employed for evaluating the warping stiffness of the floor slab, which is then incorporated into a stiffness method analysis of torsion of the core system. A comparison of analytical results conducted on a model core structure is presented with comments on convergence characteristics of finite elements.

Warping stiffness of the slab. The cross section of the core subjected to torsion suffers two distinct deformations, namely, the torsional rotation about the z axis and the warping distortion of the plane section. The distortion or the warping of the cross section is due to the longitudinal displacements of its points, and its variation across the section is given by the relation

$$u_{z,s} = -\theta_z' \omega_s \tag{10.68}$$

It is seen from Eq. 10.68 that θ_z' is a measure of the cross-sectional distortion and can be considered as a generalized displacement. A unit value of θ_z', i.e., a "unit warping displacement," imposed at any section introduces longitudinal displacements at the various points on the cross section varying in a manner similar to the ω_s diagram.

The floor slab offers no direct resistance to the rotational displacement, although its restraint to the warping displacement of the cross section is considerable.

When the core undergoes warping deformation, the floor slab, which is rigidly connected to the core, is forced to bend out of plane in resisting the warping deformation of the core. The transverse displacement of the slab and the warping displacement of the core must be compatible at the profile of the core where the two systems are interconnected. The displacement pattern of the slab at points along its connection to the wall is, therefore, known from the warping displacement of the core. For a unit warping displacement of the core, the slab is displaced along the contact boundary in a manner similar to the warping coordinate diagram ω_s of the core. This displacement gives rise to continuous interactive forces consisting of distributed axial forces and moments at the inner edges of the slab at the profile of the core. The problem of finding the warping stiffness of the slab, therefore, reduces to the determination of these interactive forces and moments. Incorporation of these forces and thus the warping stiffness of the slab in the torsion analysis of the core is greatly simplified by mathematically converting these forces into a bimoment function, as will be shown shortly.

To mathematically study the slab-core interaction, it is useful to consider the slab as an isolated two-dimensional surface element with an unknown distribution of reactive pressure which produces a known

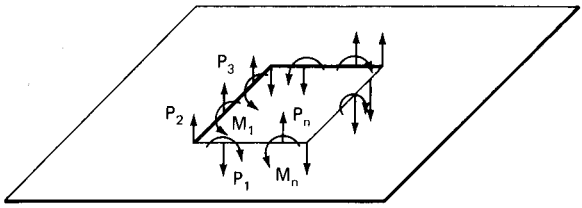

Figure 10.61 Forces and moments due to warping of floor slab.

deflection pattern at the core profile. The necessary force displacement relationship defines the required warping stiffness of the slab.

In general, the resulting force system, which consists of concentrated forces $P_1, P_2, P_3, \ldots P_n$, and moments $M_1, M_2, M_3, \ldots, M_n$ applied at the points $k = 1, 2, 3, \ldots, n$ of the cross section, is expressed as a bimoment by the relation

$$B_\omega = \sum_{k=1}^{n} P_k \omega_k + \sum_{k=1}^{n} M_k \frac{\partial \omega_k}{\partial_s} \tag{10.69}$$

where B_ω = the warping stiffness of floor slab

$\sum_{k=1}^{n} P_k \omega_k$ = the summation of the product of concentrated forces and the warping displacement

$\sum_{k=1}^{n} M_k \frac{\partial \omega_k}{\partial_s}$ = the summation of the concentrated transverse moments and the rate of change of warping function

The forces and moments are diagrammatically shown in Fig. (10.61).

The mathematical difficulties involved in even an approximate analytical solution of the bending behavior of slotted rectangular plates are too many to allow such an analysis to be used in practice. The complexity of the problem automatically precludes all methods other than a numerical procedure for the solution of the governing equation. The finite element method is one of the most powerful of these procedures; it has been adapted for the warping analysis in view of the ease of both the problem formulation and the introduction of completely arbitrary boundary conditions and loading.

The exact distribution of reactive forces even in such a numerical procedure cannot be determined precisely, requiring that the distributed reactive forces be replaced by a system of concentrated forces and moments acting at a discrete set of nodes. Generally it is to be expected

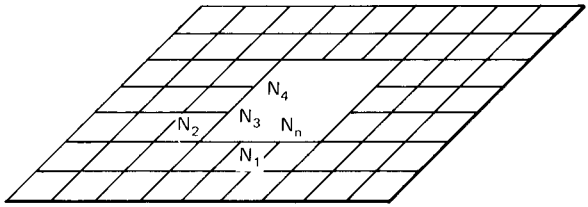

Figure 10.62 Finite element idealization of floor slab.

that such a procedure gives a progressively more accurate representation of the actual continuous pressure as the number of discretized nodes increases. An assemblage of rectangular elements has been employed in the idealization of the floor slabs. Although other finite element representations such as triangular and trapezoidal elements are available, the general success of the rectangular mesh for the idealization of isotropic rectangular plates influenced its selection.

Finite element analysis. A typical finite element idealization for the floor slab is shown in Fig. 10.62. The slab has been assumed to be free of any restraint such as may be imposed by perimeter columns, ties, etc. Hence all the nodes except those corresponding to the profile of the core are assumed to be free. The next stage is to impose unit θ_z' displacement at the inner boundary of the slab. For this purpose, transverse displacements perpendicular to the plane of the slab and equal in magnitude and sense to the warping function are introduced at the nodes common to the core and the slab (e.g., nodes N_1, N_2, . . ., N_n in Fig. 10.62). In addition to these vertical displacements, the slopes $\delta\omega/\delta x$ and $\delta\omega/\delta y$ are made equal in magnitude and sense to the slope of the ω_s diagram. Having thus given at the inner edge of the slab a displacement conforming to the warped outline of the core, the forces and transverse moments at the nodes are found from a finite element solution. The bimoment, which then corresponds to the required warping stiffness of the slab, is found from the relation given in Eq. (10.69). The effect of the floor system, which is mathematically equivalent to the bimoment, is incorporated into the analysis by adding the bimoment to the appropriate elements of the stiffness matrix of the core. A prerequisite for this operation is the derivation of stiffness coefficients for an open section. This is considered next.

Stiffness coefficients for open-section shear walls. The literature on structural analysis, especially that related to matrix methods, shows a number of methods for obtaining basic stiffness coefficients for pris-

matic members. For example, one of the fundamental methods of obtaining the basic stiffness matrix is to invert the flexibility matrix. Another method is to obtain the stiffness matrix from an assumed deformed shape of the members. However, in cases where the governing differential equation can be solved exactly, the stiffness matrix of the member can be derived by imposing appropriate boundary conditions at the member ends. This method will be used in this section to obtain the stiffness matrix for thin-walled open section subjected to torsional rotation and warping displacement at each end. Defining a member as the segment of the core between two floors, the stiffness matrix for the restrained member has to be established first. Elements of this matrix are the values of restraint exerted on the member when unit displacements are imposed in turn at each end of the member. Concentrating on the torsion analysis only, the numbers of degrees of freedom at each end will be two, namely θ_z and θ_z'. Hence, the order of the restrained member stiffness matrix will be 4 by 4. Equation (10.49) of section 10 is conveniently used for deriving the elements of the member stiffness matrix. This is reproduced here for convenience as Eq. (10.70).

$$\begin{bmatrix} \theta_z \\ \theta_z' \\ \dfrac{B_z}{GJ} \\ \dfrac{M_z}{GJ} \end{bmatrix} = \begin{bmatrix} 1 & \dfrac{l}{k}\sinh\dfrac{kz}{l} & 1-\cosh\dfrac{k}{l}z & z-\dfrac{l}{k}\sinh\dfrac{kz}{l} \\ 0 & \cosh\dfrac{kz}{l} & -\dfrac{k}{l}\sinh\dfrac{kz}{l} & 1-\cosh\dfrac{kz}{l} \\ 0 & -\dfrac{l}{k}\sinh\dfrac{kz}{l} & \cosh\dfrac{kz}{l} & \dfrac{l}{k}\sinh\dfrac{kz}{l} \\ 0 & 0 & 0 & 1 \end{bmatrix} \begin{bmatrix} \theta_0 \\ \theta_0' \\ \dfrac{B_0}{GJ} \\ \dfrac{M_0}{GJ} \end{bmatrix} \tag{10.70}$$

Now, to find the elements of the first row of the stiffness matrix, which correspond to the torque and bimoment at each end of the beam required to produce a unit rotation of $\theta = 1$ at $z = 0$ while all the other three displacements are zero, it is necessary to introduce the appropriate boundary conditions in Eqs. (10.70). Thus

$$\begin{bmatrix} 0 \\ 0 \\ \frac{B_l}{GJ} \\ \frac{M_l}{GJ} \end{bmatrix} = \begin{bmatrix} 1 & \frac{l}{k}\sinh\frac{kz}{l} & 1-\cosh\frac{k}{l}z & z-\frac{l}{k}\sinh\frac{kz}{l} \\ 0 & \cosh\frac{kz}{l} & -\frac{k}{l}\sinh\frac{kz}{l} & 1-\cosh\frac{kz}{l} \\ 0 & -\frac{l}{k}\sinh\frac{kz}{l} & \cosh\frac{kz}{l} & \frac{l}{k}\sinh\frac{kz}{l} \\ 0 & 0 & 0 & 1 \end{bmatrix} \begin{bmatrix} 1 \\ 0 \\ \frac{B_0}{GJ} \\ \frac{M_0}{GJ} \end{bmatrix}$$

(10.71)

Solving these equations, the four forces M_0, B_0, M_l, and B_l at the two ends are obtained. In the same manner, the remaining elements of the stiffness matrix are obtained by introducing the appropriate boundary conditions. These are shown diagrammatically in Fig. (10.63). Adapting the sign convention shown therein, the member stiffness matrix for the thin-walled beam subjected to torsion will take the form,

$$\left[\frac{GJ}{2+k\sinh k-2\cosh k}\right] \begin{bmatrix} \frac{k}{l}\sinh k & (1-\cosh k) & \frac{-k}{l}\sinh k & (1-\cosh k) \\ (1-\cosh k) & \frac{l}{k}(k\cosh k - \sinh k) & -(1-\cosh k) & \frac{l}{k}(\sinh k - k) \\ \frac{-k}{l}\sinh k & -(1-\cosh k) & \frac{k}{l}\sinh k & -(1-\cosh k) \\ (1-\cosh k) & \frac{l}{k}(\sinh k - k) & -(1-\cosh k) & \frac{l}{k}(k\cosh k - \sinh k) \end{bmatrix}$$

(10.72)

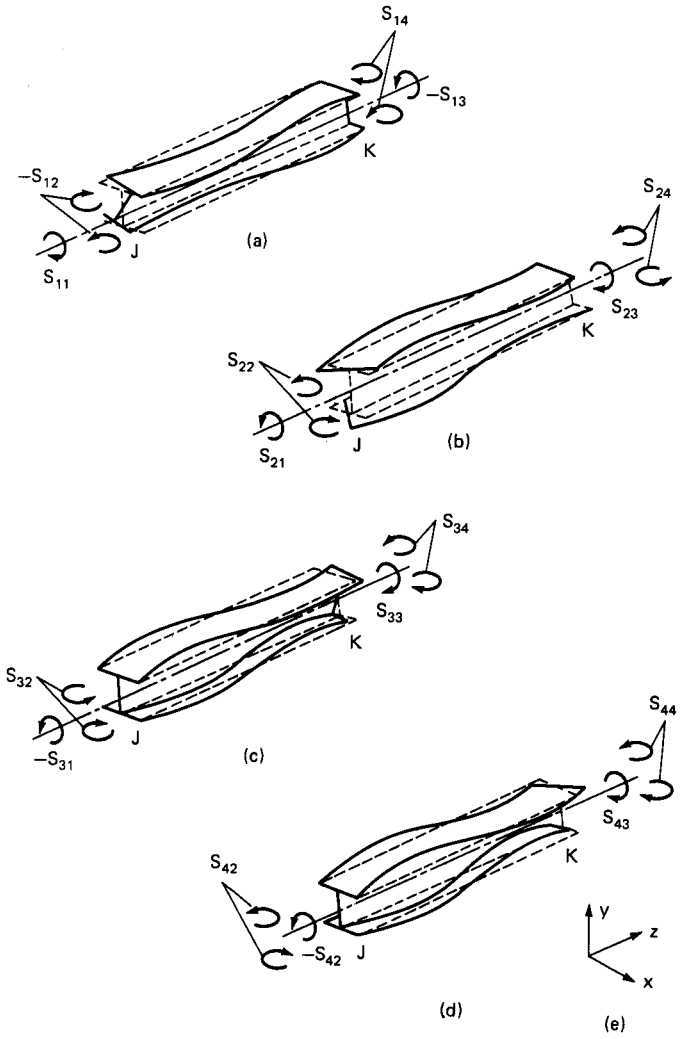

Figure 10.63 Stiffness coefficients for thin-walled open sections. (*a*) Unit rotation at J; (*b*) unit warping displacement at J; (*c*) unit rotation at K; (*d*) unit warping displacement at K; (*e*) coordinate axes.

To the best of the author's knowledge, he was the first to express the quantities θ, θ', B, and M in the form of stiffness coefficients as given in Eq. (10.72). Such a matrix is very convenient for including the effect of stiffening elements and for extending the method of analysis for interconnected open sections as will be demonstrated later in the text.

When the torsional rigidity GJ due to St. Venant torsion becomes zero, the differential equation of constrained torsion will be analogous to the equation of bending of a beam. The elements of the $[S]$ matrix

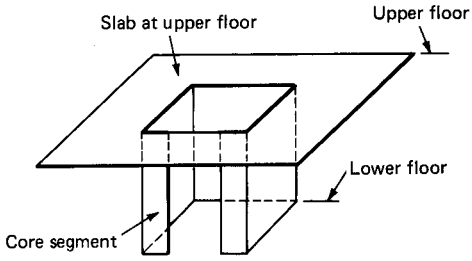

Figure 10.64 Story segment consisting of core segment between two floors and slab at upper floor.

[Eq. (10.72)] can be written directly from the beam stiffness matrix if M, B, θ, θ', and I_ω are replaced by P, M, w, w', and I_{xx}, where P is the shear force, M is the bending moment, w is the displacement, w' is the slope dw/dz, and I_{xx} is the moment of inertia. Further, this analogy can be used to check the elements of the matrix $[S]$ by writing the expanding forms for sinh k and cosh k in Eq (10.72) and taking $k \to 0$ in the limit. For example, considering one element S_{11} of Eq. (10.72) we get

$$S_{11} = \frac{GJk}{l(2 + k \sinh k - 2 \cosh k)} \sinh k$$

when $k \to 0$,

$$S_{11} = \frac{EI_\omega k^2 \left(\frac{k}{l}\right)\left(k + \frac{k^3}{6} + \frac{k^5}{120}\right)}{l^2\left[2 + k\left(k + \frac{k^3}{6} + \frac{k^5}{120}\right) - 2\left(1 + \frac{k^2}{2} + \frac{k^4}{24}\right)\right.}$$

$$= \frac{12\,EI_\omega}{l^3}$$

which is of the same form as the element corresponding to the shear force in the well-known beam stiffness matrix.

Analysis

The overall stiffness matrix. The effect of the floor slab can be incorporated into the analysis either by adding the warping stiffness to the appropriate diagonal elements of the assembled matrix or by modifying the member stiffness matrix. For ease of presentation, the latter method will be employed and the definition of a member now includes, in addition to the segment of the core between the two floor slabs, the slab itself at the top as shown in Fig. 10.64.

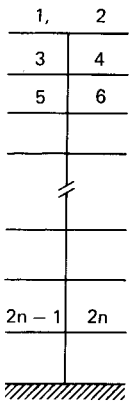

Figure 10.65 Displacement numbering sequence.

An assembly of the stiffnesses of such modified members gives the complete stiffness matrix for the structure. The modified member stiffness is simply the matrix S_M with the diagonal element S_{22} corresponding to the bimoment at the top being replaced by $S_{22} + B_\omega$. For the sequential numbering of the unknown displacements, shown in Fig. 10.65, the resulting overall stiffness matrix will be a band matrix as illustrated in Fig. 10.66. Advantage is taken of the narrow bandwidth and the symmetry of the matrix and only the half band is stored in the computer resulting in considerable saving in storage requirements as shown in Fig. 10.67.

Combined load vector. The combined load vector is the sum of the applied loads at the joints and the equivalent joint loads due to member loads between the joints. The former is known immediately from the given loads on the structure, while the latter needs to be evaluated. For this purpose, the structure is restrained against both the displacements θ and θ' at each floor level by introducing appropri-

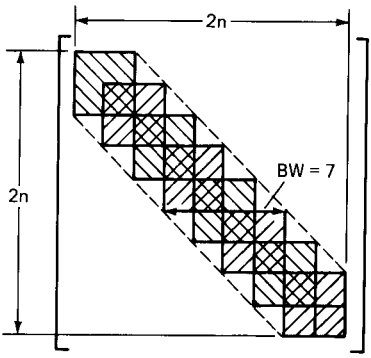

Figure 10.66 Band matrix.

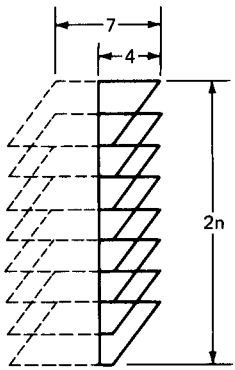

Figure 10.67 Half-band matrix.

ate restraints. The restraint action produced by the member loads is calculated using thin-walled beam formulas given in Ref. 44. The negative values of these give the equivalent joint loads. Such loads are added to the actual joint loads to give the combined loads.

Boundary conditions and solution. The heavy foundation mass for shear cores usually permits the assumption of $\theta = 0$ and $\theta' = 0$ at the base. However, for cases where the foundation is to be considered as an elastic spring, the appropriate stiffness can be incorporated readily in the analysis by modifying the boundary conditions.

The final step is the solution of the simultaneous equations:

$$[K]\,[\theta] = [F]$$

where $[K]$ is the overall stiffness matrix, $[\theta]$ the column vector of required displacements, and $[F]$ is the combined load vector. The bimoments and torques in the structure are readily obtained from the known displacements and the member stiffness matrices.

Computer programs. Two computer programs based on the above theory were written to obtain the analytical results: the first one for calculating the warping stiffness of the slabs, and the second for analyzing the core. The program for the core analysis is quite general in that it accounts for varying story heights, different slab stiffnesses, and varying moduluses of elasticity. Since the characteristic parameter k is input data for each story segment, the program can be used for obtaining approximate solutions for stepped shear walls.

Theoretical and experimental investigation. A comparison of theoretical and experimental results has been provided by a study of the 15-story model structure referred to earlier in the text (Fig 10.52). Perspex plates were attached at appropriate heights to the model and torsion

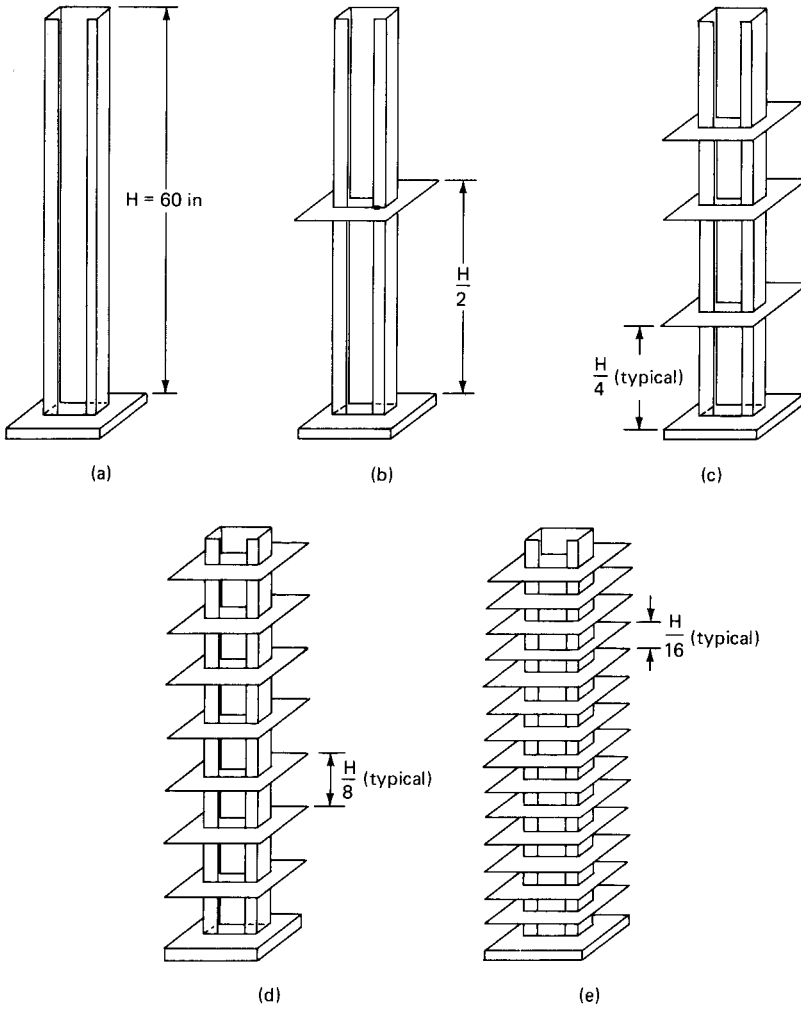

Figure 10.68 Various stages of model for torsion experiments. (*a*) Stage 1, no floor slab; (*b*) stage 2, one floor slab at midheight; (*c*) stage 3, three floor slabs; (*d*) stage 4, seven floor slabs; (*e*) stage 5, fourteen floor slabs.

tests conducted. Each plate simulating the floor slab was cut in two halves from $\frac{3}{8}$-in (9.5-mm) thick perspex sheets and was attached to the perimeter of the core using tensol cement. Altogether, 13 floor slabs at a distance of 4 in (101.6 mm) on centers were fixed, and the sequence of their fixing is shown in Fig. 10.68. Separate tests were conducted at each stage of development of the model. The loading and the measuring devices were identical to the previous setup. The various stages of the model showing the sequence of slab attachment to the

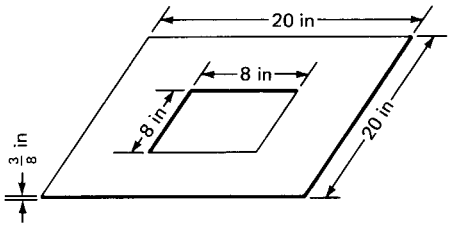

Figure 10.69 Slab dimensions.

central core are given in Fig. 10.68. The model was subjected to two tests at each stage of development by changing the direction of the loading. Good symmetry was observed in all cases.

Discussion of Results

Slab analysis. The dimensions of the slab chosen for the analysis are shown in Fig. 10.69. The dimensions correspond to those of the perspex plate of the model and were selected so that the results could be used directly in the analysis of the model. The finite element discretizations chosen to represent the plate are shown in Fig. 10.70*a* to *e*. The warping stiffness of the slab has been studied for the following three distinct cases.

1. The core inside the slab is a channel section without return walls as shown in Fig. 10.71. It is assumed that there are no moment

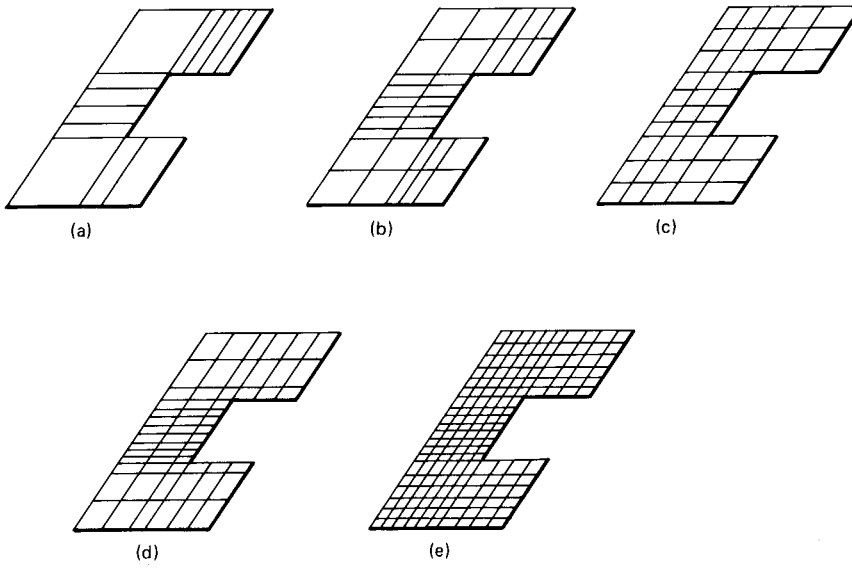

Figure 10.70 Finite element idealizations.

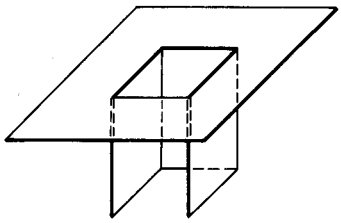

Figure 10.71 Core without return walls.

restraints at the inner boundary of the slab either along or perpendicular to the profile of the core.

2. The core consists of a channel section with return walls. The boundary conditions are similar to those in case 1, i.e., there are no moment restraints at the inner boundary of the slab.
3. The core is similar to that described in case 2, but moment restraints corresponding to the slopes $\partial\omega/\partial x$ and $\partial\omega/\partial y$ are imposed along the inner boundary of the slab.

In addition to case 3, which represents the boundary conditions of the model, cases 1 and 2 were analyzed with a view to studying the effect of the return walls and the transverse moments on the warping stiffness of the slab. For the first two cases, only vertical displacements were imposed at the nodes and the slopes $\partial\omega/\partial\chi$ and $\partial\omega/\partial\gamma$ were allowed to take any value. The bimoment was calculated from the nodal loads alone from the expression

$$B_\omega = \sum_{i=1}^{n} p_k\omega_k$$

For case 3, slopes $\partial\omega/\partial\chi$ and $\partial\omega/\partial\gamma$ were imposed in addition to the vertical displacements; the bimoment was calculated from the expression

$$B_\omega = \sum_{k=1}^{n} p_k\omega_k + \sum_{k=1}^{n} M_k \frac{\partial\omega_k}{\partial s}$$

The results of the analysis for various finite element idealizations of the three cases are shown in Table 10.2.

Comments on convergence characteristics. From Table 10.2 it is seen that the convergence for the channel-shaped core is very good; the value of bimoment obtained by using as few as 12 elements is very nearly equal

TABLE 10.2 Comparison of Bimoments for Different Finite Element Idealizations

No. of elements	Reference figure	Computed bimoments, lb · in^2		
		Case 1	Case 2	Case 3
12	10.67a	50,483	862,726	...
32	10.67b	50,412	694,193	...
42	10.67c	52,947	626,514	936,750
66	10.67d	49,914	629,650	...
168	10.67e	49,398	614,466	768,560

to the result obtained with the very close mesh idealization using 168 elements.

On the other hand, for the second case, the convergence is not as good. The presence of the return walls has radically changed the convergence pattern. This is due to the difference between the displacement patterns induced at the inner boundary of the slab for the two cases. In case 1, no drastic change of curvature occurs along the open face of core, whereas in case 2 the slab has to follow a more rapidly changing curvature pattern. The sudden change of curvature across the opening demands the use of a finer mesh for an accurate representation of the plate behavior.

From a comparison of the bimoments it is seen that the increase in the warping stiffness due to the presence of return walls is more than the increase due to the additional restraints at the interior boundary.

Core analysis. The comparison of rotations and stresses at various stages of the model are shown in Figs. 10.72 through 10.75 along with the bimoment variation. It is seen that the rotations obtained from the analysis are in very close agreement with the experimental results throughout the structure for all the stages of the model. The advantage of accounting for the warping stiffness of the slab is reflected in Figs. 10.72 and 10.75. The increase in torsional stiffness is quite astounding.

The extent of stress distribution along the length of the core can be seen from the distribution of bimoment in Figs. 10.72 through 10.75, which clearly demonstrate that the torsion effects are far from local.

Concluding remarks. On the basis of the above theory, supported by experimental results, the following conclusions are drawn.

1. The finite element method is well suited for establishing the warping stiffness of the slabs.
2. The convergence for the stiffness of the slab depends on the nature of warping displacements of the core, and the boundary conditions

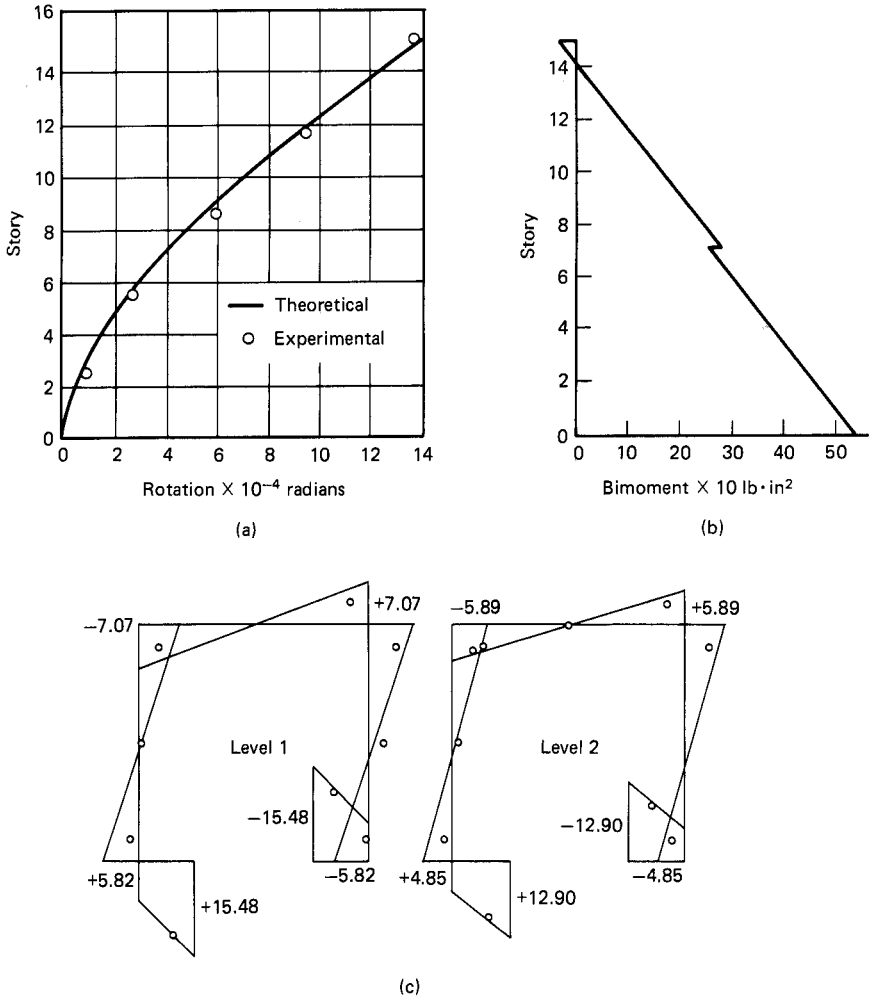

Figure 10.72 Model at stage 2. (*a*) Comparison of rotations; (*b*) bimoment variation; (*c*) comparison of stresses, in psi.

at the inner edge. A relatively fine-mesh idealization is necessary if the ω diagram for the core changes sign abruptly.

3. The moment boundary conditions at the inner edge of the slab have a profound effect on its warping stiffness.
4. The behavior of core structures surrounded by slabs can be predicted accurately by the stiffness method based on the constrained torsion theory.
5. Considerable gain in strength and stiffness is obtained by taking into consideration the warping stiffness of the slabs.

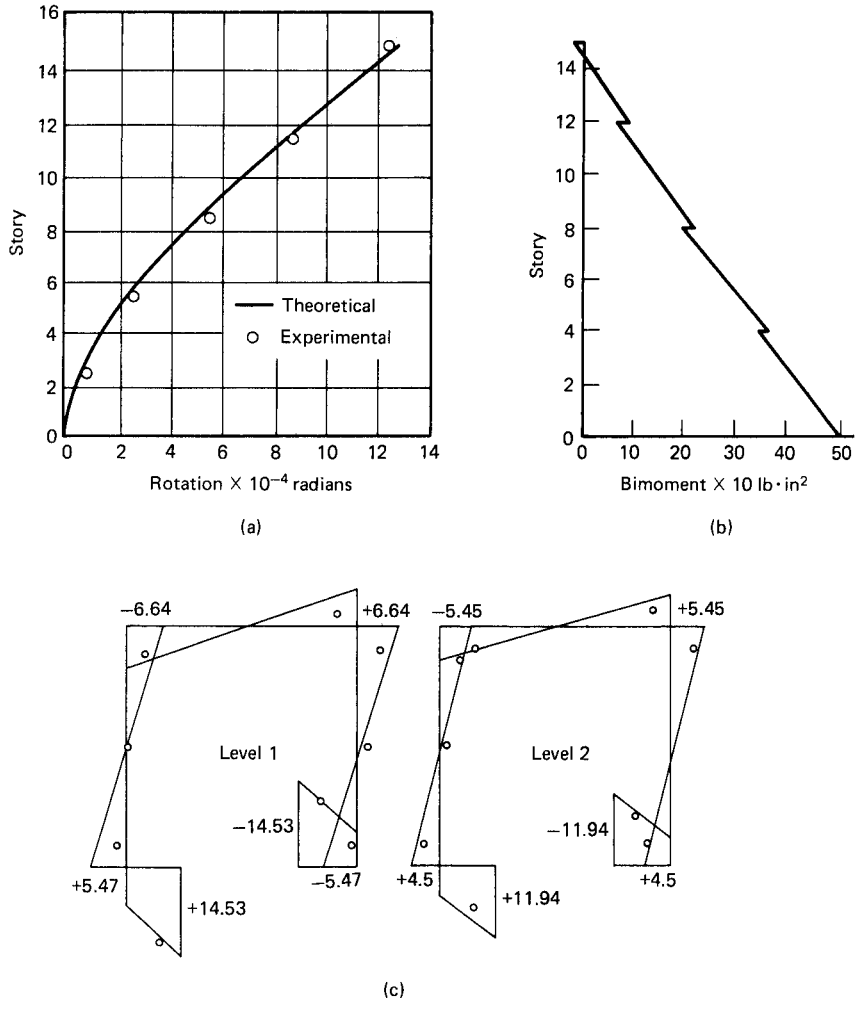

Figure 10.73 Model at stage 3. (*a*) Comparison of rotations; (*b*) bimoment variation; (*c*) comparison of stresses, in psi.

10.8.3 Twin-core systems

In certain core systems, the combined floor space required to house the stairways, duct shafts, storage and mechanical equipment, etc., can become so large that it is not architecturally feasible or structurally economic to group the services within a single core. In such circumstances it is usual to use two or more cores and distribute the services between them. The stiffness method of analysis explained in the previous section can be conveniently employed for the torsion analysis of such practical arrangements of cores.

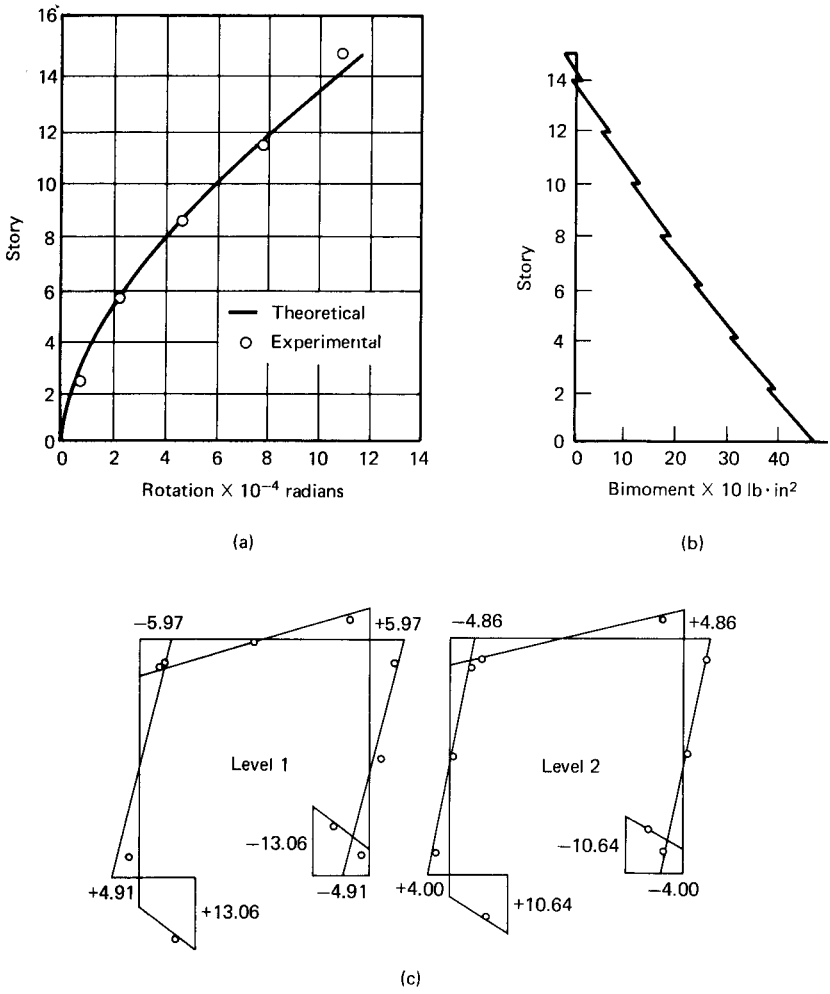

Figure 10.74 Model at stage 4. (*a*) Comparison of rotations; (*b*) bimoment variation; (*c*) comparison of stresses, in psi.

This section presents a method for the analysis of twin-core structures interconnected either through beams only or beams and slabs. Analytical results are compared with available experimental results.

Method of analysis. For a complete analysis of interconnected core systems subjected to loads producing both bending and torsion, it is necessary to resort to a three-dimensional analysis. However, leaving aside the bending part, the problem can be reduced to a unidirectional analysis. This simplification is achieved by considering the entire system of cores as a single thin-walled beam. All the elements of this

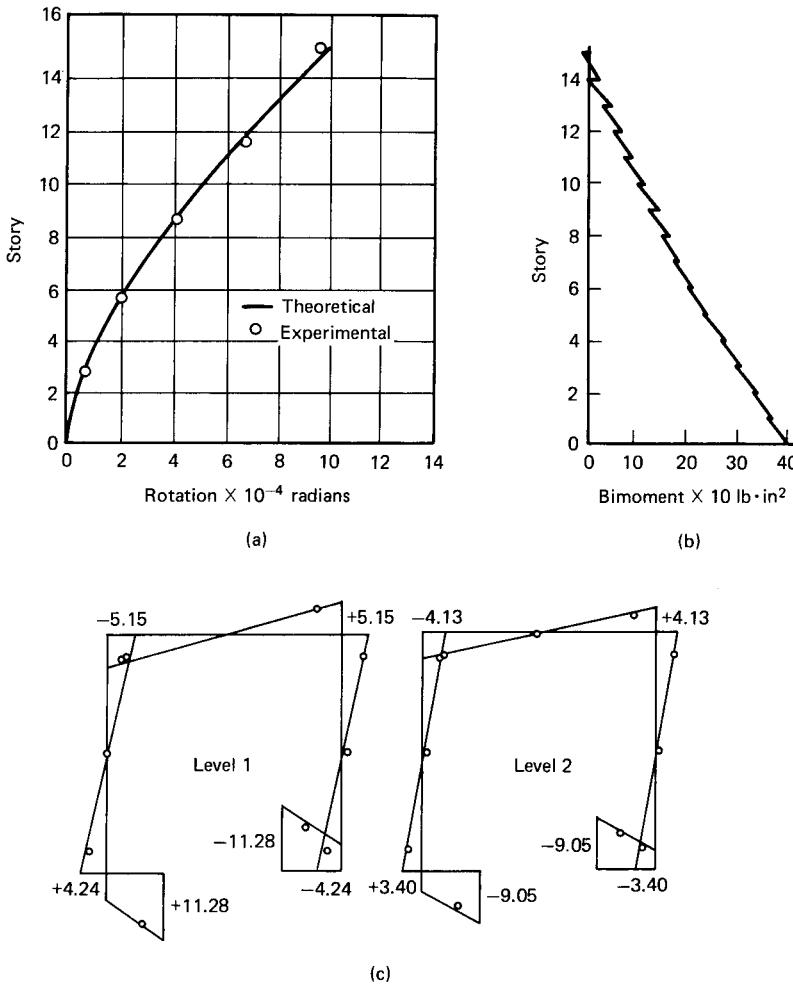

Figure 10.75 Model at stage 5. (*a*) Comparison of rotations; (*b*) bimoment variation; (*c*) comparison of stresses, in psi.

beam are then considered to rotate about a common center of rotation 0, which is located from a consideration of the shear forces in the individual elements. The sectorial properties of the complete system are found with respect to this center of rotation, and the analysis is carried out as outlined earlier for single-core systems.

The following notations are used in the development of the method

$I_{\omega 0c}$	Sectorial moment of inertia of the core with respect to 0
$I_{\omega A}$	Sectorial moment of inertia of the core with respect to A
0	Shear center of the assembly of twin cores

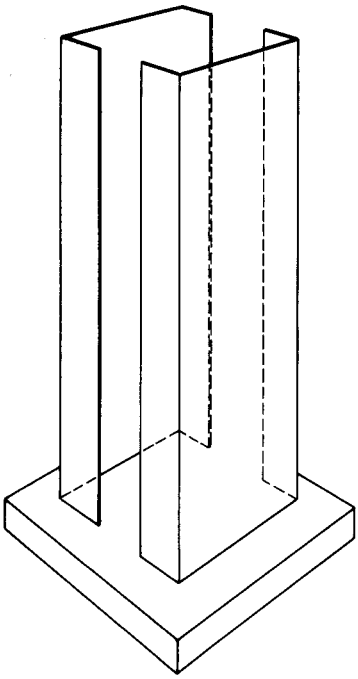

Figure 10.76 Twin cores.

A	Shear center for single core
(x_0, y_0)	Coordinates of 0
(x_A, y_A)	Coordinates of A
ξ	$(x_0 - x_A)$
ζ	$(y_0 - y_A)$
$I_{\omega 0}$	Sectorial moment of inertia of the cores
I_{xx}, I_{yy}	Moment of inertia of the core about its centroidal axis
P_1, P_2	Sectorial origins for the two cores
U	Strain energy of the plate
V	Potential energy
T	$U + V$

A system comprising two interconnected cores is shown in Fig. 10.76. Although it is possible to consider more complicated systems, this plan form has been chosen for presentation in view of the experimental and theoretical results already available for the particular arrangement.

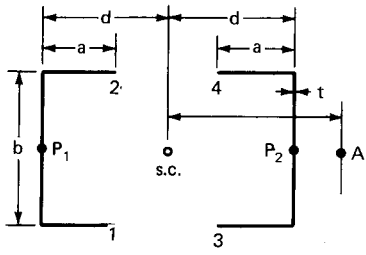

Figure 10.77 Dimensions of cores.

From a consideration of symmetry, it is seen that the shear center for the two cores coincides with the center of area of the section (Fig. 10.77). The torsional parameters, such as $\omega_{(s)}$ and I_ω, are calculated for the two cores with respect to 0, either directly or by first calculating the parameters separately for each core about its own shear center and transforming it with respect to 0. For example, the expression for the transformation of I_ω for each core will be of the form:

$$I_{\omega 0c} = I_{\omega A} + I_{xx}\xi^2 + I_{yy}\zeta^2 \tag{10.73}$$

Since in the present example, $\zeta = 0$,

$$I_{\omega 0c} = I_{\omega A} + I_{xx}\xi^2$$

and for the two cores

$$I_{\omega 0} = 2 \times I_{\omega 0c} \tag{10.74}$$

To determine the parameters directly, it is necessary to find the sectorial origin for the two cores from the condition that the sectorial static moment is equal to zero for each core

$$\int_1^2 \omega_{(s)}\, ds = 0 \qquad \int_3^4 \omega_{(s)}\, ds = 0 \tag{10.75}$$

In the case of the two cores of Fig. 10.76, these equations will fix the origins at the two web centers P_1 and P_2. The $\omega_{(s)}$ diagram is then constructed for the two cores as shown in Fig. 10.78 and the sectorial moment of inertia is calculated from the integral

$$I_{\omega 0} = \int_1^2 \omega_{(s)}{}^2\, ds + \int_3^4 \omega_{(s)}{}^2\, ds \tag{10.76}$$

The St. Venant torsional rigidity GJ for the two cores is the algebraic sum of their individual contributions. The characteristic parameter k is then calculated from the expression

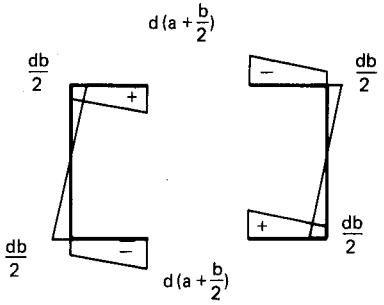

Figure 10.78 Warping coordinate ω_s diagram.

$$k = l\sqrt{\frac{GJ}{EI_{\omega 0}}} \tag{10.77}$$

l being the story height. This value of k is used in the calculation of member stiffness matrix, and the analysis carried out as outlined in the previous section.

Stiffness of interconnecting beams. Consider the case when the two cores are interconnected at each floor level by two beams as in Fig. 10.79*a*. To find the warping stiffness of the beams it is required to find the force system, and hence the bimoment generated, when a unit θ_z' displacement is given to the beams. From a consideration of $\omega_{(s)}$ diagram for the cores, it is seen that unit θ_z' corresponds to a vertical displacement equal to the magnitude of ω at 1, and a rotation of $\partial\omega/\partial x$

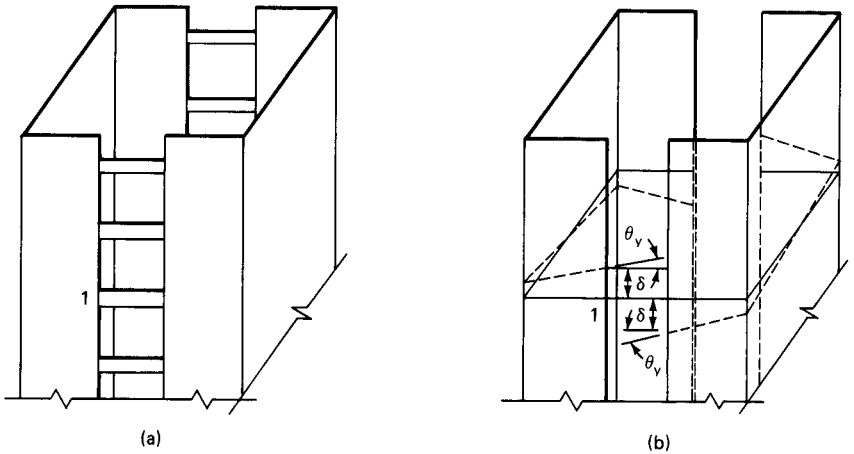

Figure 10.79 (*a*) Twin cores coupled through beams; (*b*) warping of core and resulting deflections and rotations at beam ends.

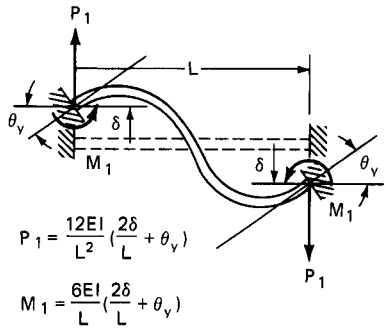

Figure 10.80 Forces and moments in beam due to warping of cores.

at each end of the beam as shown in Fig. 10.79*b*. The end moments and shear forces required to induce this displacement are found from the force-displacement relationship of a fixed-ended beam (Fig. 10.80). Using these forces, the bimoment, which is numerically equal to the warping stiffness of the beams, is found from relation

$$B_\omega = 4\left(P_1\omega_1 + M_1\frac{\partial\omega_1}{\partial y}\right) \tag{10.78}$$

The warping stiffness B_ω is introduced in the member stiffness matrix to obtain the modified story stiffness of the structure shown in Fig. 10.81. The stiffnesses of the individual story segments are then assembled to give the complete stiffness matrix; appropriate boundary conditions are introduced and the system of equations solved for the given load system. From the known displacements and the member stiffness matrix, the stress resultants at each story level are obtained.

Stiffness of interconnecting slabs. An arrangement is shown in Fig. 10.82 where the intermediate space between the beams is filled with a slab of the same depth as the beams. It is interesting to note that even when the slab-core connection is pin-jointed, there will be considerable warping stiffness due to the pure twisting of the slab. The bimoment for this type of connection can be readily found from the solution of the biharmonic equation for plate bending, as shown below.

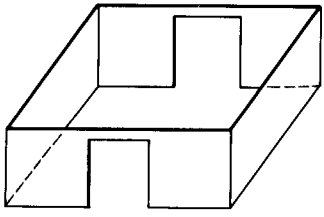

Figure 10.81 Typical story segment.

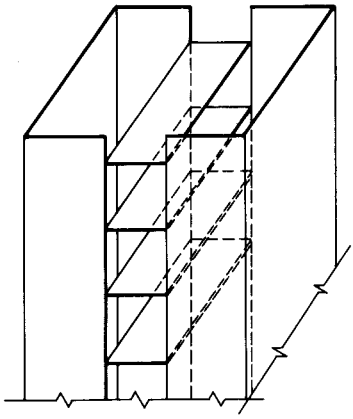

Figure 10.82 Twin cores coupled through slabs.

The deflection function for the plate, which is bending as a hyperbolic paraboloid (Fig. 10.83), is given by the relation

$$w = Cxy \tag{10.79}$$

where C is a constant. The value of C is found by substituting for w in the expression for the total potential energy and minimizing the resulting expression with respect to C.

The strain energy for the plate shown in Fig. 10.83*a* is given by

$$U = \int_{-a/2}^{a/2} \int_{-b/2}^{b/2} \frac{D}{2} \left\{ \left(\frac{\partial^2 w}{\partial x^2} + \frac{\partial^2 w}{\partial y^2} \right) - 2(1 - \mu) \left[\frac{\partial^2 w}{\partial x^2} \frac{\partial^2 w}{\partial y^2} - \left(\frac{\partial^2 w}{\partial x \partial y} \right)^2 \right] \right\} dx\, dy \tag{10.80}$$

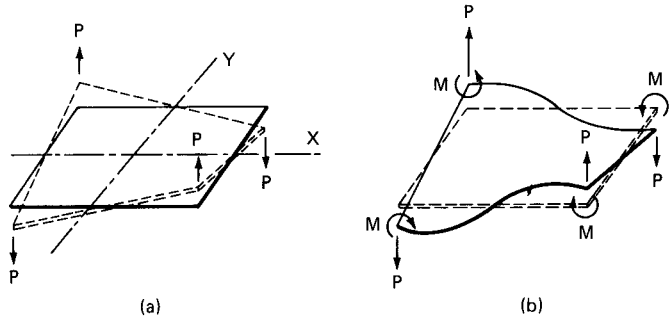

Figure 10.83 (*a*) Slab subjected to corner forces; (*b*) slab subjected to corner forces and moments.

The potential energy for the four point loads at the corners is given by

$$V = -4P\frac{a}{2}\frac{b}{2}C = -PabC$$

Substituting for ω in the expression for U, the total energy

$$T = U + V = \int_{-a/2}^{a/2}\int_{-b/2}^{b/2} D(1-\mu)C^2\,dx\,dy - PabC$$

$$= D(1-\mu)C^2ab - PabC \tag{10.81}$$

Differentiating T with respect to C and equating to zero, C is found to be equal to $P/2D(1-\mu)$.

$$w = Cxy = \frac{P}{2D(1-\mu)}xy$$

and the value of P per unit displacement becomes equal to

$$P = \frac{8D(1-\mu)}{ab} \tag{10.82}$$

The required bimoment due to the four corner forces is given by

$$B_\omega = \sum_{i=1}^{4} P_i\omega_i$$

Since $\omega_1 = -\omega_2 = -\omega_3 = \omega_4$,

$$B_\omega = 4 \times \frac{8D(1-\mu)}{ab} \times \omega_1 \tag{10.83}$$

When the slab-core joint is rigid, then it is no longer possible to find the forces and moment at the corners analytically. However, using the finite element technique, these can be readily established and the appropriate value of stiffness found.

The nodes corresponding to the corners of the plate 1, 2, 3, and 4 are given a vertical displacement and rotation equal to the warping coordinate ω and the slope $\partial\omega/\partial s$ at these points. From the finite element analysis the corner forces and moments shown diagrammati-

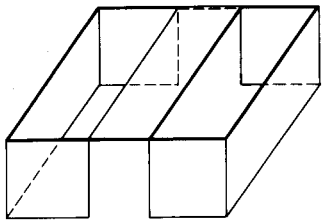

Figure 10.84 Story segment.

cally in Fig. 10.83*b* are obtained. The stiffness of the plate is then calculated from the relation

$$B_\omega = \sum_{i=1}^{4} \left(P_i \omega_i + M_i \frac{\partial \omega_i}{\partial s} \right) \tag{10.84}$$

The warping stiffness is added to the story stiffness to obtain the stiffness of modified story segment shown in Fig. 10.84. The assembly and solution of the overall matrix proceeds as before.

Experiments. The experimental results quoted in this chapter are those obtained by Jenkins and Harrison (Ref. 22), who conducted experiments on a 22-story perspex model. The model shown in Fig. 10.82 was subjected to torsion tests at the first two stages of its construction by applying a couple in the plane of the top floor. In the first stage the interconnecting medium consisted of two beams at each floor level connecting the flanges of the two cores. In the second stage, horizontal floor slabs of the same thickness as the beams were inserted between the connecting beams at each floor level.

Discussion of results. In order to investigate the convergence characteristic of rectangular elements for plates subjected to pure twisting, the slab was analyzed assuming the corners to be pin-jointed with the cores. The finite element idealizations investigated are shown in Fig. 10.85*a* to *d*. Very good convergence was observed; the result, even for the relatively coarse idealization of six elements, was also very close to the exact result obtained from the solution of biharmonic equation as shown in Fig. 10.85*e*.

The analytical results for the rotation of the model are presented in Fig. 10.86 along with the experimental results. Very good agreement is evident from Fig. 10.86 and the importance of taking the warping stiffness of the beams and slabs is emphasized even more strikingly than in the case of single cores. Analytical results for the longitudinal distribution of the bimoment, and the axial stresses at the base for the two cores are shown in Fig. 10.87*a* and 10.87*b*, respectively.

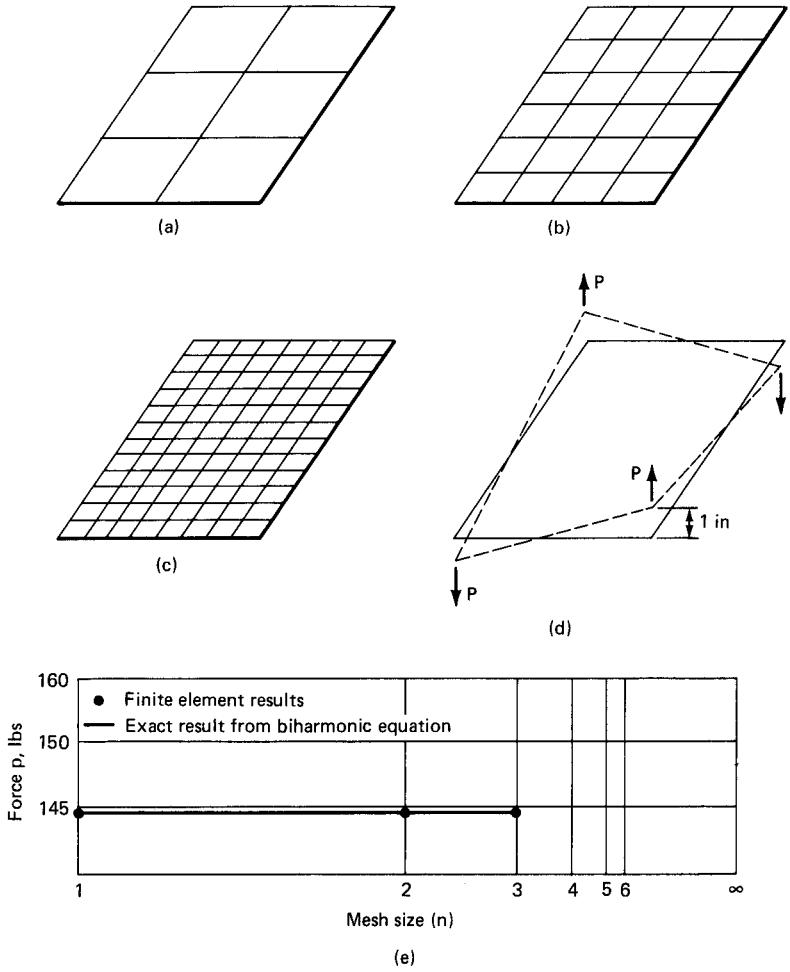

Figure 10.85 Finite element idealizations of slab subjected to pure twisting. (*a*) Six-element idealization ($n = 1$); (*b*) 24-element idealization ($n = 2$); (*c*) 96-element idealization ($n = 3$); (*d*) induced displacement at corners; (*e*) comparison of corner forces.

To demonstrate the significance of warping stresses it is instructive to consider a practical twin-core building as shown in Fig. 10.88*b*. Assume the building is 24 stories high with 12-ft (3.66-m) typical floor height for a total height of 288 ft (87.8 m). Assuming that walls are 1.5 ft (0.46 m) thick, the ratios of characteristic dimensions, length to least width of cores, and width to thickness of the cores work out equal to 16 and 12, respectively. Because of these relatively high ratios, the warping stresses are expected to be quite significant. Assume that a

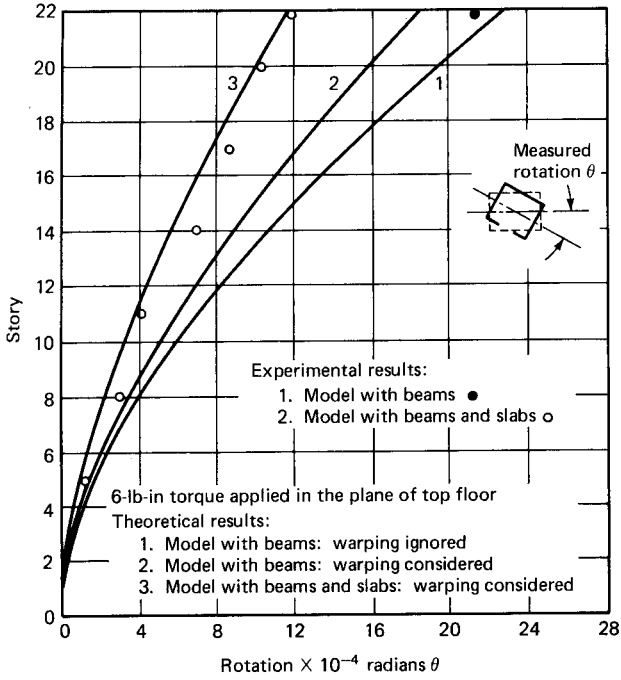

Figure 10.86 Comparison of rotations for twin-core system.

uniformly distributed wind load of intensity 25 psf (1197 Pa) is acting on the broad face of the building. Neglecting the interaction of frames and the transverse stiffness of floor slabs, the bending stresses at the base of the building work out as shown in Fig. 10.88*c*. The warping stresses at the base are shown in Fig. 10.88*d* to allow comparison. It is evident that the magnitude of warping stresses is similar to bending stresses, and therefore they are too large to be ignored in an analysis.

10.8.4 Multiple-core systems

In previous investigations of the three-dimensional behavior of shear wall structures, it has generally been assumed that at each story a shear wall has, at the most, six degrees of freedom. While this is accurate for plane shear walls or those with a T or L section, the presence of shear walls with an open section, e.g., with a U or H shape, as often used for elevator shafts, introduces the additional possibility of warping displacements. This seventh degree of freedom and its associated actions can have a significant influence on the behavior of the structure. It is necessary, therefore, that any method of analysis which aims to predict satisfactorily the behavior of such open-section systems must recognize the warping effect.

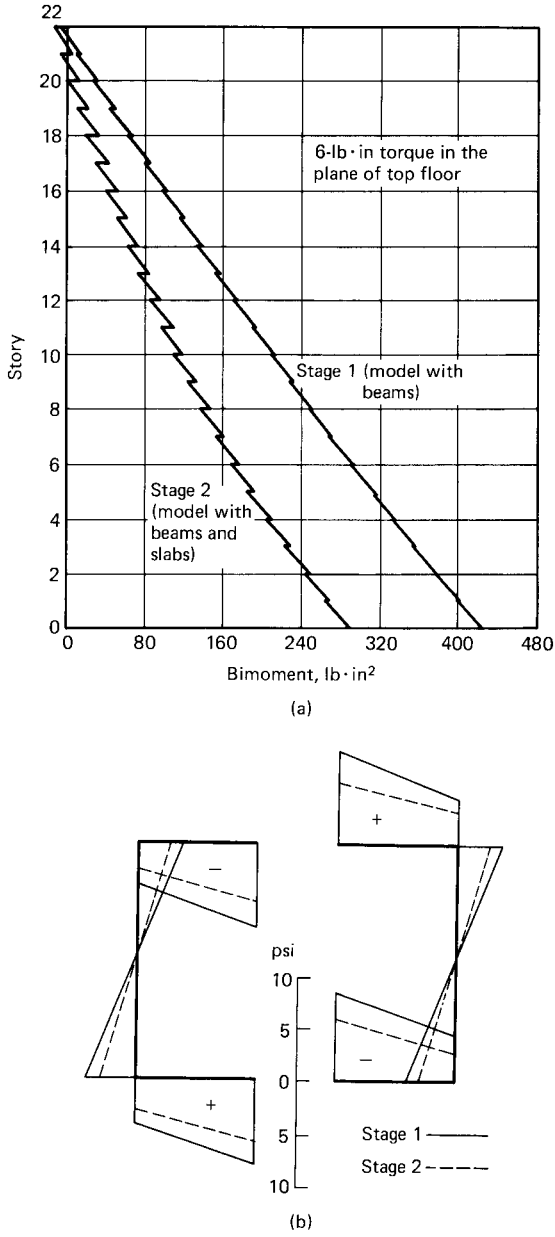

Figure 10.87 (*a*) Variation of bimoment; (*b*) axial stresses at base.

The method presented in this section considers the warping behavior as well as the warping interaction between a multiple system of open-section shear wall structures interconnected by floor slabs. The finite element technique is employed to compute the out-of-plane

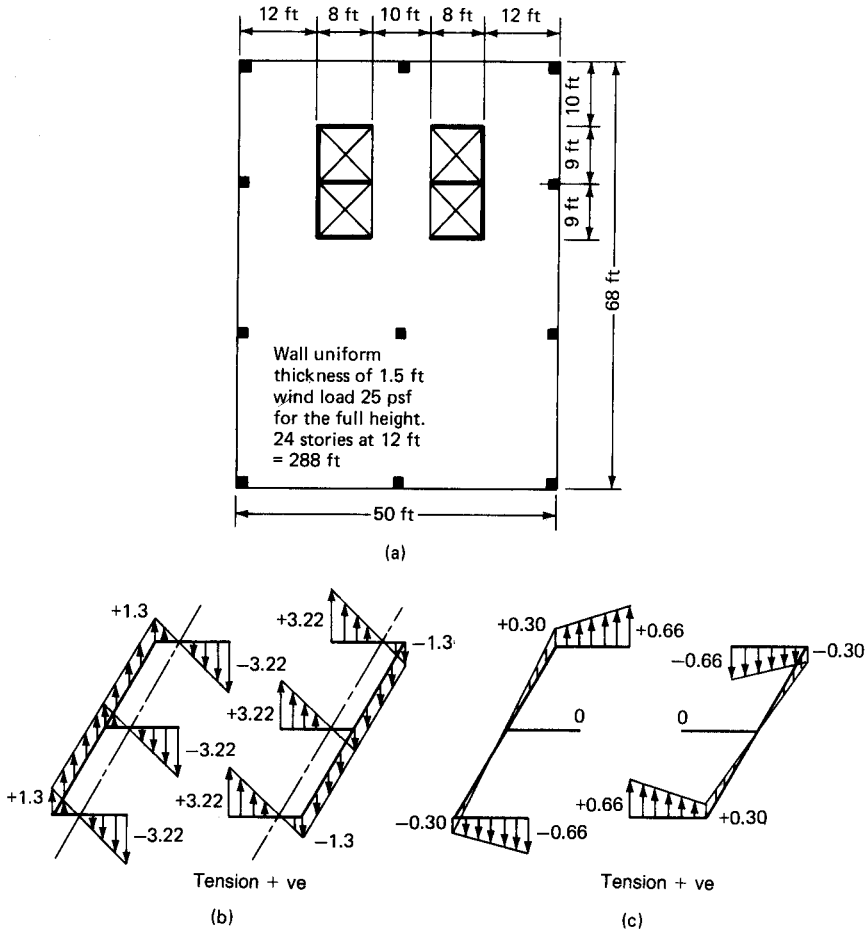

Figure 10.88 (*a*) Practical twin-core building; (*b*) dimensions and loading; (*c*) bending stresses, ksi; (*d*) warping stresses, ksi.

stiffness of floor slabs, and using a stiffness matrix approach, the complete structure is studied in a unified manner.

Method of analysis. It is convenient to develop the method of analysis with reference to a particular structural plan such as that of a hypothetical high-rise building shown in Fig. 10.89. In order to emphasize the warping phenomenon, all the shear walls are open sections. The shear walls are interconnected solely through a flat plate system, it being assumed that there are no columns or beams. The floor diaphragms are considered to be perfectly rigid in their own plane and are joined to the walls by a moment-resistant connection. The geometry of the plan, story height, member properties, elastic modulus, and

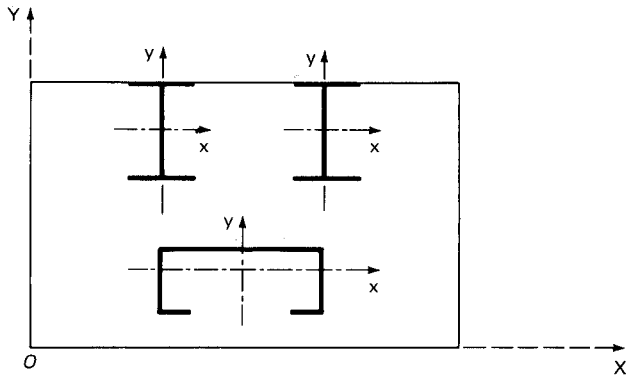

Figure 10.89 Analytical model.

Poisson's ratio are all assumed to be constant for the complete structure. The shear walls are arranged in a rectangular pattern such that each member is parallel to the three orthogonal reference axes. The regularity of geometry, E, μ, and orientation are unnecessary for the application of the method but render the problem much simpler for presentation. For the purpose of analysis, an origin of reference coordinates can be located anywhere in the plane of the floor slab and, for the present example, it is selected at the corner O of the floor slab. The origin O thus lies at the intersection of the z axis with the plane of the topmost floor slab.

In the absence of a rigid floor diaphragm, each vertical element would have seven degrees of freedom at each end; six of these are the familiar translations and rotations about three orthogonal axes, while the remaining seventh is the warping displacement. These are shown numbered for a typical open-section member in Fig. 10.90. Thus the stiffness matrix for an open-section shear wall will be of the order of 14 by 14 (for seven degrees of freedom at each end). This matrix is obtained by combining the well known 12-by-12 stiffness matrix of a prismatic member of a space frame together with the 4-by-4 torque-bimoment matrix given in a previous section. The resulting matrix is henceforth referred to as the generalized member stiffness matrix for an open section. The 12-by-12 stiffness matrix of a prismatic member and the 14-by-14 matrix for an open section are shown in Figs. 10.91 and 10.92, wherein the actions and displacements are taken to be positive in the positive sense of the reference axes.

Because the floor slab is considered to be rigid in its own plane, the displacements are such that its plan shape and the geometrical dimensions remain unchanged. The floor slab can be considered to be displaced as an absolutely rigid body whose position is defined

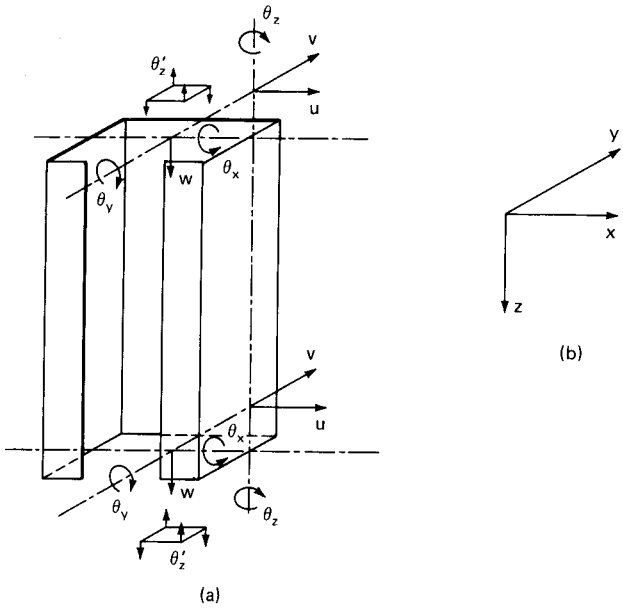

Figure 10.90 (*a*) Generalized displacements for thin-walled open section; (*b*) coordinate axes.

uniquely in the horizontal plane by the two translations and a rotation about the vertical axis.

The method for setting up the stiffness matrix for a typical segment follows the pattern employed in the earlier section. The two different steps involved are

1. Setting up the stiffness matrix for a story segment consisting of vertical elements only
2. Modifying the matrix in 1 by adding the stiffness of the floor slab to obtain the modified segment stiffness matrix

Each of the two steps will now be considered in detail.

It is to be noted that whereas the moments M_x and M_y are referred to the centroidal axes, the forces P_x, P_y, and the twisting moment M_z are referred to the shear center (Fig. 10.90). The axial force P_z is assumed to be distributed over the cross section so that no force other than a vertical force is developed when unit vertical displacement is given to the member.

Number of degrees of freedom. If there were no rigid floor diaphragms, the number of degrees of freedom at each floor would be equal to $7 \times N$ where N is the number of open sections. However, each shear wall is

		u	v	w	θ_x	θ_y	θ_z	u	v	w	θ_x	θ_y	θ_z
		1	2	3	4	5	6	7	8	9	10	11	12
u	1	$\frac{12EI_y}{L^3}$	S										
v	2	0	$\frac{12EI_x}{L^3}$	Y									
w	3	0	0	$\frac{EA}{L}$	M								
θ_x	4	0	$\frac{6EI_x}{L^2}$	0	$\frac{4EI_x}{L}$	M							
θ_y	5	$\frac{-6EI_y}{L^2}$	0	0	0	$\frac{4EI_y}{L}$	E						
θ_z	6	0	0	0	0	0	$\frac{GJ}{L}$	T					
u	7	$\frac{-12EI_y}{L^3}$	0	0	0	$\frac{6EI_y}{L^2}$	0	$\frac{12EI_y}{L^3}$	R				
v	8	0	$\frac{-12EI_x}{L^3}$	0	$\frac{-6EI_x}{L^2}$	0	0	0	$\frac{12EI_x}{L^3}$	I			
w	9	0	0	$\frac{-EA}{L}$	0	0	0	0	0	$\frac{EA}{L}$	C		
θ_x	10	0	$\frac{6EI_x}{L^2}$	0	$\frac{2EI_x}{L}$	0	0	0	$\frac{-6EI_x}{L^2}$	0	$\frac{4EI_x}{L}$	A	
θ_y	11	$\frac{-6EI_y}{L^2}$	0	0	0	$\frac{2EI_y}{L}$	0	$\frac{6EI_y}{L^2}$	0	0	0	$\frac{4EI_y}{L}$	L
θ_z	12	0	0	0	0	0	$\frac{-GJ}{L}$	0	0	0	0	0	$\frac{GJ}{L}$

(a)

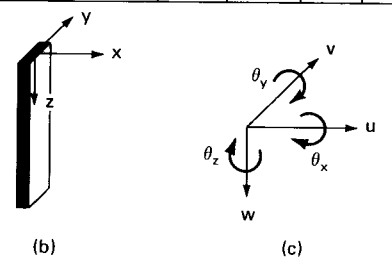

Figure 10.91 (*a*) Twelve by twelve stiffness matrix for prismatic three-dimensional element; (*b*) coordinate axes; (*c*) positive sign convention.

		u	v	w	θ_x	θ_y	θ_z	θ_z'	u	v	w	θ_x	θ_y	θ_z	θ_z'
		1	2	3	4	5	6	7	8	9	10	11	12	13	14
u	1	$\frac{12EI_y}{L^3}$		S											
v	2	0	$\frac{12EI_x}{L^2}$		Y										
w	3	0	0	$\frac{EA}{L}$		M									
θ_x	4	0	$\frac{6EI_x}{L^3}$	0	$\frac{4EI_x}{L}$		M								
θ_y	5	$\frac{-6EI_y}{L^2}$	0	0	0	$\frac{4EI_y}{L}$		E							
θ_z	6	0	0	0	0	0	S_{11}		T						
θ_z'	7	0	0	0	0	0	S_{12}	S_{22}		R					
u	8	$\frac{-12EI_y}{L^3}$	0	0	0	$\frac{6EI_y}{L^2}$	0	0	$\frac{12EI_y}{L^3}$		I				
v	9	0	$\frac{-12EI_x}{L^3}$	0	$\frac{-6EI_x}{L^2}$	0	0	0	0	$\frac{12EI_x}{L^3}$		C			
w	10	0	0	$-\frac{EA}{L}$	0	0	0	0	0	0	$\frac{EA}{L}$		A		
θ_x	11	0	$\frac{6EI_x}{L^2}$	0	$\frac{2EI_x}{L}$	0	0	0	0	$\frac{-6EI_x}{L^2}$	0	0		L	
θ_y	12	$\frac{-6EI_y}{L^2}$	0	0	0	$\frac{2EI_y}{L}$	0	0	$\frac{6EI_y}{L^2}$	0	0	0	$\frac{4EI_y}{L}$		
θ_z	13	0	0	0	0	0	$-S_{11}$	$-S_{12}$	0	0	0	0	0	S_{11}	
θ_z'	14	0	0	0	0	0	S_{12}	S_{24}	0	0	0	0	0	$-S_{12}$	S_{22}

(a)

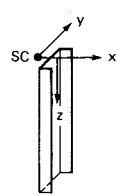

(b)

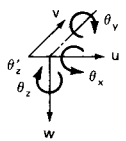

(c)

Torque bimoment relation as between P_x and θ_y.

$S_{11} = \alpha \frac{k}{\ell} \sinh k \quad S_{24} = \alpha \frac{\ell}{k} (\sinh k - k)$

$S_{12} = \alpha(1 - \cosh k)$

$S_{22} = \alpha(k \cosh k - \sinh k)$

where $\alpha = \frac{GJ}{(2 + k \sinh k - 2 \cosh k)}$

Figure 10.92 (*a*) Fourteen by fourteen stiffness matrix for thin-walled open section; (*b*) coordinate axes; (*c*) positive sign convention.

constrained by the rigid floor slab to translate and rotate in the xy plane, conforming with the rigid-body motion of the floor slab; hence all the planar displacements can be expressed in terms of the translations and rotation of the origin. The two rotations about the centroidal axes, the axial deformation, and the warping displacement referred to the shear center remain as independent displacements for each shear wall. Therefore, the number of independent displacements for each floor is $3 + 4 \times N$ instead of $7N$. For a typical segment the corresponding stiffness matrix will be of the order $(6 + 8N)$ by $(6 + 8N)$. Thus in the example problem the matrix size is 30 by 30.

Story stiffness. The evaluation of the stiffness of each single-story segment can be accomplished by any of the following two procedures. One is to employ the standard technique of matrix analysis and, since this has been well documented, the procedure is given only very briefly here. First the generalized member stiffness matrix for each shear wall is evaluated. Then using a displacement transformation matrix T, which relates the member deformation to the displacements of the structure, each member stiffness is expressed in terms of the segment stiffness coordinates as follows:

$$[K_0] = [T^*][K][T]$$

where the subscript 0 refers to the structure coordinates and $[T^*]$ is the transpose of the matrix $[T]$.

Finally, the complete segment stiffness expressed in the segment coordinates is obtained by adding together the member stiffnesses K_0. This approach is very general and suited admirably to the analysis of space structures comprising inclined beams and columns. However, when there are no interconnecting beams and the orientation of the vertical member is parallel to the reference axes, as in the present case, it is advantageous to write the elements of the segment stiffness matrix directly. This procedure will now be considered in detail.

Figure 10.93 shows a typical segment consisting of three shear walls, in which the numbering sequence of the displacements is also indicated. The displacements u_1 and u_2 are the planar displacements of the slab referred to the origin; u_3, u_4, and u_5 are the axial displacements; u_6, u_7, u_8, u_9, u_{10}, and u_{11} are the rotations of the shear walls about their respective centroidal axes; u_{12} is the rotation of the assembly about the z axis and finally u_{13}, u_{14}, and u_{15} are the warping displacements of the three walls referred to their shear centers, respectively. The displacements at the other end of the typical segment are numbered in exactly the same sequence as above. The procedure now is to induce a unit displacement $u_i = 1$ $(i = 1, 2, 3, \ldots, 30)$, restraining all other displacements and to write the expressions for the

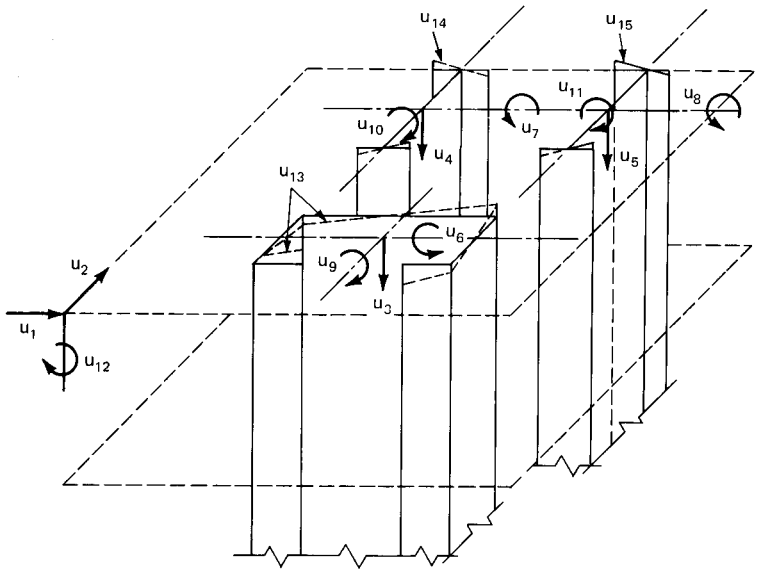

Figure 10.93 Numbering sequence for displacement.

corresponding forces developed. For example, Fig. 10.94 shows a unit displacement u_1 given to the top floor and the corresponding forces developed at that end. Imaginary supports are assumed at the origin and are supposed to restrain the displacements u_2 and u_{12}. These are shown diagrammatically in Fig. 10.94. The horizontal forces P_{x_1}, P_{x_2}, P_{x_3} are now referred to the origin giving a total horizontal force equal to $P_{x_1} + P_{x_2} + P_{x_3}$ and a torque equal to

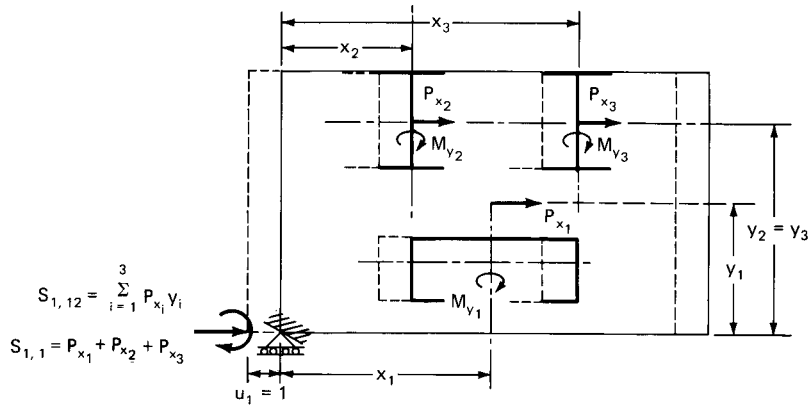

Figure 10.94 Unit horizontal displacement $u_1 = 1$.

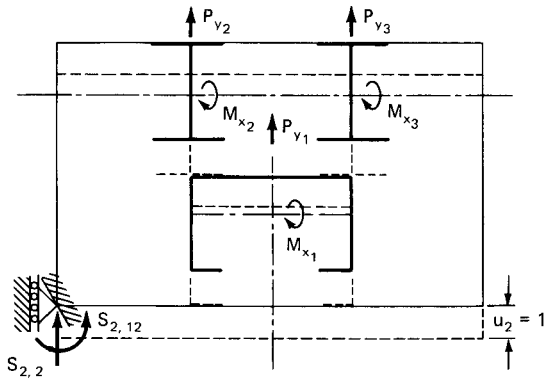

Figure 10.95 Unit horizontal displacement $u_2 = 1$.

$$\sum_{i=1}^{3} P_x y_i$$

The force and the torque correspond to the elements $S_{1,1}$ and $S_{1,12}$ of the segment stiffness matrix, while the moments M_{y_1}, M_{y_2}, and M_{y_3} are the elements $S_{1,9}$, $S_{1,10}$, and $S_{1,11}$, respectively. The forces at the other end are obtained by the equilibrium condition.

The remaining elements of the story stiffness matrix are obtained in a similar manner by giving unit displacements u_i ($i = 2, 3, 4, \ldots, 15$) to the top floor and combining the appropriate elements of the individual matrices for the three open sections. Figures 10.95 and 10.96 show the other two rigid-body displacements $u_2 = 1$ and $u_{12} = 1$ for the top floor; the forces developed owing to these displacements are also indicated in these figures.

The nonzero elements of the lower half of the first quadrant of the complete 30-by-30 story stiffness matrix are given in Table 10.3. The remaining elements of the matrix are easily obtained from considerations of symmetry and equilibrium. In Table 10.3, A, B, and C refer to the three 14-by-14 matrices for the open sections and are of the same form as given in Fig. 10.92.

Stiffness of floor slabs. If the connection between the slabs and walls is moment-resistant, then in addition to the warping restraint, the slab offers considerable resistance to other types of deformations of the walls, namely, the axial deformation and the rotations about the centroidal axes. In the previous sections it was sufficient to account only for the warping restraint, since the longitudinal deformation of the walls was only due to warping. A three-dimensional analysis,

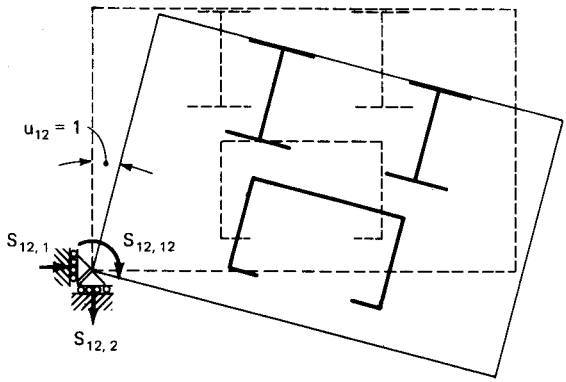

Figure 10.96 Unit rotation $u_{12} = 1$.

however, involves other forms of longitudinal displacements and it is necessary that the interaction of the slab is accounted for in all the possible displacements.

Consider the displacements of a typical floor slab interconnecting the three shear walls. Since it is assumed that the floor diaphragm is

TABLE 10.3 Nonzero Elements of the Lower Half of the First Quadrant of the Story Stiffness Matrix

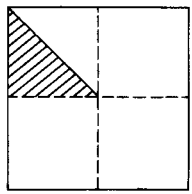

30 X 30 S matrix

$$s_{11} = A_{11} + B_{11} + C_{11}$$
$$s_{22} = A_{22} + B_{22} + C_{22}$$
$$s_{33} = A_{33}$$
$$s_{44} = B_{33}$$
$$s_{55} = C_{33}$$
$$s_{62} = A_{42}$$
$$s_{66} = A_{44}$$
$$s_{72} = B_{42}$$
$$s_{77} = B_{44}$$
$$s_{82} = C_{42}$$
$$s_{88} = C_{44}$$
$$s_{91} = A_{51}$$
$$s_{99} = A_{55}$$

$$s_{10,1} = B_{51}$$
$$s_{10,10} = B_{55}$$
$$s_{11,1} = C_{51}$$
$$s_{11,11} = C_{55}$$
$$s_{12,1} = y_1 \times A_{11} + y_2 \times B_{11} + y_3 \times C_{11}$$
$$s_{12,2} = x_1 \times A_{22} + x_2 \times B_{22} + y_3 \times C_{22}$$
$$s_{12,6} = x_1 \times A_{24}$$
$$s_{12,7} = x_2 \times B_{24}$$
$$s_{12,8} = x_3 \times C_{24}$$

$$s_{12,9} = y_1 \times A_{15}$$
$$s_{12,10} = y_2 \times B_{15}$$
$$s_{12,11} = y_3 \times C_{15}$$
$$s_{13,12} = A_{76}$$
$$s_{13,13} = A_{77}$$
$$s_{14,12} = B_{76}$$
$$s_{14,14} = B_{77}$$
$$s_{15,12} = C_{76}$$
$$s_{15,15} = C_{77}$$

$$s_{12,12} = A_{66} + B_{66} + C_{66} + x_1^2 \times A_{22} + x_2^2 \times B_{22} + x_3^2 \times C_{22} + y_1^2 \times A_{11} + y_2^2 \times B_{11} + y_3^2 \times C_{11}$$

rigid in its own plane, no strains are developed in the slab for the two x and y translations and the rotation about the z axis.

The remaining 12 displacements comprising the axial deformation, rotations about centroidal axes, and the warping about the shear centers of the three shear walls produce considerable bending and twisting of the slab. These are shown diagrammatically in Fig. 10.97*a* to *l*. Since the number of displacements capable of producing forces in the slab is 12, the stiffness matrix for the slab will be of the order of 12 by 12. Had the effect of warping been neglected, the corresponding matrix for slab stiffness would have been 9 by 9. Each of the 12 displacements gives rise to 12 forces in general, and of particular interest are the bimoments that develop not only because of warping but other displacements as well. For example, the unit vertical displacement shown in Fig. 10-97*a* induces a significant bimoment for each open section, in addition to the familiar vertical force and transverse moments. It is by recognizing this special feature that the present analysis differs from other three-dimensional analyses of shear walls.

It only remains now to find the various forces produced owing to each of the 12 displacements. This is achieved by employing the finite element analysis. The procedure is explained best by referring to Fig. 10.98, which shows a typical finite element idealization of the floor slab. It is assumed that the stiffness of the floor slab, corresponding to a unit displacement of the central core, is required.

The nodes $N_{11}, N_{12}, \ldots, N_{1,11}; N_{21}, N_{22}, \ldots, N_{27}$; and $N_{31}, N_{32}, \ldots, N_{37}$ corresponding to the profiles of the three shear walls are of particular importance in the finite element analysis, since the displacements and forces only at these nodes are of concern. A unit displacement corresponding to $u_3 = 1$ is applied to the plate by giving the nodes $N_{11}, N_{12}, \ldots, N_{1,11}$ a vertical downward displacement of unity and a zero slope along the contour. The two groups of nodes $N_{21}, N_{22}, \ldots, N_{27}$ and $N_{31}, N_{32}, \ldots, N_{37}$ corresponding to the contours of the *I*-shaped walls are held down by imposing zero deflections and rotations along the contour. However, no moment restraint is imposed in the direction perpendicular to the contour of the walls. This freedom is necessary to conform with the assumption that the longitudinal moments in the thin-walled beam are negligible. The finite element analysis of the plate is carried out for the above displacements, and the forces and moments developed at each of the nodes are found. The next step is to evaluate the four generalized forces, namely the vertical force, moments M_x and M_y, and a bimoment B_z for each of the three shear walls. This is achieved by using an appropriate transformation matrix for each wall as explained in the following.

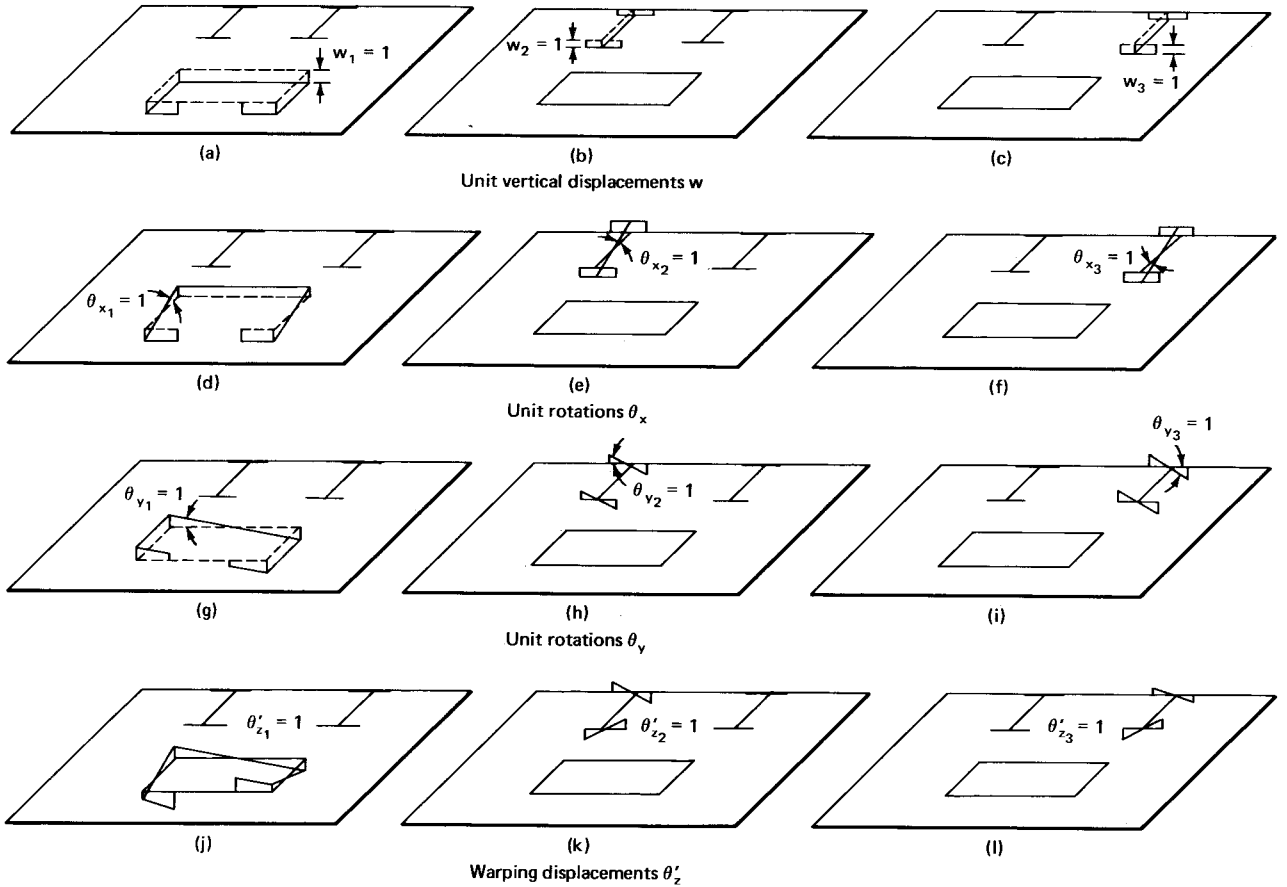

Figure 10.97 Floor slab stiffness.

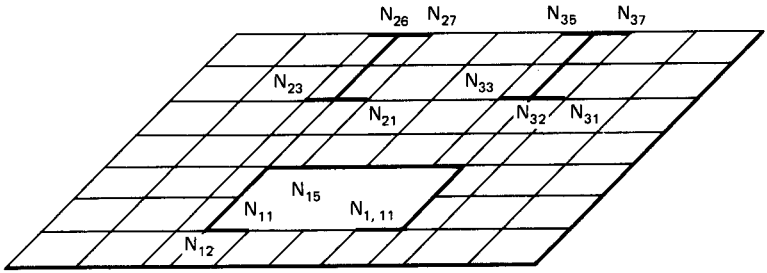

Figure 10.98 Finite element idealization of floor slab showing contact nodes.

Tranformation matrices. Figure 10.99 shows the central core wall on which, for simplicity, the nodes are designated as 1, 2, 3, . . . , n. The forces and moments at these nodes are known from the finite element solution, and it is required to express these nodal forces and moments in terms of the four generalized forces, namely, P_Z, M_X, M_Y, and B_Z. Referring to Fig. 10.99, it is seen that the vertical displacement and rotation at each node can be considered as a combination of the four generalized displacements W, θ_X, θ_Y, and θ_Z' of the core. Using the subscripts s and c to identify the displacements of the slab and core, respectively, the nodal displacements are expressed in terms of the wall displacements by the following relation:

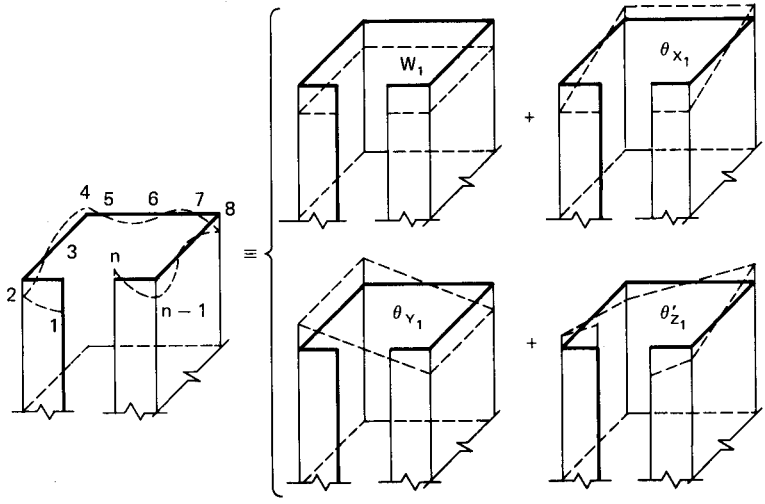

Figure 10.99 Nodal displacements in terms of generalized displacements of core.

$$\begin{bmatrix} w_1 \\ \theta_{x_1} \\ \theta_{y_1} \\ w_2 \\ \theta_{x_2} \\ \theta_{y_2} \\ \cdots \\ \cdots \\ \cdots \\ w_n \\ \theta_{x_n} \\ \theta_{y_n} \end{bmatrix} = \begin{bmatrix} 1 & \xi_1 & -\zeta_1 & -\omega_1 \\ 0 & 1 & 0 & \dfrac{\partial \omega_1}{\partial y} \\ 0 & 0 & 1 & \dfrac{\partial \omega_1}{\partial x} \\ 1 & \xi_2 & -\zeta_2 & -\omega_2 \\ 0 & 1 & 0 & \dfrac{\partial \omega_2}{\partial y} \\ 0 & 0 & 1 & \dfrac{\partial \omega_2}{\partial x} \\ \cdots & \cdots & \cdots & \cdots \\ \cdots & \cdots & \cdots & \cdots \\ \cdots & \cdots & \cdots & \cdots \\ 1 & \xi_n & \zeta_n & \omega_n \\ 0 & 1 & 0 & \dfrac{\partial \omega_n}{\partial y} \\ 0 & 0 & 1 & \dfrac{\partial \omega_n}{\partial x} \end{bmatrix} \begin{bmatrix} W \\ \theta_X \\ \theta_Y \\ \theta'_Z \end{bmatrix} \tag{10.85}$$

where ζ_i, ξ_i = the x and y coordinates of the ith node referred to the centroidal axes of the core (Fig. 10.100)

ω_i = the sectorial coordinate of the ith node referred to the shear center of the core (Fig. 10.100)

$\dfrac{\partial \omega_i}{\partial x}$ $\dfrac{\partial \omega_i}{\partial y}$ = the rates of change of the sectorial coordinate along x and y directions, respectively

w_i = the vertical displacement of the ith node

θ_{x_i}, θ_{y_i} = the rotations at the ith node with respect to a set of local orthogonal axes at i, parallel to the centroidal axes of the core

W_1 = the vertical displacement of the core

θ_{X_1}, θ_{Y_1} = the rotations of the core about its centroidal axes

θ'_{Z_1} = the warping displacement of the core referred to its shear center.

In matrix notation Eq. (10.85) can be written as

$$[U]_s = [T]\,[U]_c \tag{10.86}$$

where $[U]_s$ = the vector of nodal displacements and rotations
$[T]$ = the transformation matrix
$[U]_c$ = the vector of generalized displacement of the core

Using the contragradient relationship that exists between stress resultants and displacements, the forces and moments at the nodes of the slab are expressed in terms of the generalized forces in the core:

$$[F]_c = [T^*]\,[F]_s \tag{10.87}$$

where $[F]_c$ = the vector of generalized forces in the core
$[T^*]$ = the transpose of the transformation $[T]$
$[F]_s$ = the vector of nodal forces and moments

Equation (10.87), when expanded, takes the form

$$\begin{bmatrix} P_{Z_1} \\ M_{X_1} \\ M_{Y_1} \\ B_{Z_1} \end{bmatrix} = \begin{bmatrix} 1 & 0 & 0 & 1 & 0 & 0 & \cdots & 1 & 0 & 0 \\ \xi_1 & 1 & 0 & \xi_2 & 1 & 0 & \cdots & \xi_n & 1 & 0 \\ -\zeta_1 & 0 & 1 & -\zeta_2 & 1 & 0 & \cdots & \zeta_n & 1 & 0 \\ \omega_1 & \dfrac{\partial \omega_1}{\partial y} & \dfrac{\partial \omega_1}{\partial x} & \omega_2 & \dfrac{\partial \omega_2}{\partial y} & \dfrac{\partial \omega_2}{\partial x} & \cdots & \omega_n & \dfrac{\partial \omega_n}{\partial y} & \dfrac{\partial \omega_n}{\partial x} \end{bmatrix} \begin{bmatrix} p_1 \\ m_{x_1} \\ m_{y_1} \\ p_2 \\ m_{x_2} \\ m_{y_2} \\ \cdots \\ \cdots \\ \cdots \\ p_n \\ m_{x_n} \\ m_{y_n} \end{bmatrix} \tag{10.88}$$

where P_{Z_1} = the vertical force in the core assumed to be acting uniformly over the cross section
M_{X_1}, M_{Y_1} = the transverse bending moments about the centroidal axes of the core
B_{Z_1} = the bimoment referred to the core shear center
p_i = the vertical force at the ith node of the slab
m_{x_i}, m_{y_i} = the transverse moments at the ith node about the x and y axes, respectively.

$P_{Z_1}, M_{X_1}, M_{Y_1}$, and B_{Z_1} are the required generalized stress resultants and p_1, m_{x_1}, m_{y_1}, . . . , etc., are the forces and moments at the nodes

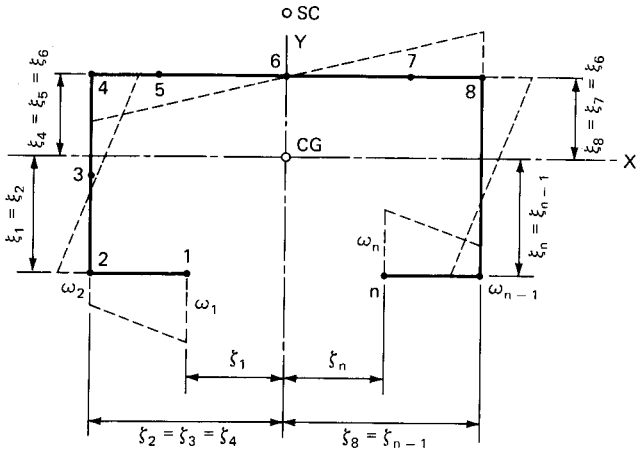

Figure 10.100 Generalized coordinates of nodes referred to the center of gravity (CG) and shear center (SC) of core.

obtained from the finite element analysis. The stress resultants P_{Z_2}, M_{X_2}, M_{Y_2} and B_{Z_2} and P_{Z_3}, M_{X_3}, M_{Y_3}, and B_{Z_3} for the other two shear walls are similarly obtained by multiplying the nodal forces and moments by appropriate transformation matrices. The resulting 12 stress resultants are the elements of the first row of the slab stiffness matrix F. The elements for the remaining 11 rows are obtained in the same manner by imposing at the nodes deformations corresponding to unit value of u_4, u_5, . . . , u_{11} and u_{13}, u_{14}, and u_{15}. Each of the displacements u_i is treated as a separate right-hand side in the finite element solution and the nodal forces and moments are found. These are multiplied by the transformation matrices to obtain the complete slab stiffness matrix.

Modified segment stiffness matrix. Having obtained the stiffness matrix for the slab, the next step is to add the appropriate elements of the slab and segment stiffnesses to form the modified story segment stiffness matrix. The addition is shown diagrammatically in Fig. 10.101.

Assembly and solution. The final part of the analysis consists of assembling the modified story segment matrices to obtain the complete stiffness matrix of the structure. Advantage is taken of the band form and symmetry of the stiffness matrix and the overall matrix is stored in the half-band form. Since the number of degrees of freedom is 15 at each story the dimensions of the stored matrix will be $(15 \times NS)$ by 30. The solution is obtained for the required number of loading cases, and from the displacements thus obtained and the generalized member

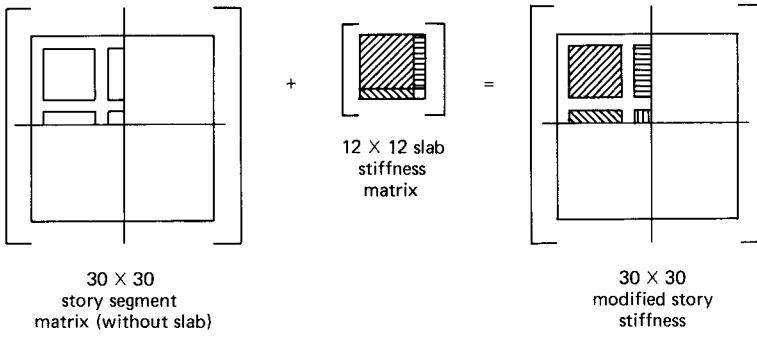

Figure 10.101 Story stiffness matrix.

stiffness matrices, the seven stress resultants for each wall throughout the structure are found.

Computer program. A program has been written using the above method. It is comprised of two parts; the first refers to the finite element solution for the stiffness of the floor slab, and the second to the three-dimensional analysis of three interconnected open sections. The input data consist of the description of the plate such as number of elements and nodes, the induced displacements at the contact nodes corresponding to this axial deformation, rotations θ_x and θ_y and the warping θ_z' for each core, and finally the description of the section and sectorial properties of the shear walls. Any number of loading cases can be treated in a single analysis operation.

Example problem. Dimensions of the structure, the finite element discretization of the slab, and the values of E and μ used in the analysis are shown in Fig. 10.102. The structure has been analyzed for a unit clockwise torque in the plane of the top floor. To illustrate the significance of warping, the model was analyzed by a separate analysis in which warping was neglected.

At the outset, it should be made clear that the stiffnesses of the slab used in the two analyses (three-dimensional analysis accounting for warping and three-dimensional analysis neglecting warping) are different. In the analysis in which warping is neglected, the stiffness of the slab is obtained on the assumption that the connection between the slab and the walls is completely rigid. In the analysis in which warping is taken into account, it is assumed that the slab is simply supported by the shear walls. The contribution to structural stiffness by the slab analyzed by the present method is, therefore, lower than the corresponding contribution in the simpler method. If the slab stiffnesses in

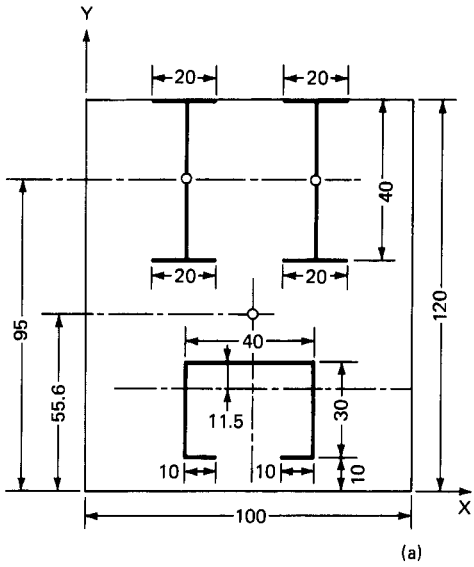

All dimensions in inches
All walls 2 in thick
Story height 12.5 in
Number of stories 20
I_x for central core 27850 in^4
I_y for central core 57578 in^4
I_x for I-shaped walls 62306 in^4
I_y for I-shaped walls 2700 in^4
I_ω for central core 12162000 in^6
I_ω for I-shaped walls 1536000 in^6
k for central core = 0.4
k for I-shaped walls = 0.11
E = 400 ksi $\mu = 0.15$
Thickness of slab 0.5 in

(a)

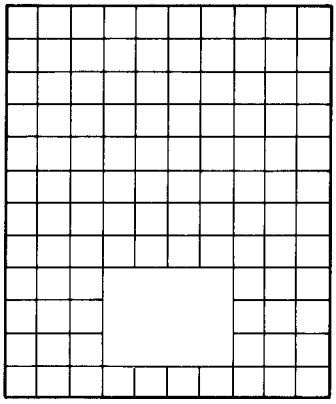

(b)

Figure 10.102 Example problem. (*a*) Dimensions and properties; (*b*) finite element idealizations.

the analyses were taken to be identical, the effect of warping would be even more striking than shown in Figs. 10.103 through 10.108.

It is seen by comparison of the displacements and rotations (Fig. 10.101) that values of stiffnesses obtained by the present warping method are around 25 percent higher than those obtained by the simpler analysis which neglects warping. It is seen (Fig. 10.102) that there is a striking difference between the values of torques for the central core given by the two analyses. The values of torque given by the analysis in which warping is considered are more than three times

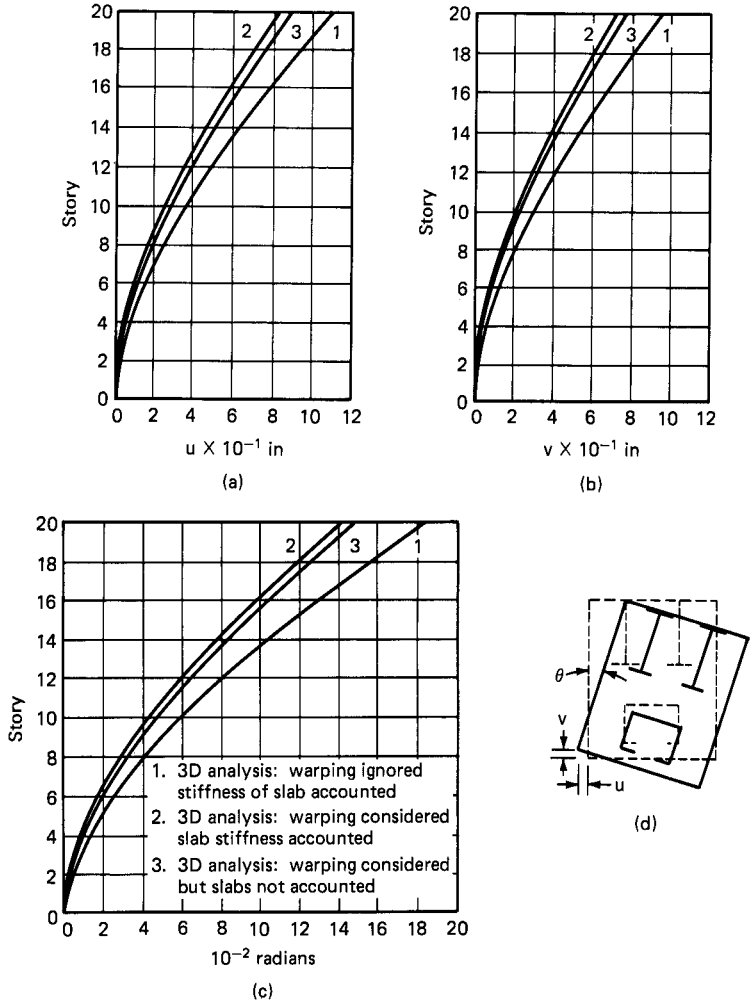

Figure 10.103 Example problem, planar displacements. (*a*) Horizontal displacement u; (*b*) horizontal displacement v, (*c*) rotation θ; (*d*) schematic plan showing planar displacements.

the corresponding values obtained by the simpler analysis. Furthermore, the torque predicted by the simpler theory decreases very rapidly until for the bottom few stories its value is negligible, whereas the torque given by the warping theory remains more or less constant for the whole height of the structure. The value of torque given by the St. Venant theory is small for the lower part of the structure because of the low relative angle of rotation in this region. The lack of torsional resistance in this region is balanced by additional shear forces. Therefore, the shear forces in the lower parts of the structure, as

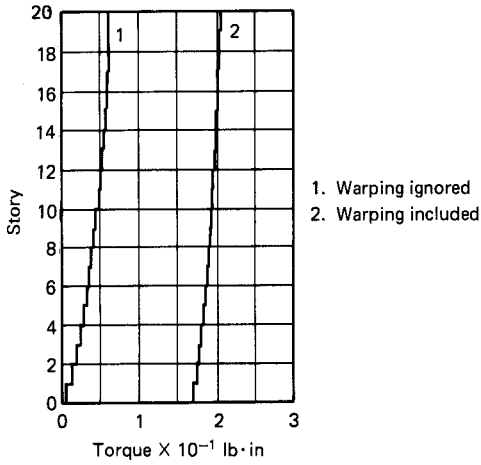

Figure 10.104 Comparison of torque in the central core.

predicted by the simpler theory, are very high (Fig. 10.106). The shear forces given by the theory in which warping is considered are not so high and remain almost constant for the whole height of the structure.

These remarks apply equally to the I-shaped walls, although the difference in values of torques and shear forces given by the two theories are not as great as those for the core. This is because the warping rigidity for the I-shaped walls is small compared with that of the core (1,536,000 in^6 compared with 12,162,000 in^6 for the core). The shear force distribution for the I-shaped wall is similar to that of the central core, its magnitude being half of that for the core.

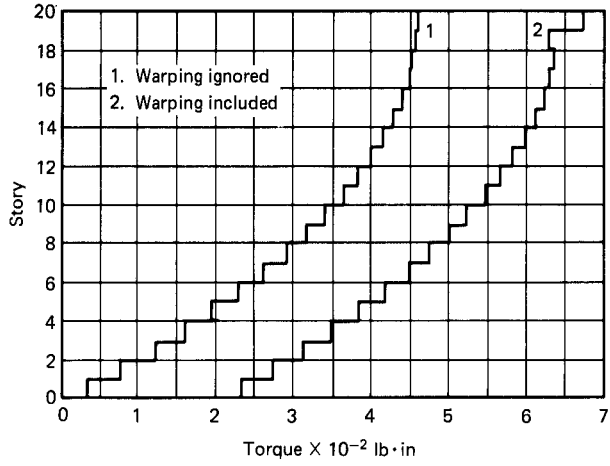

Figure 10.105 Comparison of torque in I-shaped walls.

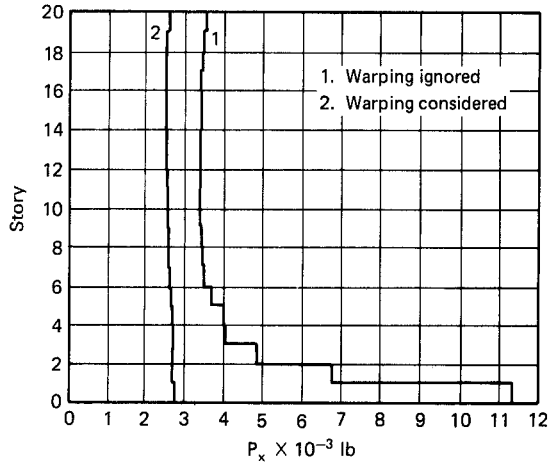

Figure 10.106 Comparison of shear force in the core.

A comparison of moment M_y and longitudinal stresses obtained by the two theories is shown in Fig. 10.107. The importance of the warping contribution is clear from this figure. The results obtained by the two analyses are summarized in Fig. 10.108.

10.8.5 Analysis of open-section and planar shear walls

In this section the three-dimensional analysis presented in the previous section is extended to analyze shear wall plate structures

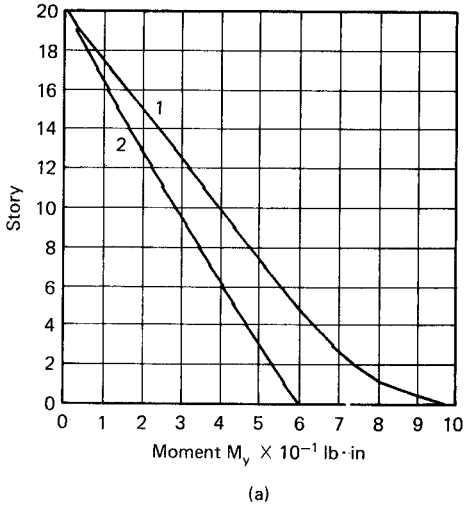

Figure 10.107 (*a*) Comparison of moment in the core.

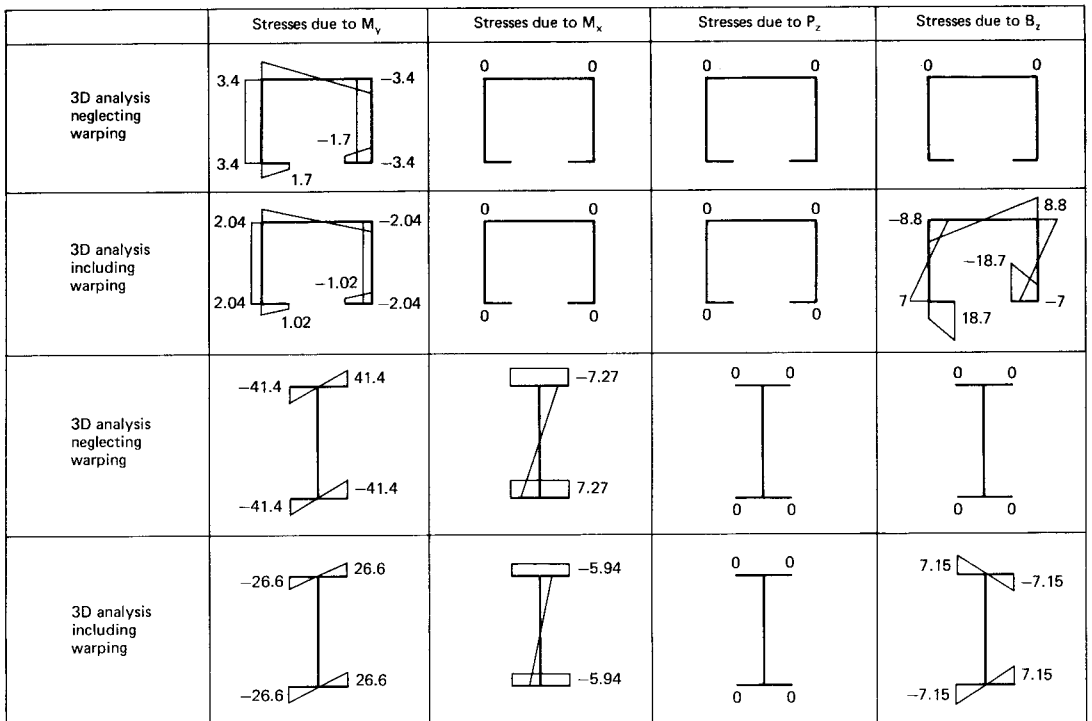

(b)

Figure 10.107 (*Continued*) (*b*) Comparison of longitudinal stresses at base.

consisting of any number of shear walls. Warping of open sections is included as an independent displacement in the analysis. In addition to the bending stiffness of flat plates, their warping interaction is considered. A stiffness method of analysis is used which employs thin-walled and conventional beam elements for shear walls and rectangular finite elements for flat plates. The importance of including the warping of open sections is shown by a comparison of analytical results of the present method with those of a conventional analysis in which warping is ignored. The notation used in this section is listed below

A	Stiffness matrix for open-section shear wall
B	Stiffness matrix for plane shear wall
B_z	Bimoment in open section
NOF	Number of degrees of freedom
NP	Number of plane shear walls
NT	Number of open-section shear walls
NW	Number of walls
$S_{1,1}, S_{1,2}$	Elements of story stiffness matrix
u_1, u_2	Shear wall displacements
W	Vertical displacement of shear wall
x_1, y_1	Coordinates of shear center
x, y, z	Reference coordinate system
θ_x, θ_y	Rotation of shear wall about the x and y axes, respectively
θ'_z	Warping displacement of open-section shear wall

Description of structure. The type of structure to which the proposed technique is applicable consists of an assemblage of vertical shear walls arranged in a rectangular pattern. Any or all of the shear walls can be open sections. At arbitrary intervals of height there are horizontal diaphragms in the form of beamless flat plates, rigid in the horizontal plane, which link together all the walls. The plan geometry, story height, and member and material properties are assumed constant throughout the height of the structure; this restriction is unnecessary for the application of the method but it keeps the presentation simple. A combination of any number of thin-walled open sections NT and any number of plane walls NP can be considered, but for illustration a structure with 2 open and 12 plane shear sections will be considered. Thus, NT = 2 and NP = 12 in the plan shown in Fig. 10.109. The origin is taken at the southwest corner of the top floor and the x, y, z coordinate system forms a left-hand system with z in the vertical downward direction. The floors are numbered from the top down; the displacements are considered positive in the positive direc-

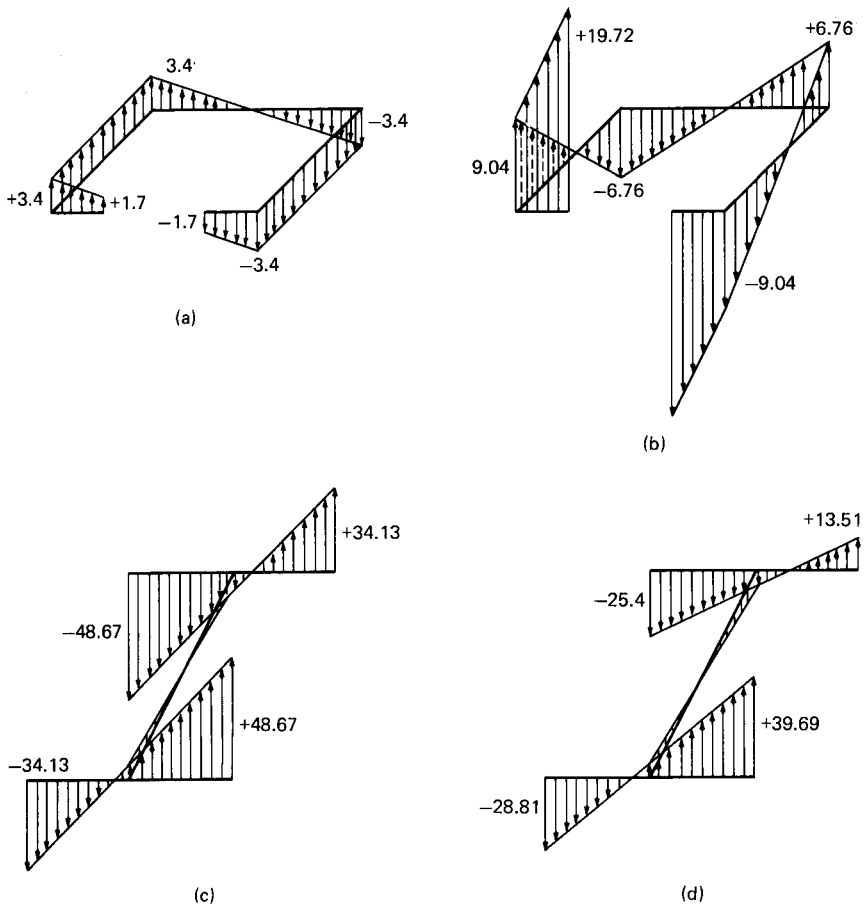

Figure 10.108 Comparison of longitudinal stresses at the base. (*a*) Central core, warping ignored; (*b*) central core, warping considered; (*c*) I-shaped walls, warping ignored; (*d*) I-shaped walls, warping considered. All units in psi.

tion of the axes. The loads applied on the structure consist of horizontal forces on the floor diaphragm in any direction and moments about the vertical axis z.

Method of analysis. First, the shear wall–flat plate system is approximated by an assemblage of three discrete elements: thin-walled beam elements for walls of open section, three-dimensional beam elements for plane walls, and rectangular bending elements for the flat plate. Individual wall stiffness matrices are evaluated in a coordinate system local to each wall and are combined appropriately in terms of the structure coordinate system. A finite element bending analysis is carried out to evaluate the out-of-plane stiffness of floor plate, and

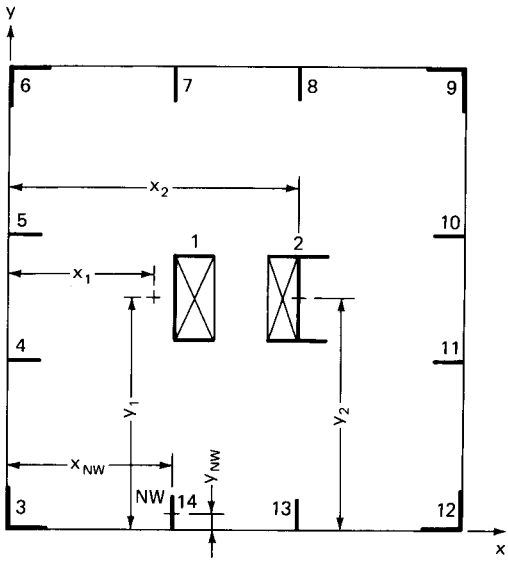

Figure 10.109 Building plan.

using a transformation technique, the plate forces are expressed in terms of well generalized forces.

The complete structure stiffness matrix is assembled and the resulting set of equilibrium equations is modified for boundary conditions and solved. Internal stresses are calculated from displacements of each element in the structure.

General structure displacement. Floor diaphragm displacements and the end displacements of the walls comprise the general displacement. In the absence of a rigid diaphragm, each open and plane shear wall would have seven and six displacements, respectively. However, because each wall is constrained to rotate and translate according to the floor diaphragm displacement, the end displacements are reduced to four (axial displacement W, rotations θ_x and θ_y, and warping displacement θ_z') for open sections and three (W, θ_x, and θ_y) for plane walls. Therefore, the total number of degrees of freedom NOF at each floor is reduced to $3 + \text{NT} \times 4 + \text{NP} \times 3$.

The numbering of the displacements follows a regular pattern: the planar displacements u, v, and θ_z of the topmost story are designated as u_1, u_2, and u_3; the vertical displacements of the walls as u_4, u_5, . . . , $u_{\text{NW}} + 3$; the rotations θ_x of the walls as $u_{\text{NW}} + 4$, $u_{\text{NW}} + 5$, . . . , $u_{2\text{NW}} + 3$; the rotations θ_y as $u_{2\text{NW}} + 4$, $u_{2\text{NW}} + 5$, . . . , $u_{3\text{NW}} + 3$; and the warping displacements for the open sections are designated as $u_{3\text{NW}} + 4$, $u_{3\text{NW}} + 5$, . . . , $u_{3\text{NW}} + 3 + \text{NT}$. The displacements for the other stories are numbered in the same sequence.

Defining a story segment as the assemblage of shear walls between two floors, the stiffness matrix for a typical segment is set up in two stages as follows:

1. Establishment of the stiffness matrix for a story segment in terms of the structure coordinate system.

2. Adjustment of the matrix in stage 1 by addition of floor slab stiffness to obtain the modified segment stiffness matrix.

The stiffness evaluation of a story segment can be accomplished by use of the direct stiffness technique. First, individual shear wall stiffnesses relating the end displacements to the forces are derived in a coordinate system that is intrinsic to the wall itself. Then each wall element matrix is expressed in the structure coordinate system by use of simple congruent transformations and the story segment stiffness is obtained by addition of individual wall contributions. This approach is quite general and is expedient when walls are located obliquely in plan. However, because the stiffness matrix for the generally regular nature of shear walls exhibits a well-defined pattern, it is convenient to generate the elements of the story segment matrix directly from the wall element matrix without recourse to transformation methods.

Because the vertical wall elements may be open or plane shear walls, it is necessary to form two types of member stiffness matrices: a 14-by-14 generalized member stiffness matrix A for an open section and a 12-by-12 matrix B for a prismatic beam element in space. For purposes of evaluating the story stiffness, the walls are numbered 1, 2, 3, . . . , NW, where NW = NT + NP, the open sections being numbered first in sequence, followed by plane walls. In the present example the open sections are number 1 and 2 and the plane walls 3 to 14. The coordinates of shear centers of the walls with respect to the origin are designated as $(x_1, y_1), (x_2, y_2), \ldots, (x_{NW}, y_{NW})$ as shown in Fig. 10.109. The procedure for formulating the elements of the story stiffness matrix S is as follows.

Member end forces generated due to a displacement $u_i = 1$ ($i = 1 -$ NOF) are evaluated in terms of the individual wall stiffness matrix and the coordinates of the shear center of the wall. Of these generalized forces, the horizontal forces and the twisting moment of each wall are combined to give equivalent horizontal forces and moments at the origin corresponding to the u_1, u_2, and u_3 displacements of the floor. The remaining forces are entered in appropriate locations of the S matrix without any transformation. Figure 10.110, for example, shows member end forces developed due to unit rotation of the top floor while imaginary restraints at the origin are assumed to suppress the planar displacements u_1 and u_2. For convenience, only the forces developed in walls 1, 2, and NW are shown in terms of the individual wall matrix and the coordinates of shear

centers. The elements $S_{1,3}$ and $S_{2,3}$ are obtained simply by summing the horizontal forces of each wall. The element $S_{3,3}$ corresponding to rotation $u_3 = 1$ is obtained by summation of torque in each wall and the moments of the shear forces about the origin. The bimoments $A_{1(6,7)}$ and $A_{2(6,7)}$ generated in the open sections are entered as elements $S_{3,47}$ and $S_{3,48}$, respectively. Explicit expressions for the elements of the S matrix due to $u_3 = 1$ are given in Eq. (10.89).

The remaining elements of the story stiffness matrix are formulated in a similar manner by putting $u_i = 1$ ($i = 1 - \text{NOF}$). The nonzero elements of the lower half of the first quadrant of the S matrix for the general case of NW shear walls are given in Eq. (10.89). The remaining elements are found from considerations of symmetry and equilibrium.

$$
\begin{aligned}
S_{1,1} &= \sum_{i=1}^{\text{NT}} A_{i(1,1)} + \sum_{i=\text{NT}+1}^{\text{NW}} B_{i(1,1)} \\
S_{2,2} &= \sum_{i=1}^{\text{NT}} A_{i(2,2)} + \sum_{i=\text{NT}+1}^{\text{NW}} B_{i(2,2)} \\
S_{3,2} &= \sum_{i=1}^{\text{NT}} - x_i \times A_{i(2,2)} - \sum_{i=\text{NT}+1}^{\text{NW}} x_{i(2,2)} \\
S_{3,1} &= \sum_{i=1}^{\text{NT}} y_i \times A_{i(1,1)} + \sum_{i=\text{NT}+1}^{\text{NW}} y_i \times B_{i(1,1)} \\
S_{3,3} &= \sum_{i=1}^{\text{NT}} [A_{i(6,6)} + x_i^2 \times A_{i(2,2)} + y_i^2 \times A_{i(1,1)}] \\
&\quad + \sum_{i=\text{NT}+1}^{\text{NW}} [B_{i(6,6)} + x_i^2 \times B_{i(2,2)} + y_i^2 \times B_{i(1,1)}]
\end{aligned}
\tag{10.89}
$$

$$
\left.
\begin{aligned}
S_{i+3,i+3} &= A_{i(3,3)} \\
S_{NW+3+i,2} &= A_{i(4,2)} \\
S_{2NW+3+i,1} &= A_{i(5,1)} \\
S_{2NW+3+i,2NW+3+i} &= A_{i(5,5)} \\
S_{3NW+3+i,3} &= A_{i(7,6)} \\
S_{3NW+3+i,3NW+3+i} &= A_{i(7,7)}
\end{aligned}
\right\} i = 1,2,\ldots,\text{NT}
$$

$$
\left.
\begin{aligned}
S_{i+3,i+3} &= B_{i,3,3} \\
S_{NW+3+i,2} &= B_{i,4,2} \\
S_{2NW+3+i,2NW+3+i} &= B_{i,5,5} \\
S_{NW+3+i,3} &= -B_{i,2,4} + x_i \\
S_{2NW+3+i,3} &= B_{i,1,5} \times y_i
\end{aligned}
\right\} i = \text{NT}+1, \text{NT}+2, \cdots, \text{NT}+\text{NP}
$$

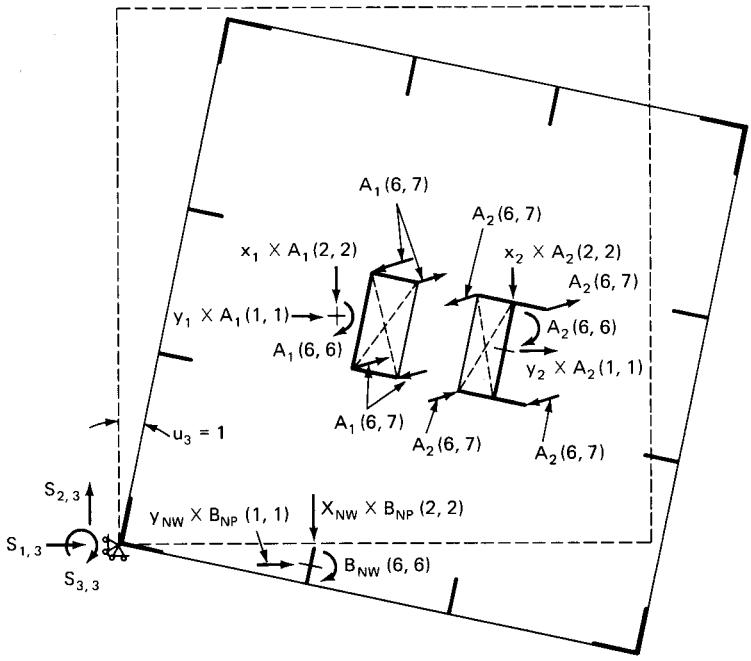

Figure 10.110 Horizontal rotation.

In these equations, $A_{i(m,n)}$ and $B_{i(m,n)}$ refer to mnth element of the 14 by 14 and 12 by 12 generalized member stiffness matrix for the open- and plane-section shear walls, respectively.

Stiffness of floor slab. Considering the displacement of each story, it is seen that of the NOF possible degrees of freedom, all but the three planar displacements u_1, u_2, and u_3 induce out-of-plane bending of the slab. Therefore, the vertical displacement W, rotations θ_x and θ_y for each wall, plus the warping displacement θ_z' of open sections are of interest in the evaluation of floor stiffness. Of particular significance is the warping because it is by recognizing this additional displacement that the present analysis differs from other three-dimensional analyses.

It is now required to find various forces produced in the floor slab due to each of the aforementioned wall displacements. In view of the complexity of the problem, a numerical procedure using rectangular finite bending elements has been adapted for evaluating the slab stiffness. First the floor slab is idealized as an assemblage of rectangular finite elements. Assume that it is required to evaluate the stiffness of slab due to a unit warping displacement of wall 2. For this purpose the nodes on the profile of wall 2 are given displacements such

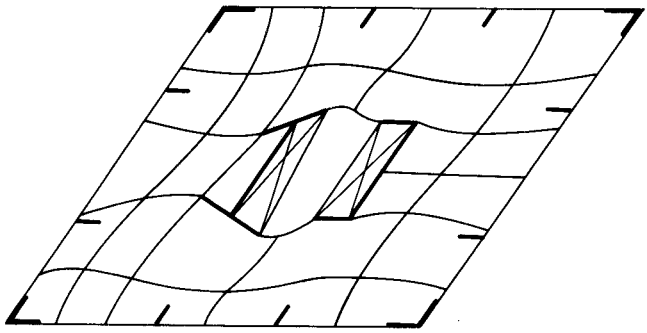

Figure 10.111 Floor slab displacement due to warping of shear wall.

that they undergo the same deformation as the warping displacement of the wall while the nodes on the profiles of the other walls are held with zero displacements as shown in Fig. 10.111. A finite element bending solution is carried out for the displacement of the slab to give forces and moments at the nodes. By using a congruent transformation, these forces and moments are condensed to give wall generalized forces, namely the axial force P_z, moments M_x and M_y for all walls, and an additional generalized force bimoment B_z for open sections. This procedure is carried out for each end displacement of wall, thus requiring $4 \times \text{NT} + 3 \times \text{NP}$ finite element solutions.

Method of solution. The condensed stiffness equation of the floor slab is added to the segment stiffness to obtain the modified story segment matrix. These matrices are assembled for each story to give the complete structure matrix. The resulting set of equations (appropriately modified for displacement boundary conditions) represents the global equilibrium equations for the discretized structure. The solution of equilibrium equations results in displacement components at each floor arising from the loads applied to the structure. When all the displacements of the structure have been defined, the forces in each shear wall are computed from the stiffness matrix of the member and the displacements.

Computer program. A general computer program based on the proposed method has been used to analyze a sample problem. The input to the program consists of the following groups of data:

1. Floor slab data: number of finite elements used to discretize the slab, total number of slab nodes, number of nodes in contact with shear wall profiles, slab thickness, and material properties

2. Geometric layout, number of floors and properties of each wall including warping moment of inertia for open sections
3. Data that describe the transformation matrices used to compute wall end forces from finite element nodal forces and moments
4. Nodal displacements that relate slab displacements to the wall end displacements
5. Applied loads on floors in the horizontal plane.

The program incorporates the standard computation technique of storing only nonzero elements of the stiffness matrix in half-band form. Several independent boundary conditions for the slab analysis are analyzed in a single analysis operation, as are several loading conditions on the structure. The output from the program consists of displacements in the horizontal plane and the wall displacements at each floor and member forces, namely, axial force, moments, shear forces for plane walls, and an additional generalized force–bimoment for open-section shear walls.

Example problem. A 15-story structure containing a single open core and eight planar shear walls was analyzed by using a purpose written computer program. The layout and dimensions of the structure and the finite element mesh pattern used in the discretization of the floor slab are shown in Fig. 10.112. Two analyses were carried out for the structure; the first analysis included the effect of warping and in order to examine its significance a second analysis was performed neglecting warping of the central core. In addition to these, to study further the effect of the floor slab, each analysis was reworked ignoring the out-of-plane stiffness of the floor slab. Thus, the example problem has been analyzed for four conditions:

1. Warping of the core considered, but out-of-plane stiffness of the slab ignored
2. Both warping of the core and out-of-plane stiffness of the slab considered
3. Both warping of the core and out-of-plane stiffness of the slab ignored
4. Warping ignored, but out-of-plane stiffness of the slab considered

All these analyses were performed for a loading condition of a unit horizontal load applied in the x direction at the origin.

The comparison of rotation curves obtained for the analysis of conditions a to d is given in Fig. 10.113. To single out the effect of

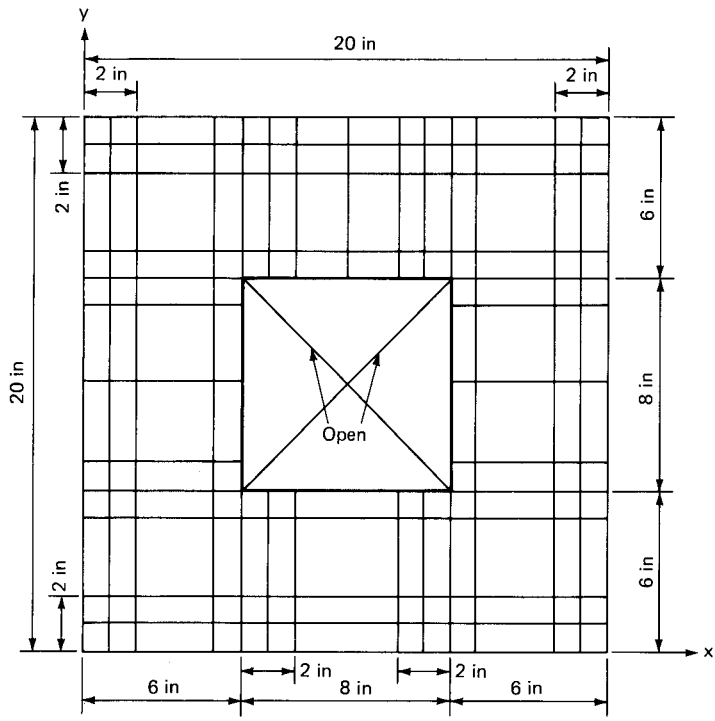

Story height	4 in
Wall thickness	$\frac{1}{4}$ in
Slab thickness	$\frac{3}{8}$ in
Young's modulus	4.25×10^5 psi
Shear modulus	1.57×10^5 psi
Number of stories	15

Figure 10.112 Finite element idealization.

warping, curve *a* should be compared with curve *c* and curve *b* with curve *d* because the analysis assumptions are identical for these two sets of curves except for the consideration of warping of the core. Comparing curves *a* and *c*, it is seen that the values of rotation given by curve *a*, which included the warping of core, are about seven times smaller than those given by curve *c* which neglected warping. The effect of warping on the stiffness of the structure is clearly too large to be ignored. The values of rotation obtained by neglecting warping do not remotely resemble those obtained by the more accurate theory. Comparing curves *b* and *d* in which the out-of-plane stiffness of slab is taken into account, it is again seen that the warping contributions are substantial; the structure stiffness values are about three times higher than those obtained by the simpler analysis. Similar results were

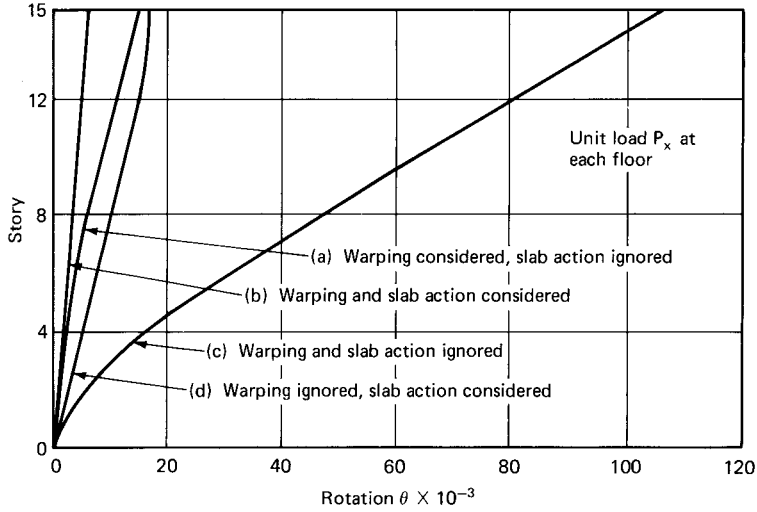

Figure 10.113 Comparison of rotations.

obtained for the other two planar displacements. Also the analyses of *a* to *d* were carried out for a unit torque loading condition in the plane of the top floor and the results were found to be of the same order of magnitude as those given in Fig. 10.113.

Consider curves *a* to *d* from another aspect to assess the importance of including the out-of-plane stiffness of the slab in the analyses. It is evident from Fig. 10.113 that the out-of-plane stiffness of the slab has a greater impact in the simpler theory than the more refined theory which accounts for warping.

Figure 10.114 shows that there is a marked difference in the values of torque obtained by using the two analyses. The values of torque at the base, given by the more exact theory in which warping of the core is taken into account, are about 10 times higher than those obtained by the simpler theory. Also the variation of torque along the height of the structure is different for the two analyses. In the simple analysis flexural torsion of the core is ignored and account is taken only of the St. Venant torsional rigidity. The corresponding St. Venant torque is a function of the core wall thickness and the relative twist of the structure. Its value is small, particularly at the lower stories, because of the small relative angle of twist at these stories. However, the torque given by the more exact theory is a function of the warping rigidity of the core and the rate at which the bimoment varies along the height of the structure. As a result of the parabolic increase of the bimoment from the top, the corresponding torque given by the more exact theory increases almost linearly from the top to the bottom of the

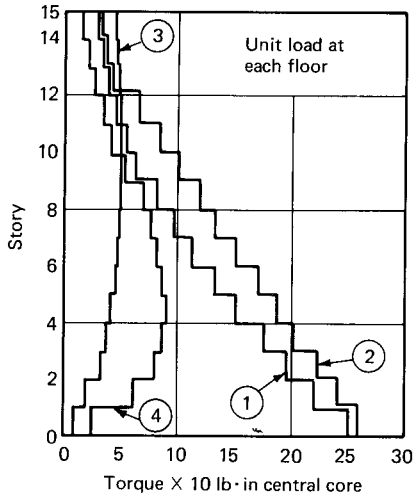

Figure 10.114 Comparison of torque in central core.

structure. The difference in the values of the torque obtained by taking the out-of-plane stiffness of the slab into consideration, although significant, is not as great as that between the two theories themselves. In other words, neglecting the out-of-plane stiffness of the slab introduces almost negligible errors compared with those introduced due to the neglect of warping.

Figure 10.115 shows the variation of bimoment along the height of the core obtained by using the exact theory. The curves are used to derive the axial warping stresses which are not predicted by the simple theory. The large values of bimoments occurring at the base again demonstrate the need for the use of warping theory in shear wall analysis.

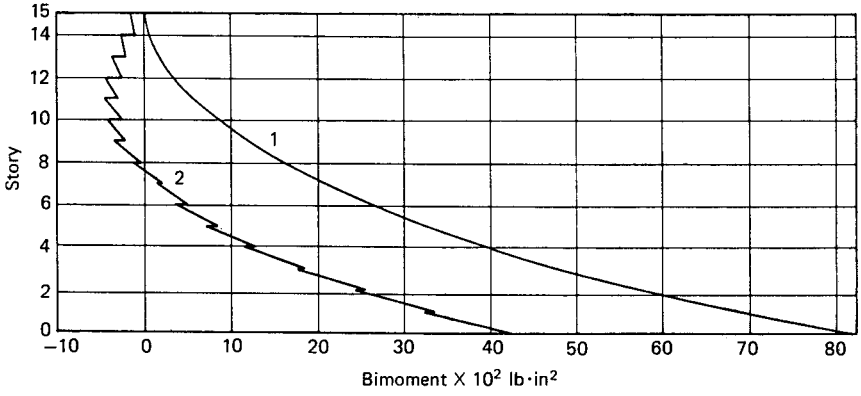

Figure 10.115 Bimoment comparison.

Summary and conclusions. An effective method for the linear structural analysis of multistory shear wall buildings has been developed. The technique is applicable to buildings with flat plates that are essentially rigid in their own plane and shear walls with either open or closed cross sections. The method of analysis differs from previously published techniques for the analysis of such structures in that it recognizes both the warping displacement of the open sections and the warping interaction associated with the flat plate; the earlier techniques either ignored one or both or used approximate methods.

From the results of the example problem, it was found that neglecting warping introduces errors for planar displacements of 300 to 700 percent depending on whether or not account is taken of the out-of-plane stiffness of the floor slab. The corresponding errors in the values of the torques in the central core were even more pronounced. In addition it was found that the variation of torque along the height of the structure given by the two theories was significantly different. Large bimoments at the base of the core were predicted by the warping theory, signifying additional longitudinal stresses in the core.

Within the confines of the assumptions made and the results of the example problem, it is evident that the warping phenomenon of open sections has a significant influence on the behavior of shear wall structures. Whether or not their effect is negligible depends on the magnitude of the warping rigidity of the cores and the torsional component of the lateral load. The height-to-width and width-to-thickness ratios of walls in elevator cores of tall buildings are of such a magnitude that they must be considered as thin-walled beams. It is recommended, therefore, that the warping phenomenon be given serious consideration in the analysis and design of open-section shear walls.

10.9 Suggested Method of Analysis

Commercially available three-dimensional frame analysis programs assume that shear walls could be modeled as prismatic beams having at the most six degrees of freedom at each end. This is true only for plane shear walls, but in practice, walls around building cores are mostly open-shaped, giving rise to warping stresses. It is necessary that the seventh degree of freedom associated with the warping displacement be included in a general analysis. Based on the results of torsion analyses presented in the previous sections, it appears that there is a definite need for a commercial three-dimensional program that takes into account the warping of shear cores and stiffness of connecting floor systems. A general analysis program requiring idealization of the whole building as an assemblage of beam, plane stress

and plate bending elements is beyond the scope of everyday engineering practice. As an alternate procedure, the author proposes the following method which attempts to capture the essential structural behavior of shear walls and floor systems in tall buildings. The method uses available commercial frame analysis programs and can be implemented as a general design office procedure without resorting to complete finite element solutions.

10.9.1 Modeling of shear walls

The first step in the analysis is to idealize the structure into a three-dimensional assemblage of vertical columns and horizontal beams at each floor. The modeling of columns and beams is a straightforward procedure, but particular care is needed in modeling shear walls. It was seen in previous sections that in a coupled shear wall system subjected to horizontal loads, each wall has a tendency to rotate about its base as a vertical cantilever, producing relative vertical displacements between adjacent wall panels. The interconnecting beams or slabs which react to diminish the relative displacement are subjected to shear forces and bending moments. In a broad sense, the action of the shear wall system is thus similar to that of a moment-resisting frame. Appreciation of this similarity of behavior led to the development of the equivalent frame concept nearly three decades ago, which even today is one of the most popular methods for idealizing shear walls.

To simulate the shear wall system as an equivalent frame it is necessary to assume the following characteristics: (1) line elements of the equivalent frame extend through the centers of gravity of the wall panels and coupling beams; (2) the cross-sectional properties of the columns are identical to those of the wall panels; (3) in representing the beams in the frame the portions of the beam falling within the wall panels are considered as haunches with large areas and moments of inertia. The purpose of stiff haunches is to provide for deflection and rotation of beam ends without bending within the wall panel. The properties of the beam between the adjacent wall panels are made the same as those of the corresponding coupling beams. The equivalent beam in the frame thus has a flexible length having the same property as the corresponding coupling beam between the wall panels and infinitely stiff haunches occurring within the limits of each wall.

Consider the I-shaped shear wall shown in Fig. 10.116. The wall can be idealized by using three vertical elements to represent the bending stiffnesses in two directions. The depth effect of wall in two directions is simulated by using rigid arms with large axial, shear, and bending stiffnesses.

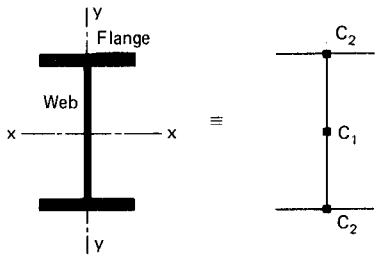

Area of C_1 = Area of shear wall web
I_x of C_1 = I_x of shear wall
I_y of C_1 = 0

Area of C_2 = Half the area of flanges
I_x of C_2 = 0
I_y of C_2 = Half the I_y of shear wall

Figure 10.116 Modeling technique for symmetric I-shaped shear wall.

In modeling the wall as a wide column, the actual values of sectional areas and flexural stiffness of the walls are assigned to the column. It is relatively easy to consider the shear deformation of the wall element by assigning equivalent shear areas to the column. All these three properties represent well both the bending and the shear deformation of the interconnected wall elements.

However, particular care is required in modeling elevator and stair cores with closed or partially closed profiles. The use of the wide-column analogy for analysis of such walls leads to poor results when such sections are subjected to torsion. For example, if a wide-column model is used to represent two I sections continuously connected at one face as shown in Fig. 10.117, there exists a discrepancy between the behavior of the actual structure and the wide-column model because of the difference in the distribution of vertical shear forces. Consider the distribution of vertical shear along the common edge of the continuously connected wall resulting from bending about the y axis. In the

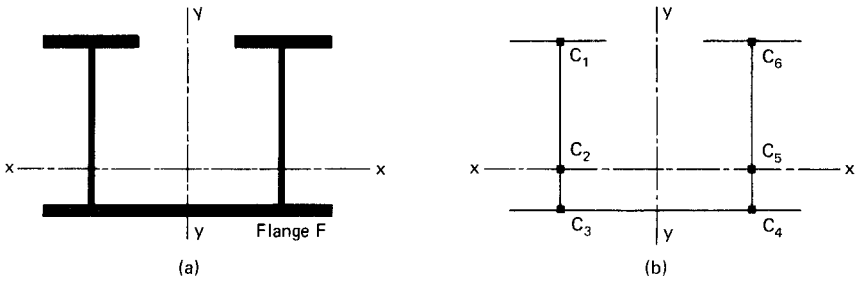

Figure 10.117 Two I sections as an example of continuously connected shear wall. (*a*) Prototype; (*b*) model.

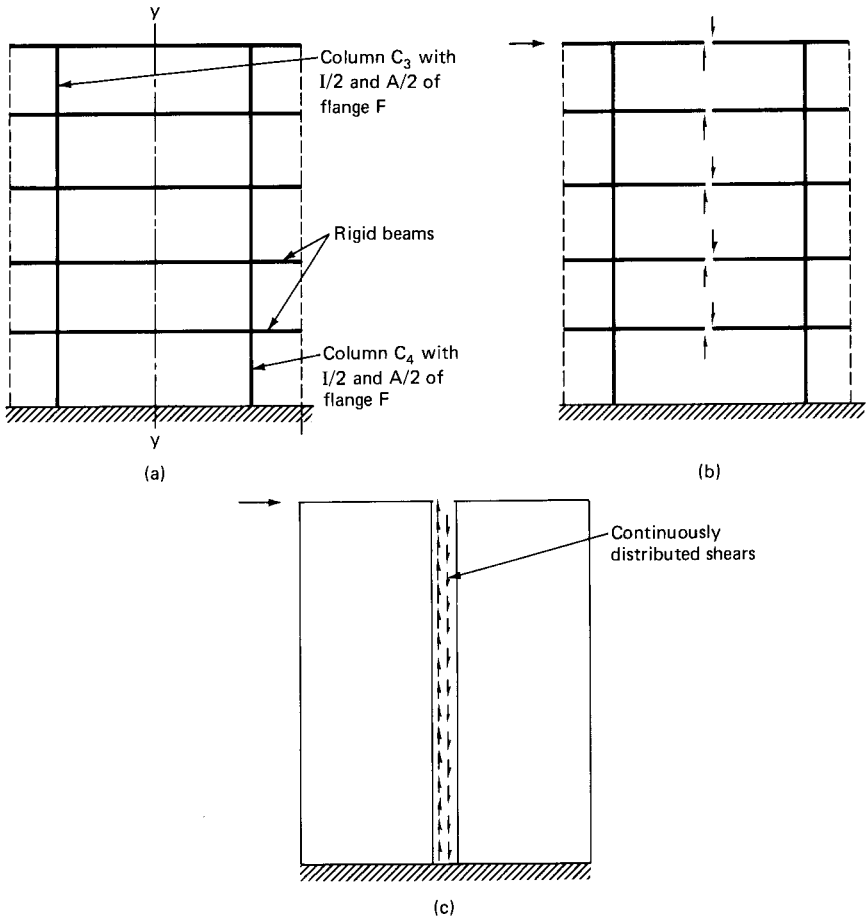

Figure 10.118 (*a*) Elevation of flange *F* showing wide-column analogy model; (*b*) vertical shear forces resulting from wide-column analogy; (*c*) distribution of vertical shear in the prototype.

actual structure these shears are continuously distributed along their junction, whereas in the discrete wide-column model, the shears are lumped into concentrated vertical shear forces at each floor acting at the intersection of two rigid arms as shown in Fig. 10.118. The lumping of uniformly distributed shear forces as a concentrated shear force results in a reverse bending of columns between the floor levels which, of course, does not occur in the real structures. However, this effect is usually negligible in planar and nonplanar shear walls and open-section cores.

Let us consider the torsional resistance of various types of shear walls. As mentioned previously, open-section cores resist torsion mainly by the out-of-plane bending or warping of the core walls. Closed

sections and those open sections subject to heavy interaction effects of surrounding beams or slabs resist torsion to a great extent by the continuously distributed membrane or St. Venant shear stresses.

Closed sections with nondeformable profiles resist torsion almost completely by membrane shear stresses. Partially closed sections (which perhaps represent the bulk of practical core structures) resist torsion both by the warping and membrane shear stresses, the portion carried by each depending upon the relative warping stiffness of the core to the flexural stiffness of the members connecting across the openings. The greater the warping moment of inertia of the core, the greater is the proportion of the torque resisted by warping, and the lesser is the proportion resisted by membrane shear forces. Therefore, when modeling a closed section or an open section with relatively stiff beams or slabs across openings, it is recommended that an alternative analogous frame that can faithfully capture the torsional behavior be used to model shear walls. A brief outline of such a model originally conceived by Stafford Smith and Amal Girgis (Ref. 59) is given in the following material.

The analogous frame is similar to the wide-column model, but with diagonal braces as shown in Fig. 10.119*a*. The addition of braces decouples the bending and shear behavior inherent in the wide-column analogy. A single module representing a story-high wall consists of a column with a rigid horizontal beam at each floor. Diagonal braces hinged at each end connect the ends of rigid beams as shown in Fig. 10.119*b* and *c*.

In common with other modeling techniques, the analogous model must be able to simulate the significant characteristics of the prototype. In the case of shear walls it is necessary to duplicate the bending, shear, and axial stiffness of the corresponding wall segment. The member properties are determined as follows.

Bending stiffness (Fig. 10.120). As in the wide column model the bending stiffness of the column is made the same as the bending stiffness of the wall,

$$I_c = \frac{bd^3}{12} \tag{10.90}$$

Shear stiffness (Fig. 10.121). In resisting the shear deformation both the column and braces of the analogous model are subjected to strains; the column is subjected to reverse bending while the braces are subjected to axial deformation. Equating the shear stiffness of the frame module to that of the wall segment we get:

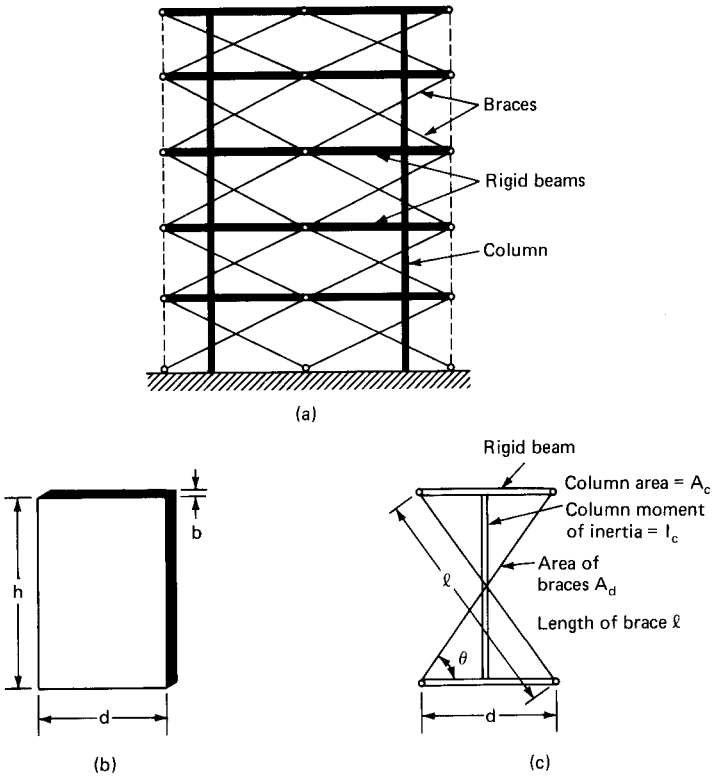

Figure 10.119 (*a*) Braced wide-column model for continuously connected shear walls; (*b*) braced wide-column model for story-high wall.

$$bd\frac{G}{h} = \frac{12EI_c}{h^3} + \frac{2\,EA_d\cos^2\theta}{l}$$

Substituting $G = 0.4E$, and $I_c = bd^3/12$ we get

$$A_d = \frac{bdl}{2h\cos^2\theta}\left(0.4 - \frac{d^2}{h^2}\right) \tag{10.91}$$

Axial stiffness (Fig. 10.122). This is provided in the analogous module by the axial stiffness of the column and the vertical stiffness of the braces. Equating the axial stiffness of the wall and the analogous frame, we get

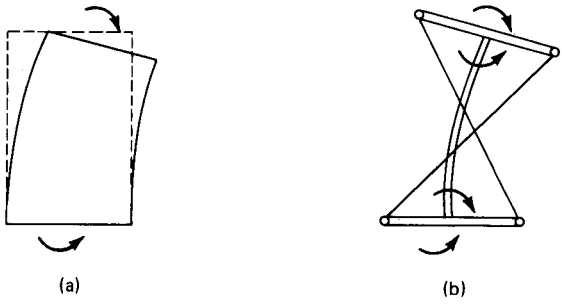

Figure 10.120 Bending stiffness. (*a*) Prototype; (*b*) braced wide-column model.

$$\frac{EA_c}{h} + \frac{2\,EA_d \sin^2\theta}{l} = \frac{EA_w}{h}$$

$$A_c = \left(A_w - \frac{2h}{l} A_d \sin^2\theta\right) \tag{10.92}$$

An analysis using the aforementioned modeling technique with judicious use of equivalent columns and braces gives more accurate results than other methods of frame analyses. Commercially available frame analysis programs can be used for this purpose without resorting to finite element programs. However, use of a finite element analysis may still be preferable for complex shear core systems with relatively flexible floor systems as in Fig. 10.123 which shows a concrete core system with a structural steel surround. The floor system consists of simple connected steel beams, metal deck, and structural concrete topping. Its out-of-plane stiffness is small and can be ignored in lateral load analysis, making it feasible to use a finite element

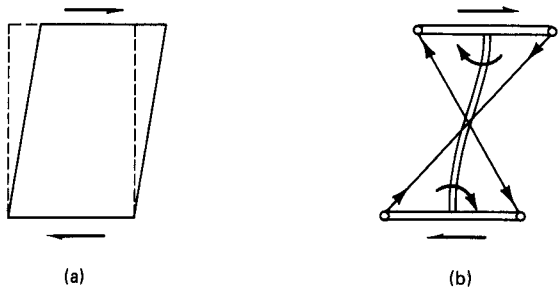

Figure 10.121 Shear stiffness. (*a*) Prototype; (*b*) braced wide-column model.

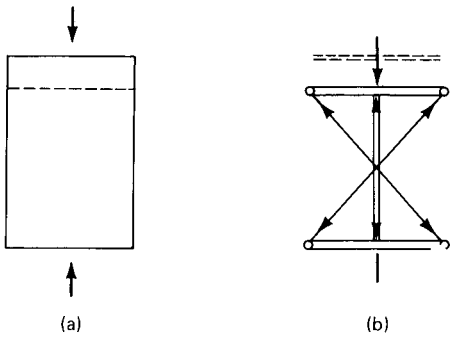

Figure 10.122 Axial stiffness. (*a*) Prototype; (*b*) braced wide-column model.

idealization as shown in Fig. 10.124. Concrete floor systems, on the other hand, possess substantial out-of-plane bending stiffness with significant contributions to structural stiffness of vertical members. A full-scale representation of finite elements for both wall and floor system gets too cumbersome and is not cost effective for routine analysis. The proposed method of modeling shear walls as modified equivalent frames may be more appropriate. The out-of-plane stiffness of the slab can be evaluated from a separate analysis and incorporated into the frame analysis as explained in the following section.

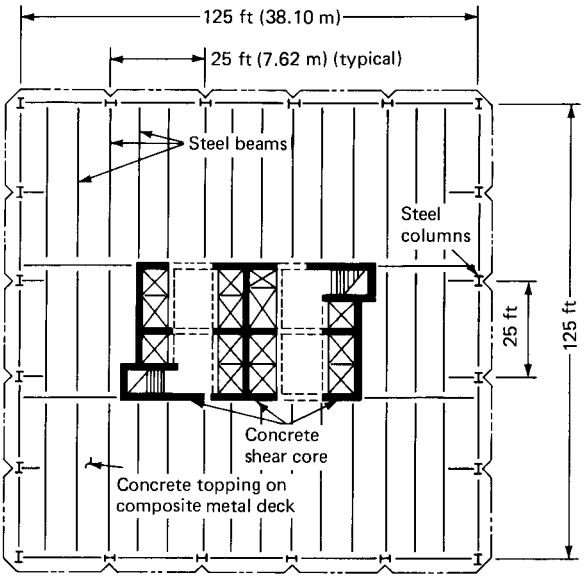

Figure 10.123 Typical floor plan of composite high-rise building with concrete core and steel surround.

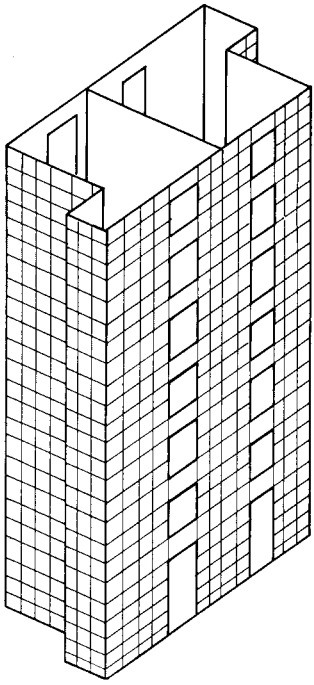

Figure 10.124 Finite element three-dimensional model of a shear core.

10.9.2 Modeling of floor systems

A two-step procedure is proposed for modeling floor systems. Step 1 is to compute the out-of-plane stiffnesses of the floor system and to express them in terms of equivalent beam stiffnesses. Step 2 is to perform a frame analysis incorporating beam stiffnesses obtained in step 1. The procedure is explained with reference first to a coupled shear wall and then to a shear wall–frame building.

Coupled shear walls. The procedure consists of idealizing the floor slab as an assemblage of finite elements or grids and applying unit displacements to the slab corresponding to the axial deformations and rotations about the centroidal axes of the walls. The finite element or grid analysis of the slab is carried out for these displacements and the nodal forces and moments at the junction of the wall and slab are found. The next step is to use the nodal forces and moments to obtain the slab stiffness. For the cross-wall system, this takes a 4-by-4 matrix form. The summation of nodal forces gives the shear force corresponding to $12EI/L$ term of a beam stiffness matrix; the summation of nodal moments and the moments obtained by the product of nodal forces and their corresponding distances from the center of gravity of the wall gives the moment term corresponding to $6EI/L$ term of the beam

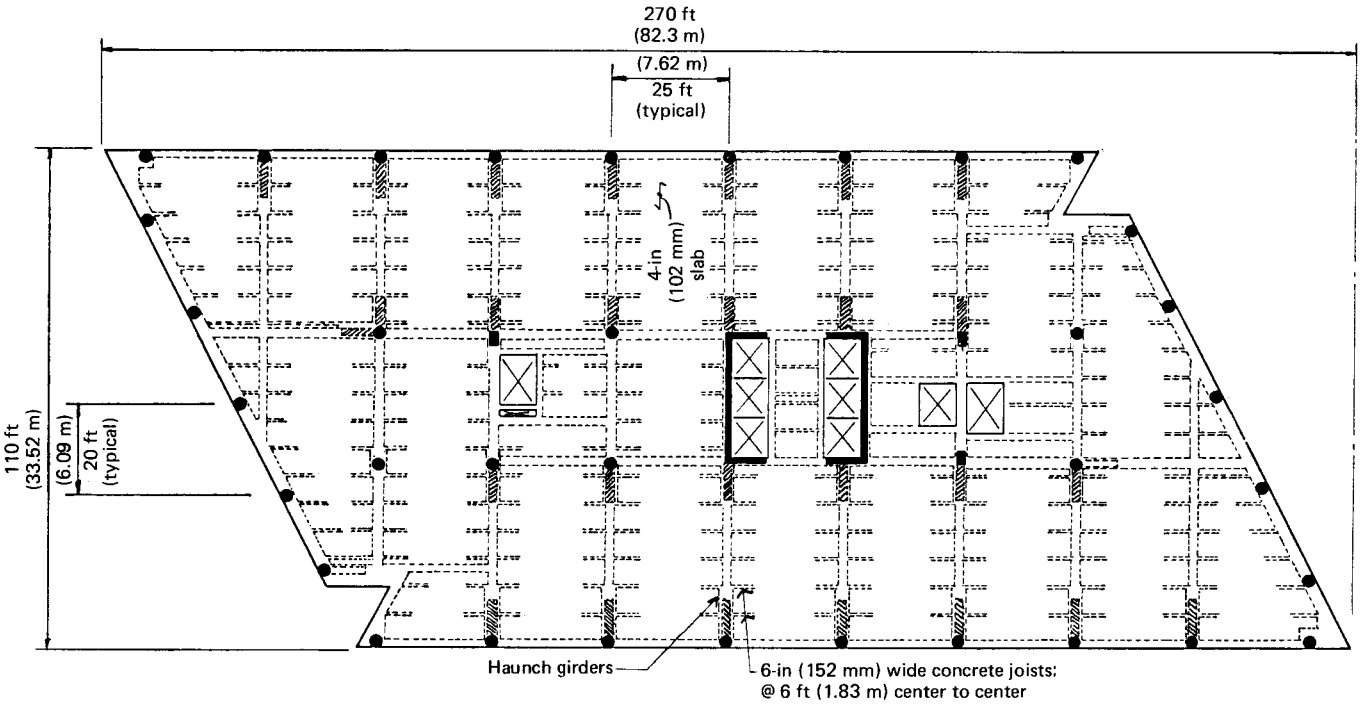

Figure 10.125 (*a*) Typical floor plan of interacting shear wall-frame system.

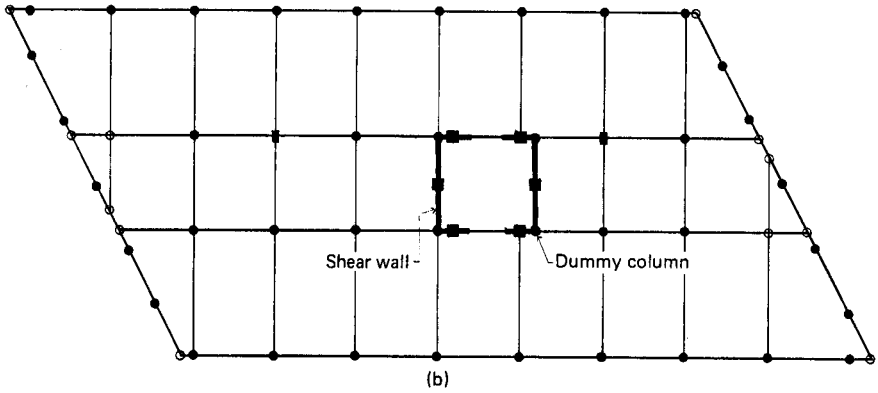

Figure 10.125 (*Continued*) (*b*) Computer model plan.

stiffness matrix. Using these values, either an equivalent moment of inertia of a beam that defines the stiffness of the connecting slab could be worked out, or the stiffness values could be incorporated directly into the frame analysis program. With this procedure the engineer will not have to worry about the many parameters that influence the effective width of the coupling slab. An added bonus from this method is that the engineer will get a better feel for the mechanism of load transfer between walls and slabs. It is necessary to design the floor system for the moments and shear forces induced because of the coupling action. The detailing of reinforcement is relatively easy because of the availability of large slab-to-wall connection areas.

Wall and frame combination. As a second example, consider a more common form of shear wall employed in a 30- to 60-story high-rise building. In these buildings lateral loads are resisted by shear walls in conjunction with frame the combination being referred to as the shear wall and frame interaction (Fig. 10.125). How does the engineer go about designing these tall buildings, taking into account all the complex interactions between the walls, floor slabs, service cores, and frames? The present-day design office practice is to use three-dimensional frame programs that employ the assumption of rigid slab by constraining the displacements at each floor to three rigid body displacements. Figure 10.125*b* shows the plan of a computer model that incorporates the effect of shear walls by using rigid links and dummy columns. It is usual practice to ignore the effect of tension cracking and to use the gross moment of inertia for beams and girders that connect the columns and walls. Some engineers use equivalent T-beam properties instead of rectangular beam properties. Although such an assumption implicitly attempts to account for the two-dimen-

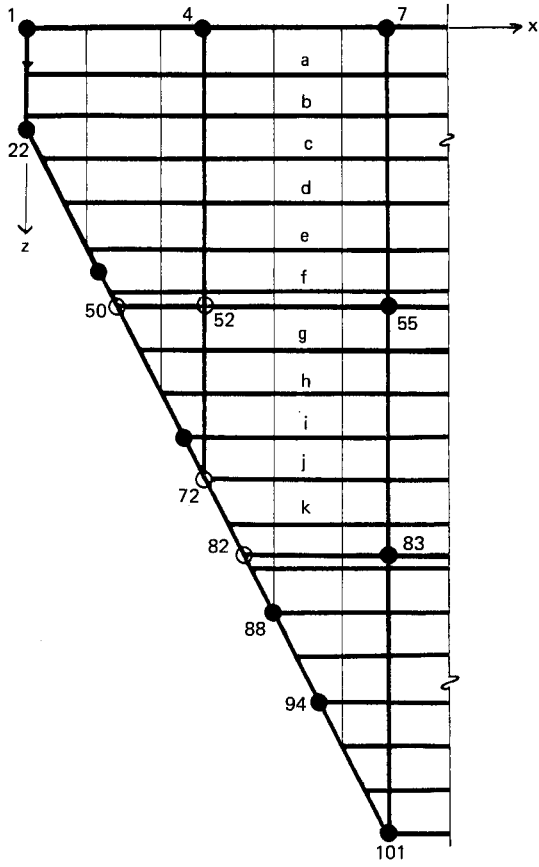

Figure 10.126 Partial slab model showing finite grid system.

sional behavior of the floor system, the analysis is inaccurate, particularly so in the case of flanged shear walls, because the contribution of the out-of-plane stiffness of the floor system is grossly underestimated in the analysis. The inaccuracy is even more pronounced in a structure with a weak frame and strong wall combination. The resulting moments and shears in the connecting beams in many cases are very high, requiring reinforcements well beyond the practical limit.

A more appropriate procedure, especially in the case of flanged shear walls, would be to use a separate analysis to obtain the equivalent stiffness of the connecting beams based on an appropriate model that captures the out-of-plane bending stiffness of the slab. Incorporating these values, a second frame analysis program is used for the solution of the problem.

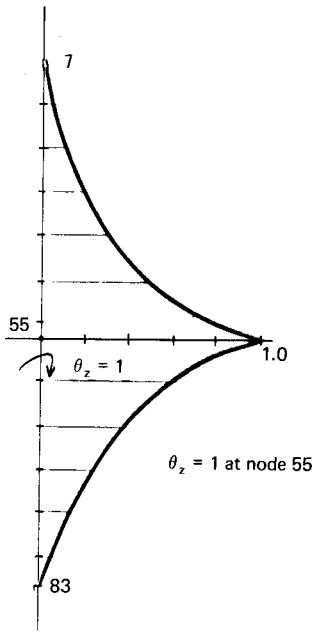

Figure 10.127 Torsional rotations along beams 55-7 and 55-83 for an imposed unit rotation at node 55.

Many times the effect of slab and joists framing between wind-resisting beams is generally ignored in the analysis leading to unnecessarily conservative designs. Ignoring the stiffness of subfloor framing turns a blind eye toward the physical behavior of the floor system. The trend today in structural analyses, especially with the availability of computers, is to account for all the significant structural interactions that exist between various elements. In keeping with this spirit, the author proposes the following method for incorporating the stiffness of subsystems between floor beams.

Consider the floor framing shown in Fig. 10.125. The subframing between main girders consists of a series of 6-in (152-mm) wide by 14-in (356-mm) deep joists at 6-ft (1.82-m) centers and a 4-in (102-mm) thick slab spanning between the joists. The basic idea of including the subframing in an analysis is to determine how much stiffer the main girders become because of the bending and twisting action of the joists and slab. For this purpose, the floor system can be idealized as a grid system, with each grid representing a joist or main beam. The enlarged section of finite grid system and nodes are shown for the two end bays in Fig. 10.126. Let us consider the grid between 52-55 which represents the beam spanning between the interior column 55 and girder 4-72 in the transverse direction. The dimensions of this beam are 18 by 18 in (457 by 457 mm). If we ignore the subframing and assume rectangular

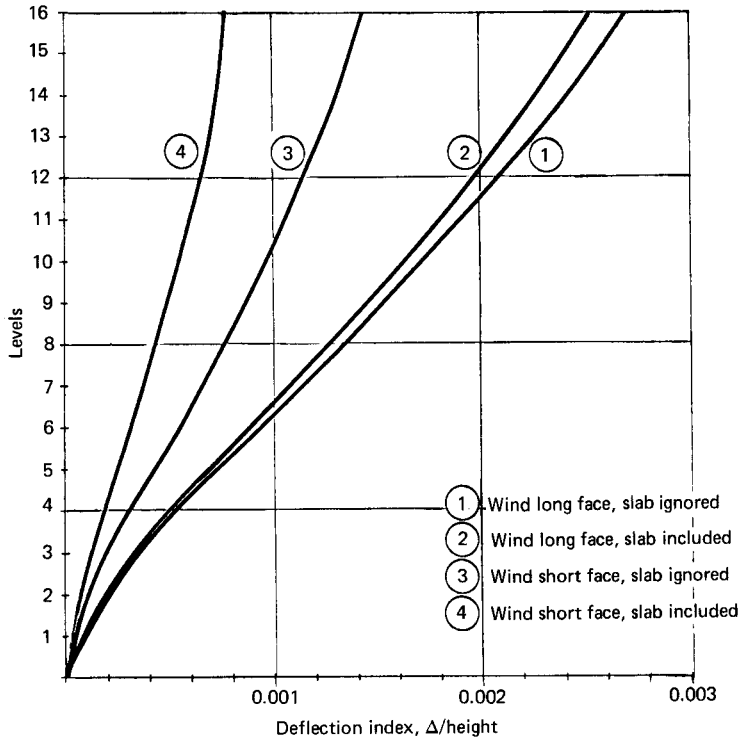

Figure 10.128 Deflection comparison.

gross properties, the value of moment of inertia for this beam works out to 8748 in^4 (3.64×10^9 mm^4) units. Assuming the modulus of elasticity E for concrete as 3700 ksi (25,517 MPa), the moment value corresponding to the beam stiffness matrix term $4EI/L$ for a unit rotation about the z axis works out to be 35,964 kft (48,778 kN·m). Note, however, a unit rotation at the node 55 in reality introduces torsional rotations along beams 55-7 and 55-83 as shown schematically in Fig. 10.127. The joists designated as a through k (Fig. 10.126) are subjected in turn to rotations compatible with the torsional rotations of beam 55-7 and 55-83 and hence give rise to bending moments at their ends. From the grid analysis we can find the values of these moments, and their summation can be physically thought of as the additional stiffness of beam 55-52 due to the bending action of the adjoining joists a through k.

In the example problem, the summation of these moments worked out to be equal to 109,668 kft (148,501 kN·m) as compared to the stiffness term of 35,964 kft (48,788 kN·m) for beam 55-52, signifying that the joists' contribution to beam stiffness is quite large. The equivalent moment of inertia for beam 55-52, which is to be used in a

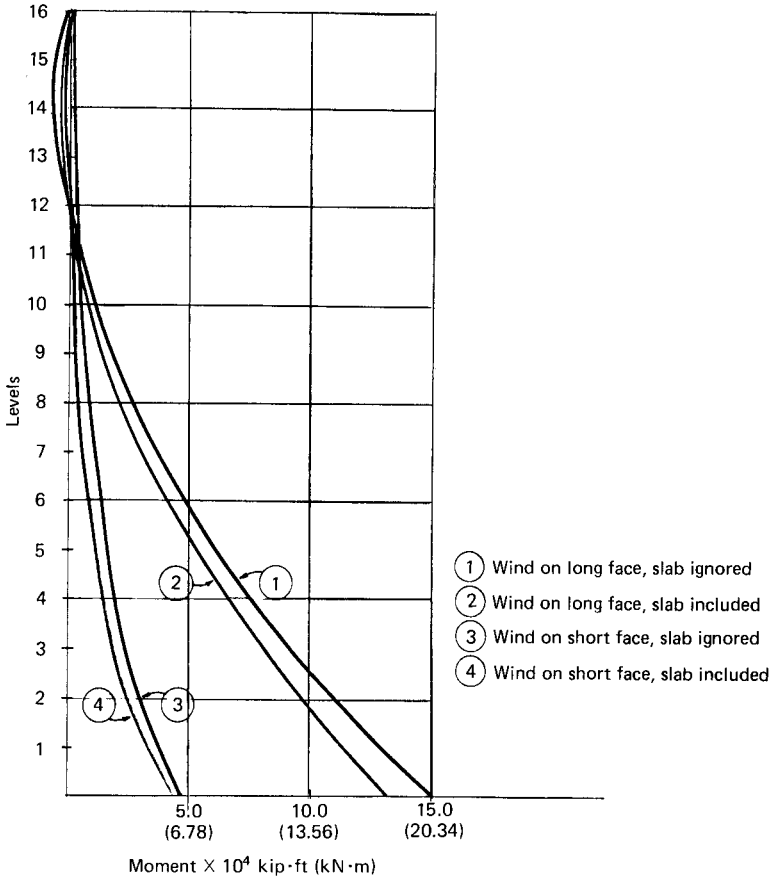

Figure 10.129 Comparison of moments in shear wall.

second analysis consisting of beam and column elements, can therefore be thought of as that value corresponding to the total of beam and joist stiffnesses. For the example problem, this worked out to be 109,668 kft (148,501 kN·m) or about three times the value for beam 55-52 alone. A similar magnitude of increase was noted for a unit vertical displacement at the ends of beam 52-55. The procedure is repeated for other beams such as 58-60 and the corresponding increases in their stiffness properties due to the joist and slab action are found. For the example problem, the magnitudes of increases in the stiffnesses of beams varied from about 2.5 to 4 times their gross properties. These values were used to compute the deflection and bending moments shown in Figs. 10.128 and 10.129. The effect of the increased beam stiffnesses is obvious as shown in Figs. 10.128 and 10.129.

10.9.3 Conclusions

An attempt has been made in this section to take the reader through the analysis of shear walls from the most elementary single shear wall case to the most complicated system of interconnected shear walls including open sections. The effect of floor systems in restraining the bending and twisting actions in shear walls is highlighted. A two-step approach is presented for a comprehensive analysis of shear wall buildings, one for assessing the out-of-plane behavior of the floor system and the other for a three-dimensional analysis using available frame analysis computer programs.

Chapter

11

Special Topics

The purpose of this chapter is twofold: (1) to examine in detail a number of special subjects which we have met in several ways in earlier chapters, and (2) to briefly touch on certain topics which are unique to the design of tall buildings. Our consideration of special topics opens with a discussion of differential shortening of columns.

A column in a tall building undergoes axial shortening considerably more than its lower brethren, requiring that special attention be paid in column design. A related problem, by no means unique to tall buildings, but one that gets aggravated to a greater extent, is the levelness of floors. Similarly, the problem of human response to transient vibration of floors is not unique to tall buildings but needs careful study because the cost of correcting the problem in a tall building with several floors is phenomenally more expensive than correcting the relatively fewer floors of a low-rise building. Next we will consider in some detail the behavior of so-called panel zones and their effect on the lateral deflections of buildings. In a rigid frame a panel zone may be defined as a structural element that is common to both a beam and column at their intersection. This element is necessary to provide a route for the transfer of moments from column to beams and vice versa.

In the next section we shall consider the nature of p-Δ effect which is not always secondary and can be large enough to require attention in

the calculation of deflection and member selection. A building frame that deflects under lateral loads has a tendency to keep moving in the same direction because of eccentricity of gravity loads from the center of gravity of the deflected frame. Its effect which is known as p-Δ effect, is to increase the deflection from about 5 to 15 percent over and above the primary deflection. Conventional effective length concepts which attempt to account for these effects are considered first, followed an explicit method called the p-Δ method in which the destabilizing forces are directly included in the design.

Next we move on to the gray area of design of curtain wall systems that brings together several diversified disciplines. The section briefly presents the design and installation aspects of metal curtain walls, stone claddings, brick veneer systems, and glass fiber–reinforced concrete systems.

The next section is introductory in its presentation of mechanical devices which are used to increase the damping and thus reduce the wind-induced sway acceleration and torsion-induced translation acceleration. Two devices, the so-called tuned mass damper and the viscoelastic damper, which are fitted to buildings to assure occupant comfort are discussed. With the additional damping provided by these devices, the peak wind-induced resultant accelerations are designed to be within benchmark limit of 20 milli-g (one-fiftieth of the acceleration due to gravity) for a recurrence interval of once in 10 years.

The last section presents a brief discussion of design aspects of two types of foundations, the drilled pier or caisson foundation, and the mat foundation.

Throughout the book all of the above subjects have been touched on at appropriate sections. However, an attempt is made in this chapter to present their special considerations in an orderly manner.

11.1 Differential Shortening of Columns

Columns in tall buildings are subjected to large axial displacements because they accumulate loads from a large number of floors and also because of their large lengths. A 60-story interior column in a steel building may shorten as much as 4 to 6 in (102 to 153 mm) because of dead and live loads, while a concrete column may experience an additional 3 to 4 in (76 to 102 mm) of shortening because of creep and shrinkage characteristics. If this frame shortening is not given due consideration, problems may develop in the performance of curtain walls and levelness of floor systems. Proper awareness of this problem is necessary on the part of the structural engineer, architect, and the curtain wall supplier to avoid lost time and money.

Assuming the building is founded on an unyielding foundation, the

maximum effect of column shortening is felt at the roof level. The roof displaces vertically toward the ground by a maximum value while each of the other floors exhibits a similar gradual displacement from the design levels. In a concrete frame this phenomenon may take several years to complete because of long-term effect of creep, although a major part of it is felt within the first few months of construction. There is very little the structural engineers can do to arrest or minimize frame shortening, but they should make the design team aware of the magnitude of frame shortening so that soft joints of appropriate widths are properly detailed between the vertical joints of the curtain walls to prevent the load from being transferred into the building facade. Before fabrication of connections of the curtain wall panels, the in-place elevations of the structure should be verified and the panels fabricated based on those elevations rather than the theoretical elevations. There must be sufficient space at the joints between the panels to allow for future movement of the structure as well as the thermal expansion and contraction of the panels themselves. Insufficient space may result in bowed curtain wall panels or in extreme cases the panels may even pop off at a later stage.

A similar problem occurs when mechanical and plumbing lines are attached rigidly to the structure. Frame shortening may force the pipes to act as structural columns resulting in their distress. A general remedy is to make sure that nonstructural elements are not brought in to bear the vertical loads. Sufficient compensation should be provided during design and construction to make sure that nonstructural elements are separated from structural elements.

The axial loads in all columns of a tall building are very seldom the same, giving rise to the problem of so-called differential shortening. The problem is more acute in a composite structure because slender steel columns are subjected to large axial loads during construction. Determining the magnitude of axial shortening in a composite system is complicated because many variables that contribute to the shortening of columns cannot be predicted with sufficient accuracy. The lower part of the column, which is encased in concrete, is continually undergoing creep, and because the age and strength of concrete keep changing, their effect on creep is difficult to predict with any precision. The steel column at any given period during construction is partly enclosed in concrete at lower floors, with the bare steel section projecting beyond the concreted levels by as many as 10 or 15 floors. Another factor difficult to predict is the gravity load redistribution due to continuity of spandrel beams. If the building is founded on compressible material, foundation settlement is another factor that influences the relative changes in the assumed elevations of the columns. The load imbalance equation continually changes, making an accurate

assessment of column shortening beyond the reach of day-to-day engineering practice. If all the variables are known, the prediction of differential shortening is no more complicated than a systematic evaluation of the *PL/AE* equation.

Although there are basic differences between the loading history of high-rise and low-rise columns, the routine method of analysis of high-rise structures is performed on the full building frame without taking into account the sequential nature of construction and the application of its weight. Ignoring the construction sequence in a 50- or 60-story concrete column would result in a calculated axial deformation of about 5 in (127 mm) of immediate axial shortening and a mind-boggling value of 10 to 12 in (254 to 305 mm) when creep effects are included in the computation. Fortunately, the method of construction more or less takes care of the immediate shortening and to a limited extent the creep effects on lower-level columns. This is because in practice a tall building is constructed one floor at a time. When a floor is constructed on top of the frame which is completed so far, the frame has already foreshortened due to the gravity loads. Since each floor is leveled at the time of its construction, in concrete construction, the column shortening which has occurred before the construction of the floor is of no consequence. Also, the lower-story columns of tall buildings have considerably smaller creep and shrinkage strains because the incremental load over a 15- to 24-month period of construction reduces creep.

As mentioned earlier, to capture the true behavior of the entire building, a series of analyses taken one story at a time is required, but cost and time constraints do not allow such an in-depth analysis for routine office practice.

In a concrete building the computation of differential shortening is even more complicated mainly because of the effects of creep and shrinkage.

Creep is difficult to quantify because it is time-dependent. Initially the rate of creep is significant and diminishes as time progresses until it eventually reaches zero. Because of sustained loads there is a tendency for additional stress to be gradually transferred to the steel with a simultaneous decrease in concrete stress. Regarding shrinkage, since evaporation occurs only from the surface of members, the volume-to-surface ratio of a member has a pronounced effect on the amount of its shrinkage.

Columns with varying percentages of reinforcement and varying volume-to-surface ratios creep and shrink differently. An increase in percentage of reinforcement and in volume-to-surface ratio reduces the strain due to creep and shrinkage under similar stresses. Differential shortening of columns produces moments in the connecting girders and

spandrels resulting in load transfer. The column which has shortened less receives more load, thus compensating for the initial imbalance. The length of construction time has considerable effect on the amount of creep, whereas shrinkage takes place independently of the construction time.

In this section we will not address the foreshortening of concrete columns because attempts to quantify the aforementioned effects are considered beyond the scope of this work. Leaving the quantification of the problem to more theoretical minds, we will proceed in this section to a brief discussion of differential shortening of steel columns. For this purpose a column is isolated from the remainder of the structural frame and studied as a cantilever by assuming it to be free of any restraint offered by moment-connected spandrels or girders. A closed-form solution for computing axial shortening of columns is presented and a numerical example is given to demonstrate the effectiveness of the method. The section concludes with suggested details for field adjustment of column heights.

11.1.1 Differential shortening

Differential rather than the *absolute* magnitude of column shortening is the most significant factor. If all the columns shorten by the same magnitude, it is unlikely that any floor-leveling problem would occur; the floors would still remain level and any elevation change at the street level would likely be too small to cause drainage or architectural problems. Relative displacement in columns occurs because of the difference between the P/A ratios of columns. If all the columns in a building have the same slenderness ratio and are sized for gravity load requirement only, there will be no relative vertical movement between different columns. All columns will undergo the same displacement because the P/A ratio is nearly constant for all columns. In a real building, this ideal condition is seldom present. Usually the design of a certain number of columns is governed by the combined gravity and lateral load requirement, whereas certain other columns are designed for gravity loads only.

For example, consider the tubular system of framing used for buildings in the 50- to 80-story range. The system typically utilizes an array of closely spaced exterior columns and widely spaced interior columns. Normally, in a steel system, high-strength steel columns up to 50 ksi are used in the interior of the building to collect gravity loads on large tributary areas resulting in a large P/A ratio. The exterior columns, on the other hand, usually have a small P/A ratio for two reasons: first, their tributary areas are small because of their close spacing of usually 8 to 12 ft (2.44 to 3.66 m); second, the columns are

sized to develop enough lateral resistance as a framed tube, resulting in areas much in excess of those required from the strength consideration alone. Because of this imbalance in the gravity stress level, these two groups of columns undergo different axial shortenings; the interior columns shorten much more than the exterior columns.

A somewhat reversed condition occurs in buildings utilizing interior-braced core columns and widely spaced exterior columns; the exterior columns experience more axial shortening than the interior columns. The behavior of columns of buildings utilizing other structural systems, such as interacting core and exterior frames, tends to be somewhere in between these two limiting cases.

In all cases, it is relatively easy to evaluate the shortening of columns and to come up with corrective lengths or shimming requirements at column splices. The procedure requires a step-by-step manipulation of the basic *PL/AE* equation as described below.

To illustrate the method of computing column shortening, let us consider a column of a hypothetical 50-story building and assume for simplicity that the variations in story heights, column areas, and the load increment at each floor are constant as shown in Fig 11.1. The calculation of the axial shortening, in itself, at any floor is trivial. It is given by the summation equation:

$$\Delta_n = \frac{PL}{AE} \sum_{i=1}^{n} (NS + 1 - i) \tag{11.1}$$

where Δ_n = the axial shortening at level n
P = the load increment assumed constant at each level
L = the story height assumed constant for the full height
A = the column area assumed constant
NS = the number of stories in the building

Using this equation, the axial shortening for the example column at different floors works out as given in Table 11.1. Having obtained these values, the next step is to evaluate the correction Δ_c required at these levels in order to compensate for the anticipated column shortening. This is given by the difference in the axial shortenings at the level and the floor immediately below it. For instance, this value at level 30 for the example column is given by PL/AE (1065−1044) = 21 PL/AE. The magnitude of this correction in a normally proportioned building is rather small, perhaps $\frac{1}{8}$ in (3.17 mm) at the most. Instead of specifying this value as a correction at each level, in practice it is usual to lump these corrections at a few floors, for example, every tenth level or so. The correction at the lumped level is simply the difference between the values of axial shortening at that level and at the lumped floor below

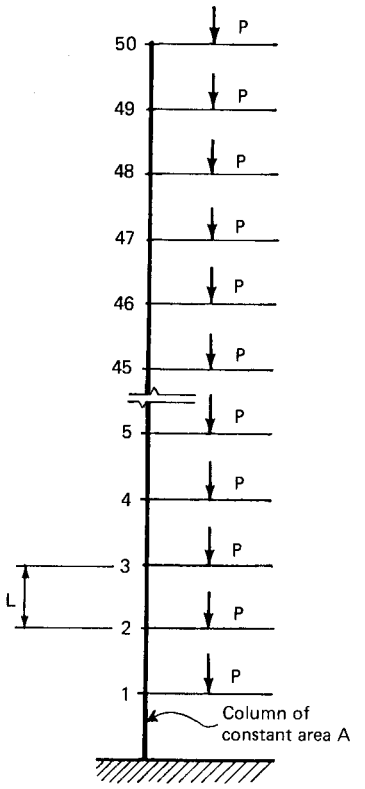

Figure 11.1 Simplified hypothetical column.

it. For example, in Table 11.1 the lumped correction of 255 *PL/AE* units at the 30th floor is equal to the column shortening at the 30th level less the shortening at the 20th level

$$\frac{PL}{AE}(1065 - 810) = 255\frac{PL}{AE} \text{ units}$$

Let us consider the practical case of a building column which has variations in story heights, load increments, and column areas as shown in Fig. 11.2. The summation equation for this general case takes the form:

$$\Delta_n = \frac{1}{E}\sum_{k=1}^{n}\frac{L_k}{A_k}\sum_{i=k}^{NS}P_i \tag{11.2}$$

Table 11.2 shows in tabular form the assumed dimensions and

TABLE 11.1 Axial Shortening Computations for Hypothetical Column

Level	Axial shortening	Column length correction at each level	Lumped column length correction
50	1275	1	55
49	1274	2	
48	1272	3	
47	1269	4	
46	1265	5	
45	1260	6	
44	1245	7	
43	1247	8	
42	1239	9	
41	1230	10	
40	1220	11	155
39	1209	12	
38	1197	13	
37	1184	14	
36	1170	15	
35	1155	16	
34	1139	17	
33	1122	18	
32	1104	19	
31	1085	20	
30	1065	21	255
29	1044	22	
28	1022	23	
27	999	24	
26	975	25	
25	950	26	
24	924	27	
23	897	28	
22	869	29	
21	840	30	
20	810	31	355
19	779	32	
18	747	33	
17	714	34	
16	680	35	
15	645	36	
14	609	37	
13	572	38	
12	534	39	
11	495	40	
10	455	41	405
9	414	42	
8	372	43	
7	329	44	
6	285	45	
5	240	46	
4	194	47	
3	147	48	
2	99	49	
1	50	50	50

NOTE: All *values* are in terms of *PL/AE*.

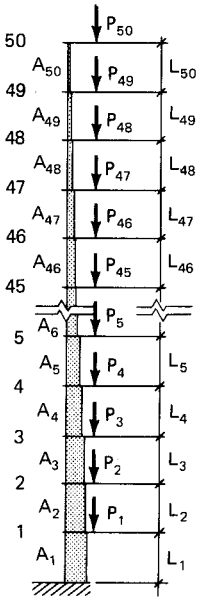

Figure 11.2 Practical example column.

loading conditions for the column and the computations for obtaining the column length shortening values. The last column shows the lumped corrections at levels 2, 10, 20, 30, 40, and the roof. Basically, these corrections represent the additional lengths over and above their theoretical lengths. For example, $\Delta_c = 1\frac{1}{4}$ in (31.75 mm) at the tenth level means that the actual fabricated length of column should be $1\frac{1}{4}$ in longer than the theoretical length given in the column schedule. This overlength could be achieved by increasing the length of column in each tier by $\frac{1}{4}$ in (6.35 mm) (ten stories equal five tiers, therefore, $\frac{1}{4}$ in times 5 gives $1\frac{1}{4}$ in). The fabricator may elect to increase the length in each story by $\frac{1}{8}$ in (3.2 mm) instead of $\frac{1}{4}$ in per tier to achieve the same Δ_c at the tenth floor.

The value of $\Delta_c = 2$ in (50.8 mm) at the 20th floor means the overlength of columns between levels 1 and 20 should be 2 in. However, an overlength of $1\frac{1}{4}$ in (31.75 mm) up to the tenth level has already been achieved by specifying $\Delta_c = 1\frac{1}{4}$ in at the tenth level. Therefore, the increment between the 10th and 20th levels should be 2 in less $1\frac{1}{4}$ in $= \frac{3}{4}$ in (19.0 mm). A correction table incorporating the above information for the example column is shown in Table 11.3.

11.1.2 Simplified approach

In a high-rise building, the distribution of material properties, such as the cross-sectional area of the column, and the loading pattern, such as the vertical load distribution, could be expressed by a simple mathe-

TABLE 11.2 Axial Shortening Computations for Practical Column

Level	Accumulated load, kips	Column section	Story height, in	Column shortening Δn, in	Column length correction each level, in	Lumped column length correction, in	Column shortening from eq. 11.4, in
50	53	W14 × 43	156	5.14	0.023	0.73	5.11
49	106	43	210	5.12	0.061		5.08
48	159	53	168	5.05	0.051		5.02
47	212	53	156	5.00	0.073		4.95
46	265	68	156	4.93	0.071		4.89
45	318	68	156	4.86	0.086		4.82
44	371	84	156	4.77	0.081		4.75
43	424	84	156	4.69	0.092		4.67
42	477	95	156	4.60	0.092		4.59
41	530	95	156	4.51	0.102		4.50
40	583	111	156	4.41	0.09	1.02	4.42
39	636	111	156	4.32	0.105		4.33
38	689	127	156	4.21	0.09		4.24
37	742	127	156	4.12	0.107		4.15
36	795	142	156	4.01	0.103		4.04
35	848	142	156	3.91	0.109		3.96
34	901	167	156	3.80	0.09		3.86
33	954	167	156	3.71	0.105		3.76
32	1007	176	156	3.62	0.105		3.66
31	1060	176	156	3.50	0.110		3.56
30	1113	202	156	3.39	0.101	1.07	3.46
29	1166	202	156	3.29	0.106		3.36

28	1219	211	156	3.19	0.106		3.26
27	1272	211	156	3.08	0.110		3.16
26	1325	228	156	2.97	0.106		3.12
25	1378	228	156	2.86	0.111		2.95
24	1431	246	156	2.75	0.107		2.85
23	1484	246	156	2.65	0.111		2.74
22	1537	264	156	2.53	0.107		2.64
21	1590	264	156	2.43	0.110		2.53
20	1643	287	156	2.32	0.104	1.06	2.42
19	1696	287	156	2.20	0.108		2.32
18	1749	314	156	2.10	0.101		2.21
17	1802	314	156	2.00	0.105		2.10
16	1855	314	156	1.90	0.108		1.99
15	1908	314	156	1.79	0.111		1.88
14	1961	342	156	1.68	0.104		1.78
13	2014	342	156	1.58	0.107		1.67
12	2067	370	156	1.47	0.101		1.56
11	2120	370	156	1.37	0.104		1.45
10	2173	370	156	1.26	0.107	0.53	1.34
9	2226	370	156	1.16	0.109		1.23
8	2279	398	156	1.05	0.104		1.12
7	2332	398	156	0.94	0.107		1.01
6	2385	398	156	0.84	0.11		0.89
5	2438	398	210	0.73	0.11		0.78
4	2491	426	168	0.62	0.11		0.67
3	2544	426	156	0.51	0.11		0.56
2	2597	500	156	0.40	0.09		0.45
Mezzanine	2650	500	240	0.31	0.15		0.17
1	2770	W14 × 500	240	0.16	0.16		0.17

TABLE 11.3 Column Length Correction Table

Level	Column length shortening, in (mm)	Correction to scheduled column lengths, in (mm)
50	5⅛ (13.75)	6 @ ⅛ = ¾ (19)
40	4⅜ (111)	8 @ ⅛ = 1 (25.4)
30	3⅜ (85.7)	8 @ ⅛ = 1 (25.4)
20	2⅜ (60.3)	9 @ ⅛ = 1⅛ (28.6)
10	1¼ (31.75)	10 @ ⅛ = 1¼ (31.75)

matical expression. Slight idealizations in the loading conditions or in the material distribution will not create meaningful deviations from accuracy.

In a normally proportioned building, the cross-sectional area of the column usually increases from a minimum value at the roof level in a steplike fashion to a maximum value at the level above foundation as shown in Fig. 11.3. These incremental steps are caused by the finite choice of material selection. In tall buildings which merit column shortening investigations, the significance of these incremental steps

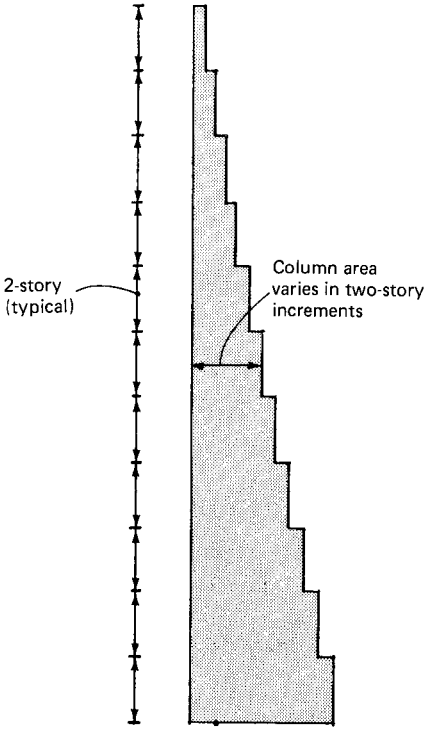

Figure 11.3 Variation of area of a high-rise column.

diminishes rather quickly as compared to a low-rise building column. Therefore, it is admissible to give the load and cross-sectional properties by continuous mathematical expressions as indicated in Fig. 11.4. The gravity load distribution could be assumed to vary linearly throughout the height of the building without any significant loss in accuracy in the computations of column shortening (Fig. 11.4). A similar linear assumption for the column area somewhat overestimates the actual column areas as shown by the dashed line in Fig. 11.5. Although mathematically it is possible to derive an equation that would fit the curvilinear variation of column areas, the author proposes a modified linear variation as indicated in Fig. 11.5. This simplification leads to less formidable expressions for the closed-form solution without any meaningful loss in accuracy. Using the subscripted notations P_t, A_t, P_b, and A_B to represent the loads and areas at the top and bottom of the column, their magnitude at any location distance x from the bottom could be expressed in the form:

$$\begin{aligned} P_n &= P_t + K_P(L - n) \\ A_x &= A_t + K_A(L - x) \end{aligned} \tag{11.3}$$

where K_p is the load increment per unit height of building, and K_A is the modified area increment per unit height of building:

$$K_A = \frac{FA_b - A_t}{L}$$

F is a modification factor varying in magnitude from about 0.9 for a pure gravity column to about 0.75 for combined gravity and wind column. By integrating the idealized load and area diagrams for the column, the column length shortening at any location n from the bottom could be shown to be of the form:

$$\Delta_n = \frac{1}{E}\left[\frac{P_b}{K_A}\ln(FA_b - K_An) + \frac{P_b}{K_A}\ln(FA_b) + \frac{K_p}{K_A{}^2}\left\{K_An + FA_B\ln(FA_b - K_An) - FA_b\ln(FA_b)\right\}\right] \tag{11.4}$$

To demonstrate the ease and accuracy of this formulation, let us rework the gravity column shown in Fig. 11.2. The different parameters for this problem are as follows:

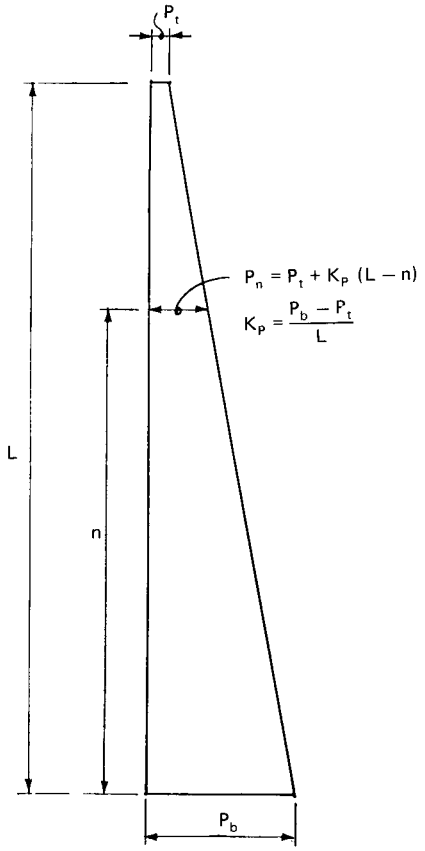

Figure 11.4 Idealized gravity load distribution.

L = 8184 in (207.8 m)
E = 29,000 ksi (200×10^3 MPa)
P = 53 kips (235.7 kN)
A = 12.48 in^2 (8052 mm^2)
P = 2770 kips (12.32×10^3 kN)
A = 147 in^2 (94.84×10^3 mm^2)
F = 0.9

The value of Δ_n obtained by using the closed-form expression is shown in column 8 of Table 11.2. It can be seen that these values correspond closely with those obtained by the long-hand method.

11.1.3 Column shortening verification during construction

Assuming that the engineer has manipulated column lengths to compensate for axial shortening, it becomes somewhat difficult during

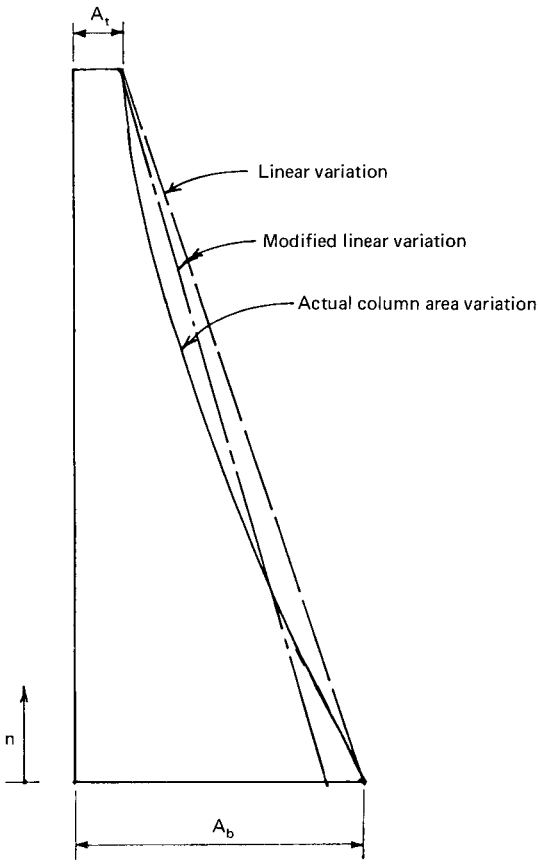

Figure 11.5 Idealized distribution of column areas.

erection to judge whether the variations in the fit-up of steel are within limits of good practice. For example, let us say the actual variation between an interior and exterior column at the time of erection is 2 in (50.8 mm) when the columns are erected halfway up a 40-story building. Let us say 1 in (25.4 mm) out of this 2 in variation is in excess of the allowable erection tolerance. It is not clear to the erector how much of this excess 1 in is due to the overlength allowed for column shortening, because the column has undergone partial shortening due to already existing dead and construction loads. There appears to be a need for a second set of column shortening computations to give the relative elevations of the columns "during erection." These values would indicate the amount by which the columns should be protruding above their theoretical location at the time of erection and, therefore, serve as a benchmark for checking the relative elevations of columns.

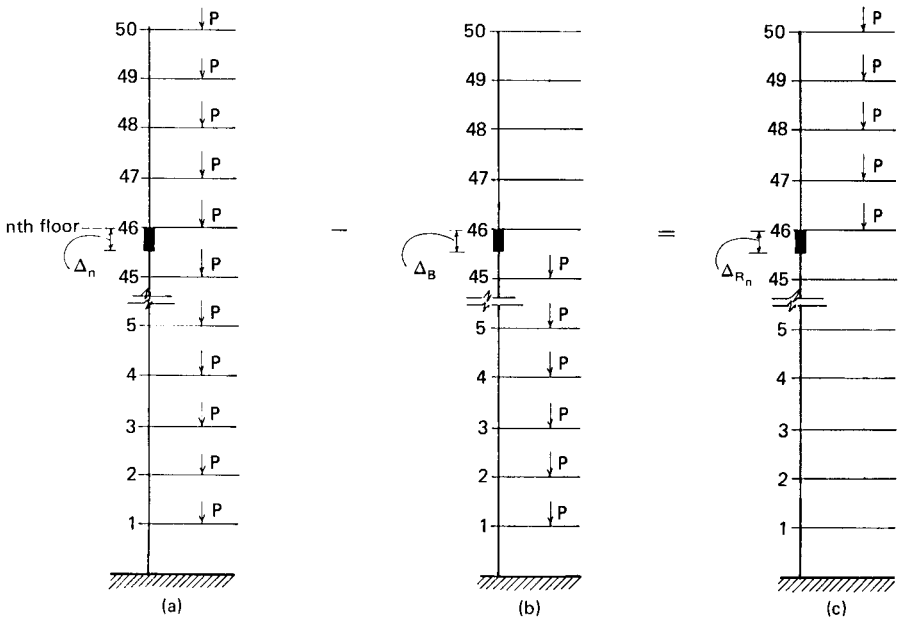

Figure 11.6 Physical interpretation of overlength. (*a*) Column shortening due to loads at all floors; (*b*) column shortening due to loads below *n*th level; (*c*) column residual overlength $\Delta_{R_n} = \Delta_n - \Delta_B$.

To illustrate the above idea, let us consider the overly simplified column of Fig. 11.1. The total overlength specified at level 30, for example, is 1065 *PL/AE* units (Table 11.1). When loads *P* are applied starting at level 1, the overlength correspondingly starts decreasing by a factor *PL/AE* units for load *P* at each level. When erection is at the 30th level, the total shortening at the level would be 855 *PL/AE* units. The residual overlength at this level will be 210 *PL/AE* units. Physically the residual overlength Δ_{R_n} at any level represents the column shortening due to loads applied at and above that level as shown schematically in Fig. 11.6.

For the general case of column shown in Fig. 11.2, the residual overlength Δ_{R_n} at any level n works out to be

$$\Delta_{R_n} = \frac{1}{E} \sum_{i=n}^{NS} P_i \sum_{i=1}^{n} \frac{L_i}{A_i} \tag{11.5}$$

Using the idealized linear variation for load and area as before, the residual overlength Δ_{R_n} at any point of distance n from the bottom works out as

TABLE 11.4 Residual Overlength of Column During Construction

Level	Residual overlength from Eq. (11.5), in	Residual overlength from Eq. (11.6), in
50	0.33	0.29
45	1.87	1.31
40	2.15	1.80
35	2.20	2.04
30	2.12	2.10
25	1.96	2.02
20	1.72	1.83
15	1.49	1.54
10	1.12	1.17
5	0.68	0.73

$$\Delta_{R_n} = \left[\frac{P_t + (L - x)\,K_p}{E}\right]\left[\frac{1}{-K_A}\ln\left(FA_B - K_A x\right) + \frac{1}{K_A}\ln\left(FA_b\right)\right] \tag{11.6}$$

Values of Δ_{R_n} calculated by using both the long-hand procedure and the short-form equation are shown in Table 11.4. There is good agreement between the two values.

11.1.4 Conclusion

Although the closed-form type of analysis presented here is based on certain simplifying assumptions, it is believed that the accuracies obtained by the use of this simple method fully justify its application to normally proportioned tall buildings. Where the material and load distribution patterns are radically different from those shown in Fig. 11.3, the application of the more accurate long-hand procedure is recommended.

As mentioned previously, a steel frame does not have the luxury of built-in compensation because steel columns are prefabricated with predetermined lengths. Therefore, a suggested method for avoiding gross inaccuracies would be to have the steel erector check the top elevation of columns at predetermined levels, say every fourth or sixth floor, and to make provisions for adjustments of column heights.

Some of the problems associated with differential shortening of columns can be eliminated in the fabrication stage. Certain columns can be made slightly longer than their nominal length to account for axial shortening. However, the uncertainties in the final structure are so many that some form of field adjustment is usually required.

For example, in steel buildings it may become necessary to place removable shims between columns and their foundations in order to

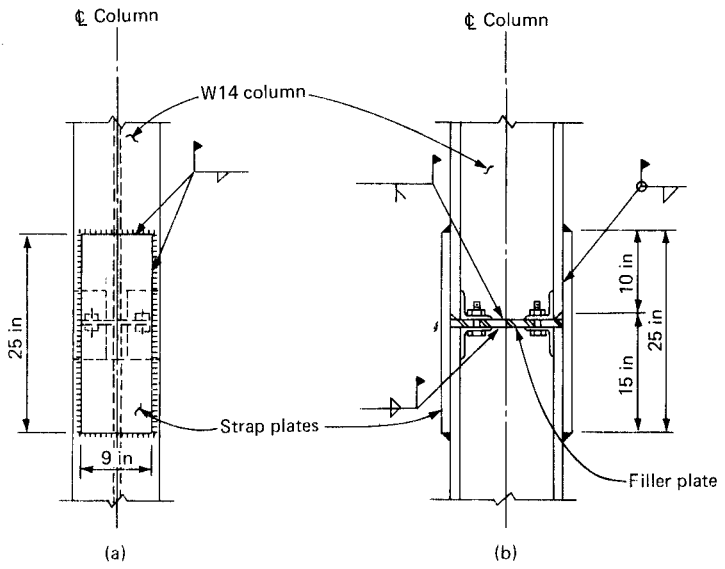

Figure 11.7 Splice detail for field correction of column lengths. (*a*) Elevation; (*b*) section.

compensate for differential shortening and to assure proper load transfer. When the erection of structural steel reaches predetermined levels, the columns are temporarily unloaded and steel shims removed. Another relatively simple method of adjusting column lengths which has been successfully used in composite construction is shown in Fig. 11.7.

11.2 Floor-Leveling Problems

Floor-leveling problems are of increasing importance as stronger building materials and more refined and sophisticated designs result in lighter construction that is more prone to deflections than earlier heavier buildings. In framed buildings considerable trouble is encountered in trying to provide a level floor system because of the many variable conditions that exist in practice. Concrete floors that are level at the time of construction may not be so at the time of occupancy. Many of the variable factors encountered are not mathematically determinable, even though an attempt is made by the engineer to compensate for such effects.

In steel buildings floor beams are furnished with a predetermined camber, while in concrete buildings the camber is built in the form work. Usually the camber specified in either type of building ranges from a minimum of ½ in (12.7 mm) to a maximum of 2.5 in (63.5 mm). Cambers smaller than ½ in (12.7 mm) are difficult to achieve, while a

camber of substantially greater than 2.5 to 2.75 in (63.5 to 69.85 mm) will result in other serviceability problems for beams in the 30- to 42-ft (9.14- to 12.80-m) span range. Cambers are specified anticipating that the loading of floors will overcome the camber, resulting in a level floor. This is not always the case because (1) rolling and construction tolerance combined with the long-term effect of creep of concrete is enough to affect the final result up or down in both steel and concrete construction. (2) Most usually, camber is calculated as if the beam were pin-connected or completely fixed. Actual erection conditions, even in simply connected steel beams, give the beam a partial fixity. Depending upon the degree of fixation the final result could again be up or down. (3) Vertical members will shorten elastically during the erection. The magnitude of elastic shortening between interior and exterior columns or between two adjacent exterior columns most usually is different, compounding the floor-leveling problems.

Because of the variable factors that are encountered, combined with the fact that none of these is mathematically determinable in the context of a practical design office, it makes it almost an accident if the floor turns out to be level. The problem is typical in most types of construction and surfaces during interior fit-up of projects. One sure method of obtaining a level floor is to float the floor to remove the lumps and fill the low spots. Cement-based self-leveling underlayments are used for this purpose. In a floor built to commercially acceptable tolerance, the average fill over the entire floor area should not exceed ½ in (12.7 mm), which translates into an additional dead load of 6 psf (287.3 mm). Depending upon the type of construction, this additional load may represent an increase of 3 to 6 percent of the total working stress load. It is recommended that an allowance be made for this additional load in the structural design.

The most commonly specified tolerance for finished floor slab surfaces is ⅛ in (3.7 mm) in 10 ft (3.048 m), which is considered too stringent for most uses. The reasons for unlevelness are manyfold, including form work sagging, deflection of members due to dead and live loads, finishing irregularities, or errors in setting of steel beams or form work. The as-built surface of the floor always exhibits bumps and dips.

In recognition of practical problems of achieving the specified tolerances, the American Concrete Institute Committee 117 is revising its "Standard Tolerances for Concrete Construction and Materials" (ACI 117-81). The most current draft of the standard includes floor finish tolerances based on two measuring methods: the F-number system and the straight-edge method. F numbers are one way of describing floor flatness. The larger the F number, the flatter the floor. An F-60 floor is roughly twice as flat as an F-30 floor. Committee 117 has voted

affirmatively on the document, and the standard is being prepared for Technical Activities Committee review. The American Society for Testing and Materials (ASTM) will include a standard test method for determining floor flatness and levelness using the F-number system (ASTM E-1155).

11.3 Floor Vibrations

Earlier chapters have dealt with the subject of vibration induced in a building by outside sources of vibrational loads such as wind and earthquakes. In addition to these forces, a building is subjected to a variety of vibrational loads that come from within. Although almost all loads except dead loads are nonstatic, the major internal sources of vibration that might be a cause of concern in an office or a residential building are the oscillation of machinery, the passage of vehicles, and various types of impact loads such as those caused by dancing, athletic activities, and even by pedestrian traffic. The trend in the design of floor framing systems of high rises is for long spans using structural systems of minimum weight. To this end, high-strength steel with lightweight concrete topping is routinely employed in the framing of floors. With the use of lightweight concrete, most building codes allow for a reduction in the thickness of slab required for fire rating. This results in a further reduction in the mass and stiffness of the structural system, thereby increasing the period of the structure, which at times may approach the period of the source causing the vibration. Resonance may occur, causing large forces and amplitudes of vibration.

The performance of such structures can be greatly improved by adding nonstructural elements such as partitions and ceilings which contribute greatly to the damping of vibrations. Nonstructural elements may also add to the mass and stiffness to produce the desired degree of solidity. Although the essential requirement in establishing the adequacy of a floor system is its strength, large deflections can be objectional for several reasons. (1) Excessive deflections and vibrations may give the user the negative impression that the building is not solid. On retail areas, for example, the china may rattle every time someone goes by, or the mirrors in the dressing rooms of clothing stores may shake, giving the customer the somewhat nebulous but real feeling that the structure is not solid. In extreme cases vibrations may cause damage to the structure as a result of loosening of connections, brittle fracture of welds, etc. It is therefore important that the structure be able to absorb impact forces and vibrations without transmitting any humanly perceptible shaking or bouncing. Monolithic concrete buildings are more solid in this respect as compared to light-framed buildings with steel or precast concrete. (2) Excessive deflection may result in curvature or misalignments perceptible to the

eye. (3) Large deflections may result in fracture of architectural elements such as plaster or masonry. (4) Large deflections may result in the transfer of load to nonstructural elements such as curtain wall frames.

It is difficult to establish general criteria for the design of a solid structure because of the human factor. Feeling of bounciness varies from person to person, and what is objectionable to some may be barely noticeable to others. Among the criteria employed in the design of floor systems are limitations on the span-to-depth ratio and flexibility which normally lead to deeper sections than would be required from strength considerations alone. It is somewhat dubious that these limitations assure occupants' comfort.

Recognizing that there is no single scale by which the limit of tolerable deflection can be defined, the AISC specification does not specify any limit on the span-to-depth ratios for floor framing members. However, as a guide, the commentary on the specification recommends that the depth of fully stressed beams and girders in floors should not be less than $(F_y/800)$ times the span. If beams of lesser depth are used, it is recommended that the allowable bending stresses be decreased in the same ratio as the depth. Where human comfort is the criterion for limiting motion, the commentary recommends that the depth of steel beams supporting large open floor areas free of partitions and other sources of damping should not be less than one-twentieth of the span, to minimize perception of transient vibration due to pedestrian traffic.

Thus there is no clear-cut requirement on the flexibility to limit the perception of vibration by occupants. Flexibility limits are given, however, from other considerations such as fracture of architectural elements like plaster ceilings. The rule-of-thumb limitations are 1/150 to 1/180 of the span for visibly perceptible curvature and 1/240 to 1/360 of the span for curvature likely to result in fracture of applied ceiling finishes.

In the design of floor systems of buildings, fatigue damage due to transient vibrations is not a consideration because it is tacitly assumed that the number of cycles to which the floor system is subjected is well within the fatigue limitations. However, damage due to fatigue can be a cause of concern in floors subjected to aerobic exercise activities.

Human response is directly related to the characteristics of the vertical motion of the floor system. Users perceive floor vibrations more strongly when standing or sitting on the floor than when walking across it. Human response to vibration seems to be a factor for consideration in design only when a significant proportion of the users will be standing, walking slowly, or seated.

Most of the experiments done on human response to vibrations are

related to the physical safety and performance abilities of physically conditioned young subjects in a vibrating environment such as the research supported by NASA and various defense agencies. Very little information is available on the comfort of humans subjected to unexpected vibrations during the course of their normal duties such as slowly walking across a floor or sitting at a desk. Comfort is a subjective human response and defies scientific quantification. Different people report the same vibrations to be perceptible, unpleasant, or even intolerable. The same vibration may bring about varying reactions among different subjects. Various investigators have established different criteria to predict the effect of vibration on human subjects. Perhaps the best currently available measure for human response to steady sinusoidal vibration is given in Ref. 60; the results are shown in Fig. 11.8. Conditions of constant peak velocity, peak acceleration, and peak jerk, which is defined as the rate of change of acceleration, are shown in the upper right-hand corner of the figure. Although there is no simple physical characteristic of vibration that completely defines the human response, there is enough evidence to suggest that acceleration associated in the frequency range of 1 to 10 Hz is preferable to the velocity and jerk criteria. This is the range for normally encountered natural frequencies of floor beams. Investigations have shown that human susceptibility to building floor vibrations is influenced by the rate at which the vibrations decay; people tend to be less sensitive to vibrations that decay rapidly. In fact, experiments have shown that people do not react to vibrations which persist for fewer than five cycles.

Human response ratings to a steady state of vibrations as originally documented by two researchers, Richer and Meister, have been found to be too severe for the design of building floors subject to transient vibrations caused by human activity. Lenzen (Ref. 61) has modified the Richer and Meister rating scale by multiplying the amplitude scale by 10 to account for the nonsteady state of vibrations. The modified curves which account implicitly for damping are shown in Fig. 11.9. In this figure the natural frequency f is plotted on the horizontal scale and the amplitude A_0 is plotted on the vertical scale. A brief discussion of evaluating these parameters follows.

The natural frequency f is given by the relation

$$f = 1.57 \sqrt{\frac{EI_b g}{W_d l^4}}$$

where f = frequency in cycles per second
E = the modulus of elasticity of the system in ksi

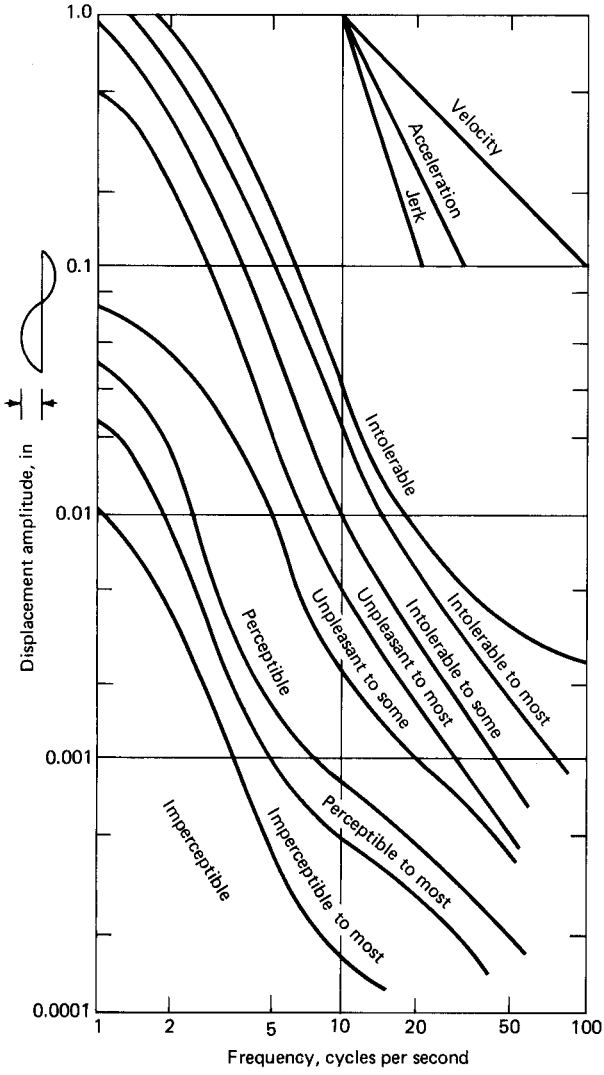

Figure 11.8 Velocity, acceleration, and jerk criteria. Response to sustained harmonic vertical vibration.

I_b = transformed moment of inertia of the beam assuming full interaction with slab system in inches
g = acceleration due to gravity, 386.4 in/s
W_d = dead load tributary to the beam in kips/in
l = effective span of beam, in inches

The design amplitude A_0 is obtained by modifying the initial amplitude of vibration of a simply supported beam subjected to the

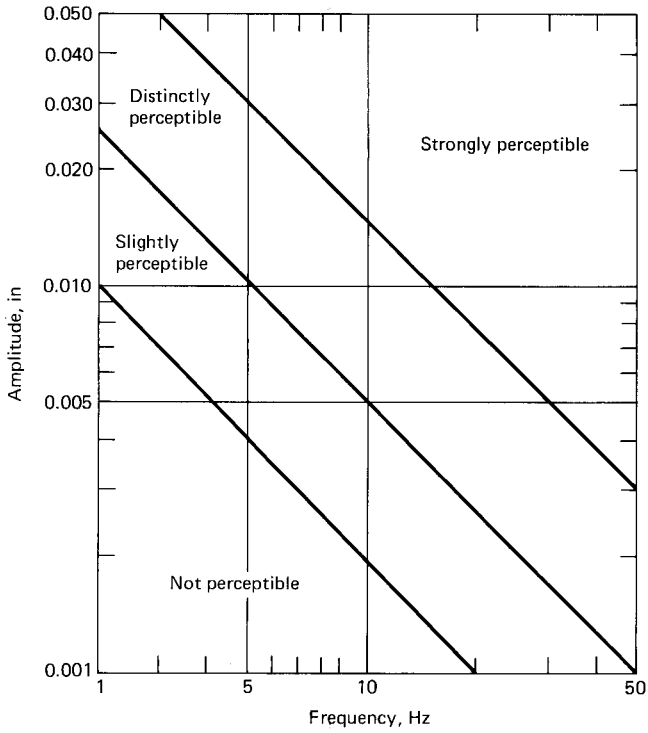

Figure 11.9 Response curves.

impact load of a 190-lb person executing a heel drop. The initial amplitude for the most common value of E of 29,000 ksi is given by the relation

$$A_{0t} = (\text{DLF})_{\max} \times \frac{l^3}{80EI_b}$$

where $(\text{DLF})_{\max}$ is the maximum dynamic factor which can be obtained from a graph given in Ref. 62.

Since a floor system usually consists of a number of parallel beams, Ref. 62 suggests that the design amplitude be obtained by dividing the initial amplitude by a factor N_{eff} to account for the action of multiple beams. Methods of estimating N_{eff} are given in Ref. 62.

The design procedure can thus be summarized as follows:

1. Compute the transformed moment of inertia of the beam under investigation. Use full composite action regardless of method of construction and assume an effective width equal to the sum of half

the distances to adjacent beams. For composite beams on metal deck use an effective slab depth that is equal in weight to the actual slab including concrete in valleys of decking and the weight of decking itself.

2. Compute the frequency from the relation $f = 1.57\sqrt{EI_b g/W_d l^4}$.
3. Compute the heel drop amplitude of a single beam by using the relation $A_{0t} = (\text{DLF})_{\max} \times l^3/80EI_b$.
4. Estimate the effective number of beams, N_{eff} (Ref. 63) and compute the design amplitude by the relation $A_0 = A_{0t}/N_{\text{eff}}$.
5. Plot on the modified Richer-Meister scale (Fig. 11.9) the computed frequency f and the amplitude A_0.
6. Redesign if necessary.

Another response rating based on experimental data has been developed by Wiss and Parmelee (Ref. 63). In their method the response rating R is given as a function of frequency, peak amplitude, and damping. Based upon the computed value of R, the expected human response is classified into one of the five following categories:

1. Imperceptible $R < 1.5$
2. Barely perceptible $1.5 < R < 2.5$
3. Distinctly perceptible $2.5 < R < 3.5$
4. Strongly perceptible $3.5 < R < 4.5$
5. Severe $R > 4.5$

The response factor R is given by

$$R = 5.08\,(FA_0/D^{0.217})^{0.265}$$

where R = response rating
F = frequency, in cycles per second
A_0 = Displacement in inches
D = Damping ratio expressed as a ratio of actual damping to critical damping

The damping coefficient D, among other things, depends on the inherent characteristics of the floor, amount of ceiling duct work, flooring, furniture, and the amount of partitions. It should be noted that it cannot be determined theoretically but can only be estimated in relation to existing floors and their contents. For a rough estimate, the Canadian Standards Association suggests the following values:

Bare floors	$D = 0.03$
Finished floor with ceiling, mechanical ducts, flooring and furniture	$D = 0.06$
Finished floor with partitions	$D = 1.13$

Floor structures subjected to rhythmic activities such as dancing, aerobics, and other jumping exercises have been a source of annoyance to owners and engineers alike. The floor vibrations could be so large as to raise some doubts about the safety of the structure due to fatigue. Unlike vibration problems encountered in office occupancies, the vibrations due to rhythmic activities are continuous. These vibrations can be greatly amplified when periodic forces are synchronized with the floor frequency, a condition called resonance. Unlike transient vibrations, continuous vibrations may not decay. The National Building Code of Canada (NBC) in its commentary recommends that floor frequencies less than 5 Hz should be avoided for light residential floors, schools, auditoriums, gymnasiums, and other similar occupancies. It recommends a frequency of 10 Hz or more for very repetitive activities because of the possibility of getting resonance when the rhythmic beat is on every second cycle of vibration.

In a paper entitled "Vibration Criteria for Assembly Occupancies," Allen, Rainer, and Pernica have presented a procedure for designing floor structures subjected to rhythmic activities. Briefly the procedure is as follows:

1. Determine the density of occupancy based on type of activity. For example, if the floor area is 30 by 60 ft (9.15 by 18.3 m) and has an aerobic class of 50 people of average weight of 120 lb, the equivalent density of occupancy works out to be

$$\frac{50 \times 120}{30 \times 60} = 3.33 \text{ psf } (159.6 \text{ Pa})$$

2. Choose an appropriate forcing frequency f and a dynamic load factor α. For aerobic exercises, the value of f suggested in the paper is between 1.5 and 3 Hz, while the value for α is given as 1.5.
3. Choose an acceptable limiting acceleration ratio, a_0/g at the center of the floor. The suggested value for physical exercise activity is 0.05.
4. Determine the lowest acceptable fundamental frequency f_0 of the floor system by the relation:

$$f_0 \geq f \sqrt{1 + \frac{1.3}{a_0/g} \frac{\alpha W_P}{W_t}}$$

where w_p = weight per unit area of participants
w_t = total weight per unit area of structure, participants, furniture, etc.

5. Determine the natural frequency f_0 of the floor structure. In addition to the weight of the floor structure itself, weights of participants and furniture, if any, are to be included in the computation of f_0.
6. The frequency f_0 should be greater than or equal to the frequency obtained in step 4. If not, the options are to stiffen the floor system, relocate the activity, convince the owner to accept a higher limiting acceleration by pointing out that no serious safety-related problems are known to have occurred for floors with frequencies higher than 6 Hz. If the frequency is less than 5 Hz, the floor system should be carefully evaluated for fatigue and other safety-related problems.

Increasing the frequency of the structure by increasing the stiffness is usually cost prohibitive. The most prudent course for the engineers is to make the owner aware of vibration-related problems during the design process.

11.4 Panel Zone Effects

Structural engineers involved in the design of high-rise structures are confronted with many uncertainties when calculating the lateral drift in tall buildings. For example, they have to decide on the magnitude of appropriate wind loads and the limit of allowable lateral deflections and accelerations. Even if it is assumed that these loads and limits are well defined, another question that often comes up in modeling of the building frames is whether or not one should consider the panel zones at the beam-column intersections as infinitely rigid.

This problem had not been of major consideration in the first generation of tall buildings built prior to the 1950s, but with the advent of the tubular structure with its closely spaced columns and deep spandrels, the problem appears to have taken on a new dimension because of the increase in the number and size of panel zones.

The panel zone can be defined as that portion of the frame whose boundaries are within the rigid connection of two or more members with webs lying in a common plane. It is the entire assemblage of the joint at the intersection of moment-connected beams and columns. It could consist of just two orthogonal members as at the intersection of a roof girder and an exterior column, or it may consist of several members coming together as at an interior joint, or any other valid combination. In all these cases, the panel zone can be looked upon as a link for transferring loads from horizontal members to vertical mem-

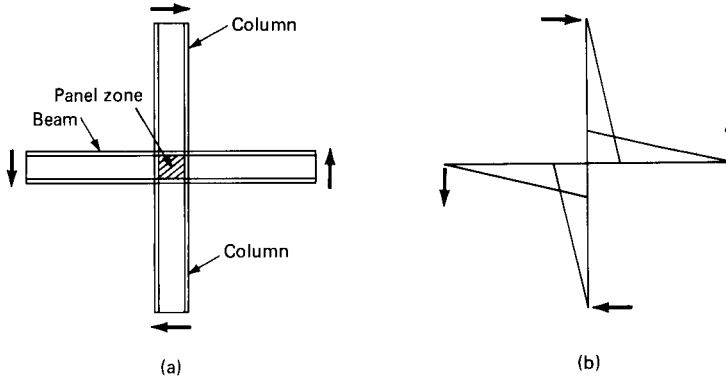

Figure 11.10 Typical frame element. (*a*) Free-body diagram; (*b*) bending moments due to shear forces in beams and columns.

bers and vice versa. For example, consider the free-body diagram of a frame element consisting of an assemblage of two identical beams and columns with points of zero moments at the ends (Fig. 11.10). These zero moment ends are, in fact, representative of points of inflection in the members.

Consider the frame element subjected to lateral loads. It is easy to see that because of these loads the columns in the frame element are subjected to horizontal shear forces and corresponding bending moments as shown in Fig. 11.10*b*. Equilibrium considerations of the frame element result in vertical shear forces in the beams at the inflection points and corresponding bending moments in the beams. The panel zone thus acts as a device for transferring the moments and forces between columns and beams. In providing for this mechanism the panel zone itself is subjected to large shear stresses.

The manifestation of high shear forces in the panel zones is best explained with reference to a straight exterior connection consisting of two wide flange sections joined together to form a right-angled connection as shown in Fig. 11.11*a*. The bending moment in the beam can be considered to be carried as tensile forces in the top flange and compressive forces in the bottom flange and the shear stresses can be assumed to be carried by the web. In the region of the panel zone, the tensile force in the top flange of the beam is carried into the web by horizontal shear forces and, by a similar action of vertical shear forces, is converted back into a tensile force in the outer flange of the column. The distribution of the actual state of stress in the panel zone is highly indeterminate, but a reasonable approximation can be obtained by assuming that the tensile stresses are reduced linearly from a maximum at the edge of the corner B or D to zero at the external corner. If the members AB and CD are assumed as stiffeners of the flange

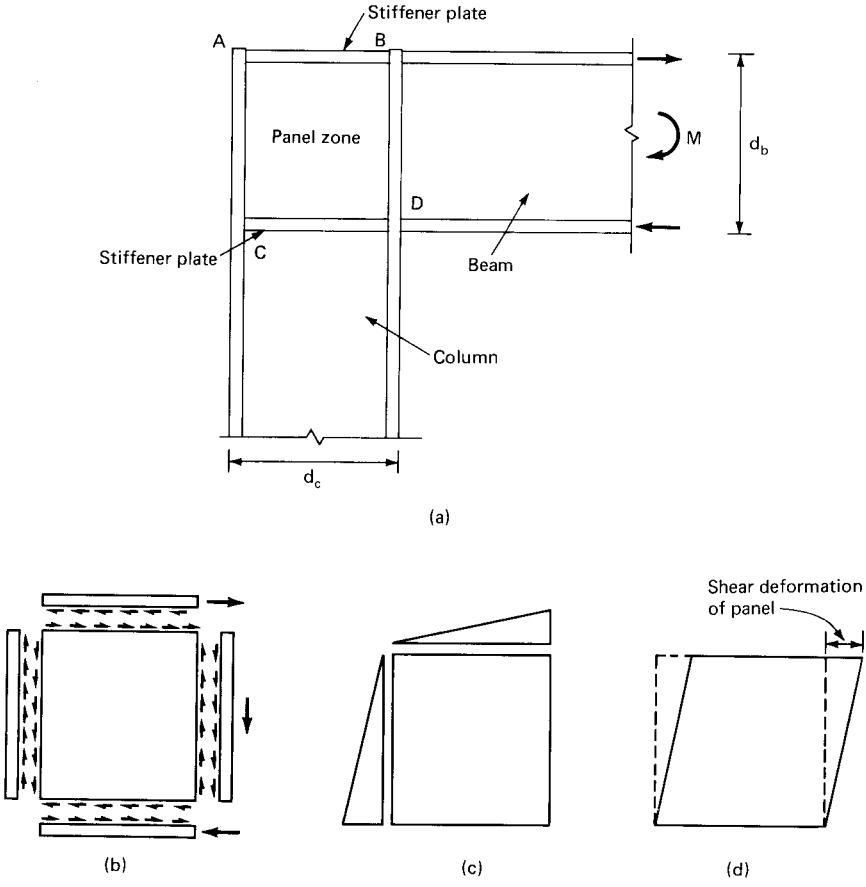

Figure 11.11 Panel zone behavior. (*a*) Corner panel at intersection of beam and column; (*b*) schematic representation of shear forces in panel zone; (*c*) linear distribution of tensile stresses; (*d*) shear deformation of panel zone.

sections of the beam, a distinct load path can be visualized for the compressive and tensile forces in the beam flange. Consideration of equilibrium of forces within the panel zone results in shear stress and a corresponding shear deformation as shown in Fig. 11.11*d*. It is this deformation that may be of considerable interest in the calculation of drift of multistory buildings.

Before proceeding with a qualitative explanation of the behavior of panel zones and their influence on building drift, it is instructive to discuss some of the assumptions commonly made in the analysis of building frames. Prior to the availability of commercial analysis programs with built-in capability of treating panel zones as rigid joints, it was common practice to ignore their effects; the frame was

usually modeled using actual properties along the centerlines of beams and columns.

If the size and number of joints in a frame were relatively large, an effort was made to include the effect of joint rigidity by artificially increasing the moment of inertia of the beams and columns; the properties were usually multiplied by a square of the ratio of centerline dimensions to clear-span dimensions.

Nowadays, it is relatively easy to model the panel zone as a rigid element because of the availability of a large number of computer programs which include this feature. Flexibility of panel zones can be considered in some of these programs, although somewhat awkwardly, by artificially decreasing the size of the panel zones. With these many options available, it becomes necessary to gain an insight into the influence of panel zone on the deflection of building frames.

Computations of beam, column, and panel zone contributions to frame drift can easily be accomplished by hand calculations by using virtual work method. For this purpose we consider again the typical frame element subjected to horizontal shear forces P_c and vertical shear forces P_b at the inflection points (Fig. 11.12*a*).

The notations used in the development of the method are as follows:

d_b = depth of panel zone
d_c = width of panel zone
h_c = clear height of column
L_c = clear span of beam
L = center-to-center span of beam
h = center-to-center height of column
I_c = moment of inertia of column
I_b = moment of inertia of beam
E = modulus of elasticity
G = shear modules
Δ_b = frame drift due to beam bending
Δ_c = frame drift due to column bending
Δ_p = frame drift due to panel zone shear deformation

The bending moment diagrams for the typical frame element can be obtained under three different assumptions.

1. The first assumption corresponds to ignoring the rigidity of panel zone; the bending moment diagrams for the external and unit loads can be assumed as shown in Figs. 11.12*c* and 11.12*g*. The bending moments increase linearly from the point of contraflexure to the centerline of the joint. By integrating the moment diagrams shown in Figs. 11.12*c* and 11.12*g*, the column and beam bending contributions to the frame drift are given by:

$$\Delta_c = \frac{P_c h^3}{12\,EI_c}$$

$$\Delta_b = \frac{P_b L^3}{12\,EI_b}$$

2. In the second case, which corresponds to assuming that the panel zone is completely rigid, we get bending moment diagrams for external and unit loads as shown in Figs. 11.12*b* and 11.12*f*. The bending moments increase linearly from the points of contraflexure but stop at the face of beams and columns. Integration of moment diagrams gives the expressions for Δ_c and Δ_b as follows:

$$\Delta_c = \frac{P_c h_c^3}{12\,EI_c}$$

$$\Delta_b = \frac{P_b L_c^3}{12\,EI_b}$$

3. The third assumption, which attempts to account for the flexibility of panel zones, results in bending moment and shear force diagrams for external and unit loads as shown in Figs. 11.12*d,h,e,i*. Integration of bending moment and shear force diagrams leads to the following expressions in Δ_c, Δ_b, and Δ_p.

$$\Delta_c = \frac{1}{12EI_c}(P_c h_c^3 + P_c h_c^2 d_b)$$

$$\Delta_b = \frac{1}{12EI_b}(P_b L_c^3 + P_b L_c^2 d_c)$$

$$\Delta_P = \frac{P_c h_c^2}{d_b t_w d_c}$$

A more accurate method of determining the effect of panel zone continuity plates is to perform a finite element analysis of a typical frame unit as shown in Fig. 11.13. A series of finite element analyses can be performed to relate the effect of panel zone to basic section properties of beam and columns of the typical unit. Halvorson (Ref. 64) indicates that for a typical 13 ft, 1 in high by 15 ft long (4 by 4.57 m) unit consisting of W 36×300 columns and W 36×230 beams, that the frame stiffness is approximately 8, 15, or 22 percent stiffer than a stick

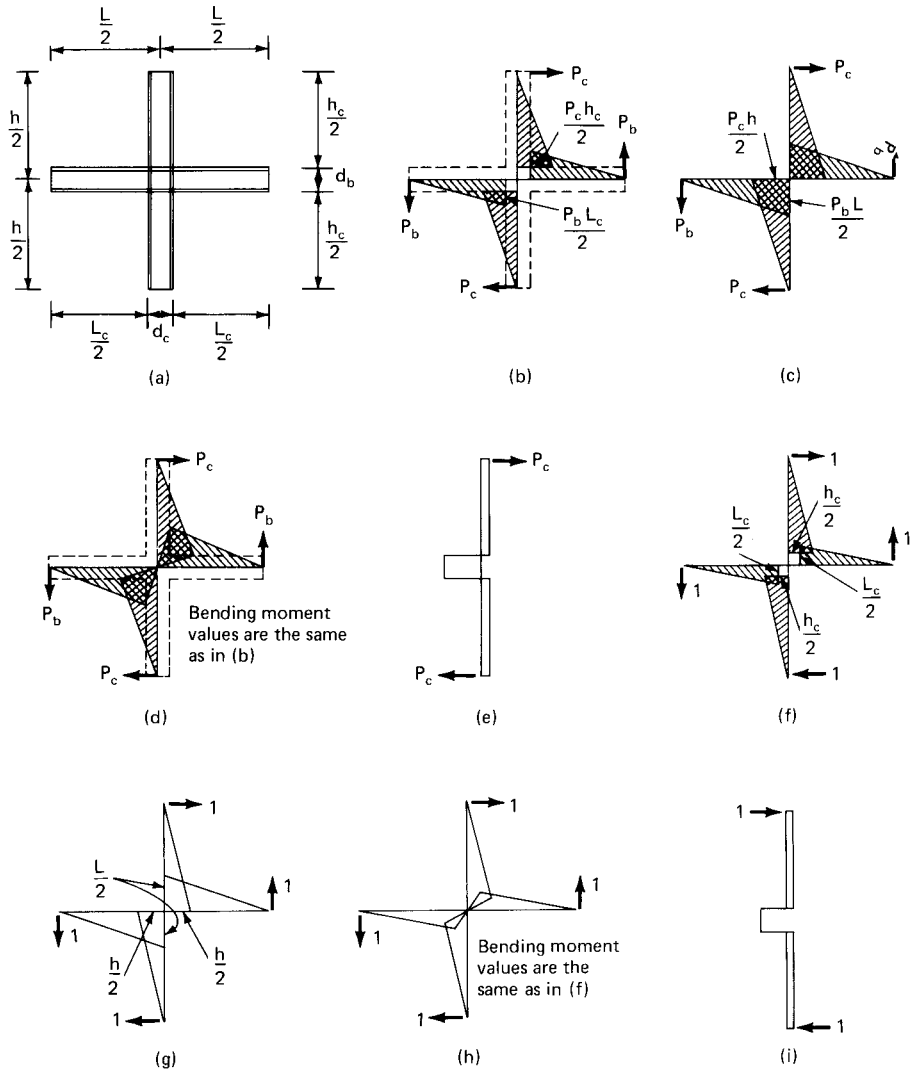

Figure 11.12. Typical frame segment. (*a*) Geometry; (*b*) bending moment diagram with rigid panel zone; (*c*) bending moment diagram without panel zone; (*d*) bending moment diagram with flexible panel zone; (*e*) shear force diagram; (*f*) through (*i*) unit load diagrams.

element model depending upon whether no, AISE minimum-, or full-continuity plates are provided, respectively.

Using the virtual work expressions given above or a finite element method it is relatively easy to compute the contribution of panel zone deformation to frame drift. The author recommends that before undertaking the analysis of large tubelike frames, representative frame elements, say at one-fourth, one-half, and three-fourths the height of

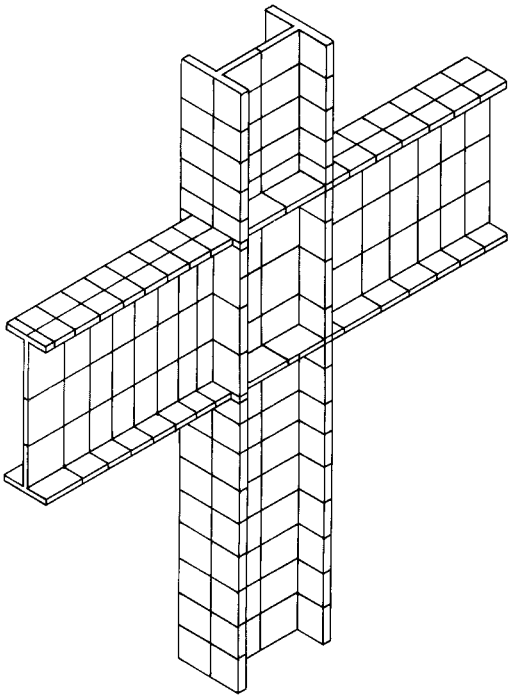

Figure 11.13 Finite element idealization of a typical frame unit.

the building be analyzed to get a feel for the contribution of panel zone deformation to frame drift. Armed with the results, it is relatively easy to modify the properties of beam and columns such that the overall behavior of the frame is properly represented in the model.

11.5 *p*-Δ Effects

Assessment of overall stability of the structure under the action of combined vertical and lateral loads or under the action of vertical load only is of importance in the design of building columns. A column is considered slender if its cross-sectional dimensions are small compared with its length. The degree of slenderness is measured in terms of the ratio l/r, where l is the unsupported length of the members and r is the radius of gyration of its cross section. Whereas a stocky column fails by crushing or yielding of the material of the column, slender columns fail by buckling, i.e., by lateral bending of the column. Various building standards such as the ACI and the AISC specifications have long recognized this phenomenon and require that the buckling or the stability of columns be considered in the design.

This section considers methods of designing for stability of frames proportioned by elastic design procedures. Conventional design methods which use the concept of effective length factor K in the interaction formulas to account for frame stability are considered first. Next, in lieu of the effective length procedure, an alternate design method called the p-Δ method, which is independent of K but requires that column destabilizing forces be applied to the structure, is considered. As a frame is displaced laterally, each story is subjected to a destabilizing or p-Δ shear equal to the product of the total vertical load on the story and the story sway deflection. Adjustments in the analysis are required to take into account the reduction in the strength of the column caused by the p-Δ effect.

Before examining these design methods, a review of the fundamentals of column behavior is useful to establish the parameters on which the ACI and AISC procedures are based. Since most of the material can be found in basic strength-of-material textbooks, we will not dwell on the derivations but emphasize only major topics.

Euler enunciated more than 200 years ago that a straight concentrically loaded pin-ended slender column fails by buckling at a critical load

$$P_c = \frac{\pi^2 EI}{l^2}$$

where E, I, and l are the familiar notations for Young's modulus, moment of inertia, and length of the column. If P_c is divided by the cross-sectional area A of the column, the expression for the critical load may be written in terms of the critical average stress f_c on the gross section of the column

$$f_c = \frac{\pi^2 EI}{l^2 A}$$

Substituting $I = Ar^2$, where r is the radius of gyration gives the stress form of Euler's equation

$$f_c = \frac{\pi^2 E}{(l/r)^2}$$

A plot of the critical stress versus the slenderness ratio, a so-called column curve, is shown in Fig. 11.14, illustrating the reduction in buckling strength as the slenderness increases. Stocky columns do not fail by buckling but do so by yielding or crushing of the material at a load much greater than the critical load. There is a limiting slender-

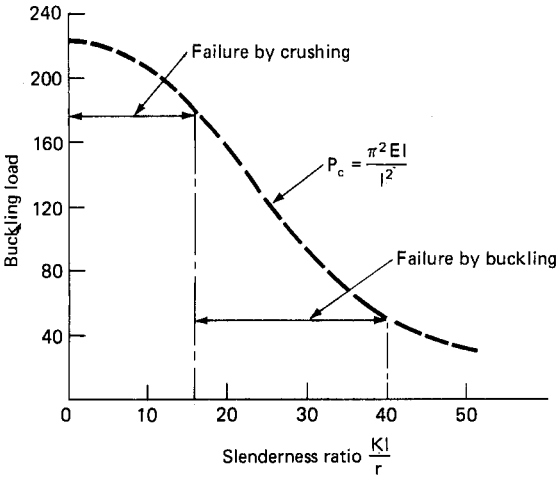

Figure 11.14 Relation between buckling load and slenderness ratio. Short columns fail by crushing, while long columns fail by buckling.

ness ratio below which failure occurs by crushing, while for larger values, the mode of failure is by buckling as shown in Fig. 11.14.

The expression for buckling load P_c holds for an idealized column supported by frictionless pins and roller; a condition that exists very rarely in practice. Building columns most often are connected to beams which restrain the rotation at the supports, thereby developing end moments. In addition, unbraced columns experience lateral deflections. In order to extend the determination of critical loads for the practical cases, the idea of effective length of column is used. The effective length is expressed as a product of actual length times a factor K, called the effective length factor. The critical load for practical cases is given by the relation

$$P_c = \frac{\pi^2 EI}{Kl^2}$$

Various design aids are available for evaluating values of K, the most popular being the alignment charts given in most building standards. The charts are entered with known values of ψ, the ratio of the sum of the relative bending stiffness of columns to that of the girders, at each end of the column, and the value of K is read by aligning the ψ values.

Many cases arise in practice in which the columns are subjected to lateral sway due to wind or earthquake loads and due to asymmetry in the geometry of the building or in the application of loading. The

effective length depends not only on the degree of restraint at the column ends but also whether it can be considered braced or unbraced against side sway. Therefore, ψ charts are given for both braced and unbraced frames.

Although in reality no building is either completely braced or unbraced, for purposes of structural analysis, building frames are divided into two categories, braced frames and unbraced frames. According to the ACI commentary, columns in a building can be considered braced if they are connected to a bracing element that is at least six times as stiff as the combined stiffness of all the columns being braced. If not, the columns are considered as part of an unbraced frame.

The values of K given separately in the alignment charts are based on the assumption that (1) for braced frames, all columns buckle simultaneously and that girders bend into single curvature with equal and opposite rotations at each end; (2) for unbraced frames the girders and columns buckle into double curvature. Situations arise in practice in which the far ends of the girders are sometimes fully fixed or pinned, requiring modification to their values of stiffness. For a braced frame, the girder stiffness should be multiplied by a factor of 2 if the far end of the girder is fixed. If it is pinned, then the corresponding factor is 1.5. For an unbraced frame, the girder stiffness should be multiplied by a factor of 0.67 if the far end of the girder is fixed and by 0.50 if the far end is hinged.

Most columns in buildings are in effect "beam-columns," i.e., they are subject to simultaneous bending caused by lateral loads or by end moments, and axial compression. Consider the column shown in Fig. 11.15*a* subjected to simultaneous action of axial load and moments at the ends. At any point, the total moment M can be considered to be a combination of the moment M_0 due to end moments plus the addition of the moment caused by P acting at an eccentricity y (Fig. 11.15*b, c,* and *d*). Thus $M = M_0 + Py$. Since the deflection is maximum at midheight, the secondary moment also reaches its maximum value at that height. A similar effect is caused when bending is caused by a lateral load as shown in Fig. 11.16. Since the deflection y and hence the magnitude of the secondary moment is itself a function of the end moments, a differential equation formulation is required for the solution of the problem. Simple cases of beam-columns subjected to end moments and concentrated loads, uniformly distributed loads, etc., have been solved by differential equation techniques. In a practical structure, such a closed-form solution is extremely complicated if not impossible. Therefore, various design standards such as the ACI and AISC specifications give provisions for approximate evaluation of the slenderness effect. The method in essence requires that the moments

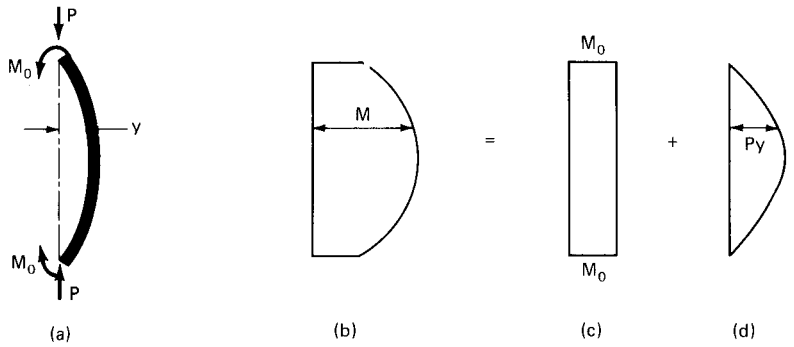

Figure 11.15 Moments in beam-columns. (*a*) Column subjected to simultaneous axial load and bending moments; (*b*) combined moment diagram; (*c*) moment diagram due to equal end moments M_0; (*d*) moment due to p-Δ effect.

obtained by a so-called first-order analysis be magnified by a moment magnification factor.

The direct addition of the maximum p-Δ moment to the maximum primary moment is correct only when the beam-column is subjected to equal moments at the ends subjecting the column to bend in a single curvature. For all other cases, it represents an upper bound, giving a moment magnification factor much larger than that which would occur in a real structure. If the two end moments at the ends of the columns are unequal but of the same sign, producing single curvature, the primary movement M_0 is certainly magnified but not to the same extent as when the moments are equal. If the end moments are of opposite sign, producing a reverse curvature in the column, the moment magnification effect will be very small. A moment magnification coefficient C_m is therefore used to take into account the relative

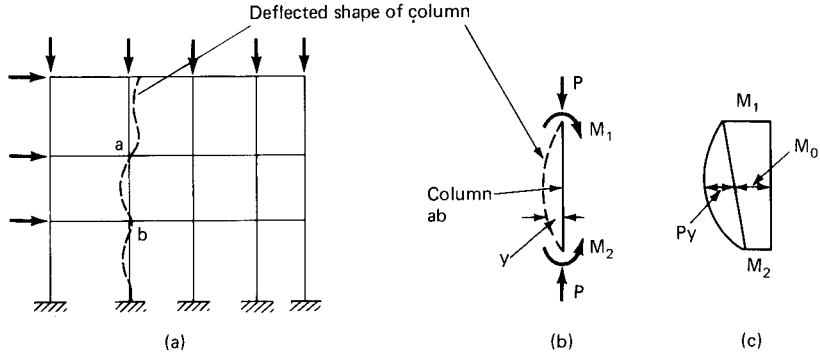

Figure 11.16 Behavior of practical building column. (*a*) Building frame showing deflected shape of column; (*b*) column subjected to simultaneous action of axial load and moments; (*c*) moment diagram due to end moments and p-Δ effect.

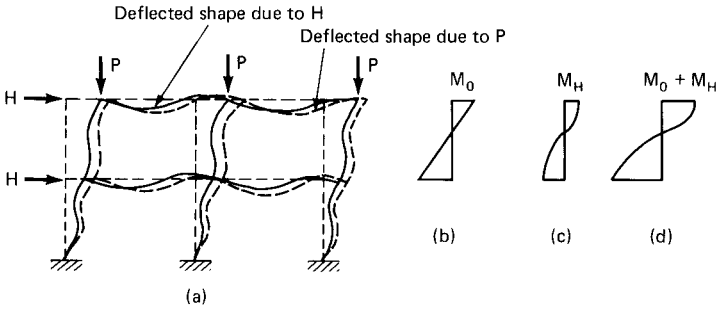

Figure 11.17 P-Δ effects in laterally unbraced portal frame. (*a*) Deflected shapes due to horizontal load H and vertical loads P; (*b*) moments at ends of columns due to horizontal load H; (*c*) moments at ends of columns due to axial loads P; (*d*) combined moment diagram due to H and P. Maximum moments due to H and P occur at ends of columns resulting in $C_m = 1.0$.

magnitude and sense of the two end moments. It is given by the expression

$$C_m = 0.6 + 0.4\, M_1/M_2 \tag{11.7}$$

In the above equation M_1 and M_2 represent the numerically smaller and larger end moments, respectively. The ratio M_1/M_2 is defined as positive when the column bends in a single curvature and negative if the moments produce reverse curvature. As can be expected, when $M_1 = M_2$ as in a column subjected to equal end moments, the value of C_m in the above equation becomes equal to 1.0. The above expression applies only to members braced against side sway. For columns which are part of the lateral resisting system, the maximum moment magnification occurs, i.e., $C_m = 1$ as illustrated in the following discussion.

Consider Fig. 11.17*a*, which shows the deflected shape of an unbraced portal frame subjected to the simultaneous action of gravity and lateral loads. Considering only the lateral loads, the deflection of the portal frame may be represented by solid lines as shown in Fig. 11.17*a*. The corresponding moments at the ends of a typical column are as shown in Fig. 11.17*b*.

When axial load is imposed on the deflected shape of the frame, additional sway occurs in the frame as shown by dashed lines in Fig. 11.17*a*. This additional deflection imposes secondary moments in the column as shown in Fig. 11.17*c*. It is seen that both the primary and secondary moments are of the same sign and have maximum values at the same locations, namely at the two ends of the columns. They are, therefore, fully additive as shown in Fig. 11.17*d*, meaning that the value of $C_m = 1$ for unbraced frames.

In American practice, both in steel and in concrete buildings, the approach to the stability problem is to modify individual member

design in a manner which approximately accounts for continuity, i.e., for frame buckling effects. This is done by mathematically isolating a compression member together with its adjoining members at both ends and determining its critical load in terms of effective length factor K. The member is then analyzed as a beam-column by a simplified interaction equation which accounts for the moment magnification caused by the p-Δ effect. Instead of frame analysis for the p-Δ method, a member analysis is substituted.

We will now review the various forms of interaction equations given in the AISC specifications. Consideration of only uniaxial bending reduces the AISC equations to the less intimidating format as follows:

$$\frac{f_a}{F_a} + \frac{C_m f_b}{(1 - f_a/F'_e)F_b} \leq 1.0 \tag{11.8}$$

$$\frac{f_a}{0.6F_y} + \frac{f_b}{F_b} \leq 1.0 \tag{11.9}$$

where f_a = axial stress in the column due to vertical loads
F_a = allowable axial stress
f_b = bending stress in the column
F_b = allowable bending stress
C_m = coefficient for modifying the actual bending moment to an equivalent moment diagram for purposes of evaluating secondary bending
F'_e = Euler's stress divided by safety factor, 23/12
F_y = yield stress of column steel

Prior to 1963, structural engineers could have made peace with the entire interaction problem by using the formula

$$\frac{f_a}{F_a} + \frac{f_b}{F_b} \leq 1.0$$

Since then, engineers have had to deal with many seemingly formidable factors which have been added on to the above interaction equation. For example, the allowable bending stress F_b now has a factor $(1 - f_a/F'_e)$ to account for the reduction in the bending capacity because of axial loads. The more the axial load in the column, the greater is the reduction of F_b. Reducing the allowable stress is mathematically equivalent to increasing the design moment for the p-Δ effects. The term F'_e contained in the reduction factor is the critical column stress divided by the factor of safety, 23/12, that governs the design of long columns.

We have seen earlier, using a total moment obtained by the direct addition of secondary and primary moments results in an overdesign if both these moments do not occur at the same location. The coefficient C_m in the interaction equation prevents overdesign by reducing the design moment by taking into account the relative magnitude and sense of the moments occurring at the ends of columns.

Values of C_m less than 1.0 increase F_b, offsetting the effects of axial load when the shape of elastic curves augments stability. Thus C_m = 0.85 when rotational restraints are present at the ends of the member. When there is no joint translation and where the shape of the curve is not affected by transverse loading, reverse curvature bending may reduce C_m to as little as 0.4.

To prevent the dramatic increase in F_b which can result in unsafe designs, Eq. (11.9), which does not contain the term C_m, is also required to be satisfied.

We will now take a brief look at the ACI procedures for designing beam-columns. First, we consider braced columns followed by a discussion of unbraced columns. The ACI procedure for designing a column in a braced portal frame can be outlined as follows:

1. Find the primary moments in the columns due to lateral loads. Include the effect of unsymmetry due to geometry and axial loads.
2. In defining the member properties, due consideration is to be given for creep and cracking effects in beams and columns. In the absence of a more detailed analysis, the ACI code permits the effective EI to be determined by either of the following two relations:

$$EI = \frac{E_c I_g/5 + E_s I_s}{1 + \beta}$$

$$EI = \frac{E_c I_g/2.5}{1 + \beta}$$

where E_c and E_s = the moduli of elasticity of concrete and steel, respectively

I_g and I_s = the moments of inertia of the gross section of concrete and reinforcement about the axis of bending

β = a ratio that takes into account the effect of creep and is equal to the ratio of maximum factored dead load moment to the maximum factored total load moment

3. From the lateral analysis obtain the moments M_1 and M_2 at the ends of the column and calculate the coefficient C_m by the relation $C_m = 0.6 + 0.4\, M_1/M_2$.
4. Determine the effective length factor K by using alignment charts. K varies from 0.5 to 1.0 for braced columns.
5. Calculate the moment magnification factor δ by the relation:

$$\delta_b = \frac{C_m}{1 - P_u/\phi P_c} \geq 1.0$$

where P_u = ultimate axial load on the column
P_c = critical load
ϕ = capacity reduction faction

6. Obtain the design moments at the ends of the column by multiplying the results of the elastic analysis by the moment magnification factor.
7. Design the column for axial loads and moments obtained in step 6.

The procedure for designing a column in an unbraced frame can be outlined as follows:

1. In a side sway mode lateral instability can occur only if all the columns in a particular story are subjected to buckling. Therefore, in calculating the moment magnification we should consider ΣP_u and ΣP_c for all the columns in that story. Steps 1, 2, and 3 are similar to those given for braced columns. The value of C_m obtained in step 3 is, however, valid for obtaining the moment magnification factor for braced columns. For moments resulting from lateral loads, $C_m = 1$ because, as explained earlier, the maximum secondary moments occur at the same locations as the primary moments.
4. From the elastic analysis find the gravity moments occurring at the ends of the columns.
5. Calculate the moment magnification factor C_m by the relation given previously for braced columns.
6. From ΣP_u and ΣP_c for all the columns in the particular story, calculate the moment magnification factor δ_s for secondary moments by the relation

$$\delta_s = \frac{1}{1 - \Sigma P_u/\phi \Sigma P_c}$$

7. Obtain the design moment M_c by multiplying the primary, i.e., the gravity moment M_g and the secondary moments M_s by their corresponding magnification factors thus:

$$M_c = \delta_b M_{2g} + \delta_s M_{2s}$$

The subscript 2 for M_g and M_s indicates that the larger of the two end moments is to be used in obtaining the design moment.

8. Design the column for the axial load and the amplified moments obtained in step 7.

Most analyses used by the designer to determine building deflections and the distribution of forces and moments throughout the structure do not include stability effects. Therefore, adjustments as outlined above are required to take into account the reduction in the strength of the structure caused by the effects of stability. The most important of these adjustments is the so-called p-Δ effect caused by additional shears and moments produced by the vertical loads acting on the laterally deformed structure. The compensation for not including the p-Δ effect directly in the analysis is made by multiplying the results of first-order analysis by the moment magnifier.

It is important to realize that the moment magnification method is an approximate method for evaluating secondary effects, and until about ten years ago it was the only practical method available for designing slender columns. The availability of commercial programs, however, has made possible a more accurate second-order analysis to be used in everyday engineering practice. It is no longer necessary to estimate the effects of axial load and of sway deflections on the bending moments. Instead, it is possible to explicitly evaluate them by the use of computers. This is considered next.

For conceptual purposes, a tall building can be considered as a cantilever with the dead and live loads acting at different floors represented as concentrated loads acting along the longitudinal axis of the cantilever column. When subjected to lateral loads such as caused by wind or earthquake, the cantilever will undergo a lateral deformation.

A conventional first-order analysis such as the stiffness method used in most commercially available programs assumes that the effect of deflections of the structural system due to external loading does not alter the magnitude of internal moments and forces in the structure. However, in reality the axial loads P acting through the deflection of the structure give rise to additional moment at the base with a consequent increase in the deflection. By invoking the basic principle

that for equilibrium to exist, the change in the externally applied moments must be equal to the change in the internal resisting moment, this change can be thought to be brought about by additional story shears called *sway forces* or p-Δ forces. The increase in deflection causes further increase in the moment and a consequent increase in the deflection. The process continues until either the structure comes to a stable equilibrium or, when the structure is very limber, it collapses. The tendency of the axial load to increase the moment and consequently the deflection of the structural system is the p-Δ effect. As mentioned earlier, until recently the only practical method of accounting for the p-Δ effect was to use the moment magnification method. However, numerous pitfalls exist in the analysis and design procedure which uses the moment magnification method. The p-Δ method, which can take into account directly the effect of axial loads, is far superior and is highly recommended for routine office use. With the results of the p-Δ analysis in hand, the engineers no longer need to worry about calculating the effective length factors through alignment charts. All columns can be designed by assuming effective length factor $K = 1$. The p-Δ method is applicable to all types of construction—steel, concrete, or composite—as a general procedure. Although the procedure itself is not described in the ACI or AISC codes, it is highly endorsed in the commentaries for the codes. Many commercially available computer programs formulate the equilibrium equations on the deflected shape to give the result in a single solution without resorting to iteration techniques. While these programs can directly include the effect of p-Δ forces and moments, they in general do not take into account the reduction in the stiffness of members due to the presence of axial loads.

If computer programs capable of performing second-order analysis are not available, the first-order analysis may be modified to include the p-Δ effect. In this method the lateral and vertical loads are applied to the structure and the relative first-order lateral displacements in each story are computed. The additional story shears caused by the p-Δ moments are computed from a knowledge of story displacement and the accumulated gravity loads at each story. The net story shear at any given level is obtained by the algebraic sum of story shears from the columns above and below the floor. The additional story shears are added to the applied loads and the structure is reanalyzed for the new set of lateral loads. Since these loads in general are larger than the first loading case, the resulting deflections are larger, requiring one or two more cycles of iteration for convergence. However, the following equation derived by various researchers can be used to obtain directly the final second-order deflection from the first-order deflection thus

$$\Delta = \frac{1}{1 - \Sigma P \Delta_i / Hh}$$

where ΣP = cumulative vertical load
Δ_i = the first-order story sway
h = story height
H = horizontal shear force

The above procedure can be outlined as follows:

1. From the first-order analysis determine Δ_i in each story.
2. Compute the second-order final deflection from the above equation.
3. Calculate the additional story shears caused by the p-Δ moments.
4. Perform another first-order analysis by subjecting the frame to the applied lateral loads plus story shears obtained in step 3.

Include gravity loads in steps 1 and 4 for unsymmetrical buildings. Step 4 gives the second-order moments and forces, which can be used in the design of members without having to resort to moment magnifier methods. What could be simpler?

The designer, however, faces a particular problem in any stability or second-order analysis of concrete structures in choosing a suitable mathematical model of flexural stiffness EI under various loading conditions. The value of EI should ideally reflect the amount of reinforcement, the extent of cracking, creep, reduction in stiffness due to axial loads and the inelastic behavior of steel and concrete. It is necessary to recognize the variation of stiffness along the entire length of each member by taking into account cracked and uncracked regions. Practical design considerations preclude the possibility of going into this detail for calculating the flexural stiffness of each and every member of a multistory building with thousands of members. Therefore, in practice, simplified methods are employed to compute EI.

When designing columns using the p-Δ method it is necessary to check the stability of individual columns by using the moment magnification procedure. This is to assure that beam-column effects for individual columns bending in single curvature are properly taken into account.

11.6 Cladding Systems

Cladding is a very expensive part of the building, making up as much as 10 to 20 percent of a building's initial cost. If the building facade is improperly designed or installed, requiring serious repairs, the repairs can cost many times more than the original cost because of the difficulties of recladding a building that is already in use. Until the

invention of structural steel building frame, about a hundred years ago, most exterior building walls were load-bearing elements pierced by windows to provide light and ventilation. The walls served the dual purpose of providing support for the upper floors and simultaneously forming an enclosing barrier. Today the only function of building exterior is to act as a filter system without having to bear any of the loads from the structure.

The performance of any wall system depends largely on the effect of natural forces on the materials constituting the wall. The natural forces are sunlight, temperature, water, wind, and seismic forces, in addition to the ever present gravity forces. Sunlight, particularly in the form of ultraviolet rays, produces chemical changes which cause fading and degradation of materials. Temperature creates expansion and contraction of materials in addition to the temperature differential between interior and exterior sides of the cladding which must be controlled to create a livable environment within the building. Water, in the form of wind-driven rain, can penetrate through the small openings and appear on the interior face of curtain walls. If trapped within the wall in the form of vapor, it can cause serious damage. Wind, acting either inward or outward, creates stresses that require the structural properties of the framing members, panels, and glass to be determined by its maximum effects. Gravity loads of cladding systems cause deflections in horizontal load-carrying members. Although gravity load itself is a one-time load, the members supporting the cladding system are subjected to variable floor and roof live loads, requiring that connections of the cladding to the frame be designed to provide sufficient relative movement to ensure that displacements do not impose vertical loads on the wall itself. In addition, concrete buildings are subjected to creep, compounding the problem of cladding design.

In the design of curtain walls there are three matters of chief concern: (1) structural integrity, (2) provision for movement, and (3) weathertightness. For structural integrity of the wall the stiffness rather than the requirement of strength is the primary concern, although anchorage failure due to inadequate strength should be given proper attention. Providing proper resistance to lateral loads is a routine procedure, especially in view of the fact that we now know more about the nature of wind loads than we did only a decade ago. The significance of negative wind pressure or suction forces acting on the wall augmented by the internal building pressure caused by air leakage is well understood, as reflected in most building codes.

In designing a curtain wall it is important to provide for ample movement between the wall components themselves, relative movements between the components, and relative movement between the cladding and the building frame to which it is attached. Although the

causes of movement are well known, it is not practical to predict the magnitude of the movements accurately. Since the movements manifest themselves at the joints of the cladding, the success of a cladding system lies in the proper detailing of the joints. Provision must be made to accommodate both the vertical and horizontal movement in the plane of the wall. Other design considerations such as weathertightness, moisture control, thermal insulation, and sound transmissions are areas normally outside the sphere of structural engineering and therefore will not be discussed here.

Common types of curtain wall failure are (1) structural failure of anchorages resulting in other wall elements disengaging from the building, creating serious hazard to the pedestrians; (2) glass breakage, which in many instances has been a safety hazard; (3) excessive air infiltration, which prevents proper conditioning of the interior space; and (4) accumulation of condensation, causing significant damage to interior finishes.

Failure of cladding can arise because of the differential movement both laterally and vertically between the building columns. Thermal movement, long-term creep of a concrete frame, and foundation settlements also contribute to the failure. The structural engineers normally do not have a direct involvement in the design of the building cladding. Typically the architect selects the cladding material for appearance and specifies requirements for the weatherproofing, performance, and durability of the cladding. From a knowledge of the weight of the cladding, the engineers designate connection points and design the structure to carry the anticipated loads. It is their responsibility to indicate the anticipated movements of the structural frame in order for the curtain wall supplier to properly detail the curtain wall connection to the structure. The effect of floor deflections due to the weight of cladding and live load, the magnitude of anticipated building drift, column shortening, foundation settlement, and thermal effects should all be taken into consideration.

The design of cladding in North America is traditionally undertaken by the architects. Many structural engineering firms specifically exclude this service by inserting a "no involvement with cladding" clause in their service contract. In spite of these attempts to keep out of conflict, if the building cladding turns out to be less than adequate, be it for watertightness, breakage, or any number of other problems, the structural engineer will be drawn into the dispute sooner or later. Therefore, it behooves the engineer to get involved, not in the sense of taking full responsibility for the design of the cladding, but by understanding all the implications involved in providing a structurally adequate and successful weatherproofing of the building.

Building cladding is one place where a number of independent

designs come together. The selection of cladding material for appearance and details for weatherproofing and performance characteristics are in the domain of the architect. The design of the structure for the weight of cladding is, of course, the responsibility of the structural engineer. It is likely that the exact weight and connection points of the cladding may not be known at the preliminary stage but may have to be conservatively assumed. Short- and long-term deflections of the structure due to gravity loads, column shortening due to creep and shrinkage in concrete and composite structures, expansion and contraction due to temperature, and lateral deflection of the building, especially the interstory drift, are some of the pieces of information required by the cladding supplier. The engineer should have a good understanding of tolerance required both horizontally and vertically for proper installation of curtain walls. In a core-braced steel frame it is likely that the perimeter spandrel is designed as a simply supported beam for gravity loads and hence somewhat limber as compared to a wind-resisting moment-connected spandrel. Even when the gravity loads are heavy, typical simple connections at beam ends have very little stiffness to prevent the rotation of spandrel beams. This is, perhaps, the single most common cause for cladding problems. Cladding problems are easily avoidable by proper detailing of connections.

The basic components that make up the exterior envelope consist of vision panels and spandrel panels. While vision panels are invariably of glass, the spectrum of materials available for spandrel panels is an ever increasing one. To name a few, spandrel panels can be made of aluminum, steel, glass, masonry, precast concrete, or glass fiber–reinforced concrete. To reduce costs, many designs use a laminated thin-gauge metal sheet bonded to a metal honeycomb backup. Typically framing employed for the mullions is aluminum because of the ease of producing complex custom shapes by extrusion.

The next sections discuss the design and installation aspects of the great diversity of exterior cladding systems. The proper design, installation, and operation of cladding in buildings is a culmination of the coordination activities among architects, engineers, cladding manufacturers, glazing contractors, building officials, and, of course, building owners. The sections briefly explain how the glass commonly used in a building is made and discusses the strength and testing aspects of glass. Other cladding systems such as metal curtain wall, stone cladding, brick veneer systems, and glass fiber–reinforced concrete systems are also briefly discussed.

11.6.1 Glass

Just as floor slabs must be designed to carry dead load and occupancy loads, or roof decks to carry dead loads and snow loads and resist uplift

forces due to wind, so must windows and spandrel panels be designed to withstand the lateral loads due to wind. Glass panels in curtain walls are structural elements insofar as they resist wind pressure or suction and transfer wind forces to the building frame. In today's high-rise architecture, glass is employed in more imaginative ways than ever before. At present, the only way to construct a building 50 or 100 stories high is to frame it on a skeleton of steel or concrete and to cloak it with a skin of relatively lightweight cladding. Glass has always been the most suitable material in the eyes of modern architects as witnessed by scores of tall buildings built within the last two decades.

To counteract the fundamental drawback of glass, namely the inordinate amount of heat loss and gain in its pure state, the glass industry has invented a whole series of products intended to make glass buildings economical. There are many tinted glasses designed to reduce the blinding effect of the sun; there are tinted-glass sandwiches, double-glazed panels designed to reduce both the blinding effect and increase the insulating value of the glass wall. All these types of glass units are commonly employed not only as vision panels but also as spandrel panels between the vision lights. There are reflective glasses coated with silver or gold mirror films and innumerable shading devices that reduce glare as well as heat gain and thus air conditioning loads.

In laying the groundwork for a discussion of glass design, it may be beneficial to explain briefly how different types of glass commonly used in building are made.

Glass is an amorphous, usually organic, transparent or translucent substance made of a mixture of silicates, borates, or phosphates and cooled from a liquid to a solid state. Archeological evidence from pre-Roman times indicates that glass making originated in the Near East, probably in the third millennium before Christ. Sand, flint, and quartz are the major sources of silica for glass manufacturing. Typical glass batches include, in addition to sand and other raw materials, up to 50 percent of broken glass of related composition, called waste. This waste promotes melting and homogenization of glass. Impurities, normally in the form of iron traces, cause the glass to be green or brown. To achieve a clear substance magnesium oxide is added to counteract the effect of iron traces. Glass can be colored by dissolving in it certain oxides and sulfides.

Carefully measured ingredients are mixed and allowed to undergo initial fusion before being subjected to full heat. In modern glass plants, the glass is melted in large tank furnaces heated by gas, oil, or electricity. Window glass, in use since the first century, was originally made by blowing hollow cylinders that were slit and flattened into

sheets. In modern process molten glass can be directly drawn into sheets. Glass thus made is not entirely uniform in thickness because of the nature of the process by which it is made. The variations in thickness distort the appearance of objects viewed through panes of glass. The traditional method of overcoming such defects has been to grind and polish the glass.

The modern procedure of making "plate glass," first introduced in France in 1668, consists of rolling the glass continuously between double rollers. After the rough sheet has been annealed, both sides of the glass sheet are finished continuously and simultaneously. *Annealing* is a process in which the glass is reheated to a temperature high enough to relieve internal stresses and then slowly cooled to avoid introducing new stresses.

Grinding and polishing are now being replaced by the more economical "float-glass" process. In this process, flat surfaces are formed on both sides by floating a continuous sheet of glass on a bath of molten tin. The temperature is high enough to allow the surface imperfections to be removed by fluid flow of glass. The temperature is gradually lowered as the glass moves along the tin bath and it passes through a long annealing oven at the end.

Annealed glass which has been reheated to a temperature near its softening point and forced to cool rapidly under carefully controlled conditions is described as "heat-treated" glass. Very often stresses are introduced intentionally in glass to impart strength to it. The objective is to introduce a surface compression because glass always breaks as a result of tensile stresses that generally originate across an infinitesimal surface scratch. Compression on the surface increases the amount of tensile stresses that can be endured before breakage occurs. One of the oldest methods of introducing surface compression is called "thermal tempering." It consists of heating the glass almost to the softening point and then cooling it rapidly with an air blast or by plunging it into a liquid bath. This process rapidly hardens the surface, and the subsequent contraction of the slower-cooling interior portions of the glass pulls the surface into compression. Surface compressions approaching 35 ksi (241.32 MPa) can be obtained in thick pieces by this method. Heat-treated glasses are classified as either "fully tempered" or "heat strengthened" according to the magnitude of compressive stresses induced during heat treatment. Federal specification DD-G-1403B 1972 calls for a minimum surface compression of 10 ksi (69 MPa) for a minimum edge compression of 9.7 ksi (66.8 MPa) for the glass to be classified as fully tempered glass. The corresponding minimum requirements for heat-strengthed glass are 3.5 ksi and 5.5 ksi (24.1 and 38 MPa). Below this level the glass is classified as annealed glass.

The fracture characteristics of heat-strengthened glass vary widely. Annealed glass fractures at about 3.5 ksi (24.1 MPa) while fully tempered glass does so at 10 ksi (69 MPa). The characteristic feature of tempered glass is that the glass fractures into small relatively harmless fragments, reducing the likelihood of injury to people. Therefore, many building regulations require the use of tempered glass for skylights, overhead glazing, sloped glazing, and other safety glazing applications.

"Laminated glass" units are made by bonding together two or more lights of glass with an elastomeric interlayer. The interlayer is commonly a plastic film of 0.030 in (0.76 mm) thickness. The laminated glass unit can be made either with annealed, heat-strengthened, or fully tempered glass sheets in any combination. The interlayer does not possess the strength or the stiffness necessary to render the composite unit as strong as an equivalent monolithic light of same thickness. The strength of a laminated unit is taken as 60 percent of the strength of a monolithic light of equal thickness. The actual strength could vary anywhere from 25 percent to full strength of an equivalent monolithic light depending upon the capacity of the interlayer to transmit horizontal shear loads.

"Insulating glass unit" consists of two lights of monolithic glass separated by a spacer and sealed around the perimeter. The sealed air space acts as a layer of insulation, greatly improving the heat-resisting properties of the unit. The edge seal may be fused glass or may be composed of elastomeric sealants and silicones capable of providing a moisture seal around the air space for the normal life of a building. The spacer contains a dessicant to absorb any moisture that may cause the fogging of the glass. Because the air space within an insulating unit is sealed, any pressure applied onto one face is effectively transferred to the other light, making the two lights share the external pressure.

"Wire glass," made by introducing wire mesh into the molten glass before it passes between the rollers, is used to prevent glass from shattering if it is struck. The presence of mesh does not increase the resistance of the light to breakage; it simply holds the pieces together should breakage occur. Building codes commonly consider the strength of wired glass as 50 percent the strength of an annealed monolithic light of the same thickness. Instead of casting a wire mesh within the glass light, an elastomeric film can be applied to the surface to improve the resistance to falling from the frame after breakage.

The strength of glass panels cannot be determined by the classical method of plate analysis because such an analysis is valid only for deflections considerably smaller than the plate thickness. Glass panels deflect many times their thickness and as a result develop membrane stresses which add significantly to their strength and stiffness. More-

over, glass is a brittle material exhibiting no observable yield strength. As such its behavior under loads is best described by evaluating the strength under full-scale test results. Test results show a wide variation of strength for the same size and support conditions of glass panels. This is because the mechanism of glass failure is complex and is highly sensitive to different characteristics of flaws such as their size, orientation, and severity. The only practical approach is to evaluate the effects using an appropriate statistical model. To incorporate the scatter of statistical analysis, a so-called design factor is correlated with probability of failure at full design load. The glass industry uses the normal distribution as the standard model in recommending glass thickness for various design conditions. The published charts of recommended thickness are based on an expected glass breakage probability of 8 lights per 1000, resulting in a design factor of 2.5.

It should be noted that from the statistical point of view, it is virtually impossible to design a glass light without some probability of its failure under design load. Therefore, in conducting a full-scale mock-up test of curtain walls, glass breakage is not considered as a cause for test failure. Glass breakage may very well occur, since the test loads are usually much larger than the design load of glass. If breakage occurs, broken glass is replaced with plywood in order to complete mock-up tests. However, if the test indicates that premature failure of glass is due to inadequate stiffness of the glass supporting system, stricter deflection control should be imposed in the supporting system.

In designing cladding systems with double-glazed insulating sandwiches, care should be taken to prevent the buildup of ultraviolet light, which is known to play havoc with the strip of sealants that completes the sides of the top edges of these sandwiches.

Tempered or semitempered glass commonly used in spandrel areas appears to be susceptible to breakage from even minute inclusions of nickel sulfide. Tempered glass is used in these areas because of the large amount of heat that builds up in the space behind the spandrel between the ceiling and floor above. Heat-strengthened glass which is not fully tempered and does not have the same mechanical and thermal endurance qualities is considered much less susceptible to breakage from infiltration of nickel and carbon sulfide.

The performance of the glass retaining members used in service may have a bearing on the actual load-carrying capacity of the window if they are significantly more flexible than the support provided in strength tests. Moreover, relatively large lateral deflections may occur under design loads, resulting in in-plane movements and a tendency for the glass to slip out of its retaining frame.

The most commonly recommended deflection limitation is 1:175 of the span. However, stiffer supports may be required for proper weathertightness, durability of sealants, or appearance.

Glass design from a structural point of view consists of selecting an appropriate thickness for a given area and design pressure from charts based on tests conducted by the glass industry.

11.6.2 Metal curtain walls

The metal curtain wall is one of the most popular methods of cladding the exterior of a building. In simple terms it consists of a metal framework in which metal, glass, and other surface material are housed. Although aluminum curtain walls of today appear to present endless variety of design, the majority of these designs can be classified into the following five generally recognized systems.

1. Stick system
2. Unit system
3. Unit and mullion system
4. Panel system
5. Column and spandrel cover system

In the stick system the vertical mullions are usually attached first to the structural frame with anchors followed by installation of the window sill and head section. Spandrel panels and vision glass are attached within the mullion framework to complete the system. In the unit system the curtain wall is preassembled into large units complete with spandrel panels and sometimes also with glass panels. The units may be one, two, or sometimes three stories in height. Typical units are designed to snap in place for a sequential interlocking installation.

The unit and mullion system, as the name implies, is a system that attempts to capture the advantages of both the stick and the unit systems. Mullions are installed first, followed by placement of preassembled frame units between them. The panel system is similar in principle to the unit system, the main difference being that the panels do not consist of vertical and horizontal mullions but are integral units formed from sheet metal or laminated aluminum honeycomb panels. Unlike the other systems, the panel system does not have the rigid discipline of vertical and horizontal grid pattern and can be made to represent a wider range of architectural design flexibility.

The column and spandrel cover system can be thought of as a response of the cladding design to the tube system of lateral bracing consisting of closely spaced columns and deep spandrels. Advantage is taken of the close spacing of columns by spanning the glazing units

directly between the column covers. The system can be engineered to clearly express the structural skeleton and permits a wide latitude of aesthetic expression for column and spandrels.

11.6.3 Stone cladding

Stone provides a distinctive alternate to glass and metal curtain walls. Distinctive pinks, reds, grays, and blacks of polished granite and the white, buff, and green of marble along with the black and blue of slate are appearing on the urban skyline. Their popularity has increased to such an extent that major glass and aluminum curtain wall manufacturers have adapted their systems to accept stone inserts. Angles, straps, anchors, and wire ties are common methods of stone erection subject to individual design considerations. New methods have been developed to cut natural stone more precisely and quickly. Because stone is a product of nature with inherent variations in physical properties, proper selection of material and its preparation as a cladding system requires careful evaluation. To this end the C-18 Committee on Natural Building Stones of the American Society of Testing and Materials has developed standards for a variety of building stones.

Stone can be finished in a variety of ways. It can be polished, honed, rubbed, flame or thermal finished, or retain the natural sawn appearance. Not all ranges of finishes are applicable to all types of stones. The wide range of finish choices applicable for dense stones such as granite diminishes to a limited choice for soft stones such as limestone and sandstone.

There are four primary types of veneer attachment to the building exterior. Two are installed piece by piece on site, while the other two types are fabricated offsite and installed as integral panels. In the conventional piece-by-piece system, the stone is installed either by using relieving angles, strap anchors, dowels, and mortar or by other mechanical systems. The standard set method is done over masonry backup with stone panels set against portland cement spots. The mechanical system utilizes a metal grid attached to the structure. The stone panel is retained in place by angles fitted into slots cut into the sides of the stone. It is important to note that noncorrosive metals must be protected from electrolytic reaction.

In the prefabricated system, panels are attached off the job site by specialty contractors. The stone is lowered, finished face down, into prepared forms. Stainless steel anchors are placed into precision-drilled holes on the back of the stone. The location and amount of anchors used are functions of the spanning capability of the stone. A bond breaker such as a liquid applied membrane or a sheet of polyethylene is laid on the back of the stone prior to concrete pour. The

purpose of bond breaker is to accommodate differential movement between the stone and the concrete backup. After the concrete is cured, the panels are trucked to the job site, hoisted into position, and secured to spandrel beams and columns.

Another method of producing a prefabricated system is to fasten stone pieces directly onto steel trusses. Yet another system is obtained by fastening a fiberglass mesh portland cement backing board to the truss and attaching the stone by using the mortar method. In the first system stone is secured to steel by fitting metal angles into slots at the top and bottom of the stone panel.

A system that is finding more and more application in high-rise buildings consists of an aluminum curtain wall system into which stone veneer is slipped instead of glass panels. The precut stone veneer is simply slipped into what would otherwise be aluminum window frame.

11.6.4 Brick veneer systems

Many problems that occur in a brick facade stem from the expansion of the brick due to moisture and direct sunlight, effects of freezing and thawing, and problems arising from insufficient firing of brick. Brick cladding attached to concrete frame buildings is subjected to serious stress buildups because the concrete will tend to creep with time while masonry has a tendency to swell. To alleviate cladding problems it is necessary to provide enough shelf angles for support and sufficient horizontal expansion joints in the wall to allow the two components—concrete and brick—to move independently.

Adequate drainage should be provided to assure that water is not trapped behind the facade of buildings in areas where winters are harsh. Otherwise water freezes and expands, dislodging the brick. A similar problem occurs if brick is supported on untreated steel structure. When steel rusts it flakes and expands, pushing out the brick. Proper coating of steel to prevent rust is necessary. The cladding joints should be detailed in such a way as not to jostle each other under building movements.

11.6.5 Glass fiber–reinforced concrete cladding

Glass fiber–reinforced concrete (GFRC) cladding is a composite material consisting of a portland cement base with glass fibers that are randomly dispersed throughout the material. The fibers add to the tensile and impact strengths, making possible the production of strong yet lightweight architectural panels. The panel can be made much thinner than a conventional precast system thus resulting in a

lightweight system. The lightweight GFRC cladding can provide significant savings by minimizing structural framing and foundation costs for multistory construction especially in areas with poor supporting soil.

11.6.6 Curtain wall mock-up tests

In high-rise construction it is a normal practice to test a full-scale mock-up of cladding at a special testing facility to evaluate the performance of cladding against the various environmental elements. Actual framing, glass, sealants, gaskets, and anchorage devices are used in an effort to simulate the actual job site conditions. In most cases, the cladding materials for a mock-up are supplied by the individual job supplier under the direction of the curtain wall subcontractor. The mock-up is erected by the subcontractor's crew. The crew erects a curtain wall of from one to four stories, which typically forms one side of a four-sided roofed test chamber.

Three performance characteristics are commonly investigated in curtain wall mock-up tests: resistance to air infiltration, resistance to water penetration, and structural performance. In addition, other characteristics such as heat and sound transmission may require testing in some cases. Traditionally structural engineers have very little input for all the tests except for the structural testing. Therefore, in this section only a brief description of the test for structural performance is given. The reader is referred to other publications, such as *Aluminum Curtain Wall Design Guide Manual*, for a description of tests not covered in this section.

The governing factor in the structural design of framing members and panels is usually the stiffness rather than strength. Analytically it is impossible to account for all the interactions that exist in a curtain wall which is comprised of many interdependent elements such as fastenings, anchors, nonrigid joints, seals, and gaskets. Physical testing is often the most reliable means of verifying the performance. Useful information can be obtained by loading the specimens to failure to get an insight into the ultimate capacity of the system and to identify its weak spots. Structural testing is conducted by the static method using an air chamber, subjecting the test specimen to both positive and negative pressures.

Air is blown into the chamber to simulate outward-acting, i.e., negative, wind loads. Air is sucked out of the chamber to simulate inward-acting, i.e., positive, wind loads. A monometer is used to measure the air pressure differential between the outside and inside of the pressure chamber. In the dynamic water test a propeller is used to create air turbulence to simulate wind blowing water against the curtain wall.

Typically, the structural test consists of positive and negative uniform static design load and a proof load of 150 percent of the design load. Seismic load test is conducted by subjecting the wall to a racking displacement in the plane of the wall equal to the calculated floor-to-floor lateral displacement and for proof load twice that displacement.

11.7 Mechanical Damping Systems

Engineers have long recognized that their design responsibility is not only to provide physically safe structures, they must also do so such that the buildings are perceived to be solid so that their earning power is not diminished at any time during their useful life.

Deflection and vibration analysis of buildings becomes very difficult for engineers who expect the same degree of dependability in their calculations as they find in formulas relating stress to strain or other well defined aspects of structural mechanics.

This is because structural response to dynamic loading is very sensitive to total damping in the system. Total damping is the sum of internal damping in the materials due to strain and aeroelastic damping resulting from wind flow around the building. If the building foundation is on compressible soils such as clay soils, the effective damping of the system is increased due to hysteretic behavior of the soil.

Although damping is an important factor in the design of tall buildings, it is at the same time a property which is relatively poorly defined—more acquired than engineered. However, there are adequate rules of thumb, and a number of useful publications exist that go deep into the mathematics of the problem. Since for many buildings several choices can yield safe designs, "better" often must be measured as either less expensive or more desirable from lateral sway and acceleration considerations.

It is not the intent here to describe the design procedures nor the installation techniques of damping systems, but to acquaint the reader with some of the systems that have been used on tall buildings. To this end a brief description of two systems is given in the following section.

Although the exact dynamic behavior of tall buildings is impossible to predict with any great certainty because of the complicated nature of wind and the uncertainty in the evaluation of stiffness of buildings, this much is well understood: Designing a tall building to meet a given drift criterion under equivalent static forces will not automatically preclude creature-comfort problems. Installation of damping systems offers a method of increasing the comfort of the occupants. Damping systems appeal to designers because of the limited control designers have in increasing the inherent stiffness or damping of the building.

The intrinsic stiffness of buildings can be increased up to a point beyond which it becomes prohibitively costly. Although sophisticated computer programs are capable of analytically determining the dynamic characteristics of buildings, it behooves us to remember that the damping characteristics cannot be estimated closer than 30 percent until the building is constructed. From the fundamental dynamic equations, it is known that the wind-induced building response is inversely proportional to the square root of total damping comprised of aerodynamic plus structural damping. To reduce the response by 50 percent, we have to increase the structural damping by four times. As the inherent damping of a building is in the range of 0.5 to 1.5 percent, it is impractical to increase this value to say 5 percent to achieve some meaningful reduction of response. Innovative engineers in their search for effective ways of increasing the comfort and safety of occupants have made use of two types of externally installed damping systems. One system is called "passive viscoelastic dampers" and was first used in the twin towers of the World Trade Center in New York. A more recent application has been in the 76-story building called Columbia Center in Seattle. Viscoelastic dampers used in this building consist of steel plates coated with a polymer compound. The plates are sandwiched between a system of relatively stationary plates. As the building sways under the action of wind loads, the steel plates which are attached to structural members are subjected alternately to compression and tension. The viscoelastic polymer is in turn subjected to shearing deformations absorbing the strain energy created in the structural members. The dissipation of energy into heat reduces the building sway.

In another system called the "tuned mass damper" or TMD, building oscillations are controlled in high winds by placing near the top a large mass that oscillates in a direction counter to the direction of building deflection. Such a system is used on two buildings—the City Corp Center in New York and the John Hancock Tower in Boston. The TMD is a huge concrete block weighing about 2 percent of the building weight and rests on a smooth concrete surface. A large spring is connected to one side of the concrete block, while a piston similar to a shock absorber is connected onto the other side. Building accelerations are continuously monitored. Accelerations in excess of 3 milli-g, indicating the possibility of a heavy windstorm, automatically activate the oil pumps which levitate the block above the concrete surface. The mass is thus free to move back and forth. The device is said to be tuned because during installation the mass of concrete and the stiffness of spring are adjusted to the period of the building. As the building sways, the mass begins to move in the opposite direction, creating a force that opposes or dampens the motion of the building.

11.8 Foundations

The structural design of a skyscraper foundation is primarily determined by loads transmitted by its many floors to the ground on which the building stands. To keep its balance in high windstorms, its foundation requires special consideration because the lateral loads which must be delivered to the soil are rather large. Where load-bearing rock or stable soils such as compact glacial tills are encountered at reasonable depth, as in Dallas with limestone with a bearing pressure of 50 tons per square foot (47.88×10^2 kPa), Chicago with hard pan at 20 to 40 tons per square foot (19.15×10^2 to 38.3×10^2 kPa), the foundation may be directly carried down to the load-bearing strata. This is accomplished by utilizing deep basements, caissons, or piles to carry the column loads down through poor soils to compact materials. The primary objective of a foundation system is to provide reasonable flexibility and freedom in architectural layout; it should be able to accommodate large variations in column loadings and spacings without adversely affecting the structural system due to differential settlements.

Many principal cities of the world are fortunate to be underlain by incompressible bedrock at shallow depths, but certain others rest on thick deposits of compressible soil. The soils underlying downtown Houston, for example, are primarily clays that are susceptible to significant volume changes due to changes in applied loads. The loads on such compressible soils must be controlled to keep settlements to acceptable limits.

Usually this is done by excavating a weight of soil equal to a significant portion of the gross weight of the structure. The net allowable pressure that the soil can be subjected to is dependent upon the physical characteristics of the soil and its previous history. Where soil conditions are poor, a weight of the soil equal to the weight of the building may have to be excavated to result in what is commonly known as fully compensated foundation. Construction of deep foundations may create a serious menace to many older neighboring buildings in many ways. If the water table is high, installation of pumps may be required to reduce the water pressure during the construction of basements and may even require a permanent dewatering system. Depending upon the nature of subsoil conditions, the water table under the adjoining facilities can be lowered, creating an adverse effect on neighboring buildings. Another effect to be kept in mind is the settlement of nearby structures from the weight of the new building.

For buildings in seismic zones, in addition to the stiffness and load distribution, it is important to consider the rigidity of the foundation. During earthquakes, the building displacements are increased by the

angular rotation of the foundation due to rocking action. The effect is an increase in the natural period of vibration of the building.

Loads resulting at the foundation level due to wind or earthquake must be delivered ultimately to the soil. The vertical component due to overturning effects is resisted by the soil in a manner similar to the effects of gravity loads. The lateral component is resisted by (1) shear resistance of piles or piers, (2) axial loads in batter piles, (3) shear along the base of the structure, (4) lateral resistance of soil pressure acting against foundation walls, piers, etc. Depending upon the type of foundation, one or more of the above may play a predominant role in resisting the lateral component.

Much engineering judgment is required to reach a sound conclusion on the allowable movements that can be safely tolerated in a tall building. A number of factors need to be taken into account. These are

1. Type of framing employed for the building
2. Magnitude of total as well as differential movement
3. Rate at which the predicted movement takes place
4. Type of movement whether the deformation of the soil causes tilting or vertical displacement of the building

Every city has its own particular characteristics in regard to design and construction of foundations for tall buildings which are characterized by the local geology and groundwater conditions. Their choice for a particular project is primarily influenced by economic and soil conditions, and even under identical conditions can vary in different geographical locations. In this section a brief description of two types, namely, the pile and mat foundations, is given, highlighting their practical aspects.

11.8.1 Pile foundation

Pile foundations using either piles or drilled piers (also called caissons) are finding more and more application in tall building foundation systems. Driven piles usually consist of prestressed precast piles, or steel piles with pipe, box, or steel H sections. Drilled piers may consist of either straight shafts or may have bells or underreams at the bottom. The number of different pile and caisson types in use is continually changing with the development of pile-driving and earth-drilling equipment.

Driven piles can be satisfactorily founded in nearly all soil conditions. When soils overlying the foundation stratum are soft, normally no problem is encountered in driving the piles. If variations occur in the level of the bearing stratum, it will be necessary to use different

lengths of piles over the site. A bearing type of pile or pier receives its principal vertical support from a soil or rock layer at the bottom of the pier, while a friction-type pier receives its vertical support from skin resistance developed along the shaft. A combination pier, as the name implies, provides resistance from a combination of bearing at the bottom and friction along the shaft. The function of a foundation is to transfer axial loads, lateral loads, and bending moments to the soil or rock surrounding and supporting it.

The design of a pier consists of two steps: (1) determination of pier size, based on allowable bearing and skin friction if any, of the foundation material, and (2) design of the concrete pier itself as a compression member. Piers that cannot be designed in plain concrete with practical dimensions can be designed in reinforced concrete in accordance with the provisions of the applicable codes, such as the ACI code. When tall buildings are constructed with deep basements, the earth pressure on the basement walls may be sufficient to resist the lateral loads from the superstructure. However, the necessary resistance must be provided by the piers when there is no basement, when the depth of basement walls below the surface is too shallow, or when the lateral movements associated with the mobilization of adequate earth pressure are too large to be tolerated. In such cases it is necessary to design the piers for lateral forces at the top, axial forces from gravity loads and overturning, and concentrated moments at the top. One method of evaluating lateral response of piers is to use the theory of beam on elastic foundation by considering the lateral reaction of the soil as an equivalent lateral elastic spring.

The effect of higher concentration of gravity loading over the plan area of a tall building often necessitates use of piles in large groups. In comparison to the stresses in the soil produced by a single pile, the influence of a group of piles extends to a significantly greater distance both laterally and vertically. The resultant effect on both ultimate resistance to failure and overall settlement are significantly different than the summation of individual pile contributions. Because of group action, the ultimate resistance is less while the overall settlement is more.

Oftentimes the engineers and architects are challenged to create a floating effect for the building. This is usually achieved by not bringing the facade right to the ground and by using glass extensively on the ground to create an open feeling in the lobby. A structural system which uses a heavily braced core and a nominal moment frame on the perimeter presents itself as a solution, the core resisting most of the overturning moment and shear while the perimeter frame provides the torsional resistance. Because of the limited width of the core, strong uplift forces are created in the core columns due to lateral loads. A

similar situation develops in the corner columns of exterior-braced tube structures. One of the methods of overcoming the uplift forces is to literally anchor the columns into bedrock. A system of post-tensioned, high-strength anchors about 30 ft or so are driven into bedrock and high-strength grout is injected at the tips to anchor the post-tensioned steel into the rock. A concrete pier constructed below the foundation is secured to the rock by the post-tensioned anchors. Anchor bolts for steel columns cast in the pier transfer the tensile forces from columns to the pier. Another method of securing the columns is to thread the post-tensioned anchors directly through the base plate assemblies of the column.

Figure 11.18 shows the plan and cross-section of a foundation system for a corner column of an X-braced tube building. The spread footing founded on limestone resists the compressive forces while the belled pier under the spread footing is designed to resist uplift forces. To guard against the failure of rock due to horizontal fissures a series of rock bolts are installed around the perimeter of spread footing.

11.8.2 Mat foundation

General considerations. The simultaneous absence of high bearing and side friction capacities of stratum at a reasonable depth beneath the footprint of the building precludes the use of piles or deep underreamed footings. In such circumstances, mat foundations are routinely used under tall buildings, particularly when the soil conditions result in conventional footings or piles occupying most of the footprint of the building. Although it may be possible to construct a multitude of individual or combined footings under each vertical load-bearing element, mat foundations are preferred because of the tendency of the mat to equalize the foundation settlements. Because of their continuous nature, mat foundations have the capacity to bridge across local weak spots in substratums. Mat foundations are predominantly used in two instances: (1) whenever the underlying load-bearing stratum consists of soft, compressible material with low bearing capacity, and (2) as a giant pile cap to distribute the building load to a cluster of piles placed under the footprint of the building.

Mat foundations are ideal when the superstructure load is delivered to the foundation through a series of vertical elements resulting in a more or less uniform bearing pressure. It may not be a good solution when high concentrations of loading occur over limited plan area. For example, in a core-supported structure carrying most of the building load, if not the entire load, it is uneconomical to spread the load over the entire footprint of the building because this would involve construction of exceptionally thick and heavily reinforced mat. A more

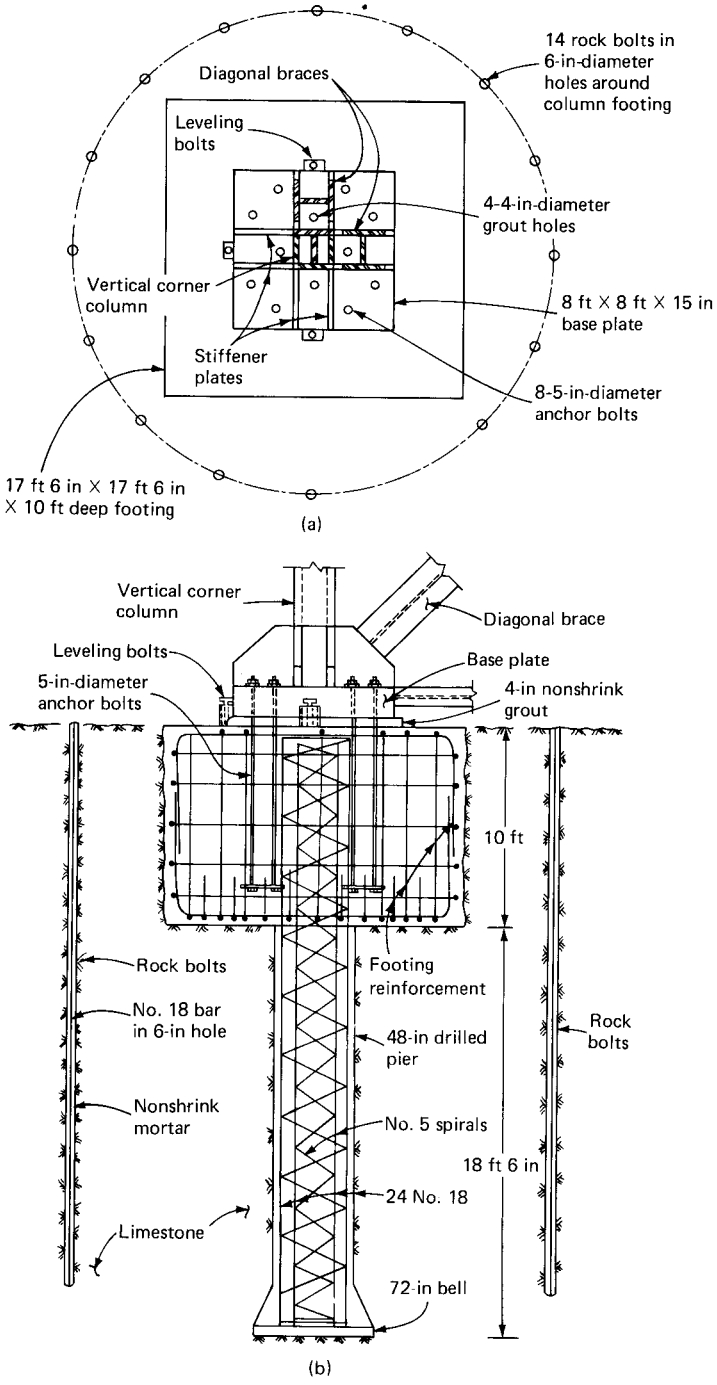

Figure. 11.18 Foundation system for a corner column of an X-braced tube building. (*a*) Plan; (*b*) section.

direct solution is to use driven piles or drilled caissons directly under the core.

The plan dimensions of the mat are determined such that the mat contact pressure does not exceed the allowable bearing capacity prescribed by the geotechnical consultant. Typically three types of allowable pressures are to be recognized: (1) net sustained pressure under sustained gravity loads, (2) gross pressure under total design gravity loads, and (3) gross pressure under both gravity and lateral loads.

In arriving at the net sustained pressure the loads to be considered on the mat area should consist of

1. Gravity load due to the weight of the structural frame
2. Weight of curtain wall, cooling tower, and other mechanical equipment
3. An allowance for actual ceiling construction including air conditioning duct work, lights, sprinklers, and fireproofing
4. Probable weight of partition based on single and multitenant layouts
5. Probable sustained live load
6. Loads applied to the mat from backfill, slab, pavings, etc.
7. Weight of mat
8. Weight of soil removed from grade to the bottom of the mat

This last item accounts for the reduction in overburden pressure and therefore is subtracted in calculating the net sustained pressure.

In calculating the sustained pressure on mats, typically less than the code prescribed values are used for items 4 and 5, requiring engineering judgment in their estimation. In the opinion of the author a total of 20 psf (958 Pa) for these items appears to be adequate. A limit on sustained pressure is basically a limit on the settlement of the mat. In practical cases of mat design it is not uncommon to have the calculated sustained pressure under isolated regions of mat be somewhat larger than the prescribed limits. This situation should be reviewed with the geotechnical engineers and usually is of no concern as long as the overstress is limited to small portions of the mat.

The gross pressure on the mat is equivalent to the loads obtained from items 1 through 7. The weight of the soil removed from grade to the bottom of the mat is not subtracted from the total load because the gross pressure is of concern. Also, in calculating the weight of partition and live loads, the code-specified values are used.

The transitory nature of lateral loads is recognized in mat design by

(a)

Figure 11.19 (*a*) Concrete placement operations for a high-rise mat.

allowing a temporary overstress on the soil. This concept is similar to the 33 percent increase in stresses allowed in most building codes for wind and seismic loads. From an academic point of view, the ideal thickness for a mat is the one that is just right from punching shear considerations while at the same time minimum reinforcement of $0.002A_c$ provided for temperature works just right from flexural considerations. However, in practice it is found that it is more economical to construct pedestals or provide shear reinforcement in the mat rather than to increase the basic mat thickness.

In detailing the flexural reinforcement there appear to be two schools of thought. One school maintains that it is more economical to limit the largest bar size to a #11 bar which can be lap-spliced. However, this limitation may force the use of as many as four layers of reinforcement both at top and bottom of mat. The other school promotes the use of #14 and #18 bars with mechanical tension splices. This requires fewer bars, resulting in cost savings in the placement of reinforcement. The choice is, of course, a matter of economy as perceived by the contractor.

Figure 11.19*a* shows concrete placement operations for a high-rise mat. A close-up view of reinforcement is shown in Fig. 11.19*b*.

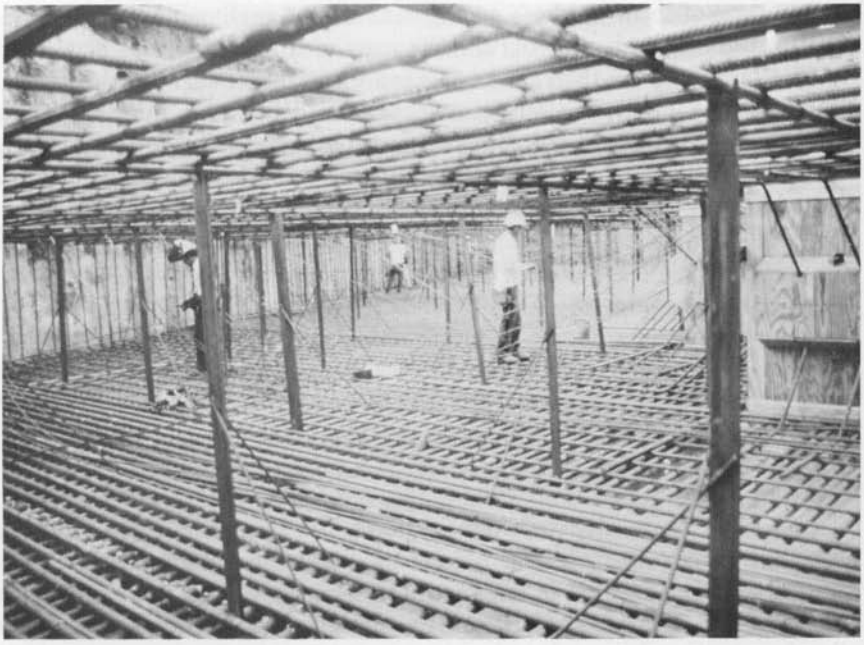

(b)

Figure 11.19 (*Continued*) (*b*) Close-up view of mat reinforcement.

Analysis. A vast majority of soil and structure interaction takes place under sustained gravity loads. Although the interaction is complicated by the nonlinear and time-dependent behavior of soils, it is convenient for analytical purposes to represent the soil as a type of elastic spring. This concept was first proposed by Winkler in 1867 and hence the name Winkler spring. He proposed that the force and vertical displacement relationship of the soil be expressed in terms of a constant K called the modulus of subgrade reaction. It is easy to incorporate the effect of the soil by simply including a spring with a stiffness factor in terms of force per unit length beneath each reaction. However, it should be remembered that the modulus is not a fundamental property of the soil but depends on many things, including the size of the loaded area and the length of time it is loaded. Consequently, the modulus of subgrade reaction used for calculating the spring constants must be consistent with the type and duration of loading applied to the mat.

Prior to the availability of finite element programs, mat analysis used to be undertaken by using grid analysis by treating the mat as an assemblage of linear elements. The grid members are assigned equivalent properties of a rectangular mat section tributary to the grid. The

magnitude of the Winkler's spring constant at each grid intersection is calculated on the basis of tributary area of the joint.

The preferred method for analyzing mats under tall buildings is to use a finite element computer program. With the availability of computers, analytical solutions for complex mats are no longer cumbersome; engineers can incorporate the following complexities into the solution with a minimum of effort:

1. Varying subgrade modulus
2. Mats of complex shapes
3. Mats with nonuniform thickness
4. Mats subjected to arbitrary loads due to axial loads and moments
5. Soil structure interaction in cases where the rigidity of the structure significantly affects the mat behavior

As in other finite element idealizations, the mathematical model for the mat consists of an assemblage of discretized elements interconnected at the nodes. It is usual practice to use rectangular or square elements instead of triangular elements because of the superiority of the former in solving plate-bending problems. The element normally employed is a plate-bending element with 12 degrees of freedom for three generalized displacements at each node. The reaction of the soil is modeled as a series of independent elastic springs located at each node in the computer model. The behavior of the soil tributary to each node is mathematically represented as a Winkler spring at each node. There is no continuity between the springs other than through the mat. Also, the springs because of their very nature can only resist compression loads although computationally it is not possible to impose this restriction in a linear elastic analysis. Therefore, it is necessary to review the spring reactions for any possible tensile support reactions. Should this have occurred in the analysis, it is necessary to set the spring constant to zero at these nodes and to perform a new analysis. This iterative procedure is carried out until the analysis shows no tensile forces in springs.

In modeling the mat as an assemblage of finite elements, the following key factors should be considered. (1) Grid lines that delineate the mat into finite elements should encompass the boundaries of the slab, as well as all openings. They should also occur between elements with changes in thicknesses. Skew boundaries of mat not parallel to the orthogonal grid lines may be approximated by steps that closely resemble the skewed boundary. (2) Grid lines should intersect preferably at the location of all columns. Minor deviations are permissible without loss of meaningful accuracy. (3) A finer grid should be used to define regions subjected to

severe displacement gradients. This can be achieved by inserting additional grid lines adjacent to major columns and shear walls.

Although it is possible to construct an analytical model consisting of both the mat and superstructure, practical budgetary and time considerations preclude use of such complex analyses in everyday practice. Admittedly the trend, with the availability of computers and general analysis programs, is certainly toward this end. However, the current practice of accounting for superstructure interaction is to simulate approximately the stiffness of superstructure by incorporating artificially stiff elements located in the plane of the mat. Although the procedure is approximate, it has the advantage of being simple and yet capable of capturing the essential stiffness contribution of the superstructure.

The complex soil-structure interaction can be accounted for in the design by the following iterative procedure. Initially the pressure distribution under the mat is calculated on the assumption of a rigid mat. The geotechnical engineer uses this value to obtain the deformation and hence the modulus of subgrade reaction at various points under the footprint of the mat. Under uniform pressure the soil generally shows greater deformations at the center than at the edges of the mat. The modulus of subgrade reaction, which is a function of the displacement of the soil, therefore has higher values at the edges than at the center. The finite element mat analysis is performed using the varying moduli of subgrade reaction at different regions of the mat. A new set of values for contact pressures is obtained and processed by the geotechnical engineer to obtain a new set of values of soil displacements and hence the moduli of subgrade reaction. The process is repeated until the deflections predicted by the mat finite element analysis and the settlement predicted by the soil deflection due to consolidation and recompression of soil stratum converge to a desirable degree.

Two examples of mat analysis are presented in the following in order to give the reader a feel for the physical behavior of mats. The first example consists of a mat for a 25-story concrete office building and the second example highlights the behavior of an octagonal mat for an 85-story composite building.

Mat for a 25-story building. The floor framing for the building consists of a system of haunch girders running between the interior core walls and columns to the exterior. The haunch girders are spaced at 30 ft (9 m) on centers and run parallel to the narrow face of the building. Skip joists spaced at 6 ft (1.81 m) center-to-center span between the haunch girders. A 4-in (101.6-mm) thick concrete slab spanning between the skip joists completes the floor framing system. Lightweight concrete is used for floor framing members while normal weight concrete is employed for columns and shear walls.

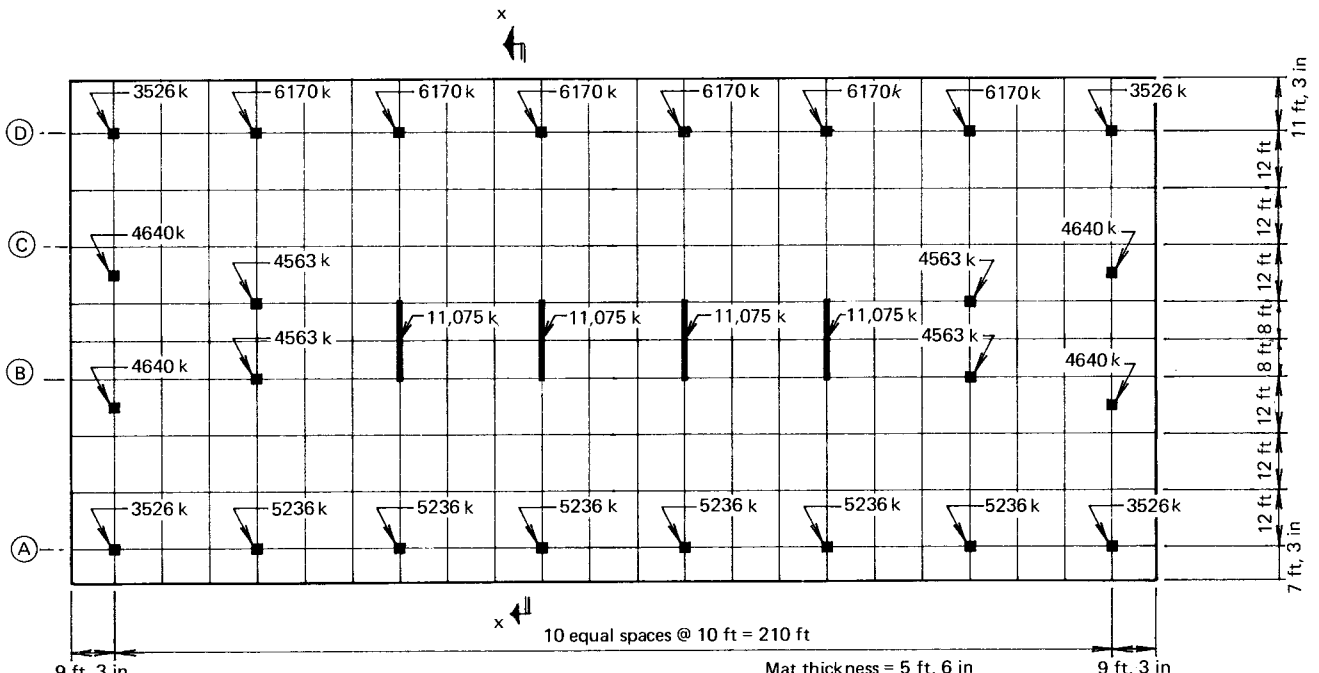

Figure 11.20 Foundation mat for a 25-story building: finite element idealization and column ultimate loads.

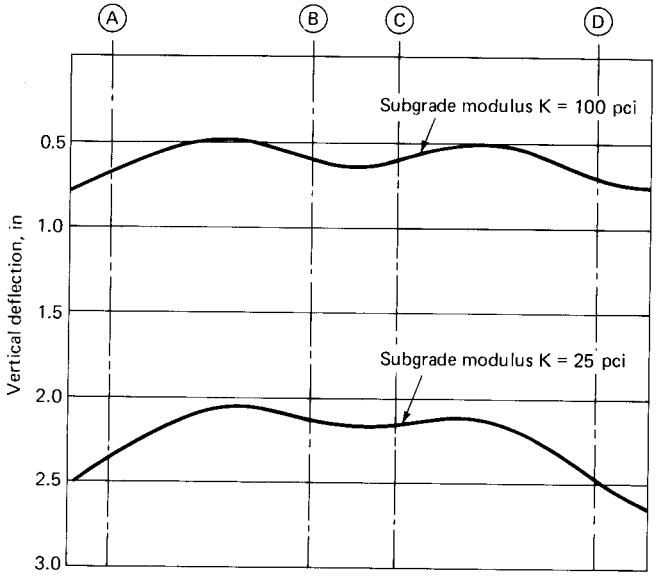

Figure 11.21 Vertical deflection of mat along section x-x.

Shown in Fig. 11.20 is a finite element idealization of the mat. The typical element size of 12 by 10 ft (3.63 by 3.03 m) may appear to be rather coarse, but an analysis which used a finer mesh in which the typical element was 3 by 2.5 ft (0.9 by 0.76 m) showed results identical to that obtained for the coarse mesh. The calculated ultimate loads at the top of the mat are shown in Fig. 11.20. It may be noted that the finite element idealization is chosen in such a manner that the location of almost all columns, with the exception of four exterior columns on the narrow face, coincide with the intersection of the finite element mesh. The loads at these locations are applied directly at the nodes. The loads on the four exterior columns are, however, divided into two equal loads and applied at the two nodes nearest to the column. The resulting discrepancy in the analytical results has very little impact, if any, on the settlement behavior and the selection of reinforcement for the mat.

Assuming a value of 100 lb/in^3 (743 kg/mm^3) for the subgrade modules, the spring constant at a typical interior node may be shown to be equal to 1728 kips/in (196×10^3 N/m). Figure 11.21 shows the mat deflection comparison for two values of subgrade reaction, namely 100 and 25 lb/in^3 (743 and 185.75 kg/mm^3). As can be expected, the mat experiences a larger deflection when supported on relatively softer springs. The variation of curvature, which is a measure of bending moments in the mat, is relatively constant for the two cases. This can be verified further by comparing the bending-moment diagrams shown

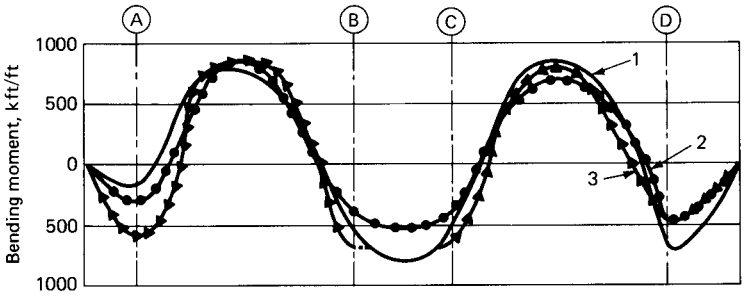

1. Modulus of subgrade reaction K = 100 pci
2. Modulus of subgrade reation K = 25 pci
3. Continuous beam analysis

Figure 11.22 Bending moment variation along section x-x.

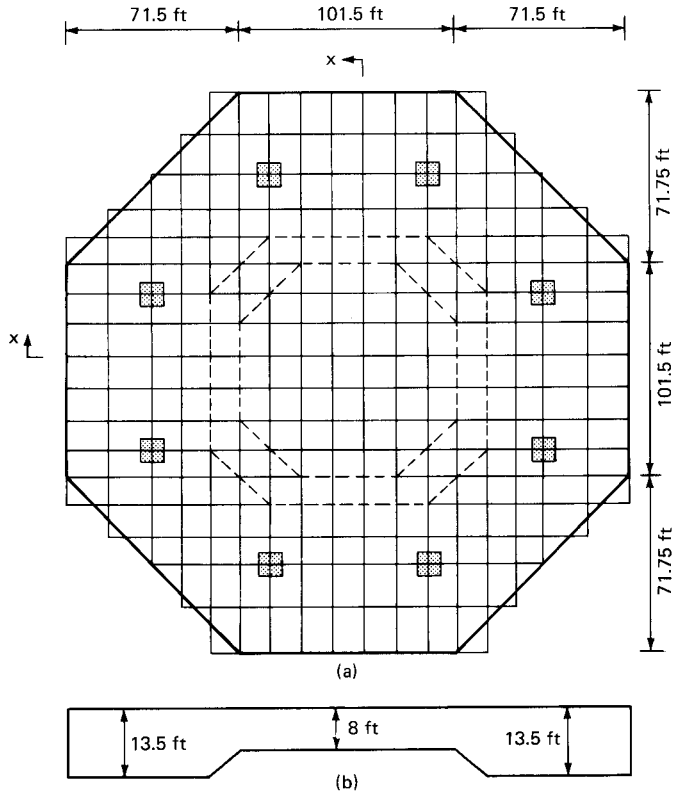

Figure 11.23 Foundation mat for a proposed 85-story office building. (*a*) Finite element idealization; (*b*) cross section x-x through mat.

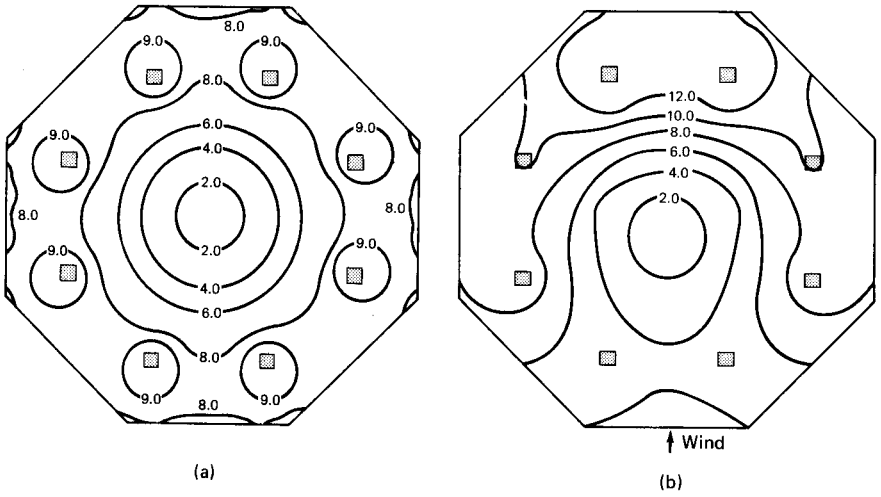

Figure 11.24 Contact pressure contour under mat (ksf). (*a*) Dead loads plus live loads; (*b*) dead plus live plus wind loads. (*Note:* $K = 100$ lb/in^3.)

in Fig. 11.22. Also shown in this figure is the bending moment variation obtained by assuming the mat as a continuous beam and supported by three rows of supports corresponding to exterior columns and interior shear walls and subjected to the reaction of the soil acting vertically upward. The results for the example mat appear to indicate that mat reinforcement selected on the basis of any of the three analyses will result in adequate design. However, in view of the ease with which the analysis can be carried out on computers, the author suggests that more than one analysis be undertaken to confirm the behavior of the mat.

Mat for an 85-story building. Figure 11.23 shows the finite element idealization of the mat for a proposed 85-story composite building, the structural system for which was described in Chap. 4. It may be noted that diagonal boundaries of the mat are approximated in a stepwise pattern using rectangular finite elements. To achieve economy in concrete and reinforcement quantities, the thickness of mat was varied; a thicker mat was proposed under the columns where the loads and thus the bending of the mat were expected to be severe. A relatively thin mat section was proposed for the center of the mat. The wisdom of choosing two mat thicknesses can be appreciated by studying the pressure contours in Fig. 11.24*a* and *b*. The pressure contours plotted in these figures were obtained from computer analyses for two different loading conditions—gravity loads acting alone and gravity loads combined with wind loads. No uplift due to wind loads was evident.

Selected References

1. Myron Goldsmith, "The Effects of Scale," ASCE National Convention, April 1977.
2. Robert A. Halvorson, "Architectural-Structural Form of Highrise Buildings—An Integrated Response," ASCE Texas Section, September 1982.
3. Uniform Building Code, 1985.
4. "Model Studies of The Dynamic Response of Tall Buildings to Wind," Proceedings of 1982 CSCE Annual Conference.
5. American National Standards Institute (ANSI) A58.1, 1982.
6. "Structuring Tall Buildings," *Progressive Architecture*, December 1980.
7. J. E. Cermak, "Applications of Fluid Mechanics to Wind Engineering," *Journal of Fluids Engineering*, March 1975.
8. "Wind Effects on High Rise Buildings," Symposium Proceedings, March 1970, Northwestern University, Illinois.
9. T. Tschanz, "Measurement of Total Dynamic Loads Using Elastic Models With High Natural Frequencies," in Timothy J. Reinhold (ed.), *Wind Tunnel Modeling for Civil Engineering Applications*, Cambridge University Press, 1982.
10. "Tall Buildings," Conference Proceedings, 1984, Singapore.
11. Robert A. Coleman, *Structural System Designs*. Englewood Cliffs, N.J., Prentice-Hall, 1983.
12. *Post-Tension Manual*. Prestressed Concrete Institute.
13. T.Y. Lin and S.D. Stotesbury, *Structural Concepts and Systems for Architects and Engineers*. New York, John Wiley, 1981.
14. James R. Libby, *Modern Pre-Stressed Concrete*. New York, Van Nostrand, Reinhold, 1984.
15. T.Y. Lin and Ned H. Burns, *Design of Prestressed Concrete Structure*. New York, John Wiley, 1981.
16. H. G. Allen, and P. S. Bulson, *Background to Buckling*. New York, McGraw-Hill, 1980.
17. George Winter and Arthur H. Nilson, *Design of Concrete Structures*. New York, McGraw-Hill, 1986.
18. Frederick S. Merritt, *Building Design and Construction Handbook*. New York, McGraw-Hill, 1982.
19. Gaylord and Gaylord, *Design of Steel Structures*. New York, McGraw-Hill, 1972.
20. S. Timoshenko, Pitt Young, and W. Weaver, Jr., *Vibration Problems in Engineering*. New York, John Wiley, 1974.
21. N. M. Newmark and E. Rosenblueth, *Fundamentals of Earthquake Engineering*. Englewood Cliffs, N.J., Prentice-Hall, 1971.
22. Coull and Stafford-Smith, *Tall Buildings with Particular Reference to Shear Wall Structures*. New York, Pergamon Press, 1967.
23. Monoru Wakabayashi, *Design of Earthquake Resistant Buildings*, New York, McGraw-Hill, 1986.
24. Kenneth Leet, *Reinforced Concrete Design*. New York, McGraw-Hill, 1982.
25. John M. Biggs, *Introduction to Structural Dynamics*. New York, McGraw-Hill, 1964.
26. Blomer W. Bodgett, *Design of Welded Structures*. Lincoln Arc Welding Foundation, 1982.

27. Gaylord and Gaylord, *Structural Engineering Handbook*. New York, McGraw-Hill, 1979.
28. John A. Blume, Nathan M. Newmark, Leo H. Corning, *Design of Reinforced Concrete Buildings for Earthquake Motions*. Portland Cement Association, 1971.
29. "Reinforced Concrete Structures Subjected to Wind and Earthquake Forces," Sp 63, ACI, 1980.
30. "Multistory Structures—Lateral Forces," Sp. 36, ACI, 1973.
31. "Analysis of Structural Systems For Torsion," Sp. 35, ACI, 1973.
32. Sol. E. Cooper with Andrew C. Chen, "Designing Steel Structures—Methods and Cases," Englewood Cliffs, N.J., Prentice-Hall, 1985.
33. Wolfgang Schueller, *High Rise Building Structures*, 1976.
34. Zbirohowski-Koscia, *Thin-Walled Beams*. Crosby Lockwood, 1967.
35. Milo S. Ketchum (ed.), *Structural Engineering Practice*. Vol. nos. 1 & 2, 1982; vol. no. 4, 1982–83; vol. nos. 1, 2, & 3, 1983; vol. no. 4, 1983–84. New York, Marcel Dekker.
36. *National Building Code Of Canada and Its Supplement*. 1985.
37. N. W. Murray, *Introduction to the Theory of Thin-Walled Structures*. New York, Oxford University Press, 1984.
38. Timothy J. Reinhold (ed.), *Wind Tunnel Modeling for Civil Engineering Applications*. Cambridge University Press, 1982.
39. M. B. Kanchi, *Matrix Methods of Structural Analysis*. New York, Wiley Eastern Limited, 1981.
40. S. L. Lee and P. Karasudhi (eds.), *Proceedings of the Regional Conference on Tall Buildings*. Bangkok, 1974.
41. "Monographs on Planning and Design of Tall Buildings." Vols. PC, SC, CL, SB, and CB, New York, American Society of Civil Engineers, 1978.
42. Mario Paz, *Structural Dynamics*. New York, Van Nostrand Reinhold, 1985.
43. J. R. Choudhury, "Analysis of Plain and Spatial Systems of Interconnected Shear Walls," Ph.D. Thesis, University of Southampton, 1968.
44. V.Z. Vlasov, *Thin-Walled Elastic Beams*. Washington, D.C., National Science Foundation.
45. Bungale S. Taranath, "Torsional Behavior of Open-Section Shear Wall Structures," Ph.D. Thesis, University of Southampton, 1968.
46. H.S. Iyengar, "State-of-the-Art report on composite or mixed steel-concrete construction for Buildings," *ASCE*, 1977.
47. Aslam Qadeer, "Interaction of Floor Slabs and Shear Walls," Ph.D. Thesis, University of Southampton, 1968.
48. Bungale S. Taranath, "A New Look at Composite High-Rise Construction," Our World in Concrete and Structures, Singapore, 1983.
49. Bungale S. Taranath et al., "A Practical Computer Method of Analysis for Complex Shear Wall Structures," ASCE 8th Conference in Electronic Computation, 1983.
50. Bungale S. Taranath, "Composite Design of First City Tower," *The Structural Engineer*, 1982.
51. Bungale S. Taranath, "Differential Shortening of Columns in High-Rise Buildings," *Journal of Torsteel*, 1981.
52. Bungale S. Taranath, "Analysis of Interconnected Open Section Wall Structures," *ASCE Journal*, 1986.
53. Bungale S. Taranath, "The Effect of Warping on Interconnected Shear Wall Flat Plate Structures," *Proceedings of the Institution of Civil Engineers*, 1976.
54. Bungale S. Taranath, "Torsion Analysis of Braced Multi-Story Buildings," *The Structural Engineer*, London, 1975.
55. Bungale S. Taranath, "Optimum Belt Truss Locations for High-Rise Buildings," *AISC*, vol. II, 1974.
56. Alexander Coull and J. R. Choudhury, "Analysis of Coupled Shear Walls," *ACI Journal*, September, 1967.
57. R. Rosman, "An Approximate Method of Analysis of Walls of Multistory Buildings," *Civil Engineering and Public Works Review (London)*, vol. 59, January 1964.
58. A. Qadeer and B. Stafford-Smith, "Bending Stiffness of Slabs Connecting Shear Wall Structures," *ACI Journal*, June 1969.

59. B. Stafford-Smith and Amal Girgis, "Simple Analogous Frames for Shear Wall Analysis," *ASCE Journal of Structural Engineering*, vol. 110, no. 11, November 1984.
60. "The Effects of Shock and Vibration on Men," in Morris and Crede (eds.), *Shock and Vibration Handbook*. McGraw-Hill, 1961.
61. Kenneth H. Lenzen, "Vibrations of Steel Joist–Concrete Slab Floors," *AISC Engineering Journal*, July 1966.
62. J. F. Wiss and R. H. Parmalee, "Human Perception of Transient Vibrations," *Journal of Structural Division ASCE*, vol. 100, April 1974, pp. 773–783.
63. Thomas M. Murray, "Design to Prevent Floor Vibrations," *Engineering Journal–American Institute of Steel Construction*, third quarter, 1975.
64. R. Halvorson and N. Isyumov, "Comparison of Predicted and Measured Dynamic Behavior of Allied Bank Plaza," in N. Isyumov and T. Tschanz (eds): *Building Motion in Wind*, New York, ASCE, 1982.

Appendix

A

Conversion Factors: U.S. Customary Units to SI Metric Units

Lengths or displacements

1 ft = 0.3048 m
1 in = 25.40 mm
1 mile (U.S. statute) = 1609.3 m (1.609 km)
1 mile (international nautical) = 1852.0 m (1.852 km)

Area

$1\ in^2 = 645.2\ mm^2$
$1\ ft^2 = 0.0929\ m^2$

Section modulus or volume

$1\ in^3 = 16.39 \times 10^3\ mm^3$
$1\ ft^3 = 0.0283\ m^3$

Moment of inertia

$1\ in^4 = 0.4162 \times 10^6\ mm^4$
$1\ ft^4 = 0.008631\ m^4$

Loads

1 lb = 4.448 N
1 kip (1000 lb) = 4.448 kN

1 lb/ft = 14.59 N/m
1 kip/ft = 14.59 kN/m
1 lb/in = 1.7513 N/m

Bending moment or torque

1 lb · in = 0.11298 Nm
1 lb · ft = 1.3558 Nm
1 kip · ft = 1.3558 kNm

Stress, modulus of elasticity, and surface loads

1 lb/in^2 = 0.006895 MPa
1 kip/in^2 = 6.895 MPa
1 lb/ft^2 = 0.0479 kN/m^2
1 kip/ft^2 = 47.88 kN/m^2

Unit weight, density

1 lb/ft^3 = 16.03 kg/m^3
1 lb mass = 0.45359 kg
1 ton mass = 907.18 kg

Index

Page references in *italic* indicate illustrations or tables.

About the Author

Dr. Bungale S. Taranath, Ph.D., PE, FI, Struct E, is a senior project manager with the structural consulting firm of John A. Martin and Associates in Los Angeles, California. He has extensive experience in the design of concrete steel and composite tall buildings and has served as principal in charge on many notable high-rise buildings. He has held positions as vice president and principal in charge with two well-known consulting firms in Houston, and as a senior project engineer with the Chicago office of Skidmore, Owings & Merrill, where his fascination with tall buildings developed under the late Dr. Fazlur R. Khan. He is a fellow of the Institution of Structural Engineers, London, England; a member of the American Society of Civil Engineers and the American Concrete Institute; and a registered professional engineer in several states. He has conducted research into the behavior of tall buildings and shear wall structures and is the author of a number of published papers on torsion analysis and multistory construction projects.

Civil Engineering
Construction
Architecture

STRUCTURAL ANALYSIS & DESIGN OF TALL BUILDINGS

Tall buildings have for decades epitomized the modern urban landscape—yet until now structural engineers and architects have lacked a targeted reference that analyzes and illustrates the full range of high-rise structural concepts and available alternatives. This first-of-its-kind in-depth sourcebook will allow both practicing professionals and engineering students to implement virtually *all* the latest ideas and methods for creating sound, cost-efficient high-rise structures.

Establishing the overriding importance of bracing for lateral loads in high-rise architecture, Dr. Taranath shows how to—

- Quantify the three-dimensional forces of wind and seismic stress—including selecting the proper wind tunnel tests and performing dynamic analysis of a building using the modal superposition method
- Handle lateral bracing systems—such as semirigid, rigid, braced frame, staggered truss, eccentric bracing, belt and outrigger truss, tube and cellular structure, and shear wall–frame interaction—using steel, concrete, and innovative combinations of both
- Incorporate gravity design of vertical and horizontal systems—using steel, concrete, and combinations of both—to enhance lateral-load-resisting effects
- Analyze, design, and detail entire structural proposals—from using basic portal and cantilever methods for preliminary engineering calculations to more complex computer techniques for modeling two- and three-dimensional formations.

Throughout, Dr. Taranath demonstrates critical principles using realistic example problems and case studies of proposed and existing tall buildings—many of which he designed himself. He tackles practical cost considerations as they arise, and draws on over 500 illustrations—structural schematics, typical floor plans, plotting graphs, and more—to provide a clear picture of system applications. Major building specifications codes and Applied Technology Council provisions are also cited and discussed where appropriate.

Lucid, systematic, and thorough, this book gives users the creative flexibility to devise almost limitless variations for the projects they encounter.

Cover Design: P.L.K. Graphics, Inc.
Cover Photo: Robert Phillips/The Image Bank

McGraw-Hill Book Company
Serving the Need for Knowledge
1221 Avenue of the Americas
New York, NY 10020

ISBN 0-07-062878-5